ELSEVIER

Coherent synchronized Oxidation Reactions by Hydrogen Peroxide

Tofik M. Nagiev

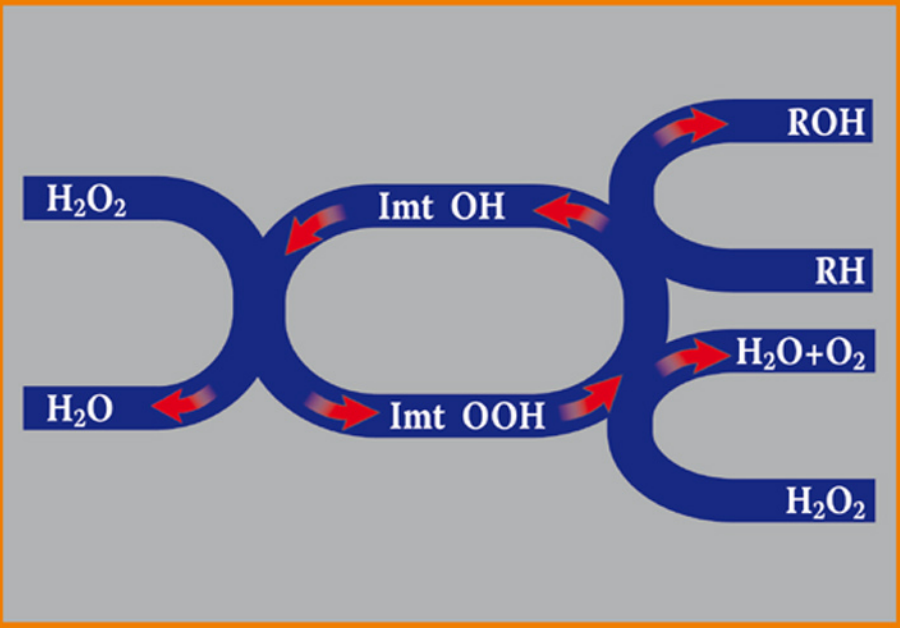

Coherent Synchronized Oxidation Reactions by Hydrogen Peroxide

This page intentionally left blank

Coherent Synchronized Oxidation Reactions by Hydrogen Peroxide

Tofik M. Nagiev
Research Center of Azerbaijani
Academy of Science
Baku, Azerbaijan

ELSEVIER
Amsterdam • Boston • Heidelberg • London • New York • Oxford
Paris • San Diego • San Francisco • Singapore • Sydney • Tokyo

Elsevier
Radarweg 29, PO Box 211, 1000 AE Amsterdam, The Netherlands
The Boulevard, Langford Lane, Kidlington, Oxford OX5 1GB, UK

First edition 2007

Library of Congress Cataloging-in-Publication Data
A catalog record for this book is available from the Library of Congress

British Library Cataloguing in Publication Data
A catalogue record for this book is available from the British Library

ISBN-13: 978-0-444-52851-3
ISBN-10: 0-444-52851-2

Printed and bound in The Netherlands

07 08 09 10 11 10 9 8 7 6 5 4 3 2 1

This book is dedicated to my
daughter Inara

This page intentionally left blank

Preface to Russian Edition

Finis libri non finis quaerendi—'The book is finished, but the investigation goes on'—this ancient Latin saying ended my previous monograph *Chemical conjugation*, published in 1989 by the Academy of Sciences of the former USSR.

Having been devoted to this scientific direction in recent decades, my colleagues and I have succeeded in obtaining a deeper knowledge of this branch of physical chemistry.

The title of the present monograph reflects the scientific concept of this book: the development of synchronously proceeding reaction interaction theory.

The title *Chemical conjugation* mainly reflects the types of interaction between synchronously proceeding complex reactions. It highlights the scientific story of the material and the most common, classical ideas.

I feel it would have been premature to use the new term *chemical interference*, which combines all types of synchronized complex reactions, in the title of this book, because the term interference is usually associated with optics. This involves efforts to find something analogous to physical (optical) interference principles in complex chemical systems.

Of course, nothing similar is found and many scientists, unselfcritical and impatient, reject this idea, taking it for just a new term.

This psychological aspect of the question made me careful when choosing the title of this book, which is *Hydrogen peroxide and phenomenon of coherent synchronization between chemical and biochemical reactions*. This title is more acceptable than *Chemical interference*.

The term chemical interference defines the interaction between synchronously proceeding complex chemical reactions. To understand this definition, one has only to reject the analogies with optics, on the one hand, and understand that chemical interference is based on ideas of chemical kinetics and the mechanism of complex chemical processes. Thus, I believe that there will be no argument about the term.

At the end of the 20th century chemistry and biology came so close that investigations developing 'molecular grounds of the sciences on life' advanced in many traditional fields of chemistry. In particular, the symbiosis of organic chemistry and catalysis with biology brought about many important discoveries and the formation of new fields in chemistry: supramolecular chemistry, computerized and combinatorial chemistry, biomimetic organic chemistry, mimetic catalysis, etc. In this context, monographs which may turn the thinking of chemists to fundamental research into living systems are in favor. In modern chemistry, many questions about the interactions of different events can be answered by an overall approach in which 'all affects all'. Periodical alteration of synchronous reaction rates, defined by their coherence degree, forms the interference pattern of two or more reactions, presented by synchronized kinetic curves. Such regularity is correct for chemical reactions implemented in the kinetic zone, when the reaction rate is limited by chemical interaction.

Another interesting example of the regularity of macroscopic chemical reactions is the Belousov–Jabotinsky reaction in which coherence is limited by the diffusion zone of the reaction run.

Chemical interference can be applied to the control of complex chemical reaction rates and be the prototype for the interpretation of analogous interactions in biochemical systems.

Chemical interference is mostly realized by selecting reactions capable of organizational interaction. Hence, an ensemble of molecules and, consequently, an ensemble of reactions, create an algorithm for implementation of interrelated spontaneous reactions able to interfere. Note that the structure of the molecular ensemble may be different, which may also affect the course of conjugated processes. The communication channels between self-organized systems (ensembles) of reactions are performed by reactive intermediate particles, general to all current processes.

These processes can be accelerated and effectively implemented with the use of catalysts or their associates similar to living systems (enzyme ensembles on cellular and subcellular membranes).

Thus, self-organization of the reaction ensemble, able to be intensified or weakened (chemical interference), may form the foundation of the principle by which the majority of enzymatic ensembles is organized.

Unfortunately, too broad an expansion of investigations tends to push fundamental research into the background.

In the present book, the viability of the new theoretical approach is illustrated by broad experimental material. Usually, a scientist chooses the level of studies with respect to the task in hand. However, progress in science is due to a combination of all levels of investigation methods in modern research, because each of them simply answers different questions.

I want very much to finish the preface with the initial sentence and do not want to say that 'there is life in the old dog yet' …

An attentive scientist will, no doubt, grasp the idea of this monograph and decide to develop and apply the theory discussed here to practical purposes. This will be the best reward for the author.

I am very grateful to those who have helped and guided me in this work. I am especially grateful to Academician J.A. Aliev for the great help and attention to the author.

T.M. Nagiev

Preface to English Edition

'A man who has to walk a thousand miles needs to think that there is something good at their end' (Leo Tolstoy, 'War and Peace'). Thus, when I made my initial steps in the branch of conjugated processes, I believed in the silliness of my tender years that something good awaited me at the end of this work.

From the very beginning, it was clear that the reaction system of two or more synchronous reactions will always find conditions and factors promoting their interaction. The level of our knowledge about kinetics and the mechanism of chemical reactions did not allow interpretation of the majority of interactions between reactions in the framework of the old concept of chemical conjugation. This prompted the question of creating a new concept which would unambiguously determine a complex interaction (coherence) between synchronous reactions.

This is the problem!

Modern chemistry is characterized by the unification of differential and integral methods in many studies. This is the most fruitful way, because it allows us to pass from the molecular mechanism of chemical and biochemical reactions (microscopic level) to their coherent synchronization (macroscopic level). This relatively new approach and its amazing efficiency for the study of complex chemical and biochemical systems are illustrated in the present monograph. It should be noted that interactions between reactions are no longer the 'wind' of scientific change, though it removes the old concepts while preserving the classical ones, for example, chemical conjugation.

To make this book clearer to understand, some parallels and differences between chemical conjugation and chemical interference are discussed. In definite conditions, chemical interference and chemical conjugation have the same objectives. Nevertheless, only chemical interference allows a deeper analysis of coherent synchronous chemical reactions.

Similar to the epoch of classical ideas, coherent synchronous reactions are divided into primary and secondary processes: the primary reaction synthesizes reactive intermediates promoting bifurcation—the process splitting to, at least, two reaction flows. One of the flows is the continuation of the primary reaction, and another is responsible for the secondary reaction proceeding. Thus, the reaction system operates in the bifurcation regime—synchronous reaction interaction (coherence).

The author does not assert that the term chemical interference is the best or the most accurate. He knows that the case is not just in the name, but in the fact of the existence of coherent chemical reactions. No doubt, they will become the essence of traditional physicochemical study (in which it is the author's hope that the present monograph will help).

As follows from the data shown, the phenomenon of synchronous reaction coherence promotes a growth of interest in selective oxidation processes with hydrogen peroxide. This direction becomes a prime importance for modern investigations.

I do not believe, of course, that hydrogen peroxide is the elixir stone, but it is able to transform and modernize oxidative process engineering.

The information on selective oxidation with hydrogen peroxide presented in this book is so full, that it could not be ignored in the framework of modern chemical technology design.

Unfortunately, applied science is not always adequately sensitive to new knowledge or to new technologies, where it tries to simulate old ideas or specifically arranged design.

It is hoped that the efforts to lay a foundation for future process design, which may change the direction of applied chemistry in many branches, will be useful. Therefore, one more question about the practical value of synchronous reaction coherence is raised in this book.

In addition, the margins between consecutive, parallel and coherent synchronous reactions are defined. Thus, this book will help chemists to resolve a problem proposed in the overall approach (i.e. 'all affects all') to the analysis of complex chemical system via a new reality of chemical interference.

The symbiosis of biology and chemistry promoted the development of a new direction in science, that of biomimetic chemistry, which is completely different from any other direction in chemistry. It is an independent branch which chemically creates models of biological objects (more or less perfect, new simulation models) differing in their physicochemical parameters from biological and chemical analogs, but possessing technological advantages.

Biomimetic chemistry is a new stage in the development of chemical ideas. In this book, new information on coherent synchronization of chemical and biochemical reactions is developed in the application of achievements of mimetic catalysis.

This book translated into English is the full copy of the Russian edition, slightly amended with respect to new experimental data obtained. I have also tried to correct mistakes found in the Russian edition.

I am very glad to thank Alexei Yu. Borissevitch for translating and editing the English version and all my colleagues and friends who have helped me in this work.

T.M. Nagiev

Contents

This page intentionally left blank

– 1 –

Historical Aspect of the Concept of Chemical Conjugation

This chapter overviews the following points:

- The origination of the chemical induction idea.
- Fundamental notions and Shilov's classification of conjugated oxidation reaction types.
- New types of conjugated reactions—conjugation on membrane catalysts, conjugated chain and induced chemical reactions.
- Some general notes.

1.1 THE ORIGINATION OF THE CHEMICAL CONJUGATION CONCEPT

Since the beginning of his scientific career, and as advised by his famous teachers, the German chemists R. Luther and V. Oswald, the outstanding Russian physicochemist N.A. Shilov devoted himself to investigating conjugated processes. In his classical monograph on conjugated oxidation reaction, published in 1905 in Moscow, Shilov presented an extraordinary review of the development of the doctrine of these processes before the 20th century.

Conjugated reactions were known about long before Shilov's time. In 1893, the German scientist Kessler primarily used the term *chemical induction* and described a series of conjugated processes. In science, almost all famous achievements that have extended the horizons of knowledge have been preceded by works which objectively contribute to the gestation of an idea and its visualization into an unambiguous fact. The grape will not ripen without the hands of the gardener, the spring air and warm sunlight. Despite excellent weather, the work of a bad gardener will affect the result and, vice versa, bad weather will render the gardener's attempts useless. It is the same in science: only a combination of the necessary conditions will provide for a high quality of scientific study and shape pathways for its modification.

The doctrine of conjugated processes by Shilov was based on all the common achievements that were known at the time. It was he who clearly determined the subject for investigation, gave accurate definitions of chemical conjugation principles and discovered the reason for the unsatisfactory conditions of the conjugated process theory. That was the subject of Shilov's book, which is still scientifically valuable. Nowadays, of course, some of its statements on the mechanism of chemical reactions may seem naive. However, the methodological approach and analysis of solutions leading to the conjugation of chemical reactions are interesting not only

from the viewpoint of studying the history of the problem, but also because of their urgency in modern investigations, especially, in the branches of physical chemistry and chemical bionics.

At the present time, the scientific interest of the overwhelming majority of chemists and physical chemists is focused mainly on studies of transformations of matter at atomic and molecular levels. This has been greatly promoted by the improved abilities of the instrumental methods of physical chemistry. Since the advent of novel methods for physicochemical investigations, chemists have regularly returned to what were thought to be thoroughly studied chemical objects. Because of the new capabilities at their disposal, they are discovering previously unknown aspects of the behavior of substances in chemically changed systems.

It is common knowledge that the investigation of functional features and the activity mechanism of a living organism as an entire system requires an understanding of the interaction laws of separate organs. In addition, besides an understanding of elementary reactions comprising overall processes, decoding of the processes proceeding in a chemical system means that the mutual influence of synchronous reactions must be accounted for.

Oswald was the first to use the term *conjugated reactions* in chemistry. Shilov, however, considered this notion in a more comprehensive sense: 'I will generally use them for denoting a system of two reactions proceeding in the same medium, one of which depends on another' [1, p. 1]. Further on, specifying this notion, he wrote: '…conjugation of the reactions is only possible in complex processes, representing a sequence of separate reactions and causing formation of intermediate products' [1, p. 2]. The greatest emphasis is placed on the following note by Shilov: 'Generally speaking, an effect of one reaction on another may be shown up by acceleration or slowing down, however, hereinafter, by conjugated reactions I will mean the only reaction couple, in which one reaction causes acceleration of another, slow one' [1, p. 2].

This classical definition of conjugated processes became common in physical chemistry. However, in the author's opinion, and in the light of our current knowledge, the second part of Shilov's statement about the possibility of both accelerating and slowing down the effect of one reaction on another becomes of equal importance. Chapter 2 of this monograph gives a theoretical discussion of various alternatives of interconnected reactions with regard to their mutual acceleration and slowing down (chemical interference).

In his further discussions, Shilov discounted the simultaneous consideration of the accelerating and slowing down effects of a pair of reactions on one another. To some extent, this can be explained by the aim of his work which was to study only the accelerating effect of the primary reaction on the secondary one, the latter being conjugated to the former. This is why when focusing his attention on the problem, Shilov substantially assigned the term *conjugated processes* to accelerating effects only, because the problems of acceleration of various oxidation reactions conjugated with other spontaneous processes were the subject of that investigation. In fact, such analysis of the mutual effect of two reactions represents a particular case, because when dealing with the intereffect in conjugated processes, only the effect of the primary reaction on the secondary one is considered. On the other hand, the secondary reaction effect on the formation of the final products of the primary one is neglected, though their formation is slowed down directly due to this effect which affects the rate of the primary (overall) reaction.

We will not discuss interconnected reactions here (refer to Chapter 2), but just note that at mutual effect of the reactions (typical of complex processes only) chemical interference proceeds, represented by a slowing down of the formation of the primary reaction products and

acceleration of secondary reaction product formation. The process in which the secondary reaction is intensified is called the conjugated process. Inherently, the secondary reaction effect on the primary reaction is one of the types of inhibiting effect that has been quite well studied in chemistry. Moreover, the interference of two overall reactions necessarily changes their effective rate constants, thus the coherence condition can be deduced (refer to Chapter 2). With respect to a particular objective, the event characterized by the reaction acceleration is called *chemical induction*; as a consequence, the event of primary reaction slow down due to the effect of the secondary reaction is called *chemical inhibition*. Thus chemical induction and chemical inhibition, proceeding in the same chemical system under the conditions of the mutual effect of two reactions, reflect different sides of the same event, i.e. *chemical interference*.

A thorough consideration of a series of conjugated processes, described by Shilov in his book, clearly indicates that when considering the interference factor, his contemporaries had mistaken the final product of the primary reaction for the intermediate product of the primary reaction; this is not correct because it conflicts with the definition of chemical induction. This contradiction, observed in the works of Shilov and other investigators, can be explained by the level of knowledge and poor experimental technology in those days. Apparently, this mistaken belief was explained by the following reasons: firstly, the final product of the primary reaction entered the secondary reaction and thus it was accepted as being the intermediate compound; secondly, it was suggested that in some cases, independently of the secondary reaction proceeding, the final products may participate in subsequent reactions ascribed to the primary process; and thirdly, highly reactive intermediate particles such as free radicals and many other intermediate complicated compounds were not then known. Nevertheless, we can only marvel at the high level and clarity of the conclusions and definitions, and the scientific sagacity of Shilov and other chemists of the past, who made such a fundamental contribution to the theory of conjugated processes, often based on very vague experimental data.

Let us now consider the basic parameters of conjugated reaction systems according to classical definitions. Shilov indicates that the number of reagents participating in the event may equal four, but in the most frequent case conjugated reactions proceed with three types of reagents. In the latter case, Shilov used the following terminology:

$$\mathrm{A} + \mathrm{B} \quad \text{(primary reaction)} \tag{1.1}$$

$$\mathrm{A} + \mathrm{C} \quad \text{(secondary reaction)} \tag{1.2}$$

Substance A participating in both reactions is called the *actor* (by Luther); substance B which, interacting with the actor, induces the secondary process is called the *inducer* (by Kessler); substance C, accepting the inducing effect of the primary reaction, is called the *acceptor* (the term introduced by Engler).[1]

[1] The minimal number of substances in conjugated processes must equal two; therefore, the inducer may be absent in the primary reaction; conjugated reactions of this type are considered in more detail in the following chapters.

According to this scheme, definite amounts of inducer affected the secondary reaction and thus for qualitative characterization of conjugated reactions Shilov introduced an important parameter, representing the relationship between the amounts of acceptor and inducer participating in the reaction:

$$I = \frac{f_{\text{acc}}}{f_{\text{in}}} \tag{1.3}$$

where f_{acc} and f_{in} are acceptor and inducer consumptions, respectively. He called it the *induction factor*. This parameter allows the separation of two similar processes: induction and catalysis.

Another problem of great importance in the investigation of conjugated processes was the determination of the connection pathways between interacting reactions. In his investigations, Shilov paid a great deal of attention to this problem and gave a complete definition as follows: 'A reaction proceeding with energy liberation may induce another process requiring expenses of even lower work, under the only condition of existence of an intermediate product' [1, p. 7]. It turns out that the primary problem facing the investigators in studies of chemical induction is the determination and identification of the intermediate substance due to which connection pathways in conjugated reactions are set.

Further on, Shilov outlined that 'under the effect of an inducer reactions aimed towards the real thermodynamic equilibrium and, besides the general methods: work consumption in the form of heat, electric and light energy, requiring one of the techniques for implementation of endoenergetic reactions are possible' [1, p. 12]. A brief explanation shall be made. Chemical reactions proceeding with a decrease of the standard free energy are called exergonic (energy-yielding) or spontaneous processes. Chemical reactions, for which variation of the free energy is positive, are called endergonic or non-spontaneous processes.

It should be noted that the overwhelming majority of chemical processes proceeding in a living organism are conjugated, i.e. they combine exergonic and endergonic reactions. To put it another way, for the initiation and acceleration of biochemical processes, besides the use of enzymatic catalysis, at some stages wild life uses chemical induction for the arrangement of the necessary processes as a whole.

At present, for the creation of completely new chemical systems, chemists adopt the principles of natural chemical reactions from nature. That is why for thriving chemical bionics such as chemical modeling methods for natural chemical processes, as well as the use of structure modeling technique, active sites and the mechanism of enzymes' action, the conjugation principles of biochemical processes are used.

In studying conjugated oxidation reactions, Shilov paid special attention to the cases in which an inducer, regenerating, enters the 'interaction cycle' again. Considering the limiting case, when the inducer is fully regenerated, Shilov came to the correct conclusion that the alternative with the infinite induction factor should correspond to the catalytic process. On this basis, he considered the catalytic process as a particular case of the conjugated process, in which 'inducer transformation proceeds by a closed cycle.'

Of course, the state of science in catalysis in those years gave Shilov no opportunity to observe the cyclic character of the catalyst state change in these processes. For example, at catalytic H_2O_2 dissociation the catalyst is alternatively oxidized and restored, and in the case of lack of any substance (for instance, in the use of the Fenton system for the oxidation reaction: iron ions—H_2O_2) the cycle is unclosed, and catalyst regeneration is disturbed and, correspondingly, its catalytic function disappears. Shilov perceived disturbances of the reduction–oxidation catalytic system of this type as the action of an inducer–reagent, but not a catalyst. Essentially, under the condition of catalyst regeneration the normal catalytic process was observed, which the scientists called the 'limiting case'. Nevertheless, two different events, catalysis and chemical induction, must not be identified. According to Shilov's definition, they are based on diametrically opposed principles: the catalytic system may not produce additional work and, vice versa, chemical induction is the source of effective power for another, non-spontaneous reaction.

Of great interest are Shilov's works in the branch of self-induction, which is a specific case of conjugated reactions. He characterized it as follows: 'Examples are known, when one of final products is the inducer and, consequently, the inducer is formed during the process itself; therefore, its concentration is increased during interaction, increasing, in turn, the secondary reaction rate, i.e. speeding it up' [1, p. 13].

Specifying the chemical conjugation mechanism, it should be noted that in this case a final product is formed in the overall reaction which acts as a reagent–inducer in the system and with the help of which active particles necessary for speeding up the secondary reaction are generated in the system.

The objectives set before investigators in the branch of conjugated processes, formulated by Shilov in the early 1900s, are generally still valid:

I. The study of various types of conjugated reactions and classification of separate cases as belonging to one type or another.
II. Determination of the origin of intermediate products, which interlink the primary and the secondary reaction.
III. Consideration of a problem, if the event is accompanied by partial increase of free energy during intermediate product formation or speeding up of the secondary reaction must be completely ascribed to elimination of passive resistances [1, p. 16].

1.2 DEVELOPMENT OF THE CONJUGATED REACTION THEORY IN LATER WORKS

Hitherto, we have only discussed Shilov's classic work in which using the example of conjugated oxidation reaction the general theory of conjugated processes was properly achieved. However, a series of subsequent works should be mentioned which developed investigations in the field of conjugated reactions. Without attempting a full treatment of the subject, let us concentrate on the most important results for scientific and applied purposes.

Zelinski and Pavlov [2] have shown that under the effect of palladium cyclohexene is fully transformed to a mixture of benzene and cyclohexane in accordance with the overall scheme (irreversible catalysis event) as follows:

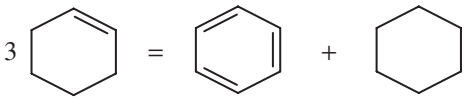

By this reaction, cyclohexadiene is transformed to the same products, the only difference being that the amount of benzene is twice as high as that of cyclohexane:

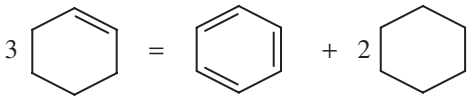

It was found that in these reactions free hydrogen is not extracted. The results of these works allowed the authors to conclude that two processes proceeded in the reaction system: dehydrogenation leading to benzene formation and hydrogenation responsible for cyclohexane accumulation. Both these reactions proceed simultaneously and are conjugated. The catalyst action is reduced to distribution of mobile hydrogen between three cyclohexadiene molecules.

The results obtained by Gryaznov *et al*. [3] on a membrane palladium catalyst showed that hydrogen redistribution was not the entire process of the transition of hydrogen atoms from one molecule of the initial substance to another, but was combined from two reactions: detachment and addition of hydrogen. These works formed the basis of a previously unknown effect of reaction conjugation on membrane catalysts, discovered by Gryaznov *et al*. [4]. For the membrane catalyst, a palladium tube was used, on the external surface of which cyclohexane transformation to benzene and hydrogen proceeded, and to the internal void toluene vapor was injected. From this vapor interacting with hydrogen, benzene and methane were synthesized. Therefore, Gryaznov *et al*. found that at simultaneous proceeding of these two reactions, the first possessed higher speed than at hydrogen occurrence inside the preliminarily evacuated palladium tube. When the reactions proceeded simultaneously, the rate of hydrogen transfer through the tube walls also increased. All this proved that both reactions had a favorable effect on one another, though they were carried out on different sides of the membrane catalyst [4].

In the study of conjugated processes, of special attention are works by Emanuel [5], who has considered conjugated chain reactions to be of great importance and promising directions of radical reactions. Emanuel *et al*. have implemented detailed studies in this area. In particular, they suggested an effective method of propylene and acetaldehyde conjugated oxidation [6] for a one-stage synthesis of propylene oxide and acetic acid [7].

1.3 ANALYSIS OF THE 'ACTIVE OXYGEN' CONCEPT FROM MODERN POSITIONS OF OXIDATION PROCESSES

In 1884, Schonbein discovered the *active oxygen*. The essence of this discovery is that a compound hardly oxidized by molecular oxygen easily reacts with it, if in the same system

simultaneously any other substance is oxidized by oxygen. For example, at room temperature As_2O_3 is inert to molecular oxygen, but if SO_2 is oxidized simultaneously in this system, then according to Shilov, the latter reaction induces the former:

$$2SO_2 + O_2 = 2SO_3 \quad \text{(primary reaction)} \tag{1.4}$$

$$As_2O_3 + O_2 = As_2O_5 \quad \text{(secondary reaction)} \tag{1.5}$$

In the first approximation, this scheme may be considered as a general one for oxidation by *active oxygen*, when only the nature of the inducer and the acceptor is changed. Schonbein [8] and Traube [9] denied the signs of chemical induction in oxidation by molecular oxygen based on the fact that oxidation products (hydrogen peroxide and organic peroxides), on the one hand, represent final products capable of oxidizing the substrate (Schonbein). On the other hand, hydrogen peroxide as a primary product has low activity unless a catalyst speeding up acceptor oxidation by hydrogen peroxide is present in the system. That is why Traube associated oxygen activation not with the primary product (hydrogen peroxide), but with a side catalytic reaction with its participation. Thus the fundamental statement in Traube's theoretical constructions was the determination of hydrogen peroxide formation as the primary product at molecular oxygen reduction. Further on, Traube has indicated that to display oxidative properties in a medium H_2O_2 almost always requires the presence of a catalyst (H_2O_2 does not react with an acceptor in the absence of a catalyst). On this basis he completely denied hydrogen peroxide properties as a strong oxidant, though he recognized that these properties may occur at its dissociation with OH formation.

Traube's observations are of great interest from two positions: oxidation by hydrogen peroxide is a slow process, requiring the presence of a catalyst; H_2O_2 may obtain the properties of a strong oxidant, if it preliminarily dissociates to OH.

Modern knowledge of kinetics and oxidation mechanisms by oxygen in gases and liquids allows us to look at this problem from a more particular position. Let us first briefly consider the basic statement of the 'active oxygen' theory, otherwise analysis of the subject will not be persuasive. Let us go back to reactions (1.4) and (1.5), related by Shilov to typical processes of chemical induction. According to Shilov's terminology, 'oxygen participating in both reactions is the actor; the substance oxidized spontaneously (sulfurous acid) is the inducer and the substance oxidized by the effect of the primary reaction (arsenous acid) is the acceptor. This scheme is also general for auto-oxidation events: in different examples the only substances playing roles of acceptors and inducers are changed; in all cases, the actor is oxygen' [1, pp. 17, 18].

Let us now trace how the 'active oxygen' concept, which in due course had been invaluable in helping chemists interpret the oxidation mechanism, led them to make outstanding discoveries, for example, that of conjugated oxidation and many other reactions and how it transformed with time into a modern theory of molecular oxygen oxidation.

In accordance with existing theories, at low-temperature oxidation (below the negative temperature parameter zone) peroxide compounds are primary products. Their further transformation leads to a formation of the entirety of the intermediate and final products observed.

Emanuel's conceptual sketch of oxidation by oxygen in liquids [10] consists of the following elementary stages:

$$\left.\begin{aligned} RH + O_2 &\rightarrow R^{\bullet} + HO_2 \\ RH + O_2 + RH &\rightarrow 2R^{\bullet} + H_2O_2 \end{aligned}\right\} \text{Chain initiation}$$

$$\left.\begin{aligned} R^{\bullet} + O_2 &\rightarrow RO_2^{\bullet} \\ RH + O_2 + RH &\rightarrow 2R^{\bullet} + H_2O_2 \end{aligned}\right\} \text{Chain propagation}$$

$$\left.\begin{aligned} ROOH &\rightarrow RO^{\bullet} + {}^{\bullet}OH \\ 2ROOH &\rightarrow RO_2^{\bullet} + H_2O + RO^{\bullet} \\ ROOH + RH &\rightarrow RO^{\bullet} + H_2O + R^{\bullet} \end{aligned}\right\} \text{Chain branching}$$

$$\left.\begin{aligned} R^{\bullet} + R^{\bullet} &\rightarrow \\ RO_2^{\bullet} + R^{\bullet} &\rightarrow \\ RO_2^{\bullet} + RO_2^{\bullet} &\rightarrow \end{aligned}\right\} \text{Chain termination}$$

Let us amplify the sketch with one more reaction of chain branching:

$$H_2O_2 \rightarrow {}^{\bullet}OH + {}^{\bullet}OH \tag{1.6}$$

Clearly the above scheme of liquid-phase oxidation by oxygen shows H_2O_2 and ROOH formed as intermediate products. However, they cannot be related to active sites of another, secondary reaction as is customary in, for example, conjugated processes. The reasons for making such comparisons are as follows: firstly, H_2O_2 and ROOH are final products of a complex reaction and initial reagents for other thermodynamically probable reactions; secondly, their formation and consumption (by the scheme selected) do not correspond to the notion of *active site* of conjugated reactions.

It should be remembered that the active site of chemical induction is a compound, playing the role of an intermediate product in two complex reactions.

It may seem difficult to imagine that, owing to their participation in chain branching, the intermediate products ROOR, ROOH and H_2O_2 of liquid-phase oxidation by oxygen are the initiators of degenerate chain reactions; hence, with respect to the length of degenerate chains H_2O_2 and ROOH may be initiators, exclusively. True enough, reactions of induced dissociation of ROOH and H_2O_2 themselves are known [11], discussion of which is of special interest. To make the discussion as full as possible, let us dwell on some aspects of these reactions.

1.4 INDUCED DISSOCIATION OF PEROXIDE COMPOUNDS

Being primary, stable, intermediate oxidation products and owing to the simplicity of their dissociation to free radicals, peroxide compounds HOOH, ROOH, ROOR (where R is alkyl, acyl, arylacyl fragments or their derivatives) possess favorable initiation properties in chain oxidation and polymerization reactions.

As an example, dissociation of the most frequently applied di-*tert*-butyl peroxide shall be considered (similarly, hydroperoxides dissociate) which independently of the fact, if the

process proceeds in the gas and liquid phase, initially dissociates to *tert*-butoxide radical $Me_3CO^{\bullet}$. The Ashmore scheme [12] shows practically all possible alternatives of further $Me_3CO^{\bullet}$ transformations (ROOH and ROOR do not participate in the chain decomposition):

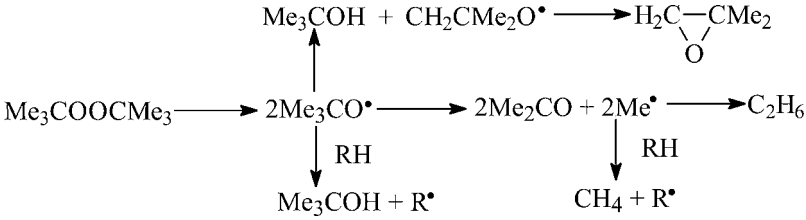

(1.7)

Nonehilbel and Walton [13] called such reactions producing free radicals *induced dissociation processes*. Hence, ROOH and ROOR dissociation is considered as induction of OH and other radicals by free radicals, generated in the chemical system by self-hemolytic break of their—O—O-bond with formation of an active site (alkoxide).

Let us ensure the accuracy of this interpretation of ROOR and ROOH dissociation mechanism in connection with a question that arises, i.e. how this statement correlates with the conditions under which chemical induction takes place.

According to Nozari and Barlett's kinetic data [14], benzoyl peroxide dissociation competes with hemolytic decomposition and a reaction with free radical participation. The kinetic dissociation equation is as follows:

$$(C_6H_5O_2)_2 - \frac{d[(C_6H_5O_2)_2]}{dt} = k_1[(C_6H_5O_2)_2 + k_2[R^{\bullet}][(C_6H_5O_2)_2]^n \qquad (1.8)$$

It is also known that the induced dissociation in various solvents proceeds with the participation of the R radical and is sufficiently dependent on both the origin of radical and solvent. Approximately the same interpretation of induced dissociation processes are caused by charge transfer, photosensitizers, etc. [13, 15].

Thus noting the abundance of induced dissociation reactions, we continue the discussion of their mechanism in the examples of radical initiator dissociation. Thus, scheme (1.7) is the most demonstrative: firstly, it indicates that the $Me_3CO^{\bullet}$ radicals formed undergo the most probable transformations to final products not involving more than one initial $Me_3COOCMe_3$ molecule; secondly, as dissociated to $Me_3CO^{\bullet}$ free radicals or transformed to Me, the initial substance may react with another substance (RH) and is thus capable of inducing its chain or radical transformation. Of course in this case, no induced radical dissociation of the initial substance happens. Actually, if the initial substance during decomposition started from dissociation to free radicals forms a definite selection of final products, the process is analogous to usual complex reactions, possessing all the inherent regularities.

However, as mentioned above, there are cases such as dibenzoyl peroxide decomposition, when primary free radicals interact with the initial substance and thus promote its faster decomposition to the same final products, as with usual decomposition (scheme (1.6)). If other reaction products are formed, untypical of decomposition of the initial substance, this means that one more complex reaction proceeds (besides decomposition), the presence of which hinders the relation of all products formed to only usual decomposition of the initial

substance. In this case, no usual decomposition may be indicated, because in one reaction the initial substance is decomposed to its final products, and in another reaction it participates as one of the reagents in a more complicated bimolecular reaction.

This is proved by the type of kinetic equation (1.7), from which it follows that the first term describes usual monomolecular dissociation, and for the second process value *n* may become equal 2/3 or 1 with respect to the solvent, i.e. induced dissociation of radical initiator obeys kinetic laws.

Let us return to scheme (1.7) and note that if initial initiator molecules play the role of RH (in this case), this will promote its inductive dissociation and formation of products not formed in usual decomposition. That is why, as a rule, with respect to kinetic experimental conditions one of the pathways will dominate in the system. Actually, the reaction:

$$Me_3COOCMe_3 + Me_3CO^{\bullet} \rightarrow Me_3COH + {}^{\bullet}CH_2Me_2COOCMe_3 \qquad (1.9)$$

is the stage of induced decomposition of the initial peroxide, and further transformation of ${}^{\bullet}CH_2Me_2COOCMe_3$ leads to formation of substances directly typical of such (induced) decomposition. Detection of isobutylene oxide in the reaction products allowed a suggestion of the mechanism of its formation, preceded by the induction stage (1.9):

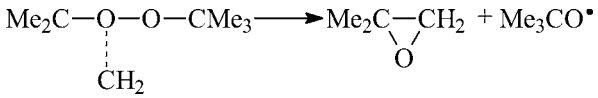

In the literature (e.g. refer to [16]), one can find analogous schemes of induced decomposition of hydrogen peroxide, the simplest representative of peroxy compounds. Nevertheless, mechanical translation of the concept of induced initiator decomposition to H_2O_2 dissociation induces conclusions contradicting the notion of chemical induction and conjugated processes.

In a broad temperature range (25–700 °C) H_2O_2 thermolysis leads to generation of ${}^{\bullet}OH$ radicals in the reaction system (reaction (1.6)).

The future fortune of these radicals depends on the conditions of reaction proceeding: for example, on the state of the reaction phase (liquid or gas), catalysts applied or thermal activation. The overall mechanism of non-catalytic H_2O_2 dissociation in a liquid is described by a selection of elementary reactions discussed in Chapter 6.

Independently of the particular combination of the stages leading to formation of final products (water and oxygen), the final equation is always presented including two molecules of hydrogen peroxide:

$$H_2O_2 + H_2O_2 = 2H_2O + O_2$$

that is stoichiometric reaction of H_2O_2 dissociation always preserves its shape independently of the transformation mechanism.

A series of signs distinguishing H_2O_2 dissociation from decomposition of its more complex derivatives shall be outlined.

The basic typical difference is that at organic peroxide dissociation (e.g. di-*tert*-butyl peroxide, scheme (1.7)) a complex set of final products—alcohols, ketones, oxides, methane and other hydrocarbons—is formed, whereas from hydrogen peroxide only H_2O and O_2 are formed.

Homogeneous decomposition of organic peroxides is developed in various directions, each characterized by a definite radical-chain mechanism determined by the final chemical equation. Hence, in every direction, in the overall reaction different active particles (free radicals) participate which, interacting with the primary initiator lead to its induced decomposition. To put it differently, when decomposing, organic radical peroxide initiators induce a series of radical and chain reactions in the system, proceeding with sufficiently high rates and requiring no additional generation of free radicals by primary break of the initial peroxide molecule by O—O-bond; instead of this reaction, an induced decomposition mechanism is actuated in the system.

The initiator interaction with free radicals, active particles of radical and chain reactions, usually forms new directions of initiator transformation different from those formed at usual initiation.

The entire complex situation is untypical of hydrogen peroxide. Decomposition of H_2O_2 starts from dissociation by O—O-bond to hydroxyl radicals, which then in gas-phase (refer to Chapter 4) and liquid-phase (refer to Chapter 6) decomposition lead to final products: H_2O and O_2. Here one deals with a single complex reaction with a definite set of subsequently proceeding elementary reactions, but not with several sets as for decomposition of organic peroxides.

For this reason, such a combination of a usual decomposition with an auto-induced one typical of organic peroxides is meaningless under consideration of decomposition. However, there are statements in the literature [17] that hydroxyl radicals of endogenous origin may participate in chain induced decomposition of H_2O_2 itself in the liquid phase. Such a presentation of the H_2O_2 decomposition mechanism is incorrect if for no other reason than in every particular case H_2O_2 decomposition proceeds by the unique pathway in accordance with the given stoichiometric equation. Therefore, the process itself cannot be divided into two independent mechanisms, as happens in the case of organic peroxide decomposition.

Only in the case where in the same reaction system hydrogen peroxide is decomposed under the effect of another substance can one speak about its induced decomposition, because such a substance may generate $^{\bullet}OH$ radicals (or other free radicals) in the system which, interacting with H_2O_2, will cause its induced decomposition.

This leads to the general conclusion typical of all peroxide compounds (including their simplest representative) that induced decomposition of H_2O_2, ROOR and ROOH takes place when it is caused by particles (free radicals, molecules, electrons, photons, etc.) of exogenic origin (the substance is injected to the system from the outside). Hence, as in the case of H_2O_2, for example, the mechanism of its dissociation to H_2O and O_2 may not change, if active sites formed in the system (owing to the presence of another substance) will induce this process. However, at induced H_2O_2 dissociation stoichiometry of the reaction necessarily changes. This circumstance will immediately allow detection of such dissociation proceeding in the system. Actually, if at usual H_2O_2 decomposition the formation of H_2O and O_2 requires the presence of two molecules of it, then at $^{\bullet}OH$ injection to the system from outside one molecule is enough. This can be illustrated by the following scheme:

$$AOH \rightarrow {}^{\bullet}OH + A \quad |2|$$

$$H_2O_2 + {}^{\bullet}OH \rightarrow H_2O + HO_2^{\bullet} \quad |2|$$

$$HO_2^{\bullet} + HO_2^{\bullet} \rightarrow H_2O_2 + O_2 \quad |1|$$

$$2AOH + H_2O_2 = 2A + 2H_2O + O_2$$

If H_2O_2 substitutes AOH, this scheme describes the reaction of usual H_2O_2 dissociation with typical stoichiometry:

$$2H_2O_2 = 2H_2O + O_2$$

that is the induction effect disappears.

Let us now trace stoichiometry of auto-induced di-*tert*-butyl peroxide decomposition:

$$\begin{array}{l} Me_3COOCMe_3 \rightarrow 2Me_3CO^{\bullet} \\ 2Me_3CO^{\bullet} \rightarrow Me_3COH + CH_2CMe_2O^{\bullet} \rightarrow H_2C\text{—}CMe_2 \\ \qquad\qquad\qquad\qquad\qquad\qquad\qquad\qquad\qquad\qquad\quad O \\ \quad \searrow \\ \quad 2Me_2CO + 2Me^{\bullet} \rightarrow C_2H_6 \\ \hline Me_3COOCMe_3 = Me_3COH + H_2C\text{—}CMe_2 \\ \qquad\qquad\qquad\qquad\qquad\qquad\quad O \qquad\qquad \text{(overall reaction)} \\ Me_3COOCMe_3 = 2Me_2CO + C_2H_6 \end{array} \qquad (1.10)$$

At usual decomposition, formation of the final products (isopropyl alcohol and isobutylene oxide or acetone and ethane) requires one initial molecule.

When $Me_3CO^{\bullet}$ attacks the initial peroxide, the following transformation scheme is realized:

$$\begin{array}{l} Me_3COOCMe_3 + Me_3CO^{\bullet} \rightarrow Me_3COH + {}^{\bullet}CH_2CMe_2OOCMe_3 \\ {}^{\bullet}CH_2CMe_2OOCMe_3 \rightarrow H_2C\text{—}CMe_2 + Me_3CO^{\bullet} \\ \qquad\qquad\qquad\qquad\qquad\quad O \\ \hline Me_3COOCMe_3 = Me_3COH + H_2C\text{—}CMe_2 \\ \qquad\qquad\qquad\qquad\qquad\quad O \end{array} \qquad (1.11)$$

Clearly, a comparison of schemes (1.10) and (1.11) shows that both pathways of decomposition are described by the same stoichiometric equation. However, there is a vital difference in decomposition mechanisms consisting of the fact that mechanism (1.10) describes the radical reaction and (1.11) the radical-chain reaction.

Thus the induced H_2O_2 dissociation and auto-induced decomposition of organic peroxides (initiators) are accompanied by a change of, at least, one of three reaction parameters: (a) stoichiometric equation of the reaction (decomposition products remain typical of the current substance); (b) reaction type and (c) reaction pathway (mechanism) with decomposition overall stoichiometric equation preserved.

Note that variation of the reaction type means the case where the initiator is attacked by another molecule or an intermediate particle generated by it, different from the particle generated by the initiator.

From these positions it becomes clear why the reaction of H_2O_2 dissociation to H_2O and O_2 cannot be induced directly by hydrogen peroxide: this is because in this case, H_2O_2 dissociation would become the primary and the secondary reaction, simultaneously.

Usually, such a situation occurs at induced decomposition of peroxides and hydroperoxides of organic substances.

As mentioned above, the secondary reaction in the system is caused by a new reaction of free radical interaction (produced in the elementary dissociation of the radical initiator) with the initiator. In this case, one more active intermediate particle (free radical), not observed at usual peroxide decomposition, is generated in the system. Owing to formation of this active site, conjugated reaction proceeds by the radical-chain mechanism. Thus products formed may be analogous to those obtained at usual initiator decomposition, or different products may be formed—this circumstance is of no importance for detection of induced decomposition.

Thus the primary reaction in di-*tert*-butyl peroxide decomposition is a usual decomposition reaction in the scheme (1.10); the secondary reaction induced by the initial one is described by the scheme (1.11). It is worthy of note that both decomposition reactions are described by the same overall equation, and free radical is the general intermediate particle.

The free radical inducing peroxide decomposition may be obtained from another substance—free radical generator. In this case, the primary reaction is the one that generates active sites, and the secondary decomposition one may proceed via formation of previously unobserved products.

1.5 HIGH-TEMPERATURE OXIDATION MECHANISM AND 'ACTIVE OXYGEN' CONCEPT

Let us now pass on to hydrocarbon oxidation mechanisms at high temperatures, when cracking and dehydrogenation become the main reactions in the system.

The chronology of investigations into this problem is as follows. For propane oxidation, Stern [18] has suggested a scheme consisting of the following elementary steps:

$$C_3H_8 + O_2 \rightarrow i\text{-}C_3H_7^{\bullet} + HO_2^{\bullet} \tag{1.12}$$

$$i\text{-}C_3H_7^{\bullet} \rightarrow C_3H_6 + H \tag{1.13}$$

However, due to high endothermicity of the step (1.13) this scheme has rightly provoked objections.

Semenov suggested the following mechanism of propane transformation to propylene [19]:

$$C_3H_8 + O_2 \rightarrow i\text{-}C_3H_7^{\bullet} + HO_2^{\bullet}$$

$$i\text{-}C_3H_7^{\bullet} + O_2 \rightarrow CH_3{-}\underset{\displaystyle O{-}O^{\bullet}}{\underset{|}{CH}}{-}CH_3$$

$$CH_3{-}\underset{\displaystyle O{-}O}{\underset{|}{CH}}{-}CH_3 \rightarrow CH_3{-}\underset{\displaystyle O{-}OH}{\underset{|}{CH}}{-}CH_2^{\bullet}$$

$$CH_3{-}\underset{\displaystyle O{-}OH}{\underset{|}{CH}}{-}CH_2^{\bullet} \rightarrow CH_3{-}CH{=}CH_2 + HO_2^{\bullet}$$

Unfortunately, neither does this scheme comply with the experimental data. In the majority of modern works, the following elementary reaction is accepted for the second step:

$$C_nH_{2n+1} + O_2 \rightarrow {}^{\bullet}C_nH_{2n} + HO_2^{\bullet} \tag{1.14}$$

For instance, in 1953, Appleby *et al*. [20] suggested a radical-chain mechanism of butane transformation to butylene, using the elementary reaction (1.14), and at 486–526 °C butylene and water were detected in the reaction products. This testified to the role of oxygen as a dehydrogenating agent.

Investigations by Knox and Wells [21, 22], devoted to the determination of alkane oxidation mechanism, led to the conclusion that alkane oxidation mainly proceeded via oxidation of corresponded olefin, transformed at the initial stage and oxidation via peroxide alkyl radicals yielded in only 20%:

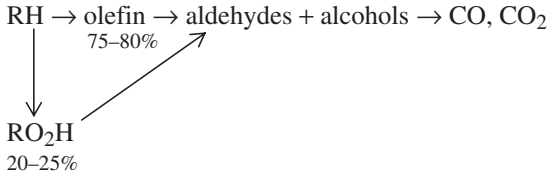

In this connection, Stern *et al*. [23] studied the problem of which alkane oxidation mechanism should be preferred: via olefin or peroxide alkyl radicals; however, they did not come to any final conclusion.

Of special attention is the work [24] in which kinetic regularities of ethane oxidation by oxygen performed at 600–630 °C in a flow reactor in the low transformation zone were successfully and semi-quantitatively explained by the radical-chain mechanism with H_2O_2 as a source of two active particles:

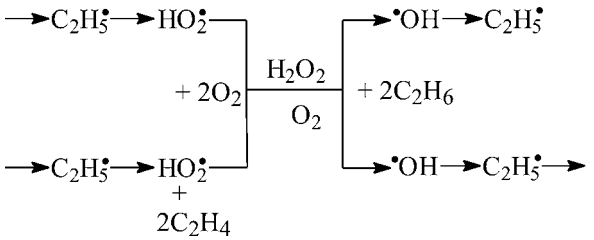

(1.15)

In this scheme, chain reactions are most probable, as well as their following stages:

$$HO_2^{\bullet} + C_2H_6 \rightarrow H_2O_2 + C_2H_5^{\bullet}$$

$$C_2H_5^{\bullet} + O_2 \rightarrow C_2H_4 + HO_2^{\bullet}$$

It should be remembered that in this case, the 'active oxygen' effect is displayed, when molecular oxygen is activated in the presence of another substance, the role of which is reduced to oxygen fixation and formation of an active site shaped as a complex or an intermediate

compound. Further transformation of the initial substance is induced by active sites—the intermediate products of the primary reaction.

In the study of conjugated dehydrogenation, the authors [25] suggested a new elementary reaction (refer to subsequent chapters for details):

$$C_nH_{2n+1} + HO_2^{\bullet} \rightarrow C_nH_{2n} + H_2O + {}^{\bullet}OH$$

From the authors' point of view, introduction of this elementary stage to mechanisms of saturated hydrocarbon gas-phase oxidation [26] makes clearer the mechanisms of such complex chemical processes, especially at olefin formation with the same number of carbon atoms as in the initial hydrocarbon.

The statements of the possible role of $HO_2^{\bullet}$ radicals in saturated hydrocarbon oxidation processes is proved by experimentally determined formation of sufficient amounts of hydrogen peroxide and $HO_2^{\bullet}$ radicals during oxidation of propane [27] and paraffin dehydrogenation products [28–30].

Before we begin to discuss the question of the oxidation mechanism of alkanes [28, 30], note that besides initial hydrocarbon (e.g. propane) and oxygen, none of the other substances are present in the system, which interaction with oxygen induces alkane oxidation. However, the initial hydrocarbon (propane) may be this third substance. Then active sites, inducing a radical-chain transformation of the hydrocarbon, are accumulated in the system. This is the approximate pathway of oxidation proceeding in gas or liquid. Modern theoretical and experimental positions indicate that at the initial stage, i.e. during oxidation initiation (according to the above schemes), active sites $HO_2^{\bullet}$ and $RO_2^{\bullet}$ are accumulated. After a definite period, which is usually called the self-induction period, oxidation is speeded up and then proceeds, as a rule, at a high rate. Fast transformation of raw materials is caused by different chain reactions, usually following the initiation stage. So what is the similarity between the notion 'active oxygen' and the self-induction phenomenon?

It is common knowledge that in the case of chemical induction, the primary reaction produces useful work for a conjugated reaction to proceed. As two chemical reactions are conjugated, they must both be rigidly connected to one another, because successful realization of this scheme permanently demands useful work to be produced by the primary reaction. Termination of active site generation in the primary reaction leads to secondary reaction termination.

At the initial oxidation stages (in the induction period) active sites are accumulated. When their concentration reaches a definite level required for a jump-like acceleration of oxidation, either chain or catalytic transformation of the substrate begins at a high rate.

In radical-chain oxidation reactions, the beginning of the process is called the initiation stage; therefore, the amount of initiator consumed in the following stages of the process development is not yet of determining significance. If chains are rather long, the raw material is consumed almost completely.

Insignificant amounts of substance (sometimes, it may be the initial oxidation stage products), generating active sites for initiation of the radical-chain reaction, may present in the system. As a rule, such substances are called initiators.

If at the initial moment of time active sites, representing a catalyst of further substrate oxidation, are formed in the system, such processes are classified as auto-catalytic processes.

They have the induction period required for active site accumulation in the system in amounts that cause a noticeable transformation of the initial substance. In both cases (for analysis, refer to the next chapter) the initial reaction is supplementary, just defining the induction period. Hence, the main oxidation reaction proceeds after the induction period, and its stoichiometric equation does not take into account the consumption of initial reagents (as well as consumption of initiators of the induction and initiation period of chain reactions). Thus at the initial stage of oxidation, initiation and auto-catalysis play the role of reaction 'launchers'.

Chemical induction displays a qualitatively different situation: the secondary reaction in the system may not proceed at any noticeable rate without a primary reaction run at any moment of the process. The first reaction is somewhat like a 'power station' for the second one. In the latter case, process of induced reaction leads to more intense actor consumption. Finally, the amount spent is much greater than in the absence of the secondary reaction.

Moreover, conjugated reactions display a specific feature, which is that, vividly expressed, both primary and secondary conjugated reactions always have the same 'the subject for adoration'—the actor.

All of this leads to the conclusion that the gas-phase oxidation mechanism of organic substrates does not fit the framework of the 'active oxygen' theory. We especially emphasize the organic origin of the substrate, because in the case of inorganic compounds the 'active oxygen' theory can be successfully applied to the interpretation of conjugated oxidation mechanisms. Such a difference in the mechanisms of oxidation processes with respect to substrate nature is explained by usual high selectivity of inorganic substance transformations and their proceeding with high yields of a single target product.

In the case of organic compounds, even at selective oxidation, secondary products occur and the target product yield is relatively low, because selectivity of the process decreases with the increase in transformation level.

To illustrate the application of the 'active oxygen' theory to inorganic oxidation, let us consider several conjugated oxidation reactions.

Based on his own experimental results and their analysis, Traube has made the correct (in terms of modern understanding) conclusion that H_2O_2 displays high reactivity in the presence of a catalyst in the system. This is the pathway of various substrate oxidations by hydrogen peroxide, proceeding in the Fenton system (iron ion + H_2O_2), and some biochemical processes.

This conclusion of Traube's is sufficient for not accepting oxidation by molecular oxygen for the primary reaction. In this reaction, H_2O_2 and other peroxides are intermediate products which, in accordance with modern terminology, may act as oxidation initiators and inducers.

Meanwhile, based on the ideas of primary oxidation by molecular oxygen in which oxidants more active than the initial O_2 were formed (e.g. H_2O_2, O_3, etc.), Shilov suggested that this fact was sufficient for consideration of these processes from the position of conjugated reactions. He believed that for chemical induction, the possibility of primary and secondary reactions proceeding separately is not of fundamental importance. Therefore, the possibility of selecting a secondary reaction for the primary one is important in this case.

It is clear from the material under consideration that there was no general point of view on the mechanism of 'active oxygen' occurrence in the literature.

As mentioned above, from a modern position, various substrates (especially of organic origin) are oxidized by molecular oxygen by radical-chain reaction mechanisms. Essentially, the use of 'active oxygen' notion in this type of reaction is of historical interest only.

Though Schonbein [8] and Traube [9] rightfully neglected chemical induction in considering oxidation reactions with molecular oxygen, nevertheless, they omitted to take account of some other examples of oxidation, where the 'active oxygen' concept was transformed to chemical induction. These cases were discovered and developed by Shilov [1], who, in turn, also made a mistake in suggesting that the primary reaction proceeded separately from the secondary one, and speeded the latter up by the effect of its final products. That is why he related oxidation processes with molecular oxygen, studied by Schonbein and Traube, to conjugated processes against which they had rightfully taken exception before.

Conjugated reactions are the only ones in which the 'active oxygen' theory preserves the meaning ascribed to it by Shilov. This fact is clearly illustrated by Shilov's examples [1], in which inorganic substances were subject to conjugated oxidation and the 'rules of the game' were strictly obeyed, conjugated reaction separation conditions, in particular.

For applied purposes, the book by Mitskevich and Erofeev [31] is of interest because it discusses conjugated reactions on the example of decarboxylation processes accompanying the liquid-phase oxidation of carboxylic acids.

It is shown that low-temperature liquid-phase oxidation of resinous acids, their salts and dicarboxylic acids, as well as their mixtures with hydrocarbons is accompanied by decarboxylation, the latter not proceeding in the absence of oxidation. The chemical conjugation mechanism in decarboxylation becomes of importance, associated with the production of fatty acids and organics oxidation.

For the first time, the monograph [32] theoretically pooled the data on interconnected synchronous reactions of various types proceeding in chemical and biochemical systems and put forward a new concept of chemical interference. It is shown how energy is accumulated, transformed and transmitted in these systems.

Of special attention were conjugated oxidation reactions by hydrogen peroxide. The possibility of using the processes described for development and modernization of various processes in chemical technology was discussed.

REFERENCES

1. Shilov, N.A., *On Conjugated Oxidation Reactions*, Mamontov Publishers Moscow, 1905, 304 pp. (in Russian).
2. Zelinski, N.D. and Pavlov, G.S., *Berichte*. 1933, Bd. 66, S. 1420–1422.
3. Gryaznov, V.M. and Smirnov, V.S., *Two Processes in One Reactor*, Znanie, Moscow, 1972, 48 pp. (in Russian).
4. Gryaznov, V.M., Smirnov, V.S., Ivanova, L.K. *et al*., *Vestn. AN SSSR*., 1971, No. 7, pp. 142–144 (in Russian).
5. Emanuel, N.M., *Combustion and Explosion*, Nauka, Moscow, 1972, 608 pp. (in Russian).
6. Blumberg, E.A., Valov, P.I., Norikova, Yu.D. and Emanuel, N.M., *Dokl. AN SSSR*., 1966, Vol. 167, No. 3, pp. 579–582 (in Russian).
7. Valov, P.I., Blumberg, E.A. and Emanuel, N.M., *Izv. AN SSSR, Ser. Khim*., 1966, No. 8, pp. 1334–1339 (in Russian).
8. Schonbein, Ch.E., *Ber. Natur. Ges. Bas*., 1844, Bd. 6, S. 16.
9. Traube, I., *Berichte*. 1883, Bd. 16, S. 123.
10. Emanuel, N.M., *Khim. Fiz*., 1982, No. 1, pp. 91–104 (in Russian).
11. Rozantsev, E.G. and Scholle, V.D., *Organic Chemistry of Free Radicals*, Khimia, Moscow, 1979, 343 pp. (in Russian).

12. Ashmore, P.A., *Catalysis and Inhibition of Chemical Reactions*, Mir, Moscow, 1966, 386 pp. (in Russian).
13. Nonehilbel, D. and Walton, G., *Chemistry of Free Radicals*, Mir, Moscow, 1977, 606 pp. (in Russian).
14. Nozari, K. and Barlett, F.D., *J. Am. Chem. Soc*., 1946, Vol. 68, pp. 1686–1689.
15. Kochi, J.K., *Ibid*., 1962, Vol. 84, p. 774.
16. Prayer, W., *Free Radicals*, Atomizdat, Moscow, 1970, 335 pp. (in Russian).
17. Emanuel, N.M. and Knorre, D.G., *The Course Of Chemical Kinetics*, Vyssh. Shkola, Moscow, 1984, 237 pp. (in Russian).
18. Stern, V.Ya., *The Mechanism of Hydrocarbons Oxidation in Liquids*, Izd. AN SSSR, Moscow, 1960, 496 pp. (in Russian).
19. Semenov, N.N., *On Some Problems in Chemical Kinetics and Reactivity*, 2nd edn, Izd. AN SSSR, Moscow, 1958, 680 pp. (in Russian).
20. Appleby, W., Avery, W., Meerbott, W. and Sartor A.T., *J. Am. Chem. Soc*., 1953, Vol. 75, pp. 1809–1814.
21. Knox, T.H., *Combust. Flame*, 1965, Vol. 9, No. 3, pp. 297–310.
22. Knox, T.H., *Trans. Faraday Soc*., 1963, Vol. 59, pp. 2786–2801.
23. Ogorodnikov, I.A., Polyak, S.S. and Stern, V.Ya., *Kinetika i Kataliz*, Vol. 10, No. 6, pp. 1210–1220 (in Russian).
24. Sompson, R.J., *J. Chem. Soc*., 1963, pp. 5095–6002.
25. Nagiev, T.M., *Azerb. Khim. Zh*., 1967, No. 1, pp. 135–141 (in Russian).
26. Nagiev, T.M., Medzhidov, N.D., Nagieva, Z.M. and Zulfuganova S.Z., *Ibid*., 1976, No. 4, pp. 153–158 (in Russian).
27. Sachyan, G.A., Shakhnazaryan, I.K. and Nalbandyan, A.B., *Dokl. AN SSSR*., 1969, Vol. 185, No. 3, pp. 647–651 (in Russian).
28. Alaverdyan, G.Sh., Sachyan, G.A. and Nalbandyan, A.B., *Ibid*., 1982, Vol. 204, No. 3, pp. 603–607 (in Russian).
29. Nalbandyan, A.B. and Mantashyan, A.A., *Elementary Processes in Slow Gas-Phase Reactions*, Izd. AN ArmSSR, Erevan, 1975, 258 pp. (in Russian).
30. Nagiev, T.M. and Mamed'yarov, G.M., *Modeling and Optimization of Chemical Processes*, Elm, Baku, 1977, pp. 145–153 (in Russian).
31. Mitskevich, N.I. and Erofeev, B.V., *Conjugated Oxidation and Decarboxylation of Carboxylic Acids*, Nauka i Tekhnika, Minsk, 1970, 188 pp. (in Russian).
32. Nagiev, T.M., *Chemical Conjugation*, Nauka, Moscow, 1989, 216 pp. (in Russian).

– 2 –

The Theory of Interaction Between Synchronous Reactions: Chemical Interference Logics

Various types of possible interactions between reactions are discussed. Some of them are united by the general idea of chemical reaction interference. The ideas on conjugated reactions are broadened and the determinant formula is deduced; the coherence condition for chemical interference is formulated and associated phase shifts are determined. It is shown how interaction between reactions may be qualitatively and quantitatively assessed and kinetic analysis of complex reactions with under-researched mechanisms may be performed with simultaneous consideration of the stationary concentration method. Using particular examples, interference of hydrogen peroxide dissociation and oxidation of substrates is considered.

2.1 INTRODUCTION

There are many types of interaction between reactions. Conjugated processes are the most demonstrative of reciprocal influence and interaction of two or more reactions.

The event when one reaction speeds up the proceeding of another reaction is shown up in non-chemical induction: e.g. via initiation or synthesis of a catalyst in a reaction for another reaction. The mutual influence of reactions synchronously proceeding in a system includes a much broader range of events than chemical induction suggests.

This chapter shows practically all kinds of possible reaction interactions, which part may be united in a general idea of interference of chemical reactions. The notion of interference includes mutual intensification or weakening of the reactions: for instance, the rate of primary reaction product formation decreases, whereas the rate of secondary, conjugated reaction product formation increases. Currently, the mutual influence of reactions synchronized in time and space will be taken for interfering chemical processes [1–3].

With this approach conjugated processes appear to be a particular case of interfering processes. As guided by the idea on chemical interference, one may define many kinds of interactions between reactions. Finally, the phenomenon may be formulated as follows: the event consisting of the fact that reactions synchronously proceeding in the chemical system

are mutually intensified or weakened is called chemical interference, i.e. interaction (e.g. interfering) reactions must be coherent.

In modern chemistry the holistic approach to chemical studies is necessitated by solutions of general, fundamental tasks. From this aspect, simultaneously proceeding chemical reactions represent the components of the entire chemical system, where, as the saying goes, 'all affects all'.

Synchronous processes represent the most demonstrative and unique example of chemical reaction ensembles, arranged in time and space. Interest in synchronous chemical reactions is also so much keener, because in biological systems many processes are synchronous. This means that biochemical reactions are arranged and performed in systems with molecular and permolecular structures, which is the chemist's 'pipe dream'. Studies performed in recent decades have allowed the development of the interaction theory for synchronous chemical reactions at two levels—microscopic and macroscopic. Strictly speaking, parallel reactions may also be taken as synchronous reactions; although proceeding simultaneously in the reaction system, they are characterized by the absence of any interaction between them. However, such synchronous reactions are trivial and of no special interest for chemistry. It is of much more importance when they interact and, therefore, induce oscillations in yields of synchronous reaction products.

It should also be noted that processes are also synchronized via interactions of physical (primary) and chemical (secondary) processes. The microscopic physical process, which induces chemical reaction, is of a quantum type, e.g. highly active intermediate compounds (intermediates) for acceleration of the secondary reaction are formed by the physical (pulse) method. This microscopic coherence of synchronous processes has been described in detail by A.L. Buchachenko [4].

Macroscopic coherence of synchronous reactions is dually displayed, because at the macroscopic level chemical processes proceed in two zones—diffusional and kinetic.

Diffusional process and chemical reaction synchronization induces oscillations of reaction product yields. This common type of synchronous reactions in the literature is referred to as the Belousov–Zhabotinsky reaction.

Meanwhile, the majority of chemical and biochemical processes proceeds in the kinetic zone. Therefore, the synchronization of two chemical reactions or more is of special importance.

As shown below, the observed intermodulation of synchronized chemical reaction yields is clearly displayed in the kinetic zone and represents a valid tool for voluntary manipulation of their rates.

For a fuller description, see the scheme shown in the next page reflecting all known types of synchronous reaction coherence.

The pulse induction and existence of the diffusional zone in a chemical reaction are conditions under which the primary physical process is synchronized with the secondary chemical reaction and, therefore, accelerates it.

Note that in the diffusional zone the chemical reaction rate is limited by the stage of initial substance supply (transport) to the place of chemical interactions, i.e. the chemical reaction rate is much higher than the rate of reagent diffusion to the active site.

On the other hand, the kinetic zone of chemical reaction proceeding is characterized by a much lower rate of chemical transformations than the rate of reagent transport to the

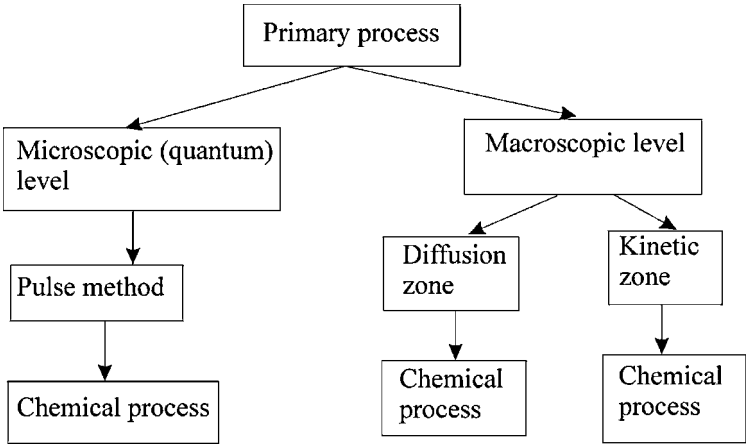

active site, i.e. the diffusion rate of reagents is much higher than the chemical reaction rate. As follows from these canonical identifications, only the kinetic zone is associated with synchronization of purely chemical reactions, two at least. This circumstance is the main reason for significant differences in coherence conditions of various synchronous processes: pulse and diffusional synchronization methods permit the only one, unique chemical reaction.

Let us discuss this principal difference of two induction systems, physical and chemical, more comprehensively. In any chemical system, physical processes associated with diffusion and activation of reacting substances proceed simultaneously with chemical transformations of reagents. Therefore, as chemical reaction is induced by the associated physical process shaped as diffusion or activation represents the potential ability of any chemical system, whereas chemical induction consists of, at least, two coherently synchronized chemical reactions. As shown below, synchronization of kinetic curves for interfering chemical reaction product yields differs radically from these curves for physical influence on the secondary chemical reaction.

Despite origination of interrelated reactions in the early 1900s, the outlook for chemical interference is expected to be, if not extraordinary, but quite useful for interpretation of complex events and voluntary control of processes proceeding in chemical and biological systems.

Until recently, the expression ‘chemical interference’ was absent from chemical dictionaries, the terms ‘complex reactions’, ‘chemical conjugation’, ‘induced reactions’ and so on being most often used. In fact, the new term occurred in the late 1980s. It unites the majority of former terms concerning interaction and mutual influence of chemical reactions. This coining of this new term, unappreciated at first sight, is not merely to be attributed to an author who has thought up a new chemical term. It is actually of deeper significance. Most likely, it is associated with the complex situation appearing in chemistry and biology, when the fundamental tendency of modern biochemical investigations concludes in the development of a holistic approach to problems. Therefore, some chemical and biochemical processes may be barely or, sometimes not at all, understood without this approach.

In fact, chemical interference united scattered ideas about interactions and reciprocal influences and, therefore, formed the general fundamental basis for them.

Chemical interference reflecting the holistic approach to complex processes proceeding in chemical and biological systems, but not to their components as is commonly practiced, characterizes the phenomenon, which real sense justifies the introduction of a new term.

At the present time, the prospect of using chemical interference as the event becomes clearer still. It should be said that it may form the basis for creation of energetically favorable, highly selective and environmentally pure processes and, therefore, may affect economic aspects of applied developments.

With the aim of providing an in-depth and complete presentation of chemical interference, let us now discuss in detail the analysis of chemical interference as the phenomenon by revealing particular spheres of its application. We will also use the terminology usual for conjugated processes.

2.2 INTER-REACTION INTERACTIONS TYPES

As stated by N.A. Shilov, one of the most important objectives of conjugated reaction studies is '… determination how processes stipulating an event (of chemical induction) may be related to one class of conjugated reactions or another'. He has distinguished three types of conjugated processes related to a chemical system with two conjugated processes with three compounds participating in them. The total scheme of the conjugated process is as follows:

$$A + In = RP \text{ (primary reaction)} \tag{2.1}$$

$$A + Acc = RP \text{ (secondary reaction)} \tag{2.2}$$

where RP are reaction products.

The following typical features of conjugated reactions may be distinguished:

1. Energy-releasing reaction performs effective work for proceeding of another (heat-absorbing) reaction, i.e. free energy drop in the primary reaction fully covers the increase of free energy in the secondary reaction. It is also possible that spontaneous (secondary) reaction is accelerated, proceeding with the free energy decrease, but under current conditions its rate may be negligibly low (for instance, equal almost zero).
2. The principle of independent proceeding of elementary chemical reactions is not fulfilled.
3. The links between reactions are set via general intermediate compounds.
4. Conjugated reactions proceed in open systems only.
5. Conjugated reactions must be complex.

As indicated in Chapter 1, principally, the reactions may be conjugated, when one of them slows another one down, and somewhat inhibits it. The mechanism of slowing down the secondary reaction may have different origins (e.g. if the target reaction is of the catalytic type, and intermediate products (IP) poisoning the catalyst are formed in the primary reaction). Another possible case is realized when IP of both reactions recombine or disproportionate (active sites are eliminated). Such negative effects of chemical reactions allow us to

call this type of interaction the 'negative chemical induction' by analogy with the 'negative catalysis' notion [5]. Of interest is that in the case of negative chemical induction both reactions must be spontaneous. Otherwise, if one of the reactions proceeds with an increase in free energy, it is senseless to speak about the slowing down effect.

It should be noted that the acceleration of one reaction by another may also be manifested without chemical induction: e.g. via induction or synthesis of a catalyst for one reaction in another. The reciprocal influence of synchronously proceeding reactions in the system comprises a much wider range of events than does chemical induction.

Obviously, chemical induction is of great interest, because, on one hand, it allows the induction and acceleration of non-spontaneous reaction and, intrinsically, remains the unique method by which to affect such reactions (except for reactions proceeding under the influence of photochemical and ionizing radiation). On the other hand, chemical induction plays a significant role in biochemical processes. The literal translation from Latin term 'interference' is mutual (*inter*) collision (*ferio*), which shows the total situation.

As follows from the definition, interacting reactions may be called coherent ones.

Let us give the general definition of chemical induction, which reflects its specific features. At chemical induction, chemical reaction spontaneously proceeding in the system performs the effective work for another, non-spontaneous chemical reaction in the same system to proceed, which may not run without the first one.

In the current definition of chemical induction, we deliberately preserved the statement that duplicates the common one in order to focus readers' attention on the key statement of the definition. What is the principal difference between saying that the primary reaction 'induces' or 'performs effective work'? In principle, another reaction may be 'induced' by initiation, as well as by synthesis of a catalyst in the primary reaction. In these cases, the primary reaction does not make (thermodynamically) effective work for the secondary reaction to proceed. As defined, catalyst is unable to make effective work, and at initiation the target reaction is developed by a self-reaction pathway and needs a 'trigger mechanism' only at the initial stage of proceeding. In both cases, the target reaction is necessarily spontaneous. At chemical conjugation, the primary reaction continuously induces non-spontaneous process, making effective work during the reaction time. This is only possible during the change of the reaction mechanism or the target reaction type.

Let us now discuss in detail the analysis of chemical interference as the event giving the areas of its display in various forms with particular examples. Therefore, let us use the general terminology, common for characterization of conjugated processes.

In principle, connections and interactions between complex chemical reactions may be most varied. Figure 2.1 gives the most significant of them, showing the layout of the most commonly known complex reactions: consecutive, parallel, consecutive–parallel, etc. At the moment, it should be noted that these schemes do not describe mechanisms of the processes at the level of elementary reactions. For consecutive reactions, IP are stable final substances of the first gross-stage, which are initial substances for the second stage. Figure 2.1 also shows another type of intermediate compounds, which display extremely low stability (free radicals, labile complex compounds, etc.) and high reactivity in relation to the substrate.

To demonstrate this more clearly, reaction arrows for consecutive and parallel reactions, also displayed in Figure 2.1, converge at a point from which, however, it does not follow that final products formed by all reactive pathways possess equal composition. Remember

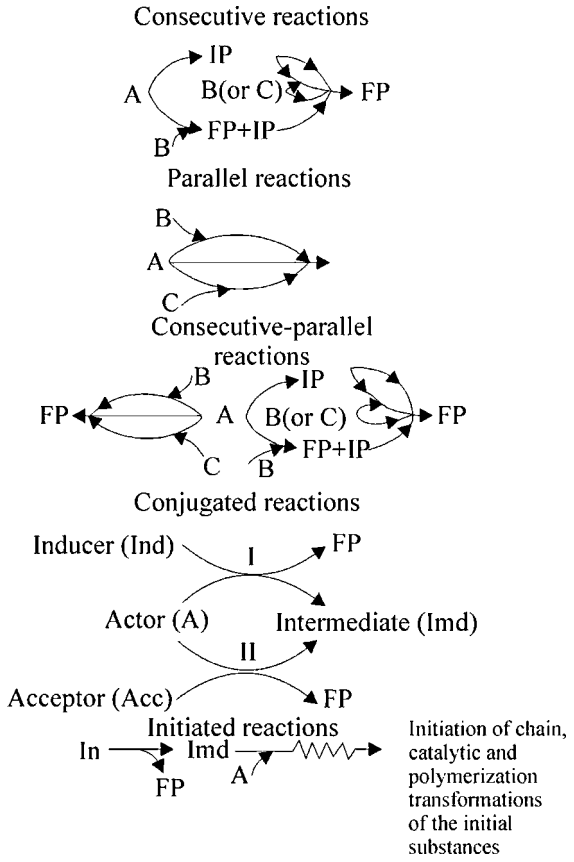

Figure 2.1 Schematic layout of interrelated reactions.

that these schemes most generally characterize complex reactions, and every direction shows formation of specific final products. As soon as these schemes obtain a particular shape, it becomes natural to indicate the corresponding final products for every reaction direction. Consecutive reactions are interconnected by synthesis of an IP at the first stage; thereafter, this product becomes the initial compound for the second stage. Intensification of the first complex reaction leads to expected intensification of another, dependent reaction. Among parallel reactions, the only reactions are reciprocally dependent, which contain even a single compound general for these reactions (A in the current scheme) in the compounding reaction.

As follows from Figure 2.1, the change in concentration of substance A caused by its general expenditure at different rates by the parallel reaction knots mentioned will affect their kinetics.

Therefore, parallel reactions implicitly affect proceeding kinetics of each other via the change of general reagent A concentration. Since consecutive–parallel reactions represent a combination of those mentioned above, the type of interaction between individual complex reactions will be similarly performed (see Figure 2.1).

In Figure 2.1, conjugated processes are shown by the scheme clearly indicating its main features. In particular, it is clear that intermediate compounds formed in the primary reaction induce and speed up non-spontaneous secondary reactions between the actor and the acceptor. Hence, the type of secondary reaction is most often changed which, in a transformed shape, becomes the spontaneous process. Initiation of spontaneous reactions is generally performed according to the mechanism plotted in Figure 2.1. As compared with the mechanism of chemical conjugation, it shows a significant difference displayed in a principally different role of intermediate compounds in the implementation of one mechanism or another.

Thus, an interaction between reactions may be performed both with the help of stable IP (consecutive reactions), intermediate compounds (initiation, conjugated reactions, etc.), and in their absence (a definite type of parallel reactions). Of special interest for us are interrelated reactions performed with the help of labile, highly reactive intermediate compounds. This question will also be discussed below.

Similar to conjugated (interfering) reactions, parallel reactions must be synchronous, which is their obvious fundamental property.

Meanwhile, consecutive reactions may never be synchronous. This is the principal difference between these two systems—synchronous and usual reactions. As a matter of fact, the final product of the first stage of consecutive reactions is the initial compound for the second stage, therefore, these stages may never be simultaneous (synchronous). Thus, the main difference between synchronous parallel and conjugated (interfering) reactions is that the first type eliminates even a possibility of interaction, whereas in the second case they may only be interacting reactions.

2.3 THREE-COMPONENT CONJUGATED PROCESSES

Let us now discuss different alternatives associated with the participation of the three main components of the conjugated reaction system (actor, inducer and acceptor) in chemical induction and other forms of chemical interference.

One of the common types of actor participation in the induction of the secondary reaction is its transformation to a reactive particle under the inducer effect. This newly formed particle then involves another substance (acceptor) in the secondary reaction. Therefore, the actor participates in gross equations of both conjugated reactions which, finally, are reduced to the widespread type of conjugated reactions (2.1) and (2.2).

Let us consider another case in which the actor does not explicitly participate in the gross equation of the secondary reaction. This type of conjugated reactions may be simply represented by the following scheme:

$$A + In = FP \text{ (final products)} \tag{2.3}$$

$$C + Acc = FP \tag{2.4}$$

Nevertheless, the actor is expended in the secondary reaction, because it participates in the formation of general active, intermediate compound X owing to which communication

channels between conjugated reactions are established. It is more desirable to present the induction action mechanism of the primary reaction by the totality of two reactions:

$$A + In \rightarrow X \rightarrow FP \qquad \text{(primary reaction)} \tag{2.5}$$

$$X + C \text{ (or Acc)} \rightarrow Y + FP \qquad \text{(secondary reaction)} \tag{2.6}$$

$$Y + Acc \text{ (or C)} \rightarrow X + FP \tag{2.7}$$

$$C + Acc = FP \qquad \text{(overall reaction)}$$

This scheme indicates that X participation in the secondary reaction may be two-fold:

1. X is synthesized at the end of the secondary reaction and, therefore, acts as a catalyst or active site of the chain reaction;
2. X takes part in formation and is exhausted in the secondary reaction, i.e. without regeneration at the end of the secondary reaction.

Then instead of stage (2.7) the following reaction may be presented:

$$Y + Acc \text{ (or C)} = FP$$

In the first case, chemical interference is displayed most effectively, because it may cause transformation of high amounts of the substance. Here we consciously use the term 'interference' instead of induction, because in this case (see below) reactions interact not by means of chemical conjugation. The second case is the most typical of conjugated processes. Therefore, it should be discussed in more detail.

Reaction (2.5) causes an inductive effect resulting in active site (IP) transfer by the reaction (2.6), which we suggest calling 're-inductive' and then, according to this approach, the general scheme (2.5) and (2.6), which takes into account two types of interaction, is transformed to the following scheme of conjugated reactions:

$$A + In \rightarrow RIn \rightarrow FP \qquad \text{(inductive reaction)} \tag{2.8}$$

$$RIn + C \rightarrow Y + FP \qquad \text{(re-inductive reaction)} \tag{2.9}$$

$$Y + Acc \rightarrow FP \tag{2.10}$$

Thus, the sequence of reactions (2.9) and (2.10) discloses the induction effect mechanism of the primary reaction (2.3) on the secondary reaction (2.4).

Substance A implicitly participates in the formation of secondary reaction (2.4) final products, shaped as Y, though, of course, a definite amount of A is expended for the formation of other final products, synthesized from A and In only.

At first sight, a quite paradoxical case is of special interest, when in conjugated reactions the functions of actor and inducer are implemented by the same substance. Such substances may simultaneously act as oxidants or reducer, or possess acid or base properties. This case

is demonstrated by the example of hydrogen peroxide (and other peroxides) dissociation, which is commonly described by the following total equation:

$$2H_2O_2 = 2H_2O + O_2$$

when one H_2O_2 molecule acts as the oxidant and another molecule as reducer. Active sites, emitted into the system during H_2O_2 dissociation, are expended for final product formation in accordance with the target (secondary) reaction [6]. This allows us to accept that one molecule is the actor and another molecule the inducer. In the author's opinion, as two functions are combined in one compound in such a manner, one may state the following about the inductive property of the substance [7]: as transformed to active sites participating in another reaction, an amphoteric substance may be selectively used up in it by a new reaction mechanism.

This type of conjugated reactions may be presented as follows:

$$A + A(In) \rightarrow X \rightarrow FP \quad \text{(primary reaction)} \tag{2.11}$$

$$A + Acc \rightarrow FP \quad \text{(secondary reaction)} \tag{2.12}$$

Usually, the primary overall reaction (2.5) consists of elementary stages which lead to X formation and its interaction with the acceptor. The latter interaction may be expressed by the following equation:

$$X + Acc \rightarrow FP \quad \text{(induced stage)} \tag{2.13}$$

As is clear from schemes (2.11) and (2.12), only two substances formally participate in such a system of conjugated reactions.

The process by which a complex monomolecular reaction is the primary one may also be related to conjugated reactions:

$$A \rightarrow X \rightarrow FP \quad \text{(primary reaction)}$$

In principle, in the alternatives under consideration, the participation of an actor in the secondary reaction, both clearly and implicitly, is permitted.

Thus, conjugated reactions may proceed without the participation of an inducer and it may be valid to assume that substance A possesses the inductive property. In practice, as is commonly known, conjugated processes are processes in which proceeding of one of the reactions induces and speeds up another reaction, not proceeding in the absence of the first one. From these classical positions, there are no arguments in principal against the statement that the primary reaction is monomolecular, e.g. might proceed without inducer.

The example demonstrating this type of conjugation is that of organic peroxide and hydroperoxide decomposition induced by radicals. These processes were discussed in Chapter 1.

The theoretical examples above most encompass the typical features of such systems. These ideas are necessary for relating conjugated processes to one type or another, which would allow specification of the mechanism of particular chemical induction display.

As follows from the last example, inducer participation in conjugated reactions is not obligatory and, therefore, expression (1.3) should be modified so that it becomes suitable for

describing all known types of interacting reactions. For this purpose, instead of inducer transformation consideration, it is suggested to take into account the actor expenditure in the denominator for every reaction. Moreover, if the actor does not clearly participate in the chemical equation of the secondary reaction, its expenditure in the form of a highly active intermediate substance must be taken into account in calculations.

2.4 THE DETERMINANT EQUATION AND COHERENCE CONDITION OF CHEMICAL INTERFERENCE

Let us discuss a three-component conjugated reaction:

$$\mathrm{A} + \mathrm{In} \xrightarrow{w_1} \mathrm{X} \xrightarrow{w_1} \mathrm{B} + \cdots \tag{2.14}$$

$$\mathrm{A} + \mathrm{Acc} \xrightarrow{w_3} \mathrm{C} + \cdots \tag{2.15a}$$

To demonstrate, the chemical conjugation mechanism may be presented by the following generalized scheme:

$$\nu\mathrm{A} + \mathrm{In} \longrightarrow \mathrm{X} \begin{cases} \xrightarrow{1} \mathrm{FP} \\ \xrightarrow[\mathrm{Acc}]{2} \mathrm{FP} \end{cases} \tag{2.15b}$$

where ν is the stoichiometric coefficient.

Comparing this scheme with its common shape expressed by reactions (2.14) and (2.15a), it should be noted that it gives the best display for the role of the intermediate substance X, which is common to both conjugated reactions as the bifurcation factor of the reaction system, and the inducer is expended in amounts providing A expenditure in both reactions.

For the scheme under consideration, the following expression may be deduced:

$$\frac{1}{\nu} f_{\mathrm{A}} = f_{\mathrm{In}} = (f_{\mathrm{A}_1} + f_{\mathrm{A}_2}) \frac{1}{\nu} \tag{2.16}$$

where f_{A_1} and f_{A_2} are amounts of actor, used for the synthesis of final products in the primary (1) and the secondary (2) reactions, respectively.

Substituting equation (2.16) into (1.3), the following expression is deduced:

$$D = \nu \left(\frac{f_{\mathrm{A}_1}}{f_{\mathrm{Acc}}} + \frac{f_{\mathrm{A}_2}}{f_{\mathrm{Acc}}} \right)^{-1}$$

or

$$D = \nu \left(\frac{w_{\mathrm{A}_1}}{w_{\mathrm{Acc}}} + \frac{w_{\mathrm{A}_2}}{w_{\mathrm{Acc}}} \right)^{-1} \tag{2.17}$$

where factor D determined in equation (2.17) is called the determinant.

As follows from equations (2.16) and (2.17), it is not obligatory to operate the amount of expended inducer in the calculations. Moreover, there are conjugated processes that proceed without inducer participation. Therefore, it is of much greater importance to account for the expenditure of compound A in both reactions and to determine the induction factor via it. From these positions, equation (2.17) is somehow universal, because it reflects chemical induction in any display. Moreover, it is shown below, how many important consequences follow from it, which may not be deduced from equation (1.3).

Another alternative is also possible, i.e. when in the primary reaction active particles representing catalysts for the secondary reaction are formed. Of course total actor expenditure will then be greater than the inducer expenditure.

Note also that for chemical induction equation (2.16) is always correct.

Note also an important point: when actor expenditure in conjugated reactions is so high, a large amount of it is used in the primary reaction, when active sites are formed. These sites are IP, and a definite part of them is spent in the formation of final products in the primary and secondary reactions.

It is common knowledge that the primary reaction usually proceeds in several stages (two, at least), and it is of importance that the reactive sites generated in it were mainly expended in the target, secondary reaction. For this purpose, the stages that cause the accumulation of active sites must proceed at a higher rate than the consecutive ones, which give final products of the primary reaction. Let us consider this possibility using the example of conjugated, type (2.14) and 2.15(a) reactions. It will be shown that relations following from these considerations are also valuable for the specific case of induction-less conjugation of chemical reactions.

When the first stage rate in the primary reaction (w_1) is lower or equals the second stage rate (w_2), the rate of the target product synthesis in the secondary reaction will be defined by w_2 and w_3 ratio. If $w_2 \approx w_3$, the final products of these conjugated reactions will be accumulated at comparable rates. As $w_2 \gg w_3$, the final products of the primary reaction will mostly be synthesized, which will minimize the induction effect. As $w_1 \gg w_2$ and $w_2 \gg w_3$, the kinetic regularities mentioned are preserved. The only difference is that high concentrations of highly active IP in the reaction system will affect induction efficiency, and the target product synthesis rate will increase somewhat.

The highest induction effect should be expected in the case of inequality $w_3 \gg w_2$ fulfillment at $w_1 > w_2$. In this regard, accumulation of final products by the overall reaction (2.15b), No. 2 under the condition of effective induction performance must proceed at an incommensurately higher rate than the primary one. As mentioned above, the induction effect at $w_2 \gg w_3$ will be insignificant, approaching the limit $I = 0$. In this consideration, it is assumed that rate constants k_1, k_2 and k_3 characterize elementary reactions of the same kinetic order; otherwise, concentration factors would also have to be taken into account which would necessarily complicate the analysis.

It should also be noted that equation (2.17) gives a more in-depth description of the physical sense of chemical induction phenomenon than equation (1.3). Thus, by introducing a qualitatively new notion of chemical induction (inducer participation is not obligatory for conjugation proceeding), equation (1.3) was modified so that it might be used to describe any type of conjugated process. On the other hand, equation (2.17) is quite universal and may describe other types of interrelated reactions (chemical interference).

Analytical consideration of equation (2.17) leads to several important consequences for various forms of chemical interference.

1. Consider the case where $f_{A_1} \gg f_{A_2}$ and $f_{Acc}; \frac{1}{v} f_{A_1} \approx f_{In}$. From equation (2.17) it then follows that:

$$D = \frac{v f_{Acc}}{f_{A_1}}$$

This means that the primary reaction mostly proceeds in the system. Hence, the higher the rate of this reaction, the lower is the induction factor (I) which approaches zero in the limit. Obviously, acceptor expenditure is low under these conditions.

2. If $f_{A_2} \gg f_{A_1}$, three alternatives of the chemical system with interrelated (interfering) reactions may be realized:

A. As we neglect the value of the actor part expended for final product synthesis in the primary reaction (f_{A_1}) and under the condition that the actor is completely spent for target product formation only according to schemes (2.11) and (2.12), the equation:

$$f_{A_2} = f_{Acc}$$

can be deduced. Then equation (2.17) is reduced to:

$$D = \frac{v f_{Acc}}{f_{A_2}} = v$$

According to equation (2.16), the real inducer consumption will equal A_2/v. In this case, chemical induction is manifested much more effectively. As a consequence, modification of the conjugated reaction system must aim to approach the above-mentioned marginal ratio.

B. At $f_{Acc} \gg f_{A_2}$ and $\frac{f_{A_2}}{v} \approx f_{ln}$, the following expression for D is deduced:

$$D = \frac{v f_{Acc}}{f_{A_2}} \gg$$

The higher the effectiveness of intermediate substance catalytic action on the secondary reaction or chain transformation of the substrate, the higher is the D value.

Let us assume that the primary reaction generates an active site in the system, which is the secondary reaction catalyst. It is known that the catalyst does not perform effective work in the reaction, but just speeds it up and remains unchanged at the end of the reaction. At the same time, one of the principles of conjugated reaction principles is that the primary reaction performs effective work for another reaction, conjugated to it, via formation of general intermediate substances consumed in both reactions.

Meanwhile, the catalyst may cause or accelerate a spontaneous reaction only and, at most, promote the achievement of outputs close to equilibrium, whereas chemical induction may cause outputs exceeding equilibrium. In this regard, if in the primary reaction, active sites representing the catalyst for another synchronously proceeding reaction are accumulated, the latter reaction must be spontaneous and the primary reaction does not perform effective work for its running. On the other hand, in chemical induction, intermediate substances are obligatorily consumed for the secondary, non-spontaneous reaction, chemical energy released in the primary reaction is consumed and, therefore, effective work is performed.

Therefore, catalyst synthesized in the primary reaction is unable to perform effective work in the secondary reaction, and such reactions may not be classified as conjugated ones, because this would entirely contradict the notion of chemical induction.

It is also known from biochemistry that the majority of processes important in biochemistry represent conjugated catalytic reactions. Conjugated catalytic reactions obey the regularities typical of chemical induction, i.e. $D \leq \nu$, and the catalyst application approaches the system to the ideal shape ($D \approx \nu$), and it should be related to the case (A). All these cases are illustrated by the expression (2.17). It is also shown below how the factor D values help in quantitative assessment of chemical interference effectiveness and determination (under particular conditions) of the type of interaction between reactions dominating in the chemical system studied.

In fact, in the latter case, the catalyst (injected into the system with initial reagents) only speeds up interaction between the IP of the primary reaction and the acceptor. Therefore, $D < \nu$ and, consequently, chemical conjugation takes place. This means that no matter how the reaction between the acceptor and the IP is intensified by the catalyst, the induction factor (the determinant) may not exceed ν.
When analyzing conjugated catalytic reactions, it should be taken into account that the amount of acceptor involved in the reaction may be significantly increased by application of a catalyst in both conjugated reactions.

Catalyst application to the primary reaction at the stage of IP formation will promote its quick accumulation in the systems in amounts much higher than for its non-catalytic run, and will soften reaction conditions. Secondary reaction is also accelerated. Its proceeding is stipulated by the presence of intermediate substance of the primary reaction.

As $D \gg \nu$, the primary reaction generates in the system a catalyst for secondary, spontaneous reaction. Hence chemical induction is absent. In this regard, a very important conclusion can be drawn: the determinant value of the chemical system characterizes conjugated reactions and represents a common induction factor only in the case where its value fulfills the inequality:

$$0 < D \leq \nu$$

Note also that this inequality is typical only of systems in which chemical conjugation occurs. The induction factor correctly describes the three-component system in which owing to the inducer action an IP is synthesized. This product is a reagent but not a catalyst. However, application of the expression (1.3) shaped equation for

the induction factor to other types of interrelated (interfering) chemical reactions leads to wrong values.

Moreover, if the primary reaction is monomolecular, and chemical induction occurs in this system, the induction factor may not be determined from equation (1.3). This is demonstrated by the limited type of equation (1.3) application range even to conjugated reactions.

Nevertheless, equation (2.17) may help in determining the determinant and detecting the type of interrelated reactions from it. It should be noted here that, in the broad sense of the word, interrelated (interfering) reactions are only those proceeding via general intermediate substances, capable reagents, initiators or catalysts of secondary reactions. Otherwise, this class of reaction may be added to by consecutive reactions, which are not coherent.

In fact, for consecutive reactions, the final product of the first stage is the initial product for the following stage and, hence, the reaction mechanism and the reaction rate remain unchanged, and the principle of independent proceeding of separate reactions is also obeyed.

The overwhelming majority of biochemical oxidation processes represent conjugated catalytic (enzymatic) reactions [8]. Therefore, of great importance is the ability to distinguish catalyst and inducer, because any mistake would cause an incorrect interpretation of the chemical mechanisms of the reactions proceeding in the biological system. For instance, redox reaction catalysts are often taken for inducers.

Among interrelated reactions, initiated radical-chain reactions are the most widespread. At the initiation process, the synthesis of highly reactive intermediate compounds (free radicals, in particular) is the necessary condition the target reaction intensification. However, initiating substances are used as additive increments, and the chain initiation stage must proceed at a much lower rate than the chain propagation stage. Otherwise, the chain length becomes shorter, and the chain transformation of the substrate becomes ineffective [9]. In other words, initiators act as 'triggers' of the radical or chain process. From these positions, interacting and initiated reactions are rather similar: catalyst is synthesized in the primary reaction, whereas other reactions generate active sites shaped as free radicals, etc.

In fact, free radicals synthesized in the initiation process may induce spontaneous chain transformation of the acceptor only, which proceeds in the case of quite long chains. Otherwise, the process will not be developed at any noticeable rate.

The determinant of initiated chain reactions will always be higher than one: the longer the chain is, the higher the determinant is. This case is analogous to catalytic influence of the primary reaction on the secondary reaction. Note also that in the case of chemical induction, the primary reaction overall accompanies the reaction to be conjugated (which may be non-spontaneous, e.g. induced) and performs effective work for it during its whole run. High amounts of the primary reaction components are taken; hence, the target reaction (if it is of the chain type) may proceed at any chain length, even very short. Thus, chemical induction allows implementation of processes proceeding with extremely short chains, which is absolutely impossible at the initiation.

Sometimes, due to special conditions, chain transformation may hardly be induced. An example of this is the reaction of propylene epoxidation. However, intense generation of active sites (HO_2) in the primary reaction gives the possibility of suppressing acceptor chain transformation to undesired products and simultaneously stimulating the main direction—epoxidation. This is obtained due to chemical induction, which induces and speeds up selective transformation of propylene (acceptor) to a quite high rate. The authors have implemented such a conjugation mechanism in propylene epoxidation by hydrogen peroxide [10].

Therefore, free-radical-chain reactions proceeding by short chains (which makes these reactions less profitable for effective transformation into desirable products) may be significantly intensified by chemical induction and, hence, heighten interest in their application.

C. Assume that $f_{A_2} = f_{Acc}$ Then:

$$D = \frac{\nu f_{Acc}}{f_{A_2}} < \nu$$

This means that, in principle, under current conditions chemical induction may take place. However, it is highly improbable that the secondary reaction requiring two actor molecules or more for its run would give a noticeable yield.

3. Finally, let us consider the case where the actor equals consumption in both reactions, e.g. $f_{A_1} = f_{A_2}$. Hence, as with previous examples, several alternatives are possible:

a) $f_{A_2} = f_{Acc}$; then $D = \dfrac{\upsilon f_{Acc}}{\left(f_{A_1} + f_{A_2}\right)} = \dfrac{\upsilon f_{Acc}}{2f_{A_2}} = \dfrac{\upsilon}{2}$

b) $f_{A_2} > f_{Acc}$; then $f_{Acc} < 2f_{A_2}, D < \upsilon$

c) $f_{A_2} < f_{Acc}$; then $\begin{cases} f_{Acc} < 2f_{A_2}, D < \upsilon \\ f_{Acc} = 2f_{A_2}, D = \upsilon \\ f_{Acc} > 2f_{A_2}, D > \upsilon \end{cases}$

We will not give a detailed analysis of case 3, because these alternatives of chemical interference have already been discussed above.

Note that the interference of chemical reactions may alter the effective rate constant of the secondary reaction and break the independence principle of elementary chemical reactions. Moreover, under these conditions non-spontaneous reactions may proceed, which are eliminated in parallel and consecutive reactions.

In case of chemical induction, secondary conjugated reaction may never be of the monomolecular type, because the IP of the primary reaction, being the reagent of the secondary reaction, is consumed in it which naturally leads to a gross equation with more than one component.

The chemical interference range is very broad. It embraces various types of interrelated reactions, including monomolecular secondary (non-conjugated) reactions. The best example

is the case in which the primary reaction synthesizes a catalyst for the secondary reaction (which, in principle, may also be monomolecular), and initiates reactions:

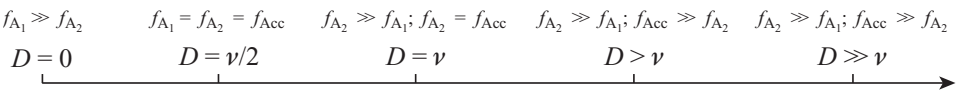

Chemical interference determinant scale; $D = 0 \div \nu$ is the chemical conjugation range $D > \nu$ is the range of other interactions proceeding

The necessary condition for chemical interference realization in the reaction system is the spontaneous type of its primary reaction.

Based on the data presented in this chapter, the above equation shows the determinant scale, which makes the detection of one type of reciprocal influence of chemical reactions (chemical interference) or another in the reaction mixture easier.

Kinetic studies of the chemical system with the interaction between reactions, based on the experimental data, allow selection between various types of interfering chemical reactions. Therefore, chemical interference investigations may be found useful for the study of reaction mechanisms.

It seems to the authors that one of the forms of self-organization in complex chemical systems may be chemical interference, described by the determinant equation (2.17). This idea is also confirmed by the fact that the overwhelming majority of enzymatic reactions *in vivo* are synchronized and conjugated. As shown below, the determinant equation is quite useful and easily adjustable for solving complex chemical tasks.

Physicochemical features of chemical interference are displayed by theoretical kinetic curves in Figure 2.2 and allow the discovery of some shapes, which will be discussed below.

These idealized curves were composed with the hypothesis that primary reaction (1) in the absence of secondary reaction (2) proceeds until the end, i.e. its initial reagents are consumed completely. Therefore, acceleration of the secondary reaction is studied under conditions in which the primary reaction runs completely to its end.

The curves in Figure 2.2a show that in the absence of the secondary reaction (2) the primary reaction (1) proceeds with almost 100% consumption of the reagents. As secondary reaction (2) products are accumulated, the quantity of primary reaction products decreases and both curves pass via extreme points (peaks). According to theoretical notions, the maximum of reaction (2) corresponds to the minimum of reaction (1). In the case where, due to kinetic reasons the reaction (2) is synchronized with the primary reaction (1) with some delay, a phase shift (Δ) occurs, shown by a dashed line in Figure 2.2a. The maximum on this curve is right shifted by Δ value. In other words, the phase shift means the difference between the primary reaction minimum and the secondary reaction maximum.

Based on kinetic regularities following from the type of these curves, one may make an important conclusion that for every particular condition, the totality of reaction products will correspond to a constant value of the actor consumption or, in accordance with stoichiometry (scheme 3) of the inducer and the assumption (e.g. postulation) of its complete consumption, the following expression becomes valid:

$$\frac{1}{\nu} f_A = f_{In} = f_{A_1} + f_{A_2} = f'_{A_1} + f'_{A_2} = f''_{A_1} + f''_{A_2} = \cdots = \text{constant} \qquad (2.18)$$

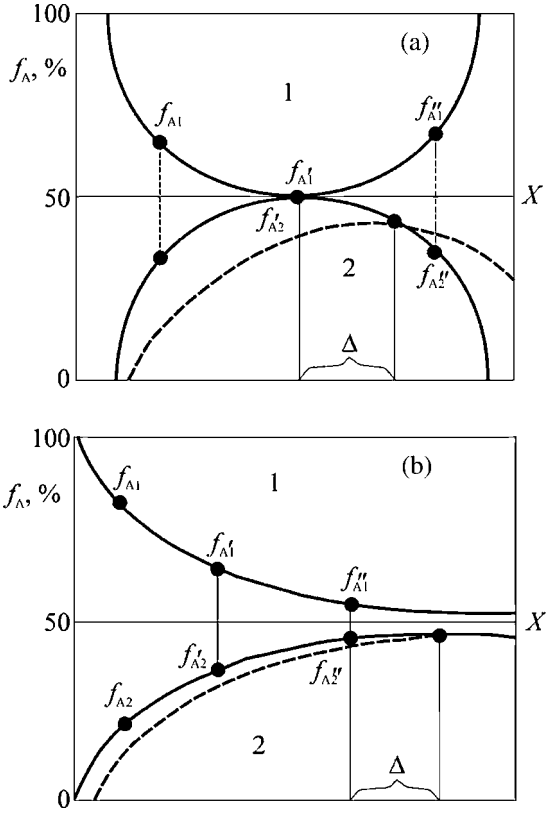

Figure 2.2 Theoretical kinetic curves for interfering reactions (primary 1 and secondary 2) of extreme (a) and asymptotic (b) type; Δ is the phase shift.

It is assumed that equation (2.18) is the coherence condition for chemical interference, at least for the case in which the D value varies between zero and ν, i.e. chemical conjugation takes place.

An important consequence of equation (2.18) should be outlined: effective interference between two chemical reactions is observed in the case where, in the absence of the secondary reaction, the primary reaction proceeds completely to its end in the whole range of conditions.

Another case, also shown in Figure 2.2b, is characterized by curves free from extreme points, approaching the X level. Such curve shapes indicate zero concentration of the actor and general highly reactive intermediate particles in the area where asymptotic curves approach the X level most closely. Therefore, at asymptotic approach no products are formed by interfering reactions. The coherence condition, displayed by equation (2.18), is also fulfilled in this case.

Other cases are mostly associated with incomplete (i.e. partial) proceeding of the primary reaction in the absence of the secondary reaction and its complication by side reactions, especially with participation of an inducer. In the cases under consideration, as actor or inducer consumptions per primary and secondary reactions are calculated, the amounts consumed

for the synthesis of side products must be subtracted from the total amount or, at incomplete consumption, the amounts of non-reacted A or In compounds.

Note that the X line in Figure 2.2b may be located above or below the 50% level of product accumulation from both interfering reactions or actor (inducer) and acceptor consumptions. Line location above the X line means that the greater part of the total, highly active intermediate particles (active sites) is consumed for secondary reaction product formation and, vice versa, when the line is below X level.

A dashed curve in Figure 2.2b shows the phase shift, the origin of which is similar to that in Figure 2.2a.

It is known that the correspondence principle suggested by N. Bohr (1923) postulates that 'any theory pretending for better description and broader application range than the older one must include the latter in the form of marginal case'.

The succession of theoretical notions may be shown by using the corresponding principle for consideration of the chemical interference theory as a more general concept of interrelated and interacting reactions. The correspondence principle applied to the interference of chemical reactions must represent a postulate, which in the marginal case of the determinant ($D \to \nu$) requires the coincidence of its chemical consequences with yields of usual chemical reactions, e.g. classical stoichiometric reaction.

For conjugated reactions, the maximum high determinant value equals ν ($D = \nu$). This means that only a secondary reaction proceeds in the system, coinciding by stoichiometric parameters with the corresponded conjugated reaction. Simultaneously, the level $D = \nu$ is the lowest for initiation, autocatalysis, chain and other types of interfering reactions which, in the previous case, are reduced to a stoichiometric reaction. Hence, when considering the suggested theory from the position of the correspondence principle, the following conclusion can be made: under the condition $D = \nu$, the conjugated, chain, initiated and autocatalytic reactions are necessarily reduced to stoichiometric reactions, i.e. described in the framework of the classical theory of chemical reactions. Formally, transition to a stoichiometric reaction happens at $D \to \nu$, which emphasizes the general type of the new notion of interfering chemical reactions.

2.5 INTERFERENCE OF HYDROGEN PEROXIDE DISSOCIATION AND SUBSTRATE OXIDATION REACTIONS

The examples given below, for instance, methane oxidation to methanol and propylene oxidation to propylene oxide, demonstrate experimental approaches to the study of interfering reaction dynamics and, with the help of the determinant equation, the potential abilities of reaction media are assessed and the type of chemical interference determined.

Monooxigenase reaction for synthesizing methanol from methane was studied in the presence of cytochrome P-450 biosimulators, such as ferroprotoporphyrin catalysts with the carriers (Al_2O_3, NaX, aluminum–chromium–silicate and aluminum–magnesium–silicate). This reaction helped in the detection of the highest catalytic activity for $PPF^{3+}OH$/aluminum–magnesium–silicate [11], which also displayed the highest catalytic activity for hydroxylation reaction. As shown, optimal hydroxylic activity of the catalyst is displayed in the initial 30 min of its operation (methanol output equals 60 wt.%, selectivity is 97 wt.%). Figure 2.3 shows that kinetic dependence of methanol output on temperature has a maximum

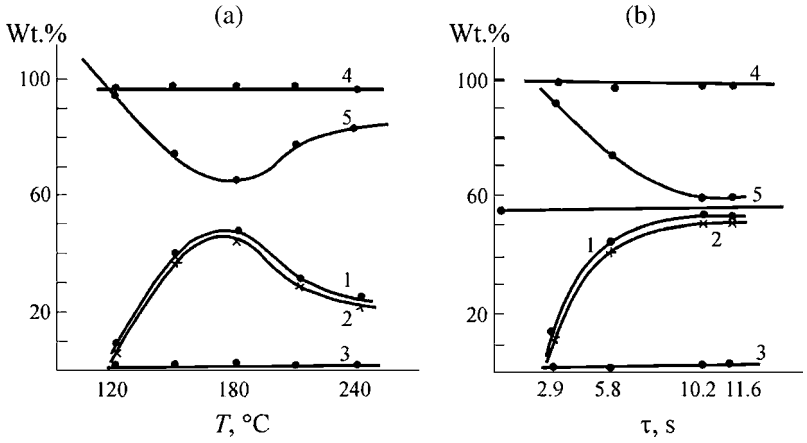

Figure 2.3 Dependencies of methane hydroxylation outputs on (a) temperature and (b) contact time at 180 °C. 1: CH_4 conversion; 2: CH_3OH output; 3: CH_2O and HCOOH outputs; 4: selectivity; 5: O_2 output Ratios: CH_4:H_2O_2 = 1:1.4 (a) and 1:1.8 (b); $V_{CH_4}V_{H_2O_2}$ = 0.8 ml/h, $[H_2O_2]$ = 20 wt.%.

at 180 °C, and the curve of molecular oxygen yield has a minimum. In this experiment, methanol yield reaches 46.5 wt.%, which at methane conversion rises to 48 wt.%. Non-target products CH_2O and HCOOH in low amounts (~1.5%) and temperature cause no effect on their yield. Comparison of the curves 2 and 5 in Figure 2.3 in the framework of the ideas discussed above shows their reliable analogy with the theoretical curves in Figure 2.2a. Some deviation of coherence (f_{Ind}) from the theoretical level may be explained by synthesis of side oxidation products and systematic errors, which usually accompany any chemical experiment. However, its value (f_{Ind}) obeys the main coherence condition following from equation (2.18). More precisely, $f_{Ind} \approx$ constant for current reaction conditions. This value may be simply calculated from the data of Figure 2.3a. A graphic presentation of chemical interference, shaped as asymptotically approaching curves in another range of the reaction conditions, is plotted in Figure 2.3b. Comparison of the experimental curves from Figure 2.3b with the theoretical ones from Figure 2.2b indicates their adequacy and relates the observable chemical interference to the case above X, i.e. when the CH_4 oxidation rate slightly exceeds the rate of molecular oxygen synthesis.

In the chemical system studied biosimulator catalyzes two interrelated (catalase and monooxygenase) reactions, which are synchronized and proceed according to the following mechanisms:

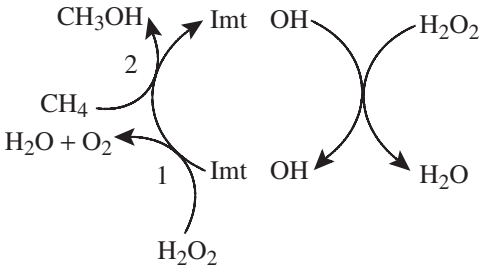

where ImtOH is $PPFe^{3+}OH/AlMgSi$ biosimulator; ImtOOH is $PPFe^{3+}OH/AlMgSi$ intermediating compound: (1) primary catalase reaction and (2) hydroxylation (secondary monooxygenase reaction).

Both reactions (1) and (2) in the scheme proceed via general $PPFe^{3+}OH/AlMgSi$ intermediating compound, which certainly is the transferring agent for the inductive action of the primary reaction to the secondary reaction. The determinant calculated by equation (2.17), which allows quantitative identification of an interaction between reactions, equals:

$$D = 0.48$$

This indicates that reactions (1) and (2) are conjugated, because the value obtained on the determinant scale of chemical interaction (Figure 2.1) falls within the range of chemical conjugation ($D < 1$), because in the current case $\nu = 1$.

The diagrams in Figure 2.4 illustrate the conjugated type of two reactions: H_2O_2 dissociation and propylene epoxidation by hydrogen peroxide [12]. Actually, the rate decrease of biosimulator catalase activity product (O_2) accumulation is accompanied by the rate increase of epoxidation product synthesis, and these processes interfere via general highly active intermediating compound: per-$FTPhFe^{3+}OOH/Al_2O_3$.

However, presenting the interference picture via a diagram has several principal disadvantages: 1. diagrams do not show how coherence is implemented; 2. phase shifts may not be shown; 3. maxima and minima in accumulation of products of both reactions and 4. the absence of asymptotic curves.

The advantage of the diagrams is that they are highly illustrative of chemical conjugation between current reactions. Thus, diagrams help in demonstrating one of the aspects of chemical interference associated with conjugation of the processes.

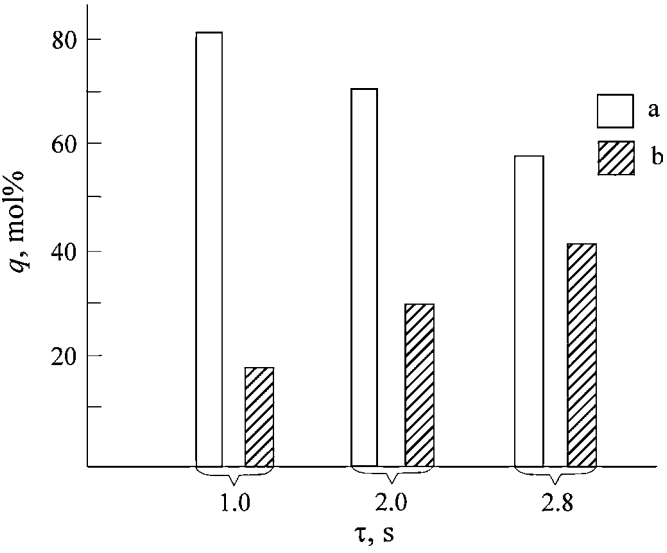

Figure 2.4 Hydrogen peroxide consumption (q) in catalase (a) and monooxygenase (b) reactions with time of contact; $T = 200°$ C, C_3H_6:H_2O_2 = 1:1.2 (mol).

Let us consider the experimental data shown in Figure 2.5a and b, obtained at homogeneous gas-phase oxidation of methane (or natural gas) by hydrogen peroxide to methanol under pressure [13, 14]. The increase in contact time to 0.95 s (Figure 2.5a) gives a maximum of methanol output and a minimum of oxygen output. A further increase in the contact time reduces methanol output, whereas molecular oxygen output increases. A similar kinetic regularity is observed in experiments with variable pressure (Figure 2.5b).

Thus, comparison of the curves of molecular oxygen accumulation and CH_4 consumption (or CH_3OH accumulation) shows that the maximum of CH_4 transformation corresponds to the minimum of O_2 accumulation.

Chemical interference is clearly displayed owing to almost 100% selectivity of reactions: increased O_2 synthesis induces a simultaneous decrease of CH_4 transformation to CH_3OH and vice versa.

As the curves in Figure 2.5a and b are considered from positions of coherence and possible phase shift, note that the particular reaction mixture differs from the mixtures considered above by relatively low (about 20 wt.%) CH_4 substrate conversion, although H_2O_2 dissociates almost completely. This circumstance must be taken into account in the framework of the approach to such a case described above.

Experimental detection of chemical interference determinant by the following equation:

$$D = \nu \left(\frac{r_1}{r_{CH_4}} + \frac{r_2}{r_{CH_4}} \right)^{-1} \tag{2.19}$$

where r_1, r_2 and r_{CH_4} are actor (H_2O_2), inducer (H_2O_2) and acceptor (CH_4) consumption rates, respectively; ν is the stoichiometric coefficient equal to 1 for the current conditions of minimal O_2 and maximal CH_3OH outputs, gave $D = 0.18$. On the chemical interference scale in Figure 2.1, this value falls within the range for conjugated reactions. It quantitatively characterizes the inductive action of H_2O_2 on CH_4 oxidation and indicates the presence of high potential abilities to increase the induction effect of the system studied (theoretically, in the current case, D may increase to 1 or will tend to approach at least the 50% level) [2]. There are physicochemical experimental techniques that allow manipulation of conjugating reaction rates. On the other hand, not applying the method of stationary concentrations, the determinant equation (2.17) gives an opportunity of analyzing the kinetics of complex reactions with insignificantly studied mechanisms. For these two reactions the conjugation mechanism is:

$$\begin{array}{l} \xrightarrow[k_2]{H_2O_2} H_2O + HO_2^{\bullet} \\ H_2O_2 \xrightarrow{k_1} 2\,{}^{\bullet}OH \\ \xrightarrow[k_3]{CH_4} H_2O + CH_3^{\bullet} \xrightarrow[k_4]{H_2O_2} CH_3OH + {}^{\bullet}OH \end{array} \tag{2.20}$$

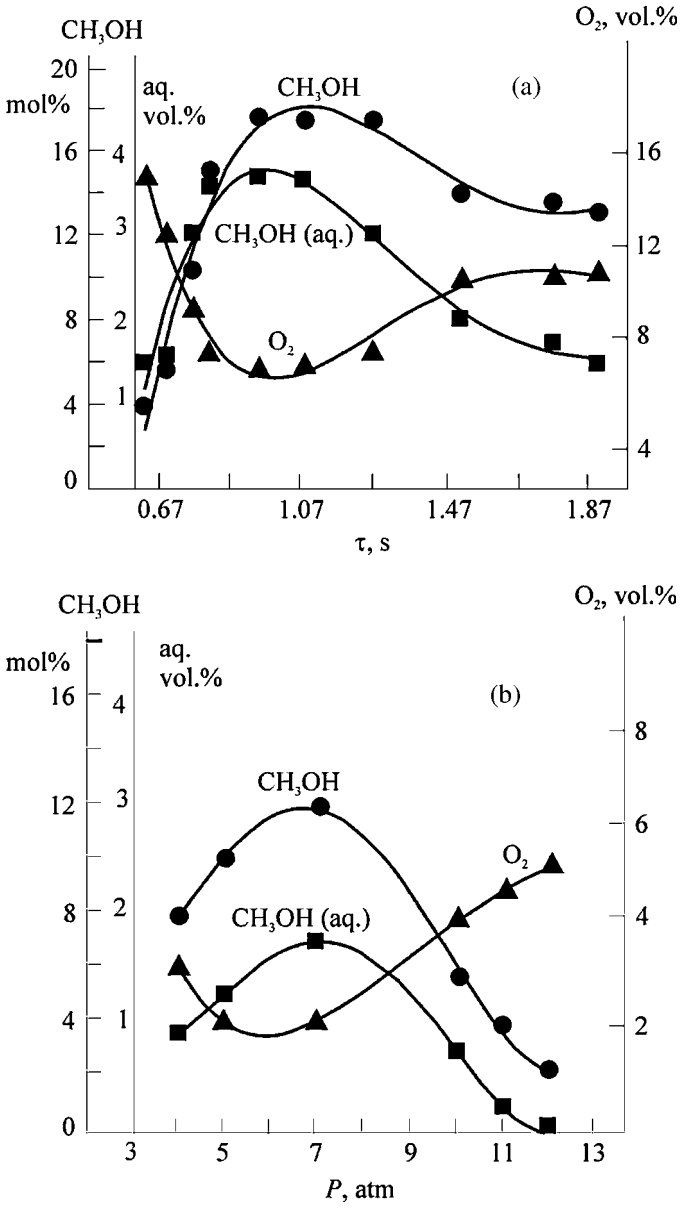

Figure 2.5 The dependence of methanol output on the contact time (a) and pressure (b); $T = 400°C$, $[H_2O_2] = 30$ wt.% (a) $p = 7$ atm; $V_{CH_4} = 31.4$ l/h; $V_{H_2O_2} = 0.18$ l/h; $CH_4{:}H_2O_2 = 1{:}1.4$ (mol) and (b) $V_{H_2O_2} = 0.18$ l/h; $V_{CH_4} = 62.4$ l/h; $CH_4{:}H_2O_2 = 1{:}0.4$ (mol).

As follows from the determinant equation:

$$r_{\mathrm{Acc}}(\mathrm{CH_4}) = \frac{D}{\nu}\left(r_{\mathrm{A}_1} + r_{\mathrm{A}_2}\right)$$

or

$$r_{\mathrm{CH_4}} = \frac{D}{\nu}(k_2[\mathrm{H_2O_2}] + k_3[\mathrm{CH_4}])[\mathrm{OH}] \tag{2.21}$$

Using experimentally obtained values of $r_{\mathrm{CH_4}}$ and D [8], the appropriate kinetic calculations were carried out. Therefore, equation (2.21) adequately describes the kinetics of interfering reaction (2.20).

Thus, the determinant equation was found useful for the analysis of the kinetics of complex reactions in that it made simpler the kinetic calculations at determination of the kinetic model of interrelated and synchronized reactions proceeding in the reaction mixture and also the qualitative and quantitative assessment of chemical interference itself.

Note also that some authors [11–14] have had to use all their inventiveness in order to impart high experimental demonstrativeness to chemical interference.

2.6 THE DIFFERENCE BETWEEN INITIATION AND INDUCTION PHENOMENA

Since no clear distinction between initiation and induction of chemical reactions is made in the scientific literature, and very often one event is taken for another, we will discuss this question in more detail.

Active sites are generated both in initiation reactions and by chemical induction, and this situation is common to all types of initiated and conjugated reactions. The main difference is related to the effect of these active sites on the target reaction (in the case of chemical induction, this is the secondary reaction). Only one aspect—generation of active sites—is very often considered. On this basis many authors make their own conclusions.

Meanwhile, only the determination of further behavior of active particles in the system—the influence on the target reaction—may exactly determine particular cases of initiation and induction.

By way of example, let us consider how radical polymerization of vinyl monomers is initiated by free hydroxyl radicals. These radicals are obtained by catalytic action of bivalent iron salts on H_2O_2 dissociation (Fenton reagent) [15]:

$$\mathrm{Fe^{2+} + H_2O_2 \rightarrow Fe^{3+} + OH^- + {}^{\bullet}OH} \quad \text{(initiation)}$$

$$\mathrm{{}^{\bullet}OH + CH_2 = CHCN \rightarrow HOCH_2\dot{C}\,HCN \xrightarrow{CH_2=CHCN}}$$

$$\rightarrow \mathrm{HO(CH_2 = CHCN)_nCH_2\,\dot{C}\,HCN} \quad \text{(chain propagation)}$$

Every free •OH radical initiates one reaction chain. After the addition of a single monomer molecule it rests at the inactive chain end and does not participate in subsequent propagation acts. A single •OH radical induces transformation of a high amount of monomer and H_2O_2 acts as the initiator, but does not participate in the gross equation of the target reaction. As suggested by Dolgoplosk and Tinyakova, H_2O_2 excess over Fe^{2+} ($[H_2O_2]/Fe^{2+} > 1$) inhibits polymerization [16, 17].

There are other examples characterizing the initiating action of H_2O_2. Ashmore [15] indicates that primary radicals do not usually induce chain degradation, because they are captured by a monomer molecule before a sufficient number of collisions with diluted initiator particles.

Therefore, H_2O_2 concentration in the system, where it acts as the initiator, is strictly limited. Initiators are applied as highly diluted solutions and accelerate only reactions, which proceed at a high rate after initiation. The initiator concentration increase in the system is limited also for chain reactions involving short chains.

This restriction for initiation reactions was set by Benson: as the chain propagation rate is 10–100 times higher than the initiation rate of active sites, propagation reactions dominate in the system and the chain process is of great importance [9]. Here, the following condition must be fulfilled for initiated chain reactions:

$$\nu = \frac{w_{\text{prod}}}{w_{\text{ini}}} > 10$$

where ν is the chain length.

From this expression it is clear that initiation is valuable for chain lengths, at least, above 10 units, i.e. the chain propagation rate must be at least 10 times above the initiation rate.

According to data by Dolgoplosk and Tinyakova [17], an increase in H_2O_2 concentration inhibits the polymerization process, initiated by low concentrations of this compound. This gives rise to the question: What is the further behavior of active sites? Ashmore suggests that in the presence of other organic substances the redox system may oxidize active sites. For example, the 'ferrous iron–hydrogen peroxide' easily oxidizes aromatic compounds [15]. Thus, an interesting interrelation between polymerization and oxidation reaction and the possibility of transferring from one reaction to another with H_2O_2 concentration change is observed.

One more example of the conjugated process is illustrated by benzene oxidation reaction in the Fenton system, which is discussed in detail in the book by Emanuel and Knorre [18]. Aqueous benzene solution does not directly interact with H_2O_2. However, as bivalent iron salt is added to the system, Fe^{2+} ion oxidation to Fe^{3+} is accompanied by benzene oxidation to phenol and diphenyl. Therefore, under these conditions H_2O_2 may not oxidize benzene. A successful oxidation performance requires H_2O_2 dissociation to hydroxyl radicals with Fe^{2+} ions as catalysts. Then free •OH radicals react with benzene inducing its oxidation. Therefore, these two reactions—H_2O_2 dissociation induced by Fe^{2+} catalyst (primary reaction) and benzene oxidation by hydrogen peroxide (secondary reaction)—are conjugated. In this case, •OH radicals are carriers of H_2O_2 inductive action on the secondary reaction.

As follows from this example, catalytic dissociation of H_2O_2 generates •OH radicals in the system and under definite conditions induces another reaction. In this regard, with respect to the particular objective of generating free radicals to the system, H_2O_2 may possess

properties of initiator (of polymerization, e.g.) and inducer (of benzene oxidation by hydrogen peroxide, e.g.).

There is a special case in which both conjugated reactions proceed at the maximal rate and, hence, chemical interference is observed in a specific manner, which is realized in the membrane catalysis of mitochondrial energetic process.

2.7 CONCLUSION

The strategy associated with imparting high efficiency and orderliness to chemical interference has proved itself:

1. the primary reaction runs with almost 100% conversion in the absence of the secondary reaction;
2. it approaches 100% selectivity for both reactions.

The study of chemical interference and its particular case of conjugated processes indicate that it may represent a simple prototype for similar systems realizable in biochemical systems.

First of all, realization of chemical interference is associated with the selection of those reactions that are capable of self-organization, i.e. to formation of complex reaction ensemble. The ensemble of molecules and, as a consequence, the ensemble of reactions is able to interfere, because aggregation of molecules in ensembles somehow creates an algorithm for the realization of mutually agreed spontaneous reactions. Contrary to free molecules, the distinctive feature of an ensemble of molecules is the fact that structural organization of an ensemble of molecules allows the running of both simple and complex reactions, chemical interference of which is vitally important for the living system activity. In this discussion we would like to indicate that chemical interference is the necessary property of biochemical systems. Note also that molecular ensembles may be differently organized structurally and, therefore, the type of ensemble from the same molecules is responsible for proceeding of one type of interrelated reactions or another (i.e. chemically interfering reactions).

The ensemble of reactions is self-organized through the intermediary of general highly active substances. These processes may be accelerated and effectively implemented with the help of catalysts similar to processes, which take part in the living systems.

Thus, self-organization of an ensemble of reactions capable of being intensified or weakened and, therefore, inducing chemical interference, may be suggested as the basis for the principle of organization of many enzymatic ensembles.

Of great interest is the creation of trigger reaction ensembles, which will not only change the interference picture but also the type of interacting reaction with respect to the action of temperature, pressure, medium pH and other important factors.

REFERENCES

1. Nagiev, T.M., *Chemical Conjugation*, Nauka, Moscow, 1989, p. 216 (in Russian).
2. Nagiev, T.M., *Zh. Fiz. Khim.*, 1994, Vol. 68, No. 3, pp. 456–460 (in Russian).
3. Nagiev, T.M., *Zh. Fiz. Khim.*, 2000, Vol. 74, No. 11, pp. 2034–2040 (in Russian).

4. Buchachenko, A.L., *Usp. Khim.*, 1999, Vol. 68, No. 2, pp. 99–118 (in Russian).
5. Boreskov, G.K., *Catalysis*, Pt. 1/2, Nauka, Novosibirsk, 1971, p. 267 (in Russian).
6. Nagiev, T.M., *Khim. Fiz.*, 1983, No. 6, pp. 823–832 (in Russian).
7. Nonhibel, D. and Walton, J., *Chemistry of Free Radicals*, Mir, Moscow, 1977, p. 606 (in Russian).
8. Nulman, B. and Pulman, A., *Quantum Biochemistry*, Mir, Moscow, 1965, p. 654 (in Russian).
9. Benson, S., *Thermochemical Kinetics*, Mir, Moscow, 1971, p. 308 (in Russian).
10. Nagiev, T.M., Mamed'yurov, G.M., Nagieva, Z.M. and Agaeva, S.I., *XII Mendeleev Council on General and Applied Chemistry*, *Thes. Rep. Inform.*, Nauka, Moscow, 1981, No. 4, p. 268 (in Russian).
11. Nagiev, T.M. and Abbasova, M.T., *Zh. Fiz. Khim.*, 1997, Vol. 71, No. 7, pp. 1213–1217 (in Russian).
12. Nagiev, T.M., Galanova, L.M., Zulfugarova, S.Z. and Mustafaeva, Ch.A., *Zh. Fiz. Khim.*, 1996, Vol. 70, No. 11, pp. 2063–2068 (in Russian).
13. Mamedov, E.M., Farajev, E.G. and Nagiev, T.M., *Azerb. Khim. Zh.*, 1997, No. 1–4, pp. 45–48 (in Russian).
14. Nagiev, T.M., Farajev, E.G. and Mamedov, E.M., *Zh. Fiz. Khim.*, 2001, Vol. 75, No. 1, pp. 50–56 (in Russian).
15. Ashmore, P.A., *Catalysis and Inhibition of Chemical Reactions*, Mir, Moscow, 1966, p. 386 (in Russian).
16. Dolgoplosk, B.A. and Tinyakova, E.I., *Generation of Free Radicals and Their Reactions*, Nauka, Moscow, 1982, p. 253 (in Russian).
17. Dolgoplosk, B.A. and Tinyakova, E.I., *Redox System as the Source of Free Radicals*, Nauka, Moscow, 1972, p. 237 (in Russian).
18. Emanuel, N.M. and Knorre D.G., *The Course of Chemical Kinetics*, Vysshaya Shkola, Moscow, 1984, p. 237 (in Russian).

– 3 –

Conjugated Chemical Reaction Morphology and Membrane Catalysis in Mitochondrial Proton Transfer

This chapter overviews the following points:

- Questions of kinetics and the mechanism of conjugated reactions.
- Conjugated chemical reactions in living nature.
- The features of simultaneous effect on chemical induction and catalysis reactions.
- Idealized model of conjugated catalytic reactions.
- The induction property of some substances for chemical reactions.
- Abilities supported by chemical induction for chemical technology development.

3.1 THE MECHANISM AND KINETICS OF CONJUGATED REACTIONS

At the present time, detection of chemical induction in complex reactions is a little-developed area in the field of conjugated reactions. Usually, difficulties occur in the interpretation of the induced reaction mechanism and its kinetic description. In fact, textbooks on chemical kinetics [1–4] either have no methodological notes on these aspects or consider only a narrow, definite type of conjugated processes.

Shilov [5] has limited considerations in regard to the final equation for conjugating reactions and determination of an intermediate substance which stipulates the initiating action of the primary reaction. However, this is not nearly complete enough to describe the secondary reaction mechanism, which should be changed during the conjugation process.

The most suitable kinetic approach was suggested in a textbook by Emanuel and Knorre [1]. It discusses a particular widespread case of conjugated processes with three components:

$$A + In \rightarrow X \tag{3.1}$$

$$X + In \rightarrow B \tag{3.2}$$

$$X + Acc \rightarrow D \tag{3.3}$$

where X is a stable intermediate substance.

For this scheme, a system of differential equations for the consumption of all initial components and an intermediate substance is presented. We will use the recommended approach for kinetic description of conjugated processes with respect to specific features typical of them.

The reduced schemes (3.1)–(3.3) does not identify each separate conjugated reaction. The solution of the problem is also complicated by the possibility of using this scheme for a scheme of consecutive–parallel reaction, if one does not know that the scheme describes chemical induction. Meanwhile, schemes (3.1)–(3.3) possess an important advantage: it shows the stages required for acceptor transformation.

In the author's opinion, Shilov's idea about conjugated reactions must be preserved shaped as separate overall reactions: primary and secondary. However, each reaction of two must be added to by a stage mechanism similar to the composition of schemes (3.1)–(3.3). Apparently, the unification of these two approaches will become the foundation stone in the chemical refinement of conjugated reactions, which will most fully describe the conjugation mechanism and preserve its individual, specific features. This description will first reflect the features of chemical induction which distinguish it from parallel and consecutive reactions. By analogy with (3.22) and (3.23), the total conjugation picture for a three-component system is most often presented in the following form:

$$\begin{aligned} A + In &\rightarrow X_1 \rightarrow FP \\ A + Acc &\rightarrow FP \end{aligned} \tag{3.4}$$

$$\begin{array}{l} A + In \longrightarrow X_i \begin{array}{l} \overset{1}{\longrightarrow} FP \\ \underset{Acc}{\overset{2}{\longrightarrow}} FP \end{array} \end{array} \tag{3.5}$$

where index 1 at X means its belonging to intermediate substances of the first kind (see below).

Every described scheme possesses definite advantages: the first scheme reflects gross transformation and the second the action mechanism of the intermediate product X_1. How can we unite them in a single scheme?

The solution to such a task may be illustrated using the example of conjugated dehydrogenation of an organic substance by hydrogen peroxide [6]. For this purpose, let us present the reaction in a traditional shape similar to schemes (3.4) and (3.5).

The primary reaction of conjugated dehydrogenation by hydrogen peroxide in the gas phase at 400–650 °C represents peroxide dissociation which generates active sites in the system:

$$\underset{\text{actor}}{H_2O_2} + \underset{\text{inducer}}{H_2O_2} \rightarrow \underset{\text{intermediates}}{[HO^{\bullet}_2, {}^{\bullet}OH]} \rightarrow 2H_2O + O_2 \tag{3.6}$$

The secondary, induced reaction represents dehydrogenation process:

$$\underset{\text{actor}}{H_2O_2} + \underset{\text{acceptor}}{\rangle HC - CH\langle} \rightarrow \rangle C = C\langle + 2H_2O \tag{3.7}$$

Experimental and theoretical justification of this scheme is presented in the next chapter. Currently, according to the objective, we may limit consideration with chemical induction mechanism. Using scheme (3.5), we obtain:

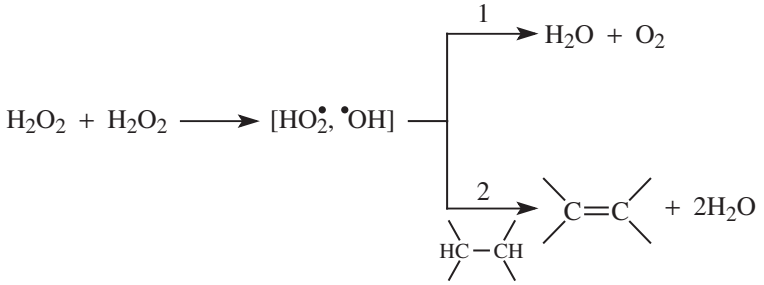

(3.8)

Schemes (3.6) and (3.7) have similar disadvantages to schemes (3.4) and (3.5). Therefore, a separate description of the mechanism of both reactions is a more rational approach embracing all features of chemical induction. Such a description preserves the individuality of each reaction and, simultaneously, clearly traces the communication channels via highly active intermediate substances. Transformation of schemes (3.6)–(3.8) [6] gives the following results:

Primary reaction

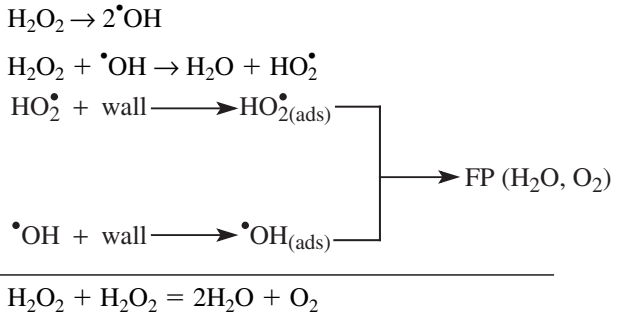

(3.9)

Here (ads) means ‘adsorbed’.

Secondary reaction

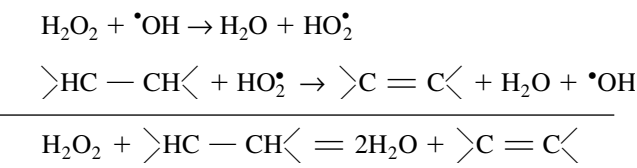

(3.10)

In this case, the secondary reaction of organic substance dehydrogenation, conjugated with the primary reaction, represents oxidative dehydrogenation. This is the key moment

for understanding the chemical oxidation mechanism and its variations from common consecutive and parallel reactions.

Let us consider some examples, such as conjugated oxidative dehydration of acetic acid [7]:

$$2CH_3COOH_{(lq)} \rightarrow (CH_3CO)_2O_{(lq)} + H_2O_{(lq)}, \tag{3.11}$$

$$\Delta G^0_{298} = 54\,\text{kJ/mol}$$

proceeding at 500–600 °C, but represents endergonic (heat-absorbing) reaction under standard conditions.

Highly exergonic process—carbon oxide oxidation—conjugated with this reaction, proceeds in the presence of palladium (II) complexes:

$$CO_{(g)} + \frac{1}{2}O_{2(g)} \rightarrow CO_{2(g)}, \tag{3.12}$$

$$\Delta G^0_{298} = -257\,\text{kJ/mol}$$

The final process represents a new reaction type—oxidative dehydration accompanied by free energy loss. Contrary to usual dehydration, this process may be performed under soft conditions at almost room temperature:

$$2CH_3COOH_{(lq)} + CO_{(g)} + \frac{1}{2}O_{2(g)} \rightarrow (CH_3CO)_2O_{(lq)} + CO_{2(g)} + H_2O_{(lq)}, \tag{3.13}$$

$$\Delta G^0_{298} = -203\,\text{kJ/mol}$$

Similarly, conjugated dehydrogenation of ethylbenzene is performed [6]. At low temperature this is an endergonic reaction requiring high temperatures (800–900 °C), at which equilibrium output is high:

$$C_6H_5C_2H_5 \rightarrow C_6H_5C_2H_3 + H_2, \tag{3.14}$$

$$\Delta G^0_{298} = 83\,\text{kJ/mol}$$

However, H_2O_2 injection to the system simultaneously with ethylbenzene sharply increases the dehydrogenation rate, whereas thermolysis of H_2O_2 is a highly exergonic process:

$$2H_2O_2 = 2H_2O + O_2, \tag{3.15}$$

$$\Delta G^0_{298} = -246.6\,\text{kJ/mol}$$

A non-spontaneous low-temperature dehydrogenation of ethylbenzene is simultaneously initiated at quite a high rate. Free radicals $HO_2^{\bullet}$—the substance mediator—induce the

primary reaction of ethylbenzene dehydrogenation, which becomes a spontaneous process due to chemical induction.

The author [6] has shown that the secondary process represents a new type of reaction—conjugated oxidative dehydrogenation, and contrary to usual thermal dehydrogenation [8], may be performed at lower temperatures and give higher yields and selectivity [9].

This example confirms the conjugated type of the secondary oxidation reactions under consideration. Meanwhile, the difference between interpretations of the gross equation for the secondary reaction given in Refs [6] and [7] is obvious.

In the first case [7], the induced reaction is indicated shaped as before the conjugation. However, chemical induction changes the secondary reaction type as exemplified by equation (3.13). As the final equation (3.13) is compared with a different, secondary reaction, a conclusion is made [7] that the conjugation process changes the target reaction type (in this case, carboxylic acid dehydration).

We suggest a different approach to the determination of the secondary (target) reaction type in the chemical induction process and interpretation of conjugating reaction mechanism (refer to equations (3.6)–(3.10)). Firstly, in schemes (3.6)–(3.7) the reaction conjugated with H_2O_2 dissociation is taken for the secondary dehydrogenation reaction. A total change in the system is determined from the final equation:

$$3H_2O_2 + \rangle HC - CH\langle \rightarrow 4H_2O + \rangle C = C\langle + O_2 \qquad (3.16)$$

One of the terms in this equation is induced reaction. Therefore, reaction (3.16) should currently be considered as a totality of two conjugated reactions.

Basing on the above-mentioned ideas, the following conclusions can be made:

- The target reaction without induction is a non-spontaneous or spontaneous reaction, but is unfortunately hard to perform for kinetic reasons.
- As the target (secondary) reaction is chemically induced, its type is changed so that the reaction is transformed from non-spontaneous to spontaneous and proceeds without any hindrances under current kinetic conditions.
- Besides the primary reaction, the conjugated process scheme is added to by the secondary reaction in induced, e.g. transformed shape, taken to be the overall reaction.
- If the secondary reaction is spontaneous, another alternative is possible, where it is not changed by conjugation but preserves its type.
- A specific feature of conjugated reactions is the fact that, contrary to consecutive and the more so parallel reactions, the induced reaction may not be performed separately from the primary reaction.

Two more conclusions can be added to this list:

1. Affected by the induction, spontaneous target reaction can also change and proceed at high rate under current conditions.
2. A system with chemical induction may have two or more components.

The last statement requires some additional explanation, because there is an opinion that conjugation of reactions is typical of three-component systems, which in the case of two

components become usual consecutive reactions. This question was partly discussed in the previous chapter; in particular, free radical induced degradation of organic peroxides and hydroperoxides [10]. In the case of active site generation by the initial substance, this degradation represents a single-component system. Conjugated reactions of oxidation by hydrogen peroxide in the gas phase and the Fenton system ($Fe^{2+} + H_2O_2$) represent two-component systems (refer to the following chapters for details).

It seems to the author that these examples confirm the existence of a broad variety of the number of conjugation components. Actually, the classical definition of conjugated processes does not limit the number of substances participating in both interrelated reactions, which may be mono-, bi- or tri-molecular.

Before passing to a kinetic description which takes into account the features of conjugated reaction mechanisms, one should clearly define the following types of complex reaction.

It is common knowledge that consecutive or consecutive–parallel reactions have intermediate products of two types:

1. Short-lived, highly reactive particles functioning *in situ*: free radicals, complexes with an inducer or a catalyst with a single or several initial reagents, extremely unstable molecular complexes, etc.
2. Valence-saturated molecules, ions and complexes.

Highly active intermediate compounds of the first kind (free radicals and complexes) are always formed in free radical and catalytic processes. These compounds induce a much higher rate of the final product synthesis compared with their absence.

There are two features distinguishing intermediate products of the first and second kinds: intermediate substances of the first kind or, as they are truly called, active sites are extremely higher reactive (they may not be separated and considered as final products); intermediate substances of the second kind are always final products of the first stage of the consecutive reaction. They are extremely more stable (they may always be extracted and studied separately).

On this basis, a qualitative criterion in a definite approximation may be applied to complex reactions. This criterion may help in setting a consecutive, parallel or conjugated type of reaction proceeding in the chemical system:

1. Intermediate products of one kind or another participate in consecutive and consecutive–parallel (complex) reactions. Participation of intermediate products of the second kind is a must, whereas participation of intermediate products of the first kind is arbitrary.
2. The mandatory requirement for parallel reaction proceeding is the obligatory participation of a unique intermediate product of the first kind in each reaction.
3. Two reactions running synchronously in the chemical system are conjugated only in the case where they include intermediate products of the first kind, general for them. The absence of intermediate products of the second kind, except for a special case, when one of conjugated reactions or, possibly, both of them are consecutive.

Note that in some cases, consecutive and parallel reactions may proceed without the formation of an intermediate product of the first kind, when interaction of the initial molecules causes formation of final products excluding the stage of active site formation (these reactions

are called molecular or simple in the literature). However, chemical reactions proceeding by the molecular mechanism are not much known. They relate to a special case and are beyond the scope of this discussion.

The kinetics of consecutive, consecutive–parallel and parallel reactions of any complexity is discussed in classical monographs on chemical kinetics [1–3, 11] and are not considered in the current monograph. The scope of kinetic regularities of these complex reactions mentioned will be minimally required for a clear understanding of their differences from kinetics of conjugated reactions.

In the literature on kinetics of conjugated reactions, they are often represented by two consecutive reactions [1, 3]:

$$\begin{aligned} A + B_1 &= X + \ldots \quad \text{(primary reaction)} \\ X + B_2 &= C + \ldots \quad \text{(secondary reaction)} \end{aligned} \tag{3.17}$$

where X is an intermediate substance of the second kind.

Kinetic equations are of the following shape:

$$\begin{aligned} -\frac{d[A]}{dt} &= k_1[A][B] \\ \frac{d[X]}{dt} &= k_1[A][B] - k_2[B_2][X] \\ -\frac{d[B_2]}{dt} &= \frac{d[C]}{dt} = k_2[B_2][X] \end{aligned} \tag{3.18}$$

where k_1 and k_2 are rate constants of primary and secondary reactions, respectively.

The results of solving these kinetic equations are shown in graph form in Figure 3.1 [3, p. 33]. Analysis of the data testifies to the kinetic uniformity of consecutive and conjugated reactions. Therefore, the conclusion [3] can be drawn that 'the latter are parallel reactions just formally'.

The similarity of the conjugated and consecutive reactions, observed in scheme (3.17), also affected the results of kinetic task (3.18) solution.

Actually, kinetic regularities resulting from the type of curves, shown in Figure 3.1, were predetermined in scheme (3.17). Therefore, kinetic indistinguishability of complex reactions of these two types is somewhat pre-programmed. Naturally, such an approach to the study of kinetic regularities of conjugated reactions may give erroneous results. For example, curve 3 (Figure 3.1) of the intermediate product accumulation has a maximum which indicates consumption of the product at the following stage. Such regularity is typical of intermediate products of the second kind, which in the case of consecutive reactions usually represent final products of the primary reaction. Consecutive reactions may be simple and complex. If they represent a sequence of simple reactions, the intermediate product is of the second kind. Scheme (3.17) contains two simple consecutive reactions.

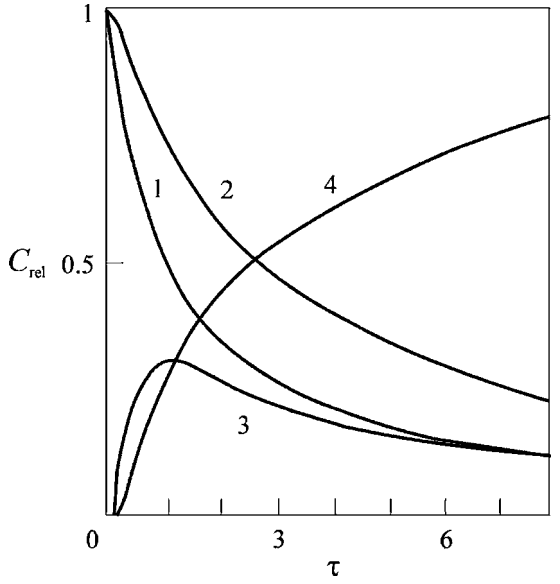

Figure 3.1 Kinetic curves of actor and inducer (1) and acceptor (2) consumption, and intermediate substance (3) and reaction product (4) accumulation in '$A + B_1 + B_2$' system (dimensionless coordinates).

In the above material we formulated basic signs of difference.

Thus, it is of great importance that the description of conjugated reactions should reflect the basic distinctive features of chemical induction, otherwise they may be taken for consecutive or parallel reactions.

Let us suggest that scheme (3.4) gives the fullest description of chemical induction features, and based on its preliminarily dividing overall reactions to elementary stages. According to current ideas, the primary reaction will consist of two processes:

Primary reaction

$$\begin{array}{lcl} A + In \rightarrow X_1 + B(In^*) & & A + In \rightarrow X_1 + B(In^*) \\ X_1 + A(In) \rightarrow B_1 + \cdots & \text{or} & X_1 \rightarrow B_1 + \cdots \\ 2A + In = B(In^*) + B_1 + \cdots & & A + In = B(In^*) + B_1 + \cdots \end{array} \qquad (3.19)$$

where X_1 is an intermediate particle of the first kind; In* is the final product mostly consisting of the inducer.

Before considering the mechanism of induced reaction, let us shape it as a secondary reaction:

$$A + Acc = C + \cdots \qquad (3.20)$$

Since the chemical induction effect is manifested via the formation of a general highly active transient formation, elementary reactions synthesizing X must be taken into account in the deduction of the stage mechanism of the induced reaction:

Secondary reaction

$$\begin{array}{l} A + In \rightarrow X_1 + B \\ \qquad X_1 + Acc \rightarrow C + \cdots \\ \hline A + Acc + In = B + C + \cdots \end{array} \tag{3.21}$$

In this case, the overall reaction (3.21) possesses inducer In as the reagent. Therefore, to avoid confusion, the final equation of the secondary reaction should be presented differently.

Note that activating the actor, the inducer transforms it to an intermediate product of the first kind, which represents a chemical active fragment of the actor.

When transforming to X under the effect of In, the actor transits to a new state (active site) and, in this shape, participates in acceptor transformation. In this case, the initial stage of the primary reaction may be presented in the following form:

$$A \underset{-In^*}{\overset{In}{\rightarrow}} X_1 \tag{3.22}$$

The notation of reaction (3.19) is suitable from positions of composing the mechanism of the secondary reaction, in which product formation is not associated with the inducer consumption, otherwise scheme (3.21) would be significant. Then for the secondary reaction, the following scheme is obtained:

$$\begin{array}{l} A \underset{-In^*}{\overset{In}{\rightarrow}} X_1 \\ X_1 + Acc \rightarrow C + \cdots \\ \hline A + Acc = C + \cdots \end{array} \tag{3.23}$$

In principle, there is a possibility of forming final products by reaction (3.22) with completely eliminated inducer or containing a part of it. This must, of course, change the right-hand parts in equations (3.22) and (3.23).

Another possibility is associated with formation of highly reactive complex which transfers the induction action of the primary reaction.

Primary reaction

$$\begin{array}{lll} A + In \rightarrow X_1 \cdot In + B & & A + In \rightarrow X_1 \cdot In + B \\ X_1 \cdot In + A \rightarrow B_1 + \cdots & \text{or} & X_1 \cdot In \rightarrow B_1 + \cdots \\ 2A + In = B + B_1 + \cdots & & A + In = B + B_1 + \cdots \end{array} \tag{3.24}$$

Secondary reaction

$$\begin{array}{l} A + In \rightarrow X_1 \cdot In + B \\ \underline{X_1 \cdot In + Acc \rightarrow C + In} \\ A + Acc = C + B \end{array} \tag{3.25}$$

Based on the comparison of schemes (3.19)–(3.25) and uniting all the above-said, one may suggest the following rules for determining the induced reaction mechanism:

- The reaction subject to induction changes its type, and its overall reaction and necessarily includes substances from the primary reactions as the initial reagents, from which a highly active intermediate particle (an active site) is formed. Usually, this is the actor. The substance promoting generation of the active site (inducer), but not being its component, is not included in the secondary reaction.
- Primary reaction products are not included in the final products of the secondary reaction.

Most frequently, a type (3.20) reaction induced by another reaction may be described by schemes (3.22) and (3.23). Therefore, in this example conjugated reactions were analyzed with preservation of specific features distinguishing it from other complex reaction:

Primary reaction

$$\begin{array}{l} A \xrightarrow[-In^*]{In} X_1 \\ \underline{X_1 \rightarrow B + \cdots} \\ A + In = In^* + B + \cdots \end{array} \tag{3.26}$$

Secondary reaction

$$\begin{array}{l} A \xrightarrow[-In^*]{In} X_1 \\ \underline{X_1 + Acc \rightarrow C + \cdots} \\ A + Acc = C + \cdots \end{array} \tag{3.27}$$

It should be remembered that these conjugated reactions are extrinsically similar to two independent parallel reactions:

$$\begin{array}{l} A + C_1 \xrightarrow{k_1} D_1 \\ A + C_2 \xrightarrow{k_2} D_2 \end{array}$$

However, the extrinsic analogy masks a principal difference consisting in the fact that in the case where chemical induction reactions are interrelated, consequently, they may not be described by two independent systems of differential equations, as for parallel reactions. If one makes an attempt to describe them by kinetic reactions for consecutive (or consecutive–parallel) reactions, similar to scheme (3.17), then conjugated reactions will be reduced to consecutive reactions, from which they principally differ. So what are the kinetic expressions that may show the individuality of chemical induction?

To solve this question, the mechanism of conjugated reactions (3.26) and (3.27) under consideration should be rewritten similar to (3.5) as follows:

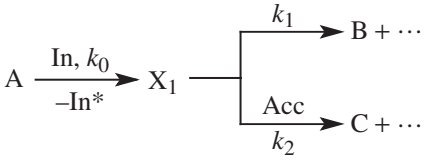

(3.28)

According to this scheme, products of two conjugated processes are synthesized by two reactions from an intermediate particle X*. We focus attention on this aspect, because this is the means of clearly delimiting consecutive–parallel and conjugated reactions.

To start with, intermediate products of the first kind are free radicals, short-lived complexes, etc., the concentration of which may not be measured using common techniques. They may not be extracted or accumulated. This is the reason why the kinetic curve for the intermediate product of the second kind (in oxidation reactions of ROOH hydrocarbons and H_2O_2) in Figure 3.1 must not be typical of conjugated reactions.

The interpretation of chemical induction phenomenon resulting from the conjugation of a reaction proceeding through general transient compounds must be added to by a condition that conjugated reactions have, at least, one more general elementary reaction.

Let us now consider a widespread type of complex reactions, the so-called competing chain reactions [12].

Actually, schemes of radical chain processes display many examples of competing elementary stages. For example, chain degradation of ethyl chloride:

$$C_2H_5Cl \rightarrow C_2H_5^{\bullet} + Cl$$

synthesizes radical R participating in the following reactions:

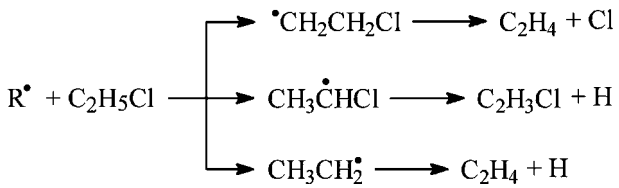

(3.29)

The type of radical R formed (H or Cl) causes formation of different reaction products. Degradation of C_2H_5Cl to $C_2H_5^{\bullet}$ and Cl is essentially the initiation reaction for C_2H_5Cl

chain transformation according to scheme (3.29). All three degradation parallel chain reactions compete with one another which correlates well with the experimental results.

Relatively large molecules are transformed by chain reactions, in which product distribution is defined by the limiting chain propagation stages. For example, Benson [12] presents the following version of *n*-butane cracking:

$$\mathrm{R^{\bullet} + CH_3CH_2CH_2CH_3} \xrightarrow{-\mathrm{RH}} \begin{cases} \mathrm{\dot{C}H_2CH_2CH_2CH_3} \longrightarrow \mathrm{C_2H_4 + C_2H_5^{\bullet}} \\ \mathrm{CH_3\dot{C}HCH_2CH_3} \longrightarrow \mathrm{C_3H_6 + CH_3^{\bullet}} \end{cases} \tag{3.30}$$

Finally, atom H detachment from the primary carbon atom causes C_2H_4 and C_2H_6 formation, whereas its detachment from the secondary carbon atom causes C_3H_6 and CH_4 formation. Note that $C_2H_5^{\bullet}$ and $CH_3^{\bullet}$ radicals easily entrap H atoms from both positions.

As mentioned in Chapter 2, chemical conjugation is absent in initiated processes. Moreover, initiated parallel chain processes (3.29) and (3.30) display the main reaction paths for reagent transformation to final products no matter what the manner of initiation. As shown by scheme (3.28), at chemical conjugation the first stage of the primary process in the mechanism and material balance equation must be taken into account by both reactions.

Discussing schemes (3.29) and (3.30) in detail we can compare with scheme (3.28) indicating their extrinsic similarity (they proceed with participation of highly active intermediate compounds) and principal difference (reactions proceeding by schemes (3.29) and (3.30) are parallel reactions and by scheme (3.28) conjugated reactions). Chain reactions shown in schemes (3.29) and (3.30) are independent of one another, whereas reactions 1 and 2 in scheme (3.28) are interrelated.

It is common knowledge that when intermediate products are highly reactive particles, a stationary mode is set in the system in a short time. In this mode concentration of active intermediate compounds is accepted as stationary, i.e. the difference in rates of their accumulation and consumption is very low compared with the reaction rates. Thus, the intermediate product concentration in the conjugated reaction may be determined by the method of stationary concentrations. On the other hand, kinetics of conjugated reactions may be described by an expression deduced from the determinant equation (2.25) not using the stationary concentration method.

Scheme (3.28) may be taken for the basic conjugation mechanism of chemical reactions, because it generally reproduces the specificity of chemical induction. Before we determine the determinant for scheme (3.28), a system of differential equations taking into account consumption of the components should be composed:

$$\begin{aligned} w_{\mathrm{In}} &= -\frac{\mathrm{d}[\mathrm{In}]}{\mathrm{d}t} = -\frac{\mathrm{d}[\mathrm{A}]}{\mathrm{d}t} = k_0[\mathrm{A}][\mathrm{In}] \\ w_{\mathrm{C}} &= w_{\mathrm{Acc}} = -\frac{\mathrm{d}[\mathrm{Acc}]}{\mathrm{d}t} = k_2[\mathrm{Acc}][\mathrm{X}] \\ w_{\mathrm{B}} &= \frac{\mathrm{d}[\mathrm{B}]}{\mathrm{d}t} = k_1[\mathrm{X}] \end{aligned} \tag{3.31}$$

Substitution of corresponding rates into the determinant equation (2.17) gives the following expression:

$$D = \left(\frac{w_{A_1}}{w_{Acc}} + \frac{w_{A_2}}{w_{Acc}} \right)^{-1}$$

or

$$D = \left(1 + \frac{k_1}{\left(k_2[Acc]\right)} \right)^{-1} \tag{3.32}$$

Expression (3.32) gives several interesting consequences.

The ratio $\frac{k_1}{\left(k_2[Acc]\right)}$ carries the main information about the induction action of the primary reaction and quantitatively estimates its efficiency. Actually, if the numerical value of the rate constant k_1 for primary reaction product formation equals (or is comparable with) the secondary reaction product formation rate multiplied by the initial acceptor concentration, then

$$D \approx \frac{1}{2}$$

This value (refer to Chapter 2) characterizes the equality of actor consumption in both reactions. Moreover, acceptor consumption also equals this value. However, this is an infrequent case of chemical induction. Most often variations of acceptor concentrations may raise the induction factor—the determinant—to its maximum (unit). For this purpose, it is enough to increase the acceptor concentration in current conjugated reactions so that the following inequality is obeyed:

$$k_2[Acc] \gg k_1$$

If the primary reaction in scheme (3.28) is bimolecular, then the denominator in the ratio $\frac{k_1}{\left(k_2[Acc]\right)}$ must obtain one more variable, depending on the concentration of either the inducer or the actor. In this case, the number of possible alternatives increases. This indicates that chemical induction may be controlled, which may be used for increasing efficiency of induction and vice versa. Thus, from the above the following recommendations can be made for the kinetic description of conjugated reactions.

First of all, differential equations accounting for final product formation in each conjugated reaction must be written down, and then using the determinant equation a relation giving a quantitative assessment of the chemical induction should be deduced. Hence, there is no need to use the stationary concentration technique.

Thus, the determinant equation represents a connecting link between differential equations (3.31) promoting their uniting in a system. To determine the determinant with sufficient

accuracy, the amount of products formed must be known in order to then calculate D with the help of equation (2.17) and scheme (3.28). With rare exceptions, when product formation in one of the reactions requires simultaneous participation of two active sites, the expression for the determinant may include intermediate product concentration. However, such situations are fairly infrequent.

Note also that if the determinant equation is used in the shape typical of the induction factor determination:

$$I = \frac{w_{\mathrm{Acc}}}{w_{\mathrm{In}}} = \frac{k_2\left[\mathrm{Acc}\right]\left[\mathrm{X}\right]}{k_0\left[\mathrm{A}\right]\left[\mathrm{In}\right]} \tag{3.33}$$

then active site concentration may hardly be determined, but if it is detected by any other method, an expression identical to equation (3.32) will be obtained.

The validity of the above may be confirmed as follows. Applying the stationary concentration method to the system of differential equations (3.31), it is deduced:

$$-\frac{\mathrm{d}\left[\mathrm{X}\right]}{\mathrm{d}t} = k_0\left[\mathrm{A}\right]\left[\mathrm{In}\right] - k_1\left[\mathrm{X}\right] - k_2\left[\mathrm{Acc}\right]\left[\mathrm{X}\right] \approx 0$$

therefore,

$$\left[\mathrm{X}\right] = \frac{k_0\left[\mathrm{A}\right]\left[\mathrm{In}\right]}{k_1 + k_2\left[\mathrm{Acc}\right]} \tag{3.34}$$

Substituting equation (3.34) into expression (3.33), the following relation is deduced:

$$I = \frac{k_2\left[\mathrm{Acc}\right]}{k_1 + k_2\left[\mathrm{Acc}\right]}$$

or

$$I = \left[1 + \frac{k_1}{k_2\left[\mathrm{Acc}\right]}\right]^{-1} \tag{3.35}$$

which is the requested result.

However, for intermediate compound concentration simple expressions are not always obtained and, moreover, the system of conjugated chemical reactions may be much more complicated than (3.28). Therefore, a guideline to the use of the determinant equation reduces the computations required for determination of the induction factor and quantitatively assesses the inductive effect, showing the ways for affecting the current system.

3.2 ENERGY TRANSFER IN CONJUGATED REACTIONS

A chemical system with conjugated chemical reactions is usually open, and a stationary state far from the chemical equilibrium is typical of it. Stationary proceeding of chemical reactions in open systems (stationary flow systems) is characterized by the equilibrated rates of the mass and energy transfer to the system from the environment and the inverse process.

Chemical energy transferred from the reaction releasing it to the one accepting it is only possible in the presence of an intermediate product general for these reactions, which represents the energy transmitter between two reactions.

The question thus arises: which transmitter form—oxidized or reduced—is more highly saturated with energy. Usually, it is the oxidized transmitter, though from positions of thermodynamics the reduced form may also accumulate high energy.

Multiple enzymatic reactions proceeding in the living cell are usually united in complex sequences of convergent and divergent reactions (when the first reaction product is the substrate of the second reaction and so on). As mentioned above, complex consecutive reactions proceed with the participation of intermediate products (intermediates): the first and the second kinds. Elementary stages proceed with the participation of highly reactive intermediate substances of the first kind; they form the mechanism of initial and subsequent stages of the consecutive reaction, and the intermediate concentration is determined by the stationary concentration method. Intermediate substances of the second kind (intermediates) are initial reagents for consecutive reactions, and their concentrations are determined by common kinetics of consecutive reactions and possess maxima.

Lehninger, the famous American biochemist, defined the 'principle of general intermediate product' in his textbook [13]: 'two consecutive reactions are conjugated, if the first reaction product represents the substrate of the second reaction:

$$A + B \rightarrow C + D$$

$$D + E \rightarrow F + G$$

Reactions are conjugated owing to the general intermediate product (currently D). There is only one method for energy transfer from one reaction to another under isothermal conditions: conjugation of two reactions via general intermediate substance. This is the way in which almost all exchange reactions run in cells.'

Further on: '… energy transfer via a general intermediate product is the universal property of consecutive chemical reactions.'

Any spontaneous reaction is associated with the free energy decrease; which means that the energy level in the reaction products is lower than in the initial compounds, i.e. they are more stable compounds. The lower is the free energy decrease, the more stable are the reaction products. In this respect, let us analyze consecutive reactions in order to clarify the intermediate product type capable of performing functions of the energy transmitter. The second type intermediate product is the final product of the primary reaction and, consequently, it accumulates chemical energy of spontaneous primary reaction. Actually, such a compound, being the initial substance for the further reaction (or an intermediate for the consequent reaction), interacts with a reagent according to the rules of any exothermic reaction ($\Delta G^0 < 0$).

The primary reaction may be exothermal, but possessing one endothermic elementary reaction synthesizing high-energy intermediate product. This product will then be used for inducing a non-spontaneous reaction.

In the literature on chemistry and biochemistry, in particular in the cited statements from Lehninger's textbook, the intermediate substance of the second kind is identified with highly reactive particles (intermediate products of the first kind). This mistake is based on fuzziness of the chemical induction definition and identification of conjugated reactions with consecutive ones. As a result, Lehninger has concluded that 'the energy transfer via general intermediate product is the universal property of consecutive reactions.'

Meanwhile, it is known [13] that the communication channels connect conjugated reactions via general reactive intermediates, which are accumulators of chemical energy, released in the primary reaction as free energy and consumed by the induced reaction. In fact, formed short-lived highly reactive particles are free radicals, complexes, charged particles, etc. and carry high energy. Chemical energy of the primary reaction is accumulated in them and, as a consequence, further transformations of the reagent have a lower-activation barrier than the molecular interaction of the initial reagents. Two or more active intermediate compounds may be involved in a complex reaction.

To demonstrate this more clearly, let us consider several typical free radical chain reactions and try to associate the high activity of free radicals and the accumulation of free energy release in a chemical reaction by them.

On the contrary, the final product of the primary reaction which is the mediator of the secondary reaction (i.e. the initial reagent) may not accumulate high energy than initial compounds of the primary reaction.

Many chemical reactions generating free radicals are described in the literature. In a homogeneous non-catalytic system, the free radical source generates active sites at one rate or another with respect to stability of molecules. Therefore, of great importance is the selection of a criterion for choosing the best source of free radicals for a particular target reaction and conditions based on kinetic characteristics. Benson [12] suggests taking activation energy and reaction order for such a criterion of 'initiation stage selection'. He concluded that monomolecular dissociation reactions will progress at higher rates that bimolecular initiation. However, there are exceptions, for example, for pyrolysis of olefins, in which the following initiation reactions compete:

$$C_3H_6 \xrightarrow{1} C_3H_5^{\bullet} + H,$$

$$2C_3H_6 \xrightarrow{2} C_3H_5^{\bullet} + C_3H_7^{\bullet}$$

According to Benson's estimate, at 900 K both initiation reactions are equally possible processes. In fact, however, the complexity of the pyrolysis reaction creates obstacles to making a conclusive decision about the initiation of processes of this type.

According to Semenov [11] at thermolysis of chain process initiators the energy of the weakest bond break in molecules of almost all substances fits the range of 209–419 kJ. In this regard, the chain initiation by initial reagents themselves may progress at a low rate. Therefore, substances promoting initiation of chain reactions are often used. For example,

Semenov took the following compounds for free radical initiators (reaction heats are in kJ/mol):

$$Na_2 \rightarrow 2Na - 73.3$$

$$(C_6H_5)_3C{-}C(C_6H_5)_3 \rightarrow 2(C_6H_5)_3C^{\bullet} - 46.1$$

$$J_2 + M \rightarrow J + J + M - 129.9$$

$$(CH_3)_3COOC(CH_3)_3 \rightarrow 2(CH_3)_3CO^{\bullet} - 150.8$$

$$C_2H_5OOH \rightarrow C_2H_5O^{\bullet} + {}^{\bullet}OH - (167.6\text{–}188.5)$$

There is no doubt that this list may be expanded, but these examples are sufficient for the current discussion. They show that synthesis of highly reactive radicals requires energy consumption. Therefore, the degradation reaction requires thermal activation of molecules. For example, gaseous sodium completely dissociates at 100 °C.

Thus, the accumulation of chemical energy of the reaction in the form of highly active intermediate compounds happens with the energy consumption. For this purpose photosensibilization, light exposure (photochemical reactions), catalysis (catalytic decay) and chemical induction (couples processes) are used.

Among the processes proceeding in living organisms at energy accumulation, catalysis and chemical induction are of the highest importance (except, of course, for photosynthesis—the unique form of energy transformation). It stands to reason that the use of a catalyst may not affect the standard free energy of the reaction and just promotes its release by decreasing the activation barrier of the reaction in which active sites are synthesized. In the case of chemical induction, the primary reaction is spontaneous and its quantitative parameter (ΔG^0) is defined by the initial and the final states of the system.

In the primary reaction, chemical energy is accumulated in one of its elementary stages. The following circumstance must be taken into account: ΔG^0 of the overall reaction depends on the reaction mechanism, whereas the energy is accumulated in one of the stages, and its ΔG_i^0 must be known. Since ΔG^0 of the overall reaction is summed up from ΔG_i^0 of each primary reaction stage, in the study of conjugated reactions it is not enough to know ΔG^0 of spontaneous primary reaction. In this case, if possible, ΔG^0 for each elementary stage should be known, in which chemical energy is accumulated as an active intermediate compound. This will allow quantitative estimation of the upper level of energy accumulated at this stage, and selection of favorable conditions and appropriate catalysts promoting decrease of the activation barrier.

Therefore, in the case of chemical induction the primary (spontaneous) reaction mechanism always includes at least a single endothermic stage, in which chemical energy is accumulated.

However, there is an alternative when chemical energy is accumulated in an intermediate particle, which is not the active site of the target (secondary) reaction. In such a case, the chemical energy of this particle is transferred to another particle which, though having lower energy, may become the active site of induced reaction. In Chapter 2, the reactions displaying such energy transfer are called re-induced reactions.

This conforms to the common rule of free radical reactions: in radical substitution reactions, i.e. when reactions between free radicals and molecules lead to atom (most often, hydrogen atom) or radical transfer from a molecule to a free radical, and the reaction progresses in the direction of lesser active radical formation.

From this point of view, it is desirable to consider two competing elementary stages of ethylbenzene conjugated dehydrogenation with participation of H_2O_2 in the example of $HO_2^{\bullet}$ radical (refer to the following chapters for more detailed consideration of this mechanism):

$$HO_2^{\bullet} + C_6H_5C_2H_5 \rightarrow C_6H_5C_2H_3 + H_2O + {}^{\bullet}OH + 111.9\ \text{kJ/mol} \quad (3.36a)$$

$$HO_2^{\bullet} + C_6H_5C_2H_5 \rightarrow H_2O_2 + C_6H_5C_2H_4^{\bullet} + 61.6\ \text{kJ/mol} \quad (3.36b)$$

The elementary reaction (3.36a) is distinguished from usual radical substitution reactions (including 3.36b) by simultaneous transfer of two hydrogen atoms from two neighboring carbon atoms (in ethylbenzene molecule) to free radical HO_2 via a hexa-site transition state:

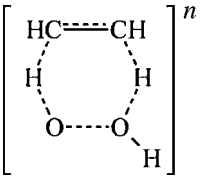

According to reaction (3.36a), this substance decomposes to two stable compounds (currently, styrene and water) and free radical ${}^{\bullet}OH$. Hence, free radicals ${}^{\bullet}OH$ released in the reaction are much more active than initial $HO_2^{\bullet}$. If we obey the above rule, it should be expected that the pathway (3.36a) is more preferable than (3.36b). However, data on heat effects of the reaction show that the stage (3.36a) is much more exothermal compared with the stage (3.36b). Therefore, if the first approximation of the equation for the activation energy:

$$E = 11.5 - 0.25|q|$$

valid for substitution radical reaction is used, then values $E_{(3.36a)} = 20.1$ kJ/mol and $E_{(3.36b)} = 32.7$ kJ/mol are obtained.

Contrary to the usual substitution radical reactions, it synthesizes more active free radical ${}^{\bullet}OH$ rather than initial $HO_2^{\bullet}$ radical by the energy profitable way.

In this regard, the rule under consideration (i.e. the radical substitution reaction is generally developed via formation of the most inactive radical), fulfilled for radical substitution proceeding with the transfer of a single hydrogen atom, is untrue if the transfer of hydrogen atoms from the donor happens simultaneously [6].

As a consequence, if the radical reaction produces two final products and a free radical, the latter may be more active than the initial one (owing to the gain in energy due to synthesis of the second product).

However, these examples are very short, and elementary reactions of this type are little known in chemical kinetics.

Thus, according to the concept suggested, the energy content of the primary active site may be enlarged by elementary reactions of the (3.36a) type, the number of which may be more than one. As a result of energy transfer from one elementary stage to another, the 'final' active site may accumulate a significant amount of energy. Thus, there is one more possibility of accumulating energy in highly active intermediate compounds (short-lived intermediates *in situ*).

Some aspects of the questions arising are illustrated by the example of conjugated oxidation reactions by hydrogen peroxide. As mentioned before, thermal dissociation of H_2O_2 generates $^{\bullet}OH$ radicals to the system by the following reaction:

$$H_2O_2 \rightarrow 2^{\bullet}OH - 217.9\,\text{kJ/mol} \tag{3.37}$$

It is known that H_2O_2 also dissociates at lower temperatures of 25–100 °C. However, in the absence of catalytic amounts of additives in H_2O_2 its chain degradation proceeds at a low rate due to the high-energy barrier of the initiated stage of thermal dissociation (3.37), which falls within the range of 188.55–217.9 kJ/mol. Therefore, redox systems which decrease the activation energy at homolysis due to electron transfer rather than thermal exposure of the substance are broadly spread. There are notes in the literature [14] that redox reactions catalyzed by iron ions possess activation energies 2–3 times lower than for thermal activation. Let us show the initial stage of H_2O_2 dissociation catalyzed by Fe^{2+} ions:

$$Fe^{2+} + H_2O_2 \rightarrow Fe^{3+} + OH^- + {}^{\bullet}OH \tag{3.38}$$

which has the rate constant:

$$k = 4.45 \times 10^8 \exp\left(-\frac{39.386}{RT}\right) \frac{1}{\text{mol s}} \tag{3.39}$$

The activation energy for stage (3.38) equals 39.4 kJ/mol only, whereas thermal homolysis of H_2O_2 by reaction (3.37) gives 188.55–217.9 kJ/mol [15].

When comparing these values, it can be observed that the catalytic alternative is much more profitable in terms of energy. Of special attention is the following circumstance: on the one hand, the reaction pathway (compare (3.37) and (3.38)) is changed, which does not affect the energy balance of the H_2O_2 dissociation overall reaction; on the other hand, such a change in the reaction target makes simpler the generation of active sites in the shape of highly active intermediate products. Though free energy of H_2O_2 dissociation is independent of the process mechanism, its value may be determined as the sum of free energies of elementary stages in the complex reaction. For the author of the present monograph such an approach is of principal importance for quantitative estimation of active site generation energy balance. In practice, if $^{\bullet}OH$ radicals are successfully accumulated in a system via a redox reaction at much lower temperatures than at thermal homolysis, the advantages of such a system need no comment. Generally speaking, radical $^{\bullet}OH$ activity is independent of its origin.

It begins interacting with the majority of organics soluble in acid media already at quite low temperatures [16].

The catalysis mechanism of H_2O_2 dissociation by bivalent iron salts differs from thermal homolysis by the number of elementary stages. If a catalyst is used, at least four more elementary stages occur.

In this regard, an important conclusion follows: the greater the number of elementary stages in the reaction mechanism, the simpler are the kinetic and energy aspects of the entire exothermal reaction.

3.3 IDEALIZED MODEL OF CONJUGATED CATALYTIC REACTIONS: THE MEMBRANE CATALYSIS IN MITOCHONDRIAL PROTON TRANSFER

Chemical conjugation theory helps in formulating the basic principles of the idealized catalytic system composition with conjugated reactions, solving theoretical tasks of composing a hypothetical, synergic, chemical system optimally combining catalysis, chemical conjugation and substance transport through a membrane. The appropriate test model for developing a similar chemical system are the respiratory process and oxidative phosphorylation and their interaction, because enzymatic catalysis, chemical conjugation and transport of initial, intermediate and final compounds though a membrane are ideally cooperated in a living cell.

The living cell may be considered as a non-equilibrium open system, a 'machine' releasing free energy from the environment. Therefore, entropy of the environment increases [13]. Like any 'machine', the cell consists of separate, interrelated 'mechanisms', which may be roughly compared with a device releasing energy from the environment, consuming it for biosynthesis purposes and other biological reactions, and re-releasing the rest of the energy to the environment in an unsuitable form (e.g. heat).

In this connection, the following discussion will be devoted to common biochemical processes connected to energy release and accumulation in adenosine triphosphate (ATP), based on the above suggestion that chemical energy is accumulated in highly active intermediate compounds.

It should be noted that the main amount of redox enzymes in animal and plant cells is accumulated in mitochondria, which are usually called the 'power plants' of the cell, because redox reactions supplying cells with energy proceed in them. Therefore, at present, mitochondria are the main source of information about biological oxidation and energetic conjugation mechanisms.

Biological oxidation is usually represented by complex chemical reactions, the staging of which allows the release of energy in portions, which are then consumed by cells for endergonic purposes.

These processes of energy accumulation and consumption by a cell are very meaningful: the energy scattering is minimal and the heat effect on the cells is eliminated (in the inorganic nature, molecular oxygen directly interacts with the substrate and releases high-energy amounts as heat). The main product of redox processes proceeding in the cell (ATP) in the energy donor for endergonic cell functions (biosyntheses, active substrate transport, bioelectric phenomena, mechanochemical processes, etc.). Hence, ATP and similar compounds may be easily extracted, which makes them intermediate products of the second kind.

Exergonic and endergonic reactions are balanced in the cell representing a complex of consecutive, parallel–consecutive and conjugated chemical reactions. Intra-mitochondrial space is divided by a complex system of inner membranes, on which redox enzymes are fixed, forming the so-called ensembles.

As shown below, strong fixing of respiratory enzymes on mitochondrial membranes is necessitated by the constancy of their contacts, which promote the most important features of the electron transfer.

Let us now briefly discuss the main enzymatic systems of mitochondria, which provide for primary dehydrogenation of substrates (tricarboxylic acid cycle dehydrogenase, fatty acid oxidation system, etc.) and proton and electron transfer from substrates to molecular oxygen (respiratory chain). For this purpose, let us use the general respiratory scheme (Figure 3.2), suggested by Lehninger [13].

Full aerobic degradation of the cell fuel (carbohydrates, fatty acids and amino acids) happens during respiration. Firstly, the fuel is involved in tricarboxylic acid cycle (the Krebs cycle, Figure 3.2) shaped as acetyl groups and oxidized to CO_2 and hydrogen. Then these gases occur in the respiratory chain, which consists of electron carriers and, therefore, they are bound by molecular oxygen. The latter process, e.g. electron transfer along the respiratory chain, proceeds with a significant free energy decrease.

The overall equation of the respiratory process is described by a chemical equation of the exergonic type:

$$CH_3COOH + 2O_2 = 2CO_2 + 2H_2O \tag{3.40}$$

$$\Delta G^0_{298} = -875.1\,\text{kJ/mol}$$

Being exergonic and spontaneous, reaction (3.40) is able to couple energetically, i.e. may induce or speed up, an endergonic reaction, namely phosphorylation. This fact is of the last importance. The substance transmitting induction from the primary reaction must be an intermediate product of the first kind, generated by the respiratory process (3.40) to the system. It should be remembered that this requires one of the primary reaction stages to be endergonic, because in this case chemical energy is accumulated as highly active intermediate products.

In accordance with these ideas, let us consider the energetic conjugation of two processes proceeding in mitochondria: the respiratory process and oxidative phosphorylation. This is the way of respiratory (primary) process development: firstly, acetic acid is dehydrogenated. During this process highly reactive hydrogen atoms are accumulated. The Krebs cycle is the catalytic system with each unit catalyzed by a specific enzyme. Moreover, intermediate products of the cycle display a catalytic effect (i.e. regenerate in the framework of a definite sequence of units). Hence, one molecule of an intermediate product participates in the oxidation of an unlimited number of acetic acid molecules. This double catalytic effect is used for dividing acetic acid dehydrogenation into the maximum possible number of elementary stages in order to make it easily realizable in the living cell.

Thus, at the initial stage of the respiration process (refer to Figure 3.2) representing acetic acid dehydrogenation (the Krebs cycle), from which molecular oxygen is excluded, chemical energy is accumulated. Then at the final stage, resulting in electron transfer along the respiratory chain to molecular oxygen, chemical energy is accumulated on ATP.

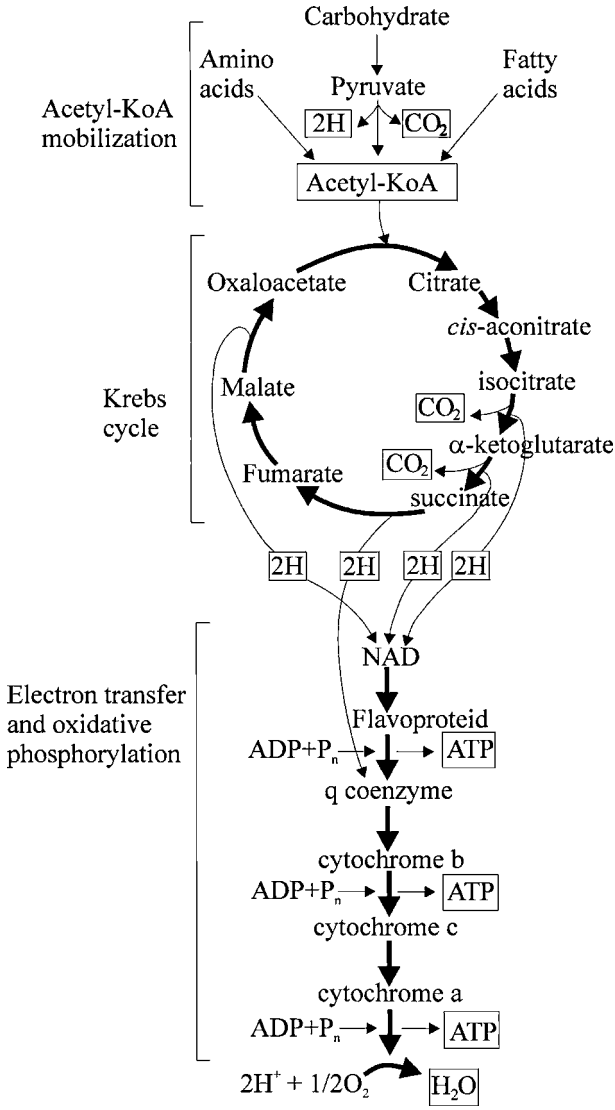

Figure 3.2 The respiratory system [13]. Final products of every reaction are given in the frames.

Figure 3.2 shows the respiratory chain. It consists of enzymes, which are electron carriers, each of which interacting with one another is capable of reversible oxidation—restoration.

The overall respiratory equation (3.40) represents the exergonic reaction, which energy in the form of highly active intermediate products is consumed by the organism.

Let us now determine what the material particle, possessing the chemical energy excess, provides for the communication channel (conjugation) between respiration and phosphorylation. According to data obtained by biochemists, there are three highly active intermediate products

of acetic acid oxidation (respiration). They are hydrogen atom, electron and proton. They are all bound in corresponding complexes with enzymes–electron carriers. Then the proton from the substrate–enzyme complex, located on the surface of mitochondrial membrane, is released to the internal cell volume and then participates in the final stage of water formation during respiration.

The electron is consecutively transferred from one respiratory chain unit to another and, finally, occurs on molecular oxygen. Therefore, it may not participate as a material particle in any other reaction outside the framework of the respiration process.

In mitochondria, hydrogen exists in two forms: proton and hydride ion bound to NADN or ADPN [17].

However, in the rest of the chains only the electron migrates along the chain. It always stays in the respiratory chain and is 'accurately' transferred by it to the 'final stop'. On the contrary, hydrogen shaped as linked proton remains on the membrane surface during some time, and then is released into the cell.

Meanwhile, H^+ is the respiration intermediate substrate and binds to oxygen at the final stage of it:

$$2\text{Cyt.a}_3\text{(II)} + 1/2\text{O}_2 + 2\text{H}^+ \leftrightarrow 2\text{Cyt.a}_3\text{(III)} + \text{H}_2\text{O} \tag{3.41}$$

where Cyt.a_3 is cytochrome.

Most likely, electrons are required for linked oxygen activation:

$$1/2\text{O}_2 + 2\text{e} \rightarrow \text{O}^{2-} \tag{3.42}$$

with further formation of water:

$$\text{O}^{2-} + 2\text{H}^+ \rightarrow \text{H}_2\text{O} \tag{3.43}$$

The overall equation describing reactions (3.42) and (3.43) is the following:

$$1/2\text{O}_2 + 2\text{H}^+ + 2\text{e} \leftrightarrow \text{H}_2\text{O} \tag{3.44}$$

When compared, reactions (3.43) and (3.44) describe the water formation process, which in both cases proceed by the same mechanism. Cytochrome a_3 (II) is the substance carrying electrons to oxygen molecules and catalyzing H_2O formation. In fact, at the final stage molecular oxygen is activated on cytochrome, and then molecular oxygen interacts with electron and, consecutively, with two protons.

At the present time, it is routinely assumed that specifically H^+ is the intermediate product, which easily releases from the respiratory catalytic system and is involved in other conjugated reactions.

The only remaining question is how proton induces the endergonic reaction and, first of all, ADP (adenosine diphosphate) and ATP phosphorylation processes. The following circumstance is of great importance: formation of a sufficient amount (generation) of H^+ results

from hydrogen atom and electron transfer along the respiratory chain with free energy decrease by a value sufficient for phosphorylation [17].

It appears to the author that not only H^+ ion generation on the mitochondrial membrane surface, but also their accumulation in the conjugation points, where oxidative phosphorylation proceeds, is of great importance for the respiration and phosphorylation conjugation mechanism. In fact, a significant decrease of electron transfer free energy along the respiratory chain makes the proceeding of these two processes simpler.

The phosphorylation reaction with respect to structural features of the substrates may be written as follows:

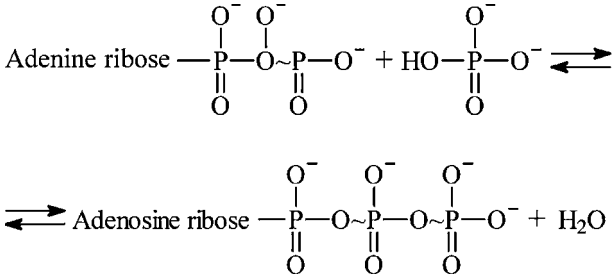

(3.45)

ATP synthesis is also conjugated with glyceraldehydes-3-phosphate dehydrogenation:

$$\text{glyceraldehydes-3-phosphate} + \text{NAD} + \text{Ph}_{\text{in}} \leftrightarrow \leftrightarrow \text{1,3-Diphosphoglycerate} + \text{NAD} \cdot 2\text{H} \tag{3.46}$$

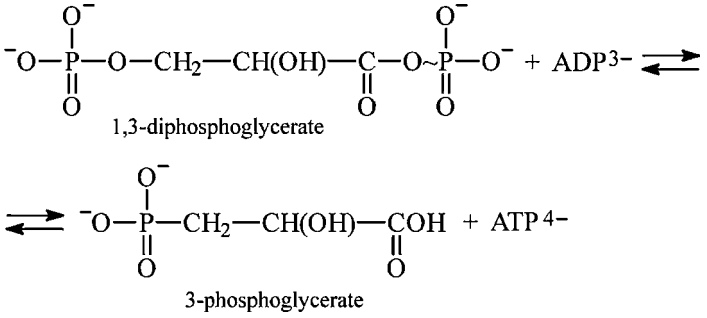

(3.47)

where Ph_{in} is an inorganic phosphate.

For reactions (3.46) and (3.47), 1,3-diphosphoglyceric acid is the general product and provides for energetic conjugation between these reactions [13].

The number of charges in the left and the right parts of chemical equation (3.47) is imbalanced. Moreover, the carboxylic fragment of the 3-phosphoglycerate molecule possesses a hydrogen atom of unclear origin, because initial substrates do not deliver it (this is observed from the hydrogen balance of initial and final reagents). It seems to the author that H^+ should

also be taken into account as the initial reagent in equation (3.47). Then the following reaction is obtained:

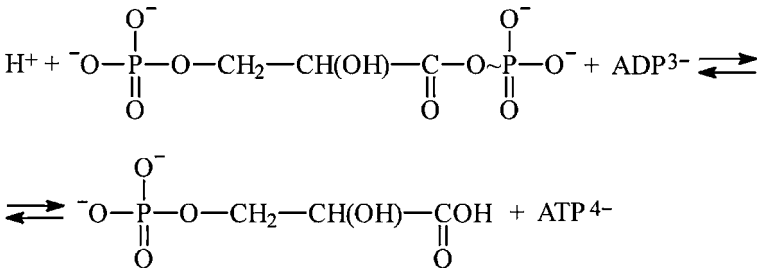

(3.48)

in which charges are balanced.

Equation (3.48) describes the elementary stage of the interaction, though if it is presented as the overall reaction taking into account the interaction between molecular substrates (similar to the monograph by Blumenfeld and Tikhonov [18]), there is no need to use the charge balance notion.

Equation (3.47) describing the elementary stage of ATP synthesis does not consider the proton consumption. Therefore, the number of charges in both parts of the equation is not balanced. Moreover, it would be more correct to take H^+ ions into account in the left part of equation (3.45). Stent [19] suggested a similar presentation for ATP hydrolysis, which is inverse to ATP synthesis:

$$ATP + H_2O = ADP + Ph_{in} + 2H^+$$

It should be remembered that oxidative phosphorylation is conjugated with the respiratory process and, therefore, the question of where H^+ ions come from can be simply answered. At ATP synthesis, the respiratory chain releases H^+ ions to the system during electron transfer, and the electron transfer energy is consumed for H^+ generation.

Thus, the excessive concentration of hydrogen ions represents a highly active intermediate compound of two conjugated reactions: the respiratory process, on the one hand, and the oxidative phosphorylation, on the other.

Since biochemists clearly understood that H^+ ion was involved in oxidative phosphorylation, the alternative ATP formation concept occurred as a counter to chemical conjugation. This concept was called the chemiosmotic hypothesis of the oxidative phosphorylation mechanism. This hypothesis was developed by Mitchell, the famous English biochemist [20], who turned is attention to the blind sides of the chemical conjugation concept.

Mitchell based his concept on the suggestion that as electron is transported along the respiratory chain, H^+ ions are 'ejected' to cytoplasm (the mitochondrion environment). As a consequence, a gradient of H^+ ion concentration occurs in external and internal mitochondrial spaces. Of course, this H^+ ion concentration gradient is supported by electron transfer free energy decrease and in the case of membrane impermeability for H^+ ions.

According to the mass action law, oxidative phosphorylation (3.45) will be accelerated, if synthesized H_2O molecules are removed immediately. In the course of these ideas, Mitchell has suggested that the ATPase, the catalyst of this reaction, is oriented in the plane

of the mitochondrial membrane so that dissociated water molecule ($H^+ + OH^-$) occurs on the membrane surface. Hence, H^+ occurs in the internal volume of the mitochondrion, decreasing pH in it and, vice versa, on its release to the environment pH increases.

Let us specify the adherent points of two hypotheses in relation to the role of hydrogen ions in oxidative phosphorylation:

- In the respiratory chain H^+ ions are generated by electron carriers.
- Electron transfer energy is accumulated in excessive H^+ concentration.
- H^+ ions take part in ATP synthesis.

Of great importance are also the differences in the approaches to molecular bases of H^+ ion action in oxidative phosphorylation:

- In the current version of chemical conjugation hypothesis, the H^+ ion represents the primary process (respiration) induction transmitter on the secondary process (phosphorylation) and, therefore, is the general, highly active intermediate product.
- The hypothesis of chemiosmotic mechanism of the oxidative phosphorylation the concentration gradient of H^+ ions, formed by the electron transfer energy, is required for speeding up ATP synthesis from ADP and phosphate according to the mechanism based on quick withdrawal of formed H_2O molecules dissociated to H^+ and OH^- ions.
- The chemiosmotic hypothesis does not use the notion of a general, highly active intermediate product.

However, it should be noted that the two hypotheses under consideration conform to each other, and they may not be considered as alternatives to one another. Most likely, they complement each other and decode the consumption mechanism of chemical energy released during respiratory processes and its accumulation shaped as high-energy bonds (ATP).

In his comments to the question, which hypothesis—chemiosmotic or chemical conjugation—is correct, Lehninger has noted that '… almost all facts concerning the features of oxidative phosphorylation, known by now, can be equally well explained by both hypotheses' [13]. Notwithstanding, the main disadvantage of a common hypothesis about chemical conjugation is its complete failure to find highly active intermediate products. Meanwhile, the typical feature of the chemiosmotic hypothesis is the absence of a concept about general, highly active intermediate products of two conjugated processes: respiration and oxidative phosphorylation.

The author thinks that, possibly, a general layout of mitochondrial processes—'accumulators of the chemical energy in the cell'—may be composed. It will unite statements of both hypotheses and describe various consecutive events of mitochondrion operation.

Modern biochemical investigations are mostly aimed at developing an entire approach to solving different problems and, hence, different biochemical reactions act as the stages of overall mitochondrial process, in which as is commonly said 'all affect all'. Therefore, some bioenergetic reactions (or events) may be difficult or even impossible to understand outside the framework of the entire approach. Note also that such an approach has become just recently predominant in biochemical investigations. In its framework, the totality of

biochemical mitochondrial processes of oxidative phosphorylation may be presented as follows:

Respiratory process, primary reaction

$$CH_3COOH + 2O_2 = 2CO_2 + 2H_2O \tag{3.49}$$

Phosphorylation (oxidative), secondary reaction

$$\begin{gathered} ADP^{3-} + p^{3-} + 2H^{+} = ATP^{4-} + H_2O \\ \uparrow \\ \text{ATP-synthase} \end{gathered} \tag{3.50}$$

H_2O dissociation

$$H_2O \xleftarrow{\text{ATP-synthase}} H^{+} + OH^{-} \tag{3.51}$$

The respiratory process (3.49) possessing the Gibbs energy:

$$\Delta G^0_{298} = -208.87\,\text{kcal/mol}$$

is usually divided into two consecutive stages:

$$CH_3COOH_{(L)}\, 2H_2O_{(L)} \rightarrow 2CO_{2(g)} + 8H_{(g)} \tag{3.52}$$

The Krebs cycle possesses:

$$\Delta G^0_{298} = 406.6\,\text{kcal/mol}$$

and the respiratory chain:

$$\begin{gathered} 4H_{(g)} + O_{2(g)} = 2H_2O_{(L)} \\ \Delta G^0_{298} = -307.73\,\text{kcal/mol} \end{gathered} \tag{3.53}$$

Enzymatic activity of the substrate in the respiratory process (3.49) is implemented by Krebs cycle hydrogenases (3.52) (the endergonic component of the respiratory process), where chemical energy is accumulated in the form of an active intermediate compound (linked hydrogen atom). There is no doubt that linked 8H and $2CO_2$ forms, in which these intermediates exist in the cell environment, will significantly decrease ΔG^0 [21]. The final product of the respiratory process is synthesized by enzymes of the respiratory chain (exergonic component).

It is found that chemical energy from the energy-producing reaction to the reaction accepting it may be transferred only if they have the general intermediate product, which is the energy transmitter from one reaction to another.

Usually, the oxidized form of the energy carrier may accumulate higher energy, though from positions of thermodynamics the reduced form may also possess high energy. Multiple enzymatic reactions proceeding in living cells are usually united in complex sequences of converging and diverging reactions.

Lehninger [17] noted that 'there is one more method for energy transfer from one reaction to another under isothermal conditions. It is conjugation of two reactions via a general intermediate product. Almost all exchange reactions in cells proceed in this way.'

Note also that a chemical system with conjugated reactions is usually open and a stationary state is typical of it. This state is always distant from chemical equilibrium, when the rates of mass and energy transfers from the system are equilibrated. Intracellular biochemical processes including mitochondrial energy reactions also represent an open system.

Meanwhile, the connection channels between conjugated reactions are set via general highly reactive intermediate particles, which accumulate chemical energy released in the primary reaction as free energy and consumed by the induced reaction. In fact, short-lived reactive particles formed—free radicals, complexes, charged particles, etc.—contain high amounts of energy. Chemical energy of the primary reaction is accumulated in them. As a result, further transformations of the reagent display a lower-activation barrier compared with molecular interaction of initial reagents. Thus, the accumulation of chemical energy of the reaction in the form of active intermediate compounds proceeds with energy consumption. Chemical energy of the primary reaction is accumulated in one of its elementary reactions. In this case, the following is of importance. The value ΔG^0_{298} of the overall reaction is independent of the reaction mechanism, and the energy is accumulated in one of the stages, therefore, ΔG^0_1 of it should be known. Since ΔG^0 of the overall reaction is summed up from ΔG^0_1 of every stage in the primary reaction, the knowledge of ΔG^0_{298} for spontaneous primary reaction is not enough for the study of conjugated processes. It is necessary to know ΔG^0 for every elementary stage, in which chemical energy is accumulated in the active intermediate compound. This allows quantitative estimation of the energy accumulation limit and appropriate catalysts which decrease its activation barrier.

Thus, in the case of chemical induction the primary (spontaneous) reaction mechanism always includes even a single endothermic stage, in which chemical energy is accumulated [21].

Therefore, in the respiratory process (3.49) the Krebs cycle (3.52) represents a totality of endothermic stages, in which chemical energy is accumulated in the form '$H^+ + e$' (or in a linked hydrogen atom, which is almost the same). When addressing the question of how the particle transferring chemical energy from one reaction to another may be identified, it should be noted that there are three material particles (hydrogen atom, electron and proton), which possess excessive chemical energy and are able to set a connection channel (conjugation) between respiration and phosphorylation. These particles are bound and form corresponded complexes with enzymes–electron carriers. Electron and hydrogen atom may not be intermediates between CH_3COOH oxidation and phosphorylation. Electron is bound to the enzymatic system of the respiratory chain, whereas hydrogen atom is always coordinated with corresponded enzymes [17]. This reasoning allows the conclusion that H^+ is the

intermediate particle, which easily releases from catalytic system of the respiratory process. Therefore, it may be involved in other conjugated reactions or take part in water molecule formation at the final respiration stage. It is also of importance that the synthesis of significant amounts (generation) of H^+ results from proton and electron (or hydrogen atoms) transfer along the respiratory chain with free energy decrease by a value sufficient for implementing phosphorylation [13]. The only question that remains is how proton may induce an endergonic reaction, first of all, ADP phosphorylation to ATP.

Skulachev [22] gave detailed consideration to the modern ideas about the mechanism of chemical energy consumption released during respiration. To put it another way, he 'traces development of the membrane bioenergetics at its main direction'. He wrote that 'When suggesting the concept of reversible H^+-ATP-synthase, Mitchell finished the proton cycle scheme, which then became the new hypothesis of energetic conjugation, which withstands the so-called chemical scheme suggesting direct chemical interaction of respiration and phosphorylation enzymes.' The main reasons for the search for alternative chemical conjugation approaches are as follows:

1. In many laboratories attempts were made to discover a high-energy intermediate consisting of a respiratory enzyme or coenzyme and ATP-synthase component. Though this intermediate is located at the central place in the chemical scheme, nobody succeeded in either observing or extracting a compound of this type.
2. The chemical scheme did not explain the requirement of closed membrane structures for oxidation and photosynthesis phosphorylation.
3. It is found that a group of compounds with different chemical structures induces typical change in mitochondrial energy state, which is called disintegration. Substances-disintegrators suppressed phosphorylation and stimulated respiration and ATP″ hydrolysis.

The idea primarily presented by Mitchell that circulation of protons overcoming the hydrophobic barrier of the membrane may be the basis for conjugation of redox reactions and ATP″ synthesis was called the chemiosmotic hypothesis. At the present time, according to Skulachev, this hypothesis 'became the leading concept in membrane bioenergetics'. He also wrote [22] that 'During the last decade disputes in bioenergetics mostly touched on the question about the fortune of H^+ ions which penetrate through the hydrophobic layer of the membrane by proton conducting paths of $\Delta\bar{\mu}H$ generators'. Of course, this is the key question, the actual meaning of which will become clear from further discussion.

The conflicting results are obtained at solving the question if H^+ ions are mixed with aqueous medium or, vice versa, are transported by the membrane–water interface (or inside the membrane) to the nearest $\Delta\bar{\mu}H$ consumer, what the accurate value of proton potential decrease on H^+-ATP-synthase molecule is, and if unmixed layers are present at the interface, and what the membrane profile complexity is [22].

It was also mentioned [22] that 'in the recent decade it was observed that $\bar{\mu}H$ is not only conjugation intermediate of oxidation phosphorylation, but also hard currency in membranes of mitochondria, chloroplasts and bacteria … It is clearly determined that $\bar{\mu}H$ can be used for implementing all types of work in the living systems: chemical, osmotic, mechanical and heat production'.

It seems to us that in the above discussion $\bar{\mu}$H potential is considered from the standpoint of two approaches: thermodynamic and chemical. The first approach operates the terms of electrochemical potential and effective work; and the second approach, the chemical intermediate.

When it is said that $\bar{\mu}$H is used for implementing effective chemical work, in particular, for inducing oxidative phosphorylation, first the energy conjugation is meant, which is of thermodynamic meaning. The energy or thermodynamic conjugation suggests the application of effective work, produced in the form of the Gibbs energy in the primary reaction, to the secondary reaction, which may be thermodynamically hindered (ΔG^0_{298}). Essentially, chemical energy represents a balance between energies of bonds formed in chemical reaction and broken bonds of the initial components.

Hence, the intermediate of chemical energy transfer is a highly active substance general for both conjugated reactions. The energetic conjugation as the intermediate term is related to the initial and final states of the system, and is associated with the determination of the potential abilities of the system, but not with the mechanisms for reaching the final state, which number may be different. Meanwhile, the chemical intermediate of conjugated reactions is always interpreted as a particularly highly active chemical particle, which induces conjugated reaction, i.e. it is simply consumed in this reaction.

If the $\bar{\mu}$H potential of the reaction is known, it can always be estimated if the work produced by it is sufficient for performing another, non-spontaneous reaction, i.e. reaching a definite final state of the system. However, the $\bar{\mu}$H potential may not relate to the realization of a particular chemical mechanism and the notion of chemical intermediate associated with it. Therefore, identification of the $\bar{\mu}$H potential with the notion of intermediate is, to choose our words carefully, incorrect and, in this connection, we may scarcely agree with the experts in bioenergetics that the $\bar{\mu}$H potential is the conjugation intermediate.

The common point of view, postulated by Mitchell, is that 'in energy-producing membranes H^+ represents the conjugation ion'. For the conjugation intermediate, biochemists upholding only the concept of energetic conjugation assumed the electrochemical potential ($\bar{\mu}$H) produced due to difference in H^+ concentrations on both sides of closed membrane.

However, the conjugation H^+ ion may also represent a chemical intermediate which induces oxidative phosphorylation. Zealous supporters of chemical conjugation were absolutely correct in their search for a chemical conjugation intermediate. Apparently, it was the search strategy and not inaccurate knowledge of the chemical conjugation theory, which is observed from the famous Lehninger monograph [13], that prevented them from deeper analysis of the unique role of H^+ ions in the chemical conjugation mechanism.

The H^+-ATP-synthase, which catalyzes ADP oxidative phosphorylation by an inorganic phosphate by means of $\Delta\bar{\mu}H^+$ energy, belongs to the group of the most studied enzymes.

It consists of two so-called sub-complexes responsible for proton transport (F_0) and ATP synthesis or hydrolysis (F_1).

According to Rucker, the part of H^+-ATP-synthase released to water from one side of the membrane represents the catalytic part of this enzyme (F_1 factor).

As separated from the membrane sector of H^+-ATP-synthase, the F_1 factor preserves the ability to hydrolyze ATP to ADP and phosphate that differentiates it from the F_0F_1 complex [23].

The F_0 factor responsible for water dissociation, apparently, suppresses hydrolytic ability of the F_1 factor, because the dissociation process loses somewhat its reagent—water.

This is also confirmed by the fact that ATP splitting by H^+-ATP-synthase 'is constrained by generated proton potential' [22]: ATP hydrolysis on catalytic site F_1 is performed via direct interaction between the water molecule and anhydride bond of ATP, i.e. which intermediate formation. It should also be noted that $\Delta\bar{\mu}H^+$ is of higher importance for ATP removal from F_1 than for ATP synthesis.

According to the concept discussed in Refs [24, 25], the F_0 factor is responsible for H^+ translocation between the environment (in relation to mitochondrion), aqueous phase and the membrane, where fixed proton-acceptor groups X are located. If H^+/ATP stoichiometry equals 2, they may be absorbed in the ATP-synthase reaction:

$$ADP^{3-} + PO_4^{3-} + 2H^+ \rightarrow ATP^{4-} + 2H_2O \tag{3.54}$$

To put it differently, more than one proton should be transferred through the membrane per molecule of synthesized ATP, i.e. the minimal ratio equals 2. At the same time, only one proton can be transferred through the membrane to mitochondrion. If this transfer is related to dissociation of the water molecule (3.51), produced during oxidative phosphorylation, the number of transferred ions must equal 1.

Analyzing the basic principles of H^+-ATP-synthase phosphorylation, Skulachev formulated them as follows [22]:

1. ADP and phosphate associated with the F_1 factor may form linked ATP without any external energy supply. From the author's point of view, the stage of 'linked ATP' formation is the dead-end form (reaction), implemented in the absence of the H^+ ion. Therefore, proton is required for synthesizing an active complex in the F_1 factor, which would prevent 'linked ATP' formation with deficient one or two protons. Hence, this 'linked ATP' is more highly ionized and capable of relatively simple formation of complexes (i.e. to be linked). Thus, proton is necessary for ATP release to the matrix, which is usually observed in the experiment.
2. Energy is required for linked ATP transfer from the active site of the F_1 factor to water or ADP transfer and phosphate from water to the active site. If energy is required for H^+ ion transfer through the membrane, the mechanism of ATP release to water may be simply explained according to the idea suggested in paragraph 1.
3. The energy must be in $\Delta\bar{\mu}H$ form, equivalent to $\Delta\psi$ and ΔpH. The mitochondrial reaction mechanism (3.54) involving H^+-ATP-synthase is illustrated [22] in Figure 3.3a. The advantage of this scheme is that it indicates ways of consumption of substrates and products in $\Delta\bar{\mu}H$ generation and utilization, i.e. protons transported by means of the F_0 factor to the water molecule are included, produced in the reaction (3.54).

Another possible scheme (3.3b) is based on a suggestion that protons transported by the F_0 factor and included in H_2O molecule in the ATP synthesis differ from one another, and $\Delta\bar{\mu}H$ is consumed for transforming the F_1 factor to a conformation making ATP release from the catalytic site easier [26]. The second scheme (3.3b) is characterized by its simplicity and conciseness if compared with scheme (3.3a). However, it possesses a serious drawback in that the conjugation idea is completely neglected, no matter if it is energetic or chemical. This contradicts the facts observed and, therefore, may not be accepted.

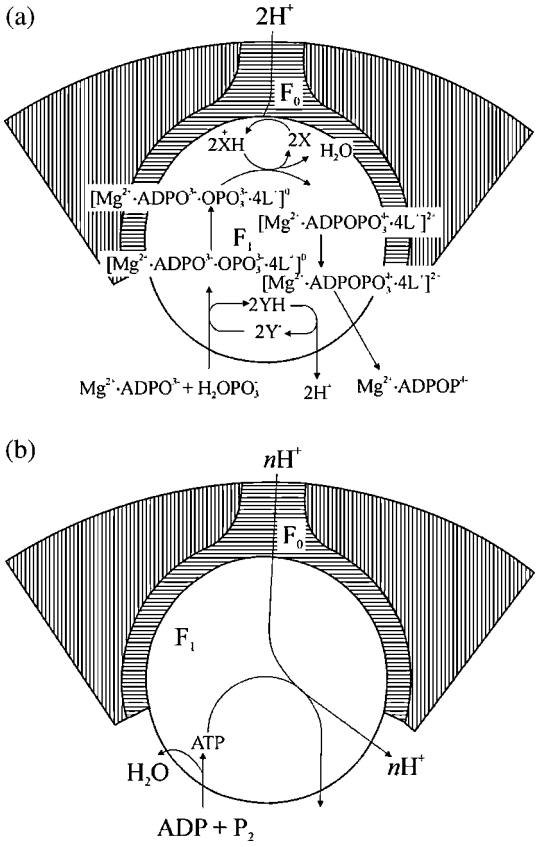

Figure 3.3 The action mechanism of mitochondrial H^+-ATP-synthase: the hypothesis of substrate translocation. (a) $2H^+$ transferred through F_0 to catalytic site F_1 are consumed in ATP synthesis (in $ADPOPO_3^{4-}$ scheme) and H_2O from ADP and phosphite ($ADPO^{3-}$ and OPO_3^{3-}, respectively). The following two H^+ ions may enter the reaction only after ATP release from the catalytic site. They rest in X groups up to the moment, when $[Mg^{2+} \cdot ADPOPO_3^{4-}]^{2+}$complex is removed from this site by electric repulsion force, which is stipulated by the presence of ^+XH group. (b) H^+ ions participating in H_2O production (not shown in the scheme) differ from those symported with synthesized ATP as it is removed from the catalytic site [22].

Of great interest is the question about local $\Delta\bar{\mu}H$ participation in ATP synthesis [13]. As stated by Skulachev '… we have to postulate the presence of respiratory enzyme complex and ATP-synthase from special mechanism of intra-membrane transfer of protons conjugation respiration and ATP synthesis'.

However, taking into account the high rate of H^+ diffusion in water the specific mechanism, which would intensify H^+ transport along the membrane, becomes useless [26]. Nevertheless, it is emphasized that local $\bar{\mu}H$ potential is unable to provide ATP synthesis, at least, without the help of delocalized $\Delta\bar{\mu}H$. Therefore, it is suggested that 'a complex profile of conjugation membranes may induce formation of small local volumes, in which pH differs from pH in the macroscopic environmental volume'.

Apparently, experiments with labeled proton donor (e.g. CD_3 or COOD) should be implemented. Then the reaction of deuterium ions will produce the expected labeled water in the respiratory process, which will unambiguously indicate the validity of the suggested mechanism.

In this regard, local volumes with appropriate ΔpH and $\Delta\psi$ should definitely be important for H^+-ATP-synthase functioning, the more so because for such an event H^+-ATP-synthase and respiratory $\Delta\bar{\mu}H$ generators are located nearby [13]. On this basis, Skulachev concludes that 'Mushroom-shaped outgrowths (of the F_1 factor) are located so close to one another in mitochondrial membranes that no one mushroom may be located between those already existing. Respiratory enzymes must somehow find room between H^+-ATP-synthase molecules. Calculations show that a local electric field, generated at the charge transfer (e.g. H^+) through the membrane may noticeably simplify the motion of another H^+, transferred in the opposite direction, if trajectories of both protons are disposed at 4 nm or closer to one another'.

This concept of local ΔpH and $\Delta\psi$ by no means revises the basic principle of the proton cycle, because protons penetrate through the membrane still.

Note also that, from a physicochemical point of view, in all schemes reflecting $\Delta\bar{\mu}H$-dependent transport systems on both sides of the membrane, H^+ ions may be taken for a catalyst, which intensifies the proceeding of definite processes, either oxidative phosphorylation, osmotic work or other types of work.

However, it is common knowledge that the catalyst does not perform any work, though the system produces thermodynamically effective work of various types. From these standpoints, such schemes are beneath the criticism and, therefore, they may not pretend to provide an adequate description of the observed processes. It should be noted that until the H_2O molecule is bound to F_1, synthesized ATP cannot leave F_1, and both processes are synchronized. Thus, dissociation of water (3.51) promotes ATP desorption to the volume and simultaneously generates H^+ ions to the matrix.

Concerning questions of membrane bioenergetics, Skulachev notes the indeterminacy in the determination of the H^+-ATP-synthase action—the main consumer of $\Delta\bar{\mu}H$. For example, with respect to H/ATP stoichiometry (values 2 and 3 are under discussion) two hypothetical mechanisms are possible (Figure 3.3a and b). There is another important observation related to reversibility of transport processes: protons overcoming the hydrophobic barrier of the membrane by H^+-conductive paths of $\Delta\bar{\mu}H$ generators are returned immediately, moving by H^+ paths of ATP-synthase and other $\Delta\bar{\mu}H$ consumers. For a clearer understanding of chemical conjugation mechanism, a scheme of structural organization of mitochondrial processes is presented in Ref. [27]. This scheme explains several principally important statements of the existing theories and prompts some new questions, for example, about a compromise decision to be made, which would allow products of conjugated reactions in a biosystem to be synthesized at the maximum possible rate. There may only be one answer: each highly active intermediate particle (currently, H^+ ions) must alternately participate in the formation of products of both reactions. The mechanism based on the chemiosmotic hypothesis of ATP synthesis allows the greatest effectiveness of use of every selected active intermediate particle (H^+ ion) in every conjugated reaction. For two conjugated reactions (3.49) and (3.50), the general intermediate particles are the H^+ ion—they occur on the membrane from cytoplasm. The substrate is presented by ADP and inorganic phosphate,

which, together with the phosphorylation reaction, correspond to the internal part of the mitochondrial surface. Though the suggested scheme [27] explains the interaction mechanism of mitochondrial processes, the H^+-ATP-synthase in it is displayed in three conjugation points by analogy with Lehninger's respiratory process scheme [13]. This conveys an impression that three H^+-ATP-synthase molecules take part in the respiratory process. Meanwhile, it is found that only one H^+-ATP-synthase molecule participates in oxidative phosphorylation, and the number of electrons transferred by the respiratory chain may be different (up to eight or higher). Apparently, additional questions are successfully answered by the scheme in Figure 3.4 [28], which represents a modified alternative of the layout in Ref. [27].

In this case, an analogy between the current idea about mitochondrial processes and common chemical phenomenon of chemical process conjugation on membrane catalysts seems to be correct. It should be remembered that at conjugation on membrane catalysts primary and secondary reactions are implemented on different sides of the membrane. The intermediate product of the primary reaction diffuses through the membrane catalyst wall to the other side, where it inductively effects the substrate transformation in the secondary reaction. Chemical reaction conjugation on membrane catalysts shows the principal possibility of inducing chemical reactions through the membrane [29].

Thus, transport of highly active intermediate product through a membrane is the necessary condition for conjugation on membrane catalysts. Moreover, understanding of the conjugation mechanism requires the reaction system to be considered as the entire system divided by a membrane into two parts. In its turn, the membrane must display catalyst properties on both sides. Specific features of catalysis on membrane catalysts allow the promotion of effective chemical conjugation.

Chemical reaction conjugation on membrane catalysts is considered [30, 31] as the simplest model of conjugated processes proceeding in mitochondria. Some functions of this model may be applied to the description of several aspects of respiration and phosphorylation conjugation mechanism.

For example, at chemical conjugation on a membrane catalyst the active intermediate product must be transported through the membrane and consumed on both sides of it. In general terms, a similar situation is most likely observed in mitochondria. Therefore, let us first outline the general moments: the intra-mitochondrial space (the matrix) is separated from

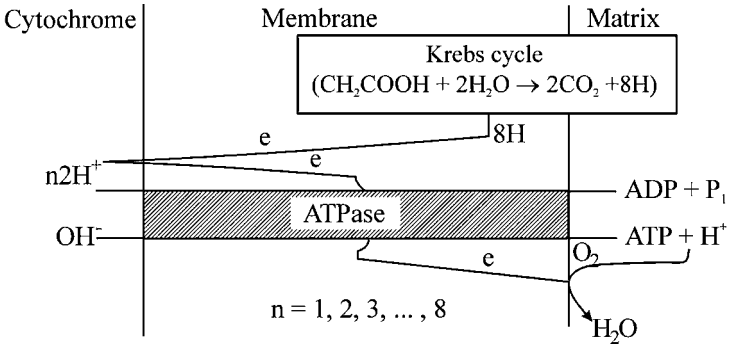

Figure 3.4 Structural organization of chemical conjugation in mitochondrial processes.

the environment (cytoplasm) by a membrane. Highly active intermediate product (H^+ ion) is synthesized on the internal side of the mitochondrial membrane. It is transported through the membrane to cytoplasm (to another part of the reaction system), where it is involved in oxidative phosphorylation. Essentially, in a living cell both conjugated reactions are of the enzymatic type and proceed on the membrane surface.

To accompany the similarity of chemical and biochemical processes proceeding with membrane catalysts, let us also indicate their specific features, which show the 'elegancy' of Nature's modernization of the chemical conjugation mechanism.

The overwhelmingly important aspect of chemical conjugation in mitochondria is the above-mentioned property: conjugated respiration and oxidative phosphorylation processes run in the matrix, i.e. in the same reaction zone. Simultaneously, in a chemical system chemical reactions conjugated on membrane catalysts proceed in different zones, separated by the membrane.

This yields an important consequence: for chemical conjugation on membrane catalysts the question about processes run in the same or in different zones of the reactor is of minor importance. Apparently, one of these possibilities will be predominant with respect to the type of conjugated reactions, for example, when strict demands are imposed on the conjugated reaction rate control.

In biochemical processes the presence of substrates and products of both conjugated reactions in the matrix (i.e. in the same zone of the reaction system) allows finer control of their rates: an increase of ADP concentration to some maximum intensifies respiration and, vice versa, ATP accumulation in sufficient amounts suppresses it.

Highly active intermediate substance, generated in the primary reaction, is always consumed for conjugated reaction product synthesis, and the higher its induction effect on the secondary reaction, the lower its consumption in the primary reaction. It follows that if products of both reactions are of great importance for consecutive biochemical reactions, in this case of chemical conjugation, in principle, the maximum effect is improbable. This gives rise to the question of whether any additional mechanism may be used to provide for effectiveness in both directions.

Let us discuss the fundamental principle of this mechanism: every active site (active intermediate compound) must take part in the synthesis of the products in both reactions, i.e. it must be alternately consumed in them. The situation seems to be rather paradoxical, because the same exclusive active particle must be consumed in both reactions. Therefore, to ensure proper reasoning of this question, some details should be explained using a particular example.

Imagine two particles of the active site (for simplicity, let them be two H^+ ions). Each of them is consumed in the synthesis of two conjugated reaction products. Then the conjugation determinant (the induction factor) calculated by the equation:

$$D = \nu \left(\frac{J_{A_1}}{J_{Acc}} + \frac{J_{A_2}}{J_{Acc}} \right)^{-1}$$

where J_{A_1} and J_{A_2} are the actor quantities consumed for final product synthesis in primary (3.49) and secondary (3.50) reactions, respectively, or determined from the determinant scale, equals $\nu/2$ [32].

It is clear that chemical conjugation characterized by the determinant value $\nu/2$ does not allow the maximum possible effect of chemical conjugation to be reached. If both active sites are consumed in the secondary reaction only, the determinant approaches the unit—its maximum value. However, this will eliminate synthesis of the primary (induction) reaction products. What is the compromise decision promoting synthesis of both reaction products in the system at the maximum rate? It is, probably, the alternate participation of every given active particle (two particles in the current case) in the synthesis of conjugated reaction products. The only way is chemical conjugation implementation on membrane catalysts: all active particles synthesized at a definite stage of the primary reaction, which runs in one part of a divided reaction system, are consumed in another part of the system. Thus, the secondary reaction is induced with the highest efficiency. Then one of the secondary reaction products should be transported through the membrane and regenerate the active site in the first zone. This newly synthesized active site will take part in the formation of products at the final stage of the primary reaction, i.e. practically the same active site takes part in both reactions. Hence, conjugated reactions must be run on different sides of the membrane, because locating in the same zone of the reaction system active sites will cause simultaneous synthesis of both reactions (in proportion with respect to their rates). Actually, in the latter case, it is senseless to speak about single particle participation in both reactions. Thus, the most important function of the membrane is transportation of active particle, where it is synthesized, to another zone, where it is consumed in the secondary reaction.

The above idea may be related to the interpretation of the conjugation mechanism of biooxidation reactions proceeding on the surface of mitochondrial membrane. It is known that Nature always displays great efficiency and rationality in the organization of biochemical processes. It is, therefore, no wonder that the same properties are observed in the structural organization of chemical conjugation, on which cell bioenergetics is based.

Saving of energy resources in the organism directly relates to the application of the same active particle—H^+ ion, both in ATP synthesis and water production, the final respiration product. No doubt, this aspect is built-in to chemical conjugation implemented in mitochondria during chemical energy accumulation in ATP.

The mechanism based on the chemiosmotic hypothesis of ATP synthesis can also be related to this class of mechanism, because it promotes the separate use of the highly active intermediate particle (H^+ ion) with the maximum effectiveness and in each of conjugated reactions.

Biochemists failed to identify high-energy intermediate substances and to explain the exclusive role of the membrane in ATP synthesis using chemical conjugation hypothesis. In the search for protein factors of conjugation which provide for oxidative phosphorylation, a specific protein was detected—H^+-ATP-synthase (the so-called F_1 factor). This caused the general picture to become even more confused. Moreover, the question arose of how and in what shape this enzyme receives energy from electron transfer for energy supply of the reaction ADP + P_i, catalyzed by it.

All the above questions can be satisfactorily answered in the framework of the chemical conjugation concept, where the central place is dedicated to H^+ ions—the conjugation intermediates. The author's hope that the concept of chemical conjugation of mitochondrial processes put forward will settle the various points between two common 'alternative' hypotheses of biochemistry: chemical conjugation and chemiosmosis [13].

This combined mechanism of chemical conjugation and chemiosmotic hypothesis gives an opportunity to give a purely chemical explanation of the respiration and phosphorylation uncoupler action. For uncouplers of respiration and phosphorylation the substances are taken whose addition to mitochondrial suspension terminates ATP synthesis and preserves respiration. It is noted that with no respect to uncoupler origin, the place of their attack on the membrane is of minor value. It is observed that places of uncoupler attacks on the membrane are of no importance. It is significant that ATP synthesis is terminated, i.e. chemical conjugation is eliminated. The physical principles fundamental for a chemiosmotic explanation of this effect are the following: uncouplers increase conductivity of biological membranes; therefore, the electric potential difference at both sides of the membrane is reduced, gradient of hydrogen ion concentration is eliminated, and ATP synthesis is terminated. To put it another way, uncouplers promote the occurrence of new channels for H^+ ion transport through the membrane.

Moreover, ATP synthesis is also terminated in the case where the mitochondrial system is open, though enzymatic ensembles necessary for respiration and phosphorylation are completely preserved. On the one hand, the open condition of the mitochondrial membrane neglects the preservation of the H^+ ion concentration gradient and electrochemical potential of the membrane. Thus, some stage of mitochondrial membrane operation on ATP synthesis (associated with the chemiosmotic mechanism) is terminated. On the other hand, kinetic conditions are changed in the system. This point requires additional discussion. If in an open mitochondrial system two conjugated reactions—respiration and oxidative phosphorylation—proceed simultaneously using a general intermediate compound (the active particle: H^+ ion), the rate of the appropriate reaction product accumulation will be defined by the kinetics of both processes. Attentive observation of this system indicates that it loses one very important property, i.e. it completely loses the ability of chemical conjugation on membrane catalysts and, therefore, other typical features such as the alternate consumption of the active particle, H^+ ion (in the reaction system divided by a membrane into two zones). This makes clear one more purely kinetic feature in mitochondrial membrane activity.

In fact, there are examples of chemical reaction in catalysis, which proceed on membranes not dividing the reaction zone into zones. They behave in the system as normal catalysts, e.g. obeying kinetic regularities of heterogeneous catalytic systems.

Therefore, as a mitochondrion membrane is broken, it somewhat disrupts communications between two conjugated reactions (respiration and phosphorylation). Hence, as expected, phosphorylation is completely terminated. This kinetic behavior of the system, both unclear and unusual at first glance, is quite logical, and is associated with the membrane origin of the ATP synthesis.

Let us start by detecting the principal difference between the two possible forms of the use of membrane catalyst: closed and open. In the case of the closed surface, active sites (H^+ ions) generated during cell nutrition oxidation are located on both sides of the membrane in almost equal amounts. This does not mean equality of their concentrations in cytoplasm and the matrix. Hence, the same pair of H^+ ions is consumed in both ATP synthesis (oxidative phosphorylation) and H_2O production (respiration). In the case in where the mitochondrial surface is open, H^+ ions would also be consumed in both reactions, the only difference being that now they begin competing for H^+ ions. In reality, oxidative phosphorylation is unable to compete for H^+ ions with respiration. The so-called proton ‘pump’, which promotes

dissociation of water produced during ATP synthesis and H^+ and OH^- ions 'draining' to the appropriate part of the reaction system, stops operating.

This explanation of ATP synthesis termination is based on the chemiosmotic hypothesis and correlates well with the experiment. It seems to us that even this very important interpretation of chemical conjugation termination is not enough, because proceeding of chemical reactions in this system preserves corresponding kinetic conditions for running ATP synthesis at a low, but different, rate. However, mitochondrion bioenergetics does not foresee such a possibility. Therefore, any obstacle to the removal of H^+ and OH^- ions from the membrane inevitably causes inhibition of the H^+-ATP-synthase reaction. Nevertheless, the question arises of why, during the evolution of the living cell, Nature did not apply this method of chemical energy accumulation. Apparently, in an open membrane several operations can be eliminated, in particular, H_2O dissociation, H^+ ion concentration gradient and the use of H^+ ions from cytoplasm by H^+-ATP-synthase. Actually, H^+ ions generated by respiration might be consumed in both reactions similar to the usual conjugation of chemical reactions.

Let us now discuss the possible disadvantages of this respiration and phosphorylation conjugation alternative for the living organism, because this analytical approach is the only way to estimate the perfection of Nature's engineering activity in the structural organization of the cell bioenergetics. Comparison of both conjugated reaction rates (respiration and phosphorylation) in the system indicates that the primary reaction (respiration) proceeds at a much higher rate than oxidative phosphorylation, and especially, at the stages in which H^+ ions participate.

In conjugated reactions active site consumption is distributed between reactions with respect to their rates. In this connection, we should discuss a hypothetical situation in which one part of the active site is consumed for H_2O production, whereas another part is consumed for ATP synthesis during the same period of time. Such a system would display simultaneous accumulation of the products of both reactions and the amount of H^+ ions consumed in the reactions would depend on the ratio of their rates.

Actually, if we denote rates of water production in the respiration process and ATP synthesis during phosphorylation by r_D and r_{ph}, respectively, the following ratios of the rates may be obtained:

$$r_D \gg r_{ph} \quad r_D \approx r_{ph} \quad r_D \gg r_{ph}$$

The latter inequality should be eliminated, because in this case chemical conjugation is ineffective.

The first inequality relates to the situation observed for an open mitochondrial membrane. In fact, as soon as the membrane becomes open, ATP synthesis is terminated, whereas respiration proceeds simultaneously at an inherently high rate. Therefore, in the author's opinion, chemical conjugation which would take place with an open membrane is hindered due to respiration proceeding at a rate much higher than the rate of ATP synthesis and actually represents the single process realized in the system.

Only the case of $r_D \approx r_{ph}$ then remains. Theoretically, active particles may be distributed in almost equal parts between both reactions. In reality, such a situation is impossible in bioenergetics of the cell, because the products of both reactions are formed not at the maximum

rate, which is possible in the case of full consumption of active sites in each reaction. Therefore, it is clear where and how the compromise decision should be looked for: one of the reaction products must be subject to further transformation in order to regenerate the active site in the system. This is not enough, however. There are the following hindrances to achieving the maximal rate of substrate transformation in the second reaction: nevertheless, a significant part of the active sites (H^+ ions) is consumed in the primary reaction and, therefore, is only partly involved in the secondary reaction. To put it another way, a part of the active sites participates in the secondary reaction, whereas all active sites, theoretically at least, may participate in the primary reaction. Hence, there occurs the problem of creating a reaction system with active sites that are also completely consumed in the secondary reaction.

Thus, these ideas give rise to the suggestion that the maximum parameters for both conjugated reactions may be obtained only in the case where active sites are guided by the following actions: the primary reaction generates active sites to the system; then the secondary reaction is induced, and active sites are completely consumed by it; afterwards, one of the products must enter the reaction, and active sites are regenerated in the system, and then participate in final product synthesis of the primary reaction. Only in the case of membrane catalysts with closed surfaces can any system operate in such a mode.

Let us analyze the ATP synthesis reaction (3.50), which, with respect to inorganic phosphate ion charge, requires one or two H^+ ions for oxidation reaction. Figure 3.4 clearly illustrates that the H^+-ATP-synthase responsible for oxidative phosphorylation consumes active H_3O^+ particles (H^+ ion) from both parts of the reaction system (matrix and cytoplasm). Specifying the work of H^+-ATP-synthase, it should be noted that H^+ ions delivered from the cytoplasm to the membrane and ADP and P_i substrates participate in phosphorylation reaction proceeding on the internal surface of the membrane. In this case, water molecules are one of the products of oxidative phosphorylation. It does not release to the volume, but dissociates to H^+ and OH^- ions immediately on the membrane. Then according to the chemiosmotic mechanism OH^- anion is desorbed to cytoplasm and H^+ ion to the matrix, where its occurrence as the active particle is associated with water production at the final stage of the respiration process.

As noted by Lehninger, the high concentration of OH^- ions in the mitochondrion promotes H^+ ion 'draining' from the H^+-ATP-synthase active site, and high H^+ concentration in cytoplasm promotes 'draining' of OH^- ions from the active site of the enzyme [17]. Thus, respiration and phosphorylation may not be conjugated without H^+-ATP-synthase. According to Mitchell, the connection channel between cytoplasm and the matrix is provided by its transverse orientation in the membrane. This event yields in H^+-ATP-synthase the ability first to 'drain' H^+ ion from cytoplasm and then to synthesize ATP. As a result of H^+ ion interaction with substrates (ADP^{3-} and HPO_4^{2-}), the oxidation energy is released and then accumulated in ATP molecules.

The respiration process produces electric potential difference on the membrane, and then H^+ ion concentration gradient is formed on the membrane sides, which plays the important role in H^+ ion transport.

The above discussion, which mostly considers kinetic and chemical aspects to explain respiration and phosphorylation unconjugation, makes clear the action of uncouplers of different origins. Moreover, no principal difference in the mechanism of uncouplers and open mitochondrial surface is observed, because uncouplers increase membrane conductivity for H^+ ions and, therefore, promote its partial break in places of uncoupler injection.

To sum up, it should be noted that the respiration process induces the occurrence of the electric potential difference H^+ concentration gradient at the membrane sides, which are of the greatest importance for H^+ transport, without which chemical conjugation is impossible. Thus, in the framework of the currently suggested concept of chemical conjugation for mitochondrial processes, the origin of the active conjugation site (H^+) is specified and the exclusive role of the membrane in conjugation structural organization is shown.

As may be ascertained by the new interpretation, these two theories are not alternative but complement each other and represent different aspects of the general mechanism of bioenergetic activity in the cell. This mechanism is associated with chemical energy accumulation, transformation and transportation.

Unfortunately, although the scheme shown in Figure 3.4 clearly presents the type of chemical conjugation between respiration and phosphorylation, nevertheless, biochemists experience difficulties with the perception of a purely chemically formulated scheme. We suggest that this very circumstance prevents them from an adequate perception of the whole scheme. All in all, this is not surprising because for biochemists scheme visualization is associated with an indication of directions or rather process routes, frequently without taking into account stoichiometry and other physical processes that are absolutely necessary for chemists.

To prove the above, let us turn to the schemes in Figure 3.3, which clearly show the structural organization of H^+-ATP-synthase. Hence, as for biochemical reactions, physicochemical analysis raises several important questions, some of which have been discussed above. Among the remaining questions is a combined structure of $[Mg^{2+} \cdot ADPO^{3-} \cdot OPO_3^{3-} \cdot 4L^+]^0$ complex and the catalytic role of active sites X and L^+ suggesting the intermediate complex to be slightly mobile. Scheme (b) in Figure 3.3 would be simpler and, therefore, more attractive. However, the H^+ ions in it represent oxidative phosphorylation catalysts, and the chemical conjugation mechanism as the means to accumulate chemical energy released during respiration is neglected. For common reasons, this latter is undesirable.

Obviously, the advantage of scheme (a) in Figure 3.3 is the demonstration of the operation of factors F_0 and F_1 at the level of the elementary act and proton travel direction to the internal mitochondrion zone. A new scheme suggested in Figure 3.5 preserves these certain advantages and includes elements from Figure 3.4. The latter mostly include the principle of chemical conjugation between respiration and oxidative phosphorylation, in which H^+ ions compose general intermediate substance.

Let us present the structural and physicochemical features, which contrary to the features of the schemes in Figure 3.3, conform to modern views and observations:

(a) The external membrane surface has a small 'bay', where H^+ and OH^- ion concentrations will differ from their concentrations in cytoplasm.
(b) It is shown how the respiration process is conjugated to phosphorylation.
(c) H^+ ions are regenerated due to dissociation of H_2O molecules formed in phosphorylation.
(d) H^+ is the intermediate of respiration and phosphorylation conjugation.

At the molecular level, the scheme of the H^+-ATP-synthase reaction mechanism is quite simple. It illustrates the interaction between two conjugated reactions: respiration and phosphorylation, and the exclusive role of the H^+ ions in the structural organization of this interrelation. Moreover, energy (i.e. thermodynamic) conjugation is reasonably substantiated from a physicochemical position.

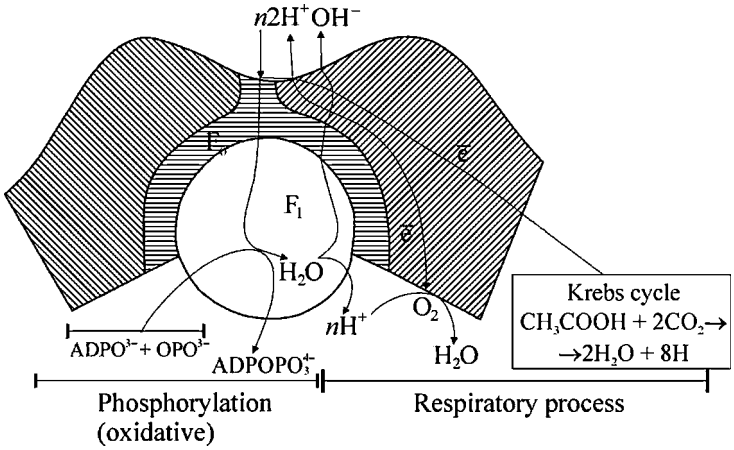

Figure 3.5 The mechanism of chemical conjugation in mitochondrial energy process.

Owing to proton generation at the external side of the mitochondrial membrane, H^+ ion concentration increases in a 'microstagnant zone' and, therefore, the proton concentration gradient at both sides of the membrane is provided. Then protons penetrate through the membrane with the help of the F_0 factor and $\bar{\mu}H^+$. However, this does not mean that the energy of the primary reaction (3.49) is consumed by the secondary reaction (3.50); the transfer of chemical energy released in one reaction to another reaction requires the participation of a general, highly active intermediate product in it. As follows from the scheme, only the H^+ ion may be the intermediate, because its oxidation energy may be used in the oxidation reaction, oxidative phosphorylation, in particular.

Thus, the 'free energy' released in the primary respiration reaction was accumulated on protons. This energy is effectively used by the factor F_1 in the secondary phosphorylation reaction. This reaction does not run without H^+ ions, because phosphorylation is an endothermic process, which requires external energy in order to proceed. Actually, owing to chemical conjugation via H^+ ions (the intermediate inducing the secondary reaction (3.50)) usual phosphorylation is transformed to oxidative phosphorylation, i.e. from endergonic to exergonic reaction.

As a consequence, besides chemical conjugation, thermodynamic conjugation happens in the reaction system. Nevertheless, though these reactions are integral parts of the same process, they display different approaches to the interpretation of the phenomenon.

Note also that chemical reactions accompanied by water formation are always thermodynamically profitable. Therefore, H^+ ion participation in water formation during the ADP phosphorylation process makes this reaction much simpler. On the other hand, the water formed is bound to the F_1 factor. It is common knowledge that the reaction is intensified by water-binding compounds. Then water is dissociated to ions, emitted to different sides of the membrane, and this process is synchronized with ATP desorption. Desorbed protons are localized at H^+-ATP-synthase, directly at the cytochrome system of the respiratory chain. Therefore, they quickly interact with activated oxygen, producing water at the final stage of respiration (3.50).

Therefore, the scheme shown in Figure 3.5 clearly illustrates mitochondrial energetic process mechanisms, and all known observations and hypotheses fall within the framework

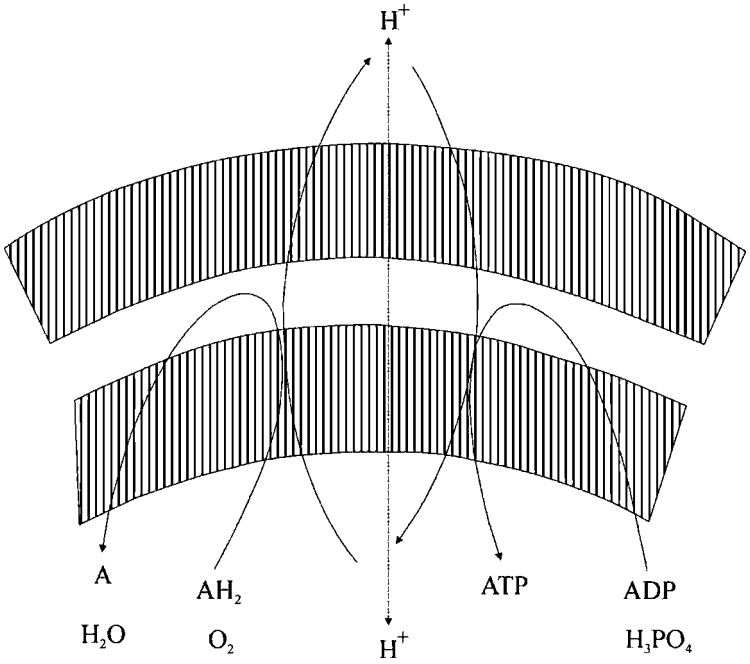

Figure 3.6 The conjugation mechanism of respiration and ADP phosphorylation. Dashed arrow shows H^+ ion leakage according to Skulachev.

of the suggested theory. This theory reconciles both common hypotheses (i.e. chemical conjugation and chemiosmotic hypothesis), indicating that they are components of this theory.

Note that though the conjugation mechanism scheme for respiration and ADP phosphorylation in Figure 3.6 [33] properly indicates the pathways of H^+ ions, their action mechanism as highly active intermediate particles (the conjugation intermediate, owing to which chemical energy of respiration is accumulated in the phosphorylation product) is not disclosed.

As discussed above, active particles $H^+ + e^-$ are generated in the Krebs cycle during the respiration process. These particles then participate in water formation, which is the secondary reaction product.

According to ideas under development, kinetic curves of both overall reactions (I: respiration and II: oxidative phosphorylation) will give the interference pattern shown in Figure 3.7.

Here curve I corresponds to water formation at a maximum rate in the respiration process. Since H^+ and e^- formation is the general process for conjugated processes, their synchronization mechanism may be presented by the following scheme:

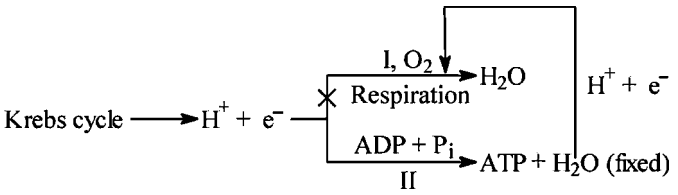

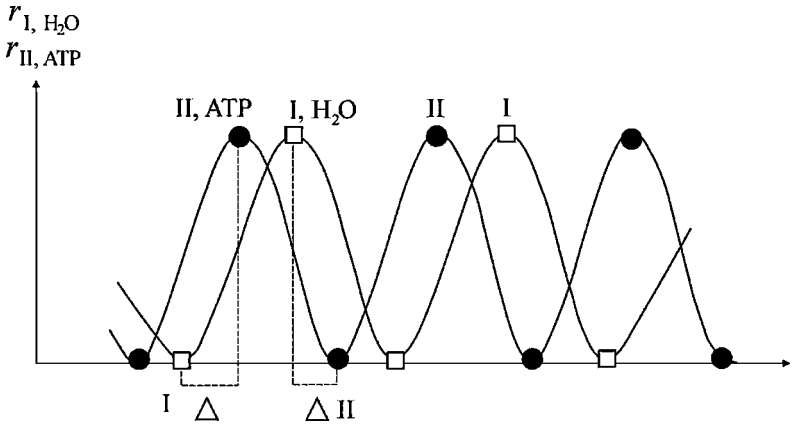

Figure 3.7 Theoretical kinetic curves for chemical interference in mitochondrial energy process.

As follows from this scheme, secondary reaction (oxidative phosphorylation) products are formed first due to the membrane catalysis effect; after bound water dissociation to H^+ and OH^- only the primary reaction (respiration) product—the water molecule—is formed with the help of H^+ ions. Thus, the maximum yield of primary reaction products is observed only in the case of the maximum yield of the secondary reaction.

The system operates in the membrane catalysis mode. Therefore, as shown in the scheme, the parallel reaction does not run by the first pathway, but implements the consecutive means of water molecule formation in the respiration process.

Water and ATP by both synchronous reactions are synthesized with some delay, given by the Δ value in Figure 3.7. This value is constant and characterizes the phase shift. However, according to practical considerations the interference pattern shown in Figure 3.7 should be presented as shown in Figure 3.8. In this case, Δ equals 0, which seems more real, though an insignificant shift between minima and maxima of synchronized curves may be suggested.

The mitochondrial process displays an untypical, more likely unique, shape of chemical interference, characterized by the highest coherence form, when the phase shift equals 0. Such a shape of the interference pattern demonstrates high conformity of bioenergetic processes and, probably, the highest symmetry in synchronized reactions. Of course, the above-mentioned interaction between synchronous reactions is possible only at membrane analysis.

The bionic aspect of the energy problem seems very attractive, because we believe it gives a good opportunity to create relatively inexpensive chemical systems, composed on the principle of mitochondria or chloroplasts. For this purpose, we have to follow a definite sequence in thermodynamic and kinetic analysis of chemical systems. From a thermodynamic position, this concludes in detecting thermochemical parameters of reactions proceeding in the system (there must be two or more). Finally, these reactions should allow the division of the system into exergonic and endergonic components (if the system possesses both types of reactions). In the case of chemical kinetics, particular conditions (temperature, reagent concentration and their ratios, pressure, solvent selection, etc.) should be determined, under which the reactions could be really conjugated. Possible effective application

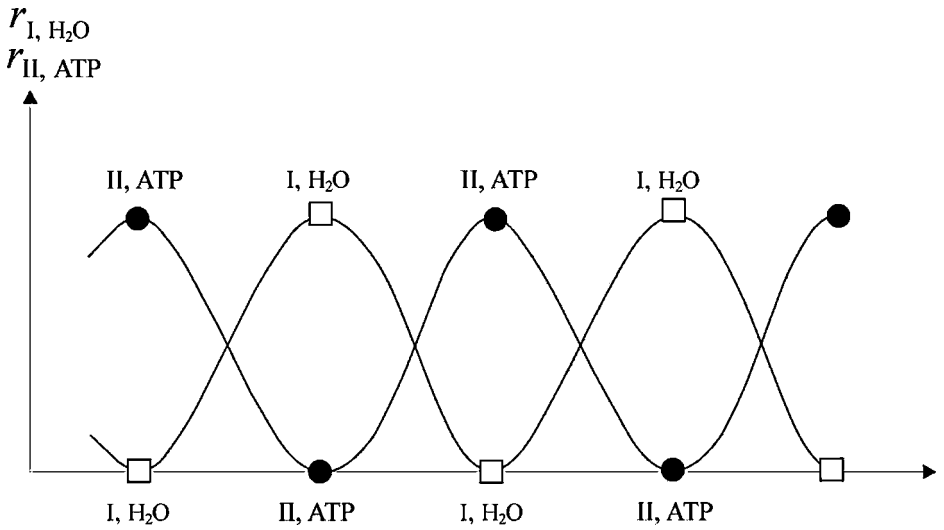

Figure 3.8 Theoretical kinetic curves of the interference pattern for mitochondrial process in the absence of the phase shift.

of usual catalytic systems, enzymes and their models to speed up and properly direct conjugated reactions should also be taken into account.

Nature suggests to us an idea to modernize already known and newly discovered catalytic reactions via chemical conjugation mechanism. In general, the task may be formulated as follows:

1. Search for reaction pairs that obey the laws of thermodynamic conjugation (a connection between exergonic and endergonic components of the system).
2. Conjugation reactions, in principle, may be known and even well investigated. Since the initial moment, the knowledge of individual features of conjugated reactions may promote the creation of more favorable conditions for chemical conjugation.
3. It is desirable to study the kinetics of conjugated chemical reactions in the absence of catalysts, because any complication of the system reduces the effectiveness of the search. Hence, any result is of interest, when the principal possibility of chemical conjugation in the system shall be detected. The induction effect is displayed via highly active general intermediate substance, which may not be described by thermodynamic investigations.
4. Conjugated reaction system may be modernized by heterogeneous catalysts, enzymes and their most effective models—the achievements of homogeneous and membrane catalysis. The catalyst application may change the type of intermediate—the active particle responsible for chemical conjugation. The catalyst application may not eliminate the ability of the system to perform chemical conjugation of reactions: it will always be a potential ability of the system. For this purpose, it is enough if active sites general to both reactions are formed on catalysts. The search for catalysts must be controlled by signs determined as a result of conjugation active particle formation. For this

purpose, it is enough if one catalytic reaction generates an inductive intermediate to the system, and then another catalyst binds it again and consumes in a conjugated reaction. Hence, a unique catalyst may be synthesized, which would be active in relation to both conjugated reactions, the more so that Nature gives such examples, shaped as enzymatic reactions.

Of course, the above list gives only the most important cases. What is obvious is that the prospective combination of catalysis and chemical conjugation methods will give a new direction for the selective transformation of substances by the oxidation mechanism.

REFERENCES

1. Emanuel, N.M. and Knorre, D.G., *The Course of Chemical Kinetics*, Vysshaya Shkola, Moscow, 1984, 237 pp. (in Russian).
2. Rakovsky, A.A., *Introduction to Physical Chemistry*, ONTI, Red. Khim. Lit., Moscow, 1938, 677 pp. (in Russian).
3. Kondratiev, V.N. and Nikitin, E.E., *Kinetics and Mechanism of Gas-Phase Reactions*, Nauka, Moscow, 1975, 559 pp. (in Russian).
4. Denisov, E.T., *Kinetics of Homogeneous Chemical Reactions*, Vysshaya Shkola, Moscow, 1978, 367 pp. (in Russian).
5. Shilov, N.A., *About Conjugated Oxidation Reactions*, Publisher A.I. Mamontov, Moscow, 1905, 304 pp. (in Russian).
6. Nagiev, T.M., *Usp. Khim.*, 1985, Vol. 54, No. 10, pp. 1654–1673 (in Russian).
7. Vol'pin, M.E., Moiseev, I.I. and Shilov, A.E., *IZh. Mendeleev VKhO*, 1980, Vol. 25, No. 5, p. 515 (in Russian).
8. Alkhazov, T.G. and Lisovsky, A.E., *Oxidative Degradation of Hydrocarbons*, Khimia, Moscow, 1980, 238 pp. (in Russian).
9. Skarchenko, V.K., *Hydrocarbon Dehydrogenation*, Naukova Dumka, Kiev, 1981, 328 pp. (in Russian).
10. Nonhible, D. and Walton, J., *Chemistry of Free Radicals*, Mir, Moscow, 1977, 606 pp. (in Russian).
11. Semenov, N.N., *On Some Problems of Chemical Kinetics and Reactivity*, 2nd edn, Izd. AN SSSR, Moscow, 1958, 680 pp. (in Russian).
12. Benson, S., *Thermochemical Kinetics*, Mir, Moscow, 1971, 308 pp. (in Russian).
13. Lehninger, A., *Biochemistry*, Mir, Moscow, 1976, 957 pp. (in Russian).
14. Dolgoplosk, B.A. and Tinyakova, E.I., *Free Radical Generation and Their Reactions*, Nauka, Moscow, 1982, 253 pp. (in Russian).
15. Kondrat'ev, V.N., *Rate Constants of Gas-Phase Reactions*, Nauka, Moscow, 1970, 351 pp. (in Russian).
16. Fridovich, I., *Free Radicals in Biology*, Pt. 1, Mir, Moscow, 1979, pp. 272–308 (in Russian).
17. Lehninger, A., *Mitochondrion*, Mir, Moscow, 1966, 316 pp. (in Russian).
18. Blumenfeld, L.A. and Tikhonov, A.N., *Biophysical Thermodynamics of Intracellular Process*, Springer Verlag, New York, 1994, 175 pp.
19. Stent, G., *Molecular Genetics*, Mir, Moscow, 1974, 525 pp. (in Russian).
20. Mitchell, P., *Trans. Biochem. Soc*., 1976, Vol. 4, pp. 399–430.
21. Nagiev, T.M., *Zh. Fiz. Khim*., 1995, Vol. 69, No. 11, pp. 1980–1983 (in Russian).
22. Skulachev, V.P., *The Energy of Biological Membranes*, Mir, Moscow, 1989, 365 pp. (in Russian).
23. Racker, E., *Mechanisms in Bioenergetics*, Academic Press, London, 1965, 259 pp.
24. Chernyak, B.V. and Kozlov, I.A., *FEBS Lett.*, 1979, Vol. 104, pp. 215–219.
25. Skulachev, V.P. and Kozlov, I.A., *Curr. Top. Membr. Transp*., 1982, Vol. 16, pp. 285–301.

26. Penefsky, H.S., *Proc. Natl. Acad. Sci. USA*, 1985, Vol. 82, pp. 1589–1593.
27. Nagiev, T.M., *Vestnik Mosk. Universiteta, Ser. 2, Khimia*, Vol. 28, No. 5, 1987, pp. 447–451 (in Russian).
28. Nagiev, T.M., *Vestnik Mosk. Universiteta, Ser. 2, Khimia*, Vol. 36, No. 5, 1995, pp. 434–440 (in Russian).
29. Nagiev, T.M., *Chemical Conjugation*, Nauka, Moscow, 1989, 216 pp. (in Russian).
30. Nagiev, T.M., Abstracts of papers, *International Symposium on Charge and Field Effects in Biosystems*, V.C.U. Richmond, Virginia, USA, 1991.
31. Nagiev, T.M., Program and abstracts, *13th International Symposium on Bioelectronics and Bioenergetics*, Ein-Gedi, Israel, 1996.
32. Nagiev, T.M., *Zh. Fiz. Khim*., 1994, Vol. 68, No. 3, pp. 456–460 (in Russian).
33. Skulachev, V.P., *Sorovsky Obozrevatel'ny Zhurnal*, No. 3, 1996, pp. 4–10 (in Russian).

– 4 –

Conjugated Reactions of Oxidation with Hydrogen Peroxide in the Gas Phase

This chapter overviews the following points:

- Hydrogen peroxide dissociation in the gas phase.
- Reactions induced with hydrogen peroxide.
- Experimental studies of conjugated reactions—dehydrogenation, oxidation, hydrogenolysis and nitrogen fixation.

Availability, ease of handling, and the combination of oxidation and reduction properties have all determined many of the traditional applications of hydrogen peroxide. Detailed investigation of the chemical properties of H_2O_2 also allows us to plumb the depths of the reaction mechanisms that proceed with its participation in order to consciously control their rate and direction. These studies may be applied as the basis for new chemical technological processes for the production of valuable chemical substances from readily available inexpensive raw materials.

Hydrogen peroxide possesses a unique multiple reactivity. Owing to the intermediate position in the redox ternary:

$$O_2 \underset{-2H}{\overset{2H}{\rightleftharpoons}} H_2O_2 \underset{-2H}{\overset{2H}{\rightleftharpoons}} H_2O$$

or

$$O_2 \underset{-2e^-}{\overset{2e^-}{\rightleftharpoons}} O_2^{2-} \underset{-2e^-}{\overset{2e^-}{\rightleftharpoons}} O^{2-}$$

it possesses dual reactivity. With respect to the substrate type, it may serve as electron donor or acceptor, i.e. enter oxidation or restoration processes. This is clearly displayed in the degradation reaction, where H_2O_2 is alternately oxidized and restored.

The role of H_2O_2 in chemical processes proceeding in both organic and inorganic nature has not yet been sufficiently studied.

4.1 HYDROGEN PEROXIDE DISSOCIATION KINETICS AND THE MECHANISM

Before passing on to the analysis of gas-phase oxidation with hydrogen peroxide, we must first obtain information about its dissociation. Hydrogen peroxide easily dissociates to water and molecular oxygen, which is the typical feature, very useful in some cases and unwanted in another. H_2O_2 can dissociate in different ways, but all of them are described by the general material balance equation as follows:

$$2H_2O_2 \rightarrow 2H_2O + O_2$$

The monographs by Shambe *et al*. [1, 2] published in 1958 give an analysis of the question before 1956. By then, the main pathways of gaseous H_2O_2 dissociation—homogeneous and heterogeneous—were known. The homogeneous process represents free radical reactions in the volume, whereas heterogeneous catalysis had only been studied qualitatively. However, much time has elapsed since those days, and our knowledge of the field of heterogeneous catalytic mechanisms of gaseous H_2O_2 dissociation have been significantly broadened. For homogeneous dissociation, ambiguous kinetic data have been specified and, for the first time, active intermediate products have been detected and identified, and their concentrations estimated using the ESR method.

Of importance for understanding kinetics and oxidation mechanism of various substrates with the participation of hydrogen peroxide are the conditions of H_2O_2 dissociation into intermediates. As already mentioned in early studies on heterogeneous gas-phase dissociation of H_2O_2 [3], the reaction is rather sensitive to the type of reactor walls and depends on their preparative treatment, which makes obtaining reproductive data more difficult.

In later works [4], Satterfield and Stein note that in flow conditions up to 723 K the homogeneous component contribution into the reaction is low and the following H_2O_2 dissociation mechanism is suggested:

$$H_2O_{2(ads)} \rightarrow 2{}^{\bullet}OH_{(ads)}$$
$${}^{\bullet}OH_{(ads)} + H_2O_{2(g)}(H_2O_{2(ads)}) \rightarrow HO^{\bullet}_{2(ads)} + H_2O$$
$$HO^{\bullet}_{2(ads)} + {}^{\bullet}OH_{(ads)} \rightarrow H_2O + O_2$$

Of interest are works [5–9] showing that at increased temperature heterogeneous dissociation reaction transits to a homogeneous reaction and the reaction degree by H_2O_2 becomes equal to 1.

Jigger and Li [60] have discovered that the transition zone is located at 673 K, and the effective rate constant of dissociation equals:

$$k = 10^{13} \exp\left(\frac{200640}{RT}\right) (s^{-1})$$

The following mechanism was suggested for homogeneous dissociation of gaseous H_2O_2 [7]:

$$H_2O_2 \rightarrow 2^{\bullet}OH$$
$$^{\bullet}OH + H_2O_2 \rightarrow H_2O + HO_2^{\bullet}$$
$$HO_2^{\bullet} + HO_2^{\bullet} \rightarrow H_2O_2 + O_2$$
$$HO_2^{\bullet} + {}^{\bullet}OH \rightarrow H_2O + O_2$$

Another chain mechanism of homogeneous H_2O_2 dissociation, slightly different from the previous one, is suggested by Satterfield and Stein [9]:

$$H_2O_2 + M \rightarrow 2^{\bullet}OH + M$$
$$^{\bullet}OH + H_2O_2 \rightarrow H_2O + HO_2^{\bullet}$$
$$HO_2^{\bullet} + H_2O_2 \rightarrow H_2O + O_2 + {}^{\bullet}OH$$
$$2^{\bullet}OH + M \rightarrow H_2O_2 + M$$
$$^{\bullet}OH + HO_2^{\bullet} + M \rightarrow H_2O + O_2 + M$$
$$2HO_2^{\bullet} + M \rightarrow H_2O_2 + O_2 + M$$

where M is the reactor wall, an inert gas, H_2O_2 or H_2O molecules. A clear transition from a heterogeneous (the order by H_2O_2 equals 1, $E = 42$ kJ/mol) to a homogeneous reaction (the order by H_2O_2 equals 3/2, $E = 230$ kJ/mol) is observed in the close range of 698 K. The order 3/2 is obtained due to the contribution of the stage of H_2O_2 dissociation to hydroxyl radicals in the presence of M [60]. This does not conform with the results from Ref. [5], where the order by H_2O_2 is assumed equals 1.

The works by Baker and Onellet [10] and Mackenzie and Ritchie [11] should be noted. These authors detected the first order by H_2O_2 in quartz reactors (up to 413 K) and the second order by H_2O_2 in approximately the same conditions, respectively. Forst [12] indicated that in the presence of inert gases (He, O_2 and H_2O) H_2O_2 dissociation rates are far different at transition from one inert gas to another. These questions are discussed in more detail in the works of Houre *et al*. [13, 14] in which it is shown that, independently of the area of gaseous H_2O_2 dissociation, the order with hydrogen peroxide equals 1, but in addition an order by the inert diluter M is also introduced. The latter also equals 1. A non-chain mechanism, which conforms to the experiment, is suggested:

$$H_2O_2 + M \rightarrow 2^{\bullet}OH + M$$
$$^{\bullet}OH + H_2O_2 \rightarrow H_2O + HO_2^{\bullet}$$
$$HO_2^{\bullet} + HO_2^{\bullet} \rightarrow H_2O_2 + O_2$$

The rate constant for the first stage ($k = K[H_2O_2][M]$) in the temperature range of 342–932 K (M = H_2O_2 or H_2O) was deduced:

$$k = 10^{15.4} \exp\left(\frac{200640}{RT}\right) \left(1/(\text{mol s})\right)$$

Further experimental studies of kinetic regularities have shown that the totality of elementary stages currently presented is the most probable and adequate describes thermolysis of gaseous hydrogen peroxide [15, 16]. Free radical decay in the gas phase on the reactor walls is more probable than the chain termination in the volume and, therefore, this circumstance should be reflected in the scheme. This was attempted in an article [17], according to which chain termination occurs by the following mechanism:

$$2^{\bullet}OH + M \rightarrow H_2O_2 + M$$
$$2HO_2^{\bullet} + M \rightarrow H_2O_2 + O_2 + M$$
$$^{\bullet}OH + HO_2^{\bullet} + M \rightarrow H_2O + O_2 + M$$

However, the physicochemical content of the termination mechanism via free radical decay is best described by the Satterfield–Stein scheme [4]. Meanwhile, the question about homogeneous dissociation of gaseous H_2O_2 is still open, because in this case $^{\bullet}OH$ and $HO_2^{\bullet}$ radicals are formed in the reactor volume first and only then are the chains terminated on the walls:

$$^{\bullet}OH + \text{wall} \rightarrow {}^{\bullet}OH_{(ads)}$$
$$HO_2^{\bullet} + \text{wall} \rightarrow HO_{2(ads)}^{\bullet}$$

Thereupon, in accordance with the Satterfield–Stein scheme the adsorbed $^{\bullet}OH$ and $HO_2^{\bullet}$ radicals give H_2O and O_2 as final products. In the above works the radical mechanism of H_2O_2 dissociation on the surface remained hypothetical. In the late 1970s studies were conducted that experimentally demonstrated the possibility of heterogeneous H_2O_2 dissociation [18] with the help of the kinetic method of radical freeze-out and accumulation combined with the ESR method. Later on, these results were confirmed in Refs [19–24].

Baldwin and Mayor [25–29] studied H_2O_2 dissociation in reactors treated by boric acid (the common technique of reducing the contribution of heterogeneous dissociation). They found that the order of surface and volumetric reaction by H_2O_2 equals 1, and the rate constant at 713–833 K and M = N_2 is the following:

$$k = (3.19 \pm 1.2) \cdot 10^{14} \exp\left(-\frac{196{,}460 \pm 2930}{RT}\right) \left(1/(\text{mol s})\right)$$

which correlates with the data from Ref. [14].

The absence of atomic oxygen in gaseous H_2O_2 dissociation is clearly proved in the work by Robertson [30] by the mass-spectrometric technique, which eliminates proceeding of the reaction:

$$H_2O_2 \rightarrow H_2O + O$$

As follows from the above analysis, gaseous H_2O_2 dissociation at temperatures above 673 K proceeds in the reaction volume by the radical mechanism and, probably, with chain termination on the reactor walls. At lower temperatures the reaction mostly proceeds on the walls.

Thus at the present time, gaseous H_2O_2 dissociation is one of the most well-studied reactions and, therefore, its mechanism can be presented with the following kinetic parameters with some confidence [31]:

	lg*A*	*E*, kJ/mol	
$M + H_2O_2 \rightarrow 2^{\bullet}OH + M$	$17.08\,[cm^3/(mol\,s)]$	188.5	
$H_2O_2 + OH \rightarrow H_2O + HO_2^{\bullet}$	$13.0\,[cm^3/(mol\,s)]$	7.5	
$HO_2^{\bullet} + wall \rightarrow HO_{2(ads)}^{\bullet}$	$1.0\,(s^{-1})$	34.3	(4.1)
$^{\bullet}OH + wall \rightarrow {}^{\bullet}OH_{(ads)}$	$1.0\,(s^{-1})$	29.3	
$2H_2O_2 = 2H_2O + O_2$			

4.2 INITIATION AND INDUCTION PROCESSES INVOLVING HYDROGEN PEROXIDE

Most studies in the branch of oxidation with hydrogen peroxide are scattered. In fact, there exists no concept that would allow consideration of the majority of these processes from a unified position and that would promote understanding of the key role of H_2O_2 in natural processes, defined by its place in the redox ternary.

This chapter gives investigation results of H_2O_2 inductive action in chemical reactions. Transforming to the active form (the primary reaction), hydrogen peroxide is selectively consumed in another, conjugated reaction. Hence, reaction products are formed with respect to the class, to which the target (conjugated) reaction belongs (dehydrogenation, hydrogenolysis, oxidative fixation of molecular nitrogen, etc.). In many ways, the conversion degree and selectivity of these oxidation reactions are determined by kinetic conjugation conditions, on the one hand, providing the highest accumulation of active sites in the system due to basic reactions (H_2O_2 dissociation) and, on the other hand, the required activation degree of the substrate, transformed in the target reaction.

From these positions, let us discuss conjugated reactions of substrate oxidation with hydrogen peroxide, which may be presented by the following generalized scheme:

$$\underset{\text{actor}}{H_2O_2} + \underset{\text{inducer}}{H_2O_2} \rightarrow \underset{\text{intermediates}}{[^{\bullet}OH, HO_2^{\bullet}]} \rightarrow 2H_2O + O_2 \tag{4.2}$$

$$\Delta G_{298}^{0} = -246.4\ \text{kJ/mol}$$
$$\underset{\text{actor}}{H_2O_2} + \underset{\text{acceptor}}{Acc} \rightarrow \text{oxidation products} \tag{4.3}$$

In both processes of initiation and chemical induction active particles are generated. This is a general feature for all types of initiated and conjugated reactions. As shown in Chapter 2, the basic difference is observed from the very moment of active particle influence on the target reaction (in the case of chemical induction on the secondary reaction). Investigation of the active particle action mechanism on the target reaction gives an opportunity to determine the cases in which initiation or chemical induction is displayed.

The induction action of H_2O_2 on many reactions implemented in the temperature range 50–115 °C [32, 33] is well known. Free hydroxyl radicals can be generated in the radical polymerization of vinyl monomers using the Fenton reagent [34, 35].

In chain reactions involving short chains an increase of the initiator concentration above a definite limit is useless. In the limit, at a chain length equaling 1, the reaction transforms from a chain to a free radical type, and H_2O_2 transforms from the initiator to one of the reagents. Dolgoplosk and Tinyakova [33] note that as H_2O_2 concentration increases, polymerization is terminated, whereas low concentrations of the substance initiate this reaction.

A question therefore arises: what is the fate of active sites in such a situation? According to Ashmore [34], if other organic compounds are present in the section system, they will be oxidized. For example, 'ferrous iron—hydrogen peroxide' easily oxidizes aromatic compounds, which usually represent solvents. Thus, an interesting transfer of one reaction type (polymerization) to another (oxidation) is observed with H_2O_2 concentration change.

In chemical conjugation the primary reaction accompanies the induced reaction (which may also be non-spontaneous) from the very beginning until the very end. If the target (secondary) reaction is of the chain type, it may principally operate chains of any length, including extremely short ones. Active particles are generated with hydrogen peroxide in concentrations sufficient to provide a high rate of non-spontaneous (secondary) reaction. Therefore, regeneration of active particles in the framework of the chain mechanism is an insignificant factor. Thus, chemical conjugation allows implementation of processes involving extremely short chains, which is absolutely impossible in the case of initiation.

In reactions (4.2) and (4.3) hydrogen peroxide represents the actor and inducer simultaneously. Such duality of H_2O_2 behavior in the chemical system is displayed only in the case of its transformation to a reactive form (active particle), which preserves amphoteric properties typical of H_2O_2. In the gas phase this particle is $HO_2^{\bullet}$, the formation of which requires the presence of two H_2O_2 molecules: the actor and the inducer. On the contrary, as H_2O_2 acts as the initiator, its dissociation to $^{\bullet}OH$ radicals is enough. This process requires one H_2O_2 molecule only and, of course, amphoteric properties of H_2O_2 are not preserved. This is also the reason why the $^{\bullet}OH$ radical may not be considered as an active form of H_2O_2. Moreover, the $^{\bullet}OH$ radical is incapable of selective interaction with various substrates due to its high reactivity [36].

Experimental studies aimed at detection of chemical conjugation in gas-phase oxidation reactions with hydrogen peroxide [31, 37] were performed in a flow system, in an integral reactor (the plug flow), which construction provided for H_2O_2 injection to the reaction zone.

Enumerated below are practically important reactions conjugated to H_2O_2 dissociation (the basic reaction). Different cases with significant speeding up of the reactions and occurrence of ionic reaction pathways were determined:

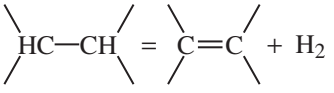

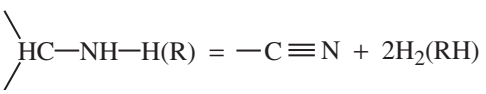

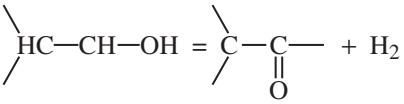

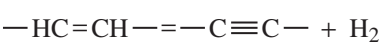

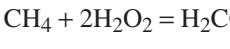

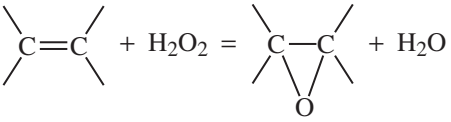

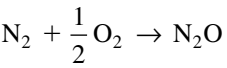

The kinetics and mechanisms of the majority of these reactions were also studied. It is shown that successful application of hydrogen peroxide is promoted by a combination of high induction properties and effectiveness and specificity of action in it, accompanied by the harmlessness of hydrogen peroxide dissociation products.

Thus, hydrogen peroxide has found application in the implementation of the well-known organic reactions in the gas phase—dehydrogenation, epoxidation, hydrogenolysis, nitrile formation from *N*-alkylbenzene, nitrogen fixation, etc.

4.3 THERMODYNAMIC ASPECTS OF CHEMICAL CONJUGATION

As mentioned in Chapter 2, there is the actual question about detection of a thermodynamic condition of conjugated oxidation of various substrates with hydrogen peroxide required for quantitative characterization of conjugation from the energy positions. For this purpose, let us show data on several non-spontaneous reactions, stimulated by chemical conjugation:

	ΔG^0_{298}, kJ/mol	
$C_6H_5C_2H_5 \rightarrow C_6H_5C_2H_3 + H_2$	83.0	(4.4)
$C_2H_5OH \rightarrow CH_3CHO + H_2$	34.8	(4.5)
$C_6H_5Cl \rightarrow C_2H_3Cl + H_2$	111.4	(4.6)
$N_2 + \frac{1}{2}O_2 \rightarrow N_2O$	59.5	(4.7)

For reactions implemented with free energy increase the source of work is required. It is common knowledge that in the reaction system consisting of the overall reactions (4.2) and

(4.3) such a source is presented by the induction reaction (4.2): free energy released at gaseous H_2O_2 dissociation by scheme (4.1) must be greater than the energy absorbed in the induced reaction (4.3).

In particular, let us concentrate on molecular nitrogen oxidative fixation, shown by reaction (4.7). Deficiency of free energy required for its implementation may be compensated by free energy of H_2O_2 dissociation, which indicates a possibility of reaction (4.7) running via conjugation. However, the use of thermodynamics gives no possibility to prove the reaction conjugation, i.e. it represents the necessary, but not sufficient, condition.

The authors of the present monograph have performed thermodynamic studies of various reactions of molecular nitrogen oxidative fixation [38]. These reactions may be executed at conjugated binding of nitrogen with hydrogen peroxide. If it is even suggested that atomic oxygen is somehow formed in H_2O_2 dissociation process (for example, on reactor walls, though this formation in the volume and on the walls is of extremely low probability), which under definite conditions is able to bind N_2 in the form of nitrous oxide, then the rate of nitrogen fixation will be negligibly low. However, oxidative fixation of nitrogen becomes principally possible in the case of chemical induction and conjugated reaction implementation under rather soft conditions for such reactions. The energetic efficiency of N_2O formation compared with the other reactions of oxidative binding of nitrogen was also observed.

Thermodynamic calculation results are shown in Table 4.1. For reaction (5), the main parameters are the following: free energy variation: 5165 kJ, equilibrium constant at 600 °C: $3.4 \cdot 10^{-3}$ and the reagent conversion to reaction products is negligibly low. Much less favorable is the equilibrium state in the reaction (6). Therefore, both reactions are not practically executed. Reaction (6) described in the monograph by Zeldovich *et al.* [39] and in the article by Anbar [40] runs at a temperature above 1273 K with nitric oxide formation by the mechanism, which includes elementary stages with atomic oxygen participation. However, atomic

Table 4.1

Thermodynamic data and equilibrium yield calculations

Reaction	Thermodynamic parameters		Equilibrium yield[a]
	ΔG^0_{873} (kJ)	K^a_p	
1. $H_2O_2 \rightarrow H_2O + \frac{1}{2}O_2$	−143.7	$2.1 \cdot 10^9$	1
2. $N_2 + H_2O_2 \rightarrow N_2O + H_2O$	−6.3	13	0.6
3. $N_2 + H_2O_2 \rightarrow N_2O + 2H_2O + \frac{1}{2}O_2$	−150.4	$3.8 \cdot 10^9$	1
4. $N_2 + O \rightarrow N_2O$	−49.0	38	0.9
5. $N_2 + \frac{1}{2}O_2 \rightarrow N_2O$	51.5	$3.4 \cdot 10^{-3}$	~0
6. $N_2 + O_2 \rightarrow 2NO$	157.5	$1.3 \cdot 10^{-9}$	~0

[a] At 1 atm pressure and 873 K.

oxygen may cause nitrous oxide formation with higher yield at lower temperatures. The fact of N_2O formation from N_2 and atomic oxygen is experimentally proved and thermodynamically possible. Therefore, reaction (4) in Table 4.1 should be taken into account when considering the oxidative fixation mechanism, where atomic oxygen is formed.

All of the above actualizes the question about detection of thermodynamic conditions for conjugation reactions (4.2) and (4.7). Thermodynamic study of these reactions shows that the under-mentioned conditions (refer to Table 4.1) are quite executable and the equilibrium yield of N_2O, for example, equals 60%, whereas in the overall reaction (3) it equals 100%, but this reaction not known to be conjugated.

Let us consider reactions (4.2) and (4.7). Basing on the following expression:

$$A = RT \ln\left(K_p C_{A_1}^{v_1} C_{A_2}^{v_2} C_{A_3}^{-v_3} C_{A_4}^{-v_4}\right)$$

deduced for the chemical reaction:

$$v_1 A_1 + v_2 A_2 = v_3 A_3 + v_4 A_4$$

the following chemical affinity equations will be obtained:

$$A_1 = RT \ln\left(K_p C_{H_2O_2} C_{H_2O}^{-1} C_{O_2}^{-0.5}\right)$$
$$A_2 = RT \ln\left(K_p C_{N_2O}^{-1} C_{N_2} C_{O_2}^{0.5}\right)$$

Kinetic equations for reactions (4.2) and (4.7) (with respect to reverse reactions) are shaped as follows [29, 41, 42]:

$$w_1 = \vec{w} - \overleftarrow{w} = \vec{k}_1\left(C_{H_2O_2} - K_p^{-1} C_{H_2O_2} C_{O_2}^{0.5}\right) \tag{4.8}$$

$$w_2 = \vec{w} - \overleftarrow{w} = \overleftarrow{k}_2\left(C_{N_2} C_{O_2} K_p - C_{N_2O}\right) \tag{4.9}$$

where $\vec{k}_1 = 10^{13} \exp\left(-\dfrac{201120\,\text{J}}{RT}\right)(\text{s}^{-1})$

and $\overleftarrow{k}_2 = 10^{9.6} \exp\left(-\dfrac{219556\,\text{J}}{RT}\right)(\text{s}^{-1})$

where

Concentrations of reagents and products in reactions (4.2) and (4.7) were determined from their known conversions in the equilibrium state (refer to Table 4.1). From the above expressions (4.8) and (4.9) the following values are deduced [38]:

$$A_1 = 149744; w_1 = 14.3$$
$$A_2 = -199523; w_2 = 0.17 \cdot 10^{-14}$$
$$A_1 w_1 = 21.4 \cdot 10^5 \gg 0; A_2 w_2 = -3.39 \cdot 10^{-10} \ll 0$$
$$A_1 w_1 + A_2 w_2 = 21.4 \cdot 10^5 \gg 0$$

Therefore, the restriction imposed by Prigozhin's inequality:

$$A_1 w_1 + A_2 w_2 \gg 0 \text{ [43, 44]}$$

is obeyed for the chemical system under consideration. Hence it appears that for conjugated reactions (1) and (5) (Table 4.1), the latter may run opposite to its direction without conjugation.

Thus, kinetic conditions in oxidation with hydrogen peroxide must be selected in a manner providing, on the one hand, accumulation of $HO_2^{\bullet}$ free radicals in the system in amounts required for the target (secondary) reaction execution at the maximum possible rate and, on the other hand, forming less favorable conditions for recombination of $^{\bullet}OH$ and $HO_2^{\bullet}$ radicals, which may cause their loss and induce O_2 formation.

Experimental studies, which revealed the chemical conjugation in oxidation reactions with hydrogen peroxide in the gas phase, were performed in open systems in reactors providing non-dissociated H_2O_2 supply directly to the reaction zone.

Figure 4.1 shows the design of an integral-type flow reactor, which provides non-dissociated gaseous H_2O_2 supply to the reaction zone. Hydrogen peroxide occurs directly in the pre-reaction zone through a quartz tube separately from a substrate to be oxidized.

A high linear rate of H_2O_2 supply by the quartz tube (determined experimentally for every particular reactor) usually eliminates any possibility of its dissociation. Moreover, to prevent heterogeneous decomposition of H_2O_2, in some cases the internal walls of the tube are treated with boric acid [45]. If these conditions are maintained, H_2O_2 concentration remains

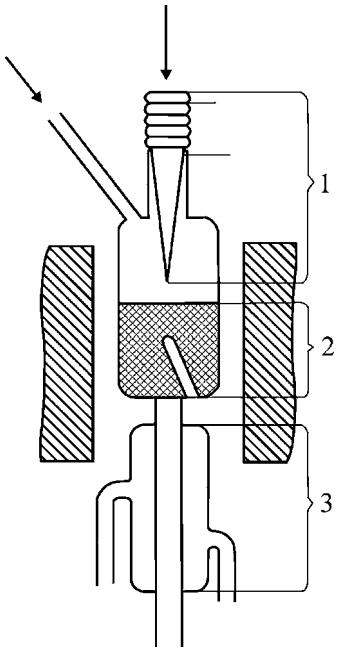

Figure 4.1 Basic diagram of the quartz flow reactor (1: heating up zone; 2: reaction zone and 3: induration zone).

at the given level. As a consequence, sufficient supply of non-dissociated H_2O_2 to the reaction zone almost eliminates the participation of molecular oxygen occurring from the outside. The initial oxygenizing substance in the form of heated-up gas is injected to the reaction zone through another quartz tube separated from H_2O_2.

The induration zone should be as close to the reaction zone as possible. Such an induration system is applied to prevent oxidation of the reaction products outside the reaction zone.

4.4 CONJUGATED DEHYDROGENATION WITH HYDROGEN PEROXIDE

4.4.1 Specific features of dehydrogenation mechanism

Initially, the investigations of organic substance dehydrogenation mechanisms in the presence of hydrogen peroxide require an answer to the question: what is responsible for (oxidative) dehydrogenations, H_2O_2 or final product of its dissociation—molecular oxygen? Conditions were formed [46, 47] providing non-dissociated H_2O_2 supply to the reactor. However, *a priori* probability of molecular oxygen participation in reaction product synthesis may not be neglected. Molecular oxygen is the recombination product of H_2O_2 decomposition intermediate products ($^{\bullet}OH$ and $HO_2^{\bullet}$), formed directly in the reaction zone. Therefore, its participation in oxidation must be determined experimentally. For this purpose, we took conjugated ethylbenzene dehydrogenation for model one. The study was performed as follows [46]:

1. Conjugated ethylbenzene dehydrogenation by 15% aqueous hydrogen peroxide.
2. Oxidative ethylbenzene dehydrogenation by oxygen in an amount equivalent to its concentration in 15% aqueous hydrogen peroxide at complete dissociation of the latter.
3. Ethylbenzene dehydrogenation in the simultaneous presence of hydrogen peroxide and molecular oxygen.

Experimental results on conjugated ethylbenzene dehydrogenation with hydrogen peroxide, shown in Table 4.2 (experiments 1 and 2), indicate that the use of 15% aqueous hydrogen peroxide promotes high yields of styrene for both the missed and the converted ethylbenzene: 36.3% and 90%, respectively[1].

Thus, for this reaction H_2O_2 is a highly active dehydrogenating agent.

In the second series of experiments (Table 4.2, experiments 3–6) on ethylbenzene dehydrogenation by molecular oxygen, styrene yields were much lower than in the first series. On the quartz reactor walls condensation product precipitation in amounts up to 1.7% was observed. Moreover, if molecular hydrogen was absent in the products of conjugated dehydrogenation, the total amount of hydrogen equals 78–82% of the whole volume of gaseous products (2.2% in total products).

Analysis of the results of this series of experiments leads to the conclusion that, in conditions of high-temperature oxidation of hydrocarbons by oxygen, the latter is a less active dehydrogenating agent and splits the process into several parallel reactions.

[1] Hereinafter, reaction product yields are given in weight percents (wt. %).

Table 4.2

Oxidative ethylbenzene dehydrogenation (EB) results

Number	Volume rate of EB supply (ml/(ml h)	$[H_2O_2]^a$ (%)	O_2 consumption (l/h)	Volumetric ratio of the components		Reaction products (%)	
				EB:H_2O_2	EB:O_2	Styrene	EB
1.	0.2	15	–	1:3	–	36.3	60.9
2.	0.4	15	–	1:3	–	35.3	62.1
3.	0.2	–	0.22	–	1:3	10.0	74.8
4.	0.4	–	0.45	–	1:3	7.4	79.9
5.	0.4	–	0.5	–	1:3	7.9	78.2
6.	0.4	–	0.5	–	1:3	8.0	78.3
7.	0.1	7.5	0.05	1:3	–	17.4	69.9
8.	0.2	7.5	0.11	1:3	–	15.0	76.2
9.	0.4	7.5	0.22	1:3	–	11.8	79.2
10.	0.4	10.0	0.45	1:3	–	12.8	78.3

Number	Reaction products (%)								Selectivity by styrene (%)
	Toluene	Benzene	CP^b	H_2	CO_2	CH_4	C_2H_6	C_2H_4	
1.	1.2	1.6	–	–	0.7	0.1	0.1	0.1	90
2.	0.8	1.8	–	–	0.8	0.1	0.1	0.1	91
3.	2.0	3.0	1.7	2.0	1.0	2.5	2.5	0.5	40
4.	0.8	1.4	1.5	2.2	1.5	2.4	2.4	0.5	37
5.	1.9	1.6	1.6	2.2	1.5	2.3	2.3	0.5	36
6.	1.7	1.8	1.6	2.2	1.5	2.3	2.3	0.5	36
7.	0.9	1.9	Traces	1.7	1.8	3.4	3.3	0.7	56
8.	0.7	2.5	Traces	1.5	1.3	1.7	1.7	0.4	61
9.	1.0	2.2	Traces	1.2	1.5	1.4	1.4	0.3	57
10.	1.0	2.1	Traces	1.5	1.6	1.2	1.2	0.3	60

[a] In aqueous solution.
[b] Condensation products.

However, the situation may arise in the system whereby H_2O_2 will display the initiating influence on oxidative ethylbenzene dehydrogenation by molecular oxygen, formed as a product of partial H_2O_2 dissociation. This question was studied in the third series of experiments (refer to Table 4.2, experiments 7–10), in which oxygen was injected together with H_2O_2 in amounts corresponding to a dissociation degree of 15% aqueous H_2O_2 equal 0.5. Moreover, in experiment 10 molecular oxygen and hydrogen peroxide were injected in equimolar amounts. As shown by the results of this series, styrene yield increased 1.5–2-fold and benzene selectivity to 56–64%; traces of condensation products were detected and the amount of H_2 formed slightly decreased.

Comparison of the data of the third experimental series with conjugated dehydrogenation results (experiments 1 and 2) indicates a quantitative difference in the composition of the reaction products. Styrene is the main product of the conjugated dehydrogenation (90–91%

selectivity). This indicates that the process mostly runs as dehydrogenation, and detached hydrogen atoms are associated to water molecules. In all experiments with O_2 participation the products contain molecular hydrogen, and styrene yield in the process is much lower.

Taken together, these investigations thus allow the statement that the conjugated dehydrogenation of hydrocarbons with hydrogen peroxide runs by a mechanism that is principally different from high-temperature oxidation by molecular oxygen. As a consequence, the conclusion is confirmed that intermediate products of H_2O_2 dissociation—free radicals $^{\bullet}OH$ and $HO_2^{\bullet}$—are responsible for the accumulation of unsaturated compounds in this chemical system [47].

The next basic aspect in the studies of dehydrogenation mechanism is the determination of the H_2O_2 interaction type with hydrocarbons. Under high-temperature oxidation conditions this interaction produces unsaturated compounds. Is this reaction the chain of a simple bimolecular type? If the process is chain, variations of experimental conditions (presence of inert diluters, small additives, treatment of the reactor surface by various salts, the effect of the 'surface:reaction zone volume' ratio—the so-called *S*/*V* factor, etc.) must significantly change the initiation and chain termination rates.

For this purpose, conjugated dehydrogenation of some alkylbenzenes was executed in reactors treated by various inorganic compounds [48]. The experimental results indicate that in all cases the reaction proceeding is highly sensitive to the reactor surface type. For example, target product yields decreased in the following sequence with respect to salt selected for treatment of the reactor:

$$B_2O_3 > \text{untreated reactor} > K_2B_4O_7 > KBr > KCl > BaBr_2$$

The results obtained [48] correlate with the data from the literature [49], which prove that a quartz surface treated with the above-mentioned salts displays different activity in $HO_2^{\bullet}$ radical recombination. This activity decreased in the reverse sequence:

$$BaBr_2 > KBr > KCl > K_2B_4O_7 > \text{untreated reactor} > B_2O_3$$

Comparison of the sequences indicates that the surfaces most active in $HO_2^{\bullet}$ radical recombination are the worst for the implementation of hydrocarbon conjugated dehydrogenation on them.

Based on these investigations, the conclusion about free radical, chain mechanism of the reaction is that its rate is mostly determined by $HO_2^{\bullet}$ radical concentration in the system [50].

The activity in this direction led to the discovery of a reaction pathway (mechanism) in dehydrogenation of various substrates involving hydrogen peroxide, which apparently may be widely applied in the interpretation of conjugated dehydrogenation of a wide class of organic substances, including those containing heteroatoms.

The possibility of synthesizing unsaturated hydrocarbons and some derivatives from them via conjugation of organics dehydrogenation and H_2O_2 dissociation reactions leads us to consider that this reaction pathway is somewhat universal. This is also confirmed by some theoretical ideas: reactions proceeding with the participation of free radicals are much more sensitive to electron density variations on substrate molecules compared with reactions in which intermediate compounds of polar origin are formed [51].

Let us discuss in general gas-phase processes of oxidative dehydrogenation of hydrocarbons involving as reagents substances that easily induce free radical transformations of substrates. Many such substances are known that dissociate to free radicals or induce free radical reactions. However, the most widespread in investigations are compounds that are able to shift dehydrogenation and cracking product ratios toward the first process.

This question is discussed in detail in the book by Skarchenko [52]. It is noted that dehydrogenation of paraffin hydrocarbons dominates by selectivity over thermal cracking in the presence of iodine or other halogens, sulfur-containing compounds, oxygen and nitrous oxide. For example, in the presence of iodine dehydration dominates in the system, whereas in the case of other additives, independently of their amounts—oxygen, ethylene oxide and nitric acid—the main shift of the process toward cracking is preserved.

Of greatest interest for investigators is the oxygen action mechanism at different temperature intervals for paraffin hydrocarbon oxidation: at 300 °C or lower oxygen-containing compounds—aldehydes, ketones, alcohols, CO_2, CO, etc.—are formed; at 500 °C or higher—cracking and dehydrogenation products are synthesized. The transition zone between the lower- and the higher-temperature oxidation falls within the interval of 350–500 °C [53]. In this zone, due to chain branching suppression by chain propagation processes, an anomalous (negative) temperature coefficient (NTC) is observed. This phenomenon is comprehensively explained using the kinetic method of radical freeze-out combined with ESR [54] and its unambiguous dependence on the ratio of $RO_2^\bullet$ and $HO_2^\bullet$ radicals formed during oxidation. It is found that reduction of the oxidation rate in the NTC zone is associated with $RO_2^\bullet$ concentration decrease. In high-temperature oxidation $HO_2^\bullet$ radicals mostly dominate, which are not formed at low temperatures.

Thus, in the range of relatively high temperatures, when oxidative dehydrogenation and cracking are the main directions of the process development, one of the basic active sites of the reagent radical transformation becomes $HO_2^\bullet$ radicals, which are produced by H_2O_2 dissociation. Therefore, the studies of oxidation of various substrates with hydrogen peroxide make the question about $HO_2^\bullet$ action mechanism on various substrates clearer.

4.4.2 Alkane and alkene dehydrogenation

Since the mid-1960s, the increasing shortage of butylenes and, especially, isoamylenes as initial materials for divinyl and isoprene production has encouraged investigations into the one-stage oxygen dehydrogenation of butane and isopentane. Of increased difficulty is work with relatively low-reactive paraffins. Their activation requires high temperatures, which usually reduces the selectivity of the process. Comprehensive data on catalysts for oxygen dehydrogenation of paraffin hydrocarbons and the influence of industrial parameters on the process are given in Ref. [55].

Oxidative catalytic dehydrogenation of butane in the presence of iodine and oxygen (other halogens may also be used) is effectively executed with divinyl yields up to 40% with selectivity approaching 70%. However, selectivity is low and, moreover, used halogens are not ecologically friendly oxidants. Oxidants that do not transform into aggressive substances and toxicants are most attractive for application. Hydrogen peroxide in particular conforms to these requirements, being the oxidant that dissociates to ecologically

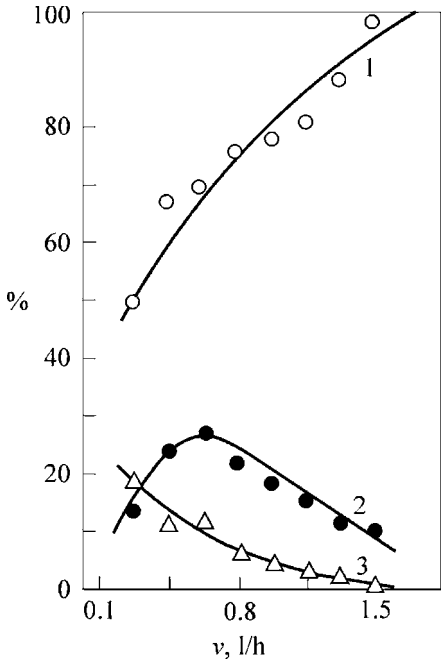

Figure 4.2 Dependence of conjugated dehydrogenation selectivity (1), isoprene yield (2) and total side products yield (3) on isoamylenes and nitrogen mixture rate. $T = 553$ °C; volume ratio C_5H_{10}:N_2 = 1:10; 20% aqueous H_2O_2 rate is 0.185 ml/h.

friendly substances—H_2O and O_2, and possesses high effectiveness in its interaction with butane [56, 57].

With the aim of creating a mainly new method for the one-stage divinyl synthesis from butane and isoprene synthesis from isoamylenes, conjugated dehydrogenation of alkanes and alkenes was investigated [58, 59]. Studies of kinetic regularities for butane conjugated dehydrogenation with hydrogen peroxide in the presence of nitrogen as a diluter revealed the way of effective divinyl synthesis at 590 °C with a yield of about 30% and selectivity approaching 85%.

Figure 4.2 shows the kinetic dependencies of target and side product yields, and the process selectivity on the volume rate of isoamylenes and N_2 mixture in the presence of 20% aqueous H_2O_2. It can be concluded from these data that H_2O_2 participates in the conjugated dehydrogenation of isoamylenes as dehydrogenating agents. The conversion degree of some isomers per corresponding initial isomer equals: 32 mol.% for 3-methylbutene-1, 38 mol.% for 2-methylbutene-1 and 30 mol.% for 2-methylbutene-2. The composition of side products in the experiment with the highest yield of isoprene (25 mol.% with 75% selectivity) is the following: 6.1 mol.% divinyl, 1.2 mol.% α-butylene, 3.4 mol.% β-*cis*-butylene and 1.3 mol.% β-*trans*-butylene. Molecular hydrogen (H_2) and oxygen-containing compounds (including CO and CO_2) were not detected in the reaction products. Coke formation of the reactor walls was not also observed.

Thus, it may be concluded that conjugated dehydrogenation of isoamylenes similar in isomeric composition to industrial fractions gives a high isoprene yield. Despite relatively

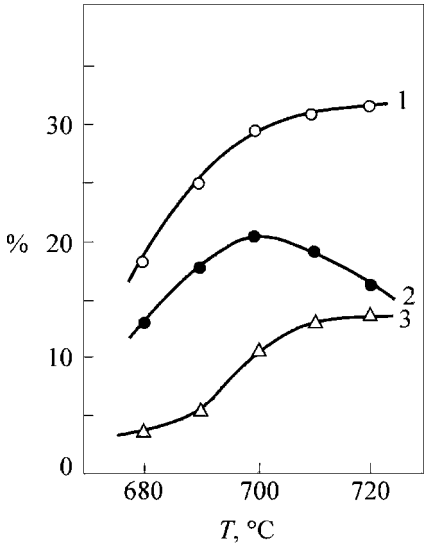

Figure 4.3 Temperature dependencies of propylene conversion (1), allene (2) and methyl acetylene (3) yields in conjugated dehydrogenation of propylene. Time of contact $t = 0.045$ s.

low selectivity, the advantage of this reaction before oxidative catalytic dehydrogenation is in the absence of process suppression by reaction products and the lack of a need for expensive catalysts, as well as in the process independence of isomeric composition of raw materials.

The efficiency of conjugated dehydrogenation of olefins with hydrogen peroxide was also confirmed in studies of propylene dehydrogenation to allene [60]. The well-known process of propylene oxidative dehydrogenation to allene in the presence of iodine [61] at 625–700 °C gives low yields of the target product (3.6% allene) at low selectivity of the process (6%).

In the case of conjugated dehydrogenation of propylene under optimal conditions (700 °C), allene and methyl acetylene yields equal 20% and 10%, respectively (Figure 4.3) [62]. Methyl acetylene yield increases with temperature, whereas allene yield decreases.

There are many other examples of olefin derivative production by the conjugated dehydrogenation technique. For example, because chlorolefin yield growth produced by existing technology [63] is limited by chlorine loss for side products, there are good prospects for the development of chloroalkane dehydrogenation methods, which do not display this disadvantage. Oxidative degradation of ethyl chloride in air above a catalyst (chromium oxide applied on Al_2O_3) [64] displays low yield and selectivity, because at the optimal temperature of 367 °C the vinyl chloride yield equals 17% at 21% conversion. Some of these disadvantages are eliminated in a newly designed method for vinyl chloride production. It is conjugated dehydrogenation of ethyl chloride with hydrogen peroxide [65]. Under optimum conditions at 450 °C vinyl chloride yield reaches 37.8% at 52% conversion, which is twice as high as the parameters of the process described above. It should be taken into account that haloalkanes of more complex structure may also be synthesized in this reaction.

4.4.3 Naphthene hydrocarbon dehydrogenation

The study of conjugated dehydrogenation of naphthene hydrocarbons with hydrogen peroxide was implemented for model compounds—cyclopentane and cyclohexane. The products of their incomplete dehydrogenation and the final products (cyclopentadiene and benzene) possess high activity. This property as well as the possibility of producing many valuable substances from them are attracting great attention from investigators.

Among primary works on cyclopentane dehydrogenation, the studies by Zelinsky [66] should be mentioned. He showed that at 300 °C and atmospheric pressure, in the presence of platinum and palladium catalysts, cyclopentane and its homologs are unable to hydrogenate. Multiple investigations of the cyclopentane dehydrogenation process were carried out by Shuikin and Naryishkina [67]. For example, they first showed that under definite conditions platinum charcoal is able to catalyze dehydrogenation of cyclopentane and its homologs with 9–17% conversion. They have also found that activated coal is able to catalyze dehydrogenation of penta- and hexatomic naphthenes at increased temperatures: at 600 °C, cyclopentane conversion approached 18%. However, it is indicated that applied catalysts were easily poisoned, and their lifetime was short. Shuikin [67, 68] carried out one more study of cyclopentane dehydrogenation, which displayed cyclopentane and cyclopentadiene yields above chromia-alumina-potassium catalyst equaling 7% and 4%, respectively.

Wanae and Walters [69] studied the thermal degradation of cyclopentane in a static system at 438–548 °C and under pressure of 38–244 mmHg. It is shown that under these conditions the cyclopentane conversion degree was below 25%. There are some other works [70, 71] devoted to cyclopentane dehydrogenation; here, however, the cyclopentadiene yield does not exceed 3–11%.

Studying cyclopentane pyrolysis processes, Frey [72] has found that in a hollow reactor about 5.4% of olefins and diolefins are formed, among which only 2.7% are formed by cyclopentadiene and 66.5% of cyclopentane remain unconverted. Thermal degradation of cyclopentane was thoroughly studied by Japanese scientists [73].

A brief review of the literature shows that cyclopentadiene synthesis by thermal or catalytic dehydrogenation is unsuccessful either due to low yields or because of the short lifetime of applied catalysts. In this connection, searching for new effective pathways of cyclopentane dehydrogenation is the principal task both in scientific and applied aspects. It is to be expected that application of the gas-phase conjugated dehydrogenation method, which allows process execution under atmospheric pressure, will give the desired result: high yields and selectivity. Since cyclopentane dehydrogenation is a consecutive process and passes through cyclopentene formation, in order to simplify kinetic studies of the reaction, conjugated dehydrogenation of cyclopentane with hydrogen peroxide was studied [74], including the effect of factors such as raw material volume rate, component ratio, temperature, H_2O_2 concentration and quartz reactor surface conditions on the process run.

As observed from these investigations, the initial material velocity variation from 0.05 to 0.52 ml/(ml h) at 450 °C and 500 °C does not noticeably affect cyclopentadiene yield. At higher temperatures (550 °C and 600 °C) the reaction rate significantly increased within the range of the volume rates mentioned and a higher yield of the target product was reached.

However, the reaction rate sharply increases with temperature (from 450 °C to 600 °C). For example, for the volume rate of 0.08 ml/(ml h) and the component ratio C_5H_8:20% H_2O_2 = 1:3,

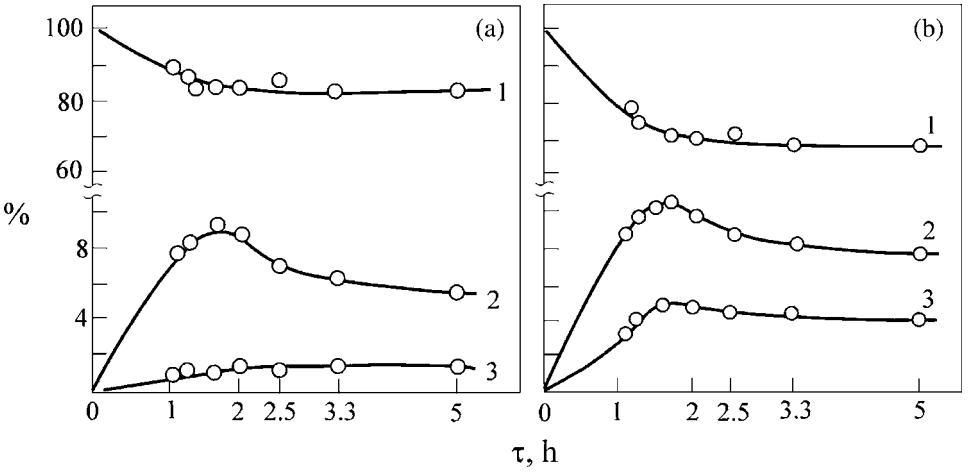

Figure 4.4 Kinetic curves for conjugated dehydrogenation of cyclopentane at (a) 450 °C and (b) 600 °C (1: unreacted cyclopentane; 2: cyclopentene yield (per involved cyclopentane) and 3: cyclopentadiene yield (per involved cyclopentane)).

cyclopentadiene yield is 7.46% at 450 °C and 40.6% at 600 °C. The data obtained also indicate, besides dehydrogenation, proceeding of cyclopentene decyclization with temperature increase. In this process the following compounds are synthesized: CH_4, C_2H_4, C_3H_6, CO_2.

These studies determined the range of parameters of cyclopentane conjugated dehydrogenation with hydrogen peroxide [75].

Figure 4.4 shows that accumulation of cyclopentene as an intermediate product increases in the initial period only and reaches its maximum when accumulation and consumption rates equalize. Further on, cyclopentadiene yield is equalized with increasing conditional contact time τ ($\tau = 1/\upsilon$, where υ is the liquid cyclopentane volume rate). For example, at 600 °C cyclopentene and cyclopentadiene yields equaling 10.5% and 5%, respectively, at 54.35% selectivity are reached at $\tau = 1.66$ h. The rates of cyclopentene and cyclopentadiene synthesis increase first and reach their maxima at the inflection point. Cyclopentene, cyclopentadiene, methane, ethylene, carbon dioxide and unidentified hydrocarbons in the amount about 5% are synthesized in the reaction.

The kinetic curves in Figure 4.4 show that the cyclopentene consumption rate decreases insignificantly after reaching its maximal yield. This testifies to an insufficient concentration of H_2O_2 at the stage of cyclopentadiene formation. The kinetic curves of cyclopentadiene accumulation are S-shaped, which indicates autocatalytic type of the process with an autoacceleration period from the beginning of these curves to inflection points.

Of special interest for petrochemical and organic synthesis is the implementation of thermodynamically hindered reactions, among which incomplete benzene hydrogenation or incomplete cyclohexene and cyclohexadiene dehydrogenation should be mentioned. Cost-effective methods of cyclohexene production would stimulate the creation of new processes of phenol, cyclohexanol, cyclohexene oxide, pyrocatechol synthesis, cyclohexadiene application in synthetic rubber production, and a possibility for designing caprolactam synthesis from cyclohexene and cyclohexadiene via combined epoxidation. At present, the most

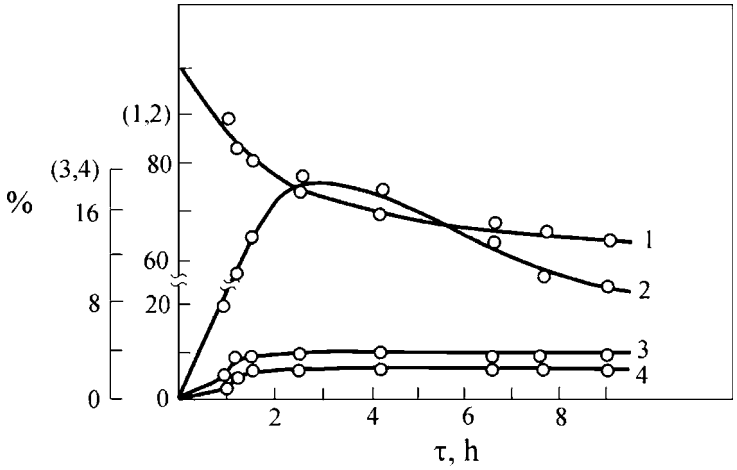

Figure 4.5 Kinetic curves of cyclohexane conjugated dehydrogenation (1: cyclohexane; 2: cyclohexene; 3: benzene and 4: cyclohexadiene).

widespread pathways for cycloolefin synthesis are heterogeneous catalytic and oxidative dehydrogenation on solid catalysts. However, the methods for cycloolefin synthesis described in the literature do not find industrial application due to their multistage type, small yields and low selectivity.

Minachev *et al*. [76] studied oxidative dehydrogenation of cyclohexane on zeolite cationic forms at 300–475 °C, the main reaction product of which is cyclohexene. Cyclohexadiene and CO_2 are also formed, and at long-term contacts benzene is detected. Cyclohexene yield and selectivity of the reaction depend on zeolite structure and composition, reaction temperature and oxygen:cyclohexane ratio in the reaction mixture. Among alkaline cationic forms of zeolite, the highest cyclohexene yield (21%) is observed for NaA zeolite (66% selectivity).

As shown above, the principal task is the search for mainly new effective ways of cyclohexene and cyclohexadiene synthesis. Based on the execution principles of conjugated oxidation reaction, the authors of the current monograph performed conjugated dehydrogenation of cyclohexane with hydrogen peroxide to cyclohexene and cyclohexadiene [77–79]. The reaction was studied in the temperature range of 450–650 °C proceeding with various volume rates and ratios of initial reagents.

Figure 4.5 shows that the process is of consecutive autocatalytic type with a self-acceleration period (kinetic curves for cyclohexadiene and benzene). Under optimal conditions, target product yields approach 19.4% for cyclohexene, 3.4% for cyclohexadiene and 2.4% for benzene; selectivity by target products is almost 100%. Cyclohexene is synthesized in the temperature range of 450–500 °C. As temperature increases from 560 °C to 650 °C, cyclohexene is added to by other dehydrogenation products: cyclohexadiene and benzene. It follows that cyclohexane conjugated dehydrogenation with H_2O_2 can be aimed at cyclohexadiene synthesis with respect to the process conditions. An insignificant amount of carbon dioxide (mostly as traces) was detected in gaseous reaction products.

One may suggest that the reaction products (cyclohexene, cyclohexadiene and benzene) are synthesized in a step-by-step dehydrogenation of higher saturated analogs. In this connection,

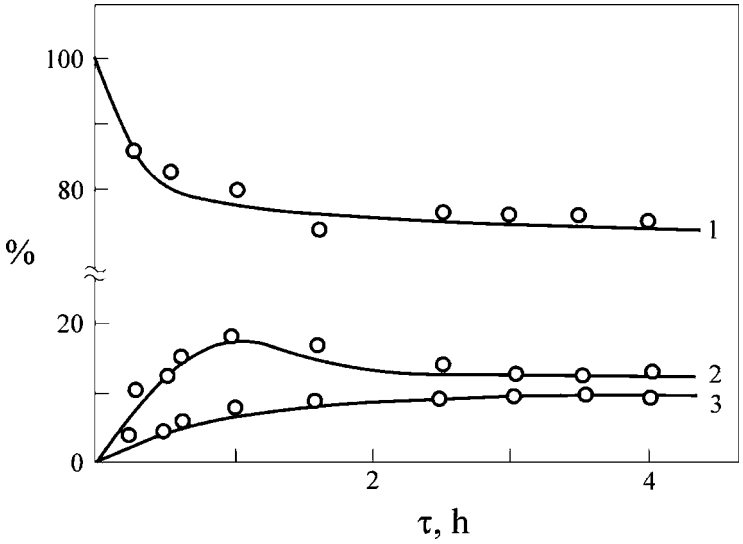

Figure 4.6 Kinetic curves of cyclohexene consumption and reaction product accumulation at 580 °C (1: cyclohexene consumption; 2: cyclohexadiene accumulation (kinetic curve) and 3: benzene yield).

of interest is the study of cyclohexene dehydrogenation to cyclohexadiene as one of the intermediate stages of cyclohexane conjugated dehydrogenation [80]. It has been shown [81] that the highest yields of target products in conjugated dehydrogenation of cyclohexane with hydrogen peroxide are obtained for 20% aqueous H_2O_2 and the volumetric ratio cyclohexane:aqueous H_2O_2 = 1:3. Therefore, conjugated dehydrogenation of cyclohexane with hydrogen peroxide was studied under analogous conditions: 500–630 °C temperature interval and various cyclohexene volume rates [80, 81].

Figure 4.6 presents kinetic curves of cyclohexadiene accumulation at an optimal temperature of 580 °C. It is shown that in the initial period cyclohexadiene accumulation as an intermediate product is intensified until its consumption and accumulation rates are equalized and cyclohexadiene concentration reaches the maximum. Further increase of conditional contact time reduces cyclohexadiene concentration. For example, at 580 °C and $\tau = 0.7$ h the cyclohexadiene yield is 17.5%, decreasing to 9.5% with τ increased to 2.5 h. Under optimal conditions ($T = 580$ °C, cyclohexene volume rate 1.4 ml/(ml h), cyclohexene:20% aqueous H_2O_2 = 1:3), yields were 17.1% for cyclohexadiene and 5.8% for benzene. The reaction selectivity approached 100%. The entire process was of a consecutive autocatalytic type.

A possibility of intensifying the reaction by silica glass granules was also determined (yields are 25.7% for cyclohexene and 7% for cyclohexadiene).

4.4.4 Alkylbenzene dehydrogenation

The above discussed were several aspects of ethylbenzene conjugated oxidation (dehydrogenation) with hydrogen peroxide. This reaction was studied in detail in many investigations

[31], because its final product—styrene (as well as other vinyl-aromatic hydrocarbons)—has found wide industrial application, for example, in the production of synthetic rubbers, blow and heat-resistant plastics.

The main production techniques for alkenyl benzenes both in Russia and abroad are heterogeneous catalytic and oxidative dehydrogenation of alkylbenzenes. There processes have been comprehensively studied from various positions [55, 82], so we will not dwell on them here. We will refer only to one of the oxidative dehydrogenation processes, in which the bound form of oxygen (SO_2) is used as the oxidant. It is soft oxidant compared with O_2 and J_2, and this allows increase of the process selectivity. In fact, it had already been noted in the 1940s [31] that sulfur dioxide significantly intensified dehydrogenation processes. In the late 1960s, the interest in these processes increased owing to works by Adams [83], who disclosed sulfur dioxide effectiveness as the dehydrogenating agent in the example of ethylbenzene oxidative dehydrogenation by this compound. In his experiments styrene yield reached 80–85% and selectivity approached 90%. Carbonaceous deposit formation is explained by the presence of reaction products in the mixture—H_2S, S and SO_2 reagent—which induces quick deactivation of the catalyst [84]. On the contrary, in the following works [85] it is stated that styrene synthesis is significantly intensified on the condensation products, deposited on γ-Al_2O_3 during oxidative dehydrogenation of ethylbenzene by sulfur dioxide. In this case, the catalytic action mechanism of the condensation products is analogous to oxidation catalysis on polyconjugated polymers, and catalytic activity of the condensation products depends on their formation conditions. Under optimal conditions at $T = 550\,^{\circ}C$, styrene yield on Mg–Al-oxide catalyst approaches 85 mol.% and selectivity raises to 94–95 mol.%. Ethylbenzene oxidative dehydrogenation with participation of SO_2 and other sulfur-containing compounds is described by the gross equation as follows:

$$3C_6H_5C_2H_5 + SO_2 \rightarrow 3C_6H_5C_2H_3 + 2H_2O + H_2S$$

As is obvious, hydrogen sulfide active under current conditions is one of the reaction products. Its aggressiveness, the ability to interact with SO_2 even under natural conditions, promotes sulfur accumulation in the system, affects synthesis of condensation products and can alter their catalytic activity. Therefore, despite high effectiveness, oxidative catalytic dehydrogenation of ethylbenzene by sulfur dioxide may be found unacceptable for production management in relation to ecology and protection of the environment.

Thus, the tasks of ecologically friendly oxidant selection for the production of alkenyl-aromatic hydrocarbons, modernization of common catalytic dehydrogenation of alkyl-aromatic hydrocarbons are of the highest importance. The purpose is to raise selectivity of the processes to 100%. The most likely processes are oxidative dehydrogenation applying bound forms of oxygen (as the factor increasing selectivity) combined with the new principles, such as chemical conjugation, which may help in creation and development of a principally new, up-to-date technique.

The authors [86] studied ethylbenzene conjugated dehydrogenation with H_2O_2 in the quartz reactor in the temperature range of 500–640 °C, at liquid ethylbenzene volume rates of 0.2–0.8 ml/(ml h) and volumetric ratios $C_6H_5C_2H_5$:15% aqueous H_2O_2 from 1:1 to 1:4, and the influence of *S/V*-factor on the process. Under the conditions mentioned, the reaction runs with a high conversion degree, 40% yield of the target product and high selectivity (up to 90%).

Diethylbenzenes (DEB) dehydrogenation with hydrogen peroxide was studied [88, 89] in the broad ranges of initial reagent volume rate, reagent ratio, temperature and *S/V*-factor variations.

Initial DEB had the following isomeric composition: 53.5% *m*-DEB, 40.9% *o*- and *n*-DEB, and 5.6% additives (the rest for losses).

Figure 4.7 shows that accumulation of vinylethylbenzenes as intermediate products at the initial stage of the process increases until equalizing their accumulation rate and liquid DEB consumption rate at conditional contact time $\tau = 3.3$ h and reaching a maximum of vinylethylbenzene concentration. Further increase of contact time τ reduces vinylethylbenzene concentration. For example, at 640 °C *m*-isomer yield and a total yield of *o*- and *n*-isomers of vinylethylbenzene (calculated per corresponded initial isomers) at $\tau = 5$ h equal 40.5% and 25.9%, respectively.

The rates of divinylbenzenes and vinylethylbenzenes synthesis increase first with their concentrations and reach a maxima at the inflection point. However, since H_2O_2 takes part in the synthesis of divinylbenzenes and its concentration is decreased with the reaction run, the inflection point on the kinetic curve gives divinylbenzene concentration below the real maximum.

Figure 4.7 shows that after reaching the maximum yield the consumption rate of vinylethylbenzenes decreases only slightly. This indicates deficient H_2O_2 concentration at the stage of divinylbenzene synthesis. The S-shape of the kinetic curves obtained testifies to the autocatalytic type of the process with the autoacceleration period from the beginning of these curves to inflection points.

Experimental data [90] that give an opportunity of analyzing kinetics of the above processes were also obtained for conjugated dehydrogenation of vinylethylbenzenes.

In the example of DEB dehydrogenation with hydrogen peroxide, a possibility of reaction intensification on the quartz glass was determined [91].

The high efficiency of hydrogen peroxide in conjugated dehydrogenation of ethyltoluenes was also shown [92]. For example, under optimal conditions at 640 °C the yield of vinyltoluenes equaled about 40% with the reaction selectivity approaching 90%. For industry, of interest is conjugated dehydrogenation of diisopropylbenzene industrial fraction containing 57% *n*-diisopropylbenzene and 34% *n*-diisopropylbenzene [93]; *n*-diisopropylene benzene in dehydrogenate reaches 30%. Comparison of the results obtained with the data on diisopropylbenzene catalytic dehydrogenation on *Shell-105* catalyst leads to the conclusion that the yield and selectivity are much higher for conjugated dehydrogenation of *n*-diisopropylbenzene.

4.4.5 Dehydrogenation and oxidation of heterocyclic compounds

At the present time, the economic demand for nitrogen-containing heterocyclic compounds is prompting the search for new effective techniques for their production. The known techniques of pyridine bases production are not effective enough and display several disadvantages associated with deactivation of catalysts, application of diluters, polymerization inhibitors and reduced pressure that makes the process more complicated. Therefore, synthesis of pyridine bases and their derivatives (N-oxides, in particular) via rather simple transformations, for example, dehydrogenation of appropriate higher saturated compounds, is the actual point. For instance, implementation of the chemical conjugation mechanism in 4-ethylpyridine

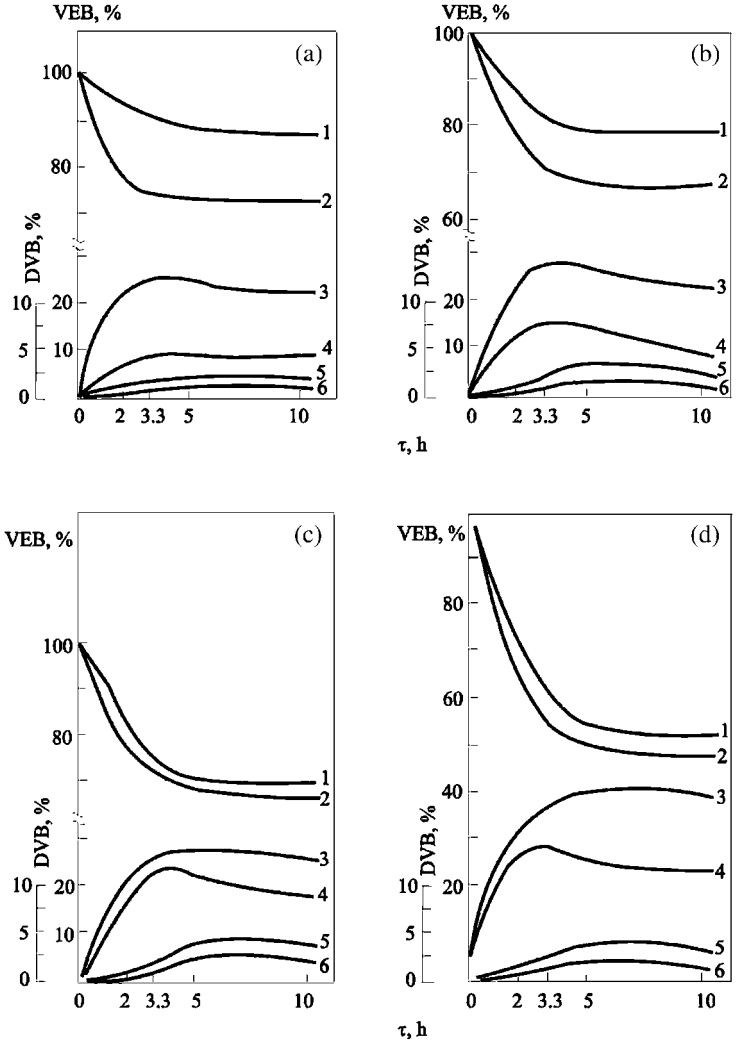

Figure 4.7 Kinetic curves for DEB conjugated dehydrogenation. Experimental conditions: volumetric ratio DEB:20% H_2O_2 = 1:3: (a) 580 °C; (b) 600 °C; (c) 620 °C and (d) 640 °C (1: unreacted *o*- and *n*-DEB; 2: unreacted *m*-DEB; 3: *m*-vinylethylbenzene (VEB) yield per used *m*-DEB; 4: *o*- and *n*-VEB yields per used *o*- and *n*-DEB; 5: *o*- and *n*-divinylbenzene (DVB) yields per used *o*- and *n*-DEB and 6: *m*-DVB yield per used *m*-DEB).

Conjugated dehydrogenation of isopropylbenzene was planned [87] by the method of experiments with the minimal number of tests. Total yields of styrene and α-methylstyrene per injected isopropylbenzene were taken for optimized parameters, because these monomers are equally valuable. At the gradient motion (T = 640 °C) the highest yield of the target products (styrene + α-methylstyrene) equaled 56.8% with about 90% selectivity. Further gradient motion was of no practical interest due to a process selectivity decrease down to 80%.

(EP) and piperidine oxidation helps in synthesizing 4-vinylpyridine (VP), 4-VP N-oxide and pyridine.

The results of studies of this reaction in a hollow reactor show high selectivity up to 640 °C in the range of 4-EP volume rate from 0.065 to 0.78 h^{-1} and at 4-EP:20% aqueous H_2O_2 = 1:3 [94]. Under optimal conditions at 620 °C, 4-VP yield equals 20.9% with 92% selectivity. Injection of quartz granules to the reactor raises the yield to 44.3% and selectivity to 96%. This is because the total surface on which, probably, the chain initiation reaction:

$$H_2O_2 + M \rightarrow {}^{\bullet}OH + M\text{-}OH$$

proceeds, increases.

Concentration of active sites increases with the *S/V*-factor, all other parameters being equal. As a consequence, the target product yield also increases. Therefore, all following experiments were implemented in a reactor filled with quartz granules [95]. A temperature increase above 640 °C abruptly reduces 4-VP yield and the process selectivity, and increases the amounts of side products (pyridine, in particular), which indicates that under definite conditions in the presence of hydrogen peroxide alkylpyridine dealkylation reaction may be implemented.

As shown in the literature [96, 97], at low-temperatures liquid hydrogen peroxide participates in N-oxidation of pyridine bases, and the process is catalyzed by organic acids and their anhydrides.

Of practical interest is synthesis of N-oxides without the mentioned acids and anhydrides, because they include odd ingredients, which themselves and their degradation products may hardly be eliminated. Low-temperature 4-EP dehydrogenation with hydrogen peroxide was carried out in a quartz reactor [98]. As determined in the study of temperature influence in the range of 200–400 °C on conjugated N-oxidation, the highest yield of 4-VP N-oxide (Figure 4.8) is observed at 300 °C. Temperature increase from 200 °C to 300 °C increases the target product yield due to active site generation rate increase at thermal dissociation of hydrogen peroxide. Apparently, low yields of 4-VP N-oxide at temperatures below 300 °C are associated with predominant heterogeneous mechanism of hydrogen peroxide decomposition to final products (H_2O and O_2). As a result, concentration of active particles in the volume decreases. At a temperature increase from 300 °C to 400 °C the yield and selectivity of N-oxide synthesis also decreases: at 400 °C the yields are 19.8% for 4-VP, 9.1% for pyridine and about 7% for N-oxide.

Thus, in low-temperature oxidation (200–400 °C) of 4-EP with hydrogen peroxide the main direction is 4-VP N-oxide synthesis with 33% yield at 300 °C and selectivity above 98%.

Finally, the above investigations show that conjugated 4-EP oxidation with hydrogen peroxide with respect to reaction conditions may be targeted both to 4-VP and 4-VP N-oxide synthesis.

The reaction of piperidine conjugated dehydrogenation with hydrogen peroxide [99] opens the way to dehydrogenation of natural compounds, which include piperidine fragments. As shown by experimental data, pyridine yield increases from 45% to 65.2% with hydrogen peroxide concentration from 20% to 25%, respectively, with reaction selectivity above 98%. A further increase of H_2O_2 concentration reduces pyridine yield to 59%. It follows from these

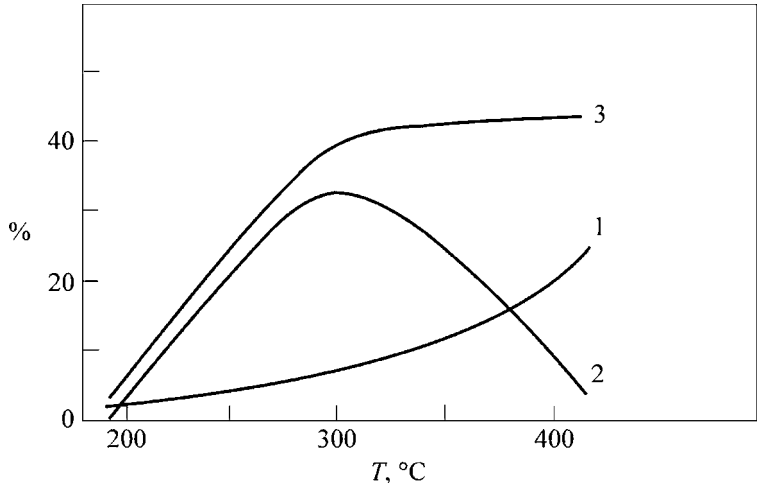

Figure 4.8 Temperature dependence of EP conjugated dehydrogenation product yield. Molar ratio 4-EP:30% H_2O_2 = 1:3, 4-EP volume rate is 0.045 h^{-1} (1: 4-VP; 2: 4-VP N-oxide and 3: total conversion of 4-EP).

results that conjugated dehydrogenation with hydrogen peroxide can be successfully applied to analogous transformation in fragments of natural compounds.

Of interest is the application of the conjugated dehydrogenation technique to transformations of more complex objects, for example, *N*-alkylanilines, for *N*-ethylaniline dehydrogenation, in particular. Besides illustrating new possibilities of the technique mentioned, all the above would help to solve several theoretical questions associated with *N*-alkylaniline behavior under reaction conditions.

The possibility of *N*-ethylaniline conjugated dehydrogenation [100] with a high conversion degree, 50–60% benzonitrile yield and 85% selectivity is shown. Figure 4.9 shows the kinetic curves of this process. In the initial period of the reaction, benzonitrile yield increases with conditional contact time. After a definite period, τ_{cond} increase to 5 h changes just slightly the target product yield. With a further increase in the contact time, the benzonitrile yield even decreases slightly.

Based on the investigations performed and analysis of data from the literature, a plausible mechanism of *N*-ethylaniline conversion to benzonitrile is suggested [101]. According to this mechanism, the conversion passes through several intermediate stages. The first stage represents conjugated dehydrogenation of *N*-ethylaniline with the participation of a $HO_2^{\bullet}$ radical—the product of H_2O_2 dissociation. Then under experimental conditions intermediate dehydrogenation products (*N*-vinylaniline and *N*-ethylidenaniline) are quickly dealkylated producing isonitrile group, which easily isomerizes to nitrile (—C≡N) group at raised temperatures.

The suggested mechanism of *N*-ethylaniline conversion to benzonitrile is proved by conjugated dehydrogenation of *N*-methylaniline and benzylaniline in the presence of H_2O_2 [102]. Hence, data from the literature were taken into account, which confirmed the mechanism

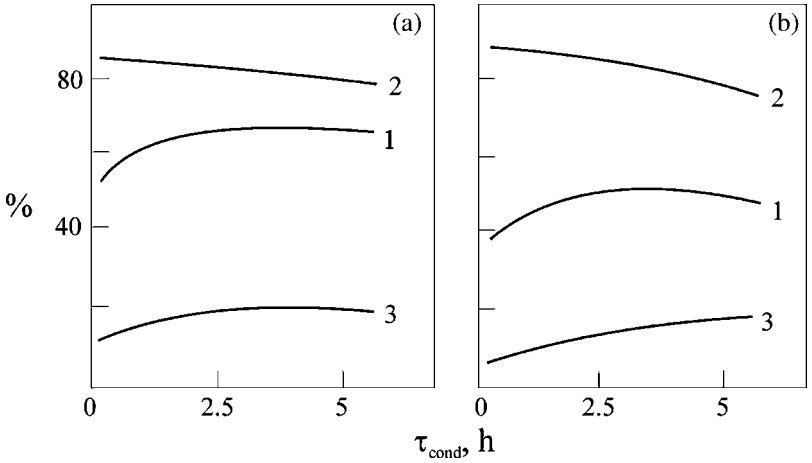

Figure 4.9 The dependence of yields and selectivity of *N*-ethylaniline dehydrogenation on conditional contact time: (a) 600 °C and (b) 640 °C (1: benzonitrile; 2: selectivity and 3: side product yield).

of benzonitrile formation from these products. For instance, conjugated dehydrogenation of benzylamine with hydrogen peroxide produces benzonitrile indicating, therefore, that the main direction of the reaction is C—N bond dehydrogenation. The formation of significant amounts of benzonitrile in *N*-methylaniline reaction with hydrogen peroxide confirms the suggestion that the first stage of *N*-ethylaniline conjugated dehydrogenation is dehydrogenation by C—N bond, but not dealkylation with forming methane. Methane is formed at the second stage. On the contrary, conjugated dehydrogenation of *N*-methylaniline would possess no benzonitrile, and a great quantity of methane would be synthesized.

These experiments with chemical conjugation have helped to develop a new highly efficient method of benzonitrile production. This provides a new effective engineering decision for benzonitrile production, which does not require application of an ammonia–oxygen explosive mixture and simplifies the technological maintenance of the process. Moreover, conjugated dehydrogenation allows the obtaining of various deficient or difficult to synthesize aromatic nitriles derived from corresponding *N*-alkylanilines.

4.4.6 Dehydrogenation of alcohols

Oxidative dehydrogenation of alcohols is a new approach in the development of industrial processes for the synthesis of aldehydes and ketones [103–105]. In this regard, the technologically most suitable is the method of acetaldehyde synthesis in the presence of melted vanadium oxide, alkaline metals with promoting additives, alkaline metal sulfates or chlorides as catalysts [105]. The target product yield equals 65.9% per used alcohol at 69.2% conversion. The disadvantage of the method is the relatively low yield of the target product

and the complication of the process by using expensive catalysts. To simplify the process and increase product yield, oxidative dehydrogenation of ethanol was carried out with H_2O_2 participation by the conjugated mechanism [106]. It is shown that in the temperature range 450–550 °C variations of reaction parameters may provide for reaching high acetaldehyde yields using no catalysts (up to 87% with 97% selectivity or higher). The great effectiveness of H_2O_2 application to oxidation of alcohols may also be illustrated by the example of *sec*-butanol dehydrogenation to methyl ethyl ketone (MEK). At present, oxidative dehydrogenation is implemented with gold and silver as catalysts [107, 108]. In the temperature range 520–600 °C MEK yield equals 70–85% with 93–96% selectivity. Despite high selectivity and conversion degree of alcohol, the occurrence of various side products such as acetaldehyde, acetone, diacetyl, CO, CO_2 makes additional technological difficulties for MEK extraction from the reaction mixture.

Though precious metal catalysts can be eliminated from the liquid-phase oxidation of *sec*-butanol [109], nevertheless, the process parameters (23.5% MEK yield and 79.4% selectivity) are lower compared with catalytic processes. Moreover, at 115–130 °C process implementation requires application of 9–20 atm pressure and, to reduce the induction period, the use of initiating additives.

Conjugated dehydrogenation of *sec*-butanol with hydrogen peroxide is free from the majority of these disadvantages. Hydrogen peroxide allows selectivity increase to 99%, simplifies technology of the process by implementing it under atmospheric pressure and neglects catalysts and special additives. The process is executed in the gas phase at 400–500 °C, giving a yield of 26–44% [110].

Thus, it may be concluded that dehydrogenation of organic substances in the homogeneous phase by the radical-chain mechanism using chemical induction possesses several essential advantages, for example:

- No catalysts and associated costs for their synthesis and regeneration are required.
- Kinetics and mechanism of the reaction may be studied on the basis of well-developed, clearly formulated statements of fundamental investigations in the branch of radical-chain processes.
- Kinetic models of reactions reproduce well the experimental results and, consequently, allow conscious control over rates and directions of the reactions studied.
- High selectivity of the process gives an opportunity to exclude several processing steps, in which noticeable amounts of hardly separable components are produced. Moreover, selectivity increase provides for fuller use of raw material resources of the process.
- The specific feature of the suggested method is invariance of its relative yields independently of reactor productivity. This is of extreme importance for transferring the laboratory results to industry without multistage pilot investigations. Thus, a mathematical model of the process allows reliable reproduction of laboratory data on any larger scale, whereas heterogeneous catalytic processes of monomer production require tests on pilot sets and consecutive correction of the mathematical model, using up time and resources.
- Conjugated dehydrogenation makes it possible to obtain unsaturated compounds, which either cannot bez synthesized by traditional methods or their synthesis is of little effectiveness.

4.5 CONJUGATED OXIDATION WITH HYDROGEN PEROXIDE

4.5.1 Methane and methanol oxidation to formaldehyde

Formaldehyde is one of the most important and large-tonnage products in the chemical industry and is widely used in all branches of organic synthesis. Despite the great amount of formaldehyde produced, growing industrial demands for this valuable monomer are not being fully met. The slow pace of formaldehyde production is due to several reasons, basic among them being the high cost of the existing production technique (oxidative dehydrogenation of methanol in the presence of silver or iron–molybdenum contacts), required by the deficiency of initial reagent and catalysts, and the multistage nature of the process.

Formaldehyde production from natural gas is one of the most promising directions in modern chemical industry. However, the industrial realization of producing formaldehyde from methane is hampered by severe disadvantages, among which the most important are the low yields of the target product and multiple side reaction products. Therefore, the task in hand is the development of direct selective oxidation of methane to formaldehyde without formation of admixtures, which require additional thorough purification.

In this connection, it should be expected that the application of chemical conjugation will allow oxidation of methane to formaldehyde with hydrogen peroxide according to a new reaction mechanism.

In recent decades many investigations have been devoted to incomplete methane oxidation. The intense interest in the development of this method is encouraged by the fact that methane reserves are almost unlimited and can meet the demand of the national economy for methanol and formaldehyde. The study of methane oxidation by oxygen in the presence of small H_2O_2 additives [111] indicates a hydrogen peroxide promoting effect on formaldehyde formation. The intermediate particles formed in the reaction are $HO_2^{\bullet}$ and $CH_3O_2^{\bullet}$ free radicals, transformations that give the final reaction product—formaldehyde. In this reaction H_2O_2 is synthesized in very small amounts [111]. The main oxidant is molecular oxygen and the oxidation mechanism with H_2O_2 additives differs just slightly from O_2 oxidation mechanism without H_2O_2. Methane oxidation to formaldehyde is a highly effective conjugated process proceeding in the presence of H_2O_2 [112, 113].

Figure 4.10 shows temperature influence on the process results: formaldehyde yield reaches its maximum (about 40%) with temperature raise to 520 °C and total methane conversion increase. Above 520 °C, CO and CO_2 are detected in reaction products. Their formation rates noticeably increase with temperature. The occurrence of these compounds in the system is explained by sequential formaldehyde transformation to intense degradation products in the high temperature range. After-oxidation of methanol synthesized in the system also contributes to formation of these products.

The results of experiments on the contact time effect on methane oxidation reaction (Figure 4.11) show that formaldehyde yield increases to some extent (39%) with the contact time. Maximal yield of formaldehyde is reached at $\tau = 1.2$ s, which is optimal for execution of the reaction at selected parameters. As the contact time exceeds 1.2 s, side products occur in the system: CO, CO_2 and CH_3OH; concentration of the last compound reaches its maximum at $\tau = 1.4$ h. The above results show that methane is oxidized to formaldehyde

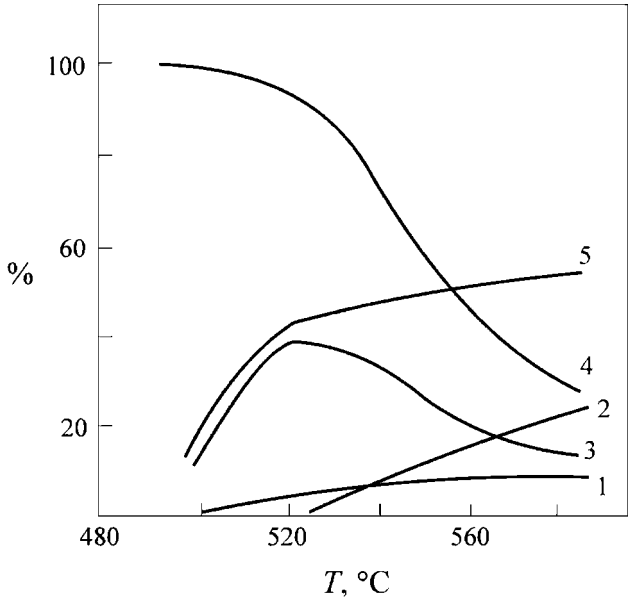

Figure 4.10 Temperature dependencies of reaction product yields and selectivity at methane oxidation: molar ratio CH_4:25% H_2O_2 = 1:1, τ = 1.2 s (1: methanol; 2: CO + CO_2; 3: formaldehyde; 4: selectivity by formaldehyde and 5: total methane conversion).

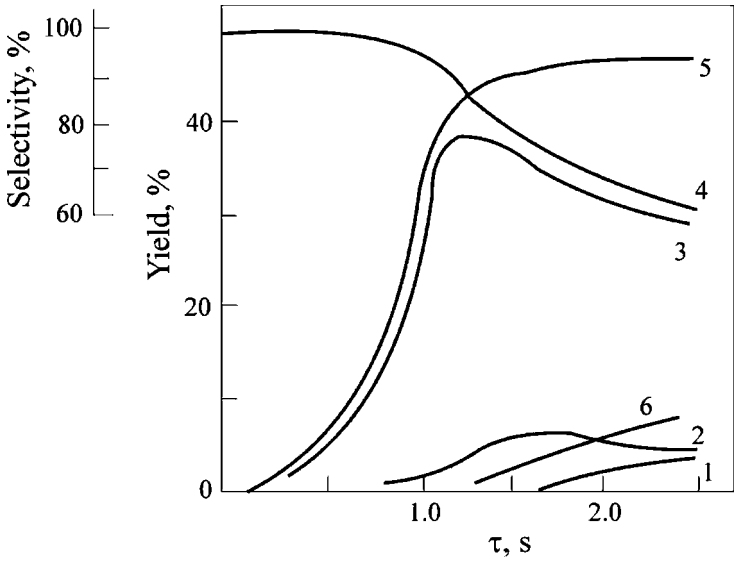

Figure 4.11 Contact time dependence of reaction product yields and selectivity at methane oxidation: T = 520 °C; molar ratio CH_4:25% H_2O_2 = 1:1 (1: CO_2; 2: methanol; 3: formaldehyde; 4: selectivity by formaldehyde; 5: total methane conversion and 6: CO).

with almost 100% selectivity and without side product formation under the following conditions: T = 500–520 °C, contact time τ = 0.88–1.1 s, 15–25% aqueous H_2O_2.

From the above data it may be concluded that under optimal conditions formaldehyde is synthesized directly from methane without intermediate methanol formation. At higher temperatures (above 520 °C) and long-term contact, formaldehyde is synthesized according to parallel scheme with further transformation to severe degradation products, CO and CO_2. For example, the target product is mostly after-oxidized to CO and its contribution to the CO_2 formation rate is low, whereas for methanol the opposite situation is observed. This conclusion may be indirectly proved by the results of special tests [113, 114] carried out on conjugated oxidation of methanol without methane and by its low additions to the reaction mixture CH_4–H_2O_2–H_2O (Table 4.3). It is observed that the CO_2 amount formed from methane is much greater than the CO amount. As CH_3OH is added to the reaction mixture, the following side products are formed in low amounts: C_2H_6, C_3H_6 and C_3H_8.

It also follows from these experiments that the formation of formaldehyde in low amounts is explained by the presence of methanol in the initial mixture, because under current conditions H_2O_2 is mostly consumed for its deep oxidation. Similar results were obtained at methanol oxidation with hydrogen peroxide in the absence of methane (Table 4.3, tests 9–11). Comparison of these data with the results of methane oxidation with hydrogen peroxide under identical conditions (tests 1 and 2) indicates qualitative and quantitative differences in reaction products.

Based on the above results, it may be concluded that selective oxidation of methane to formaldehyde with hydrogen peroxide is implemented by a mechanism different from that in which methanol is formed as the intermediate oxidation product [115].

Thus, a predominantly new means of formaldehyde production by direct methanol oxidation with hydrogen peroxide under homogeneous conditions without methanol formation stage was suggested.

Methanol oxidation with hydrogen peroxide was studied under conditions equal to methane oxidation [116]. The results given in Figure 4.12 show that the maximal formaldehyde yield is determined at a high temperature range (580–600 °C). The amount of formaldehyde synthesized is affected by the ratio of components in the alcohol–hydrogen peroxide mixture: for all temperatures maximal yield is observed for the ratio CH_3OH:H_2O_2=1:0.5.

Experiments determining temperature dependence of methanol oxidation with hydrogen peroxide were carried out under the same conditions. Figure 4.13 shows methanol conversion and formaldehyde yield (10%) maxima at 590 °C. A further increase of temperature decreases formaldehyde content in the reaction mixture. This testifies to the process proceeding by the consecutive scheme with further transformation of formaldehyde, CO and CO_2 concentration increasing simultaneously.

Thus, the decrease of formaldehyde yield with increasing temperature after reaching the yield maximum is explained by an increase of CO concentration in the products of its conversion. CO_2 yield is greater than CO yield, hence, in low temperature ranges its amount increases proportionally with temperature, but at 600 °C the formation rate is stabilized. At high temperatures (600–620 °C) the amount of CO_2 remains constant, and above 620 °C CO_2 yield may be reduced. As a consequence, CO_2 is mostly formed at severe oxidation of methanol, but not from CO, because in that case CO concentration increase in the contact zone would increase CO_2 yield at 610–620 °C.

Table 4.3

Conjugated oxidation of methane and methanol by 25% hydrogen peroxide

Test number	n	CH_4 (l/h)	H_2O_2 (ml/h)	CH_3OH (ml/h)	Reaction products (%)				$^aCH_4$ (%)	CH_3OH (%)	γ (%)
					CH_2O	CH_3OH	CO_2	CO			
CH_4—H_2O_2—H_2O (520 °C)											
1	1:0.24	1.2	1.44	–	6.8	–	–	–	6.8	–	100
2	1:0.5	1.2	3.2	–	14.0	1.0	–	–	15.3	–	97.5
3	1:1	1.2	5.74	–	39.0	2.4	–	–	41.4	–	94
4	1:1.2	1.2	7.2	–	35.5	7.5	–	3.2	45.5	–	78
5	1:1.6	1.2	9.5	–	30.5	13.0	2.4	5.6	50.0	–	60
CH_4—H_2O_2—H_2O (500 °C)											
6	1:1	1.0	4.79	–	10.2	–	–	–	10.2	–	100
7	1:1	1.2	5.74	–	14.6	–	–	–	14.8	–	99
8	1:1	1.4	6.72	–	19.1	0.6	–	–	19.7	–	97
CH_3OH—H_2O_2—H_2O (520 °C)											
9	1:0.25	–	1.44	1.44	4.5	–	2.0	–	–	6.5	69
10	1:0.5	–	2.32	1.44	9.2	–	4.0	1.6	–	14.0	67.5
11[b]	1:1	–	4.72	1.44	7.9	–	5.8	2.5	–	16.2	48.8
CH_4—CH_3OH—H_2O_2—H_2O (520 °C)											
12[c]	0.7:0.39:1	0.8	5.74	0.72	2..5	–	5.9	0.5	4.3	16.1	–
13[c]	0.8:0.2:1	0.82	5.74	0.36	3.7	–	4.3	1.6	6.2	13.4	–

Notes: [a]CH_4 is methane conversion; γ is selectivity; n is molar ratio of the following reaction products (1–8: CH_4:H_2O_2; 9–11: CH_3OH:H_2O_2 and 12, 13: CH_4:CH_3OH:H_2O_2).

[b]Products contain 1.3% HCOOH.

[c]Products contain 0.9% and 0.7% C_2H_6, 0.17% and 0.1% C_3H_6, 0.25% and 0.2% C_3H_8, respectively.

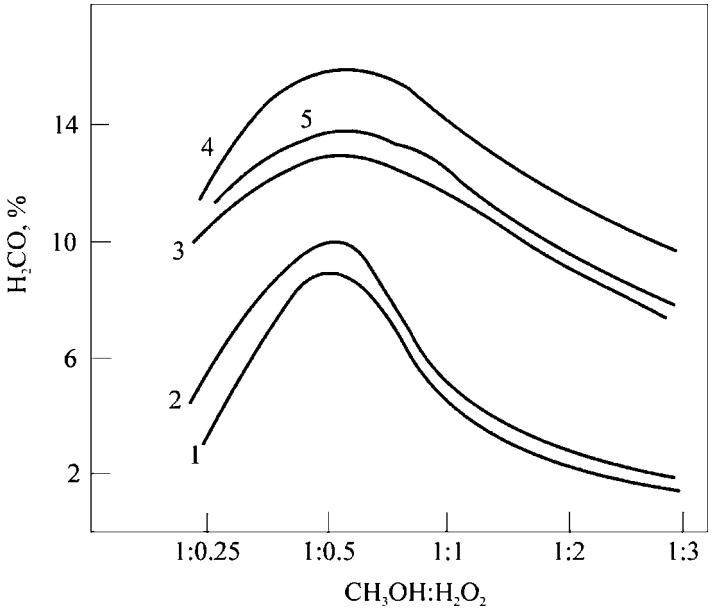

Figure 4.12 The dependence of formaldehyde yield on molar ratio $CH_3OH:H_2O_2$ at different temperatures: 25% aqueous H_2O_2, v_{CH_3OH} = 1.44 ml/h, $v_{H_2O_2}$ = 2.32 ml/h (1: 500 °C; 2: 520 °C; 3: 580 °C; 4: 590 °C and 5: 600 °C).

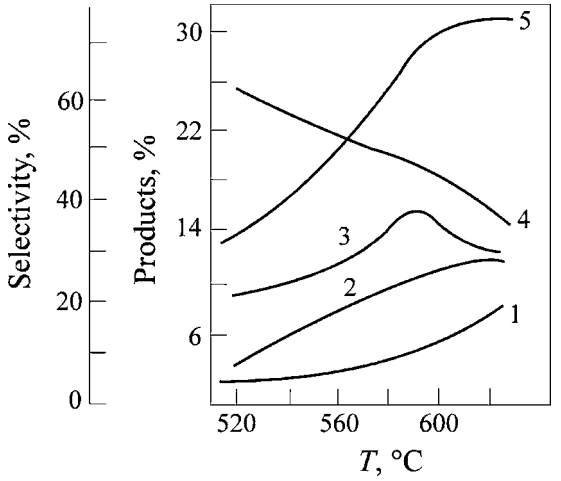

Figure 4.13 Temperature dependence of reaction product yields and selectivity at methanol oxidation: molar ratio CH_3OH:25% aqueous H_2O, v_{CH_3OH} = 1.44 ml/h, $v_{H_2O_2}$ = 2.32 ml/h (1: CO; 2: CO_2; 3: formaldehyde; 4: selectivity and 5: total methanol conversion).

Let us note once again that comparison of the results on methanol oxidation with hydrogen peroxide with methane oxidation data under atmospheric pressure (refer to Table 4.3, Figures 4.10 and 4.11) indicates significant differences in these processes. Methane is oxidized to formaldehyde at a higher rate and higher selectivity than at methanol oxidation. Low methanol yields at methane oxidation compared with formaldehyde confirm parallel proceeding of formaldehyde and methanol synthesis from methane.

4.5.2 Direct pressurized oxidation of methane to methanol with hydrogen peroxide

In the theory and practice of free radical-chain reactions the influence of increased pressure on the oxidation mechanism is known. For example, based on direct single-stage oxidation of methane to methanol with hydrogen peroxide under pressure [117, 118], a new highly selective and high-conversion process allowing pressure and temperature reduction, and processing simplification was developed for a pilot unit. It was found experimentally that methane is oxidized according to a chemical conjugation mechanism in which the inducing intermediate is free hydroxyl radical. Kinetic simulation of methane oxidation with hydrogen peroxide disclosed the most probable free radical mechanism. This kinetic model conforms to experimentally determined regularities in a wide range of oxidation parameter variation under pressure. Kinetic analysis applying the determinant equation to a description of interrelated and synchronized reactions of H_2O_2 dissociation and methane oxidation gives an opportunity to make qualitative and quantitative assessment of chemical induction efficiency ($D = 0.18$) and indicates the great potential to intensify the induction effect.

Methane is a practically inexhaustible natural material from which many valuable organic compounds are produced. One of the products is methanol used in the production of formaldehyde, synthetic rubber, acetic acid, methyl acetate, etc. In this connection, investigators have aimed their recent efforts at intensifying existing production techniques and developing new economic processes for its production. Creation of such technologies will solve the actual problems of the modern chemical industry related to natural gas conversion to more easily transportable fuels, industrial supply of valuable semiproduct and expanded production of high-octane fuels [119].

Besides gasoline, methanol is the most promising alternative fuel. Unfortunately, there are only a few industrial units all over the world that process natural gas to motor fuels based on its preliminary conversion to synthetic gas. This is a multistage, power-consuming process, which requires high pressure and temperature, expensive catalysts, etc.

In addition to the search for ways of creating economic technology for natural gas processing to methanol with an intermediate synthesis gas stage, recent investigations have been aimed at direct methane oxidation by pure oxygen or in air [120, 121].

Direct one-stage oxidation of methane to methanol is performed by two methods: catalytic and thermal. Modernization of the process of methane conversion to methanol using various catalysts is ineffective, because in this case methane conversion is usually below 13%. At the present time, methane conversion to methanol has been raised to 24% [122]; however, this is still insufficient for an economic assessment of the process. Hence, thermal

oxidation of methane to methanol is being studied well. Unfortunately, the conditions under which conversion and selectivity of the process may reach acceptable levels have not yet been determined. This is the basic reason for the delay in manufacturing application of this technique.

Analysis of the literature on natural gas oxidation to methanol indicates the following main points:

1. Operating industrial facilities (units), designed for natural gas oxidation to methanol, do not currently meet the demand of national economies in methanol and other chemical products.
2. Currently existing industrial processes for methanol production are multistage, expensive, complicated for design and engineering, and require high investment for production intensification.
3. Studies aimed at creating methods for direct methane oxidation to methanol are not implemented in industry because of high pressure, relatively low yields of target products and great amounts of side products.

In this connection, one of the significant future ways of solving the problem of methanol production may be the creation of largely new selective techniques of natural gas oxidation with hydrogen peroxide.

Typical advantages of non-catalytic conjugated processes are:

- No catalysts are required; therefore, all associated expenses for their synthesis and regeneration are eliminated.
- High selectivity of the process allows elimination of many process operations releasing multiple hardly separable components.
- Selectivity increase also allows fuller consumption of raw materials.
- Simplified technology.

The reaction of methane oxidation with hydrogen peroxide under pressure was studied on an automated micropilot flow unit with integral reactor based on the standard double reactor OL 105/02 system. The OL 105/02 system is usually used in studies of pressurized homogeneous and heterogeneous processes in gas and liquid [123]. The micropilot unit has two equal reactors of 250 cm^3 volume and is equipped with standard metering, recording and control instruments.

Aqueous hydrogen peroxide of a given concentration was poured into a vessel with a piston pump, which continuously injected it into the reactor. Methane was supplied from a gas cylinder with pressure sensors at the output. It was purified and dried, then heated and injected into the reactor. The reaction system is of a homogeneous (non-catalytic) flow type and operates in plug flow mode.

A gas–liquid mixture yielded from the reactor is immediately quenched in a flow cooling device, then occurs in a separator, where it is finally separated into gas and liquid reaction products.

The bulk of experimental data makes possible the detection of several nontrivial kinetic regularities, among which the synchronized curves shown in Figures 4.14–4.17 are of special

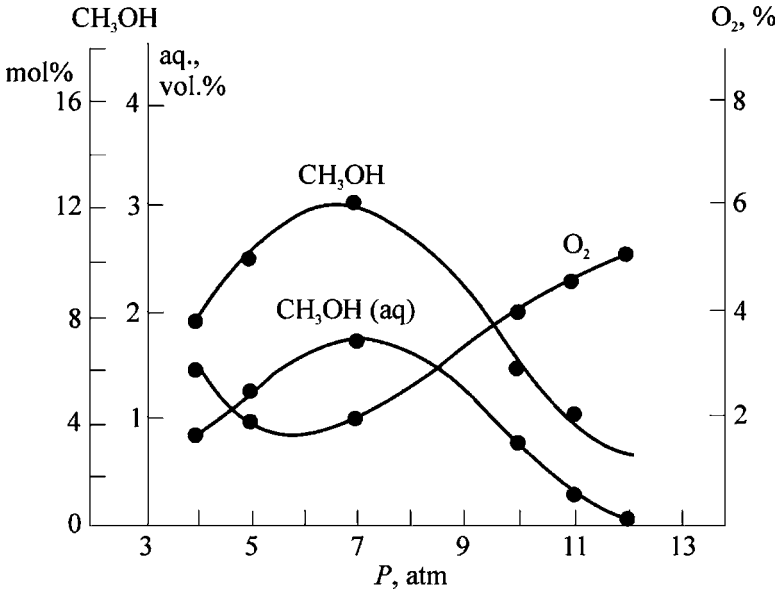

Figure 4.14 Pressure dependencies of reaction product accumulation.

importance. These curves demonstrate the inductive effect of the primary (inductive) reaction of hydrogen peroxide dissociation on the secondary (induced) reaction of CH_4 hydroxylation.

Comparison of the pressure-dependent molecular oxygen accumulation and CH_4 consumption (or CH_3OH accumulation) curves in Figure 4.14 shows a correspondence of the O_2 accumulation minimum to the maximum of CH_4 conversion to CH_3OH.

Figure 4.15 presents experimental data on the contact time influence on the methane oxidation process. At contact time $\tau = 0.95$ s, the maximum methanol yield is observed. Further increase of this parameter reduces methanol yield.

Analyzing the dependencies deduced, it may be concluded that the yield of oxygen formed at hydrogen peroxide dissociation decreases with the increase in methanol yield.

The influence of temperature on the reaction product yield is shown in Figure 4.16. The studies were implemented for a temperature range of 350–475 °C. Hence, values of the remaining parameters were kept identical for all experiments. It is clear from the curves that maximal methanol yield falls within the range of 400–425 °C. Methanol yield decreases with temperature increase, which is explained by recombination of reacting radicals and H_2O_2 dissociation rate increase.

Owing to almost 100% selectivity of the reaction chemical interference [9] is clearly illustrated in these plots: intensification of O_2 formation causes simultaneous decrease of CH_4 conversion to CH_3OH, and vice versa. Chemical interference determinant (D), deduced from the equation:

$$D = v\left(\frac{r_1}{r_{CH_4}} + \frac{r_2}{r_{CH_4}}\right)^{-1} \tag{4.10}$$

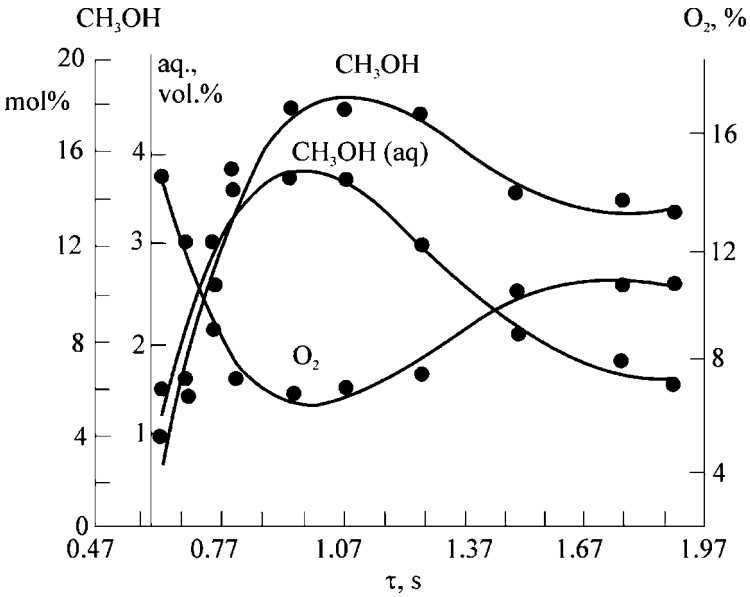

Figure 4.15 Dependence of methane oxidation on contact time.

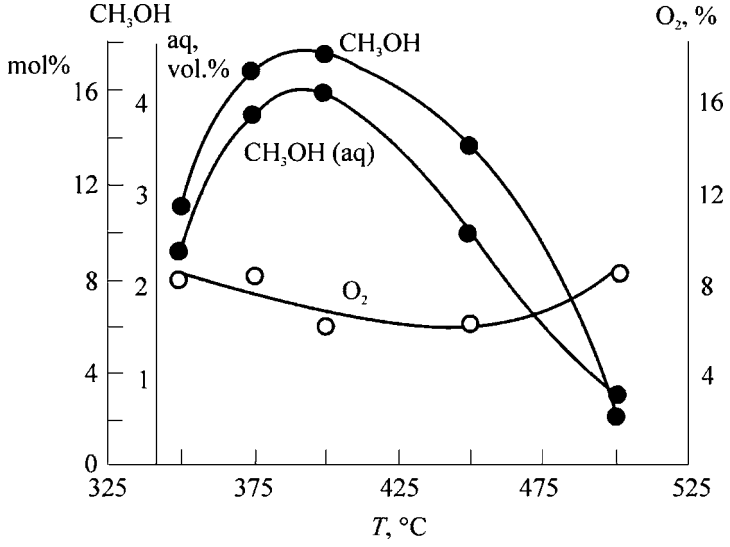

Figure 4.16 Temperature dependence of methanol yield.

(where r_1, r_2 and r_{CH_4}. are consumption rates of actor (H_2O_2), inducer (H_2O_2) and acceptor (CH_4); ν is the stoichiometric number, currently equals 1) equals 0.18 under current test conditions corresponding to the minimum of O_2 formation and CH_3OH maximum. On the chemical interference scale this value falls within the area of conjugated reactions [7]. This

value quantitatively characterizes the H_2O_2 induction effect on CH_4 oxidation and indicates high potential for intensification of the induction effect in the system studied (theoretically, *D* may increase to 1, but in practice try to reach at least 0.5). There are experimental, mostly kinetic methods, which allow manipulation of the rates of conjugated reactions [124].

Gross equations proceeding in the reaction system of conjugated process can be expressed as follows:

$$\underset{\text{actor}}{H_2O_2} + \underset{\text{inducer}}{H_2O_2} = 2H_2O + O_2 \quad \text{(primary reaction)} \tag{4.11}$$

$$\underset{\text{actor}}{H_2O_2} + \underset{\text{acceptor}}{CH_4} = CH_3OH + H_2O \quad \text{(secondary reaction)} \tag{4.12}$$

where H_2O_2 is both the actor and the inducer and CH_4 is the acceptor.

However, Equations (4.11) and (4.12) do not show how inter-reaction communication is set. For this purpose, highly active intermediate compounds should be identified. They will detect connection channels between reactions (4.11) and (4.12).

It is known [9] that the primary reaction of H_2O_2 dissociation generates to the system highly active sites of two types—$^{\bullet}_{2}OH$ and $HO^{\bullet}_{2}$ free radicals, which easily react with methane molecule (substitution reaction) under current experimental conditions forming new free radicals—$CH^{\bullet}_{3}$ and $CH_3O^{\bullet}$. High selectivity of methane oxidation to methanol allows us to limit consideration of the reaction mechanism by free methyl and methoxy radicals. A series of experiments was devoted to the study of the reactor wall origin effect on methane oxidation. As follows from experimental data (Figure 4.17), quartz walls cause

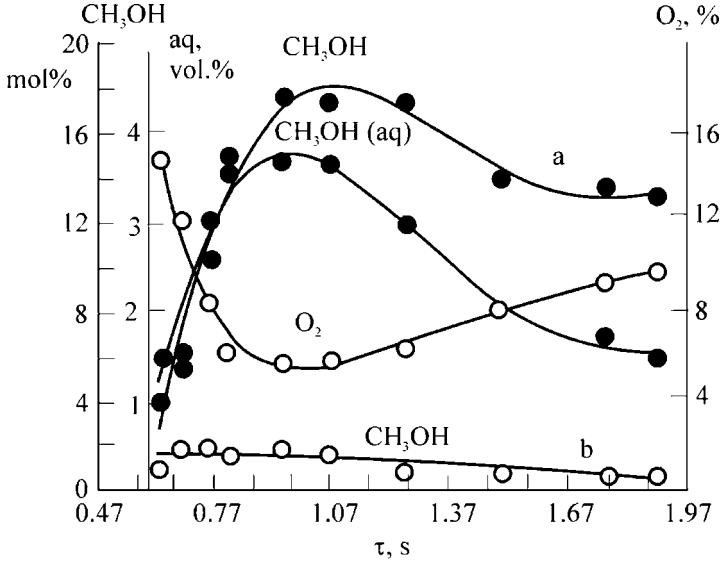

Figure 4.17 Dependence of reaction product yield on contact time with reactor walls, a. CH_3OH yield in a reactor filled with quartz granules; b. CH_3OH yield in an empty quartz reactor.

a significant influence on the course of oxidation and unambiguously indicate free radical-chain oxidation type.

4.5.3 High-temperature oxidation of natural methane with hydrogen peroxide

The increasing demand for hydrogen and CO_2 in the metallurgic, petroleum refining and power industry requires the development and investigations of new and less expensive hydrogen production processes. One of the promising processes for hydrogen production is non-catalytic conversion of natural gas (methane) in the presence of oxygen [125–128]. However, it has been shown above that incomplete methane oxidation to formaldehyde is of great effectiveness in the presence of hydrogen peroxide in the temperature range of 480–540 °C. The kinetics and mechanism of this slow reaction indicate that methane oxidation with hydrogen peroxide is a conjugated reaction based on the initiating action of hydrogen peroxide [8, 9].

Nevertheless, the area of methane high-temperature oxidation with hydrogen peroxide and associated kinetic and mechanism questions have not yet been comprehensively studied. The works mentioned below describe the manner of conjugated H_2 and CO_2 production in natural gas high-temperature homogeneous oxidation with hydrogen peroxide.

The process was studied in a flow quartz reactor [129]. Natural gas of the following composition was taken as the raw material: 96% methane, 2.0% nitrogen, 1.0% oxygen, 1.5% propane and 0.5% propylene.

The study of the aqueous H_2O_2 concentration effect on the course of the reaction shows almost full methane conversion with high hydrogen yield (74%) and a carbon dioxide concentration decrease to 0.4% in the presence of 15% hydrogen peroxide at 880 °C [130].

Experimental results from temperature influence on methane oxidation to hydrogen-containing gas are presented in Figure 4.18. It is obvious that besides total methane conversion,

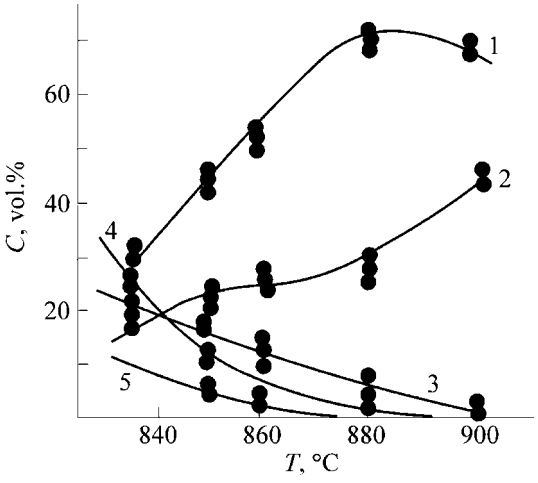

Figure 4.18 Temperature dependence of reaction product concentration (vol.%) in the reaction gas mixture with 15% H_2O_2: v_{CH_4} = 0.38 l/h; $v_{H_2O_2}$ = 0.2 ml/min (1: H_2; 2: CO_2; 3: CO; 4: CH_4 and 5: O_2).

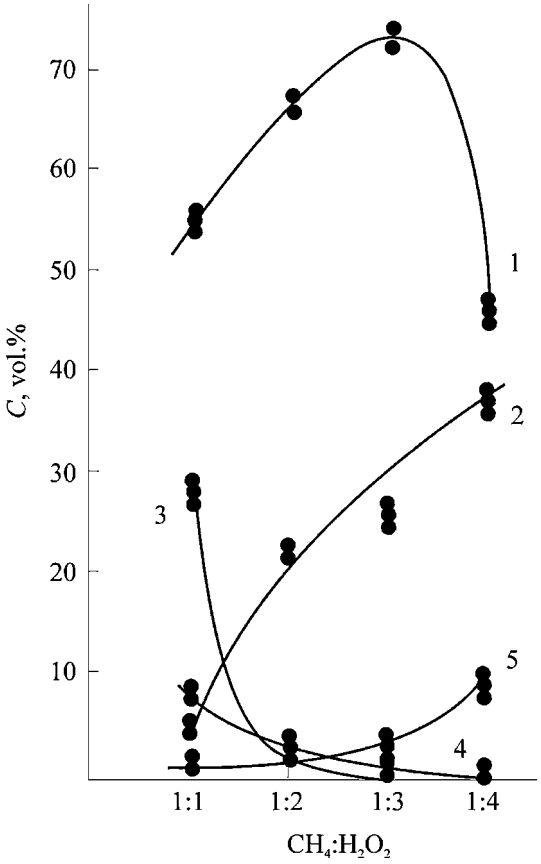

Figure 4.19 Dependencies of reaction product yields on CH_4:H_2O_2 ratio at 880 °C: v_{CH_4} = 0.38 l/h; $v_{H_2O_2}$ = 0.2 ml/min (1: H_2; 2: CO_2; 3: CO; 4: CH_4 and 5: O_2).

hydrogen content in converted gas also increases with temperature. Hence, the quantity of carbon oxide formed is gradually reduced, and the H_2:CO ratio increases. At 880 °C full conversion of methane is observed, and hydrogen yield (74%) approaches the stoichiometric parameter. A temperature increase from 860 °C to 900 °C reduces carbon oxide concentration to a negligibly small value. This makes synthesized gas applicable (of course, after purification from carbon dioxide without secondary CO conversion) to ammonia synthesis.

The influence of the CH_4:H_2O_2 ratio on the course of the reaction was also studied. Figure 4.19 shows that the ratio change from 1:1 to 1:3 raises H_2 yield to its maximum. A further change of the ratio to 1:4 increases conversion and decreases the amount of synthesized hydrogen due to its gradual oxidation. The results indicate that the ratio CH_4:H_2O_2 = 1:3 is the best value for reaching maximal hydrogen yield.

The experimental data on the effect of the contact time on the methane oxidation process (Figure 4.20) show increasing dependence of methane conversion on the contact time (τ). Carbon oxide formed in the system is after-oxidized to CO_2 with the contact time. Therefore,

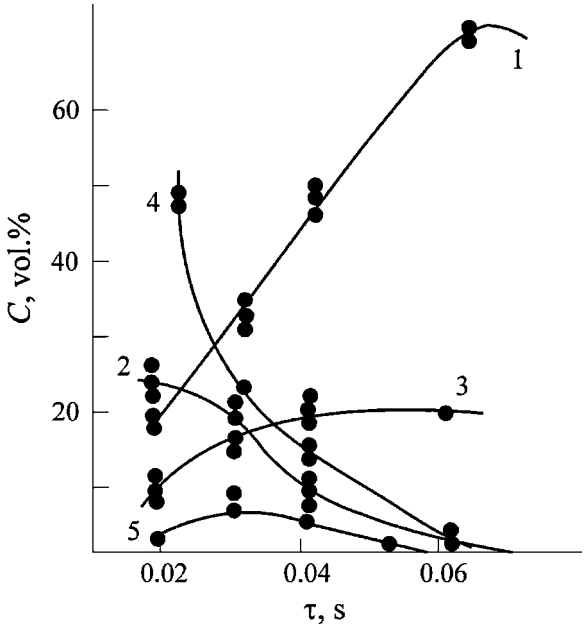

Figure 4.20 The change in gas concentrations (vol.%) in the reaction gas mixture with contact time: T = 880°C; 15% H_2O_2; CH_4:H_2O_2 = 1:3 (1: H_2; 2: CO_2; 3: CO; 4: CH_4 and 5: O_2).

already at τ = 0.0–6 s, when hydrogen yield is maximal (74 vol.%), CO concentration is reduced to a very small value.

Carbon oxide may be converted not only with hydrogen peroxide, but also by excessive aqueous vapor present in the system:

$$CO + H_2O_2 \rightarrow CO_2 + H_2O$$
$$CO + H_2O \rightarrow CO_2 + H$$

As observed in the experiment, a variation of H_2O_2 concentration in the aqueous solution and other basic parameters of the process may induce the synthesis of gas with given H_2:CO ratio for its further application in methanol or ammonia synthesis. In the latter process, low CO concentration is required.

Compared with the common high-temperature conversion of natural gas and further carbon oxide conversion on a catalyst [131], the current process promotes process simplification: the reaction is implemented at relatively low temperature (860–900 °C instead of 1400–1600 °C for existing non-catalytic processes of methane conversion) and an additional unit for catalytic conversion of carbon oxide is excluded (in NH_3 production).

4.5.4 Lower olefin oxidation

Catalytic epoxidation of olefins by various forms of bound oxygen (ROOH, H_2O_2, peroxy acids) in the liquid phase was comprehensively studied in a review [132, 133] in which

detailed information about the kinetics and mechanism of homogeneous catalysis in the presence of compounds of the V–VI group elements is provided. To explain the mechanism of homogeneous catalysis proceeding during epoxidation by hydroperoxide, several suggestions about the origin of active particles were put forward in the work mentioned.

Of special attention is the single-stage method of olefin oxide production by their conjugated oxidation with another, more easily oxidizing compound (aldehyde, ketone, etc.) [134, 139]. For the epoxidation of an olefin, active oxygen of peroxy radicals is used in such a system:

The principal possibility of olefin epoxidation by peroxy radicals is indicated. The simplest representative of this class can be obtained from H_2O_2.

For reasons of economy and availability, selective oxidation of propylene is most frequently implemented with H_2O_2 as a catalyst [135]. Hydrogen peroxide has low reactivity for direct epoxidation in liquid; therefore, various activation methods are applied. Activation is usually performed with the help of carboxylic acids or some inorganic anhydrides with active compound formation. Studies have been described [136, 137] in which peroxy acids derived by H_2O_2 interaction with formic or acetic acid are used as epoxidation agents. In this connection, of special interest are reactions of olefin epoxidation by peroxy acids at the moment of their formation from acid anhydride and H_2O_2. Tungstic acid and its salts are the most effective catalysts for olefins conversion to olefin oxides by H_2O_2 in the presence of Ti, W, V, Ge, Mo, U and Ru oxides [138].

Taking into account the applied value of low-molecular olefin oxides, a possibility to synthesize the first homolog in this sequence (ethylene oxide) was studied [139]. The implementation of such a reaction is of interest for a deeper understanding of the mechanism of substrate conjugated oxidation with hydrogen peroxide and expansion of the sphere of its practical application. In the example of ethylene oxide synthesis it was found [140] that, depending on kinetic conditions, in the presence of olefins, conjugated oxidation with hydrogen peroxide may be aimed at epoxidation.

The gas-phase propylene oxidation with hydrogen peroxide according to the conjugated mechanism is one of the major ways of synthesizing such valuable products as propylene oxide, acrolein and allene [124, 141, 142].

Experimental studies [31] (Figure 4.21) have determined the effect of the following parameters on the oxidation rate and mechanism: temperature, initial reagent feeding rate, the reagent ratio, H_2O_2 concentration in aqueous solution and *S/V*-factor.

Conjugated propylene epoxidation with hydrogen peroxide is the main reaction proceeding in the temperature range of 500–580 °C; under optimal conditions the average propylene oxide yield reaches 50%.

As mentioned above, at gas-phase conjugated oxidation with hydrogen peroxide in a flow system with stationary mode $HO_2^{\bullet}$ radical concentration is several orders of magnitude higher than $^{\bullet}OH$ radical concentration. Based on this fact and literary data on olefin epoxidation

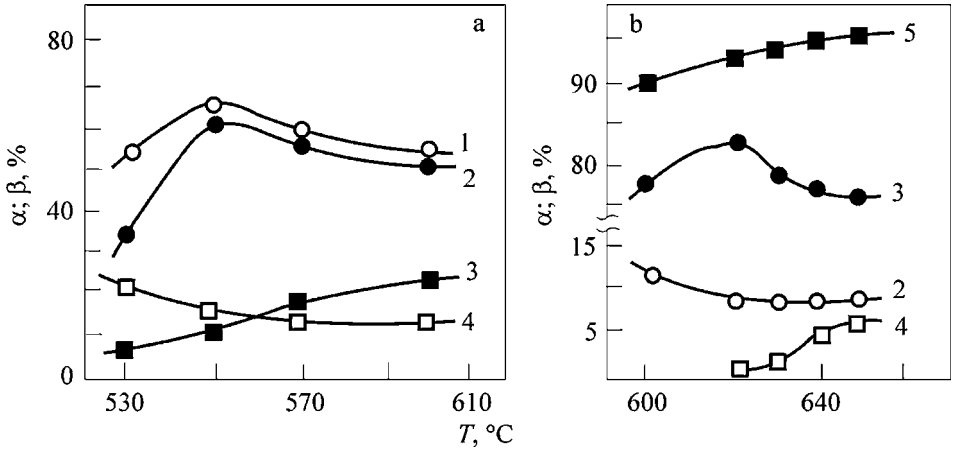

Figure 4.21 Temperature dependencies of selectivity (γ) (1), yields (β) of propylene oxide (2), acrolein (3) and side products (4), and propylene consumption (α) (5) for conjugated oxidation with hydrogen peroxide. (a) 30% H_2O_2; $v_{H_2O_2}$ = 1.3 ml/h; $v_{C_3H_6}$ = 150 ml/h and (b) 10% H_2O_2; $v_{H_2O_2}$ = 3.78 ml/h; $v_{C_3H_6}$ = 900 ml/h.

by alkylperoxy radicals, it may be suggested that the elementary act of olefin epoxidation by $HO_2^{\bullet}$ radicals in the gas phase is described by the following equation:

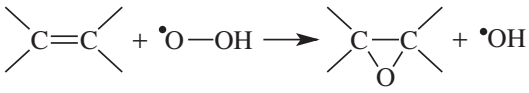

In fact, the mechanism of olefin epoxidation by alkylperoxy radicals accepted in the literature is generally presented by the following scheme [143]:

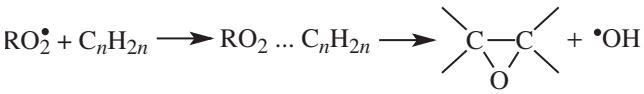

It is common knowledge that the rate of epoxidation by alkylperoxy radicals is defined by their structure. The simplest representative and the parent radical of this class is the $HO_2^{\bullet}$ radical. In the case of propylene epoxidation with hydrogen peroxide in the gas phase at 500–580 °C and contact time τ = 4.4 s, the epoxidating particle is, probably, the $HO_2^{\bullet}$ radical whose activity in the absence of catalysts is higher than the $RO_2^{\bullet}$ activity.

In accordance with the accepted mechanism, the course of conjugated epoxidation must be affected by the type of oxidable object, which is olefin.

In fact, the experimental data [124] show that all other factors being equal in the reaction mixture, propylene oxide yield is higher than ethylene oxide yield. This is explained by the

easier proceeding of propylene elementary epoxidation reaction with $HO_2^{\bullet}$ radicals rather than ethylene epoxidation, because the presence of methyl group at ethylene bond in propylene causes loosening of the π-bond and makes its break with addition of perhydroxy radical 'active oxygen' easier. Higher reactivity of propylene is the reason for fuller conversion of it. Selectivity changes insignificantly with the conversion increase. This testifies to the target reaction rate increase with the olefin conversion. However, a further increase of epoxidation rate with the radical length or olefin branching degree can scarcely be suggested, because the course of the reaction may also be affected by other factors, including steric ones.

In the temperature range of 580–600 °C, propylene oxidation to acrolein proceeds at the commensurable rate simultaneously with propylene epoxidation. At 600–640 °C and $\tau = 1.2$ s acrolein is the predominant product with 80% average yield.

A temperature rise above 680 °C (at $\tau = 0.45$ s) induces allene and methyl acetate synthesis by propylene conjugated dehydrogenation reaction (refer to Figure 4.3), the yield of which under optimal conditions equals 20% and 10%, respectively [62].

Basing on investigations carried out, it is shown that the conjugated oxidation of propylene is a controllable process and, with respect to particular conditions, secondary reaction may display three dominant propagation directions as follows:

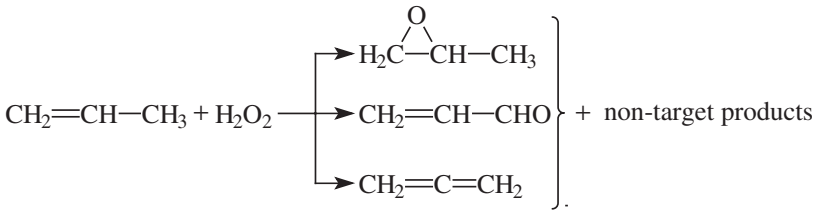

Similar to the other reactions of oxidation with hydrogen peroxide considered above, in this reaction system chemical conjugation is implemented according to schemes (4.2) and (4.3) [144]. Finally, these investigations defined the borders of various mechanisms for conjugated oxidation with hydrogen peroxide with respect to conditions (temperature and contact time). They also showed transition areas in epoxidation and soft oxidation mechanisms. Moreover, implementation of olefin conjugated epoxidation in the gas phase opens a predominantly new method of olefin oxide synthesis, because changing the kinetic conditions along the reaction zone will allow a combination of olefin synthesis (conjugated dehydrogenation with hydrogen peroxide) and olefin conjugated epoxidation.

As mentioned above, investigators have paid attention recently to the homogeneous gas-phase oxidation of propylene, which is much simpler and requires no great expense. If we learn how a definite kind of free radicals can be generated to the system and forecast the reaction they enter with respect to conditions (reactor operation mode), high selectivity of homogeneous gas-phase oxidation can be obtained. If active sites are able to implement two-electron oxidation in a single stage, selectivity will be provided, because many elementary stages will be neglected, which takes place at one-electron oxidation. The solution to this question is of great importance for determining the process mechanism and finding effective pathways of olefin conversion to oxides via direct oxidation.

4.6 CONJUGATED HYDROGENOLYSIS OF TOLUENE TO BENZENE WITH HYDROGEN PEROXIDE

Great progress in organic synthesis and synthetic material production results in an intense growth of aromatic hydrocarbon consumption, especially benzene.

At the present time, the industrial production of benzene and its homologs is implemented by coal carbonization, dehydrocyclization of the usual paraffin hydrocarbons and dehydrogenation of cyclohexane hydrocarbons with catalytic reforming of directly distilled gasoline fractions. The petroleum refining industry is the main source for meeting the demand for benzene and its reserves can fully meet the increasing demand for this compound.

The basic raw materials for benzene production in the petroleum industry are low-octane direct distilled gasoline fractions, boiling away at 62–85 °C or 62–105 °C. For benzene yield the fraction with a 62–85 °C boiling away interval is more economically profitable rather than the 62–105 °C fraction, but a lack of resources makes manufacturers also use the latter fraction. However, 62–105 °C fraction processing gives high yields of toluene, the demand for which is relatively low. The ratio between gasoline, toluene and xylene quantities in the mixture obtained by 62–105 °C fraction platformating equals 1:4:5, i.e. the yields of toluene and xylenes exceed benzene yield. Therefore, homogeneous and catalytic processes of toluene dealkylation have been developed. These processes give high yields of benzene per both injected (40–80%) and converted (at least 90%) toluene. However, they require high pressures and high hydrogen consumption, and there are heavy capital costs associated with the synthesis and regeneration of catalysts.

Among the processes suggested, homogeneous hydrodealkylation of toluene is the most economic reaction, for which kinetic regularities, optimal conditions for maximal benzene yields and effects of various factors on the reaction run are determined. However, this technique has not found an industrial application because of the high pressure needed and high hydrogen consumption. Since hydrodealkylation causes a break of the side chain with the follow-up hydrogen addition to the bond break location, this reaction can be called toluene hydrogenolysis to benzene.

With the aim of developing a new, higher effective method of toluene hydrogenolysis, homogeneous hydrogenolysis to benzene with hydroperoxide participation under atmospheric pressure was studied [145, 146].

For the first time hydrogen peroxide was studied as the reagent of toluene hydrogenolysis. Since this reaction belongs to the class of conjugated processes, it is called the ‘conjugated hydrogenolysis of toluene to benzene’. Both combined and separate actions of hydrogen peroxide on toluene were studied [147]. The investigation results for reactions:

$$C_6H_5CH_3 + H_2O_2 \quad \text{and} \quad C_6H_5CH_3 + H_2$$

proceeding in a hollow reactor are presented in Figure 4.22. Clearly, the highest yield of benzene in the reaction:

$$C_6H_5CH_3 + H_2O_2$$

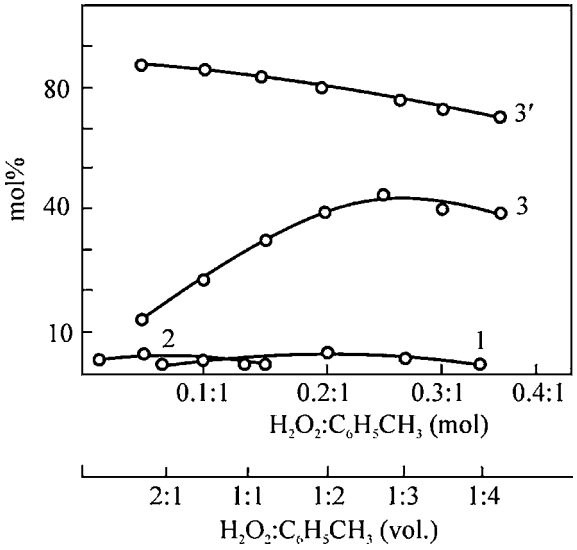

Figure 4.22 Dependence of benzene yields on molar ratio H_2O_2:toluene: $T = 680\,°C$; molar ratio $C_6H_5CH_3$:H_2 = 1:4.85; liquid toluene volume rate equals $0.02\,h^{-1}$ (1: autohydrogenolysis of toluene (without H_2) in the presence of H_2O_2; 2, 3: 3′-conjugated hydrogenolysis of toluene per injected and converted toluene, respectively).

is reached at the volumetric ratio between aqueous H_2O_2 and $C_6H_5CH_3$ varying within the range of 1:2 to 1:3. Data from these tests gave an opportunity to select conditions for studying conjugated hydrogenolysis of toluene to benzene at H_2 and H_2O_2 co-participation. Curves 2 and 3 in Figure 4.22 obey the same regularities. The maximum on curve 3 corresponds to H_2O_2:$C_6H_5CH_3$ = 0.25:1 molar ratio. The curve 3 shift in relation to curve 2 is explained by the presence of the third component (H_2), the role of which in hydrogenolysis is well known. It is also shown that a temperature rise from 680 °C to 730 °C causes a significant increase of the main reaction rate, though side reactions are intensified simultaneously, which noticeably reduces the main process selectivity. Under studied conditions, the quartz reaction surface or, to put it differently, the *S/V*-factor, does not in practice affect the reaction rate. The experiments studying short-term initiating effect of H_2O_2 on toluene homogeneous hydrogenolysis to benzene show that even after initiation stop during a long time benzene yield remains high compared with homogeneous hydrogenolysis.

According to test results, benzene yield per injected toluene in conjugated hydrogenolysis increases 5–6-fold compared with common hydrogenolysis of toluene. The reaction also possesses high selectivity which, accompanied by atmospheric pressure, makes it more economic than homogeneous hydrogenolysis of toluene to benzene under high pressure.

4.7 NITROGEN FIXATION AT CONJUGATED OXIDATION

The problem of nitrogen fixation is one of the most important scientific and technical tasks. The nitrogen and nitrogen-compound-making industry is one of the leading branches of the

modern chemical industry. The state of the art of it is the main factor affecting the supply of nitrogenous fertilizers to agriculture and of various nitrogen-containing substances to industry.

D.I. Mendeleev was the first to bring up the question of nitrogen fixation from air: '… time will come, when nitrogen compounds will be produced from air nitrogen. This will be a great success for practical life, because having nitrogen compounds and using them as fertilizers one can obtain high crops of cultivated plants … One of the tasks of applied chemistry is searching for technically advantageous method of obtaining nitrogen compounds containing assimilable nitrogen from the air nitrogen … The fortune of agriculture is mostly dependent on discovery of such a method' [148, pp. 361–362].

It is common knowledge that both shapes of mineral bound nitrogen—ammonia and nitrate—are directly accessible for plants. Therefore, at present, the question of nitrogen fixation in inorganic compounds is urgent. The problem is that human and animal organisms are unable to use nitrogen from inorganic compounds for protein synthesis. As for nitrogen nutrition, its resources are limited by assimilating activity of plants and weed-eating animal proteins. Therefore, meeting human and animal demand for proteins depends on the level of meeting the demand of plants for mineral fixed nitrogen [149].

The following methods of nitrogen fixation are developed: ammonia, arc, cyanamide, plasmatic, thermal and nitric oxides synthesis in a nuclear reactor. However, besides ammonia synthesis, no other methods have found wide industrial application. This method has many disadvantages, for example: multistage type and production awkwardness, the necessity for specific materials, equipment and machinery suitable for working under high pressure and temperature conditions, inexpensive raw material demand in the form of natural gas, coke oven gas or petroleum residues, high investments, etc. Therefore, research into new, simpler and more economic methods of atmospheric nitrogen fixation are continuing. Direct air nitrogen oxidation can be implemented at high temperatures and under the influence of high-velocity electrons and γ-radiation, in a nuclear reactor, etc. [150].

Thermal oxidation of nitrogen was studied by Gabor Nernst, Zeldovich and others [39, 151]. Various methods of atmospheric nitrogen thermal fixation in regeneration ovens and reactors of various constructions and principles of operation were suggested. The essence of all methods consists in obtaining equilibrium values of nitric oxide concentrations at different temperature modes. In a plasma jet, bulk mean air temperature can simply be raised to 3000–4000 K and pressure boosted to several tens of atmospheres. This increases nitric oxide concentration in nitrous gas to 5%. Compared with the ammonia method, the advantage of the plasmatic method is the presence of almost inexhaustible resources of raw materials, simplicity of formation and an opportunity for plant construction in close proximity to the customer.

Among methods of nitrogen chemical fixation, direct nitrogen oxidation by air oxygen giving nitric oxide is of special attention for application purposes. The wide distribution of the initial products and their low cost are obvious. The problem is reduced to reaction implementation with the lowest costs. In the USA, the Bradley–Lovejoy [152] method of atmospheric nitrogen fixation by oxygen in a high-voltage discharge was applied in industry.

Stokes and Knipe [153] obtained nitric oxides by mixing nitrogen plasma jet with oxygen. The average conversion of O_2 in these experiments equaled 2%. La Roche [154] obtained higher yields in high-quality discharge plasma. Maximal concentration in a sample with low

quenching rate just slightly exceeded 2%. The use of devices providing high quenching rate increases NO concentration above 4% which testifies to the importance of quenching for this process.

A possibility of NO synthesis from the air was studied [155, 156]. Fromens [155] used thermal reaction, the so-called Wisconsin process, which at maximal temperature 2500 K gave an NO yield equals 1.9% and at 1900 K—below 0.45%.

Thompson [156] described a thermal process in a flow oven with a temperature up to 3000 K. Under favorable experimental conditions, NO concentration in nitrous gases reached 3.7%.

Analysis of the works in which NO formation is studied [157] in the nitrogen–oxygen system at high temperature shows NO concentrations ranging within 2–4%.

There were experiments [158] studying formation of nitric oxides in nitrogen plasma jet with injected oxygen, oxygen–nitrogen mixture and water. In this case, NO concentration in nitrous gases reached 8%.

According to data by Polak and Shipachev [159], the main object of expenditure in the production of nitrogen from air in plasma jets is electric power.

The works by Volpin and Shur [160] as well as by Shilov [161] on molecular nitrogen fixation via complexing with transition metals indicates nitrogen readily reacting with low-valence organometallic compounds of titanium, chromium, molybdenum, wolfram and iron.

More investigations of nitrogen reactions with transition metal compounds [162] confirmed the capability of nitrogen to readily enter reactions and reduction by many organometallic and inorganic coordination compounds of transition metals [163].

Shilov *et al*. [164] displayed the possibility of synthesizing stable ruthenium complex with molecular nitrogen.

Thus, at present, the task of atmospheric nitrogen fixation has mainly been developed in two directions: reduction and oxidation fixation. Chemical fixation of molecular nitrogen by the reduction mechanism on transition metals is a comprehensively studied branch of physical chemistry, displaying several discoveries made in this direction [165].

Meanwhile, another direction, that of oxidative fixation of nitrogen, has been poorly studied, because only several oxidation reactions are known; for example, the above-described reactions in electric arc, plasma or induced by ionizing radiation [166]. They are all endothermic oxidation reactions, consuming high energy and possessing low selectivity and yield.

The analytical analysis in methods of nitrogen fixation methods prompts the conclusion that all currently existing techniques possess specific disadvantages. Therefore, besides modernization of synthetic ammonia production process, new methods of molecular nitrogen fixation are also searched for. In this connection, of interest is the development of chemical-engineering processes in which conjugated reaction principles will be used and, therefore, non-spontaneous oxidative fixation of nitrogen will be implemented with the help of chemical induction (similar to biological systems).

As shown below, the application of this principle to nitrogen oxidation by hydroperoxide has helped in discovering a new method of nitrogen fixation, mainly shaped as N_2O, other oxides with low admixtures or nitrogen-containing acids under conditions, which are relatively soft for such reaction type. The method is also energy saving and ecologically friendly [167, 168].

For the sake of comparison, let us briefly consider the commonly known method of nitrous oxide synthesis [169] by thermal decomposition of ammonia nitrate at 523–533 K by the following reaction:

$$NH_4NO_3 \rightleftharpoons N_2O + 2H_2O$$

Admixtures are 1–2% nitrogen and NO, which can be removed by passing bivalent iron sulfate through the solution. Moreover, N_2O is also produced by nitrates and nitrites reduction under definite conditions or by hyponitrite decomposition.

It is shown [31] that besides N_2O, an acid suggested to be hyponitrous acid ($H_2N_2O_2$) is formed in the aqueous part of products of molecular nitrogen oxidative fixation with hydrogen peroxide. This acid then dissociates to N_2O and H_2O. Acid formation is also indicated by predominant presence of N_2O in the aqueous phase in amounts significantly exceeding its solubility in water. The presence of soft acid (which is $H_2N_2O_2$) may be judged by changes in the pH of the solution (3–4). Hence, direct detection of $H_2N_2O_2$ was reduced to qualitative reaction of yellow-colored silver hyponitrite ($Ag_2N_2O_2$) precipitation [170]. Taking into account the fact that silver cation also gives a yellow deposit with nitrite anion NO_2^- as well as some technical difficulties associated with $Ag_2N_2O_2$ (which is an extremely unstable salt) extraction from the solution, titration by lithium and potassium hydroxides was performed in one part of the reaction product. Hyponitrites of lithium and potassium hydroxides display high thermal stability up to 260 °C [171]. X-ray diffraction analysis of these salts, extracted by solvent evaporation, showed the presence of NO_2^- and NO_3^- anions in them shaped as KNO_2, KNO_3 and $LiNO_3 \cdot 2H_2O$. According to the analyses discussed below, the main part of these salts consists of alkaline metal hyponitrites.

In alkaline metal salts, hyponitrite-ion $N_2O_2^-$ was detected using IR-spectroscopy technique (by the presence of intensive absorption bands at 500 and 1000 cm^{-1}) [171] and from qualitative reactions.

HJ and starch action. As HJ and starch are poured into a potassium hyponitrite solution, the latter is colored blue 2–3 min afterwards, which is a result [171, 172] of insignificant amounts (traces) of NO_2^- anion presence, which were formed in the following reaction [171–174]:

$$3K_2N_2O_2 + 2H_2O \rightleftharpoons 2KNO_2 + 2KOH + 2N_2$$
$$K_2N_2O_2 + O_2 = 2KNO_2$$

The action of concentrated H_2SO_4. Potassium hyponitrite decomposes completely under the effect of concentrated H_2SO_4. The reaction is outrage and releases nitrous oxide, which unambiguously indicates its origin, because interaction with H_2SO_4, KNO_2 and KNO_3 does not release N_2O. The main reaction is described by the following equation [172]:

$$K_2N_2O_2 + H_2SO_4 = K_2SO_4 + H_2O + N_2O$$

Oxidation with $KMnO_4$. The solution used contained 0.2 g $KMnO_4$ and 30 ml H_2SO_4. As $K_2N_2O_2$ and KNO_2 were poured into the solution, it became colorless. Then for the purpose

of HNO_3 detection, which may be formed in the reactions below [171], the aliquot part was extracted [172]:

$$H_2N_2O_2 \xrightarrow{O_2} HNO_3$$
$$HNO_3 \xrightarrow{O_2} HNO_2$$

In the case, when only $KMnO_4$ solution (0.2 g in 30 ml H_2SO_4) is poured to the mixture, outrage release of gases is observed. Chromatographic analysis of these gases indicated the presence of equal parts of N_2O and N_2. After pouring H_2SO_4 to the system this ratio shifts toward nitrous oxide.

Thus, the results of above analyses of aqueous reaction products and salts extracted by hydroxide titration indicate the presence of $N_2O_2^-$, NO_2^- and NO_3^- anions in the reaction products. The latter anion can also be obtained in another reaction [173, 174]:

$$KNO_2 + K_2N_2O_2 + H_2O = KNO_3 + 2KHOH + N_2$$

It may be concluded from generalized results that the conjugated reaction of molecular nitrogen oxidative fixation with hydrogen peroxide mostly produces nitrous oxide (N_2O) in concentrations below 19%. In the quenching zone, most of the nitrous oxide is converted to $H_2N_2O_2$ due to the action of active sites ($HO_2^{\bullet}$ and $^{\bullet}OH$) and H_2O_2. Small amounts of HNO_2 and HNO_3 (up to 0.1%) are also detected [175].

Figure 4.23 shows the dependence of molecular nitrogen conversion on its volume rate in the temperature range of 773–873 K. It is clearly observed that the quantity of fixed nitrogen per injected molecular nitrogen increases to some extent with the amount of injected molecular nitrogen. A further increase of raw material rate does not change the level of nitrogen fixation. Despite shorter contact time, the increase of N_2 volume rate from 1 to 4 l/h intensifies the reaction. The aqueous hydroperoxide rate is constant for all nitrogen rates. However, at a nitrogen rate of 4–5 l/h the fixed nitrogen yield is altered.

Thus, chemical induction is the main factor promoting N_2 fixation in a N_2—H_2O_2—H_2O system. It manifests itself owing to conjugation of H_2O_2 dissociation reactions, which generate the intermediate—$HO_2^{\bullet}$ radical—to the system. This intermediate transfers the induction action of the primary reaction to the N_2 oxidation process. In this case, H_2O_2 is injected in amounts much greater than demanded by N_2 oxidation, because the main requirement for effective chemical conjugation is the presence of $HO_2^{\bullet}$ in high concentration.

To conclude the discussion, it should be noted that oxidative fixation of molecular nitrogen with hydrogen peroxide is fairly simple for process-engineering design, usually proceeds under homogeneous conditions without any catalyst under atmospheric pressure, and produces high yields of fixed nitrogen.

Among other aims, the author attempted in this chapter to give a simple phenomenological description of the kinetic regularities of conjugated oxidation with hydrogen peroxide in the gas phase with time, plotted as curves in the figures above. Thus, the quantitative data accumulated in kinetic investigations must be transformed to qualitatively absolutely different results, associated with the decoding of the chemical conjugation mechanism in reactions of oxidation with hydrogen peroxide and the basic principles of its operation.

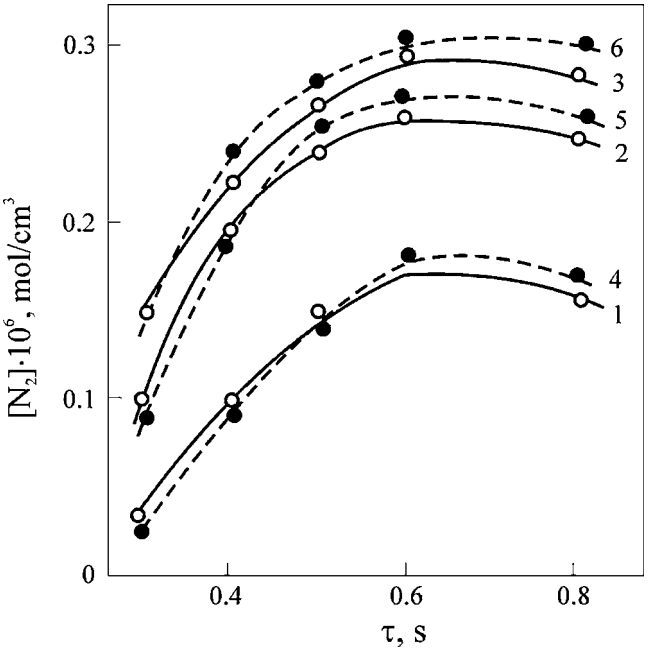

Figure 4.23 Kinetics of nitrogen fixation with hydrogen peroxide: molar ratio N_2: 30% H_2O_2 = 1:1.6 (1–3: T = 773, 823 and 873 K, respectively, and 4–6: theoretical curves at these temperatures).

REFERENCES

1. Shambe, U., Satterfield, C. and Ventvorse, R., *Hydrogen Peroxide*, Inostrannaya Literatura, Moscow, 1958, 578 pp. (in Russian).
2. Berenblit, V.M., Burdin, V.V., Vishnyakov, V.M. *et al*., *Chemistry and Technology of Hydrogen Peroxide*, Khimia, Leningrad, 1984, 200 pp. (in Russian).
3. Kistakowsky, J.B. and Bosenberg, S.L., *J. Am. Chem. Soc*., 1937, Vol. 59, pp. 442–450.
4. Satterfield, C.N. and Stein, S.W., *Ind. Eng. Chem*., 1957, Vol. 49, pp. 1173–1180.
5. McLance, C.K., *J. Chem. Phys.*, 1949, Vol. 17, pp. 379–385.
6 Harris, E.S., *Trans. Faraday Soc*., 1948, Vol. 44, pp. 754–766.
7. Jiguerre, P.A. and Liu, G.D., *J. Chem. Phys*., 1957, Vol. 35, pp. 283–293.
8. Satterfield, C.N. and Stein, S.W., *J. Phys. Chem*., 1957, Vol. 51, pp. 537–540.
9. Connway, D.C., *Ibid.*, Vol. 61, pp. 1579–1580.
10. Baker, B.F. and Onellet, C., *Canad. J. Res. B*, 1945, Vol. 23, pp. 167–182.
11. Mackenzie, R.C. and Ritchie, M., *Proc. Roy. Soc. London A*, 1946, Vol. 185, pp. 207–224.
12. Forst, W., *Canad. J. Chem*., 1958, Vol. 36, pp. 1308–1319.
13. Houre, D.E., Prothero, J.B. and Walch, A.D., *Nature*, 1958, Vol. 182, No. 4636, pp. 654–658.
14. Houre, D.E., Prothero, J.B. and Walch, A.D., *Trans. Faraday Soc*., *Arch. Combust* 1959, Vol. 55, pp. 548–557.
15. Baldwin, R.R. *et al*., *Combust. Flame*, Vol. 15, 1970, pp. 113–142.
16. Baldwin, R.R., Walker, R.W. and Webster, S.I., *Ibid.*, pp. 167–182.
17. Satterfield, C.N., Kavanagh, J.M. and Resnick, H., *Ind. Eng. Chem*., 1951, Vol. 43, pp. 2507–2514.
18. Grigor'yan, G.L. and Nalbandyan, A.B., *Dokl. AN SSSR*, 1977, Vol. 235, No. 2, pp. 381–383 (in Russian).

19. Minasyan, V.T., Grigor'yan, G.L. and Nalbandyan, A.B., *Arm. Khim. Zh.*, 1978, Vol. 31, No. 1, pp. 45–48 (in Russian).
20. Carlier, M., Sahetchian, R. and Sochet, L., *Cr. Acad. Sci. C*, Vol. 286, pp. 123–126.
21. Carlier, M., Sahetchian, R. and Sochet, L., *Chem Phys. Lett.*, 1978, Vol. 6, pp. 557–560.
22. Savvin, N.N., Myasnikov, I.A., Gutman, E.E. and Bazov, V.P., *Kinetika i Kataliz*, 1978, Vol. 19, No. 3, pp. 802–804 (in Russian).
23. Chaltykyan, M.T. and Samvelyan, S.Kh., *Arm. Khim. Zh.*, 1979, Vol. 32, No. 11, pp. 840–884 (in Russisan).
24. Vartikyan, L.A., Minasyan, V.T., Grigor'yan, G.L. and Nalbandyan, A.B., *Thes. Rep. XII Mendeleev's Congress on General and Applied Chemistry*, Nauka, Moscow, 1981, No. 3, p. 17 (in Russian).
25. Baldwin, R.R. and Mayor, L., *VII International Symposium on Combustion*, Liverpool, 1959, pp. 8–12.
26. Baldwin, R.R. and Mayor, L., *Trans. Faraday Soc*., 1960, Vol. 56, pp. 80–92.
27. Baldwin, R.R., Mayor, L. and Doran, P., *Trans. Faraday Soc*., 1960, Vol. 56, pp. 93–102.
28. Baldwin, R.R., Mayor, L. and Doran, P., *Trans. Faraday Soc*., 1960, Vol. 56, pp. 103–114.
29. Baldwin, R.R. and Brattan, D., *VIII International Symposium on Combustion*, Baltimore, MD, 1962, pp. 110–119.
30. Robertson, A.J., *Trans. Faraday Soc*., 1952, Vol. 42, pp. 228–234.
31. Nagiev, T.M., *Usp. Khim.*, 1985, Vol. 54, No. 10, pp. 1654–1673 (in Russian).
32. Dolgoplosk, B.A. and Tinyakova, E.I., *Free Radical Generation and Reactions*, Nauka, Moscow, 1982, 253 pp. (in Russian).
33. Dolgoplosk, B.A. and Tinyakova, E.I., *Redox Systems as the Source of Free Radicals*, Nauka, Moscow, 1972, 237 pp. (in Russian).
34. Ashmore, P.A., *Catalysis and Inhibition of Chemical Reactions*, Mir, Moscow, 1966, 386 pp. (in Russian).
35. Baxendale, J.H. *et al*. *Trans. Faraday Soc*., 1946, Vol. 42, p. 155.
36. Sychev, A.Ya., Isak, V.G. and Porannmler, U., *Zh. Fiz. Khim.*, 1979, Vol. 53, No. 11, pp. 2790–2794 (in Russian).
37. Nagiev, T.M., *Arch. Combust*. 1984, Vol. 4, No. 3, pp. 211–219.
38. Kuliev, A.M. and Nagiev, Ch.M., *Dokl. AN SSSR*, 1981, Vol. 258, No. 2, pp. 339–401 (in Russian).
39. Zeldovich, Ya.B., Sadovnikov, P.Ya. and Frank-Kamenetsky, D.A., *Nitrogen Oxidation at Combustion*, Izd. AN SSSR, Moscow, 1947, 148 pp. (in Russian).
40. Anbar, M., *J. Amer. Chem. Soc.*, 1966, Vol. 88, pp. 5924–5926.
41. Nagiev, T.M. and Nagiev, Ch.M., *Azerb. Khim. Zh.*, 1974, No. 2, pp. 141–146 (in Russian).
42. Vedeneev, V.I. and Kibkalo, A.A., *Rate Constants of Gas-Phase Monomolecular Reactions*, Nauka, Moscow, 1972, 164 pp. (in Russian).
43. Prigozhin, I., *Introduction in Thermodynamics of Irreversible Processes*, Moscow, Inostrannaya Literatura, 1960, 127 pp. (in Russian).
44. Jones, M., *Biochemical Thermodynamics*, Mir, Moscow, 1982, 440 pp. (in Russian).
45. Nagiev, T.M., Nagiev, M.F. and Mejidov, N.D., *Dokl. AN SSSR*, 1972, Vol. 205, No. 1, pp. 116–118 (in Russian).
46. Nagiev, T.M., Mejidov, N.D., Nagieva, Z.M. and Zulfugarova, S.Z., *Azerb. Khim. Zh.*, 1976, No. 4, 153–159 (in Russian).
47. Nagiev, T.M. and Nagiev, M.F., *Dokl. AN SSSR*, 1970, Vol. 195, No. 3, pp. 640–642 (in Russian).
48. Nagiev, M.F., Nagiev, T.M., Mejidov, N.D. and Iskenderov, R.A., *Azerb. Khim. Zh.*, 1971, No. 5–6, pp. 183–188 (in Russian).
49. Vardanyan, I.A., Sochyan, G.A. and Nalbandyan, A.B., *Dokl. AN SSSR*, 1970, Vol. 193, No. 1, pp. 123–127 (in Russian).
50. Nagiev, T.M. and Mejidov, N.D., *Zh. Fiz. Khim*., 1973, Vol. 42, No. 2, pp. 439–440 (in Russian).
51. Semenov, N.N., *On Some Questions of Chemical Kinetics and Reactivity*, 2nd edn, Izd. AN SSSR, Moscow, 1958, 680 pp. (in Russian).
52. Skarchenko, V.K., *Dehydrogenation of Hydrocarbons*, Naukova Dumka, Kiev, 1981, 328 pp. (in Russian).

53. Stern, V.Ya. and Lisichkin, A.M., *Question of Chemical Kinetics*, Nauka, Moscow, 1979, pp. 284–293 (in Russian).
54. Nalbandyan, A.B. and Mantashyan, A.A., *Elementary Processes in Slow Gas-Phase Reactions*, Izd. AN ArmSSR, Erevan, 1975, 258 pp. (in Russian).
55. Alkhazov, T.G. and Lisovsky, A.E., *Oxidative Dehydrogenation of Hydrocarbons*, Lhimia, Moscow, 1980, 238 pp. (in Russian).
56. Kolobikhin, V.A., Stepanov, G.A. and Chugunnikov, R.V., *Khim. Promst.*, 1966, No. 4, pp. 225–257 (in Russian).
57. Stepanov, G.A., Baranova, P.S., Shishkina, I.M. *et al*., *Ibid.*, 1967, No. 8, pp. 568–570 (in Russian).
58. Nagiev, M.F., Nagiev, T.M., and Bairamov, N.V., *Azerb. Khim. Zh*., 1976, No. 1, pp. 102–108 (in Russian).
59. Nagiev, T.M. and Bairamov, N.V., *Ibid.*, 1978, No. 2, pp. 94–95 (in Russian).
60. Nagiev, T.M., Agaeva, S.I., Kasimova, V.P. *et al.*, 'The method of allene and methyl acetate production', *Patent No. 722,890* (USSR), M.Kl[2] C07c11/14; C11/22; C07C5/42; No. 2651216/23-04, Publ. B.I. 1980, No. 11 (in Russian).
61. Tmenov, D.N., Raevskaya, L.N., Shipovalova, L.P. *et al*., *Neftepererabotka i Neftekhimia*, Minneftekhimprom SSSR, Moscow, 1975, No. 4, pp. 33–34 (in Russain).
62. Nagiev, T.M., Nagieva, Z.M. and Agaeva, S.I., *Neftekhimia*, 1986, Vol. 26, No. 2, pp. 176–180 (in Russian).
63. Yukelson, I.I., *The Main Organic Synthesis Technology*, Khimia, Moscow, 1968, 846 pp. (in Russian).
64. Castaneu, R. and Wandamme, R., *Cr. Acad. Sci*., 1965, Vol. 261, pp. 4729–4733.
65. Nagiev, M.F., Nagiev, T.M., Mamed'yarov, G.M. and Kalantarov, R.F., 'The method of vinyl chloride production', *Patent No. 503,842* (USSR), MKI, C07C21/06, No. 1745444/23-4, Publ. B.I. 1976, No. 7 (in Russian).
66. Zelinsky, N.D., *Zh. RKhO*, 1911, Vol. 43, pp. 1220–1222 (in Russian).
67. Shuikin, N.I. and Naryishkina, T.N., *Dokl. AN SSSR*, 1961, Vol. 136, No. 4, pp. 849–853 (in Russian).
68. Timofeeva, E.A., Shuikin, N.I. and Smirnov, V.S., *Izv. AN SSSR*, *Ser. Khim*., 1958, No. 7, pp. 893–896 (in Russian).
69. Wanae, D.W. and Walters, W.D., *J. Am. Chem. Soc*., 1948, Vol. 70, pp. 4035–4038.
70. Kazansky, B.A. and Plate, A.F., *Uchen. Zap. MGU*, 1934, No. 3, pp. 213–216 (in Russian).
71. Balandin, A.A. and Fedorov, V.S., *Dokl. AN SSSR*, 1941, Vol. 30, No. 1, pp. 21–25 (in Russian).
72. Frey, F.E., *Industry and Chemistry*, 1934, Vol. 26, pp. 198–202.
73. Tandzi, Kh., Uziyama, M. and Amono, A., *J. Chem. Soc. Jpn*, 1967, Vol. 70, pp. 3–8.
74. Nagiev, T.M., Sultanova, A.I., Nagieva, Z.M. and Ramazanova, Z.Yu., *Azerb. Khim. Zh.*, 1969, No. 5, pp. 115–119 (in Russian).
75. Nagiev, T.M., Sultanova A.I., Nagieva, Z.M. and Ramazanova, Z.Yu., *Azerb. Khim. Zh.*, 1974, No. 1, pp. 26–29 (in Russian).
76. Minachev, Kh.M., Tagiev, D.B., Zulfugarov, Z.G. and Kharlamov, V.V., *Kinetika i Kataliz*, 1979, Vol. 20, No. 2, pp. 399–404 (in Russian).
77. Nagiev, T.M., Agaeva, S.I., Nagieva, Z.M. *et al*., *Thes. Rep. Republ. Conf. to the Memory of Academician M.F. Nagiev*, Elm, Baku, 1976, p. 14 (in Russian).
78. Nagiev, T.M., Agaeva, S.I., Bairamov, F.G. and Nagieva, Z.M., *Azerb. Khim Zh*., 1977, No. 4, pp. 16–21 (in Russian).
79. Nagiev, T.M., Bairamov, F.G., Nagieva, Z.M. and Agaeva, S.I., *Azerb. Khim Zh*., 1980, No. 2, pp. 32–36 (in Russian).
80. Nagiev, T.M., Agaeva, S.I., Nagieva, Z.M. and Bairamov, F.G., *Azerb. Khim Zh*., 1977, No. 6, pp. 7–12 (in Russian).
81. Nagiev, T.M. and Bairamov, F.G., *Neftekhimia*, 1987, Vol. 27, No. 2, pp. 170–171 (in Russian).
82. Skarchenko, V.K., *Dehydrogenation of Hydrocarbons*, Naukova Dumka, Kiev, 1981, 328 pp (in Russian).
83. Adams, C.R. and Jennings, T.J., *J. Catal*., 1970, Vol. 17, pp. 158–177.

84. Flkhazov, T.G., Lisovsky, A.E. and Talyibov, Z.A., *Neftekhimia*, 1977, Vol. 17, No. 5, pp. 687–689 (in Russian).
85. Talybova, E.A., *Thes. Rep. 4th Conf. Oxid. Heterogen. Catalysis*, Azneftekhim, Baku, 1978, No. 2, pp. 25–29 (in Russian).
86. Nagiev, M.F. and Nagiev, T.M., *Adv. Chem. Ser. Am. Chem. Soc.*, 1974, pp. 137–148.
87. Nagiev, T.M., Mejidov, N.D. and Nagi-zade, N.S., *Azerb. Khim. Zh.*, 1971, No. 1, pp. 77–82 (in Russian).
88. Nagiev, T.M. and Iskenderov, R.A., *Azerb. Khim. Zh.*, 1972, No. 2, pp. 36–41 (in Russian).
89. Nagiev, T.M., *Azerb. Khim. Zh.*, 1973, No. 2, pp. 59–63 (in Russian).
90. Nagiev, T.M., Mejidov, N.D. and Iskenderov, R.A., *Azerb. Khim. Zh.*, 1974, No. 4, pp. 102–108 (in Russian).
91. Sultanova, A.I. and Nagiev, T.M., *Azerb. Khim. Zh.*, 1964, No. 4, pp. 17–20 (in Russian).
92. Nagiev, M.F., Nagiev, T.M. and Iskenderov, R.A., *Azerb. Khim. Zh.*, 1969, No. 1, pp. 35–41 (in Russian).
93. Dimov, A. and Aleksandrov, I., *Azerb. Khim. Zh.*, 1983, No. 1, pp. 131–136 (in Russian).
94. Nagiev, T.M., Mame'yarov, G.M. and N.I. Ali-zade, 'The method of 4-vinylpyridine production', *Patent No. 547,446* (USSR), M. Kl^2 C07D213/24, Publ. July 18, 1977, Bull. No. 7 (in Russian).
95. Nagiev, T.M., Mame'yarov, G.M. and Ali-zade, N.I., *Azerb. Khim. Zh.*, 1977, No. 5, pp. 13–18 (in Russian).
96. Chumakov, Yu.I., *Pyridine Bases*, Tekhnika, Kiev, 1965, 191 pp. (in Russian).
97. Mosher, G., Turner, L. and Carliemitte, A., *Syntheses of Organic Preparations*, Inostrannaya Literatura, Moscow, 1954, Vol. 5, 56 pp. (in Russian).
98. Nagiev, T.M., Mamed'yarov, G.M., Nagieva, Z.M. and Ali-zade, N.I., 'The method of 4-vinylpyridine N-oxide production', *Patent No. 1,068,430* (USSR), M.Kl^2 C07D213189, Publ. January 23, 1984, Bull. No. 3 (in Russian).
99. Nagiev, T.M., Mame'yarov, G.M., Ali-zade, N.I. *et al*., *Azerb. Khim. Zh.*, 1978, No. 3, pp. 16–21 (in Russian).
100. Nagiev, T.M., Mamed'yarov, G.M., Kasimov, R.M. *et al*., *Azerb. Khim. Zh.*, 1978, No. 3, pp. 16–21 (in Russian).
101. Nagiev, T.M., Mamed'yarov, G.M., Salakhov, V.A. *et al*., *Azerb. Khim. Zh.*, 1984, No. 2, pp. 67–73 (in Russian).
102. Nagiev, T.M. and Mamed'yarov, G.M., *Modeling and Optimization of Chemical Processes*, Elm, Baku, 1982, pp. 77–86 (in Russian).
103. Borisov, A.M., Lapshev, A.I., Malyutin, N.R., Karasev, V.I., Gaivorozhsky, V.I., Nikitin, Yu.S. and Bashirov L.S., 'The method of acetaldehyde production', *Patent No. 618,363* (USSR), MKI S 07 S47106; S 07 S45116, Publ. 1978, Bull. No. 29 (in Russian).
104. Kurina, L.N. and Morozova, E.P., *Zh. Fiz. Khim.*, 1977, Vol. 51, No. 9, pp. 2257–2260 (in Russian).
105. Koz'minykh, O.K., Makarevich, N.A., Ketov, A.N., Kostin, L.P. and Burnyishev, 'The method of acetaldehyde production', *Patent No. 352,874* (USSR), MKI C07C47/06, Publ. 1972, Bull. No. 29 (in Russian).
106. Nagiev, T.M., Zul'fugarova, S.Z. and Iskenderov, R.A., 'The method of acetaldehyde production', *Patent No. 891,623* (USSR), MKI^3 C07C47/06; C07C47/07, Publ. December 23, 1981, Bull. No. 47 (in Russian).
107. *US Patent No.* N4154762 (1979)
108. Gvozdovsky, G.N., Gushchevsky, A.B., Mushchenko, D.V., Petrov, A.N. and Malov, Yu.I., 'The method of aliphatic saturated ketones production', *Patent No. 482,434* (USSR), MKI C07C49/04, C07C49/08, C07C49/10, Publ. 1975, Bull. No. 32 (in Russian).
109. Pneva, E.Ya., Selyutina, L.P., Andrianova, N.A., Krokhmalyuk, A.E., Sisin, M.Ya., Leont'ev, A.S. and Yudaev, A.I., 'The method of methyl ethyl ketone production', *Patent No. 697,494* (USSR), MKI C07C49/10; C07C45/16, Publ. 1979, Bull. No. 42 (in Russian).
110. Nagiev, T.M., Zulfugarova, S.Z. and Tagieva, Sh.A., 'The method of methyl ethyl ketone production', *Patent No. 1,074,858* (USSR), M.Kl^2 C07C49/10; C07C45/29, Publ. February 23, 1984, Bull. No. 7 (in Russian).

111. Vardanyan, I.A. and Nalbandyan, A.B., *Kinetika i Kataliz*, 1981, Vol. 22, No. 5, pp. 1100–1103 (in Russian).
112. Nagiev, T.M. and Gasanova, L.M., 'The method of formaldehyde production', *Patent No. 1,011,627* (USSR), M.Kl^2 C07C47/048, Publ. April 15, 1983, Bull. No. 14 (in Russian).
113. Nagiev, T.M. and Gasanova, L.M., *Khim. Fiz.*, 1984, Vol. 3, No. 10, pp. 1455–1461 (in Russian).
114. Nagiev, T.M. and Gasanova, L.M., *Thes. Rep. All-Union Meeting on Chemical Synthesis Based on One-Carbon Molecules*, Nauka, Moscow, 1984, p. 73 (in Russian).
115. Khachatryan, L.A., Niazyan, O.M. and Mantashyan, A.A., *Arm. Khim. Zh.*, 1981, Vol. 34, No. 4, pp. 267–272 (in Russian).
116. Nagiev, T.M. and Gasanova, L.M., *Azerb. Khim. Zh.*, 1984, No. 3, pp. 31–37 (in Russian).
117. Mamedov, E.M., Farajev, E.G. and Nagiev, T.M., *Ibid.*, 1997, No. 1–4, pp. 45–48 (in Russian).
118. Nagiev, T.M., Farajev, E.G., Gasanova, L.M. and Mamedov, E.M., *Ibid.*, 1998, No. 1, pp. 101–108 (in Russian).
119. Vedeneev, V.T., Basevich, V.Ya. and Aruthyunov, V.S., *Usp. Khim.*, 1996, Vol. 65, No. 3, pp. 211–238 (in Russian).
120. Shcherbakov, P.M., Egorov, S.A. and Borbova, S.R., *Neftyanaya i Gazovaya Promyishlennost*, 1986, No. 1, p. 40 (in Russian).
121. Crunvald, V.R., Vedeneev, V.I., Krylov, I.Yu. *et al*., *Khim. Promst*., 1993, No. 11, p. 543 (in Russian).
122. Marchionna, M., Aragno, A. and Basini, L., In: *IX International Symposium on Alcohol Fuels*, Firenze, Italy, 1991, Vol. 1, No. 1, p. 68.
123. Mamedov, E.M., Kasimov, R.M. and Shakhtakhtinsky, T.N., *Khim. Promst.*, 1988, No. 12, p. 50 (in Russian).
124. Nagiev, T.M., *Chemical Conjugation*, Nauka, Moscow, 1989, p. 216 (in Russian).
125. Egerton, G.J., Minkoff, H.C. and Salooja, *Proc. Roy. Soc. London*, 1956, Vol. H235, p. 158.
126. Baldwin, R.R., Fuller, S.C., Longthorn, D. and Walzer, R.W., *J. Chem. Soc. Faraday Trans. I*, 1972, Vol. 68, pp. 1362.
127. Basevich, V.Ya., Kogarko, S.M. and Neigauz, M.G., *Izv. AN SSSR, Ser. Khim*., 1976, No. 1, p. 42 (in Russian).
128. Basevich, V.Ya., Kogarko, S.M. and Berezin, O.Yu., *Izv. AN SSSR, Ser. Khim*., 1979, No. 9, p. 1986 (in Russian).
129. Nagiev, T.M., Gasanova, L.M. and Ramazanova, Z.Yu., *Zh. Fiz. Khim*., 1994, Vol. 68, No. 1, pp. 23–28 (in Russian).
130. Nagiev, T.M., Gasanova, L.M. and Ramazanova, Z.Yu., 'The method of hydrogen production', *Patent No. 1,444,294* (USSR), B.I. 1988, No. 46 (in Russian).
131. Temkin, M.I., Shyb, F.S., Khomenko, A.A. and Apelbaum, L.O., *Scientific Bases of Hydrocarbon Catalytic Conversions*, Naukova Dumka, Kiev, 1977, pp. 3–27 (in Russian).
132. Skibida, I.P., *Usp. Khim.*, 1975, Vol. 44, No. 10, pp. 1729–1747 (in Russian).
133. Maslov, S.A., Vasil'chenko, S.A., Byumberg, E.A. and Dryuk, V.G., *Izv. AN SSSR, Ser. Khim*., 1972, No. 11, pp. 2467–2472 (in Russian).
134. Bobolev, A.V., Blyumberg, E.A., Norikov, Yu.D. and Emanuel, N.M., *Zh. Fiz. Khim*., 1970, Vol. 44, No. 1, pp. 1028–1035 (in Russian).
135. Griesbaum, K., *Petrol. Chem.*, 1980, No. 33, pp. 34–40.
136. Svern, D., Scaplan, J.T. and Dickel, G.B., *Syntheses of Organic Preparations*, Inostrannaya Literatura, Moscow, 1961, Col. 11, p. 75 (in Russian).
137. Fernhol, H., *Berichte*, 1951, Bd. 4, S 110–112.
138. Ctall, F. and Greenspan, M., *Ind. Eng. Chem*., 1955, Vol. 47, pp. 147–150.
139. Nagiev, T.M., Mamed'yarov, G.M. and Rzabekova, N.N., *Thes. Rep. 4th Republ. Conf. on Oxid. Heterogen. Catalysis*, Azneftekhim, Baku, 1978, pp. 103–104 (in Russian).
140. Nagiev, T.M. and Mamed'yarov, G.M., *Azerb. Khim. Zh*., 1981, No. 1, pp. 51–55 (in Russian).
141. Nagieva, T.M., Zulfugarova, S.Z. and Nagieva, Z.M., *Ibid*, 1980, No. 6, pp. 16–22 (in Russian).
142. Nagiev, T.M., *Ibid.*, 1979, No. 1, pp. 60–70 (in Russian).
143. Emanuel, N.M., *Neftekhimia*, 1977, Vol. 13, No. 3, pp. 323–338 (in Russian).
144. Nagiev, T.M., *Khim. Fiz*., 1983, No. 6, pp. 823–832 (in Russian).

145. Nagiev, M.F., Nagiev, T.M. and Aliev, A.M., *Azerb. Khim. Zh.*, 1968, No. 5, pp. 94–97 (in Russian).
146. Nagiev, M.F., Nagiev, T.M. and Aliev, A.M., *Ibid.*, 1969, No. 2, pp. 22–25 (in Russain).
147. Nagiev, M.F., Nagiev, T.M. and Aliev, A.M., *Dokl. AN SSSR*, 1970, Vol. 193, No. 1, pp. 151–155 (in Russian).
148. Mendeleev, D.I., *Tractates*, Izd. AN SSSR, Moscow, 1949, Vol. 13, p. 362 (in Russian).
149. Zhavoronkov, N.M., *D.I. Mendeleev ZhVKhO*, 1978, Vol. 23, No. 1, pp. 9–22 (in Russian).
150. Hartreck, P. and Dondes, S., *Nucleonics*, 1956, Vol. 14, No. 7, pp. 22–25.
151. Atroshchenko, V.I., Alekseev, A.M., Zasorin, A.P. *et al*., *The Course of Fixed Nitrogen Technology*, Khimia, Moscow, 1969, 384 pp. (in Russian).
152. Curtis, H.A., *Fixed Nitrogen, No. 4, The Chem. Cataloqueco*., 1932, Chap. 4, p. 463.
153. Stokes, C.S. and Knipe, W.W., *Ind. Eng. Chem*., 1960, Vol. 52, pp. 287–288.
154. La Roche, N.G., Etude de la torche electronique, la chemie des hautes temperatures, *Proc. CNRS*, 1955, 212 pp.
155. Fromens, E.D., *Chem. Eng. Prog*., 1956, Vol. 52, pp. 149–156.
156. Thomson, A.L., Formation and quenching of nitric oxide in a continuous flow furnace, *Spring Meeting of Western States Combustion Institute*, 1965, p. 243.
157. Polak, L.S., *Plasma Use in Chemical Processes*, Nauka, Moscow, 1970, 253 pp. (in Russian).
158. Gulyaev, G.V., Kozlov, G., Polak, L.S. *et al*., *Kinetics and Thermodynamics of Chemical Reactions in Low-Temperature Plasma*, Nauka, Moscow, 1965, pp. 132–151 (in Russian).
159. Polak, L.S. and Shipachev, V.S., *Ibid*., pp. 151–166 (in Russian).
160. Volpin, M.E. and Shur, V.B., *Dokl. AN SSSR*, 1964, Vol. 156, No. 5, pp. 1102–1105 (in Russian).
161. Shilov, A.E., *Usp. Khim.*, 1974, Vol. 43, No. 5, pp. 863–902 (in Russian).
162. Brintzinger, H., *J. Am. Chem. Soc*., 1966, Vol. 88, pp. 4305–4307.
163. Osborn, J.A., Jardine, F.H., Joung, J.F. and Wilkinson, G., *J. Chem. Soc*. A, 1966, No. 12, pp. 1711–1732.
164. Shilov, A.K., Shilov, A.E. and Brod'ko, Yu.G., *Dokl. AN SSSR*, 1967, Vol. 176, No. 6, pp. 1297–1299 (in Russian).
165. Hardy, R. and Bottomly, F., *The Questions of Nitrogen Fixation*, Mir, Moscow, 1982, 734 pp. (in Russian).
166. Chatt, J., Camara, P. and Richards, R., *New in Chemical Fixation of Nitrogen*, Mir, Moscow, 1983, 304 pp. (in Russian).
167. Nagiev, M.F., Nagiev, T.M., Bairamov, V.M. and Iskenderov, R.A., *Dokl. AN SSSR*, 1973, Vol. 213, No. 5, pp. 256–260 (in Russian).
168. Nagiev, T.M. and Shakhtakhtinsky, T.N., *Thes. Rep. 4th Intern. Symp. on Homogen. Catalysis*, Nauka, Leningrad, 1984, Vol. 2, p. 133 (in Russian).
169. *Nitrogen User Guide*, Khimia, Moscow, 1969, Vol. 2, 131 pp. (in Russian).
170. Aleshin, V.V., SHirokova, G.N. and Rosolovsky, V.Ya., *Zh. Neorg. Khim.*, 1981, Vol. 26, No. 8, pp. 2051–2058 (in Russian).
171. Partington, J.R. and Shach, C.C., *J. Chem. Soc*., 1931, Vol. pt. II, pp. 2071–2075.
172. Ushakova, N.N., Nikolaeva, E.R. and Morosanova, S.A., *Guidelines on Analytical Chemistry: Qualitative Analysis*, Izd. MGU, Moscow, 1981, 152 pp. (in Russian).
173. Hugnes, M.N. and Stedman, G., *J. Chem. Soc*., 1963, Vol. 8, pp. 4230–4236.
174. Addison, C.C., Camlen, G.A. and Thompson, R., *Ibid.*, 1952, pp. 346–354.
175. Nagiev, T.M., Zokhrabbekov, S.Z. and Shakhtakhtinsky, T.N., *Dokl. AN SSSR*, 1987, Vol. 292, No. 6, pp. 1392–1395 (in Russian).

This page intentionally left blank

– 5 –

Kinetics and the Mechanism of Synchronous (Interfering) Reactions of Hydrogen Peroxide Dissociation and Oxidation of Substrates in the Gas Phase

This chapter overviews the following points:

- Free-radical (chain) mechanism of oxidation with hydrogen peroxide.
- The role of $HO_2^{\bullet}$ radicals in gas-phase oxidation reaction control.
- Kinetic model of conjugated dehydrogenation of compounds.
- Unification of the model and its typical features.
- Detection and identification of $HO_2^{\bullet}$ radical as the main active site of both conjugated reactions and determination of its ability to dehydrogenation, epoxidation and nitrogen fixation.
- Bivalent oxidation with participation of $HO_2^{\bullet}$ radical and gas-phase, $HO_2^{\bullet}$-dependent elementary reactions.
- Probable mechanism of nitrous-oxide- and nitrogen-containing acid formation. Hydrogen peroxide ability to induce free-radical oxidation reactions.

5.1 DEHYDROGENATION MECHANISM AND GAS-PHASE $HO_2^{\bullet}$-DEPENDENT ELEMENTARY REACTIONS

Currently, the idea that the $HO_2^{\bullet}$ radical plays a key role is the foundation stone in the interpretation of multiple mechanisms for gas-phase oxidation reactions, which may scarcely be explained on the basis of different suggestions.

For example, in oxidation reactions proceeding at relatively high temperatures mostly as oxidative dehydrogenation and cracking (above 500 °C), $HO_2^{\bullet}$ radicals become the main active sites of the substrate radical transformation. As is known, these radicals are produced

by H_2O_2 vapor dissociation. Therefore, the study of various substrate oxidations with hydrogen peroxide can clarify the question about $HO_2^{\bullet}$ radical action on various substrates.

As is obvious from the previous chapter, dehydrogenation of various substrates in the presence of H_2O_2 is implemented by the free-radical mechanism, the rate of which is mostly defined by $HO_2^{\bullet}$ radical concentration in the system. Moreover, it is noted that conjugated dehydrogenation with hydrogen peroxide is performed by a mechanism that is principally different from high-temperature homogeneous oxidation of hydrocarbons by molecular oxygen. This is discussed in detail in two monographs [1, 2]. The processes of oxidation by molecular oxygen are complicated; therefore, some features of their mechanism should be taken into account when considering reactions with hydrogen peroxide.

Atomic oxygen formation from H_2O_2 at conjugated dehydrogenation of hydrocarbons on the reactor walls is of low probability, but to justify the possibility of oxygen participation in dehydrogenation, nitrous oxide decomposition [3]:

$$N_2O \rightarrow N_2 + O$$

was taken for its source. In the presence of butane or cyclohexane at 500–600 °C, N_2O decomposes by 25 and 30 mol.%, respectively [4, 5], i.e. N_2O decomposition is independent of hydrocarbon presence in the mixture.

Cyclohexane dehydrogenation in the presence of H_2O_2 displays higher selectivity at higher conversion level than in the presence of N_2O [5]:

	C_6H_{10} (%)	C_6H_8 (%)	C_6H_6 (%)	Selectivity (%)
$C_6H_{12} + H_2O_2$	20	4	3	98
$C_6H_{12} + N_2O$	9	2	7	80

Thus, dehydrogenation with hydrogen peroxide displays a mechanism that differs from oxidative dehydrogenation by molecular oxygen in the presence of nitric oxide. As a consequence, oxygen atom participation as an active site in conjugated oxidation of a substrate with hydrogen peroxide is almost improbable, and elementary reactions with it must not be taken into account in the mechanism. This conclusion is justified by butane dehydrogenation process in both presence of hydrogen peroxide and nitrous oxide [6]. In the second case, many side products were detected.

In accordance with the above, of special interest is kinetic assessment of H_2O_2 dissociation to $HO_2^{\bullet}$ and $^{\bullet}OH$ free radicals. Dissociation of H_2O_2 in the gas phase is a comprehensively studied reaction proceeding by the mechanism (4.1), from which the following equation is deduced:

$$\frac{\lfloor HO_2^{\bullet} \rfloor}{\lfloor {}^{\bullet}OH \rfloor} = \frac{k_1}{k_2}[H_2O_2] \tag{5.1}$$

This gives an opportunity to assess the concentration ratio of active sites in the system. It is found [6, 7] that the ratio in equation (5.1) falls within the range of between 10^3 and 10^7,

i.e. in the gas phase $HO_2^{\bullet}$ radical concentration is higher by many orders of magnitude than $^{\bullet}OH$ concentration.

Let us illustrate the mechanism of substrate dehydrogenation with hydrogen peroxide on the model hydrocarbon—ethylbenzene. Presumably, the process consists of the following stages [7] (the heat effect of the reaction is given in kJ/mol):

$$H_2O_2 \rightarrow 2^{\bullet}OH - 217.9 \tag{5.2}$$

$$H_2O_2 + {}^{\bullet}OH \rightarrow HO_2^{\bullet} + H_2O + 107.7 \tag{5.3}$$

$$C_6H_5C_2H_5 + {}^{\bullet}OH \rightarrow C_6H_5C_2H_4^{\bullet} + H_2O + 179.75 \tag{5.4}$$

$$C_6H_5C_2H_4^{\bullet} \rightarrow C_6H_5C_2H_3 + H - 52.7 \tag{5.5}$$

$$C_6H_5C_2H_5 + HO_2^{\bullet} \rightarrow C_6H_5C_2H_3 + H_2O + {}^{\bullet}OH + 220.8 \tag{5.6}$$

$$H_2O_2 + H \rightarrow H_2O + {}^{\bullet}OH + 286.6 \tag{5.7}$$

$$C_6H_5C_2H_5 + HO_2^{\bullet} \rightarrow C_6H_5C_2H_4^{\bullet} + H_2O_2 + 61.6 \tag{5.8}$$

$$\left.\begin{array}{l} HO_2^{\bullet} + \text{wall} \rightarrow HO_{2(\text{ads})}^{\bullet} \\ {}^{\bullet}OH + \text{wall} \rightarrow {}^{\bullet}OH_{(\text{ads})} \end{array}\right\} \rightarrow \text{products} \quad \begin{array}{l} (5.9) \\ (5.10) \end{array}$$

This scheme takes into account three directions of styrene chain formation in the $C_6H_5C_2H_5-H_2O_2-H_2O$ system. The hydroxyl radical formed at the elementary stage (5.2) is consumed in the volume in two possible reactions (5.3) and (5.4). Comparison of kinetic parameters of elementary stages (5.3) and (5.4), activation energies of which equal 4.2–8.4 [8] and 21–33.5 kJ/mol [9], respectively, shows that the rate of reaction (5.3) is much higher than the rate of reaction (5.4). Therefore, stage (5.3) is the most probable means of $^{\bullet}OH$ radical consumption in the system under consideration.

Of special attention is that the formation of hydrocarbon radicals in the reaction:

$$RH + {}^{\bullet}OH \rightarrow R^{\bullet} + H_2O$$

would cause synthesis of new $RO^{\bullet}$ and $RO_2^{\bullet}$ free radicals at the following stages of the process. Besides unsaturated compounds, the conversion of these free radicals will induce the formation of oxygen-containing substances and oxidative cracking products [10]. However, in ethylbenzene dehydrogenation products organic oxygen-containing compounds are absent; in the area of relatively low styrene yields (about 20%) oxidative cracking products were also not detected [11]. Taking this circumstance into account, it may be suggested [7] that the elementary stage (5.6) is the most probable one. Actually, activation energy of stage (5.8) usually exceeds 52.4 kJ/mol ($\log A_{(5.8)} = 9.4$ ($cm^3/(mol\,s)$)) [12, 13], and the activation

energy of stage (5.6) is below 46.1 kJ/mol [7, 14] ($\log A_{(5.8)} = 9.6$ (cm^3/(mol s))). For chain termination reactions due to $^{\bullet}OH$ and $HO_2^{\bullet}$ free radical recombination on the quartz reactor walls the probabilities of their arrest were determined as follows: $\varepsilon_{^{\bullet}OH} = 0.5 \times 10^{-6}$ and $\varepsilon_{HO_2^{\bullet}} = 0.2 \times 10^{-5}$ [7, 15]. Thus, an assessment of the results of the rates of elementary stages (5.2)–(5.10) suggests that conjugated dehydrogenation of ethylbenzene is a non-branched chain reaction with two stages of chain propagation as follows:

$$\begin{array}{r} H_2O_2 + {}^{\bullet}OH \xrightarrow{k_{(5.3)}} HO_2^{\bullet} + H_2O \\ C_6H_5C_2H_5 + HO_2^{\bullet} \xrightarrow{k_{(5.6)}} C_6H_5C_2H_3 + H_2O + {}^{\bullet}OH \\ \hline C_6H_5C_2H_5 + H_2O_2 = C_6H_5C_2H_3 + 2H_2O \text{ (the overall reaction)} \end{array}$$

Basing on the mechanism suggested and with the help of the stationary concentration method, the following kinetic equation of the reaction rate was deduced:

$$-\frac{d[EB]}{dt} = k_{eff}[EB][H_2O_2] \tag{5.11}$$

$$k_{eff} = k_{(5.2)}k_{(5.6)}k_{(5.9)} = 0.35 \times 10^{16} \exp\left(-\frac{231{,}707}{RT}\right), \text{ l/(mol s)}$$

This equation adequately describes the experimental data within the range 500–620 °C [6, 16].

Obviously, the expression for k_{eff} does not include the rate constant of reaction (5.3) and, therefore, reaction (5.6) running with participation of the $HO_2^{\bullet}$ radical represents the limiting stage of chain propagation.

Let us consider more comprehensively the role of the $HO_2^{\bullet}$ radical in the kinetics of the gas-phase oxidation reaction. In 1926, $HO_2^{\bullet}$ radical formation by the reaction below was initially suggested in the investigations of hydrogen oxidation by molecular oxygen:

$$H + O_2 + M \rightarrow HO_2^{\bullet} + M$$

Lloyd then applied this reaction to the description of the second limit of self-ignition [18], and Voevodsky [19] used it for an explanation of hydrogen peroxide formation mechanism at the third limit of self-ignition. In 1947, Eltenton made the first attempt at $HO_2^{\bullet}$ direct detection [20] using the mass-spectrometric method in C_3H_8 and O_2 flame. In the early 1960s, Panfilov [21], using the electron spin resonance (ESR) method, succeeded in detecting $HO_2^{\bullet}$ radicals in frozen products of hydrogen combustion.

The kinetic method of $HO_2^{\bullet}$ and $RO_2^{\bullet}$ radical freezing out and an analysis of their ESR spectra in relation to the oxidation of lower hydrocarbons are presented in detail in a monograph [22]. It was unambiguously shown for the first time (via direct measurements) that the areas of negative temperature coefficient occurrence in low- and high-temperature oxidation depend on the ratio $\lfloor HO_2^{\bullet} \rfloor / \lfloor RO_2^{\bullet} \rfloor$: at high-temperature oxidation, this ratio sharply increases and $HO_2^{\bullet}$ radicals become the active sites in chain propagation reactions.

Tal'rose [23] and many other authors [24, 25] presented an interesting sphere of $HO_2^{\bullet}$ radical participation: non-linear reactions and ozonosphere processes proceeding at ozone formation in the Earth atmosphere and chemical lasers.

As follows from a brief consideration of the role of $HO_2^{\bullet}$ radicals in gas-phase oxidation reactions, they are the key active sites in the high temperature range, and studies of homogeneous oxidative dehydrogenation of hydrocarbons allocate the dominating role in unsaturated compound formation to them.

In this regard, the above-suggested mechanism of ethylbenzene conjugated dehydrogenation with hydrogen peroxide presents a satisfactory explanation of styrene formation. Here the central place belongs to a new elementary reaction:

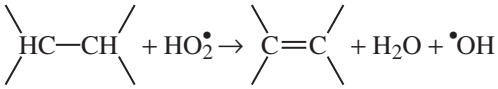

(5.12)

It is common knowledge that radical substitution reactions (where in the resulting interaction between free radicals and molecules an atom—most frequently a hydrogen atom—or a radical is transferred from a molecule to a free radical) mostly proceed towards the formation of a less active radical. From this point of view, two competing elementary stages (5.6) and (5.8), should be discussed.

Stage (5.6) is distinguished from common radical substitution reactions (including stage (5.8)) by simultaneous transfer of two hydrogen atoms (or $H^+ + e$) from two neighboring carbon atoms (in ethylbenzene molecule) to $HO_2^{\bullet}$ free radical via hexasite transition state (I) formed (according to (5.6) this state dissociates to two stable compounds, currently styrene and water):

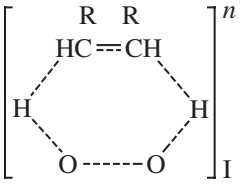

and $^{\bullet}OH$ free radical, which is much more active than the initial $HO_2^{\bullet}$ radical. If we are guided by the rule that radical substitution reaction is mostly developed toward the formation of a less active radical [26], the predominance of stage (5.8) rather than (5.6) may be expected. However, as follows from the data on heat effects of the reactions, stage (5.6) is a little more highly exothermal than (5.8). Then, if in the first approximation we use the equation of activation energy:

$$E = 11.5 - 0.25|q|$$

which is true for radical substitution reactions, the following values are deduced:

$$E_{(5.6)} = 20.1\,\text{kJ/mol} \quad \text{and} \quad E_{(5.8)} = 32.7\,\text{kJ/mol}$$

This indicates a preference of the chain process with stage (5.6) over that with stage (5.8). Moreover, stage (5.6) has one more specific feature. Contrary to common radical substitution reactions, it forms more active $^{\bullet}OH$ free radical than the initial radical. Hence it follows that the rule (radical substitution reaction is mostly developed toward the formation of less active radical) valid for radical substitution with transfer of only one hydrogen atom, is invalid for simultaneous transfer of two hydrogen atoms from the donor.

Integrating the above ideas, the authors conclude that if two final products and a free radical are synthesized in the radical reaction, the latter radical may possess higher activity compared with the initial radical (owing to energy gain at the second substance formation). The principle of indestructibility of the free valence [27] typical of the molecule-radical system is also preserved in this case, the only difference being that the substrate molecule in action (5.12) is subject to two-electron oxidation, contrary to the usual radical substitution reactions of types (5.4) and (5.8).

As a rule, it is assumed that if the substrate is subject to two-electron transfer in one stage, oxidation is implemented by the molecular mechanism. The validity of this statement is unambiguous; however, in the context of elementary reactions of type (5.12) it should be noted that the substrate is really oxidized with two-electron transfer in one chemical action, but at the reaction end free valence is preserved due to the second substance formation (H_2O in the case of reaction (5.12)).

From these positions, it is observed in reaction (5.12) that both molecular products result from the redox action between the substrate and radical. Such a paradoxical, at first glance, interaction in the molecule-radical system possesses all the advantages of molecular redox actions, because it allows the transformation of the substrate molecule to the final product omitting the stage of intermediate reactive particle formation ($C_6H_5C_2H_4^{\bullet}$ for the reaction (5.8)). These reactions are always highly selective and consume relatively low energy. Thus, the uniqueness of the $HO_2^{\bullet}$ radical is that, with respect to substrate type and reaction conditions, it can be both a one-electron (e.g. in reaction (5.8)) and a two-electron oxidant (reaction (5.12)). To put it another way, though the $HO_2^{\bullet}$ radical interacts with the substrate by the radical mechanism, the substrate itself is transformed by the molecular mechanism.

For the purpose of theoretical (quantum-mechanical) study of the $HO_2^{\bullet}$ radical's ability to detach two hydrogen atoms from substrate molecule in one stage, in the framework of non-empirical scheme [28] and on the basis STO-3G the heat effect of the following model reaction was calculated:

$$C_2H_6 + HO_2^{\bullet} \rightarrow C_2H_4 + {}^{\bullet}OH + H_2O$$

All initial and final compounds were calculated for optimal geometrical dimensions of the reacting particles. As a result, it is found that this reaction is exothermal ($\Delta q = 261.4$ kJ/mol). This value correlates well with $\Delta q = 199$ kJ/mol, deduced from the referenced data on chemical bond break energies.

As a result of these investigations, it is concluded that there are no quantum-mechanism restrictions of the existence of elementary reaction (5.12). Moreover, good quantitative correlation indicates the possibility of its proceeding.

Furthermore, a question was cleared up [28] about the probability of hexasite transition complex (II) formation.

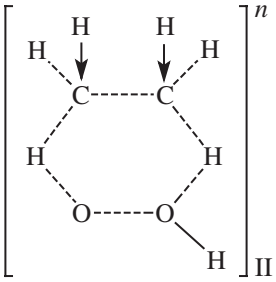

Preliminary approximate calculations of the transition state in $C_2H_6 + HO_2^{\bullet}$ reaction, also executed by the Partial Reservation of Double-Centered Differential Overlap (PRDDO) method [29, 30] indicate the interaction between masked ethane conformation (with a calculated internal rotation barrier equal 1.3 kJ/mol) and the $HO_2^{\bullet}$ radical approaching it in the C—C plane. The distance between C—C and O—O bond sites was taken as the reaction coordinate. It is found that planar structure (II) corresponds to the transition state in the $C_2H_6 + HO_2^{\bullet}$ reaction.

For transition state (II) the following structural parameters were determined: $r_{(C—C)} = 1.5$ Å; $r_{(O—O)} = 1.51$ Å; $r_{(C—H)} = 1.07$ Å; $r_{(O...H)} = 1.19$ Å. The formation of fixed planar complex (II) testifies to the simultaneous detachment of two hydrogen atoms from the C_2H_6 molecule. The energy of this complex is higher by approximately 838 kJ/mol than the total energy of the reaction product formation and may be taken as the upper border of the reaction. Full optimization of the transition state geometry may cause some deviations from the planar structure. However, this will not affect the principal possibility of the existence of a hexasite transition state (II). As products come closer, the O—O bond and two C—H bonds will break forming H_2O and $^{\bullet}OH$, and calculation data will approach the real energy barrier value.

Thus, for the first time, quantum-mechanical investigations have outlined the possibility of two-electron transfer in one stage by elementary reaction (5.12), which has expanded our knowledge of the properties of the $HO_2^{\bullet}$ free radical, still relatively poorly studied, in radical-chain oxidation processes.

Elementary reaction (5.12) was successfully applied to the kinetic description of the conjugated dehydrogenation of various substrates using corresponding interaction rate constants between $HO_2^{\bullet}$ and RH.

Propylene thermal oxidation with hydrogen peroxide is implemented with formation of propylene oxide, acrolein and allene, and C_3H_6 present in the system plays the role of the 'active oxygen' acceptor from $^{\bullet}O—OH$. To put it another way, the conjugated oxidation of propylene with hydrogen peroxide is also a $HO_2^{\bullet}$-dependent reaction [31].

Reaction	A (cm^3/mol s)	E (kJ/mol)
1. $C_3H_6 + HO_2^{\bullet} \rightarrow$ 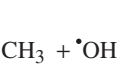 $+ {}^{\bullet}OH$	0.152×10^{10}	54.4
2. $C_3H_6 + HO_2^{\bullet} \rightarrow CH_2{=}C{=}CH_2 + H_2O + OH$	0.154×10^{14}	65.7
3. $C_3H_5^{\bullet} + HO_2^{\bullet} \rightarrow CH_2{=}C{—}CHO + H_2O$	–	–

It should be noted that for elementary reactions (1) and (2) the kinetic parameters determined to some extent conform to the theory [32] and the results recently obtained in the work [33] on Arrhenius parameters of $HO_2^{\bullet}$ radical addition to ethylene (400–500 °C). For the reaction:

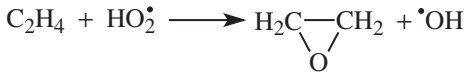

the values of the pre-exponential factor and the activation energy equal $10^{-12 \cdots 0.56 \pm 0.35}$ $cm^3/mol\,s$, respectively, were obtained.

However, the somewhat underestimated value of the pre-exponential factor of the elementary reaction (1) may be explained by the type of $HO_2^{\bullet}$ radical interaction.

The study of the kinetics and mechanism of high-temperature methane oxidation with hydrogen peroxide to a hydrogen-containing gas considers that a new elementary reaction is responsible for the final product formation, H_2 and CO_2:

$$CH_2O + HO_2^{\bullet} \rightarrow H_2 + CO_2 + {}^{\bullet}OH$$
$$\log A = 10.3\ (cm^3/(mol\,s))$$
$$E = 14.2\ kJ/mol$$

The kinetic model derived from the free-radical mechanism includes this stage as one of the basic steps of the reaction and adequately describes experimentally observed regularities. Moreover, the suggested mechanism contains one more elementary stage with $HO_2^{\bullet}$ radical participation:

$$CO + HO_2^{\bullet} \rightarrow CO_2 + {}^{\bullet}OH$$
$$\log A = 14.18\ (cm^3/(mol\,s))$$
$$E = 99.1\ kJ/mol$$

To sum up, it should be noted that the implementation of selective gas-phase oxidation reactions containing $HO_2^{\bullet}$-dependent elementary stages, which control the reaction run, demonstrates their versatility with respect to high synthesis abilities.

This is also proved by theoretical ideas: reactions implemented with the participation of free radicals (including $HO_2^{\bullet}$) are much less sensitive to changes in electron density in substrate molecules compared with the reactions that include intermediate compounds of polar origin.

5.2 CONJUGATED DEHYDROGENATION AND OXIDATION WITH HYDROGEN PEROXIDE

Let us now show the methodology for the thermodynamic and kinetic determination of chemical conjugation in the reaction mixture and some features of the treatment of theoretical and experimental results using the examples of analysis of self-kinetic experiments in the field of conjugated dehydrogenation and oxidation with hydrogen peroxide. The most

widespread and applied processes are discussed in detail, whereas the remaining processes are mentioned only in order to arouse interest in further investigations.

5.2.1 Dehydrogenation alkylbenzenes

The study of chemical conjugation between two or more reactions in the reaction system consists of the following steps:

1. First, the free energy change ΔG^0_{873} of the primary reaction (4.2) equal -246.4 kJ/mol fully compensates for the free energy 'deficiency' in the secondary reaction. For this purpose, let us calculate ΔG^0_{873} at test temperatures for each of the following reactions:

$$\left.\begin{array}{l} C_6H_5C_3H_7 \\ CH_3C_6H_4C_2H_5 \\ C_6H_4(C_2H_5)_2 \\ C_6H_4(C_2H_3)C_2H_5 \end{array}\right\} \rightarrow H_2 + \left\{\begin{array}{ll} C_6H_5C_3H_5 & -7.5 \quad (5.13) \\ CH_3C_6H_4C_2H_3 & -26.8 \quad (5.14) \\ C_6H_4(C_2H_3)C_2H_5 & - \quad (5.15) \\ C_6H_4(C_2H_3)_2 & - \quad (5.16) \end{array}\right.$$

(ΔG^0_{873}, kJ/mol)

For conjugated reactions (4.2), (5.13) and (5.14), we obtain:

$$\Delta G^0_{873(4.2)} + \Delta G^0_{873(5.13)} = -238.8\,\text{kJ/mol} < 0$$

$$\Delta G^0_{873(4.2)} + \Delta G^0_{873(5.14)} = -219.5\,\text{kJ/mol} < 0$$

Clearly, all ΔG^0_{873} values were below zero and according to theoretical notions about conjugated processes (refer to Chapters 2 and 3) these reactions can be chemically conjugated. However, this suggestion is a necessary but by far insufficient condition, because in principle, the infinite number of non-conjugation reactions can obey this rule.

2. The second and most complicated step is the determination of thermodynamic conjugation in the framework of irreversible process thermodynamics due to the possible absence of data on reactions (5.13)–(5.16).

   Actually, if Aw can be calculated for every reaction of (5.13)–(5.16) (refer to Chapters 2 and 3) and the following inequality fulfillment can be shown (thermodynamic conjugation condition):

$$A_1 w_1 + A_2 w_2 > 0$$

   then such a pair of reactions has connection channels and must be conjugated. However, kinetic data for the calculation of w_1 and w_2 may be absent. Then approximate values which can always be found should be used. *A priori* this inequality is fulfilled for all the reactions under consideration. Thus, as the principal question about the possibility of chemical conjugation in the current reaction mixture is decided, kinetic conditions should be found under which the system will operate. This requires additional experimental studies.

Table 5.1

Conjugated dehydrogenation of alkylbenzenes at 600 °C

Alkylbenzene	Reagent rate (mol/h)		Reaction product yield (mol/h)				f_{A_1}	f_{A_2}	$\frac{f_{A_1}}{Acc}$	$\frac{f_{A_2}}{Acc}$	D
	Acc	H_2O_2	Styrene	Vinyltoluene	Divinylbenzene	Vinyl ethylbenzene					
Ethylbenzene	0.065	0.155	0.019[a]	–	–	–	0.06783	0.019	3.5	1	0.22
Isopropylbenzene	0.013	0.086	0.004	–	–	–	0.0409	0.004	9.5	1	0.1
Ethyltoluene	0.007	0.0259	–	0.002	–	–	0.0119	0.002	5.9	1	0.14
Vinyl ethylbenzene	0.018	0.0729	–	–	0.006	–	0.03345	0.006	5.57	1	0.15
Diethylbenzene	0.018	0.0729	–	–	–	0.05 (*m*)	0.0339	0.005	6.8	1	0.13
						0.03 (*o*, *n*)	0.02145	0.003	7.15	1	0.12

[a]Side products at the rate of 0.01 mol/h are formed.

3. Let us consider the kinetic features of isopropylbenzene, diethylbenzene and vinyl ethylbenzene dehydrogenation. Table 5.1 presents experimental data obtained under optimal conditions, which indicate successful implementation of the process. However, experimental justification of the results of a dehydrogenation reaction performed with hydrogen peroxide and thermodynamic conjugation are insufficient for making the final conclusion about the conjugation of these reactions. As follows from previous chapters, in principle, dehydrogenation can be initiated or radical chain, the reactor wall catalysis is also possible, etc.
4. The final conclusion requires calculation of the determinant using equation (2.17) and experimental data (Table 5.1) and determination by the scale (see Figure 2.2) the interval of its occurrence. All D values found (Table 5.1) fall within the range 0.1–0.2, which is the quantitative characteristic of chemical conjugation.
5. The next investigation step concludes in identification and quantitative assessment of reactive intermediate compounds operating *in situ*, which is general for both conjugated reactions.

   The mechanism of H_2O_2 dissociation has already been discussed in detail. Note only that this reaction generates two types of free radicals in the reaction system—$^{\bullet}OH$ and $HO_2^{\bullet}$—and their ratio is calculated by equation (5.1). In this case, the ratio $\lfloor HO_2^{\bullet} \rfloor / \lfloor {}^{\bullet}OH \rfloor$ falls within the same range, mentioned above, i.e. between 10^{-5} and 10^{-7}. From this it follows that $HO_2^{\bullet}$ radicals are the main active sites in the system. Essentially, the presence of substrate will affect the ratio value, but as shown in calculations, for current H_2O_2 concentration the order of magnitude is preserved. Hence, after identifying the intermediate that transmits the induction effect of the primary reaction on the secondary reaction and quantitatively assessing its concentration, the reaction mechanism of the intermediate must be determined.
6. It should be taken into account that $HO_2^{\bullet}$ radicals will be consumed in the secondary reaction and change its type. Therefore, the elementary stages responsible for their formation should be indicated. After adding the elementary reaction (5.11), by which the dehydrogenation product is synthesized, to these stages, the following scheme is obtained:

$$H_2O_2 + {}^{\bullet}OH \rightarrow H_2O + HO_2^{\bullet}$$

$$HO_2^{\bullet} + \begin{Bmatrix} C_6H_5C_3H_7 \\ CH_3C_6H_4C_2H_5 \\ C_6H_4(C_2H_5)_2 \\ C_6H_4(C_2H_3)C_2H_5 \end{Bmatrix} \rightarrow H_2O + {}^{\bullet}OH + \begin{Bmatrix} C_6H_5C_3H_5 \\ CH_3C_6H_4C_2H_3 \\ C_6H_4(C_2H_3)C_2H_5 \\ C_6H_4(C_2H_3)_2 \end{Bmatrix}$$

Therefore, the overall reaction is the following:

$$H_2O_2 + \begin{Bmatrix} C_6H_5C_3H_7 \\ CH_3C_6H_4C_2H_5 \\ C_6H_4(C_2H_5)_2 \\ C_6H_4(C_2H_3)C_2H_5 \end{Bmatrix} \rightarrow 2H_2O + \begin{Bmatrix} C_6H_5C_3H_5 & -352.4 & (5.17) \\ CH_3C_6H_4C_2H_3 & -333.1 & (5.18) \\ C_6H_4(C_2H_3)C_2H_5 & - & (5.19) \\ C_6H_4(C_2H_3)_2 & - & (5.20) \end{Bmatrix}$$

ΔG^0_{873} (kJ/mol)

Comparison of overall reactions (5.13)–(5.16) and (5.17)–(5.20) shows that (5.13)–(5.16) transform from common dehydrogenation to oxidative dehydrogenation with hydrogen peroxide participation. Such transformation of the target, secondary reaction in the reaction system becomes possible owing to the induction effect of the primary reaction of H_2O_2 dissociation.

7. For each of reactions (5.17)–(5.20), by analogy with kinetics of conjugated dehydrogenation of ethylbenzene, kinetic equation (5.11) is deduced, the solution of which determines the kinetic parameters, for example [6]:

$$k_{\text{eff}(5.18)} = 0.52 \times 10^{20} \exp\left(-\frac{230500}{RT}\right)$$

Here, conjugated dehydrogenation of ethylpyridine (EP) might be considered, but because of the task of solution identity we will limit our consideration to the kinetic parameters of the overall reaction and the stage of interaction between 4-EP and $HO_2^{\bullet}$ radicals [6]:

	$\log A$ (cm^3/mol s)	E (kJ/mol)
4-EP + $H_2O_2 \rightarrow$ 4-VP + $2H_2O$	23.8	213.7
4-EP + $HO_2^{\bullet} \rightarrow$ 4-VP + H_2O + $^{\bullet}OH$	10.8	42.7

Thus, taken together, the theoretical and experimental studies carried out lead to a new, chemically particularized mechanism of conjugated dehydrogenation, which consists of the primary (induction) reaction of H_2O_2 dissociation and the secondary (inducible) reaction of conjugated dehydrogenation.

5.2.2 Cyclohexane and cyclopentane dehydrogenation

1. The usual step-by-step dehydrogenation of cyclohexane to cyclohexene, cyclohexadiene and benzene is a thermodynamically hindered reaction:

	ΔG^0_{298} (kJ/mol)
$C_6H_{12} \rightarrow C_6H_{10} + H_2$	–
$C_6H_{10} \rightarrow C_6H_8 + H_2$	80.4
$C_6H_8 \rightarrow C_6H_6 + H_2$	57.5

Actually, from an energy-gaining position, it is desirable to carry out such reactions conjugated with another reaction, which can be hydrogen peroxide dissociation.

2. Experimental data shown in Chapter 4 testify to the formation of reaction products (cyclohexadiene and benzene) via consecutive conjugated dehydrogenation of higher saturated analogs.
3. The conjugation determinant calculated from these data equals $D \approx 0.1$ under optimal conditions, which indicates the induced type of cyclohexane dehydrogenation.

4. The mechanism of formation of the reaction products represents the following consecutive reactions:

$$H_2O_2 + \begin{Bmatrix} C_6H_{12} \\ C_6H_{10} \\ C_6H_8 \end{Bmatrix} \rightarrow 2H_2O + \begin{Bmatrix} C_6H_{10} \\ C_6H_8 \\ C_6H_6 \end{Bmatrix}$$

ΔG^0_{873} (kJ/mol)
−373.5
−271.9
–

Comparison of conjugated and usual dehydrogenation results indicates the desirability of the oxidation method. Each consecutive reaction described by the chain non-branched scheme represents a combination of initiation, propagation and chain termination stages.

5. The system of kinetic equations, which adequately describes experimental data, is as follows [6]:

$$-\frac{d[C_6H_{12}]}{dt} = k_{eff_1}[C_6H_{12}][H_2O_2]$$
$$-\frac{d[C_6H_{10}]}{dt} = k_{eff_1}[C_6H_{12}][H_2O_2] - k_{eff_2}[C_6H_{10}][H_2O_2]$$
$$-\frac{d[C_6H_8]}{dt} = k_{eff_2}[C_6H_{10}][H_2O_2] - k_{eff_3}[C_6H_8][H_2O_2]$$

where

$$k_{eff_1} = 10^{24.9} \exp\left(-\frac{264000}{RT}\right) \text{ cm}^3/(\text{mol s})$$
$$k_{eff_2} = 10^{23.9} \exp\left(-\frac{222000}{RT}\right) \text{ cm}^3/(\text{mol s})$$
$$k_{eff_3} = 10^{22.8} \exp\left(-\frac{205000}{RT}\right) \text{ cm}^3/(\text{mol s})$$

The gross dehydrogenation process is well described by the chain radical scheme possessing the following rate constants of $HO_2^{\bullet}$ radicals with cyclohexane and cycloolefins:

$$HO_2^{\bullet} + \begin{Bmatrix} C_6H_{12} \\ C_6H_{10} \\ C_6H_8 \end{Bmatrix} \rightarrow {}^{\bullet}OH + H_2O + \begin{Bmatrix} C_6H_{10} \\ C_6H_8 \\ C_6H_6 \end{Bmatrix}$$

$\log A$ ($\text{cm}^3/(\text{mol s})$)	E (kJ/mol)
11.65	63.7
10.65	63.7
9.86	40.2

This example shows the extent to which conjugated reaction study is simplified, if scientists have data on general regularities of conjugated oxidation with hydrogen peroxide.

Conjugated dehydrogenation of cyclopentane to cyclopentadiene passes through an intermediate formation of cyclopentene, and kinetic regularities of this reaction are identical to those for cyclohexane:

	$\log A$ (cm^3/(mol s))	E (kJ/mol)
$H_2O_2 + \begin{Bmatrix} C_5H_{10} \\ C_5H_8 \end{Bmatrix} \rightarrow 2H_2O + \begin{Bmatrix} C_5H_8 \\ C_5H_6 \end{Bmatrix}$	23.73 23.39	216.0 238.8
$HO_2^{\bullet} + \begin{Bmatrix} C_5H_{10} \\ C_5H_8 \end{Bmatrix} \rightarrow {}^{\bullet}OH + H_2O + \begin{Bmatrix} C_5H_8 \\ C_5H_6 \end{Bmatrix}$	23.73 23.39	216.0 238.8

The possibility of obtaining unsaturated hydrocarbons and their derivatives by conjugation H_2O_2 dissociation and dehydrogenation of organic compounds indicates the definite versatility of this method. This is also confirmed by theoretical notions: reactions proceeding with the participation of free radicals are much less sensitive to changes in electron density of substrate molecules compared with the reactions including intermediate compounds of polar origin.

5.2.3 Methane oxidation to formaldehyde

The process of incomplete oxidation of methane to formaldehyde by molecular oxygen has been studied in numerous works and has always been presented by the unique stoichiometric equation:

$$CH_4 + O_2 = H_2CO + H_2O \qquad (5.21)$$
$$\Delta G^0_{800} = -268\,\text{kJ/mol}$$

Obviously, this reaction is spontaneous and under definite kinetic conditions is implemented in the presence of catalysts in two stages with low conversion and selectivity (refer to Chapter 4):

$$CH_4 + \frac{1}{2}O_2 = CH_3OH$$
$$CH_3OH + \frac{1}{2}O_2 = H_2CO + H_2O$$

It is shown that methane oxidation to formaldehyde may be implemented with great efficiency by a conjugated process in the presence of H_2O_2. As mentioned in Chapter 3, spontaneous reactions may also be induced for which conditions with advantageous kinetics cannot be selected. The low-effective reaction (5.21) unambiguously belongs to this class of processes.

Chapter 4 presents experimental data on methane oxidation to formaldehyde with hydrogen peroxide. We shall not discuss them here again, but use them only for determinant D calculation. The calculated D value is 0.2 which, according to currently developed ideas, indicates the conjugated type of CH_4 oxidation with hydrogen peroxide.

In accordance with the chemical conjugation concept applied to processes of oxidation with hydrogen peroxide, H_2O_2 dissociation by Scheme (4.1) is the primary process, and for methane the following reaction becomes of great importance:

$$\begin{aligned} &CH_4 + {}^{\bullet}OH \rightarrow CH_3 + H_2O \\ &\log A = 12.5\,(\mathrm{cm^3/(mol\,s)}) \\ &E = 8.4\,\mathrm{kJ/mol} \end{aligned} \tag{5.22}$$

The concentration of $HO_2^{\bullet}$ radicals in the system H_2O_2–H_2O–CH_4 will be defined by the ratio of the rates of reactions (5.3) and (5.2). At the molar ratio CH_4:H_2O_2 = 1:1, corresponding to optimal conditions of formaldehyde production,

$$\frac{\left\lfloor HO_2^{\bullet} \right\rfloor}{\left\lfloor {}^{\bullet}OH \right\rfloor} = 0.22 \cdot 10^4$$

and the rates of elementary stages (5.3) and (5.22) with respect to the reaction:

$$CH_3^{\bullet} + HO_2^{\bullet} \rightarrow H_2CO + H_2O \tag{5.23}$$

are nearly equal and fall within the range between 0.46×10^{-6} and 0.60×10^{-6} mol/(cm^3 s). As a consequence, $^{\bullet}$OH radicals formed in reaction (5.2) interact with H_2O_2 and CH_4 with almost equal rates [34].

In this context, CH_4 oxidation with hydrogen peroxide holds a special place, because in the presence of other compounds (ethylbenzene, cyclohexane, etc.) the ratio:

$$\frac{\left\lfloor HO_2^{\bullet} \right\rfloor}{\left\lfloor {}^{\bullet}OH \right\rfloor} >> 10^4 \text{ [35]}$$

that is $HO_2^{\bullet}$ is the leading active site. Under optimal conditions at methane oxidation, the concentration ratio between $CH_3^{\bullet}$ and $HO_2^{\bullet}$ is the following:

$$\frac{\left\lfloor HO_2^{\bullet} \right\rfloor}{\left\lfloor CH_3^{\bullet} \right\rfloor} < 10^2$$

This circumstance indicates that cross recombination by reaction (5.23) is the main means of formaldehyde formation. Other alternative pathways of formaldehyde formation were also considered:

	$\log A$ [cm^3/(mol s)]	E (kJ/mol)	
$CH_3^{\bullet} + HO_2^{\bullet} \rightarrow CH_3O^{\bullet} + {}^{\bullet}OH$	13.51	0	(5.24)
$CH_3O^{\bullet} + CH_3^{\bullet} \rightarrow H_2CO + CH_4$	13.40	0	(5.25)

Apparently, elementary stages (5.24) and (5.25) are not of very great significance, because $CH_3O^\bullet$ formation by reaction (5.24) ought to cause methanol accumulation in the system:

$$CH_3O^\bullet + CH_4 \rightarrow CH_3OH$$

which is not observed in the experiment [34].

The results of methanol addition to the system H_2O_2—H_2O—CH_4 lead to an unambiguous conclusion about the non-intermediate role of CH_3OH in the selective oxidation of CH_4 with hydrogen peroxide [36, 37]. This reaction does not produce CO and CO_2, therefore, in conditions of relatively low temperatures and short contact times the elementary stages of their formation were not taken into account in the suggested mechanism of CH_4 oxidation. Moreover, the following reaction was also excluded from the oxidation scheme:

$$\begin{aligned} &CH_4 + HO_2^\bullet \rightarrow CH_3^\bullet + H_2O_2 \\ &\log A = 13.3\,(\mathrm{cm^3/(mol\,s)}) \\ &E = 75.4\,\mathrm{kJ/mol} \end{aligned}$$

This probably happens because of high activation energy. The list of elementary stages (5.2), (5.3), (5.9), (5.10), (5.22) and (5.23) must be added to by the chain termination reaction due to $CH_3^\bullet$ radical recombination [36, 37]:

$$\begin{aligned} &CH_3^\bullet + \mathrm{wall} \rightarrow CH_{3(\mathrm{ads})}^\bullet \\ &\log A = 0.68\ [\mathrm{s^{-1}}] \\ &E = 55.7\,\mathrm{kJ/mol} \end{aligned} \tag{5.26}$$

The overall equation of conjugated methane oxidation with hydrogen peroxide including all necessary stages is the following:

$$CH_4 + 2H_2O_2 = H_2CO + 3H_2O \tag{5.27}$$

As a result of these investigations, the most probable mechanism was suggested. According to this mechanism, H_2O_2 dissociation and methane oxidation (5.27) reactions are chemically conjugated via general intermediates – $^\bullet OH$ and $HO_2^\bullet$ free radicals.

Based on the suggested mechanism of formaldehyde formation, the following scheme of kinetic equations which adequately describe the experimental data (Figure 5.1) was suggested [36, 37]:

$$\begin{aligned} -\frac{\mathrm{d}\left[CH_4\right]}{\mathrm{d}t} &= k_{(5.22)}[CH_4][^\bullet OH] \\ -\frac{\mathrm{d}\left[^\bullet OH\right]}{\mathrm{d}t} &= 2k_{(5.2)}[H_2O_2][\mathrm{M}] - k_{(5.3)}[H_2O_2][^\bullet OH] \\ &\quad - k_{(5.22)}[CH_4][^\bullet OH] - k_{(5.10)}[^\bullet OH] \end{aligned}$$

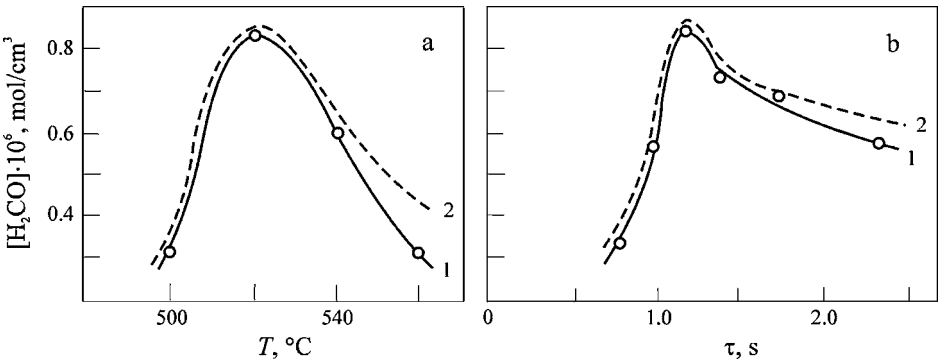

Figure 5.1 Dependencies of formaldehyde concentration on (a) temperature and (b) contact time. Molar ratio CH_4:25% H_2O_2 = 1:1 (1: experimental data and 2: calculated data).

$$-\frac{\mathrm{d}\lfloor \mathrm{HO}_2^{\bullet} \rfloor}{\mathrm{d}t} = k_{(5.3)}[\mathrm{H_2O_2}][^{\bullet}\mathrm{OH}] - k_{(5.23)}[\mathrm{CH}_3^{\bullet}][\mathrm{HO}_2^{\bullet}] - k_{(5.9)}[\mathrm{HO}_2^{\bullet}]$$

$$-\frac{\mathrm{d}\lfloor \mathrm{CH}_3^{\bullet} \rfloor}{\mathrm{d}t} = k_{(5.22)}[\mathrm{CH_4}][^{\bullet}\mathrm{OH}] - k_{(5.23)}[\mathrm{CH}_3^{\bullet}][\mathrm{HO}_2^{\bullet}] - k_{(5.26)}[\mathrm{CH}_3^{\bullet}]$$

For kinetic calculations [38] it was suggested that pre-exponential coefficients of the elementary stages (5.23) and (5.24) are equal:

$$\log A_{(5.23)} = \log A_{(5.24)}$$

The activation energy of free radical recombination approached zero. As a result of these investigations, the conditions for selective conjugated oxidation of methane to formaldehyde with hydrogen peroxide were determined and the process mechanism was suggested. The example is notable, because two types of free radicals ($CH_3^{\bullet}$ and $HO_2^{\bullet}$) are reactive particles in it.

5.2.4 Direct methane oxidation to methanol under pressure

The experimental results on conjugated methane oxidation under pressure with hydrogen peroxide displayed the most probable mechanism of methanol synthesis.

The scope of the experimental data allowed the determination of several kinetic regularities, among which the synchronized curves (Figure 5.2) are of special interest which demonstrate the induction effect of the primary reaction (hydrogen peroxide dissociation) on the secondary (inducible) reaction of CH_4 hydroxylation.

The comparison of molecular oxygen accumulation and CH_4 consumption (or CH_3OH accumulation) curves displays correspondence between O_2 accumulation minimum and the maximum of CH_4 conversion to CH_3OH.

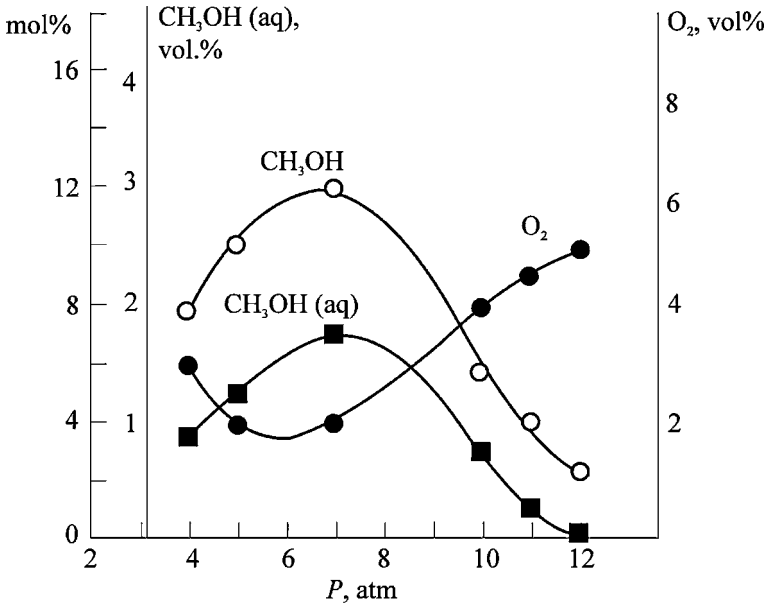

Figure 5.2 Pressure influence on methanol yield. $T = 400\,^{\circ}C$; $c_{H_2O_2} = 30\%$; CH_4:H_2O_2 = 1:0.4; $v_{H_2O_2} = 0.18$ l/h; $v_{CH_4} = 62.4$ l/h.

Due to 100% selectivity of the reaction, chemical interference is clearly displayed: intensification of O_2 formation causes simultaneous decrease of CH_4 conversion to CH_3OH and vice versa. The determinant (D) of chemical interference found from the equation:

$$D = \nu\left(\frac{r_1}{r_{CH_4}} + \frac{r_2}{r_{CH_4}}\right)^{-1} \tag{5.28}$$

equaled 0.18 (where r_1, r_2 and r_{CH_4} are consumption rates of the actor (H_2O_2), inducer (H_2O_2) and acceptor (CH_4), respectively; ν is the stoichiometric number, equal one in the current case, under the test conditions corresponded to maxima of O_2 and CH_3OH synthesis).

Lying in the area of conjugated reactions on the chemical interference scale, this value characterizes the induction effect of H_2O_2 on CH_4 oxidation and indicates great potential ability to intensify the induction effect of the system studied (theoretically, D may increase to 1, but in practice attempts to reach, at least, a level of 0.5). Of course, there are kinetic experimental methods, which give an opportunity to manipulate the rates of conjugated reactions.

Overall reactions proceeding in the reaction system can be presented in the following form:

$$\underset{\text{actor}}{H_2O_2} + \underset{\text{inducer}}{H_2O_2} = 2H_2O + O_2 \quad \text{(primary reaction)} \tag{5.29}$$

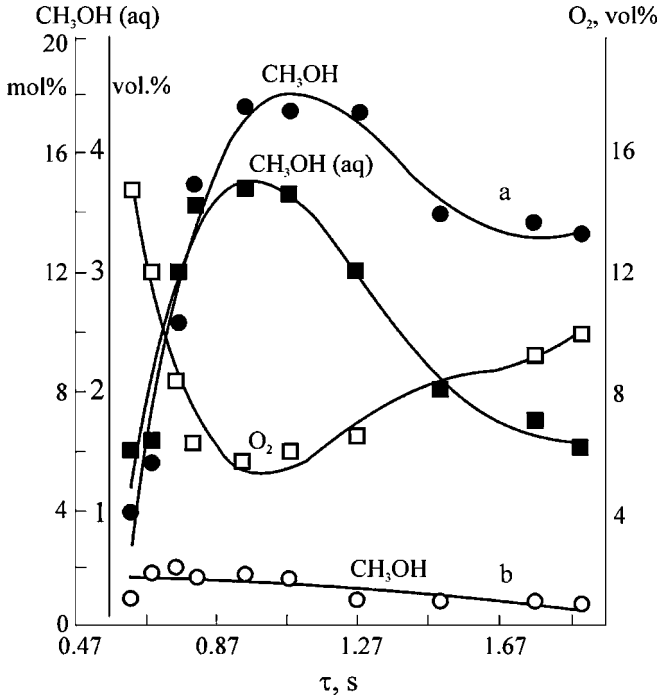

Figure 5.3 The dependence of methanol and O_2 yields on the contact time on: (a) quartz and (b) metal walls of the reactor. $T = 400\,°C$, $P = 7\,atm$; molar ratio CH_4:H_2O_2 = 1:1.4; $c_{H_2O_2} = 30\%$.

$$\underset{\text{actor}}{H_2O_2} + \underset{\text{acceptor}}{CH_4} = CH_3^{\bullet}OH + H_2O \quad \text{(secondary reaction)} \tag{5.30}$$

where H_2O_2 represents both the actor and the inducer, and CH_4 is the acceptor.

Equations (5.29) and (5.30) do not show the means of setting the inter-reaction communication. For this purpose, active intermediate compounds should be identified, the kinetic studies of which will help in determining connection channels between reactions (5.29) and (5.30).

It is common knowledge that the primary reaction of H_2O_2 dissociation generates active sites of two types in the system—$^{\bullet}OH$ and $HO_2^{\bullet}$ free radicals, which easily react with methane molecules (substitution reaction) under current experimental conditions and form new free radicals $CH_3^{\bullet}$ and $CH_3O^{\bullet}$. Methane is oxidized to methanol with 100% selectivity that allows us to limit with free methyl and methoxy radicals. Since this is a homogeneous (non-catalytic) flow reaction system operating in the plug flow mode, a series of experiments was devoted to the study of reactor wall influence on methane oxidation. The data presented in Figure 5.3 show that quartz walls of the reactor induce a significant effect on the course of oxidation and unambiguously indicate the free-radical type of the reaction.

Table 5.2

Elementary reactions of H_2O_2 dissociation and methanol synthesis from methane

No.	Reaction	$\log A$ (cm^3/mol s)	E (kJ/mol s)
1	$H_2O_2 \xrightarrow{k_1} 2^{\bullet}OH$	15.1 (s^{-1})	197.4
2	$H_2O_2 + {}^{\bullet}OH \xrightarrow{k_2} HO_2^{\bullet} + H_2O$	10.59	2.14
3	$CH_4 + {}^{\bullet}OH \xrightarrow{k_3} CH_3^{\bullet} + H_2O$	12.5	10.7
4	$CH_4 + HO_2^{\bullet} \xrightarrow{k_4} CH_3O^{\bullet} + H_2O$	17.3	77.04
5	$CH_3^{\bullet} + {}^{\bullet}OH \xrightarrow{k_5} CH_3O^{\bullet}$	13.16	0
6	$CH_3^{\bullet} + HO_2^{\bullet} \xrightarrow{k_6} CH_3O^{\bullet} + H_2O$	11.2	0
7	$CH_3^{\bullet} + H_2O_2 \xrightarrow{k_7} CH_3OH + {}^{\bullet}OH$	12.02	6.21
8	$CH_3^{\bullet} + CH_4 \xrightarrow{k_8} CH_3OH + CH_3^{\bullet}$	12.1	46.65
9	$CH_3^{\bullet} + H_2O_2 \xrightarrow{k_9} CH_3OH + HO_2^{\bullet}$	11.15	16.69
10	$CH_3^{\bullet} + \text{wall} \xrightarrow{k_{10}} CH_{3(ads)}^{\bullet}$	0.68 (s^{-1})	59.41
11	${}^{\bullet}OH + \text{wall} \xrightarrow{k_{11}} {}^{\bullet}OH_{(ads)}$	0.3 (s^{-1})	31.37
12	$HO_2^{\bullet} + \text{wall} \xrightarrow{k_{12}} HO_{2(ads)}^{\bullet}$	1.0 (s^{-1})	36.72
13	$CH_3O^{\bullet} + \text{wall} \xrightarrow{k_{13}} CH_3O^{\bullet}_{(ads)}$	0.68 (s^{-1})	0

Table 5.2 summarizes elementary radical reactions with participation of the above-mentioned free radicals and their kinetic parameters, taken from the periodicals.

Based on the elementary reactions shown in Table 5.2, a sketch of H_2O_2 dissociation and CH_4 oxidation mechanism is compiled (Figure 5.4). It shows possible methods of methyl alcohol synthesis and the role of suggested conjugation intermediates in the implementation of the cyclic process. Figure 5.4, in which the central places of active sites are devoted to really existing free radicals – ${}^{\bullet}OH$, $HO_2^{\bullet}$, $CH_3^{\bullet}$ and $CH_3O^{\bullet}$, helps to compose a kinetic model, shaped as a system of differential equations in approximation suggesting stationary concentrations of free radicals:

$$-\frac{dN_{CH_4}}{dV} = k_3[CH_4][{}^{\bullet}OH] + k_4[CH_4][HO_2^{\bullet}] + k_8[CH_3O^{\bullet}][CH_4] \tag{5.31}$$

$$\begin{aligned} -\frac{d\left\lfloor CH_3^{\bullet}\right\rfloor}{d\tau} = {} & k_3[CH_4][{}^{\bullet}OH] + k_4[CH_4][HO_2^{\bullet}] - k_5[CH_3^{\bullet}][{}^{\bullet}OH] \\ & - k_6[CH_3^{\bullet}][HO_2^{\bullet}] - k_7[CH_3^{\bullet}][H_2O_2] + k_8[CH_3O^{\bullet}][CH_4] \\ & - k_{10}[CH_3^{\bullet}] \approx 0 \end{aligned} \tag{5.32}$$

$$\begin{aligned} -\frac{d\left\lfloor {}^{\bullet}OH\right\rfloor}{d\tau} = {} & 2k_1[H_2O_2] - k_2[H_2O_2][{}^{\bullet}OH] - k_3[CH_4][{}^{\bullet}OH] \\ & - k_5[CH_3^{\bullet}][{}^{\bullet}OH] + k_6[CH_3^{\bullet}][HO_2^{\bullet}] + k_7[CH_3^{\bullet}][H_2O_2] \\ & - k_{11}[{}^{\bullet}OH] \approx 0 \end{aligned} \tag{5.33}$$

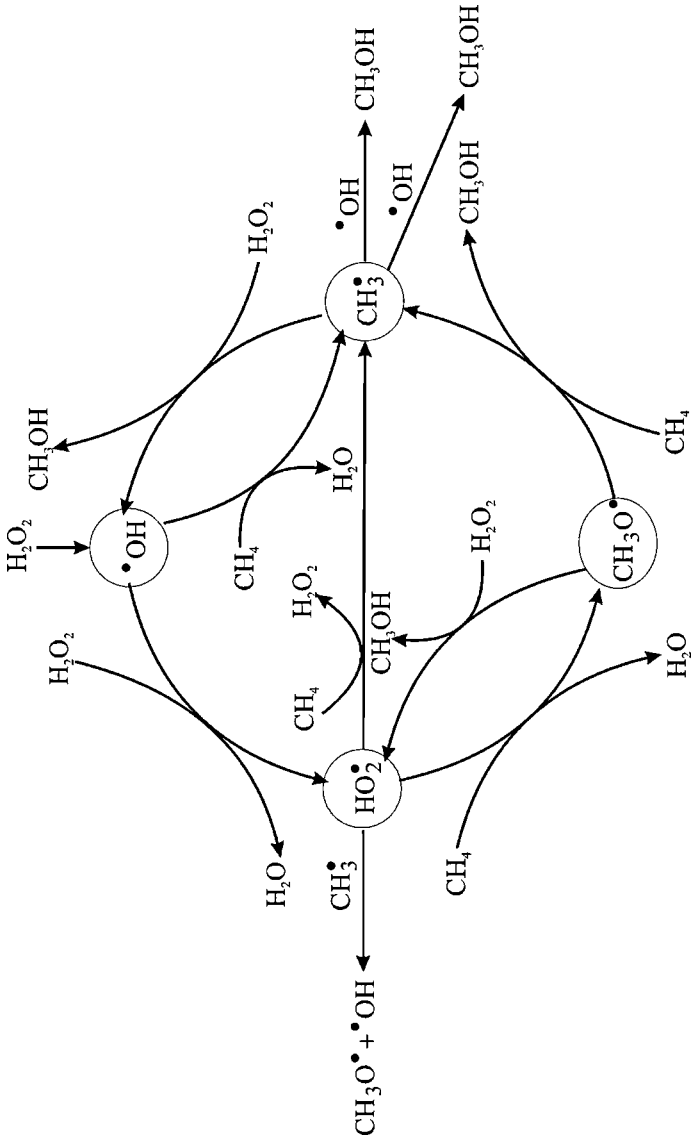

Figure 5.4 Sketch of H_2O_2 dissociation and CH_4 oxidation mechanism.

$$-\frac{\mathrm{d}\left\lfloor \mathrm{HO}_2^{\bullet} \right\rfloor}{\mathrm{d}\tau} = k_2[\mathrm{H_2O_2}][{}^{\bullet}\mathrm{OH}] - k_4[\mathrm{CH_4}][\mathrm{HO}_2^{\bullet}] - k_6[\mathrm{CH}_3^{\bullet}][\mathrm{HO}_2^{\bullet}] + k_9[\mathrm{CH_3O}^{\bullet}][\mathrm{H_2O_2}] - k_{12}[\mathrm{HO}_2^{\bullet}] \approx 0 \quad (5.34)$$

$$-\frac{\mathrm{d}\left\lfloor \mathrm{CH_3O}^{\bullet} \right\rfloor}{\mathrm{d}\tau} = k_6[\mathrm{CH}_3^{\bullet}][\mathrm{HO}_2^{\bullet}] - k_8[\mathrm{CH_3O}^{\bullet}][\mathrm{CH_4}] - k_9[\mathrm{CH_3O}^{\bullet}][\mathrm{H_2O_2}] - k_{12}[\mathrm{CH_3O}^{\bullet}] \approx 0 \quad (5.35)$$

Here N is the methane quantity in moles; V is the volume of the reaction zone; τ is the contact time.

Using the kinetic system (5.31)–(5.35) and kinetic data from Table 5.2 the unique solution for the direct kinetic task was found. The results are shown in Figure 5.5. The comparison

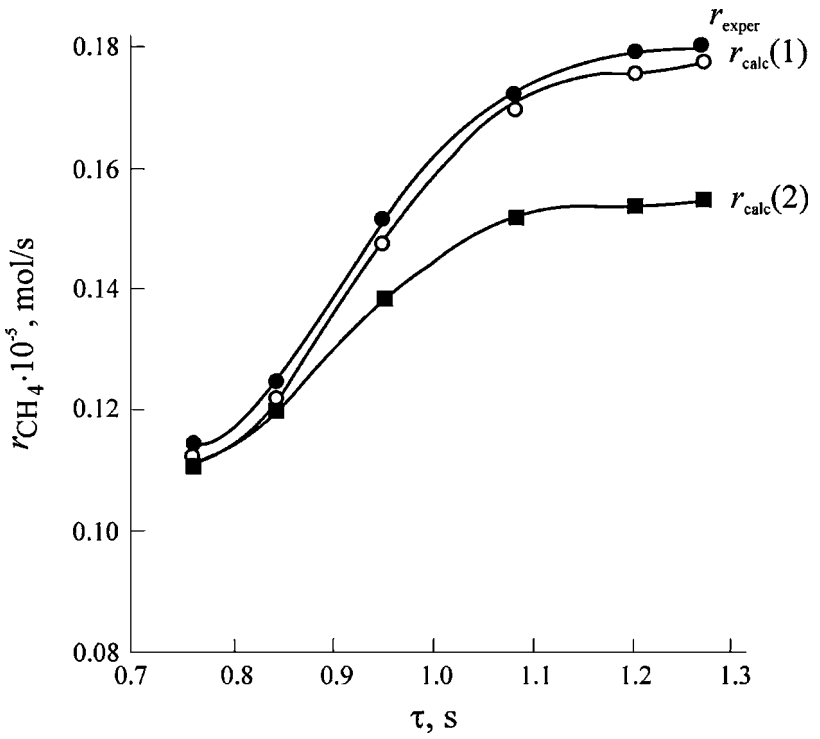

Figure 5.5 Dependence of experimental and calculated rates of methane consumption on the contract time: r_{exp} is the experimental rate; $r_{calc}(1)$ is the rate calculated from equations (5.31)–(5.35) and $r_{calc}(2)$ is the rate calculated from equation (5.36).

shows the identity of kinetic parameters measured in the experiment and calculated by equations (5.31)–(5.35) for a broad range of conditions of CH_4 oxidation to CH_3OH.

The mechanism of CH_4 oxidation with hydrogen peroxide shown in Figure 5.4 assumes proceeding of several radical-chain reactions of methanol synthesis. In analyzing kinetic equations (5.31)–(5.35) the following inequalities were deduced:

$$k_3[CH_4][^\bullet OH] >> k_4[CH_4][HO_2^\bullet]$$

and

$$k_3[CH_4][^\bullet OH] >> k_8[CH_3O^\bullet][CH_4]$$

Moreover, the ratios of free radical formation rates:

$$\frac{\lfloor {}^\bullet OH \rfloor}{\lfloor HO_2^\bullet \rfloor} = 0.25 \cdot 10^3 \qquad \frac{\lfloor {}^\bullet OH \rfloor}{\lfloor CH_3^\bullet \rfloor} = 0.9 \cdot 10^2$$

allow consideration of $^\bullet OH$ as the basic reactive intermediate in methane oxidation. Therefore, the following chain reaction scheme is, most probably, responsible for methyl alcohol synthesis:

Chain initiation

$$H_2O_2 \xrightarrow{k_1} 2^\bullet OH + \cdots$$

Chain propagation

$$CH_4 + {}^\bullet OH \xrightarrow{k_3} CH_3^\bullet + H_2O$$
$$CH_3^\bullet + H_2O_2 \xrightarrow{k_7} CH_3OH + {}^\bullet OH$$

Chain termination

$$CH_3^\bullet + \text{wall} \xrightarrow{k_{10}} CH_{3(ads)}^\bullet$$
$$^\bullet OH + \text{wall} \xrightarrow{k_{11}} {}^\bullet OH_{(ads)}$$

Kinetic equation:

$$r_{CH_4} = k_7[CH_3^\bullet][H_2O_2]$$
$$[CH_3^\bullet] = \frac{2k_1k_3[CH_4][H_2O_2]}{k_{10}k_3[CH_4] + k_{11}k_7[H_2O_2]} \tag{5.36}$$

deduced from this chain scheme also gives an adequate description of the process (Figure 5.5).

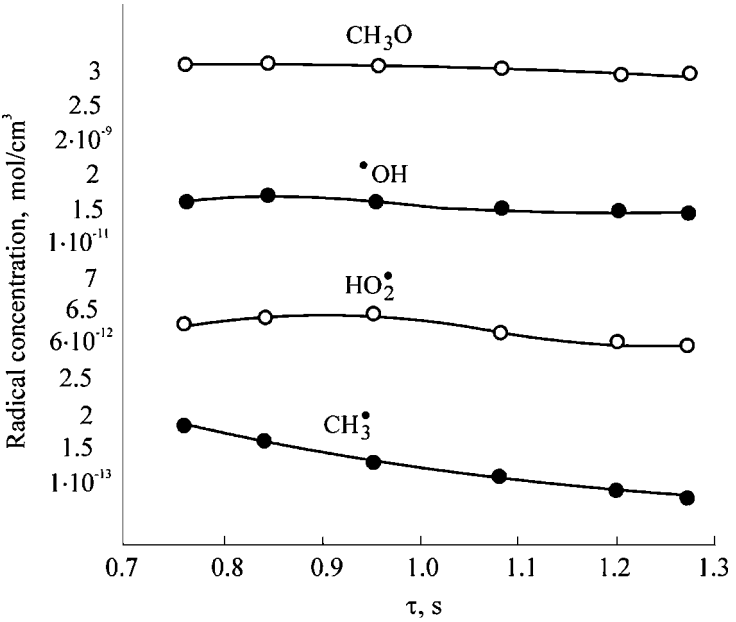

Figure 5.6 Kinetic dependencies of intermediate radical accumulation and accumulation on the contact time. $T = 400\,^{\circ}C$; $c_{H_2O_2} = 30\%$.

Thus, kinetic analysis of the free-radical mechanism of methane oxidation to methanol with hydrogen peroxide under pressure shows that under current conditions the complex cyclic scheme consisting of several chain reactions is reduced to a short scheme.

Under different oxidation conditions other chain reactions may be implemented with confidence (refer to Figure 5.4). The fact that kinetic curves of free radicals (Figures 5.6 and 5.7) obey regularities, directly following from the experiment, also confirms the above ideas.

On the other hand, the determinant equation (5.28) allows the study of complex reaction kinetics with incompletely studied mechanisms neglecting the assumptive stationary concentration method. Let us assume that the most probable mechanism of methane oxidation to methanol with hydrogen peroxide is unknown. Then equations (5.29) and (5.30) should be presented in the form that discloses the conjugation mechanism of these two reactions:

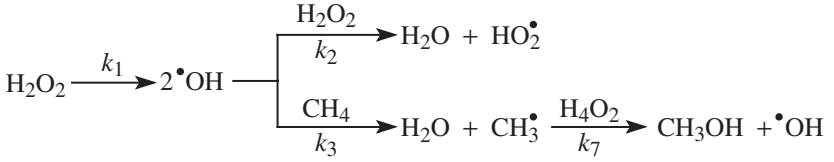

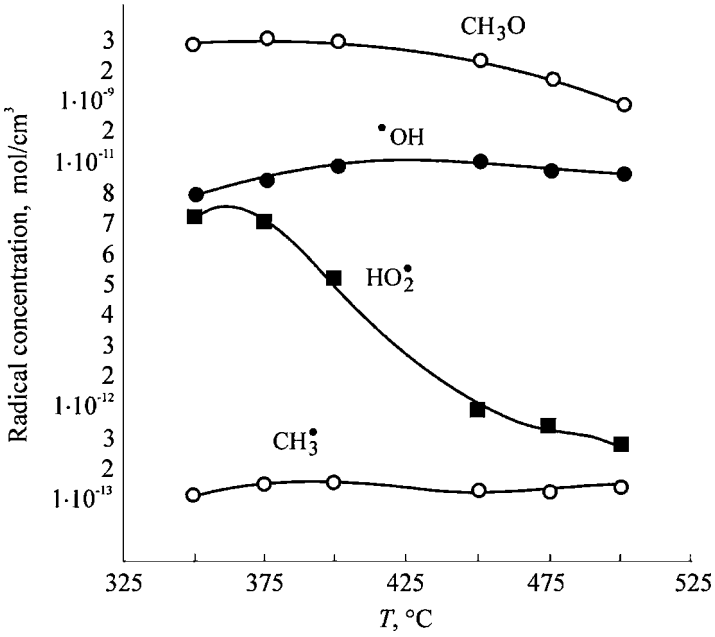

Figure 5.7 Temperature kinetic dependencies of intermediate radical accumulation and accumulation on the contact time. $\tau = 0.76$ s; $c_{H_2O_2} = 30\%$; $P = 7$ atm.

As deduced from the determinant equation:

$$r_{\mathrm{Acc(CH_4)}} = \frac{D}{v}\left(r_{A_1} + r_{A_2}\right)$$

$$r_{CH_4} = \frac{D}{v}(k_2[H_2O_2] + k_3[CH_4])\left[{}^{\bullet}OH\right]$$

$$\left[{}^{\bullet}OH\right] = \frac{r_{CH_4} v}{D(k_2[H_2O_2] + k_3[CH_4])}$$

Substituting corresponding k values and CH_4 and H_2O_2 concentrations in these equations for the case of the highest methanol yield ($T = 400\,^{\circ}C$; CH_4:H_2O_2 = 1:1.4; $\tau = 0.95$ s), the following values are obtained:

$$r_{CH_4} = 0.17 \times 10^{-5} \text{ mol/s}$$

$$\left[{}^{\bullet}OH\right] = 0.179 \times 10^{-10} \text{ mol/cm}^3$$

Comparison of these values with corresponding r_{CH_4} and $\lfloor {}^{\bullet}OH \rfloor$, obtained from the data in Figure 5.6, displays their close similarity.

Thus, the application of the determinant equation (5.28) enables the possible deduction of kinetic equation (5.36), which adequately describes the kinetics of conjugated reactions (5.29) and (5.30), not involving the stationary concentration method.

To conclude, it should be noted that the application of the determinant equation to the analysis of complex reaction kinetics is quite suitable for simplifying the calculation of the kinetic model of interrelated and synchronized reactions and quantitative assessment of chemical induction efficiency.

5.2.5 Methane oxidation to H_2, CO and CO_2

Methane oxidation with hydrogen peroxide belongs to two-component conjugated reactions, where H_2O_2 represents both the actor and the inducer [39]. According to this concept, the chemical conjugation mechanism for high-temperature methane oxidation in a CH_4—H_2O_2—H_2O system can be described by the following overall scheme [40]:

$$\underset{\text{actor}}{H_2O_2} + \underset{\text{inducer}}{H_2O_2} \rightarrow [{}^{\bullet}OH, HO_2^{\bullet}] \rightarrow 2H_2O + O_2 \tag{5.37}$$

$$\underset{\text{actor}}{H_2O_2} + \underset{\text{acceptor}}{CH_4} \rightarrow CO_2 \rightarrow 3H_2 \tag{5.38}$$

This conjugation mechanism is based on two complex overall reactions, one of which is H_2O_2 dissociation (primary reaction) induces the secondary reaction of methane oxidation.

The mandatory requirement for chemical conjugation in the current reaction system is its quantitative parameter, determined from the determinant equation [40]:

$$D = \nu \left(\frac{W_{A_1}}{W_{Acc}} + \frac{W_{A_2}}{W_{Acc}} \right)^{-1}$$

where W_{A_1} and W_{A_2} are the rates of actor (A) consumption for formation of the final products in the primary and the secondary reactions, respectively; W_{Acc} is the quantity of consumed acceptor; ν is the stoichiometric coefficient of the actor ($\nu = 1$ in this case).

The value obtained for high-temperature methane oxidation under optimal conditions is $D = 0.5$. According to the determinant scale of chemical interference [40], this value lies in the area of chemical conjugation ($D = 0 \div 1$). Therefore, this investigation unambiguously determines and gives the quantitative assessment of chemical conjugation phenomenon in the CH_4—H_2O_2—H_2O system studied.

Chemical conjugation channels between two overall reactions (5.37) and (5.38) are formed with the help of highly active intermediate ${}^{\bullet}OH$ and $HO_2^{\bullet}$ free radicals, generated to the system by H_2O_2 dissociation (primary reaction).

Based on these ideas, a free-radical mechanism for high-temperature methane oxidation with hydrogen peroxide was composed. It considers possible ways of initial material expenditure and formation of intermediate and final products (Figure 5.8).

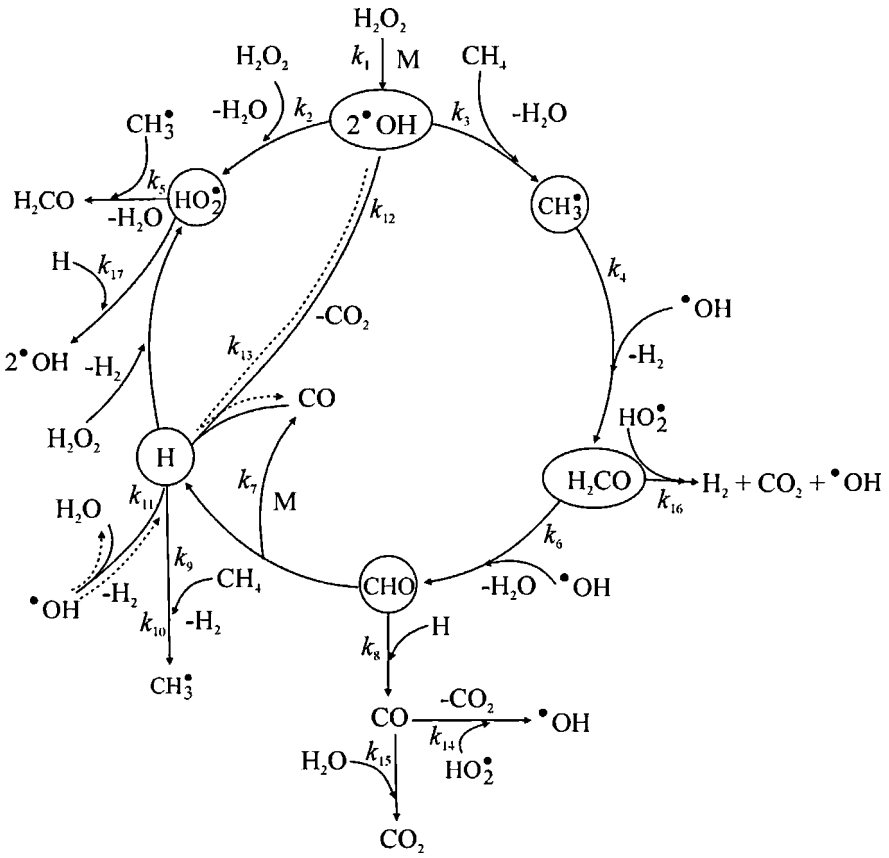

Figure 5.8 The mechanism of conjugated methane oxidation with hydrogen peroxide to hydrogen-containing gas.

This mechanism should also be supplemented by the following stages of linear and quadratic chain termination:

Stage	$\log k_0$	E (kJ/mol)
$HO_2^\bullet + H^+ \xrightarrow{k_{17}} 2^\bullet OH$	14.4	0
$^\bullet OH + H^+ \xrightarrow{k_{18}} H_2O$	12.7	32.42
$HO_2^\bullet + \text{walls} \xrightarrow{k_{19}} HO_{2(ads)}^\bullet$	1.0	34.3
$^\bullet OH + \text{walls} \xrightarrow{k_{20}} {}^\bullet OH_{(ads)}$	0.3	29.3
$CH_3^\bullet + \text{walls} \xrightarrow{k_{21}} CH_{3(ads)}^\bullet$	0.68	55.5

Here 'walls' means the reactor walls; k_{17} and k_{18} are of $cm^3/(mol\,s)$ dimensionality, and k_{19}, k_{20} and k_{21} of s^{-1}.

Table 5.3

Experimental data on the study of formaldehyde addition influence on high-temperature oxidation of methane (860 °C, 15 wt.% H_2O_2)

No.	Molar ratio	v_{CH_2O}	Reaction product yield (wt.%)					η
			CO	CO_2	H_2	CH_4	CH_2O	
1	CH_4:H_2O_2 = 1:3	–	13.6	27	51.8	7.6	–	92.4
2	CH_4:CH_2O:H_2O_2 = 1:0.76:3	0.025	18.6	7.2	72	0.7	2.5	99.0
3	CH_2O	0.5	48	–	50	–	2.0	100.0
4	CH_2O:H_2O_2 = 1:3	0.031	–	50	50	–	–	100.0

Flow velocities are 0.38 l/h for CH_4 and 0.2 ml/min for H_2O_2; v_{CH_2O} is CH_2O flow velocity, ml/min; η is conversion, wt.%.

As observed from the suggested mechanism, methane oxidation to H_2, CO and CO_2 runs through the intermediate product CH_2O, and $^{\bullet}OH$ and $HO_2^{\bullet}$ radicals are basic sites in the reaction and actively participate in formaldehyde formation and consumption. To obtain an unambiguous confirmation that formaldehyde is the basic intermediate product on the way of hydrogen-containing gas synthesis, the influence of formaldehyde increments on the course of the process was studied (Table 5.3). The concentration of added formaldehyde was enough for obtaining yields, observed in the experiment. For the purpose of determining final products by CH_2O thermal decomposition in a reactor at 860 °C, only aqueous formaldehyde was injected. In this case, the formaldehyde supplied completely decomposes to H_2 and CO (test 3, Table 5.3). A mixture of formaldehyde with hydrogen peroxide heated to the same temperature was then injected into the system. Under equal conditions aqueous formaldehyde, injected into the reactor, completely decomposes to H_2 and CO, whereas in the presence of H_2O_2 full conversion of produced CO to CO_2 is observed (test 4, Table 5.3). As formaldehyde is added to the CH_4—H_2O_2 reaction mixture (test 2, Table 5.3), hydrogen yield sharply increases and, correspondingly, carbon oxide yield increases.

The results obtained confirm the mechanism by which formaldehyde as the intermediate product is directly responsible for H_2 and CO formation.

The comparison of free energies and exothermicity of reactions with constants k_4 and k_5 (Figure 5.8) shows that formaldehyde formation by the reaction (k_5) displays higher exothermicity (512.6 kJ/mol compared with −288.7 kJ/mol for the reaction (k_4)) and is accompanied by a significant reduction of the Gibbs energy (−487.92 kJ/mol).

Carbon oxide can afterwards be oxidized to CO_2 in two stages (k_{12}) and (k_{14}) (Figure 5.8), where the thermodynamic characteristics of the reaction (k_{12}) ($\Delta H^0_{298} = -104.03$ kJ/mol; $\Delta G^0_{298} = -88.53$ kJ/mol) yield the reaction (k_{14}) ($\Delta H^0_{298} = -264.93$ kJ/mol; $\Delta G^0_{298} = -235.77$ kJ/mol). Later, the initial product CH_4 can be consumed in both reactions (k_3) ($\Delta H^0_{298} = -72.36$ kJ/mol; $\Delta G^0_{298} = -80.15$ kJ/mol) and (k_9) ($\Delta H^0_{298} = -9.51$ kJ/mol; $\Delta G^0_{298} = -15.96$ kJ/mol) (Figure 5.8). However, comparison of their thermodynamic data leads to the conclusion that the main direction of methane consumption is its interaction with the active $^{\bullet}OH$ radical.

Thermodynamic parameters of formyl radical dissociation by the reaction (k_7) (Figure 5.8) at 298 K ($\Delta H^0_{298} = 30.16$ kJ/mol; $\Delta G^0_{298} = 93.14$ kJ/mol) show enthalpy and Gibbs

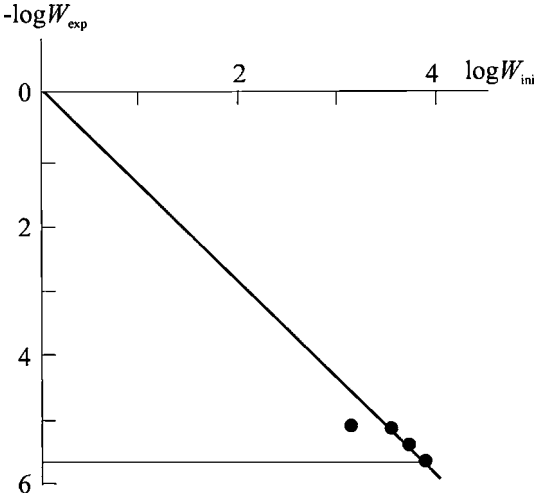

Figure 5.9 The dependence of methane oxidation rate with hydrogen peroxide on the chain ignition rate.

energy increase in the reaction. As a consequence, at 298 K this reaction may barely be performed. Nevertheless, at 1000 K it is accompanied by a significant decrease of the Gibbs energy due to increasing $T\Delta S$ member ($\Delta G_{1000} = -77.09$ kJ/mol). From a practical point of view, this means that at the process temperature formyl radical will spontaneously dissociate to CO and H^+. Note that the initially suggested elementary stage (k_{16}) (Figure 5.8) is spontaneous ($\Delta G_{1000} = -263$ kJ/mol).

Thus, in the scheme shown in Figure 5.8, more preferable stages are those considered to be more highly exothermal and displaying abrupt reduction of standard Gibbs energy.

For the purpose of determining the chain termination type, Figure 5.9 shows the dependence of the methane oxidation rate on the chain initiation rate, which is characterized by the elementary reaction of H_2O_2 dissociation (k_1) to hydroxyl radicals and described by the following kinetic equation:

$$W_{\text{ini}} = 10^{17.08} \exp\left(-\frac{E}{RT}\right)[H_2O_2]$$
$$E = 190 \text{ kJ/mol}$$

The value $\text{tg}\,\alpha \approx 1$ obtained shows that the chain termination order by means of $^{\bullet}OH$, $HO_2^{\bullet}$ and $CH_3^{\bullet}$ radical recombination equals one, i.e. termination is of a linear type.

As a consequence, the CH_4 oxidation mechanism presented in Figure 5.8 is described by a system of kinetic equations that takes into account linear chain terminations only:

$$-\frac{d[CH_4]}{d\tau} = k_3[CH_4][^{\bullet}OH] + k_9[CH_4][H^+]$$
$$-\frac{d[^{\bullet}OH]}{d\tau} = 2k_1[H_2O_2][M] - k_2[H_2O_2][^{\bullet}OH] - k_3[CH_4][^{\bullet}OH]$$

$$- k_6[CH_2O][^{\bullet}OH] - k_{10}[H_2][^{\bullet}OH] + k_{11}[H^+][H_2O]$$
$$+ k_{14}[CO][HO_2^{\bullet}] + k_{16}[CH_2O][HO_2^{\bullet}] - k_{20}[^{\bullet}OH] \approx 0$$
$$- \frac{d[HO_2^{\bullet}]}{d\tau} = k_2[H_2O_2][^{\bullet}OH] - k_5[CH_3^{\bullet}][HO_2^{\bullet}] - k_{16}[CH_2O][HO_2^{\bullet}] \approx 0$$
$$- \frac{d[H^+]}{d\tau} = k_7[CHO^{\bullet}][M] - k_8[CHO^{\bullet}][H^+] - k_9[CH_4][H^+] - k_{21}[CH_3^{\bullet}] \approx 0$$

In kinetic calculations, rate constants of elementary reactions present in reference books and periodicals [41] are used, except for k_{16}.

Concentrations of active intermediate radicals were determined by the stationary concentration method. Solution of this system of equations determines both active radical concentration and the rate constant (k_{16}) of the new elementary reaction:

$$CH_2O + HO_2^{\bullet} \xrightarrow{k_{16}} CO_2 + H_2 + {}^{\bullet}OH$$

($\log k_0 = 10.3$; $E = 14.2$ kJ/mol). The rates of CH_4 consumption calculated by kinetic equations conform to the experimental rates with the maximum 20% deviation.

Comparison of elementary reaction rates indicates reactions (k_5) and (k_{14}) (Figure 5.8) as the most significant processes for intermediate CH_2O and final H_2 and CO_2 products synthesis under current experimental conditions. This is associated with $HO_2^{\bullet}$ radical predominance in the reaction system with $\lfloor HO_2^{\bullet} \rfloor / \lfloor {}^{\bullet}OH \rfloor = 10^3 \div 10^4$.

Figure 5.10 shows temperature dependencies of final and intermediate product accumulation or consumption. As should be expected, rate increase with temperature is accompanied by increase in concentration of the main active sites ($HO_2^{\bullet}$ radicals) in the system. Maximal CH_2O yield corresponds to lower temperatures. Concentration of CH_2O increases to its maximum with temperature first and then abruptly decreases due to intensification of its consumption, because it interacts with ${}^{\bullet}OH$ and $HO_2^{\bullet}$ radicals. Synthesis of CO and CH_2O is of extreme type, and temperature increase reduces CO yield. As CO is consumed, the contribution of stages with high activation energies increases, for example, the reaction:

$$CO + HO_2^{\bullet} \rightarrow CO + {}^{\bullet}OH$$
$$E = 99.1 \text{ kJ/mol}$$

causes a sharp increase of CO concentration in the system.

Thus, current kinetic regularities correspond to the suggested mechanism, according to which ${}^{\bullet}OH$ and $HO_2^{\bullet}$ radicals are the main active sites in the CH_4—H_2O_2—H_2O system.

5.2.6 Oxidative fixation of molecular nitrogen

With regards to thermodynamic aspects, Chapter 4 discussed practically all known oxidation pathways of molecular nitrogen fixation, including reaction with hydrogen peroxide.

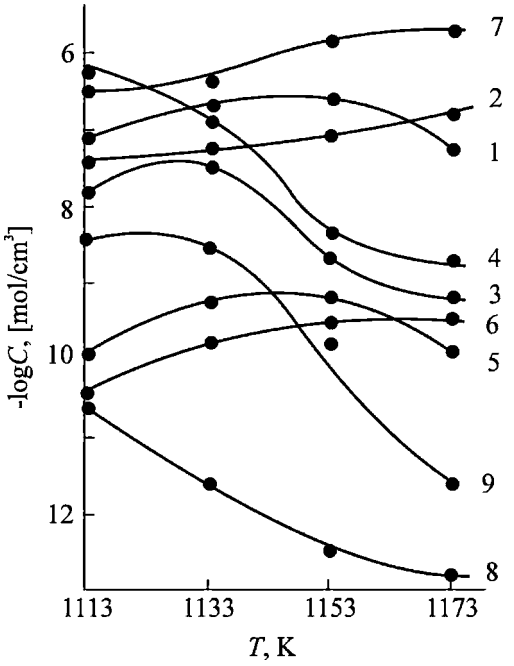

Figure 5.10 Temperature dependencies of accumulation and consumption of final and intermediate reaction products. CH_4:H_2O_2 = 1:3; $c_{H_2O_2}$ = 15 wt.%; v_{CH_4} = 0.38 l/h; $v_{H_2O_2}$ = 0.2 ml/min (1: H_2; 2: CO_2; 3: CO; 4: CH_4; 5: H^+; 6: $^{\bullet}OH$; 7: $HO_2^{\bullet}$; 8: $CH_3^{\bullet}$ and 9: CH_2O).

It is shown that at nitrogen fixation with hydrogen peroxide, the thermodynamic conjugation condition is fulfilled and, therefore, in principle, chemical induction can be used for oxidative N_2 fixation in N_2O under quite soft conditions. The formation of N_2O is more energy preserving compared with other reactions of nitrogen oxidative fixation proceeding simultaneously with triple bond dissociation in the nitrogen molecule.

The experimental studies considered in Chapter 4 clearly display the applied capabilities of this reaction [42–44].

The determinant values lie in the range $0.5 < D < 1$. Therefore, the chemical conjugation requirement is fulfilled and, probably, $HO_2^{\bullet}$ radicals represent the general intermediate substance for both reactions: H_2O_2 dissociation and N_2 oxidation.

To explain the mechanism of N_2 oxidative fixation with hydrogen peroxide, the fact should be applied that the stage mechanism of unsaturated compound epoxidation includes elementary reactions involving $HO_2^{\bullet}$ and $RO_2^{\bullet}$ free. These radicals are able to break the O—O bond with further addition of oxygen to epoxidized compound.

Of special importance in this connection is the study of the interaction mechanism between H_2O_2 and NO at 633 K or higher. It is found [45] that the elementary reaction:

$$HO_2^{\bullet} + NO = NO_2 + {}^{\bullet}OH$$

is responsible for NO_2 formation in the system. It proceeds at a higher rate compared with other processes involving $HO_2^{\bullet}$ radicals. The overall shape of the reaction, taking into account gross transformations in the system, is as follows:

$$NO + H_2O_2 = NO_2 + H_2O$$

It is noted [45] that the reaction is developed according to the free-radical chain mechanism.

As shown in the previous chapter, besides N_2O, a soft nitrogen-containing acid (pH 3–4 suggested to be hyponitrous acid $H_2N_2O_2$) is present in the products of molecular nitrogen oxidative fixation with hydrogen peroxide.

Therefore, the specific feature of the mechanism, by which N_2O and $H_2N_2O_2$ are synthesized, is that H_2O_2 thermal dissociation by the radical mechanism is the main reaction in the reaction system of conjugated oxidation with hydrogen peroxide. The products of this reaction are intermediate active sites representing hydroxide and perhydroxide radicals. In the gas phase, H_2O_2 dissociates by the elementary stages (5.2), (5.3), (5.9) and (5.10). Quantitative assessment of active sites present in the system displayed [46] a ratio $\lfloor HO_2^{\bullet} \rfloor / \lfloor {}^{\bullet}OH \rfloor$ lying in the range between 10^5 and 10^6.

Thus, $HO_2^{\bullet}$ radicals are predominant active sites in the H_2O_2—H_2O—N_2 system. It is probable that these radicals interact with molecular nitrogen forming nitrous oxide in two possible directions:

$$N_2 + HO_2^{\bullet} \xrightarrow[HO_2^{\bullet}]{} N_2O + {}^{\bullet}OH \qquad (5.39)$$

$$N_2 + H_2O_2 \longrightarrow N_2 + H_2O \qquad (5.40)$$

$$N_2 + H_2O_2 = N_2 + H_2O \qquad (5.41)$$

$$\Delta G^0_{298} = -18\,\text{kJ/mol}$$

The disadvantage of the elementary reaction (5.39) is its relatively high endothermicity (the heat effect equals −79.6 kJ/mol), which makes the implementation of this reaction mechanism ambiguous. However, chemical induction provides products of the induced reaction with the ability to form in concentrations exceeding thermodynamically equilibrium concentrations. This allows implementation of chemical processes with the equilibrium essentially shifted towards the initial substances [27].

This fundamental statement of the conjugated process theory explains reaction (5.39) proceeding under chemical conjugation conditions, when $HO_2^{\bullet}$ radicals (owing to the primary reaction proceeding) are formed in a much higher concentration than the equilibrium one for the overall reaction (5.41). Thus, the latter reaction can be implemented by the mechanism including the elementary stage (5.39).

Thus, N_2O synthesis from N_2 requires the presence of sufficient amounts of $HO_2^{\bullet}$ free radical in the system. However, this amount can be significantly decreased by quadratic chain termination ($HO_2^{\bullet}$ radical recombination), which leads to molecular oxygen formation. It is common knowledge that molecular oxygen interacts with nitrogen only at

high temperatures. Therefore, accumulation of oxygen in the system due to the primary reaction rate increase at high temperatures reduces the target product yield.

Syrkin and Moiseev [47] show that in some cases $HO_2^{\bullet}$ radicals may be catalysts for molecular transformations of the reagents. They also considered the reaction mechanism with hydrogen peroxide and formulated the concept, according to which '… due to O—O bond low energy molecular reactions with participation of peroxide compounds can display the activation energy much lower than the effective energy of the radical reaction …'. From this point of view they considered hydrogen peroxide addition to carbonyl compounds via formation of an active cyclic complex in which an acid-catalyst reacts and regenerates in the same act.

If the elementary stage (5.41) is considered from these positions, one may suggest possible molecular interaction between H_2O_2 molecule and substrates, with nitrogen molecule, in particular, via linear complex (III) formation:

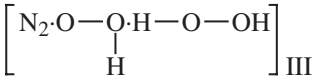

III

in which some bonds break and others form simultaneously. According to this mechanism, the $HO_2^{\bullet}$ radical represents something like a catalyst, which reacts and regenerates in the same elementary action (5.41). This is promoted by high reactivity of the O—O bond both in $HO_2^{\bullet}$ and H_2O_2.

Based on the above nitrogen oxidation mechanism with hydrogen peroxide, a kinetic model [46] was suggested, which allows the calculation of pre-exponential parameters and activation energies for elementary stages (5.39) and (5.40):

$$\ln A_{(5.39)} = -32.15 \quad E_{(5.39)} = 286.76\,\text{kJ/mol}$$
$$\ln A_{(5.40)} = 10.41 \quad E_{(5.40)} = 42.99\,\text{kJ/mol}$$

The comparison of experimental [46] and theoretical data (refer to Figure 4.23) indicates an adequate description of the experimental results in the framework of the kinetic model.

Calculated $k_{(5.39)}$ value is extremely low, therefore, the contribution of stage (5.39) to nitrous oxide formation is negligibly small. As $k_{(5.39)} \approx 0$, nitrous oxide synthesis rate will be determined from the following equation:

$$w_{N_2O} = k_{(5.40)}[N_2][H_2O_2]$$

Concentrations of highly reactive sites presented by $^{\bullet}OH$ and $HO_2^{\bullet}$ radicals in the reaction system depend on the contact time (Figure 5.11). For instance, concentrations sharply increase when the contact time is increased from 0.3 to 0.6 s, and $HO_2^{\bullet}$ concentration is higher by six orders of magnitude than $^{\bullet}OH$ concentration. The final product (fixed nitrogen) concentration also increases in the same interval of the contact time, but above 0.6 s a tendency to decrease is observed.

It may be suggested that the elementary stage (5.40) is responsible for N_2O synthesis. At this stage the role of $HO_2^{\bullet}$ radical is limited only by the catalytic effect.

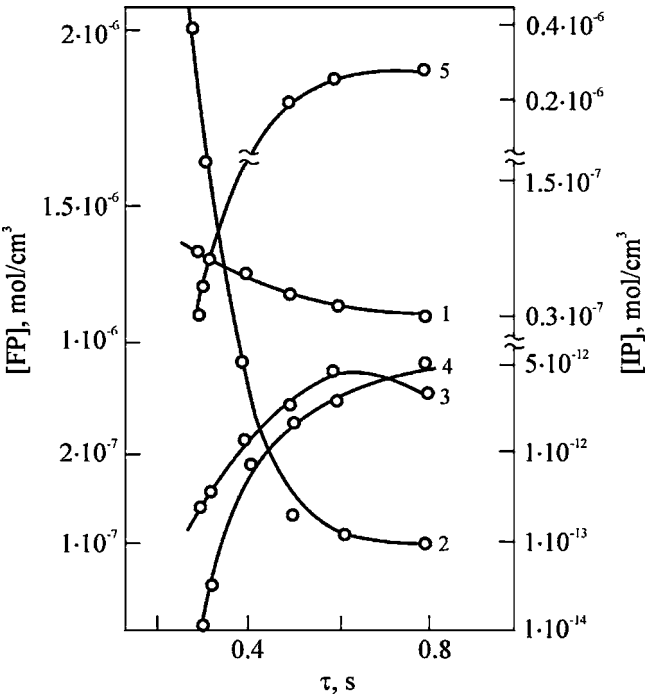

Figure 5.11 Kinetic curves of N_2 and H_2O_2 consumption, final product (FP) and intermediate product (IP) accumulation. $T = 873$ K; molar ratio N_2:H_2O_2 = 1:1.6 (1: $[N_2]$; 2: $[H_2O_2]$; 3: $[N_2]_{fixed}$; 4: $[^{\bullet}OH]$ and 5: $[HO_2^{\bullet}]$).

Figure 5.12 shows temperature dependencies of final and intermediate product accumulation or consumption for N_2 hydroperoxide oxidation. Fixed nitrogen concentration in the reaction mixture reaches the maximum at 873 K and then decreases with a temperature increase to 923 K. Hence, hydrogen peroxide concentration decreases abruptly, which is associated with its consumption in the target reaction of nitrogen fixation; $HO_2^{\bullet}$ and $^{\bullet}OH$ radical concentrations sharply increase with temperature.

The reaction kinetics of nitrogen fixation with hydrogen peroxide is defined by the quantity of fixed nitrogen. The primary fixation product is N_2O which is uniquely formed in the reaction zone, whereas secondary products ($H_2N_2O_2$, HNO_2, HNO_3) are, as shown below, formed in the quenching zone [44].

The value ΔG^0_{298} of nitrogen fixation in N_2O form by the equation (5.41) is much below zero (−18 kJ/mol). On the contrary, for $H_2N_2O_2$ formation by the equation:

$$N_2O + H_2O = H_2N_2O_2 \qquad (5.42)$$

ΔG^0_{298} is much above zero (170 kJ/mol). Therefore, though $H_2N_2O_2$ synthesis via direct interaction between N_2O and H_2O is thermodynamically hindered, under current experimental

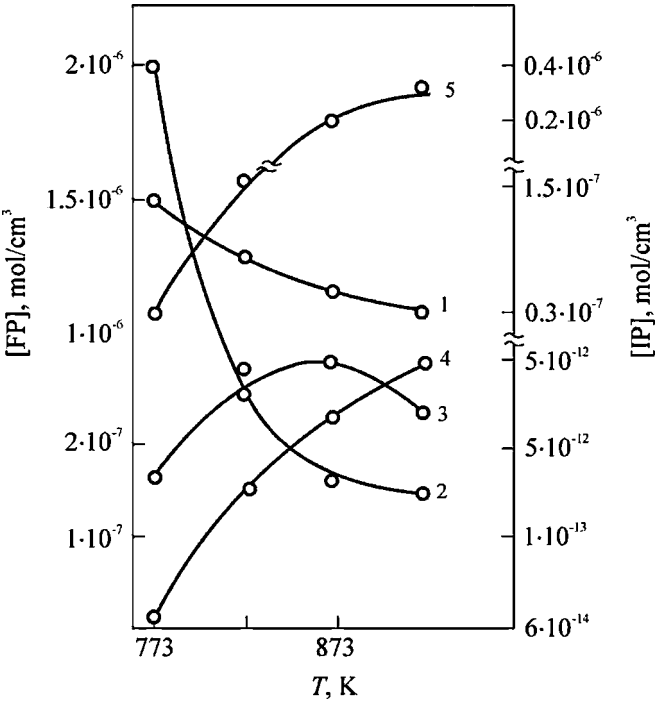

Figure 5.12 Temperature dependencies of N_2 and H_2O_2 consumption, final product (FP) and intermediate product (IP) accumulation. $\tau = 0.6$ s (optimal condition); molar ratio N_2:H_2O_2 = 1:1.6 (1: $[N_2]$; 2: $[H_2O_2]$; 3: $[N_2]_{fixed;}$ 4: $[^{\bullet}OH]$ and 5: $[HO_2^{\bullet}]$).

conditions [44] N_2O can dissociate by the following reaction [48]:

$$N_2O \rightarrow N_2 + O \tag{5.43}$$

and oxygen atom in the presence of water may be the active site responsible not only for N_2O dissociation product formation. To check this suggestion, the authors carried out N_2O dissociation in the presence of water under conditions identical to nitrogen fixation by reaction (5.41). In fact, similar to reaction (5.41), $H_2N_2O_2$, HNO_2 and HNO_3 were detected in the products [46]. To explain the formation of these products a mechanism is suggested in which the central place is occupied by N_2O_2 dimer. Under equal experimental conditions, oxygen atoms generated in reaction (5.43) easily interact with water vapor [49]:

	ΔG^0_{298} (kJ/mol)	
$O + H_2O \rightarrow {}^{\bullet}OH + {}^{\bullet}OH$	−70.8	(5.44)
$O + H_2O \rightarrow H_2O_2$	−142	(5.45)

It follows that particles typical of an N_2–H_2O_2 system are also present in an N_2O–H_2O system. Hence, the presence of reactive sites may bring about the following spontaneous reactions:

	ΔG^0_{298} (kJ/mol)	
$N_2O + H_2O_2 = N_2O_2 + H_2O$	−22.9	(5.46)
$N_2O + O = N_2O_2$	−131.3	(5.47)
$N_2O + HO_2^{\bullet} = N_2O_2 + {}^{\bullet}OH$	−335.0	(5.48)

which synthesize unstable reactive compound N_2O_2. Taking into account the specific features of N_2O_2 [49], it is suggested that $H_2N_2O_2$ can be synthesized in the following reactions:

$$N_2O_2 + {}^{\bullet}OH \rightarrow [{}^{\bullet}OH \cdot N_2O_2] + {}^{\bullet}OH \rightarrow [{}^{\bullet}OH \cdot N_2O_2 \cdot {}^{\bullet}OH] \rightarrow H_2N_2O_2 \quad (5.49)$$

$$\Delta G^0_{298} = -141.4\,\text{kJ/mol}$$

$$N_2O_2 + H_2O_2 = H_2N_2O_2 + O_2, \quad (5.50)$$

$$\Delta G^0_{298} = -141.4\,\text{kJ/mol}$$

Of course, the possibility of NO_2 formation by the well-known reaction should be taken into account:

$$N_2O_2 + O_2 = 2NO_2 \quad (5.51)$$

Interacting with water by the following reaction:

$$2NO_2 + H_2O = HNO_3 + HNO_2$$

it then forms two acids. This coincides with the results obtained, because in the aqueous part of reactions (5.41) and (5.42) products possess anions of three acids: $N_2O_2^{2-}$, NO_2^- and NO_3^-; hence, the two last anions can be formed in the further oxidation of $N_2O_2^{2-}$ radical [49–52].

All secondary reactions (5.46)–(5.50), and N_2O_2 and $H_2N_2O_2$ formation proceed at almost room temperature. Therefore, quenching of the reaction mixture becomes of great value. It concludes in a rapid temperature decrease of the gas reaction mixture coming from the reactor. For the reaction (5.41) carried out under optimal conditions, Table 5.4 shows the temperature dependence of the fixed nitrogen quantity change in the aqueous part of the product in the quenching zone. As temperature in the quenching zone increases from 0 to 22 °C, the quantity of fixed nitrogen in the aqueous part decreases from 15% to 3.4%, whereas in the gas phase it increases from 4% to 15.8%.

Thus, the gas-phase oxidation of nitrogen with hydrogen peroxide is rather complicated and consists of primary nitrous oxide formation (up to 20%). When nitrous oxide with the

Table 5.4

Temperature dependence of fixed nitrogen quantity ratio in gaseous and aqueous equation products on the quenching zone

Temperature in quenching zone (°C)	Fixed nitrogen (%)	
	In gas	In aqueous solution
0	4.0	15.0
5	8.5	10.7
10	12.0	7.2
15	14.2	5.0
22	15.8	3.4

Note: The reaction conditions are: $T = 873$ K; $v_{N_2} = 3$ l/h; $v_{H_2O_2} = 22$ ml/h.

reaction mixture is yielded by the reaction (high-temperature) zone, it enters secondary reactions with other reagents in the mixture and, on rapid cooling, forms $H_2N_2O_2$ and HNO_2 acids.

Finally, the conditions for the oxidative fixation of nitrogen with hydrogen peroxide and the probable reaction mechanism were determined.

REFERENCES

1. Alkhazov, T.G. and Lisovsky, A.E., *Oxidative Dehydrogenation of Hydrocarbons*, Khimia, Moscow, 1980, 238 pp. (in Russian).
2. Skarchenko, V.K., *Dehydrogenation of Hydrocarbons*, Naukova Dumka, Kiev, 1981, 328 pp. (in Russian).
3. Kaufman, F., *Prog. React. Kinet*., 1961, No. 1, p. 1.
4. Nagiev, M.F., Nagiev, T.M., Babeva, R.M. and Tagieva, Sh.A., *Azerb Khim Zh*., 1973, No. 5/6, pp. 139–143 (in Russian).
5. Nagiev, M.F., Nagiev, T.M. and Poladova, L.M., *Ibid.*, 1975, No. 3, pp. 153–158 (in Russian).
6. *Usp. Khim*., 1985, Vol. 54, No. 10, pp. 1654–1673 (in Russian).
7. Nagiev, T.M. andMejidov, N.D., *Zh. Fiz. Khim*., 1973, Vol. 42, No. 2, pp. 439–440 (in Russian).
8. Hoare, D.E., *Proc. Roy. Soc. London A*, 1966, Vol. 291, pp. 73–78.
9. Anber, M. and Neta, P., *Int. J. Appl. Radiat. Isotope*., 1967, No. 18, pp. 493–497.
10. Medli, G.D. and Kuli, S.D., *Modern Achievements in Petrochemistry and Oil Refining*, Vol. 3, Gostekhizdat, Moscow, 1962, pp. 190–232 (in Russian).
11. Nagiev, M.F. and Nagiev, T.M., *Adv. Chem. Ser. Am. Chem. Soc.*, 1974, pp. 137–148.
12. Sampson, R.J., *J. Chem. Soc.*, 1963, pp. 5095–6002.
13. Nagiev, T.M., *Azerb Khim Zh*., 1978, No. 6, pp. 32–38. (in Russian).
14. Nagiev, T.M., *VI International Symposium on Combustion Processes*, Karpacz, 1979, pp. 18–19.
15. Cheany, D.E., Davies, D.A., Hoare, D.E. *et al*., *VII International Symposium on Combustion*, London, 1959, pp. 183–187.
16. Nagiev, T.M., *The Study on Kinetics, Simulation and Optimization of Chemical Processes*, Vol. 2, Elm, Baku, 1974, pp. 187–229 (in Russian).
17. Marshall, A.L., *J. Phys. Chem.*, 1926, Vol. 30, pp. 1078–1082.
18. Lloyd, A.C., *Int. J. Chem. Kinet.*, 1974, Vol. 6, pp. 169–174.
19. Voevodsky, V.V. and Tal'rose, V.L., *Zh. Fiz. Khim*., 1948, Vol. 22, No. 10, pp. 1192–1204 (in Russian).

20. Eltenton, G.C., *J. Chem. Phys.*, 1947, Vol. 15, pp. 455–458.
21. Panfilov, V.N., *Kinetika i Kataliz*, 1964, Vol. 5, No. 2, pp. 211–214 (in Russian).
22. Nalbandyan, A.B. and Mantashyan, A.A., *Elementary Processes in Slow Ga-Phase Reactions*, Izd. AN ArmSSR, Erevan, 1975, 258 pp. (in Russian).
23. Tal'rose, V.L. and Poroikova, A.I., *Usp. Khim.*, 1978, Vol. 47, No. 6, pp. 955–966 (in Russian).
24. Hampson, R. and Garvin, D., *Chemical Kinetic and Photochemical Data for Modeling Atmospheric Chemistry*, NBS, Washington, DC, 1975, pp. 124.
25. Kapralova, G.A., Trofimova, E.M. and Shilov, A.E., *Kinetika i Kataliz*, 1965, Vol. 6, pp. 977–981 (in Russian).
26. Semenov, N.N., *On Some Questions of Chemical Kinetics and Reactivity*, 2nd edn, Izd. AN SSSR, Moscow, 1958, pp. 680 (in Russian).
27. Emanuel, N.M. and Knorre, D.G., *The Course of Chemical Kinetics*, Vysshaya Shkola, Moscow, 1984, pp. 237 (in Russian).
28. Nagiev, T.M. and Smolyar, A.E., *Azerb Khim Zh.*, 1985, No. 6, pp. 12–16 (in Russian).
29. Zyubin, Z.S., *Zh. Strukt. Khim.*, 1979, Vol. 20, No. 2, pp. 195–202 (in Russian).
30. Halgen, T.A., Kleler, D.A., Hall, T.H. *et al.*, *J. Am. Chem. Soc.*, 1978, Vol. 100, pp. 6595–6598.
31. Nagiev, T.M., *Vestnik MGU, Ser. Khim.*, 1993, Vol. 34, No. 3, pp. 260–266 (in Russian).
32. Baldwin, R.R., Stout, D.R. and Walken, R.W., *J. Chem. Soc. Faraday Trans.*, 1991, Vol. 87, p. 9147.
33. Benson, S., *Thermochemical Kinetics*, Mir, Moscow, 1971, p. 308 (in Russian).
34. Charies, K., *Combust. Ind.*, 1982, Vol. 6, pp. 191–196.
35. Vardanyan, I.A., Sochyan, G.A. and Nalbandyan, A.B., *Dokl. AN SSSR*, 1970, Vol. 193, No. 1, pp. 123–127 (in Russian).
36. Nagiev, T.M. and Gasanova, L.M., *Khim. Fiz.*, 1984, Vol. 3, No. 10, pp. 1455–1461 (in Russian).
37. Nagiev, T.M., Shakhtakhtinsky, T.N. and Gasanova, L.M., *Thes. Rep. I All-Union Symposium on Macroscopic Kinetics and Chemical Gas Dynamics*, Alma-Ata, 1984, Vol. 2, Pt 1, p. 378 (in Russian).
38. Basevich, V.Ya. and Kocharko, S.M., *Izv. AN SSSR, Ser. Khim.*, 1982, No. 12, pp. 2658–2662 (in Russian).
39. Nagiev, T.M., Farajev, E.G. and Mamedov, E., *Zh. Fiz. Khim.*, 2001, Vol. 75, No. 1, pp. 45–51 (in Russian).
40. Nagiev, T.M., *Chemical Conjugation*, Nauka, Moscow, 1989, pp. 33–39 (in Russian).
41. Kondrat'ev, V.N., *Rate Constants of Gas-Phase Reactions*, Reference Book, Nauka, Moscow, 1970, p. 209 (in Russian).
42. Nagiev, T.M. and Shakhtakhtinsky, T.N., *Thes. Rep. 4th International Symposium on Homogenetic Catalysis*, Nauka, Leningrad, 1984, Vol. 2, p. 133 (in Russian).
43. Ushakova, N.N., Nikolaeva, E.R. and Morosanova, S.A., *Manual on Analytical Chemistry Quantitative Analysis*, Izd. MGU, Moscow, 1981, pp. 152 (in Russian).
44. Nagiev, T.M., Zakhrabbekov, S.Z. and Shakhtakhtinsky, T.N., *Dokl. AN SSSR*, 1987, Vol. 292, No. 6, pp. 1392–1395 (in Russian).
45. Ashmore, P.L. and Tyler, B.J., *Trans. Faraday Soc.*, 1962, Vol. 58, pp. 1108–1112.
46. Nagiev, T.M. and Zakhrabbekov, S.Z., *Khim. Fiz.*, 1988, Vol. 7, No. 11, pp. 1528–1532 (in Russian).
47. Syrkin, Ya.K. and Moiseev, I.I., *Usp. Khim.*, 1960, Vol. 29, No. 4, p. 425 (in Russian).
48. Robinson, P.L. and Smith, J., *J. Chem. Soc.*, 1955, pp. 3895–3901.
49. Poltorak, O.M. and Kovba, L.M., *Physicochemical Fundamentals of Inorganic Chemistry*, Izd. MGU, Moscow, 1984, pp. 288 (in Russian).
50. Karapetyants, M.Kh. and Drakin, S.M., *General and Inorganic Chemistry*, Khimia, Moscow, 1981, pp. 632 (in Russian).
51. Hugness, M.N. and Stedman, G., *J. Chem. Soc.*, 1963, pp. 1239–1240.
52. Buchhol, J.K. and Powell, R., *Ibid.*, 1963, pp. 509–515.

– 6 –

The Phenomena of Interference in Chemical and Biochemical Redox Reactions with Hydrogen Peroxide

This chapter overviews the following points:

- Dissociation of H_2O_2 in the liquid phase.
- Critical review of oxidation reactions in the Fenton system.
- Epoxidation with hydrogen peroxide, Ruff hydrocarbon degradation, α-degradation of hydroxy acids and other reactions.
- Hydrogen peroxide induction effect on oxidation reactions in the liquid phase.
- Enzymatic H_2O_2 dissociation.
- Action mechanisms and kinetic features of catalases, peroxidases and monooxygenases. Catalytic system selection for conjugated dehydrogenation, epoxidation and monooxygenation reactions.
- Co-factors and their role in synchronization of biochemical reactions.

6.1 HYDROGEN PEROXIDE DISSOCIATION IN THE LIQUID PHASE

The liquid-phase free radical dissociation of aqueous H_2O_2 predominantly occurs at room temperature. It is initiated by the effect of vessel walls or particles suspended in the mixture [1, 2]. However, Kazarnovsky [3] suggested that purified aqueous H_2O_2 dissociates homogeneously according to the following mechanism:

$$\begin{aligned} H_2O &\rightleftharpoons H^+ + OH^- \\ H_2O_2 + OH^- &\rightleftharpoons HO_2^- + H_2O \\ OH^- + HO_2^- &\rightleftharpoons O_2^{2-} + H_2O \\ O_2^{2-} + H_2O_2 &\rightleftharpoons O_2^- + OH^- + {}^\bullet OH \\ {}^\bullet OH + H_2O_2 &\rightarrow H_2O + OH^- \\ O_2^{\bullet-} + H_2O &\rightarrow HO_2^\bullet + OH^- \\ 2HO_2^\bullet &\rightarrow H_2O_2 + O_2 \end{aligned} \qquad (6.1)$$

In the framework of this mechanism, a proper explanation can be found based on experimental facts: H_2O_2 dissociation catalysis by alkaline additives and stabilization by small increments of acids and $^{\bullet}OH$ radical acceptors.

It is common knowledge that transition metals are effective catalysts for redox processes, including H_2O_2 dissociation. Of the greatest interest is catalytic dissociation of H_2O_2 in the liquid phase in the presence of small amounts of bi- and trivalent iron salts (the Fenton reagent [4]). The reaction mechanism primarily suggested by Haber and Weiss [5] was then complemented by Bard [6]:

$$\begin{aligned} Fe^{2+} + H_2O_2 &\rightarrow Fe^{3+} + OH^- + {}^{\bullet}OH \\ H_2O_2 &\rightleftharpoons H^+ + HO_2^- \\ {}^{\bullet}OH + H_2O_2 &\rightarrow H_2O + HO_2^{\bullet} \\ HO_2^{\bullet} + H_2O_2 &\rightarrow O_2 + H_2O + {}^{\bullet}OH \\ Fe^{3+} + HO_2^- &\rightleftharpoons Fe^{2+} + HO_2^{\bullet} \end{aligned} \tag{6.2}$$

Dissociation of H_2O_2 can be catalyzed by compounds of copper, chromium, vanadium, cobalt, titanium or other transition metals.

Many works are devoted to the detection and identification of $^{\bullet}OH$ and $HO_2^{\bullet}$ radicals. For example, using the ESR method, they were detected in the following systems: Ti^{3+}–H_2O_2 and Ce^{4+}–H_2O_2 [7–10]. It is also shown that $^{\bullet}OH$ and $HO_2^{\bullet}$ radicals form complexes with group IV and V metal ions [11, 12]. Complexes including Mn^{2+} and Co^{2+} ions are rather active in the H_2O_2 dissociation process [13–15], whereas the ions of these metals themselves display very low catalytic activity in solutions.

According to Weiss the use of heterogeneous catalysts in H_2O_2 is associated with electron transitions between surface ions and atoms of the solid and components of the liquid. The suggested mechanism of H_2O_2 dissociation of metals consists of the following stages [16]:

$$\begin{aligned} M + H_2O_2 &\rightarrow M^+ + OH^- + {}^{\bullet}OH \\ {}^{\bullet}OH + H_2O_2 &\rightarrow H_2O + HO_2^{\bullet} \\ HO_2^{\bullet} &\rightarrow H^+ + O_2^{\bullet-} \\ M^+ + O_2^{\bullet-} &\rightarrow M + O_2 \\ M + HO_2^{\bullet} &\rightarrow M^+ + HO_2^- \\ M + HO_2^- &\rightarrow M + HO_2^{\bullet} \end{aligned} \tag{6.3}$$

where M and M^+ are reduced and oxidized forms of metals.

Comparison of H_2O_2 homogeneous dissociation (6.2) with heterogeneous mechanism (6.3) shows their unique difference: in that heterogeneous mechanism electrons are transferred from the solid, but not from the metal ion in solution. It is also concluded [17, 18] that the adsorbed oxygen speeds up the H_2O_2 dissociation and is partly converted to O_2 [19]. An interesting reaction for $HO_2^{\bullet}$ radical yield to the volume is suggested:

$$\begin{aligned} O_{2\,(ads)}^{\bullet-} + H_2O &\rightleftarrows HO_{2(ads)}^{\bullet} + OH^- \\ H_2O_{2(ads)} + HO_{2(ads)}^{\bullet} &\rightarrow H_2O_{2(ads)} + HO_2^{\bullet} \end{aligned}$$

In this context, works [20, 21] should be mentioned, in which $O_2^{\bullet}$ ion-radicals were ESR detected in all samples of solution quickly frozen after initiation of H_2O_2 catalytic dissociation on metals and oxides (applied on Al_2O_3). The ion-radicals mentioned occur on the surface and desorb to the liquid phase, where, with high probability, they induce free radical processes. These results conform to the Weiss mechanism (6.3) of H_2O_2 dissociation on heterogeneous catalysts.

Using the ESR method, Kaitmaziv and Prokhorov [22–24] detected $HO_2^{\bullet}$ radical formation in the experiment, in which concentrated (98%) hydrogen peroxide was preliminarily frozen at liquefied nitrogen temperature and exposed to ultraviolet (UV) light. The absorption spectrum of diluted aqueous hydrogen peroxide changed, which was attributed to the $^{\bullet}OH$ radical band which occurred, according to the authors, because of the following elementary stage de-emphasis:

$$H_2O_2 + {}^{\bullet}OH \rightarrow HO_2^{\bullet} + H_2O$$

In all cases, $^{\bullet}OH$ and $HO_2^{\bullet}$ free radicals were formed as intermediate particles only and participated in the formation of the final products, H_2O and O_2.

However, it should be noted that scheme (6.2), which in general correctly reflects the homogeneous dissociation of H_2O_2 in the liquid phase in the presence of transition metal ions, for instance, Fe^{2+} or Fe^{3+}, must be complemented by the stages, suggested later on Ref. [25]:

$$\begin{aligned} Fe^{3+} + H_2O_2 &\rightarrow Fe^{2+} + HO_2^{\bullet} + H^+ \\ Fe^{2+} + {}^{\bullet}OH &\rightarrow Fe^{3+} + OH^- \\ Fe^{3+} + HO_2^- &\rightarrow Fe^{2+} + H^+ + O_2^{\bullet} \\ H_2O_2 + O_2^{\bullet} &\rightarrow O_2 + OH^- + {}^{\bullet}OH \end{aligned} \qquad (6.4)$$

Thus, the homogeneous-catalytic generation of $^{\bullet}OH$ radicals, which proceeds owing to the alteration of oxidation and bi- and trivalent iron ion recombination stages, produces free radicals at temperatures much lower than for thermal homolysis. Hence, the elementary stage, at which $^{\bullet}OH$ radicals are generated to the system,

$$Fe^{2+} + H_2O_2 \rightarrow Fe^{3+} + OH^- + {}^{\bullet}OH$$

displays the following temperature dependence of the reaction rate constant [26]:

$$k = 4.45 \cdot 10^8 \exp\left(-\frac{39386}{RT}\right)$$

Free radicals formed in the reaction can interact with any organic compounds in acid solutions [27]. To explain the mechanism of homogeneous catalysis, two general theories are advanced:

1. Formation of higher peroxy compounds from H_2O_2 and catalyst with consequent interaction of a complex with the substrate (S) in the catalyst regeneration process.

2. Alternate catalyst oxidation–reduction by the overall scheme:

$$\text{Reduced catalyst} + H_2O_2 \rightarrow \text{oxidized catalyst} + H_2O$$
$$\text{Oxidized catalyst} + S \rightarrow \text{reduced catalyst} + \text{oxidized product (SO)}$$

$$H_2O_2 + S = H_2O + SO \text{ (overall reaction)}$$

Though homogeneous-catalytic processes can be explained by one of these two theories [28], in practice, the mechanism is more complex.

Thus, development of the investigations in this branch is not an extensive process. Interest in this problem is regularly kept alive by new theoretical ideas. All currently known elementary reactions proceeding in the Fenton system are shown by the overall sketch in Figure 6.1 which presents the whole variety of highly active intermediate particles, synthesized in seemingly simple reactions. However, it should be noted that the fate of free radicals and charged particles in the mechanism is determined by the process kinetics, where the basic factors are the reactor operation mode and physicochemical parameters of the catalyst.

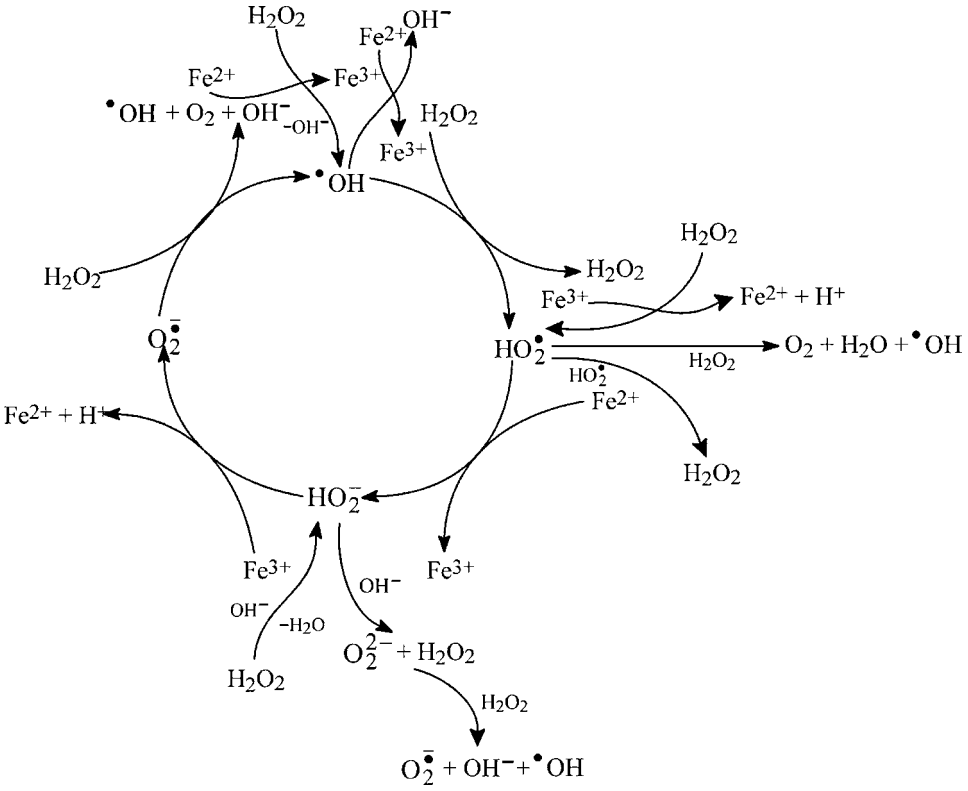

Figure 6.1 The mechanism of hydrogen peroxide dissociation in the Fenton system. The sketch is based on the data by Kazarnovsky [7], Haber–Weiss [9], Bard [6] and Uri [25].

Figure 6.1 also shows the uniqueness of H_2O_2 as oxidant or reducer: in molecular shape it is a strong oxidant and reducer, a reliable and suitable generator of $^{\bullet}OH$, $HO_2^{\bullet}$ and $O_2^{\bar{\bullet}}$ free radicals; dissociated H_2O_2 is the electron donor. The system in Figure 6.1 is incomplete because of the absence of active 'superoxide' and 'peroxide' intermediate complexes, occurring in metal ion interaction with H_2O_2 and O_2. The detailed mechanism of their formation is unclear, though they are registered *de visu* in many metal-peroxide systems.

6.2 OXIDATION WITH HYDROGEN PEROXIDE

Let us consider the reaction of benzene oxidation with hydrogen peroxide in the Fenton system as the classical situation [30]. In the absence of iron ions benzene does not in practice interact with H_2O_2. The addition of bivalent iron salt to the system C_6H_6–H_2O_2–H_2O induces benzene oxidation to phenol and diphenyl according to the following mechanism:

$$\begin{aligned} Fe^{2+} + H_2O_2 &\rightarrow Fe^{3+} + OH^- \\ Fe^{2+} + {}^{\bullet}OH &\rightarrow Fe^{3+} + OH^- \\ C_6H_6 + {}^{\bullet}OH &\rightarrow C_6H_5^{\bullet} + H_2O \\ C_6H_5^{\bullet} + {}^{\bullet}OH &\rightarrow C_6H_5OH \\ C_6H_5^{\bullet} + C_6H_5^{\bullet} &\rightarrow C_6H_5\text{–}C_6H_5 \end{aligned}$$

The chemical conjugation observed in the system is considered [30] to be a result of the combined proceeding of two reactions: Fe^{2+} and C_6H_6 oxidation, in which $^{\bullet}OH$ radicals participate. In fact, the $^{\bullet}OH$ radical is the general intermediate. It takes part in the oxidation reactions currently mentioned and in many others. Usually, Fe^{2+} ions catalyze H_2O_2 dissociation. In the Fenton system, they are unable to perform effective work for the secondary reaction. Therefore, benzene oxidation requires H_2O_2 dissociation to $^{\bullet}OH$ radicals with the participation of Fe^{2+} ions as the catalyst. The process of H_2O_2 dissociation induced by Fe^{2+} catalyst (the primary reaction) is 'conjugated' to benzene oxidation with hydrogen peroxide (the secondary reaction). In this case, the $^{\bullet}OH$ radical is the carrier of the H_2O_2 induction action to the secondary reaction.

Thus, the scheme presented in Chapter 4 including reactions (4.2) and (4.3) describes chemical conjugation in oxidation with hydrogen peroxide in both gas and liquid phases. This gives an opportunity to consider conjugated oxidation with hydrogen peroxide in both phases from general positions. The rational question arises: why does application of the liquid-phase Fenton system not induce selective oxidation with hydrogen peroxide similar to reactions in the gas phase?

As noted in the previous chapter, substrate interaction with $^{\bullet}OH$ and $HO_2^{\bullet}$ radicals produces different products, which composition depends on H_2O_2 dilution. Hence, $^{\bullet}OH$ radicals participate in nonselective oxidation, whereas $HO_2^{\bullet}$ promotes selective gas-phase oxidation of substrates with hydrogen peroxide [32]. This situation is observed for both low H_2O_2 concentrations in the reaction mixture and liquid-phase oxidation in the Fenton system, where the $^{\bullet}OH$ radical is the key active site. In the Fenton system, connection channels between two reactions are set with the help of a general intermediate, the $^{\bullet}OH$ radical, which represents a nonselective active site due to the ability to attack another complex molecule by various

bonds. This is the reason why the selectivity of oxidation with hydrogen peroxide depends on the phase state of the reaction mixture's components. According to the data in Chapter 5, the $HO_2^{\bullet}$ radical is the selective oxidant preserving the donor–acceptor (amphoteric) properties of H_2O_2. In fact, it represents the active form of hydrogen peroxide. Thus, selective oxidation with hydrogen peroxide in the gas phase is explained by the presence of active, chemically bound oxygen—the 'active oxygen' of perhydroxide $HO_2^{\bullet}$ radical.

As follows from the above, there is no principal possibility of implementing high selectivity oxidation of the substrate in the Fenton system.

Rakovsky [33] gives the following example: '… hydrogen peroxide always oxidizes ferrous oxide salt (e.g. Fe SO_4) but it does not directly affect HJ; if HJ is added to H_2O_2 and $FeSO_4$ mixture, the reaction between H_2O_2 and HJ will also proceed …'. In this case, hydrogen peroxide becomes the secondary reaction reagent in the Fenton system only. However, initially, redox catalysis by iron ions was identified with a stoichiometric reaction. As follows from the above examples on benzene and HJ oxidation in the Fenton system, H_2O_2 does not interact directly with the substrates. Implementation of the secondary reaction requires H_2O_2 dissociation, which induces H_2O_2 interaction with C_6H_6 and HJ. Therefore, in the absence of chemical induction H_2O_2 is not a reagent in $C_6H_6 + H_2O_2$ and HJ + H_2O_2 reactions.

The works devoted to catalytic hydroxylation of aromatic and heterocyclic compounds with hydrogen peroxide under soft conditions should be mentioned [34]. The authors showed that the main experiments were performed in the Fenton system and the process can be described by the following generalized mechanism:

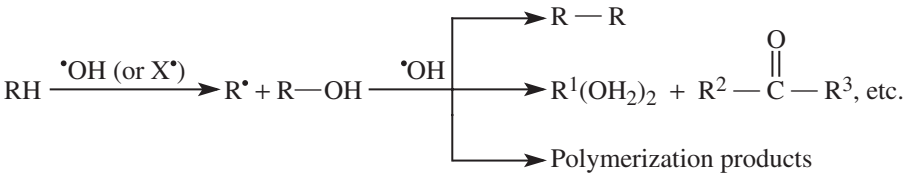

For phenol hydroxylation it is shown that Fe^{2+} and Fe^{3+} ion activity increases in the presence of other ions, among which the highest activity is displayed by salts and complexes of the following metals: Co, Mn, Mo, Cu, Fe, etc. In aqueous solution Fenton's reagent oxidizes substrates according to the radical mechanism in which reactions with $^{\bullet}OH$ radicals play the central role. In aprotic solvents oxidation with Fenton's reagent suggests the participation of different intermediates—complexes with iron ions, Fe═O, for example.

Of special attention is one more reagent containing Fe^{2+}, H_2O_2 (or O_2), ascorbic and ethyl diamino tetraacetic acids (the Udenfried system) [29]. In this system, Fe^{2+} and Fe^{3+} display equal catalytic activity. The authors of the review [34] conclude that purely hydroxylating catalytic systems containing Fe^{2+} possess a limited activity and, consequently, reaction product yields and selectivity are low.

In this connection, of greatest interest are catalytic systems based of Fe^{3+} complexes (the Hamilton system) with phenol, pyrocatechol, hydroquinone, etc. These compounds provide for higher yields at benzene hydroxylation in the Hamilton system compared with

the Fenton and Udenfried [29]. Hamilton's reagent activity strictly depends on the reaction conditions, ferric salt composition, mixture and solvent pH. The efficiency of Hamilton's reagent operation was increased by a catalyst (Fe^{3+} complexes with quinine and its derivatives) applied on silica gel [35, 36].

For benzene hydroxylation an analytical system [37] was successfully used at the interface. This system contains Fe^{3+} hydrophobic complexes, which promote the process intensification. It is shown [38, 39] that compared with hydrophobic complexes, Fe^{3+} complexes with the phase transfer—tertiary ammonium salts and crown ethers—display more effective action. At 20–50 °C, owing to the use of trimethylacetylammonium bromide as the phase transferring agent, benzene is successfully hydroxylated in the two-phase water–benzene system in the presence of Fe^{3+} ions [40]. Hence, it is Shilov's opinion [41] that in the case of cytochrome P-450 a radical reaction is probable. It produces radicals, which then transform in the cell, as follows:

$$Fe^{2+} + O_2^{\bullet-} + RH \rightarrow [FeOOH + R^{\bullet}] \rightarrow FeO^{+} + ROH$$

For monooxygenating systems, Hamilton suggested the so-called oxynoid mechanism [42], in which the hydroxylating intermediate represents heme iron coordinated an atom or a molecule of oxygen. The question of the oxynoid intermediate origin is still disputed. This intermediate helps the oxygen atom to intercalate into the substrate by a C—H bond, by analogy with free carbene reactions (intercalation by C—H bond). It is apparent that the intermediate can participate in monooxygenase oxidation, epoxidation and hydroxylation of aromatic hydrocarbons. Combined use of the Hamilton system and the phase transfer reagents makes possible high selectivity and high conversion of benzene hydroxylation.

Of interest is the idea [34] that since the catalyst activity strictly depends on the pH of the medium and initial salt composition, then it turns out that hydrolyzed Fe^{3+} ions are responsible for the active form of the catalyst, because iron ions are easily hydrolyzed [43]. Catalytic activity is maximal in the pH range in which Fe^{3+} ions are fixed in a dimer hydroxoform $[Fe_2(OH)_2]^{4+}$, and different catalytic activity of Fe^{2+} and Fe^{3+} ions is caused by the difference in their hydroxoforms [34]. Milas's reagent, consisting of catalytic quantities of OsO_4, H_2O_2, acetone and *tert*-butanol [44], also performs with high activity in hydroxylation reactions.

It is stated [45] that 2-amino-3,4-dihydroquinoxaline is quite easily dehydrogenated to 2-aminoquinoxaline with the help of H_2O_2 in the presence of trace amounts of iron ions:

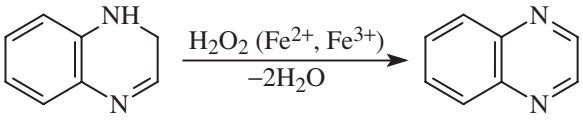

In this case, the origin of the 'dehydrogenating effect' displayed in the interaction between hydrogen peroxide and the substrate and conjugated dehydrogenation of hydrocarbons in the gas phase is the same.

In fact, bivalent iron ions intensively catalyze H_2O_2 dissociation to free radicals (Fenton's reagent) and then oxidize themselves to Fe^{3+} ions. Free radicals can be coordinated with iron ions and implement a dehydrogenation reaction interacting with hydrogen atoms in positions

3 and 4 in 2-amino-3,4-dihydroquinoxaline molecule. Therefore, H_2O_2 dissociation is conjugated with the substrate dehydrogenation, and $^{\bullet}OH$ is again the general intermediate compound. This clearly reveals the origin of the true oxidant: it can be presented by $^{\bullet}OH$ radicals—the semi-product of H_2O_2 dissociation. It is also possible that iron ions can activate a substrate molecule in a different way. As is expected, this reaction is of low selectivity, which is explained in the framework of the ideas stated above.

For another reaction, i.e. Ruff's carbohydrate degradation [46], the origin of the true oxidant is also unclear. The reaction between α-oxyacids and H_2O_2 in the presence of trivalent ferric salts is presented by the following overall reaction:

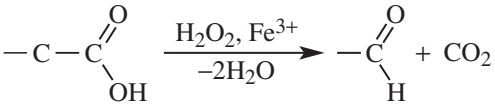

For example, the consecutive conversion of D-glucose to D-arabinose is a complex process:

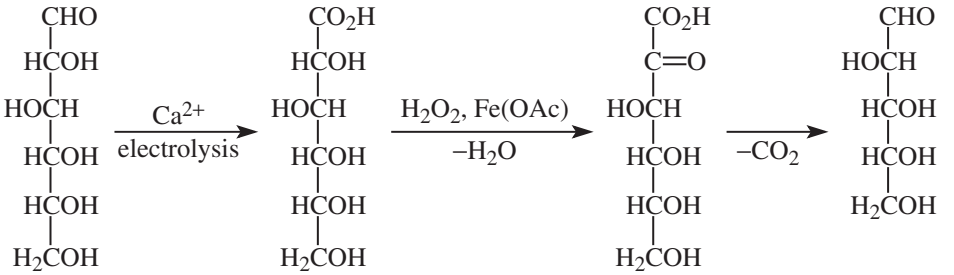

D-glucose (aldose) | aldonic acid | 2-ketoaldonic acid | D-arabinose

Hence, the stage of aldonic acid conversion to 2-ketoaldonic acid is a typical dehydrogenation reaction. The authors suggest that the role of H_2O_2 is analogous to that described above: in this case, the true oxidants are again highly active particles, formed as a result of H_2O_2 dissociation with iron ions as catalysts.

Of special interest are olefin epoxidation with peroxy acids at the moment of their formation from acid anhydrides and hydrogen peroxide. Among the catalysts of olefin oxide formation from olefins interacting with H_2O_2 in the presence of metal (Ti, W, V, Ta, Ge, Mo, U, Ru) oxides or acids are tungstic acid and its salts [47]. Epoxidation is described by the following mechanism:

$$H_2WO_4 + H_2O_2 \xrightarrow{\text{fast}} H_2WO_5 + H_2O \tag{6.5}$$

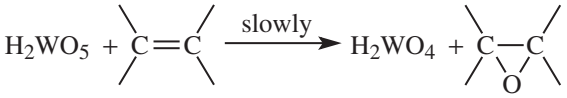

(6.6)

In a rapid reaction (6.5) H_2O_2 dissociates to H_2O and oxygen atom, which is fixed in peroxy tungstic acid and represents the intermediate state on the way of free (molecular) oxygen formation. Thus, peroxy tungstic acid is the active intermediate substance in H_2O_2 dissociation, catalyzed by tungstic acid. Then peroxy tungstic acid promotes accelerated oxidation of olefins. In this aspect, of great interest are works by Sapunov and Lebedev [48] who studied the kinetics and catalytic mechanism of olefin epoxidation with hydrogen peroxide in the presence of tungstenites. As shown by the scheme (6.5)–(6.6), peroxy tungstate and olefin participate in the stage defining the epoxidation rate. Hence, the actor of catalysis is the HWO_5^- anion. Neutralization of the acid salt reduces epoxidation catalyst activity, whereas H_2O_2 dissociation is intensified. Thus, despite lower acidity of the medium, acid salts of tungstic acid ($NaHWO_4$ or NH_4HWO_4) intensify epoxidation due to its high solubility in water. Based on the idea about two shapes of peroxy tungstate ion:

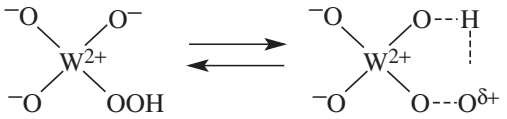

the authors conclude that electrophilic attack on olefin double bond becomes easier owing to intramolecular hydrogen bond and the presence of partial positive charge at peroxide oxygen atom. Most probably, this attack happens via formation of the following transition state:

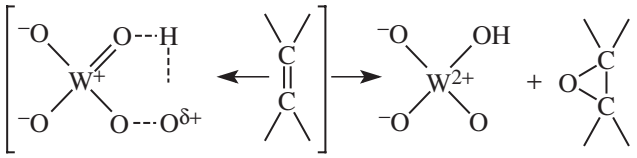

which then decomposes to reaction products.

This system contains two chemically conjugated reactions: H_2O_2 catalytic dissociation in the presence of HWO_4 and olefin epoxidation. For these reactions, peroxy tungstic acid or, most likely, peroxy tungstate ions form the general intermediate substance.

Epoxidation of olefins by peroxy acetic acid, formed in the reaction mixture on catalytic (with H_2SO_4 or lower alkylsulfonic acids as the catalysts) interaction between H_2O_2 and CH_3COOH, is described [49]:

$$H_2O_2 + AcOH \rightleftharpoons H_2O + AcOOH;$$

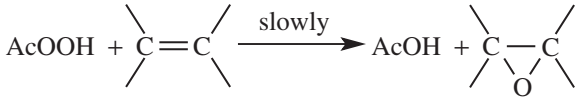

A hydrogen peroxide and acetic acid mixture is also used in the following reactions: carbon–carbon bond break [50], aromatic hydrocarbon and phenol oxidation to *n*-quinones [51], 2,6-dihaloanilines oxidation to nitroso-compounds and synthesis of N-oxides of pyridine

derivatives [52]. These reactions are possible in the H_2O_2–AcOH system owing to peroxy acetic acid formation only.

Under alkaline conditions, H_2O_2 produces perhydroxide anion, which playing the role of the intermediate substance epoxidizes α-unsaturated ketones and interacts with nitriles giving amides and O_2 [59]. In the two latter cases, the perhydroxide anion helps in setting the inter-reaction communication required for conjugation.

A series of olefin oxidation reactions with H_2O_2 and SeO_2—hydroxylation and oxidation, including cycle contraction, should be noted [53, 54]. It is the author's opinion that selenium dioxide catalyzes H_2O_2 dissociation to free radicals and, therefore, promotes H_2O_2 induction influence on oxidation of olefins.

The course of conjugated H_2O_2 dissociation and H_2CO and HCOOH oxidation in the presence of platinized graphites and spongy platinum with lead additives is shown [55]. Graphite trademark, platinum deposition conditions, reagent concentrations and percent content of additives significantly influence the ratio of oxidation products.

The detailed mechanism of dehydroxyfumaric and tartaric acid oxidation with hydrogen peroxide is considered [56] in the presence of ferric and copper ions.

Kinetic study of the self-oscillating reaction observed in a potassium iodate–hydrogen peroxide–cysteine–sulfuric acid (acid medium) system was carried out [57]. It is found that according to an adequate model the feedback mechanism is associated with autocatalytic reaction

$$H_2O_2 + KJO$$

and one-electron transfer stage

$$—SH \rightleftharpoons S—S—$$

at cysteine conversion to cystine. Autocatalytic reaction is inhibited due to free (peroxide) radical recombination and dissolved molecular nitrogen accumulation in the system. It is the authors' opinion that the mechanism of this outstanding reaction must be specified from positions of conjugated processes.

Based on kinetic studies of H_2O_2-ion–molecular decomposition by manganese ions, the following chain mechanism is suggested [58]:

$$\begin{aligned}
Mn^{3+} + HO_2^- &\rightarrow Mn^{2+} + HO_2^\bullet \\
Mn^{2+} + H_2O_2 &\rightarrow Mn^{4+} + H_2O + O^{2-} \\
Mn^{4+} + H_2O_2 &\rightarrow Mn^{3+} + HO_2^\bullet + H^+ \\
Mn^{3+} + O_2^{\bar{\bullet}} &\rightarrow Mn^{2+} + O_2 \\
Mn^{2+} + HO_2^\bullet &\rightarrow Mn^{3+} + HO_2^-
\end{aligned}$$

This mechanism is notable for a possibility of molecular H_2O_2 to participate in two-electron oxidation implemented in one-stage ion, a mononuclear metal complex.

In the framework of the theory of elementary open catalytic system self-development suggested by Rudenko [59] evolutionary changes in homogeneous catalytic systems based on hydrogen peroxide dissociation are indicated [60]. Hence, it is suggested that formation of amino acids, for example, is associated with the transformation of components in the

system $H_2CO + KNO_3$. The following work [61] is devoted to determining the possibility of glycine synthesis also based on H_2O_2 dissociation, but, on the contrary, via interaction between formaldehyde and hydroxyl amine catalyzed by bi-, (tri-)valent iron ions.

Glycine synthesis is concluded to be associated with the basic reaction (H_2O_2 dissociation), without which the secondary reaction (glycine synthesis) almost stops. For instance, glycine yield depends heavily on the duration of H_2O_2 dissociation: the longer H_2O_2 dissociation and the higher H_2O_2 concentration, the higher the level of glycine accumulated in the system. Glycine formation can be presented by the totality of the following consecutive reactions:

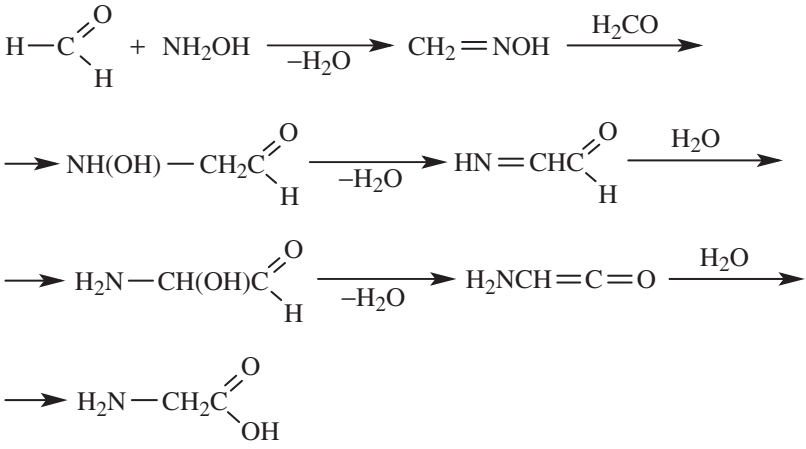

(6.7)

Obviously, reaction (6.7) is chemically conjugated with H_2O_2 dissociation.

The conclusion that Rudenko made on the basis of these studies is quite original [59]: 'The observed synthesis phenomenon in the course of hydrogen peroxide dissociation in a multicomponent catalytic system containing Fe^{3+} ions, formaldehyde and hydroxyl amine at 30 °C in aqueous solution testifies to the possibility of abiogenic synthesis of amino acids under soft conditions with consumption of energy of chemical processes. As a consequence, the sources of energy for abiogenic synthesis of amino acids in conditions of the germ of life on Earth are not only common (*T. Nagiev* in Ref. [62]) UV light, ionizing radiation, electric charges, volcano heat and meteorite deceleration energy, but also chemical energy of catalytic processes'.

The next work [63] discusses the use of hydrogen peroxide and alkyl peroxides as effective oxidants in applied studies. Effective oxidation catalysts consisting of promoter transition metals are described.

Later, these studies were developed in work [64, 65] in which Pt(II) diphosphine complex was used as the catalyst of oxidation with hydrogen peroxide. Modifications of the catalytic system mentioned were applied to enantioselective oxidation [66]. However, these catalytic systems find limited application, because they are active in transformations of cyclic ketones only [67].

Selective oxidation of aromatic amines to nitroso-derivatives with hydrogen peroxide and a catalyst is also studied [68, 69]. In kinetic systems with transition metal complexes substrate oxidation is accompanied by H_2O_2 dissociation to H_2O and O_2. Therefore, in this case, the occurrence of chemical induction would be expected.

The authors suggest that every last reaction of oxidation with hydrogen peroxide must be studied for the presence of chemical induction in the reaction system, and the absence of this phenomenon should be proved experimentally.

Any simplified consideration of the oxidation mechanism with hydrogen peroxide causes inadequacy, and the more so when searching for any additional factors affecting the course of the reaction, which are most frequently thought out in order to obtain even a satisfactory kinetic model of the reaction.

Propylene epoxidation with hydrogen peroxide on titanium–vanadium catalyst applied on silica gel is described [70]. Apparently, in this reaction mixture epoxidation of propylene is accompanied by H_2O_2 dissociation to molecular oxygen and water. It is common knowledge that as dissociated H_2O_2 generates to the system highly active intermediate—hydroperoxide—fixes on the catalyst surface. This very intermediate possesses the epoxidizing property. This reasoning allows the assumption that chemical induction occurs in the system.

Unfortunately, the absence of kinetic data in Ref. [70] does not allow more comprehensive consideration of the interaction between synchronously proceeding H_2O_2 dissociation and propylene epoxidation processes.

These studies simulate several of the most important functions of redox enzymes (catalases, peroxidases and monooxygenases) develop their biological simulators and explain some aspects of the action mechanism of these enzymes.

As shown for liquid-phase oxidation reactions of various organics with hydrogen peroxide and homogeneous and heterogeneous catalysts, they are conjugated with H_2O_2 dissociation, in the absence of which they either cannot or can hardly be implemented.

Thus, the experimentally determined ability of hydrogen peroxide to induce oxidation reactions in the gas phase is also observed for liquid-phase oxidation of substrates.

6.3 THE MECHANISMS OF CATALASE, PEROXIDASE AND MONOOXYGENASE REACTIONS

The history of the development of physical chemistry for enzymatic processes and composition of their chemical models shows that the foundation was laid in the works studying catalase reactions. Catalase enzyme is present in all aerobic organisms and catalyzes dissociation H_2O_2, toxic for living cells [31].

It is known that, because of spin forbidding, molecular oxygen is weakly active in the normal state. However, when possible, it enters oxidation reactions much more easily by the one-electron rather than by the two-electron mechanism [71]. In this connection, it is believed that not so much molecular oxygen is toxic as reactive intermediates $O_2^{\bullet}$, $HO_2^{\bullet}$ and $^{\bullet}OH$, occurring in the course of its reduction to water. The radicals $O_2^{\bullet-}$ and $HO_2^{\bullet}$ are equivalent; therefore, in the redox medium $O_2^{\bullet-}$ possess the same unique properties, i.e. can be the oxidant and the reducer simultaneously. Thus, in principle, molecular oxygen is incapable of two-electron oxidation (because of spin forbidding), whereas H_2O_2 has this ability. This is the principal difference in the oxidation mechanisms of these radicals.

Many enzymatic oxidation processes proceed by a multielectron mechanism. For example, bielectron reduction of O_2 to H_2O_2 and tetraelectron reduction to H_2O produce short-lived

intermediates bound to the enzyme. However, these intermediates can only be fixed, and active oxygen-containing radicals do not freely occur in the solution. Meanwhile, there are biological oxidation reactions in which $O_2^{\bullet-}$ radicals are synthesized capable of interacting with H_2O_2 by the following reaction:

$$O_2^{\bullet-} + H_2O_2 \rightarrow O_2 + {}^{-}OH + {}^{\bullet}OH$$

and generating reactive $^{\bullet}OH$ radicals to the system [72]. Fridovich [31] notes that H_2O_2 hazard concludes not in the possibility of its direct influence on the cell components, but most likely in the interaction with $O_2^{\bullet-}$ or Fe^{2+} that can synthesize the extremely reactive hydroxide radical.

Spontaneous reactions of $O_2^{\bullet-}$ synthesis and consumption are rapid. As a rule, stationary concentrations of $O_2^{\bullet-}$ or its protonated form ($HO_2^{\bullet}$) in chemical and biological systems are low [73].

The high reactivity of the $^{\bullet}OH$ radical may be illustrated by numerical values of reaction rate constants with ethanol, acetic and phenylformic acids at 25 °C: $1.85 \cdot 10^9$ [74], $1.9 \cdot 10^7$ [75] and $6.0 \cdot 10^9$ l/(mol s) [74], respectively. The cell protection system against the toxic action of $O_2^{\bullet-}$ and H_2O_2 is based on the operation of the so-called enzymatic 'traps' for $O_2^{\bullet-}$ and H_2O_2. Entrapping enzymes are superoxide dismutases (arresting $O_2^{\bullet-}$), catalases and peroxydases (fixing H_2O_2). Essentially, after $O_2^{\bullet-}$ and H_2O_2 arrest, the Haber–Weiss reaction (scheme (6.2)) in biological systems is practically absent [76, 77]. In some cases, however, a positive role of $O_2^{\bullet-}$ and H_2O_2 in the organism activity was noted [78].

The cell metabolism is based on the oxidation–reduction enzyme activity. These enzymes are called oxidoreductases and divided into the following groups:

1. Dehydrogenases—catalyze hydrogen transfer from one substrate to another.
2. Oxygenases—catalyze inclusion of a single atom from molecular oxygen to the substrate, the remaining atom forms a water molecule.
3. Oxidases—catalyze hydrogen transfer from the substrate to oxygen molecule. The final product can be water or hydrogen peroxide with respect to the enzyme specificity.
4. Peroxidases and catalases—catalyze reactions with H_2O_2 as the oxidant.

We will limit our discussion to catalase and peroxidase as the enzymes—hydrogen peroxide killers. In its turn, hydrogen peroxide is formed *in vivo* in two-electron O_2 reduction and enzymatic dismutation of $O_2^{\bullet-}$ radicals in accordance with the mechanism, which includes alternating reduction and Cu^{2+} reoxidation in the active site of the enzyme during consecutive acts of interaction with $O_2^{\bullet-}$ [79, 80]:

$$\text{E-Cu}^{2+} + O_2^{\bullet-} \rightarrow \text{Cu}^{+} + O_2$$
$$\text{E-Cu}^{+} + O_2^{\bullet-} + 2H^{+} \rightarrow \text{E-Cu}^{2+} + H_2O_2$$

where E-Cu^{2+} is the enzyme.

Note that many animal oxidases, such as D-amino-acid oxidase, α-oxyacid oxidase, etc., promote H_2O_2 synthesis in the course of molecular oxygen reduction [81]. In some plants H_2O_2 is formed abundantly. Mitochondria, in which the greater part of the oxygen is reduced, and peroxisomes are the cell organelles displaying noticeable formation of H_2O_2 with concentrations falling within a range of between 10^{-9} and 10^{-7} mol/l [77].

Let us now consider the questions of the biological oxidation of various substrates with hydrogen peroxide in the presence of catalases and peroxidases. As Pratt notes [82], this group of enzymes is unique in that it is the only one in which intermediates are detected, and all stages of catalytic process are determined, identified and studied. Of special value is the characteristic that catalase consists of four subunits, whereas peroxidase possesses only one subunit. Using special technique, it is also shown that every iron atom (heme) binds one H_2O_2 molecule [83].

In biological and, less frequently, in chemical systems the term 'peroxidase activity' is used. It means that the reaction with H_2O_2 does not produce molecular oxygen. If dissociation of H_2O_2 gives oxygen and water, 'catalase activity' is outlined. Considering the catalase role in biological processes from these positions, one may indicate its catalytic properties, if two H_2O_2 molecules fall on one catalase molecule. Catalase displays peroxidase activity *in vitro* exclusively in relation to methanol, ethanol, nitrite and formate ions [84], whereas peroxidase possesses much broader substrate specificity. It is also found that at relatively low H_2O_2 concentrations catalase displays the catalase activity only; at higher concentrations of hydrogen peroxide it can function as peroxidase.

In the context of the above, the authors suggest that consideration of catalase and non-classical peroxidase reactions from positions of the ability of H_2O_2 to induce chemical conjugation in oxidation reactions broadens our knowledge about the role and mechanism of catalases and peroxidases.

Not all aspects of biooxidation with the hydrogen peroxide mechanism in the presence of catalase are clear yet. The following mechanism is accepted in the biochemical literature [82], which illustrates formal iron valences in catalase and peroxidase reactions:

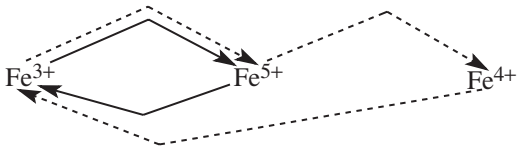

where Fe^{4+} and Fe^{5+} are iron porphyrin complexes; continuous lines show catalase and dashed lines peroxidase reactions.

Note that mechanisms of these reactions are disputable. The Chance mechanism is most frequently used in the literature [85]:

$$E\text{-}Fe^{3+}\text{—}OH^- + H_2O_2 \rightarrow E\text{-}Fe^{3+}\text{—}OOH^- + H_2O \tag{6.8}$$

$$E\text{-}Fe^{3+}\text{—}OOH^- + H_2O_2 \rightarrow E\text{-}Fe^{3+}\text{—}OH^- + O_2 + H_2O \tag{6.9}$$

$$E\text{-}Fe^{3+}\text{—}OOH^- + H_2D \rightarrow E\text{-}Fe^{3+}\text{—}O^- + DH + H_2O \tag{6.10}$$

$$E\text{-}Fe^{3+}\text{—}O^- + H_2D \rightarrow E\text{-}Fe^{3+}\text{—}OH^- + DH \tag{6.11}$$

$$DH + DH \rightarrow H_2D + D \tag{6.12}$$

where H_2D is an organic substrate, two hydrogen atom donor.

The single intermediate form Fe^{5+} is synthesized in catalase and non-classical peroxidase reactions (contrary to peroxidase, peroxidase action of catalase is called non-classical). In the course of the one-stage two-electron reaction this form is reduced to Fe^{3+}, whereas in classical peroxidase reactions two intermediates (Fe^{4+} and Fe^{5+}) are synthesized, and the process has two consecutive stages [86].

Of special importance is the example of catalase interaction with formate ion [87], because it represents a substrate for non-classical peroxidase reaction and, probably, the interaction mechanism between formate ion and Fe^{5+} complex is identical to the reaction mechanism with H_2O_2 [82].

Critically analyzing the mechanism (6.8)–(6.12), one may note the unsuitability of the currently presented interaction between complexes E-Fe^{3+}—OH^- and E-Fe^{3+}—OOH^- and substrates (H_2O_2 and H_2D), because it is unclear how the substrate is activated. Moreover, intensification of the catalase reaction induces a non-classical peroxidase activity increase in ethanol and formic acid oxidation reactions. This indicates the existence of a unit common to these two processes [82, 83]. The alternative action of catalase (catalase of peroxidase reaction) in the biosystem with solidarity of elementary stage mechanisms should be noted [88, 89]. Peroxidase action of catalase requires a continuous supply of H_2O_2 for ethanol and formic acid oxidation, which can be explained by oxidation according to conjugated mechanism [90].

It is the opinion of Chance *et al.* [91] that the key to an understanding of useful catalase functions in the organism are such features such as its high local concentration, extremely high effectiveness by H_2O_2 and extremely low H_2O_2 concentration. Such conditions can be achieved only in the case of H_2O_2 generation in mitochondria accompanied by further H_2O_2 diffusion through cell elements [91] into peroxisomes at low and moderate H_2O_2 concentration.

One of the amazing features in Nature is the realization of the cycle of various reactions involving H_2O_2 in a living organism by means of two enzymes: catalase and glutathione peroxidase. Catalase promotes H_2O_2 dissociation and ethanol oxidation, whereas glutathione peroxidase is responsible for the degradation of long-chain peroxides. Their co-action is one of the admirable achievements of Nature, especially if one accounts for H_2O_2 synthesis in both mitochondria and peroxisomes [91].

Later mechanisms of biooxidation with catalase are associated with attempts to explain some interesting experimental data and show the enzymatic activation mechanism of interacting substances. In this context, the work by Poltorak and Chukhrai [92] is of great importance; they present an in-depth study of the question and suggest the alternative mechanism of the catalase reaction. It is noted, however, that although the mechanism suggested by Jones and Sugget [93] correctly shows catalase reaction proceeding with the help of acid–base protein groups, the elementary degradation stage is presented as the result of two protons transfer from one H_2O_2 molecule to another instead of co-transfer of proton and hydride ion, as it really is.

Studies of hematin associates [94] indicate their inactivity in the catalase reaction. The interaction by the Fe–O–Fe mechanism, the existence of which was confirmed by the Mössbauer spectroscopy method, also disproves the idea of two hematin group interaction in the active site of catalase [92].

As mentioned above, the mechanisms of catalase and peroxidase reactions are similar at particular stages, and differences are observed at the stage of final alternative product formation:

$$E + H_2O_2 \xrightarrow[-H_2O]{} [E \cdot OOH] \rightarrow \tag{6.13}$$

$$\begin{array}{l} \xrightarrow{1\ H_2O_2} E \cdot (HO_2^{\bullet}) \cdot H_2O_2 \longrightarrow E + H_2O + O_2 \\ \xrightarrow{2\ C_2H_5OH} E \cdot (HO_2^{\bullet}) \cdot C_2H_5OH \longrightarrow E + H_2O + CH_2CHO \end{array}$$

where 1 is catalase reaction and 2 is non-classical peroxidase reaction.

Possible structures of ferroxygen complexes formed at H_2O_2 dissociation with Fe^{3+}—O, Fe^{4+}—O or Fe^{5+}—O enzyme can be generally shaped as $[Fe{-}O]^{3+}$. The specific feature of this complex is the existence of only six valent electrons at oxygen atom. Hence, electrophilic properties are displayed in hydroxylation reaction (because porphyrin structure is charge 2−, and total charge of the oxynoid complex is 1+). Such complexes are called 'oxynoid' (or 'oxene' by analogy with carbenes and nitrenes). Hydroxylation with these complexes passes through formation of stereospecific complex with the substrate.

At the corresponding stage of the oxidation cycle, all three types of heme enzymes (peroxidases, oxygenases, and oxidases) form ferroperoxy complexes with further O—O bond break. This is the reason for higher effectives of H_2O_2 that of O_2 in catalytic oxida-tion of cytochrome with cytochrome oxidase. An analogous phenomenon is observed for cytochrome P-450 [95, 96]. This reasoning leads to the suggestion about formation of unitypical peroxy complexes for all heme-containing proteins under consideration, and then they are hydrolytically degraded to initial heme and protein with a free radical site.

It should be noted that cytochrome-c–peroxidase complex and catalase possess two amino-acid residues in the ligand surrounding the active site: Arg (arginine) 48, His (histidine) 552 in cytochrome-c–peroxidase and His 74 and Asn (asparagine) 147 in catalase. These residues participate in the acid–base catalysis of the charge stabilization. As indicated in model studies [97], the higher is the polarity of peroxidase and catalase polarity, the more probable is the O—O bond break. For this reason, the fact that myoglobine is a weak peroxidase is explained by the absence of polar residues in it, which promote O—O bond polarization. On the contrary, myoglobine has an active site rounded by hydrophobic distal fragments, which promote reversible oxygen fixation. Thus, due to polar surrounding of the active site, heme-containing fragments lose the ability of reversible O_2 fixation, polarize O—O bond and, therefore, promote oxidative conversion of the substrate and iron ion of the active site.

In this context, let us discuss Poulos and Finzel's [98] analysis of the mechanism for complex I cytochrome-c–peroxidase formation (Figure 6.2). Here the reasons for such great differences are analyzed via comparison of the second-order rate constants in H_2O_2

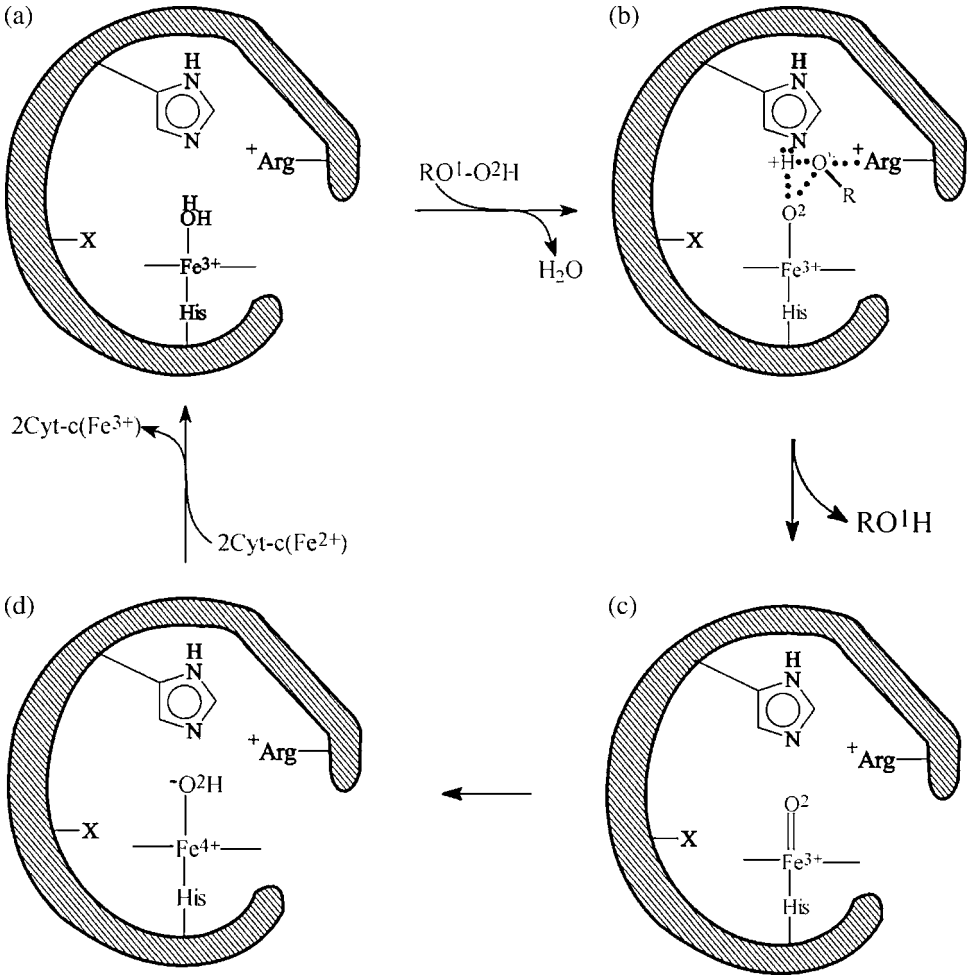

Figure 6.2 The mechanism of cytochrome-c–peroxidase complex formation. (a) Native enzyme. (b) Activated complex with the acid–base catalytic function of distal histidine (His) and stabilization of negative charge by arginine (Arg) residue of the active site. (c) Hypothetic intermediate oxene complex. (d) Complex I after intramolecular electron regrouping of oxene complex with Fe^{4+} and free radical $X^{\bullet}$ fragment formation.

dissociation reactions in the presence of the cytochrome-c–peroxidase complex (10^7–10^8 M/s) and heme (10^{-3} M/s):

1. Coordination of O^2 atom in peroxide (RO^1—O^2H) with Fe^{3+} iron ion makes O^2—H bond much weaker;
2. His 552 residue promotes direct proton transfer;
3. Arg 48 residue provides for charge stabilization;
4. Proximal histidine provides for iron stabilization in the higher oxidized state Fe^{4+}.

All the above statements are illustrated by Figure 6.2, where a probable mechanism for complex I cytochrome-c–peroxidase formation and conversion is shown. The participation of two water molecules was not shown in the layout (H_2O 595 and H_2O 648) [98]. One of these molecules (H_2O 595) is axially bound to iron ion and by hydrogen bonds to His 552 and Trp (tryptophane) 51 fragments. The second molecule (H_2O 648) is bound by hydrogen bonds to the axial water molecule and Arg 48. It is the authors' opinion [98] that fixed positions of these water molecules form something of a model of the enzyme–substrate complex I, in which O^2 atom in the substrate $RO^1—O^2H$ substitutes axial water molecule 595, and O^1 atom–water molecule 648.

Of the same importance is another component of the mechanism—the display of acid–base properties of His 552 fragment. According to X-ray patterns, among two probable mechanisms of distal histidine interaction with hydrogen bond formation:

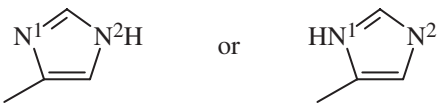

(a) (b)

Alternative b is the most probable for cytochrome-c–peroxidase complex. Here, the N^2 atom is the basic site of the catalytic act (which promotes specificity of the cytochrome-c–peroxidase complex) and the proton donor, simultaneously. It should be noted that in other heme-containing enzymes N^2 atom of His 552 (fragment a) may be of the amphoteric type.

Figure 6.2 also shows $X^\bullet$ radical formation. For heme enzymes, this radical is described from positions of location and origin of distal amino-acid residues. For example, in the case of the cytochrome-c–peroxidase complex above discussed, this Trp 51 is easily forming an indole radical. In the case of catalase and vegetable peroxidase this position is occupied by Phe (phenylalanine) which is oxidized much harder than tryptophane. Hence, heme oxidation becomes predominant.

In the general case, synthesis of radical forms can be presented as follows [98]:

$$\underset{\text{red}}{X \cdot \text{heme}} \rightleftharpoons \underset{\text{green}}{X\text{heme}^\bullet} \tag{6.14}$$

For the cytochrome-c–peroxidase complex this equilibrium is shifted to the left, whereas for catalase and vegetable peroxidase to the right. Further on, Poulos and Finzel show that though electron transfer with participation of conjugated bonds and a system of hydrogen bonds in inorganic and organic models are well known, it is absent in enzymatic systems. Since the importance of proton and electron transfers for biological processes is great, the participation of amino-acid fragments of the protein carcass in proton and electron transfer reactions contributes to the energy of activated enzyme–substrate complex.

In the course of developing the idea of the enzymatic catalysis mechanism Poltorak [99] stated the uniformity of enzymatic catalysis mechanisms in the framework of suggested notion of linear chain of bond redistribution (linear CBR). Actually, this idea laid the foundation for the catalase reaction mechanism suggested by Poltorak. In this mechanism, owing to composition of linear CBRs he showed the means for effective proton transfer between

catalytic groups and substrate molecules in the catalysis act. The main advantage of this mechanism is reflection of the acid–base protein group participation in proton transfers, which accompany the Chance complex synthesis.

Fita and Rossmann [100] presented a comprehensive analysis of the catalase active site and discussed probable catalytic mechanisms with the participation of acid–base catalytic groups in the redox transformations of the substrate. Figure 6.3 is a diagram of catalase redox transformation with formation of intermediate complexes II, III and IV. Note that in this work the experimentally found analogy of complex II formation for catalase and cytochrome-c–peroxidase complex is applied to particular simulations [101, 102].

Figure 6.3 shows catalase transformation under the substrate (ROOH) effect in complex II to be the predominant pathway. For neutral substrates, which are hydroperoxides, the rate of complex II formation is independent of pH and is usually described by the second-order equation [103, 104]. Complex II is the general intermediate for catalase and peroxidase reactions with the only difference that for catalase it is colored green (unpaired electron is localized on heme) and for peroxidase it is red (unpaired electron is localized on distal amino-acid fragment). Complex III is also colored red for peroxidase. However, the formation mechanism is different. Complexes II, III and IV are typical of peroxidases, whereas for catalase only complex II is formed. At the stage of complex II formation, the general properties and distinctive features of catalase and peroxidase were determined.

The general features are as follows:

- Imidazole ring of distal cystidine participates in the reaction shaped as fixed tautomeric form III.
- In both cases, H_2O_2 interacts with two amino-acid fragments (His 74 and Asn 147 for catalase, and His 552 and Arg 48 for peroxidase). Hence, N^2 atom in the imidazole ring acts as hydrogen acceptor.
- In both cases, histidine fragment is activated by the corresponding amino-acid fragment (Ser (serine) 113 for catalase and Asn 82 for peroxidase).

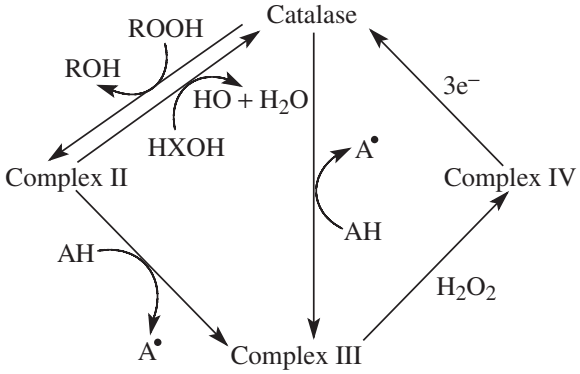

Figure 6.3 Catalase redox transformation diagram. Compounds II, III and IV represent complexes of the enzyme with H_2O_2 and iron valence states, Fe^{5+}, Fe^{4+} and Fe^{6+}, respectively; HXOH is a two-electron donor (reducer): X═O, NH, C═O, $H(CH_2)_nCH$, where $n = 1, 2, 3$; AH is a single-electron donor (reducer); ROOH is hydroperoxide (R is alkyl or acyl radical) and ROH is alcohol.

The distinctive features are:

- The participation of peroxidase Arg 48 in complex II formation is less expressed than for Asn 147 of catalase.
- Parallel disposition of imidazole ring and heme planes is typical of catalase.
- Tyrosine and histidine are proximal ligands of catalase and peroxidase, respectively.
- Heme surrounding of catalase possesses much lower polarity than for peroxidase and, therefore, is less affected by the solvent.
- Different localization of unpaired electrons.

The general features are responsible for the equal mechanism of complex II formation, whereas the distinctive features define the fate of the mechanism.

Figure 6.4 shows the suggested mechanism of Rossmann's complex V formation, in which acid–base distal surrounding properties are not taken into account.

Further reduction of the catalase complex VI is shown in Figure 6.5 (peroxidase reaction) and Figure 6.6 (catalase reaction). These diagrams show that peroxidase and catalase reactions of catalase proceed by two-electron transfer mechanism in one stage and are practically equal.

Note that if for complex VI reduction, catalase applies substrates representing two-electron donors, then peroxidase applies single-electron donors with complex II reduction in two stages through complex III formation (refer to Figure 6.3).

It is the author's opinion that the disadvantage of the Rossmann mechanism is the absence of any particularization of hydrogen transfer from substrate to Fe^{4+}—O and proton transfer with the participation of catalytic group distal fragments.

According to Rossmann, the C_2H_5OOH molecule is converted to one CH_3CHO molecule and H_2O, whereas a catalase reaction requires two H_2O_2 molecules for H_2O and O_2 synthesis. Thus, ethanol produced in complex V synthesis is immediately oxidized to aldehydes. In the analysis of both reactions of special attention is the circumstance that in a stoichiometric aspect, the Rossmann reaction represents dehydrogenation:

$$C_2H_5OOH \rightarrow CH_3CHO + H_2O + 243\,\text{kJ/mol}$$

whereas peroxidase reaction represents oxidative degradation:

$$C_2H_5OOH + H_2O_2 \rightarrow CH_3CHO + H_2O + 315\,\text{kJ/mol}$$

Comprehensive consideration of C_2H_5OOH dehydrogenation displays its consecutive nature:

$$C_2H_5OOH \rightarrow [C_2H_5OH \cdot \overset{\overset{|^{+}}{|}}{Fe^{4+}}\text{—O}] \rightarrow CH_3CHO + H_2O$$

As the authors suggest [100], C_2H_5OH is not released to the volume, though it is the intermediate product and is highly stable. Apparently, no matter how strongly C_2H_5OH is bound to the active site of the enzyme, some part of it can be fixed in products. Obviously, this would be additional proof of the Rossmann and Fit mechanism. Moreover, if forced injection of

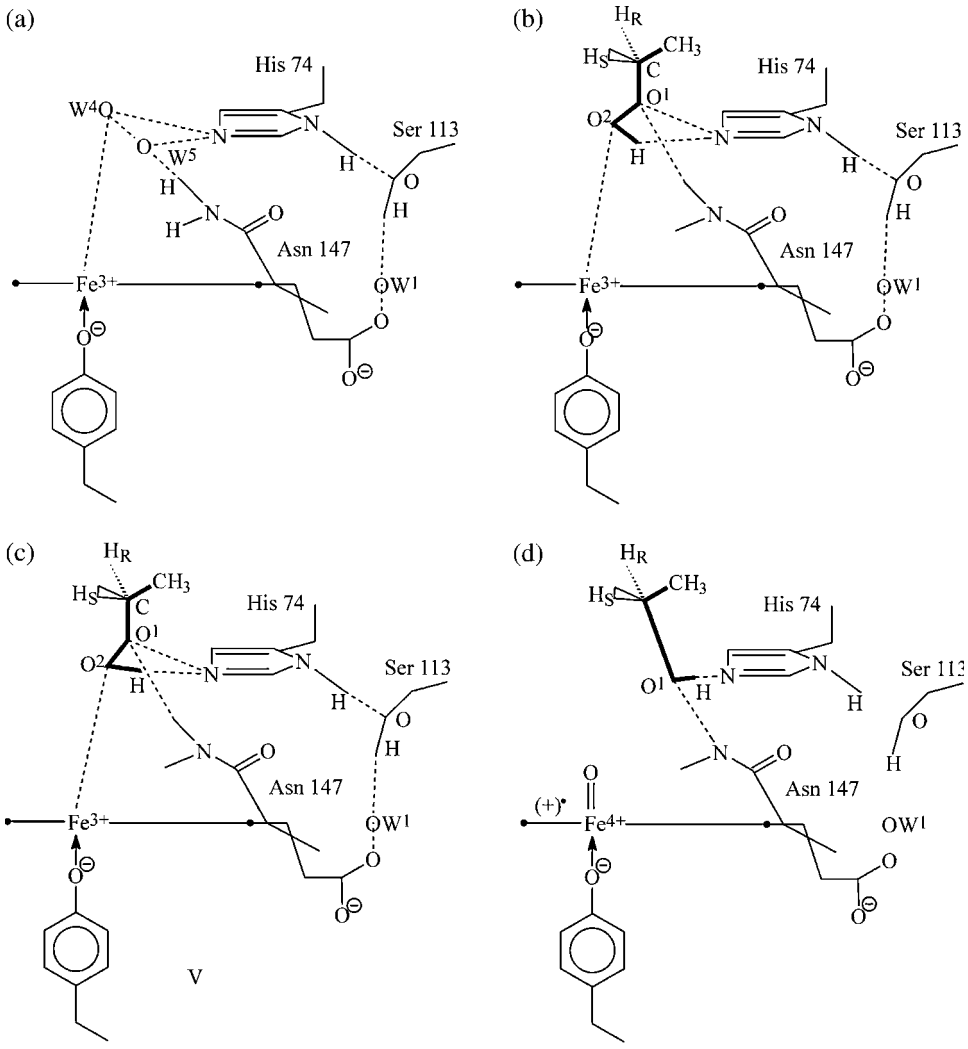

Figure 6.4 Diagrams for hypothetical stages of complex V formation. (a) The enzyme with suggested water molecules (W) in the distal part (W^4 and W^5). (b) The enzyme–substrate complex. (c) Hydrogen atom transfer between oxygen atoms in peroxide (H is bound to O^1 and O^2). (d) Complex V formation.

small amounts of ethanol to the C_2H_5OOH–catalase system intensifies CH_3CHO synthesis, this would eliminate any uncertainties.

Homogeneous catalytic degradation of ethyl hydroperoxide:

$$C_2H_5OOH \rightarrow C_2H_5OH + \frac{1}{2}O_2 - 215\,\text{kJ/mol}$$

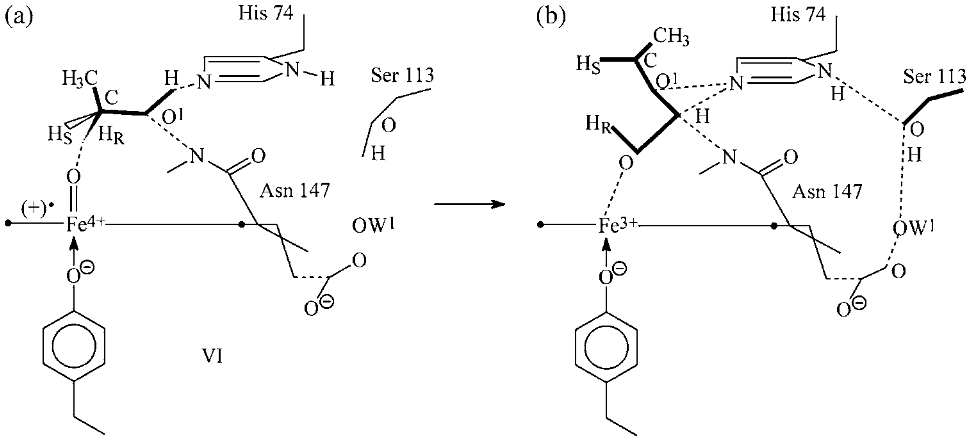

Figure 6.5 Diagram for hypothetical stages of complex VI reduction. (a) Hydrogen H_R detachment by oxygen of Fe═O group. (b) Hydrogen transfer from alcohol to oxygen of the oxide group (or hydroxide ion) with aldehydes formation.

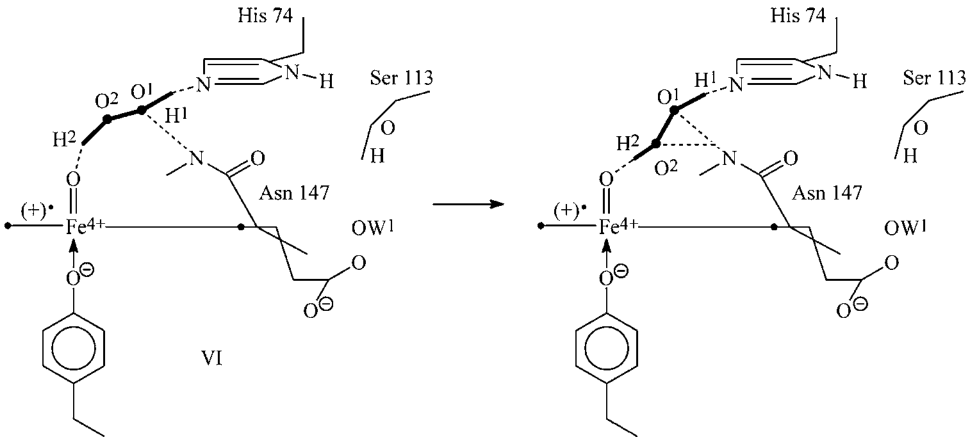

Figure 6.6 Models of two probable routes of H_2O_2 fixation at catalase reduction of complex VI.

is a strongly endothermic reaction. In the enzymatic form of this reaction and in the framework of Rossmann's opinion on its mechanism, both products are fixed to catalase with the energy gain. However, compensation over 209 kJ/mol with preservation of extremely high C_2H_5OOH degradation rate seems to be problematic.

As an alternative mechanism the following is assumed by the authors:

$$\overset{|}{\underset{|}{Fe^{3+}}}—OH + C_2H_5OOH \rightarrow \overset{|}{\underset{|}{Fe^{3+}}}—O^1—O^2C^1H_2C^2H_3 + H_2O \rightarrow$$

$$\rightarrow \overset{|}{\underset{|}{Fe^{3+}}}—OH + CH_3CHO \quad (6.15)$$

This mechanism is highly attractive owing to the simplicity of the Fe^{3+}—$O^1OC_2H_5$ complex formation and its conversion to reaction products with an eliminated stage of fixed ethanol formation by means of intramolecular regrouping.

The presentation of the enzyme active site in the Fe^{3+}—OH shape is debatable, contrary to the Rossmann mechanism, where Fe^{3+} has no extraligand at all.

It is the author's opinion that the following reasons prove the presence of the Fe^{3+}—OH complex in the native catalase form:

- Iron ions (Fe^{2+} or Fe^{3+}) are easily hydrolyzed with hydroxide formation.
- In a mildly alkaline mixture hemin forms hematin easily adding OH^- group.
- In the liquid-phase oxidation (see above) one of the hydrolyzed F^{3+} forms is responsible for the catalyst activity.
- Catalase simulator $PPFeOH/Al_2O_3$ possesses hydroxide in the fifth coordination position of the ion. In this form, the catalyst displays high catalase and peroxidase activity (see below).

Based on a consideration of the possible reactions between catalase and C_2H_5OH from chemical kinetics positions, Kremer [105] drew conclusions about the high probability of the following mechanism:

$$\begin{aligned} E + C_2H_5OOH &\rightarrow IP \\ IP &\rightarrow E + CH_3CHO + H_2O \\ IP + C_2H_5OOH &\rightarrow \text{side products} \end{aligned} \qquad (6.16)$$

where E is the enzyme and IP are intermediate products.

There are works [106] that show the mechanism of fixed heme ionization in the complex VII of horse-radish peroxidase. The absorption bans of F^{4+}═O bond in the complex VII change with respect to pH in accordance with the following formulae:

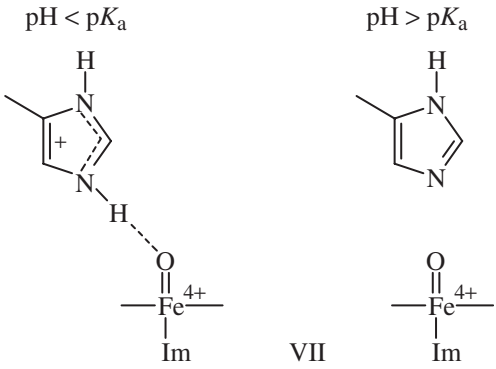

Using the Raman scattering method and the example of ferrimyoglobine–horse-radish peroxidase complex VII, Terner has proved the existence of heme in Fe^{4+}═O in the catalytic site.

According to Terner, reduction of intermediates of the complex VII type proceeds by the following reaction:

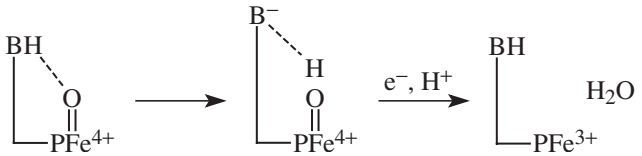

in the alkaline medium

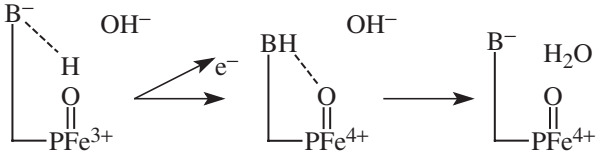

According to Terner's data [107], the lifetime of the horse-radish peroxidase complex VII is 2–3 min.

The authors of the present monograph suggested [108] a nontrivial mechanism of catalase and non-classical peroxidase reactions using BRC complexes in the design.

The BRC concept [99] allows the analysis of the elementary actions of chemical transformation at the level of active complexes, in which electron density is redistributed in accordance with bond multiplicity change. Generally, this is expressed by the rule of multiplicity alternating change:

$$\Delta = \pm a \; (\Delta = \pm 1; \; \Delta = \pm 0.5)$$

The acid–base catalysis is carried out in BRC, with H^+ or $2H^+$ ion transfer. Poltorak notes [99] that when H^+ and e^- or H^+ and H^- are transferred, the reaction mechanisms relate to H^+-dependent redox type. BRC with electron transfer describes heterolytic oxidative processes.

In enzymatic catalysis, the amazing unity of acid–base and redox mechanisms, in one of BRC H^+ and e^- or H^- are transferred to prosthetic groups of enzymes, which results in redox transformations of the substrate.

Considering the mechanism of the abundance of enzymatic reactions in the framework of the BRC theory, Poltorak [99] has separated three types of 'admirably standard BRC', to which enzymatic reaction can be related:

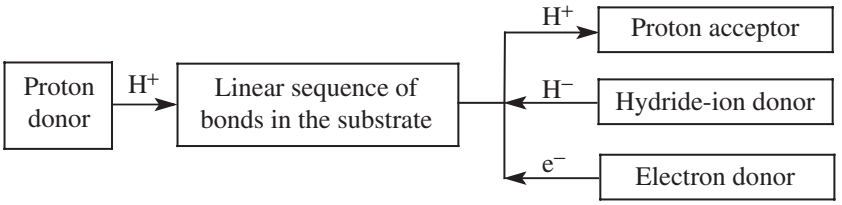

Such structure of enzyme catalytic sites causes a 'stereotype' of chemical mechanisms of the substrate enzymatic transformations, which 'is associated with the unique individuality of their adsorption sites in relation to substrate fixation'. It is common knowledge that donors and acceptors of catalytic groups exchanging protons, electrons and hydride ions with the substrates have different origins in different enzymes.

The catalase action mechanism is developed [108] with the help of BRC composition principles. According to this mechanism, reaction products are formed at a single stage resulting in two-electron transfer from H_2O_2 to the acceptor. The native diagram of catalase is presented in Figure 6.7, where the active site is accepted to represent a hydrolyzed form of Fe^{3+} ion, bound to Asn 147 by two hydrogen bonds of two fixed water molecules. Shown below are distances in angströms [109] between the catalytic groups, various atoms and ions, required for stereochemical analysis of the catalase action mechanism:

Fe^{3+} 1.95 OH Asn 147 5.64 Fe^{3+}
Fe^{4+} 1.60 O
Fe^{3+} 1.95 OOH Asn 147 5.37 (N) His 74
Fe^{3+} 1.49 OH
H 0.97 O 1.49 H Fe^{3+} 4.90 (N) His 74
H 0.99 OH

Figure 6.8 shows a stoichiometric diagram, which reflects an attempt to make the H_2O_2 molecule interact with Fe—OH. Obviously, the Van der Waals radius of the OH group, shown by points in the figure, does not allow effective performance of such interaction.

The mechanism of complex VIII formation is shown in Figure 6.9. It is the author's opinion that it gives a satisfactory explanation to the Chance complex formation at combined action of acid–base catalytic groups (His and Asn fragments), two water molecules and ferric

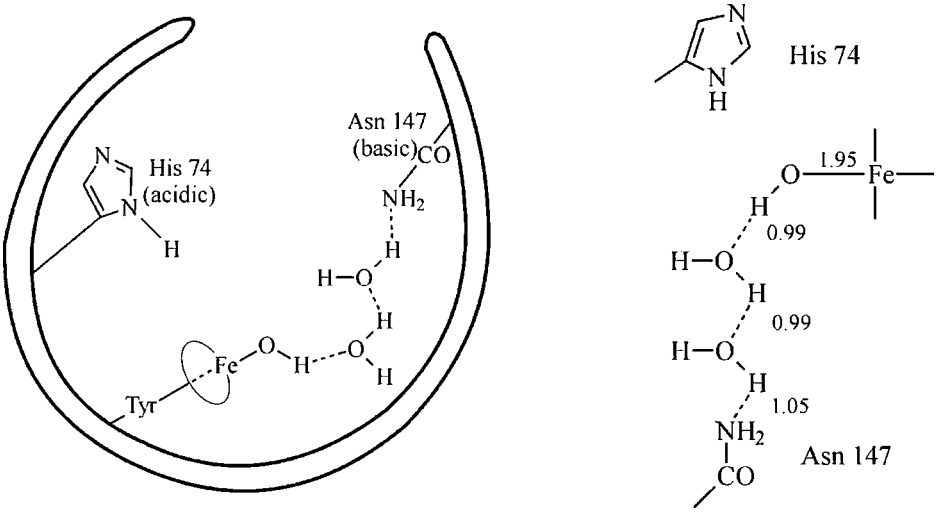

Figure 6.7 The suggested native diagram of catalase.

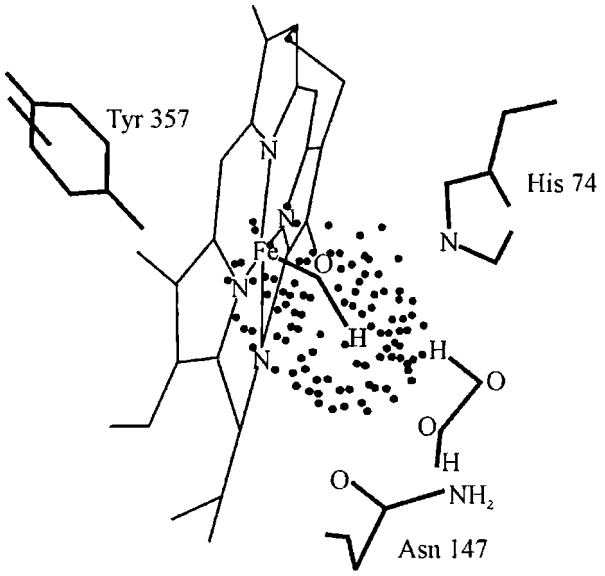

Figure 6.8 Stereochemical image reproducing H_2O_2 molecule attack on Fe–OH catalytic site.

protoporphyrin hydroxoform in BRC. The results of computerized stoichiometric analysis of this diagram are shown in Figure 6.10. As indicated, based on interatomic distances (in angströms) and spatial disposition of reacting particles, the Chance complex can be formed by the mechanism designed in the framework of the BRC theory.

The Oguri complex formation with respect to requirements relating to the synthesis of the products via the one-stage transfer of two electrons is presented diagrammatically in Figure 6.11. The stoichiometric image taking into account optimal interatomic distances (in angströms) and bond angles is shown in Figure 6.12.

It may seem strange in Figure 6.11 that one of the arrows showing electron transportation in BRC indicates electron transfer from the hydrogen atom in the hydrogen peroxide molecule to the oxygen atom bound to iron ion. To explain this, at first sight unusual, part of the electron pathway in BRC, the whole sequence of this transfer must be traced.

Proton transfer from the hydrogen peroxide molecule to His 74 is accompanied by O—H bond break and electron transfer to the oxygen atom. Then owing to the following O—H bond break and O═O bond formation this electron is transferred to the hydrogen atom with simultaneous hydride-ion transfer. The whole sequence of electron transfer in BRC is implemented without high-energy consumption.

Therefore, according to this idea, two differently shaped hydrogen atoms (proton and hydride-ion) are transferred simultaneously from the hydrogen peroxide molecule. Primarily, hydride-ion formation and participation of acid–base sites in the catalysis act were noted in the works [82, 110, 111], where the key role of hydride ion in the mechanism of enzymatic H_2O_2 dissociation was suggested.

This circumstance is a strong argument for the benefit of hydride-ion participation in linear BRC.

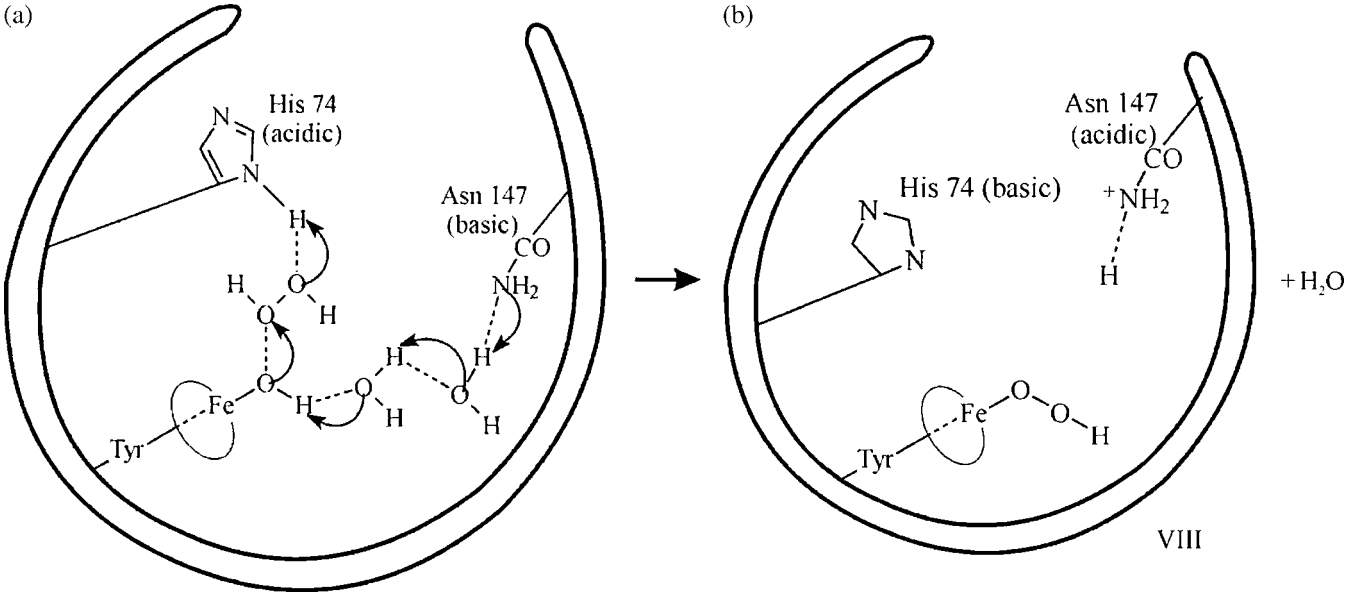

Figure 6.9 The formation mechanism of complex VIII (Chance). (a) Active complex with distal histidine and asparagine as acid–base sites. (b) Active intermediate—complex VIII (Chance).

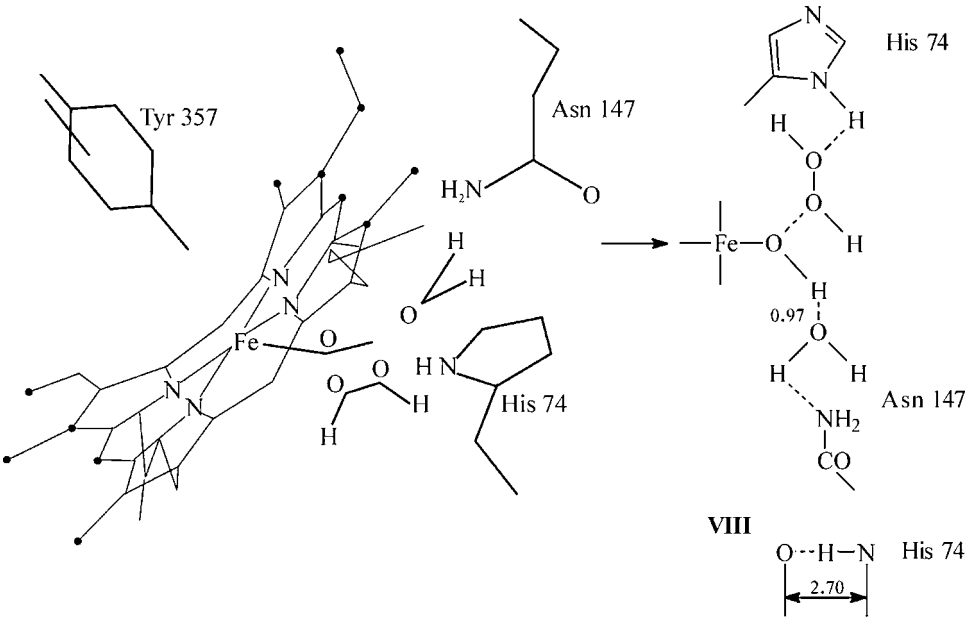

Figure 6.10 Stoichiometric image of complex VIII (Chance) formation.

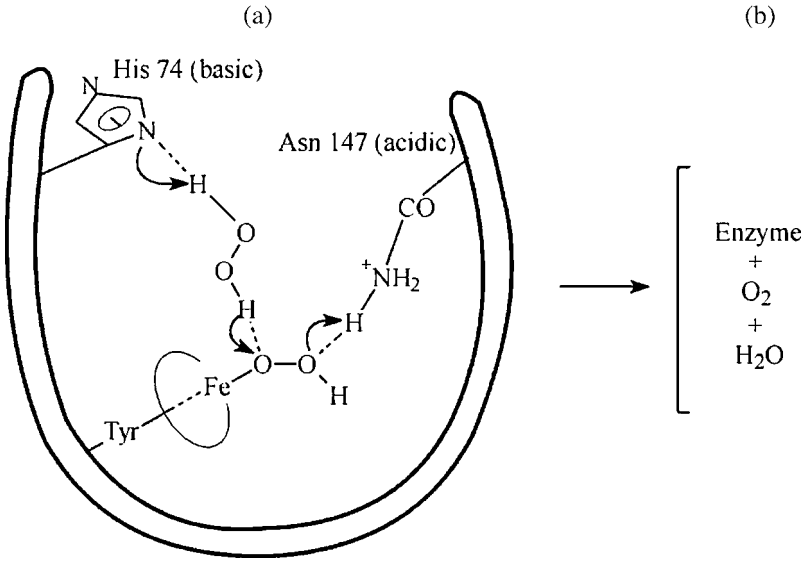

Figure 6.11 The formation mechanism of catalase reaction products. (a) The Oguri complex formed with the second H_2O molecule. (b) H_2O and O_2 formation, and native enzyme synthesis.

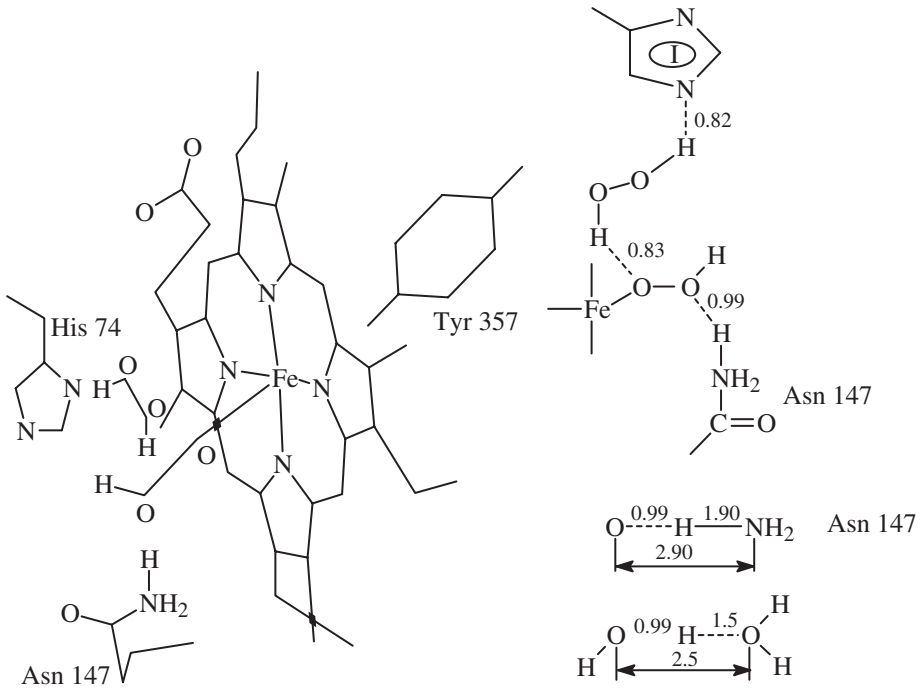

Figure 6.12 Stoichiometric image of the Oguri complex.

BRC formed by catalytic His 74 and Asn 147 groups correspond to these schemes (Table 6.1).

In both diagrams the change of bond multiplicity in the catalysis act meets the rule ± 1, which reflects the condition of BRC conductivity for electron.

In the suggested mechanisms, rearrangement of the bond system in BRC is stipulated by transfers of two protons and one hydride ion, which is accompanied by electron transfer from one BRC end to another.

The mechanisms of catalase and non-classical peroxidase reactions shown in Figures 6.11 and 6.13 explain a sequence of observable key factors:

- Two-electron oxidation of the substrate (i.e. H_2O_2 and C_2H_5OH) in one stage.
- Oxidation associated with hydride-ion detachment from H_2O_2.
- The synthesis of reaction product H_2O and O_2 in a single act of catalysis.
- The analogy of catalase and non-classical peroxidase reaction mechanisms.

The mechanism of the elementary reaction suggested (refer to Figure 6.11) has a very important feature: both atoms of the oxygen molecule formed belong to the same hydrogen peroxide molecule. This experimental result conforms to isotopic investigations of the homogeneous degradation of the $H_2{}^{18}O_2$–H_2O_2 mixture. Hence, independently of the reaction pathway both atoms of molecular oxygen ($^{18}O_2$ and O_2) belong to the same hydrogen peroxide molecule [112, 113]. This statement can also encompass the catalase reaction. This will be one more urgent argument for the benefit of the mechanism shown in Figure 6.11.

Table 6.1

Conditions of meeting the rule '±1' for BRC

State	Activity	
	Catalase	Peroxidase
Initial	His 74 H–O–O–H O–O H–Asn 147 0 1 1 1 0 1 0 1	His 74 H–O–O–H O–O H–Asn 147 0 1 1 1 0 1 0 1
Final	His 74 –H O=O H–O O–H Asn 147 1 0 2 0 1 0 1 0	B–H C=O H–O O–H Asn 147 1 0 2 0 1 0 1 0
Multiplicity variation	+1 −1 +1 −1 +1 −1 +1 −1	+1 −1 +1 −1 +1 −1 +1 −1

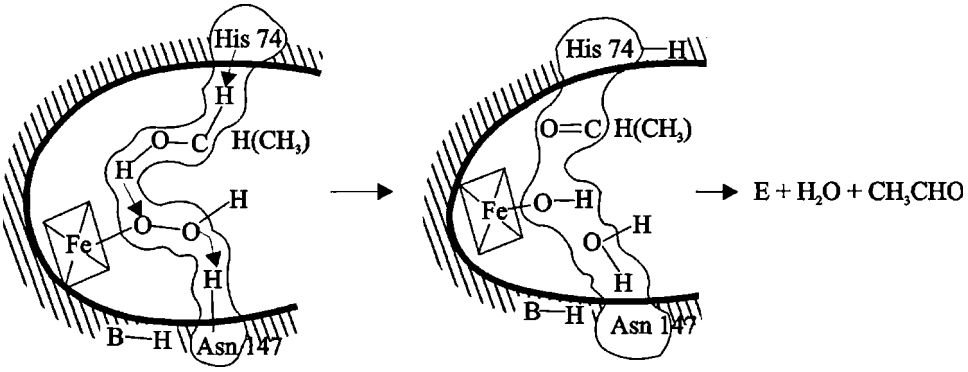

Figure 6.13 The mechanism of non-classical peroxidase reaction. B is acidic or basic site.

Of the highest urgency is the question of complex VIII composition: either it is Fe^{4+}═O or Fe^{3+}OOH. The authors assume that the complex Fe^{4+}═O is less suitable as an active intermediate for the following reasons:

- The lifetime of the complex is several minutes; therefore, it is doubtful that such a relatively stable intermediate product can provide for such a high catalase reaction rate.
- The Fe ═ O bond is strong enough and fixed in space.
- The distance between the oxygen atom of the Fe^{4+}═O complex and His and Asn catalytic groups is greater than for Fe—OOH. It is not inconceivable that the spectroscopically detected intermediate product Fe ═ O is formed by the following reaction:

$$\text{Tyr} - \overset{|}{\underset{|}{Fe^{3+}}} - O - O - H \xrightarrow{H^+,\ \text{quickly}} \text{Tyr} - \overset{|^+}{\underset{|}{Fe^{4+}}} = O + H_2O$$

if H_2O_2 concentration in the reaction mixture is extremely low to run the catalase reaction.

In this context, in the case of catalase the Fe═O complex may be considered as a dead-end intermediate, though for peroxidases it most likely represents the catalytic site for one-electron oxidation.

The intermediate Fe—OOH is a mobile compound. Therefore, stereochemical diagrams show satisfactory interatomic distances and bond angles. It is obvious that the complex Fe—OOH is better adapted for two-electron reactions proceeding in one stage. Unfortunately, it has not yet been detected by spectroscopy methods because of its high activity in the reaction mentioned. There is a possibility of solving this question using catalase simulators [114, 115].

Reactions 1 and 2 in the diagram shown in Figure 6.13 can be easily reduced to gross equations, identical to conjugated oxidation reactions [115]:

$$H_2O_2 + H_2O_2 \xrightarrow{\text{catalase}} 2H_2O + O_2 \tag{6.17}$$

$$H_2O_2 + C_2H_5OH \xrightarrow{\text{catalase}} CH_3CHO + 2H_2O \tag{6.18}$$

If the diagram is analyzed in the context of the principles of conjugated reaction, it may be concluded that conjugated biooxidation with hydrogen peroxide consists of the basic (primary) catalase reaction of H_2O_2 dissociation (reaction (6.17)). Owing to the Chance complex formation [116, 117], this primary reaction induces the secondary non-classical peroxidase reaction (6.18).

Thus, the Chance complex [116, 117] is the general highly active intermediate compound transmitting the inductive action of the primary reaction (6.17) to the conjugated secondary reaction (6.18), which is also indicated in the work [108].

In the [E—OOH · C_2H_5OH] complex ligand OOH is the electron acceptor particle, whereas ligand C_2H_5OH (DH_2 in the general shape) is the electron donor. Their interaction regenerates active sites of catalase, produces H_2O and oxidizes the substrate.

An analogous diagram is presented by Kremer [118], where catalase and peroxidase reactions are considered to be competitive processes. The statement about competition between these reactions eliminates the possibility of peroxidase reaction speeding up by means of catalase reaction intensification.

Meanwhile, the data obtained [87, 116] unambiguously indicate that the catalase activity increase is associated with non-classical peroxidase activity intensification. It is obvious that the last circumstance casts some suspicion on the interpretation of reactions (6.17) and (6.18) as the competing ones, because in this case, intensification of one reaction should cause suppression of the other. Moreover, as follows from Kremer's data [118], the catalase reaction rate is five orders of magnitude higher than the peroxidase reaction rate. Therefore, comparison of these reactions from competition positions is very suspect. An article by Chance and coworkers [119] can be mentioned as evidence that a H_2O_2 concentration increase in the system in the presence of ethanol intensifies peroxidase activity (hence, intensification of the catalase activity is implied). Because catalase activity increase causes the Chance complex formation at higher rate, the peroxidase reaction (6.18) rate is also increased owing to chemical induction principle.

Thus, both processes of H_2O_2 dissociation and C_2H_5OH oxidation proceed in two stages: general intermediate (Chance) complex formation responsible for chemical conjugation in the system and Oguri complex formation, which induces the one-stage synthesis of the final oxidation products.

The typical feature of the substrate oxidation mechanism in aqueous solutions is electron transfer from the substrate to the oxygen molecule that forms H_2O_2 or H_2O, whereas in an organic medium the hydrogen atom is fixed on the substrate. In this connection, the main function of metalloporphyrin-containing enzymes (catalase and peroxidase) is substrate oxidation without addition of oxygen atoms to it. The process must be run in aqueous solution. The function of iron protoporphyrin—the active site for these enzymes—concludes in making electron transfer from the substrate to oxygen with water formation easier.

It is common knowledge [41, 120, 121] that hydroxylating enzymatic systems, cytochrome P-450 and analogs, in particular, have the prospect of a broad field of practical application. For example, they can be used in the synthesis of various medical preparations, detoxication of living organisms and development of highly selective process techniques for the production of epoxides, alcohols and ketones.

However, there are many obstacles in the way of creating catalytic systems simulating the unique properties of cytochrome P-450. Many works [41] have been devoted to the task of overcoming them, and more and more articles are issued every year. Listed below are the most significant disadvantages that create obstacles to the development of simple analogs of cytochrome P-450 with preservation of its basic functions.

Enzymes monooxygenating with molecular oxygen usually function in the presence of organic and inorganic reducers. This imposes the additional limitations on reducer selection and makes the process more complicated for laboratory performance. Moreover, metalloporphyrins initiate substrate chain autooxidation with molecular oxygen, varying qualitative and quantitative reaction indices. Hence, free radicals occurring in the reaction mixture can destroy the enzyme and, apparently, model catalytic systems. Neither can the probability of side reactions between oxidation products and the reducer be excluded. The question of the mechanism of oxygen transfer present in the complex with heme to oxidized substrate (S) is still unclear. The problem of the necessary reducer presence is solved by using organic hydroperoxides and peroxy acids reacting with the substrate according to the following process:

$$S + ROOH \rightarrow SO + ROH \tag{6.19}$$

As observed from reaction (6.19) and experimental data [41, 120, 121], ROOH satisfactorily replaces molecular oxygen and the reducer. When oxidized with hydroperoxides in the presence of iron porphyrin catalysts (cytochrome P-450 analogs), olefins mostly convert to allyl oxidation products, namely unsaturated alcohols and ketones, whereas the quantity of epoxides does not exceed 1% [122]. According to current suggestions [121] such behavior of iron porphyrin catalysts is explained by olefin epoxidation with the catalyst–ROOH complex by the heterolytical mechanism according to the following equation:

$$[PPFe^{3+} \cdot ROOH] + \begin{array}{c} \diagdown \quad \diagup \\ C = C \\ \diagup \quad \diagdown \end{array} \longrightarrow \begin{array}{c} \diagdown \quad \diagup \\ C = C \\ \diagup \; O \; \diagdown \end{array} + ROH + PPFe^{3+} \tag{6.20}$$

where PP is protoporphyrin.

The same complex degrades with free radical formation according to the following reaction:

$$[PPFe^{3+} \cdot ROOH] \rightarrow PPFe^{3+} + RO_2^{\bullet} + H^+ \quad (6.21)$$

and can initiate the radical-chain conversion of olefins to allyl oxidation products. Both reactions of olefin oxidation are implemented in catalysis by cytochrome P-450, where the predominant formation of one product or another is defined by the contribution of each reaction. In the present case, $PPFe^{3+} \cdot OH$ catalyst is more active in reaction (6.21) than in epoxidation reaction (6.20). In this connection, it is believed that formation of allyl oxidation products from olefins is observed in the presence of catalysts promoting ROOH homolytical degradation by reaction (6.21). The radical-chain oxidation mechanism casts some suspicion on the conclusion that the reaction represents a model of the enzymatic process. It is also noted that the oxynoid mechanism of monooxygenase reactions has not yet been confirmed, and the analogs of monooxygenase reactions should be searched for among monooxygenase models in conjugated oxidation of organic compounds with metal ions in case of low degrees of oxidation. In fact, the data from many works in which conjugated processes are considered as simple models of monooxygenase reactions confirm the above idea.

6.4 CO-FACTORS AND THEIR ROLE IN THE INTERACTION AND SYNCHRONIZATION OF BIOCHEMICAL REACTIONS

Various biochemical reactions interact in all living organisms. Therefore, it is desirable to determine the chemical interference or chemical conjugation in such systems.

Thus, a logical question arises: what is newly introduced by the theory of synchronous chemical reaction interaction to decoding of the mechanism and functions of enzymatic systems?

First of all, the interference pattern of the biochemical interaction between reactions will shed light on their synergic mechanism and the associated effect on the control functions of enzymatic systems, especially those immobilized on membranes: the overwhelming majority of the enzymes' work on the surface of cell and sub-cell membranes. Moreover, interference presentation allows the detection of the origin of active intermediate substances, which form and operate the communication channels between two or more biochemical reactions, defines the co-factor role and gives an opportunity to induce thermodynamically hindered biochemical reactions.

Co-factors, as a rule, are the integral part of enzymes, without which the cell metabolism is impossible.

Co-factors are metal ions or non-protein organic compounds; however, many enzymes require the presence of both co-factors.

Co-factors are added to the catalytically inactive protein part of enzymes, the so-called apoenzyme. In cases where this bond in a complex is strong enough, it is called the prosthetic group.

In the framework of the currently developing concept of chemical interference, of primary interest are co-factors transferring chemical groups, hydrogen atoms or electrons.

The key role of co-factors concludes in the formation of the active catalytic site of the enzyme, with the help of which substrate is fixed and its conversion is simplified and intensified.

It should be noted that derivatives from vitamins possessing relatively more complex structures are also co-factors. Unfortunately, they cannot be synthesized in animal organisms.

Naturally, organisms are supplied with vitamins in food, and vitamin deficiency can cause specific diseases.

As mentioned above, redox enzymes (oxidoreductases) are divided into four large groups: dehydrogenases, oxygenases, oxidases, and peroxidases and catalases.

Dehydrogenases responsible for hydrogen transfer between substrates possess NAD^+ (nicotinamide) as the coenzyme, owing to which chiral alcohols are formed from ketones and aldehydes.

Participating in dehydrogenase reactions, the NAD^+ coenzyme is reduced to NADN by the following biochemical reaction:

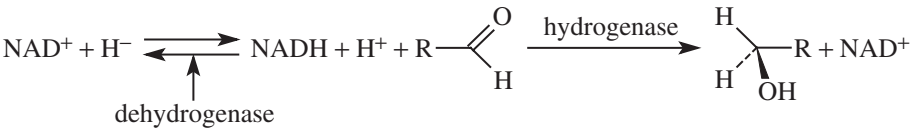

(6.22)

This reaction is stereospecific and synthesizes one of two possible isomers in α- or β-position.

To analyze reaction (6.22) in the framework of the chemical interference concept, it should be divided into two component processes: the primary and the secondary overall reactions.

In this case, the primary reaction is presented by the so-called citric acid cycle with the participation of various NAD^+-dependent dehydrogenases synthesizing corresponding final products typical of this cycle. However, active intermediate NAD^+H^- and H^+ particles formed in the course of these reactions are able to induce reduction of aldehydes and ketones to corresponding chiral alcohols with the simultaneous regeneration of the NAD^+ co-factor.

Thus, the secondary overall reaction will represent a complex biochemical reaction consisting of elementary stages in which NADH and H^+ are formed and consumed for reduction of aldehydes and ketones.

Using experimental data, the interference pattern demonstrates kinetic curves of the primary and secondary reactions. Hence, it reflects the mechanism of possible control influences on the system, for example, by means of concentration of one initial substrate or another and final products of both reactions.

The above indicates the importance of specific requirements to the synthesis of enzyme biosimulators.

The problem of biomimetic model design simulating the action mechanism of corresponding enzymes is based on the idea of structural–functional conformity. In 1971, alcohol dehydrogenase was primarily synthesized [123]. In this biomimetic system the product is formed due to direct electron transfer from the reduced co-factor (NADH) analog to aldehyde. Note that the display of alcohol dehydrogenase catalytic activity requires the presence of zinc (II) ion.

Simulation of the reverse dehydrogenase reaction induced the use of crown ethers as NADH models [124]. It is shown that hydride-ion transfer by crown ethers happens 3000 times faster than in the case of different carriers. It is believed that crown ether provides for the required

cation complex formation level, which displays some typical features of simulated enzymes. In particular, on the one hand, crown-ether biosimulator is an acceptor site for substrate fixing; on the other hand, it is a catalytic site for fixed substrate conversion. Thus, similar biosimulators are of dual interest: as simulation enzyme models and effective chemical agents [125].

Of course, the creation of co-factor models requires a comprehensive knowledge of structural and catalytic properties of corresponding enzymes. For example, postulated hydride ion may be opposed by a simpler reduction mechanism involving two-electron transfer. In this connection, Hamilton believes that if hydride ion is really directly transferred in dehydrogenase reactions, this mere process is unique not only in biology, because $H^+ + 2e^-$ transfer is more favorable [126]. However, the author failed to distinguish these two possibilities. Broadly speaking, it is very difficult to judge this unambiguously.

When simulating the alcohol dehydrogenase, the investigators met with economic problems because the NAD^+ co-factor is very expensive. Therefore, several methods of its regeneration were developed, among which the most effective method is non-enzymatic continuous regeneration of catalytic amounts of NADHL and NAD^+ with sodium dithionite [127]. This method can be used for HLADH synthesis, used in the catalytic reduction of a wide selection of aldehydes and ketones.

However, the reverse reaction of alcohol oxidation in this system can be performed with flavin co-factor added ($FMNH_2 \rightarrow FMN$), where molecular oxygen is reduced to H_2O_2. The entire biomimetic process under consideration is well illustrated by the following diagram [128]:

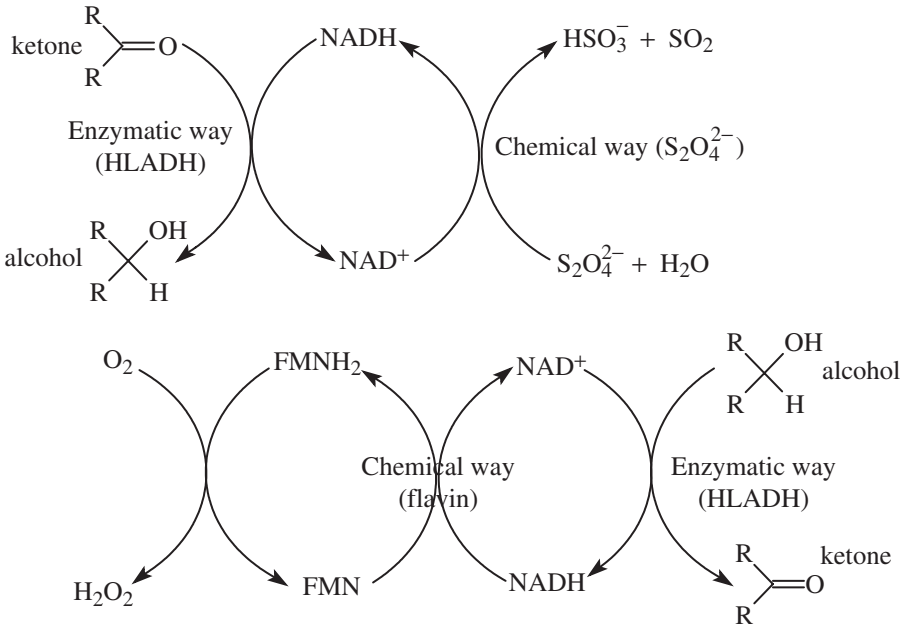

(6.23)

The absolute advantage of the biomimetic systems suggested above is that they possess a set of properties that cannot be reproduced in one stage by traditional methods of chemical

catalysis. Similar to corresponding enzymes, these properties help the systems mentioned to effectively convert the substrate.

Let us now apply these ideas about the features of co-factor mechanism of enzymatic reactions and their analogs to the analysis or interpretation of substrate conversion in terms of synchronous reaction interaction (chemical interference). As usual, we first need to identify the primary reaction which synthesizes NADH, the highly active intermediate compound, to the system. A primary reaction shaped as follows can be simply deduced from the diagram (6.23):

$$RCH_2OH + NAD^+ \xrightleftharpoons{\text{dehydrogenase}} R{-}C(=O){-}H + \underbrace{NAD^+H^- + H^+}_{\text{intermediates}}$$

where RCH_2OH and $R{-}C(=O){-}H$ are the substrate and the product, respectively.

The secondary reaction is carried out with the direct involvement of the intermediate generated to the system according to the following process:

$$NAD^+H^- + R{-}C(=O){-}H \xrightleftharpoons[\text{dehydrogenase}]{H^+} NAD^+ + RCH_2OH$$

In the primary reaction two electrons are transferred in one stage from the substrate by NAD^+ in the form of hydride ion (H^-); the second hydrogen atom is detached from the substrate molecule as proton (hydrogen ion H^+). Note that NAD-dependent dehydrogenases participate in the citric acid cycle, carbohydrate exchange, etc. in mitochondria.

Generalizing the above, it can be shown that cellular dehydrogenases transfer hydrogen atoms from various substrates by NAD^+, in NADH form, which is the unique (general) intermediate, among those generated by various NAD^+-dependent dehydrogenases to the system. This statement does not exclude H^- from the reaction volume, where it is also formed in dehydrogenase reactions.

At the next stage, two electrons fixed by hydride ion (H^-) in NADH coenzyme are transferred to flavin adenine dinucleotide (FAD) dependent dehydrogenase, located on the internal mitochondrial membrane. In this reaction the strongly bound prosthetic group of FAD-dehydrogenase is reduced. The role of the FAD-dehydrogenase prosthetic group is played by FAD; hence, two electrons (by analogy with hydride ion) are transferred from NADH to FAD by the reaction:

$$NADH + FAD + H^+ \rightleftharpoons NAD^+ + FADH_2$$

In the Hamilton mechanism, widely applied by biochemists, one proton and two electrons are or hydride ion is transferred. It is justified by the fact that proton has no electron cover and, therefore, is quite movable and more highly effective in biological media [126].

This question will be more or less cleared up only after model reaction investigations. The majority of oxidases are FAD dependent and able to transfer oxygen to the substrate molecule. NAD^+ coenzyme does not possess this property. For example, flavin-dependent monooxygenases activate molecular oxygen so that one atom of oxygen can be added to the substrate molecule hydroxylating or epoxidizing it, whereas the second atom of oxygen is reduced to H_2O.

The cyclic mechanism of monooxygenase reactions performed in flavin-dependent systems is shown in the diagram below [128]:

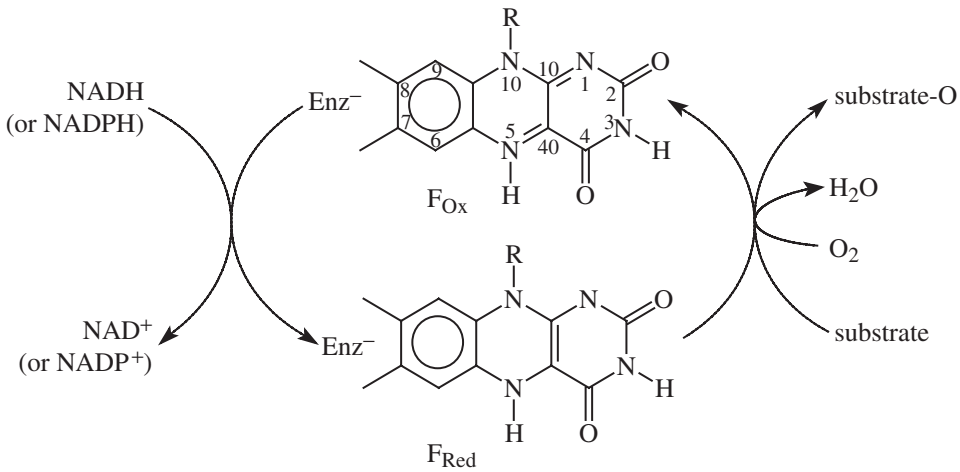

where:

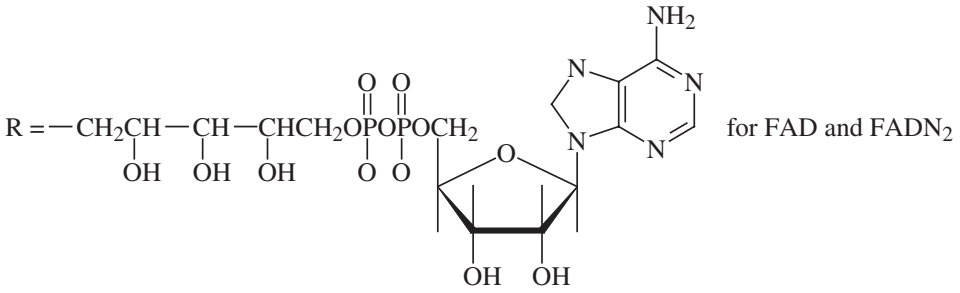

By analogy with carbenes, this mechanism is known by the name ‘oxene mechanism’. The diagram shows that the oxygen molecule reacts with the reduced flavin is activated and

only then oxidizes the substrate in accordance with the ion mechanism; hence, free electron spins in O_2 are necessarily preserved. Thus, it is suggested that reduced flavin forms fixed H_2O_2 via interaction with O_2. In this form, H_2O_2 is regrouped to flavin-4a-hydroperoxide (HO_2) and, therefore, obtains higher reactivity. In its turn, affected by H^+, flavin hydroperoxide is regrouped to carbonyl oxide, which is a hydroxylating and an epoxidizing agent. To prove the reality of such a system, the mechanism developed for ozone reaction with unsaturated compounds is shown:

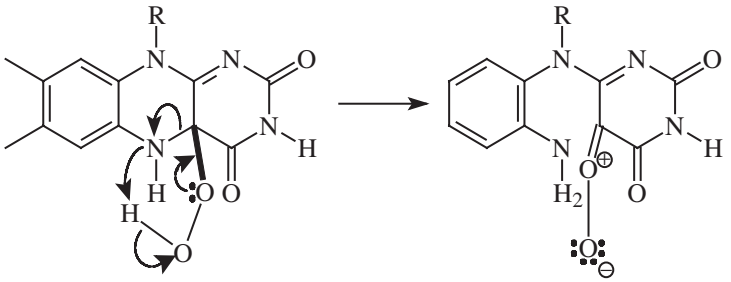

flavin hydroperoxide — carbonyl oxide

The main disadvantage of Hamilton's mechanism [126] is the existence of an open flavin ring shape. Moreover, Hamilton's mechanism is based on the idea that there is no direct oxygen transfer to the substrate, which is clearly illustrated by the following expression:

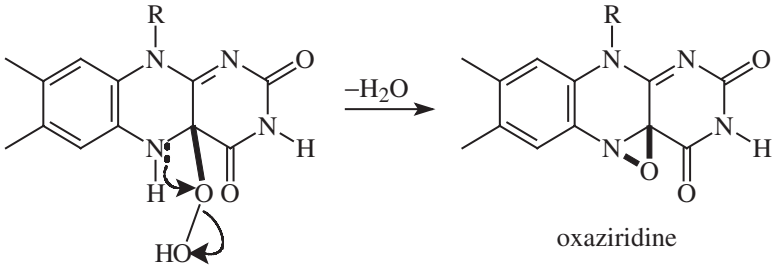

oxaziridine

The mechanism suggested in Ref. [129] does not imply the formation of an intermediate product with an open ring. Active oxaziridine-4a,5-flavin benzoxide formed from flavin hydroperoxide is assumed to be the intermediate. This mechanism based on the electrophilic type of the oxaziridine system is justified in multiple examples, united in the following diagram [128]:

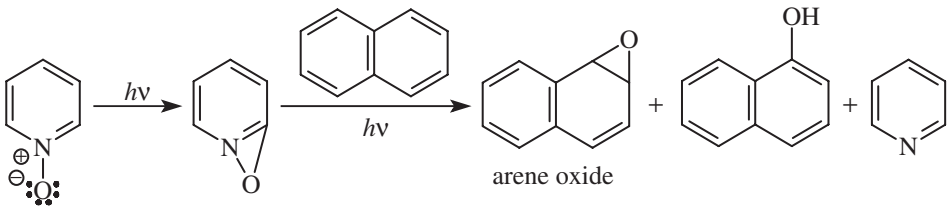

arene oxide

In the framework of these ideas, the phenol hydroxylation mechanism is implemented by oxygen transfer from the oxaziridine intermediate to phenol giving different intermediate compounds—benzene epoxide:

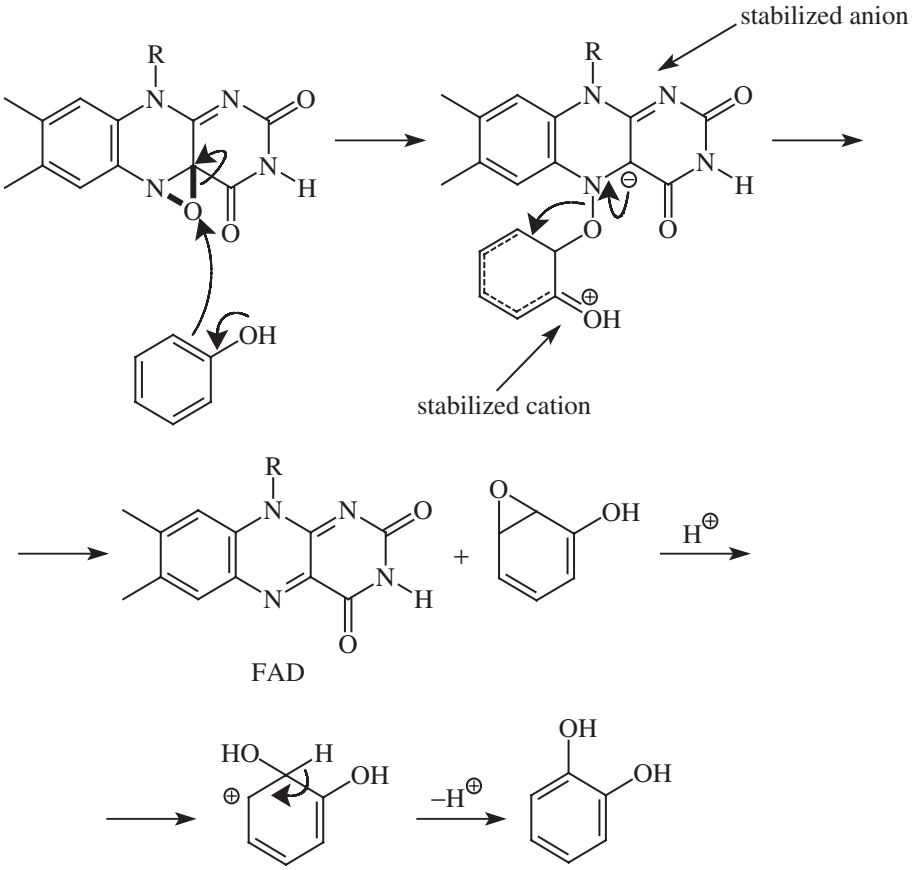

This suggestion is already known. Indeed in 1969, it was stated [130] that monooxygenase oxidation of some aromatic compounds produced intermediates, shaped as epoxides of these aromatics:

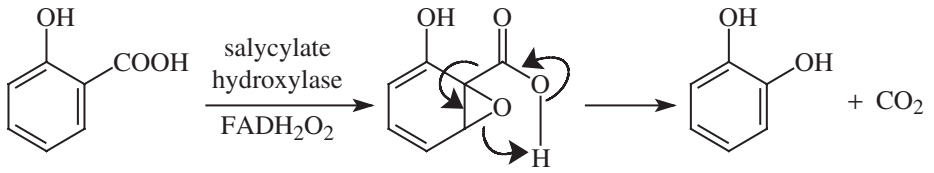

Another idea, theoretically justified by Goddare [131], about the hydroxylation mechanism of phenol compounds is based on the suggestion that the active intermediate compound is presented by biradical particles.

As shown by this method, besides biradical, another intermediate compound is formed. It represents a complex of flavin bound to phenol by two atoms of oxygen:

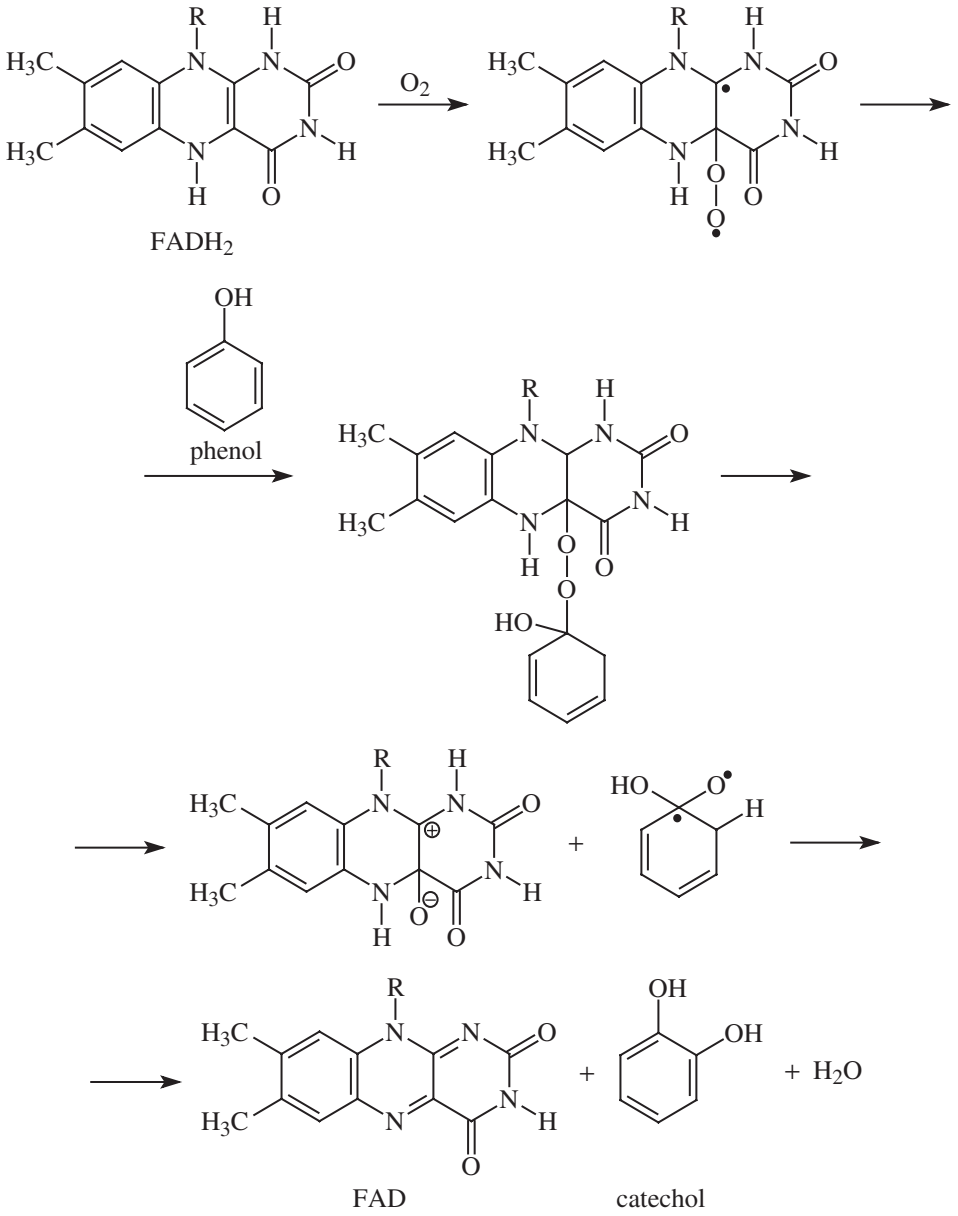

This is the multistage method. It suggests the formation of several active intermediate substances, including biradical particles, which in the author's opinion has less probability for enzymatic transformation of the substrate.

REFERENCES

1. Shamb, W., Satterfield, C. and Wentware, R., *Hydrogen Peroxide*, Inostrannaya Literatura, Moscow, 1958, 578 pp. (in Russian).
2. Pozin, M.E., *Hydrogen Peroxide and Peroxy Compounds*, Goskhimizdat, Moscow, 1951, 475 pp. (in Russian).
3. Kazarnovsky, I.A., *Dokl. AN SSSR*, 1975, Vol. 221, No. 2, pp. 353–356 (in Russian).
4. Fenton, H.S., *J. Chem. Soc*., 1894, p. 899.
5. Haber, P. and Weiss, J., *Proc. Roy. Soc. London A*, 1934, Vol. 147, pp. 332–352.
6. Bard, W.L., Baxendale, J.H., Jarge, P. and Hargave, K.R., *Trans. Faraday Soc.*, 1951, Vol. 47, pp. 462–500.
7. Benson, H.J., Bielski, B.H. and Saito, E., *J. Phys. Chem*., 1962, Vol. 66, pp. 2266–2270.
8. Dixon, W.J. and Noiman, R.O.C., *J. Chem. Soc*., 1963, No. 5, pp. 3119–3124.
9. Saito, E. and Bielski, B.H., *J. Am. Chem. Soc*., 1961, Vol. 83, pp. 4467–4470.
10. Chang, J.S., Iraddock, D. *et al*., *J. Chem. Soc*., 1966, Vol. 70, pp. 3509–3513.
11. Shuvalov, V.F., Bazhin, N.M., Berdnikov, V.M. *et al*., *Zh. Strukt. Khim*., 1969, Vol. 10, No. 3, pp. 548–549 (in Russian).
12. Merkulov, N.M., Bazhin, N.M. and Berdnikov, V.M., *Ibid.*, 1970, Vol. 11, No. 6, pp. 1121–1122 (in Russian).
13. Sychev, A.Ya. and Isak, V.G., *Zh. Fiz. Khim*., 1973, Vol. 47, No. 3, pp. 593–597 (in Russian).
14. Sychev, A.Ya. and Isak, V.G., *Zh. Fiz. Khim*., 1977, Vol. 51, No. 2, pp. 363–366 (in Russian).
15. Pantaler, R.P., Alerimova, L.D. and Bulgakova, A.M., *Ukr. Khim. Zh*., 1975, Vol. 41, No. 8, pp. 800–805 (in Russian).
16. Weiss, J., *Adv. Catal*., 1952, Vol. 4, pp. 343–365.
17. Danilova, M.M., Mikhacheva, Yu.V. and Tsyirul'nikova, P.G., *Kinetika i Kataliz*, 1975, Vol. 16, No. 14, pp. 1082–1084 (in Russian).
18. Sadyikhov, V.A. and Tsyirul'nikova, P.G., *Ibid.*, 1976, Vol. 16, No. 3, pp. 626–633 (in Russian).
19. Legenchenko, I.A. and Stupichenko, R.N., *Zh. Fiz. Khim*., 1978, Vol. 52, No. 10, pp. 2524–2529 (in Russian).
20. Ono, J., Matsumura, T., Kitajima, N. and Fukuzumi, S., *J. Phys. Chem*., 1977, Vol. 81, pp. 1307–1311.
21. Kitajima, N., Fukuzumi, S. and Ono, J., *Ibid.*, 1978, Vol. 82, pp. 1505–1509.
22. Kaitmaziv, S.D. and Prokhorov, A.M., *Zh. Eksperim. Teoret. Fiz*., 1954, Vol. 26, No. 4, pp. 1331–1332 (in Russian).
23. Kaitmaziv, S.D. and Prokhorov, A.M., *Zh. Fiz. Khim*., 1960, Vol. 34, No. 1, pp. 227–228 (in Russian).
24. Kaitmaziv, S.D. and Prokhorov, A.M., *F. T. T.*, 1963, Vol. 5, No. 1, pp. 347–348 (in Russian).
25. Uri, N., *Chem. Rev.*, 1952, Vol. 50, pp. 375–446.
26. Semenov, N.N., *On Some Questions of Chemical Kinetics and Reactivity*, 2nd edn, Izd. AN SSSR, Moscow, 1958, 680 pp. (in Russian).
27. Huang, R.L., Goh, S.H. and Org, S.H., *The Chemistry of Free Radicals*, Arnold Publishers, 1974, p. 244.
28. Baxendale, T.H., *Adv. Catal*. 1952, Vol. 4, pp. 31–50.
29. Udenfried, S., Clark, C.T., Axelrod, J. and Brodie, B.B., *J. Biol. Chem.*, 1954, Vol. 208, pp. 731–737.
30. Emanuel, N.M. and Knorre, D.G., *The Course of Chemical Kinetics*, Vysshaya Shkola, Moscow, 1984, 237 pp. (in Russian).
31. Fridovich, I., *Free Radicals in Biology*, Vol. 1, Mir, Moscow, 1979, pp. 272–308 (in Russian).
32. Vol'pin, M.E., Moiseev, I.I. and Shilov, A.E., *D.I. Mendeleev ZhVKhO*, 1980, Vol. 25, No. 5, p. 515 (in Russian).
33. Rakovsky, A.A., *The Introduction to Physical Chemistry*, ONTI Red Khim. Lit., Moscow, 1938, 677 pp. (in Russian).
34. Karakhanov, E.A., Volkov, S.M. and Dedov, A.G., *Catalysis*, Izd. MGU, Moscow, 1987, pp. 147–172 (in Russian).

35. Hamilton, G.A., Workman, R.J. and Wool, L., *J. Am. Chem. Soc*., 1964, Vol. 86, pp. 3390–3394.
36. Tamagaki, S., Heotta, K. and Tagaki, W., *Chem. Lett.*, 1982, No. 5, pp. 651–654.
37. Tamagaki, S., Suzuki, K., Okamota, H. and Tagaki, W., *Tetrahedron Lett*., 1983, Vol. 24, No. 44, pp. 4847–4850.
38. Heotta, K., Tamagaki, S., Suzuki, K. and Tagaki, W. *Chem. Lett.* 1981, No. 6, pp. 789–790.
39. Karakhanov, E.A., Narin, S.Yu., Filipov, T.Yu. and Dedov, A.G., *Thes. Rep. VI International Conference on Organic Synthesis*, Nauka, Moscow, 1986, p. 219. (in Russian).
40. Karakhanov, E.A., Narin, S.Yu., Filipov, T.Yu. and Dedov, A.G., *Dokl. AN SSSR*, 1987, Vol. 292, No. 6, pp. 1387–1391 (in Russian).
41. Shilov, A.E., *Redox Metalloenzymes and Their Models*, Pt. 2, Chernogolovka, Russia, 1982, pp. 3–19 (in Russian).
42. Hamilton, G.A., *Adv. Enzymol.*, 1962, Vol. 32, pp. 55–76.
43. Scheider, W., *Comment. Inorg. Chem*., 1984, Vol. 3, pp. 205–211.
44. Milas, N.A. and Sussman, S., *J. Am. Chem. Soc.*, Wiley, N.Y., 1936, Vol. 58, pp. 1302–1306.
45. Pfister, K., Sulliran, A.P., Weiland, I. and Tishler, M., *Ibid.*, 1961, Vol. 73, pp. 4955–4959.
46. Fizer, L. and Fizer, M., *A Reagent for Organic Synthesis*, Mir, Moscow, 1970, Vol. 2, p. 478 (in Russian).
47. Jean-Rierre Schirmann et Serge, *von Delavarenne Nouvean procede d'epoxidation des olefins parle peroxide d'hydrogene*. Demande de Brevet D'Invention N 76 35668, B.O.P.I.-Listen N 25 dn.
48. Sapunov, V.N. and Lebedev, N.N., *Zh. Org. Khim*. 1966, Vol. 2, No. 2, pp. 273–280 (in Russian).
49. Swern, D., *J. Am. Chem. Soc*., 1947, Vol. 69, pp. 1692–1695.
50. Holleman, A.F., *Rev. Trav. Chim.*, 1904, Vol. 23, pp. 169–172.
51. Arnold, R.T. and Lawson, R., *J. Org. Chem*., 1940, Vol. 5, pp. 250–256.
52. Holmes, R.R. and Bayer, R.P., *J. Am. Chem. Soc.*, 1964, Vol. 82, pp. 3454–3458.
53. Fiesev, L.F., *J. Biol. Chem.*, 1940, Vol. 133, pp. 391–395.
54. Smith, C.W. and Holm, R.T., *J. Org. Chem.*, 1957, Vol. 22, pp. 746–752.
55. Khorozova, E.G., Shchereb, G.I., Elerimova, N.I. and Bogdanovsky, G.A., *Thes. Rep. All-Union Conference on Catalytic Reactions*, Alma-Ata, 1978, p. 95 (in Russian).
56. Sychev, A.Ya., Travin, S.O., Duka, G.G. and Skuratov, Yu.I., *Catalytic Reactions and Protection of the Environment*, Kishinev, Shtinitsa, 1983, 271 pp. (in Russian).
57. Protopopov, E.V., Zueva, T.S. and Moshkovich, F.S., *Thes. Rep. IV International Symposium on Homogenous Catalysis*, Leningrad, 1984, Vol. 1, p. 159 (in Russian).
58. Tiginyants, Ya.D., Berdnikov, V.M. and Lozovan, V.P., *Ibid.*, p. 184 (in Russian).
59. Rudenko, A.P., *The Theory of Self-Development of Open Catalytic Systems*, Izd. MGU, Moscow, 1969, 276 pp. (in Russian).
60. Mamatov, Yu.I. and Rudenko, A.P., *Vestnik MGU*, *Ser. 2, Khimia*, 1975, Vol. 16, No. 2, pp. 96–100 (in Russian).
61. Mamatov, Yu.I. and Rudenko, A.P., *Ibid.*, 1977, Vol. 18, No. 4, pp. 451–455 (in Russian).
62. Pavlovskaya, T.E., *The Questions of Initiation and the Essence of Life*, Nauka, Moscow, 1973, pp. 38–42 (in Russian).
63. Strukul, G., In: *Catalytic Oxidation with Hydrogen Peroxide As Oxidant*, Ch. 6, Ed. G. Strukul, Kluwer, Dordrecht, 1992, p. 177.
64. Del Todesco Frisone, M., Giovanetti, R., Pinna, F. and Strukul, G., *Stud. Surf. Sci. Catal.*, 1991, Vol. 66, p. 405.
65. Del Todesco Frisone, M., Pinna, F. and Strukul, G., *Organometallics*, 1993, Vol. 12, p. 148.
66. Gusso, A., Baccin, C., Pinna F. and Strukul, G., *Organometallics*, 1994, Vol. 13, p. 3442.
67. Herrmann, W.A., Fischer, R.W. and Correid, J.D.G., *J. Mol. Catal.*, 1994, Vol. 94, p. 213.
68. Tollari, S., Vergani, D. and Porta, F., *J. Chem. Soc. Chem. Commun*., 1993, p. 442.
69. Maldotti, A., Amadelli, R., Varani, G., Tollari, S. and Porta, F., *Inogr. Chem*., 1994, Vol. 33, p. 2968.
70. Nemeth, L.T., Lewis, G., Rosin, R.R. and Ringwelski, A., *The 3rd World Congress on Oxidation Catalysis*, Abstract, Pt. 2, San Diego, CA, 1972.
71. Taube, H., *Oxygen: Proc. Symp. N.* Heart Assoc., Little Brown, Boston, MA, 1965, pp. 29–33.
72. Fridovich, I., *Adv. Enzymol.*, 1974, Vol. 41, pp. 35–56.

73. Czapski, G., *Ann. Rev. Phys. Chem.*, 1971, Vol. 22, pp. 171–179.
74. Neta, P. and Dorfman, L.M., *Adv. Chem. Ser.*, 1968, Vol. 81, pp. 222–240.
75. Borggaard, O.K., *Acta Chem. Scand.*, 1972, Vol. 26, pp. 3393–3397.
76. Beauchamp, C. and Fridovich, I., *J. Biol. Chem.*, 1970, Vol. 245, pp. 4641–4646.
77. Oshono, N., Chance, B., Sies, H. and Bucher, T., *Arch. Biochem. Biophys.*, 1973, Vol. 154, pp. 117–123.
78. Valenta, K.J., Bode, H., Vickery, A.L. *et al*., *J. Clin. Endoerinol. Metabol.*, 1973, Vol. 36, pp. 830–833.
79. Fielden, E.M., Reberts, P.B., Bray, R.C. and Rotili, O.G., *Biochem. Soc. Trans.*, 1973, Vol. 1, pp. 52–56.
80. Klug, D., Fridovich, I. and Rabani, J., *J. Am. Chem. Soc.*, 1973, Vol. 95, pp. 2786–2791.
81. Fridovich, I., *J. Biol. Chem.*, 1970, Vol. 245, pp. 4053–4057.
82. Pratt, G., *Methods and Achievements of Bioenergy Chemistry*, Mir, Moscow, 1978, pp. 132–252.
83. Nicholls, P. and Schonbaum, G.R., *The Enzymes*, 2nd edn, Vol. 8, Academic Press, NY, 1963, pp. 147–158.
84. Oshino, N., Oshino, R. and Chance, B., *Biochem. J.*, 1973, Vol. 131, pp. 555–559.
85. Roughton, F.W. and Chance, B., *Technique of Organic Chemistry*, Vol. 2, Eds S.L. Friss *et al*., NY, 1969.
86. George, P., *Oxidases and Related Redox Systems*, Wiley, NY, 1965, 136 pp.
87. Ricketts, C.R., Cos, J.S.G., Fitzmaurice, C. and Moss, G.F., *Nature*, 1965, Vol. 208, pp. 237–241.
88. Keilin, D. and Hartee, E.F., *Biochem. J.*, 1955, Vol. 60, pp. 310–316.
89. Chance, B., *Adv. Enzymol.*, 1951, Vol. 12, pp. 153–158.
90. Satterfield, C.N. and Stein, J.W., *Ind. Eng. Chem.*, 1957, Vol. 49, pp. 1173–1180.
91. Chance, B., Sies, H. and Boveris, A., *Physiol. Rev.*, 1979, Vol. 59, pp. 527–605.
92. Poltorak, O.M. and Chukhrai, E.S., *Vestnik MGU Ser. 2, Khimia*, 1971, Vol. 12, No. 6, pp. 656–660 (in Russian).
93. Jones, P. and Sugget, A., *Biochem. J.*, 1968, Vol. 110, pp. 621–627.
94. Veselova, M.N., Chukhrai, E.S. and Poltorak, O.M., *Vestnik MGU Ser. 2, Khimia*, 1970, Vol. 11, No. 1, pp. 14–18 (in Russian).
95. Bickar, D., Bonaventura, J. and Bonaventura, C., *Biochemistry*, 1982, Vol. 21, pp. 2661–2666.
96. Ori, I., *J. Biol. Chem.*, 1982, Vol. 257, pp. 9246–9248.
97. Lee, W.A., *Dr. Phylos. Thesis*, San Diego, CA, 1982.
98. Poulos, T.L. and Finzel, B.C., *Peptide and Protein Rew*, 1984, Vol. 4, pp. 115–171.
99. Poltorak, O.M., *Catalysis*, Izd. MGU, Moscow, 1987, pp. 7–38 (in Russian).
100. Fita, L. and Rossmann, M.G., *J. Mol. Biol.*, 1985, Vol. 185, pp. 21–37.
101. Poulos, T.L. and Kraunt, J., *J. Biol. Chem.*, 1980, Vol. 225, pp. 8199–8205.
102. Poulos, T.L., Freer, S.T., Alden, R.A. *et al*., *Ibid.*, Vol. 155, pp. 575–580.
103. Chance, B., *Ibid.*, 1950, Vol. 182, pp. 649–658.
104. Chance, B., *Ibid.*, 1952, Vol. 194, pp. 471–481.
105. Kremer, M.L., *J. Chem. Soc. Faraday Trans.*, Pt. 2, 1985, Vol. 81, pp. 91–104.
106. Sitter, A.J., Reczek, C.M. and Terner, J., *J. Biol. Chem.*, 1985, Vol. 260, pp. 7515–7522.
107. Terner, J., Sitter, A.J. and Reczek, C.M., *Biochim. Biophys. Acta*, 1985, Vol. 828, pp. 73–80.
108. Nagiev, T.M., *Vestnik MGU, Ser. 2, Khimia*, 1984, Vol. 25, No. 3, pp. 254–258 (in Russian).
109. *Iron Porphyrins*, Pt. 1, Eds A.B.P. Lever and H.R. Grey, Addison-Wesley, Reading, MA, 1983, p. 283.
110. Brown, S.B., Jones, P. and Sugget, A., *Trans. Faraday Soc.*, 1968, Vol. 64, pp. 986–990.
111. Deno, N.G., Peterson, H.J. and Saines, G.S., *Chem. Rev.*, 1960, Vol. 60, pp. 7–15.
112. Jarnagin, R.C. and Wang, J.H., *J. Am. Chem. Soc.*, 1958, Vol. 80, pp. 786–787.
113. Hager, L.P., Doubek, D.L., Silverstein, R.M. *et al*., *Ibid.*, 1972, Vol. 94, pp. 4364–4367.
114. Nagiev, T.M., *Vestnik MGU, Ser. 2, Khimia*, 1990, Vol. 31, No. 3, pp. 237–245 (in Russian).
115. Nagiev, T.M., *Vestnik MGU, Ser. 2, Khimia*, 1995, Vol. 36, No. 5, pp. 434–440 (in Russian).
116. Chance, B., *Arch. Biochem. Biophys.*, 1952, Vol. 41, pp. 416–422.

117. Chance, B., *J. Biol. Chem.*, 1943, Vol. 151, pp. 553–559.
118. Kremer, M.L., *Biochim. Biophys. Acta*, 1970, Vol. 198, pp. 157–165.
119. Oshino, N., Jamieson, D., Sugano, T. and Chance, B., *Biochem. J.*, 1975, Vol. 146, pp. 67–77.
120. Metelitsa, D.I., *Redox Metalloenzymes and Their Models*, Pt. 1, Chernogolovka, Russia, 1982, pp. 39–52 (in Russian).
121. Enikolopyan, N.S., Bogdanova, K.A., Karmilova, L.V. and Askarov, K.A., *Uspekhi Khimii*, 1985, Vol. 54, No. 3, pp. 369–395 (in Russian).
122. Gold, A., Ivey, W. and Bowen, M., *Chem. Commun.*, 1981, No. 6, p. 293–295.
123. Greighlon, D.J. and Sigman, D.S., *J. Am. Chem. Soc.*, 1971, Vol. 93, pp. 6314–6316.
124. Van Bergen, J.T. and Kellogg, R.M., *J. Am. Chem. Soc.*, 1977, Vol. 99, pp. 3882–3884.
125. Behr, J.P. and Lehn, J.M., *Chem. Commun.*, 1978, No. 3, pp. 143–146.
126. Hamilton, G.A., *Progress in Bioorganic Chemistry*, Vol. 1, Wiley Interscience, New York, 1971.
127. Jones, J.B. and Beck, J.F., Applications of biochemical systems in organic chemistry, In: *Techniques of Chemistry Series*, Pt. 1, Wiley, New York, 1976, pp. 107–401.
128. Prelog, V., Specification of the stereochemistry of some oxidoreductases by diamond lattice sections, *Pure Appl. Chem.*, 1964, Vol. 9, pp. 119–130.
129. Orf, H.W. and Dolphin, D., *Proc. Nat. Acad. Sci. USA*, 1974, Vol. 71, pp. 2646–2650.
130. Terina, D.M., Daly, J.W., Witkop, P., Zaltzman-Nirenberg, S. and Udenfriend, S., *Biochemistry*, 1969, Vol. 9, pp. 147–156.
131. Fox, J.L., Chemists attack complex organic mechanisms, *Chem. Eng. News*, 1978, May 22, pp. 28–30.

– 7 –

New Approaches to Simulation of Enzymatic Reactions: Mimetic Catalysis

The area between enzymatic and chemical catalyses, associated with simulation of biochemical processes by their basic parameters, is accepted as mimetic catalysis. The key aspect of the mimetic catalyst is diversity of enzyme and biomimetic function processes, which principally distinguishes the mimetic model from traditional full simulation. Based on the analysis of conformities and diversities of enzymatic and chemical catalysis, the general aspects of mimetic catalysis are discussed. An idealized model of the biomimetic catalyst and the exclusive role of the membrane in its structural organization are considered. The most important achievements in the branch of catalysis are shown, in particular, new approaches to synthesis and study of biomimetic catalase, peroxidase and monooxidases reactions.

It is suggested that the catalysis approach, originating from the simulation of biochemical processes, is called 'mimetic catalysis'.

Mimetic catalysis designs a real model (a mimic) which simulates objects and processes of enzymatic catalysis by their basic (but deficient) characteristics (selectivity, mildness of condition, active site action mechanism, etc.). Since only definite properties of the enzyme are simulated, it does not profess to a complete enzyme description, though optimal parameters by some properties may be approached. The mimetic model of enzyme helps in synthesizing suitable catalysts using inaccurate and sometimes ambiguous information.

The overwhelming majority of biomimetics operate in liquid. Their activity depends on the origin of solvents, reaction mixture and cell effects. Gas-phase oxidation processes are less dependent on these effects and in the first approximation can be considered as oxidation under quasi-ideal conditions. It goes without saying that enzymatic reactions do not proceed in gases. However, it is possible to simulate catalytic functions in the gas phase. This simplifies the decoding of the reaction mechanism, not complicated by factors accompanying the liquid-phase oxidation [1].

7.1 CRITERIA OF MIMETIC CATALYSIS BASED ON CONFORMITIES AND DIVERSITIES BETWEEN ENZYMATIC AND CHEMICAL CATALYSES

Undoubtedly, mimetic models of enzymes must conform to definite physicochemical features of the target enzyme. The specific feature of any biomimic is its relatively small size and simpler structure.

According to the definition by Dugat and Peeny [2]: 'simulation of enzymes is an attempt to reproduce at much simpler level some key parameter of the enzymatic function.'

One may agree with this definition, if the main task of the simulation is that it approaches as closely as possible the simulated object in physicochemical characteristics. In this case, of course, if corresponding models of every catalytic parameter are obtained, it is possible not only to estimate their relative importance, but by combining them, also to update the model structure in order to approach the efficiency of the simulated enzyme.

It is the author's opinion [3] that this means of creating 'miniature enzymes' is accessible to chemists, who are experts in synthesis. In this case, the mandatory requirement is the following: active catalytic groups of the biomimic must be oriented to conform to the geometry of the active site of the enzyme consisting of catalytic groups.

The study of biochemical processes by simulating their structural–functional features is called biomimetic chemistry in the literature [4].

To successfully resolve biomimetic tasks one must understand the mechanism of the biological object simulated, including enzymes. In this regard, the main approaches to associating the structure and functions of bioorganic molecules are formulated [5]. For this purpose, the following must be known: structure of the active site and enzyme–substrate complex, data on the substrate specificity of the enzyme and kinetics of various stages in the determination of the most probable highly active intermediates.

It is common knowledge that the protein part of the enzyme consists of functional groups participating in catalytic transformation of the substrate. They are imidazole fragment, aliphatic and aromatic hydroxide groups, carboxylic, sulfohydride and amino groups.

As noted [6], two fundamental requirements are imposed on bioorganic model development:

(a) The model must generally reproduce the enzymatic reaction mechanism.
(b) It must answer the question about the interrelation of enzymatic reaction and structural–functional organization of the enzyme.

It is naturally concluded [7] that, finally, all the information obtained with the help of the model must be compared with the behavior of the enzymatic system studied *in vivo* in order to achieve bioorganic models of systems existing in the nature. The difficulty of such an approach to the design of highly effective biomimics—the catalysts of chemical reactions—will be justified below.

Model systems frequently possess properties typical of more than one enzyme. This feature, typical of numerous models, allowed the formulation [2] of approaches to the development of effective enzyme models in the form of the following criteria:

1. Since biological mobility and specificity are based on non-covalent interactions, the model must possess a good (hydrophobic) fixation area.

Here the author may contemplate the fact that almost all enzymatic reactions are implemented in aqueous medium where, in the presence of the hydrophobic surrounding of the active site, water molecules can occupy the substrate place.

Apparently, it is sufficient for the model if water is slightly coordinated with the active site and, therefore, can be substituted by the substrate with higher coordinated properties.

The reach of hydrophobicity in the model can severely complicate its synthesis. This criterion makes sense in the case of the task of achieving as close a correspondence as possible between the model and the simulated enzyme. However, a more particular objective is often assigned for the synthesis of mimics. It consists of synthesizing an effective catalyst simulating a definite (useful) enzyme property. Therefore, it seems more desirable to replace hydrophobic tub synthesis by more accessible methods, developed in chemical catalysis, particularly in coordination and heterogeneous catalysis.

2. The model must provide for electrostatic and hydrogen bonding in order to fix the substrate properly.
3. Catalytic groups must be thoroughly selected and properly disposed in the model to provide for catalytic reaction run.
4. The model must have rigid structure and strictly correspond to substrate orientation and structure.

   In heterogeneous inorganic biomimics objectives (2)–(4) are resolved more easily than for organic mimics. Many acidic and basic sites on an inorganic carrier (matrix) form a situation in the biomimetic system when a definite quantity of these sites will display the required geometry for substrate-activated complex formation.

   This condition is met in the case of heterogeneous inorganic biomimics—the surface on which the adsorbed active site has a rigid structure, and catalytic activity of the surface always depends on the site catalytic domain correspondence to the substrate structure and orientation.
5. It is desirable to make the model compound water-soluble and catalytically active at physiological pH and temperature.

As indicated below, for heterogeneous inorganic models of enzymes this circumstance is of practically no importance, i.e. the model operates in a broad range of reaction mixture parameter variation. In some cases, high effectiveness is displayed even in the gas phase (at relatively high temperature).

Thus, if it is taken into consideration that the overwhelming majority of enzymes is adsorbed on cell membranes and sensationally execute the functions under these conditions, this situation is of importance for enzymes (due to their sensitivity to the medium) rather than for their models, especially inorganic biomimics.

It is suggested [5–9] that though such criteria are rather conditional, nevertheless, they allow the synthesis of an effective catalyst by correct matrix selection, which promotes the drawing together of the catalytic groups and substrate.

It is the author's opinion that the matrix does not actively participate in catalysis, but only brings together and strongly fixes the substrate and the catalytic group (or groups), and orients them properly in relation to one another.

With this reasoning, when speaking about non-participation of the matrix in catalysis, the author [5–9] allow principal discrepancy. As a rule, amino acid fragments of polypeptide

chain (protein) are always involved in the enzyme effect on the substrate as catalytic sites of the acidic–basic origin.

To put it another way, synchronously with the prosthetic group, acidic–basic active sites of the protein participate in the substrate conversion.

Therefore, geometrical adequacy of the model and the substrate active sites will mean an increase in specificity. Of course, this reasoning is of the fundamental importance for the design of biomimics.

To date, a great scope of computerized information on enzyme structure has been accumulated. This should stimulate organic chemists to create such highly structured molecular complexes as, for example, proteins and nucleic acids.

It would seem that the use of synthetic organic polymers as a matrix in biomimetic models would lead to the creation of effective catalysts. Although an affinity between natural and synthetic macromolecular systems with catalytic groups added to them is sometimes observed, nevertheless, they were found less effective.

In the simulation of enzymes attempts have been made to use steroid matrices and biomimetic reactions of polyene cyclization, comprehensively described in Ref. [10].

Similar to simulated enzymes, their biomimetic analogs frequently implement synchronous mechanism of the substrate transformation rather than the stage-by-stage one. Many metal ions enter to the composition of enzymes. As a rule, they form a coordination bond, preserve neutrality of charges and participate in catalytic processes.

In particular, metal ions in the metalloporphyrins under consideration (prosthetic groups) execute two functions: orientation (matrix) and concentration of accumulated nucleophile in a catalytic domain. In these enzymatic systems, they are superacid (Louis acids) catalytic factors.

The question about the substrate fixation site (matrix or catalytic domain?) is always debatable for biomimetic catalytic systems.

Because of its rigid three-dimensional structure, an enzyme forms highly active catalytic site. Short peptide oligomers possess a more mobile structure, but, nevertheless, are also catalytically active.

This property of organic ligands (peptides, in particular) and their oligomers, coordinated with metal ions, opens up good possibilities for the development of highly active catalytic systems. Hence, such systems can be well soluble in water and operate at biologically suitable pH.

The basic question of mimetic catalysis is the determination of physicochemical properties of enzymes to be simulated in the synthesized biomimic in accordance with the reaction modeled. Firstly, let us try to answer one of the key questions that arise in biomimic construction: how important is it to reach the enzymatic specificity in the synthesis of their analogs? To put it another way, should the dynamic (tertiary) structure of the enzyme responsible for the selectivity control mechanism be simulated by active site protection from competitive admixtures? This feature of the enzymes distinguishes them from usual catalysts.

Another difference associated with the first one is defined by the presence of a gap above the active site, which allows us to distinguish adsorption and catalytic sites in enzymes. The question of reacting molecule recognition by the enzyme also relates to specificity and selectivity. The author of ‘aromatic’ mechanism of the substrate recognition call it ‘aromatic targeting’ [11].

Shilov devoted his review [12] to the development of selective and non-waste processes. He discusses the questions of organized molecular system (or ensembles) construction. Note that in the case of usual catalysis, catalytic sites freely interact with substrate molecules. This process is characterized by the absence of complementary activity. This is the reason for the relatively low selectivity of catalytic reactions. However, from positions of applied catalysis, such a catalytic system possesses clear advantages:

1. It does not make the system excessively strict in relation to selectivity.
2. It allows the use of a single catalyst for analogous molecule transformation.
3. It functions at any concentrations of reagents.

Common catalytic systems are characterized by the presence of reagent molecules only, whereas the enzymatic system is multicomponent and possesses low concentrations of the substrates in water. The interaction between a substrate with an oxidant or a reducer is most often considered. This makes unnecessary simulation of the enzyme selectivity. However, free contact of reagent molecules with active sites preserves the possibility of various mechanism realizations which is the reason for decrease of the process selectivity. Apparently, a compromise should be found in resolving the question of selectivity in biomimics development in suggesting that, though complex gap mechanism is the effective method for distance and mutual orientation control of reactive groups in the enzyme, it may hardly be implemented in synthetic systems.

Implementation of the enzyme mechanism is the means of increasing selectivity of chemical catalysis, because in this case substrate is converted to product in one catalytic stage, bypassing the formation of substrate intermediates (mediators may be formed).

To date, the composition of active sites is known for many enzymes, the most probable action mechanisms are suggested, and comparison data exist on catalytic group properties in enzymes and free molecules in solutions. Note also that the chemical composition of catalytic active sites of enzymes is independent of the presence of any specific compounds. Moreover, the majority of them are the well-known compounds for homogeneous catalysis: histidine imidazole, carboxylic groups of aspartic and aminoglutaric acids, flavins, hemins, etc. However, as homogeneous catalysts, they possess rather moderate or even poor catalytic activity in appropriate reactions.

Thus, differences of enzymes from chemical catalysts are stipulated by the reasons, according to which catalytic groups of enzymes display properties untypical for their free state, and the enzymes themselves are much more effective than any homogeneous catalysts. The advantage of heterogeneous catalytic systems over homogeneous ones consists of the ability to simulate analogous catalytic sites of the protein part of enzymes by means of acidic–basic groups of the matrix (carrier), whereas homogeneous catalysts either have no such ability or display low effects induced by a solvent or injected additives. However, the absence of acidic–basic groups fixed in the volume decreases the catalytic effectiveness of the active site, because the optimal distance and aligning of reagent groups (both the catalyst and the substrate) can hardly be arranged for the active complex of homogeneous catalytic reaction. Here homogeneous and heterogeneous catalysts (biomimics) simulating definite functions of corresponded enzymes are discussed.

The application of a prosthetic group of simulated enzyme or its modified synthetic analog on the surface of heterogeneous acidic–basic carrier allows the simulation of acidic–basic sites of the protein. Such a system contains fixed forms of acidic and basic catalytic groups, which together with the applied complex can compose the active catalytic site of the synthesized biomimic. In this method of biomimic preparation positional relationship and alignment of catalytic groups can vary widely. Hence, some quantity of them may locate on the catalyst surface in positions close to optimal for the main reaction. Then selective conversion of the substrate will occur on the active site. It is the author's opinion that the reach of high selectivity requires implementation of the enzymatic mechanism in the substrate conversion, when all catalytic groups of the active site affect the substrate simultaneously and transform it to the final product. Therefore, the applied catalytic site of the biomimic must possess properties that can be displayed only in association with the acidic–basic catalytic groups, otherwise this site will be inactive in catalysis.

According to the composition, structure and the effect on substrate, it is suggested that the ensemble of catalytic groups, simulating the active site of the corresponding enzyme, is called the mimetic domain (a small area of the catalyst surface differing in physicochemical properties from neighboring zones). Note that the catalytic material of the biomimic requires great conservatism in order to provide stability of mimetic domain operation. However, stability may be reached only in the final time interval. Nevertheless, the biomimic is subject to the united effects of the reaction mixture. These effects induce its evolution which reduces the selectivity or activity of the catalyst in the main process. This circumstance should be taken into account in relation to both mimetic and general catalysis. For example, one accepts that for heterogeneous catalysis the reaction mixture positively affects the catalyst activity, i.e. qualitative and quantitative parameters of the process are improved. In this case, unitypical active sites reform and intensify in the course of the reaction (e.g. amplification takes place). Of the greatest importance for catalysis is separation of proton addition and detachment places by restructuring chemical bonds: splitting and bond formation in the active complex due to alternating multiplicity ± 1. Such a bond aggregate is called the bond redistribution chain (BRC) [13].

In homogeneous model systems, this mechanism is scarcely realized because of proton exchange simplicity between the donor and the acceptor. It proceeds without substrate and, therefore, the efficiency of the push–pull mechanism in solution is reduced. Moreover, both the donor and the acceptor of protons are usually located far from the places required for proton transfer in solutions. This hinders the required alignment of reacting molecules being achieved.

In principle, more or less stable BRC structures can be obtained in heterogeneous biomimics, especially when adsorption and catalytic sites are combined, i.e. active sites perform both functions: fixation and transformation of the substrate. To put it another way, the above enumerated restrictions typical of homogeneous catalysis are absent in heterogeneous mimic-substrate complexes, where acidic–basic sites are fixed in required points of the active site.

In fact, heterogeneous models (biomimics), where catalytic groups of the active site are not fixed so regularly as in enzymes, will possess part of the catalytic groups (due to their dispersion on the carrier surface) located in positions favorable for BRC formation. An important consequence follows: the heterogeneity of biomimics is a mandatory feature providing for catalytic group fixation.

7.2 BIOMIMETIC CATALYSTS (BIOMIMICS) FOR CATALASE, PEROXIDASE AND MONOOXYGENASE REACTIONS

Recently, many articles have been devoted to the synthesis and investigations of active site models of catalase, peroxidase and cytochrome P-450 enzymes. Based on structural modeling of the enzymes mentioned, the following ideas are mainly applied:

1. Catalytically functional acidic–basic and redox groups must possess advantageous geometry (disposition) structurally shaped similar to the active zone of the appropriate enzyme [14].
2. The structure of the activated complex must conform to a biochemical analog.
3. It must have structural components preventing adverse interactions of catalytic groups with other particles in the reaction mixture [15].

At the present time, there are many examples of super-structured hemes, highly stable in interactions with molecular oxygen at room temperature [16–19].

Progress in decoding the mechanism of cytochrome P-450, which catalyzes epoxidation and hydroxylation of various hydrocarbons, has stimulated the search for comparatively simple and effective iron porphyrin systems [20–24]. The reaction mechanism of monooxygenation can be illustrated by the following diagram:

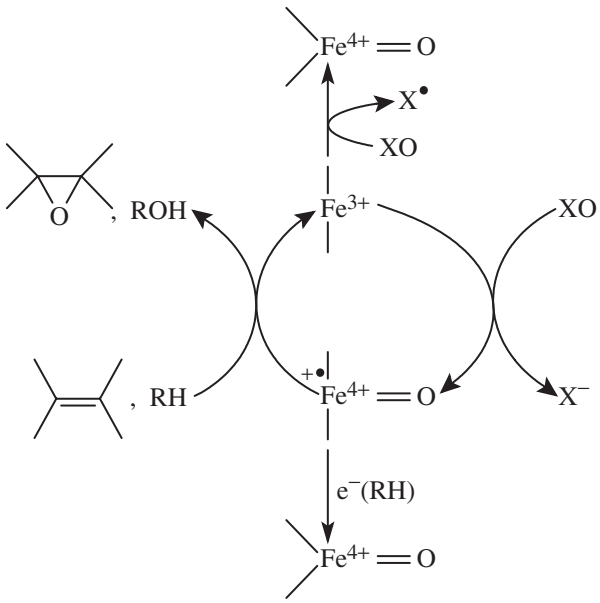

where:

$^{+\bullet}$Fe^{4+} = O is the two-electron oxidized hemin form;


$Fe^{4+}=O$ is the single-electron oxidized hemin form;

XO is the general oxidant shape; RH is the substrate.

The intermediate:

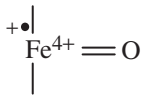

represents [25–27] the two-electron oxidized form of iron(III) porphyrin. Possessing an Fe=O bond and positive charge on the porphyrin ring, it essentially represents a cation-radical particle. Hence, the intermediate:

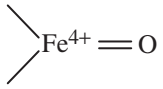

is the reduced form of the above compound. As observed from the diagram, the central place in the studies of monooxygenation belongs to the elementary stages of the intermediate synthesis mentioned.

For preparation of stable liquid biomimics [15], it should be noted that the substrate (S) must be much more sensitive to oxidation than the catalyst:

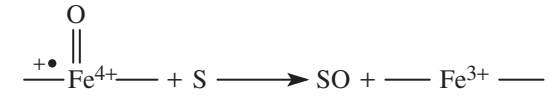
(7.1)

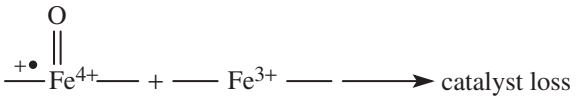
(7.2)

It should be noted that the mechanism of catalyst deactivation (7.2) is a particular case, because the immobilized biomimic is protected from this danger.

According to the diagram, intermediates are formed by both heterolytical dissociation of oxidants (hydroperoxides, peroxy acids and iodosylbenzenes):

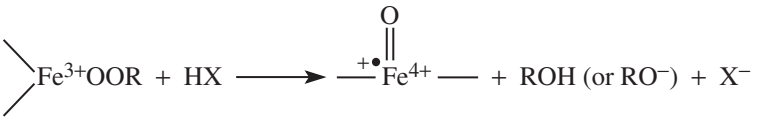
(7.3)

and homolytical process:

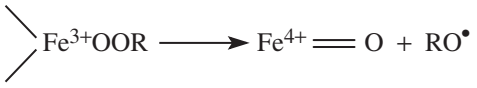
(7.4)

Note also that prior to dissociation hydroperoxide reversibly adds to iron [28].

It is noticed that when $Fe^{3+}OOR$ is formed in aprotic diluters (under strongly basic conditions) at low temperature, degradation products are synthesized by reaction (7.4) [29]. However, in hydroxide diluters oxidants dissociate heterolytically by reaction (7.3) [30, 31], which is proved by the formation of the following products: epoxides from alkenes and alcohols from ROOH.

It is justified [32, 33] that electron demand of Fe(III) decreased by injection of electron donor substituting groups to the porphyrin ring increases the oxidation reaction rate. Moreover, it is found that at ROOH degradation alcohols and water manifest properties typical of acid catalysis. Besides epoxides, *N*-alkyl hemins were detected [28], formed as a result of hemin *N*-alkylation by 1-alkenes according to the following reaction [34, 35]:

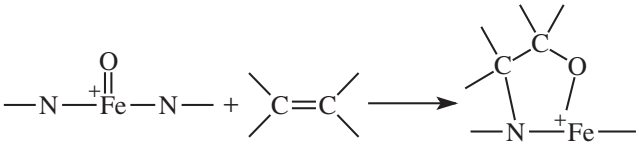

As indicated [36], intermediates in the above mechanism play different oxidant roles. For example, in the reaction ROOH + *meso*-tetraphenylporphyrin (Fe(III)(TPhPFe^{3+})) in the absence of imidazole ROOH dissociates homolytically in the reaction mixture to alkoxy radicals and TPhPFe^{3+}═O. These intermediates then interact with ROOH giving peroxy radicals (ROO$^{\bullet}$), which afterwards nonspecifically epoxides *cis*-stylbene. In the presence of imidazole TPhPFe^{3+} also degrades ROOH to alcohol and TPhP$^{+\bullet}$Fe^{4+}═O, which sterospecifically epoxides *cis*-stylbene. In both directions, the epoxide synthesis stage is illustrated by the following reactions:

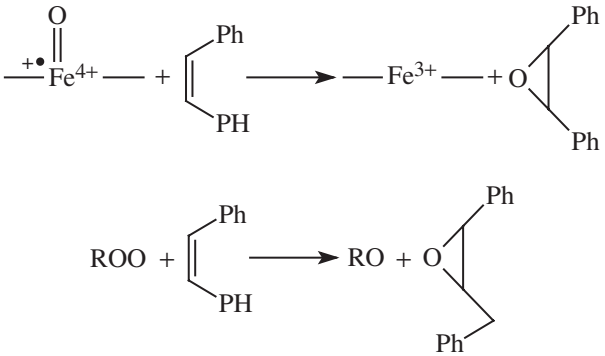

These studies show how sensitive heme catalytic systems are to environmental effects, which marks the manner of hemin catalytic activity control. For example, the above diagrams show that if the intermediate:

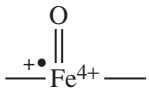

strips a single electron from the substrate, it indicates the peroxidase reaction. Electronegative substitution in iron porphyrins promotes a significant increase of epoxidation activity (norbornene, cyclohexene, etc.), but not allyl oxidation, and manifests high selectivity by *cis*-alkenes [37].

Intermediate formation mechanisms indicated in the monooxygenation diagram relate to the class of reactions in non-aqueous solvents. This is the reason why the hemin form of iron porphyrin is absent in it. Hence, hemin is present, of which the intermediate formation shaped as Hm^+O (where Hm is heme) is typical.

There are data [30] indicating the homolytical reaction:

$$\rangle Fe^{3+}OOR \rightarrow \rangle Fe^{3+} = O + RO^{\bullet} \tag{7.5}$$

for AlkylOOH (or H_2O_2)—PFe(III) system in a neutral aqueous medium or alcohol diluters not competing with heterolytical degradation in the presence of methanol. Intermediate $Fe^{3+}OOR$ was detected at low temperature [28]. Activation energy estimation for homolysis (7.5) gave $E < 10$ kcal/mol. Heterolytical ROOH and peroxy acid degradation in alcohol solution for acid medium formation is considered [28] as a sequence of the following elementary reactions:

$$\rangle Fe^{3+} + ROOH \leftrightarrows \rangle Fe^{3+}\overset{\overset{\displaystyle H}{|}}{O}OR \leftrightarrows Fe^{3+}OOR + H^+ \xrightarrow{BH^+} \rangle Fe^{4+} = O + ROH + B$$

Sometimes homolysis (7.5) is displayed under the same conditions in nonpolar solvents and in the absence of proton donors.

Using crystalline cytochrome-c peroxidase [38] and catalase [39], it is shown that intermediates are formed according to the general mechanism of acidic–basic catalysis:

$$B \rightarrow \underset{|}{\overset{|}{Fe^{3+}}} — O + \overset{\overset{\displaystyle Im}{|}}{O} — H \rightarrow B \rightarrow \underset{|}{\overset{|}{Fe^{4+}}} = O + H_2O \tag{7.6}$$

In a neutral solution, reaction (7.6) is reversible; the intermediate for H_2O_2 dissociation, ROOH and peroxy acid degradation is most likely ($Fe^{3+}OOH$) peroxy form [1]. In the absence of a buffer or a solvent, HmOOR complex degrades by the homolytical manner [38, 39].

Of special interest are monooxygenase reactions involving Mn(II) porphyrins and various oxygen donors, such as PhIO, ClO^- and H_2O_2 [40–42]. High yields of monooxygenase products indicate the good potential abilities of these biomimetic systems for preparative oxidation in organic chemistry. It is also shown [43] that manganese complexes with proximal

nitric ligand possess higher efficiency in dismutase and oxidation reactions than corresponding iron derivatives. The methods of stable porphyrin preparation by replacing pyrrole ring hydrogen atoms with electronegative groups and bridge hydrogen with phenyl radicals are described [44, 45]. This strategy allows the synthesis of highly stable perfluorinated iron(III) tetraphenylporphyrin, which catalyzes benzene hydroxylation to phenol with hydrogen peroxide [46]. The stereochemical mechanism of catalase complex formation is computer simulated [47]. It is shown that in the framework of optimal interatomic distances and spatial disposition of reactive particles, complexes can be formed by a mechanism designed in accordance with the BRC theory [48]. For catalase reaction, heterogenized iron protoporphyrin biomimic is suggested [49, 50].

The questions of activation and stabilization of such catalase biomimics were studied [46] using the example of heme-containing catalysts applied on various inorganic acidic–basic supports (Al_2O_3, $Al_2O_3 \cdot SiO_2$, SiO_2). The reported data show [51] the highest activity of $PPFe^{3+}$ OH/Al_2O_3. Aluminum oxide is apparently a better acidic–basic site of the catalase reaction.

The study of tyrosine-modified $PPFe^{3+}$ OH/Al_2O_3 catalyst indicated its extremely low peroxidase activity, whereas catalase activity of unmodified catalyst was 3 times higher [52].

Similar to enzymes, the biomimetic catalysts mentioned operate in liquids. Their activity depends on the diluter origin, reaction mixture pH and cell effects. Gas-phase oxidation is free from these effects, which can be considered in the first approximation as oxidation under quasi-ideal conditions [53]. The study of resonance Raman spectra [54] of $PPFe^{3+}$ OH/Al_2O_3 catalase mimic indicated its clear analogy with the fifth coordinate high-spin heme Fe^{3+} ion, bonded to tyrosine in catalase.

The use of organic hydroperoxides ROOH in the organic substrate oxidation process in the presence of chemical analogs of cytochrome P-450 has unambiguous advantages over molecular oxygen as the oxidant. However, the use of hydroperoxides causes additional problems which affect selectivity of the process. Among them the most important points are the following: porphyrins initiate ROOH chain radical degradation (besides autooxidation of the substrate) in various directions with formation of appropriate products. Hence, several active particles (free radicals) are usually formed. Then transforming in the presence of substrate they give side products [55, 56]. If organic hydroperoxides and peroxides are used as components of soft oxidation, the occurrence of abundant active particles in the homolytical degradation of ROOH and ROOR will become a serious obstacle for selective implementation of the process [57].

In previous chapters conjugated oxidation processes of various substrates with hydrogen peroxide were considered. It is shown that H_2O_2 is effective for the oxidation process intensification and for making it simpler. General signs of chemical conjugation mechanism at oxidation with hydrogen peroxide in gas and liquid are also formulated.

The most ambiguous point in the oxynoid hydroxylation mechanism with cytochrome P-450 is the question about the formation and origin of the oxygen intermediate Fe^{3+}—O, where the oxygen atom (possessing six electrons in the external cover) is coordinated with Fe^{3+}.

Apparently, electrophilic oxygen in the oxynoid complexes of catalase, peroxidase and cytochrome P-450 occurs at heterolytical degradation of the iron-peroxidase complex with proton consumption for formation of the water molecule.

All known hydroxiding catalysts, which simulate monooxygenases, are homogeneous compounds and participate in oxidation in liquids. In all cases, oxynoid complex is suggested to participate in the introduction of the oxygen atom to the C—H bond of the substrate.

Poltorak *et al*. [49, 50] developed a heterogenized version of metalloporphyrin catalyst for catalase reaction. The catalytic system suggested possesses an important advantage over other catalase, peroxidase and monooxygenase analogs: possessing acidic–basic properties, aluminum oxide in its structure is principally capable of simulating functions of the protein part of the above-mentioned enzymes. However, tests on the catalase activity of this catalyst were performed in liquid only, whereas it may also be tested in the gas phase for catalase, peroxidase and monooxygenase activity. It is suggested that the creation of heterogeneous catalysts—the analogs of redox enzymes, for use in selective oxidation in gases gives rise to development of new highly effective epoxidation, hydroxylation, dehydrogenation and soft oxidation processes with the full set of industrial advantages of gas-phase heterogeneous catalytic reactions.

A catalase mimic, similar to that described above, was synthesized on five forms of aluminum oxide: α-, β-, acidic, basic and neutral. The neutral and basic forms of Al_2O_3 were found to be the most active sorbents. Prior to adsorption, hemin was dissolved on an aqueous alcohol solution (pH 9), where it transformed to hematin, and then applied on Al_2O_3 forming catalase mimic $PPFe^{3+}OH/Al_2O_3$. According to this technique, iron protoporphyrin was applied on SiO_2.

Tests on synthesized biomimics indicated their high catalase activity (specifically for these applied on Al_2O_2) in H_2O_2 dissociation. It is the author's opinion that these studies gave essentially important results for explaining the Chance complex formation. It consists of bonding of Fe^{3+} ion in the sixth coordinate position in the biomimic to hydroxide anion. In this very form it manifests catalase activity.

If only hemin or adsorbent (Al_2O_3 or SiO_2) affects aqueous hydrogen peroxide, at room temperature catalase reaction is not practically observed.

The question of whether the sixth coordinate position of Fe^{3+} ion in native catalase is open (i.e. free) or is occupied by hydroxide is partly resolved in these studies. On all occasions, the possibility of Fe^{3+} hydroxo-form realization in the active site of catalase is confirmed, and this fact may not be neglected.

Thus, the debatable question about the state of iron ion at native catalase and the form of it responsible for enzyme activity requires further study.

Studies of resonance Raman spectra (Figure 7.1) of catalase $PPFe^{3+}OH/Al_2O_3$ give the following frequencies: $\nu_4 = 1372\,cm^{-1}$; $\nu_3 = 1491\,cm^{-1}$; $\nu_2 = 1574\,cm^{-1}$; $\nu_{37} = 1593\,cm^{-1}$; $\nu_{10} = 1631\,cm^{-1}$, typical of iron protoporphyrin catalase [58]. It is also shown that high-spin heme Fe^{3+} ion locates in the fifth coordinate position. Frequency ν_4 decrease to $1361\,cm^{-1}$ at the complex reduction testifies to involving iron ion π-donor axial ligand, most likely, Fe^{3+}—O—Al. Thus, a clearly indicated analogy with the fifth coordinate high-spin heme Fe^{3+} ion, bound to tyrosine in catalase, is determined.

It is shown that with the model system [38, 59] heme iron reaction with hydrogen peroxide is promoted by acidic catalytic sites, which are replaced by distal amino acid group bound to heme [60]. Here experimentally observed two-electron oxidation substrate in one stage and corresponded hydride-ion transfer is confirmed [61, 62]. In the example of catalase reaction the transfer mechanism of two electrons simultaneously was discussed above

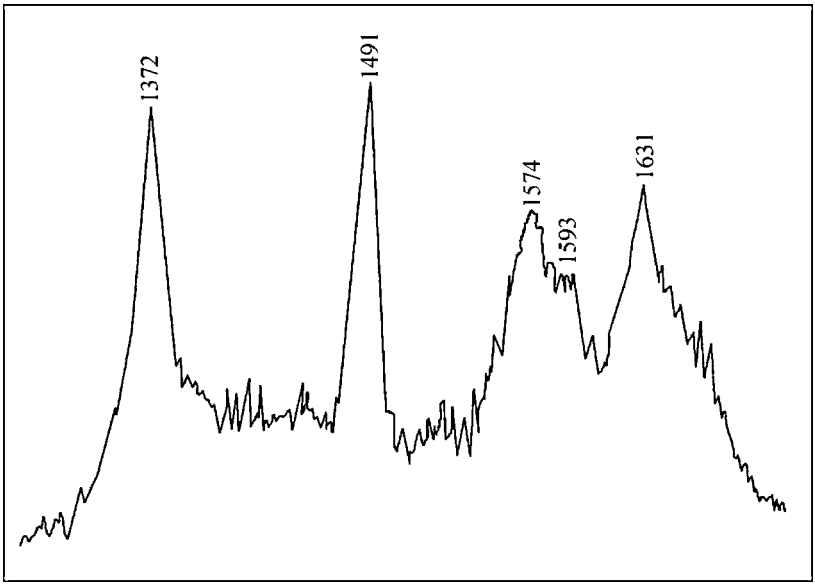

Figure 7.1 Resonance Raman spectrum of $PPFE^{3+}$ OH/Al_2O_3.

[63]. It seems plausible that amphoteric aluminum oxide plays the role of catalase amino acid fragments: the acidic–basic sites.

Slightly different models of catalase and H_2O_2 and ROOH disproportionation are discussed by Traylor and Xu [64]. Based on an analysis of the literature and his own data, he concludes that the main stages of model catalase reactions are the following:

$$\rangle Fe^+ + H_2O_2 \rightarrow \rangle Fe^+ = O + H_2O$$
$$\rangle Fe^+ = O + H_2O_2 \rightarrow HOO^\bullet + \rangle Fe^+ — OH$$
$$[\rangle Fe^+ \, OH \cdot OOH]_{cell} \rightarrow \rangle Fe^+ — OH_2 + O_2$$
$$[\rangle Fe^+ \, OH \cdot OO — H \ldots B]_{cell} \xrightarrow{e^-, \text{transfer}} \rangle Fe - OH + O_2 + BH^+$$

where B is the base. The weakest points in the Traylor mechanism are the absence of a deeper analogy with distal acidic–basic sites of catalase and the suggestion of $HOO^\bullet$ free radical formation during the catalase reaction.

Aqueous alcohol iron protoporphyrin solutions with pH $>$ 10 (14 in the limit), required for preventing their interaction with one another, are most frequently used in the synthesis and reactions with biomimics. On the contrary, H_2O_2 dissociation was implemented in the presence of 5,10,15,20-tetrakis-(2,6-dimethyl-3-sulfonatophenyl)porphynato-$Fe^{3+} \cdot H_2O$ $[(P)Fe^{3+}(H_2O)]$ in a pH range of between 1 and 12 [65]. This porphyrin is easily soluble in water and does not form dimeric and polymeric associates. Of interest are transition states shown in Figure 7.2. It is the author's opinion that the mechanism with heterolytical O—O bond break is the most preferable.

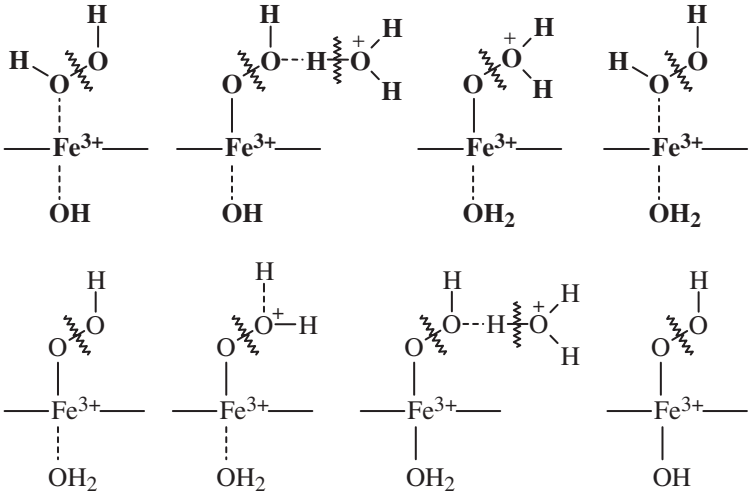

Figure 7.2 Possible transition state structures in PFe^{3+}—H_2O_2 system.

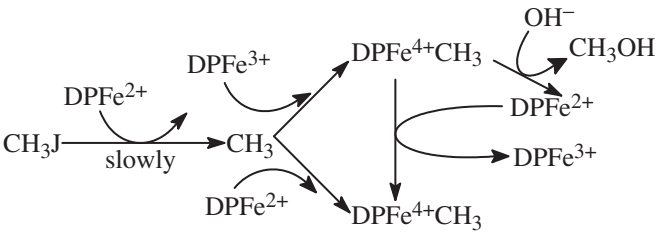

Figure 7.3 Methyl radical reactions with iron porphyrins.

Among the works devoted to cytochrome P-450 modeling, the article by Cook *et al.* [66] should be mentioned. It is indicated that the series of Mn- and Fe-porphyrins with sterically protected 'tubs' are selective catalysts of alkane hydroxylation. In the case where iodosylbenzene is used as the oxidant, quite high regioselectivity of alkane hydroxylation by the lower shielded methyl group is observed. The process is performed with sterically hindered catalyst—Mn^{3+} 5,10,15,20-tetra-2,4,6-triphenylporphyrin acetate. For Fe derivatives, slightly lower selectivity was observed. The article by Karasevich *et al.* [67] should also be mentioned, in which the authors suggest a catalytic system of O_2 activation. This promotes the simulation of monooxygenase reaction of alkane oxidation in the presence of cytochrome P-450.

Of definite interest are reactions of iron porphyrins containing methyl radicals, because the question is in the mechanism of the toxic impact of the haloalkanes on living organisms (Figure 7.3) [68]. They are formed by the following reaction:

$$DPFe^{2+} + CH_3J \rightarrow DPFe^{4+}CH_3 + J^-$$

where DP is deuteroporphyrin.

These reactions are useful as models for interpretation of the organic radical effect on metalloporphyrin systems.

Superoxide dismutase (SOD) mimic, synthesized from ferrioxamine B and Mn^{4+}, which catalyzes $O_2^{\bullet}$ is of special interest. Hence, the activity of this compound equals about 0.1% of SOD activity (calculated per Mn content) [69].

A significant result was obtained in the study of manganese porphyrin behavior in aqueous solutions [70]. Manganese porphyrins ($Mn^{3+}P$) in aqueous alkaline solutions are easily oxidized to corresponded $Mn^{4+}P$, which, in their turn, are able to catalyze H_2O_2 synthesis in accordance with the following reaction:

$$Mn^{4+}P + 2H_2O \rightarrow Mn^{3+}P + H_2O_2 + 2H^+$$

The results from the publications mentioned are of interest because they can help in the creation of effective catalytic systems containing porphyrins, which combine functions typical of multienzyme systems. The task in hand is the possible synthesis of bifunctional catalysts based on metalloporphyrin systems, when with the help of manganese porphyrins, for example, or SOD mimic, hydrogen peroxide is accumulated in the system. Afterwards, the accumulated hydrogen peroxide is used in oxidation reactions of various substrates with iron porphyrin components of the catalyst.

In this regard, studies carried out by the Du Pont Company (USA), headed by Tolman [71] are of high scientific value. In these studies inorganic mimics of enzymes were derived from iron-zeolite structures for selective and partial oxidation of some hydrocarbons under soft conditions, including high selective transformations of end methyl groups of linear hydrocarbons to CH_2OH groups.

Primarily synthesized catalysts, which contain iron phthalocyanine on zeolites X, possessed a low catalytic effect. They were followed by a series of highly selective oxidation catalysts containing iron ions without organic ligand in narrow zeolite gaps with channels 5 Å in diameter [72]. This catalyst was also added to with Pd(0), necessary for oxygen fixation in the presence of a reducing co-factor—molecular hydrogen. Tolman suggests that the Pd(0) catalyzes the reaction between oxygen and hydrogen, in which hydrogen peroxide is synthesized. Then it reacts with iron, forming a reactive intermediate oxidation product Fe═O, required for hydroxylation of the end methyl group of *n*-octane at 25 °C.

Romanovsky and Zakharov [73] believe that, being the unique system for arranging the interrelations of the 'guest-host' type, zeolites promote synthesis of unusual catalysts, in which molecules—'guests' are frequently presented by transition metal complexes with organic ligands, disposed inside zeolite structures and impart them with an affinity to enzymes.

Enzyme mimics have not yet been applied in practice, but they are catalytic systems with interesting prospects from both theoretical and practical points of view.

The production of various half-finished products of petrochemical synthesis and liquid fuels from natural gas is the most important objective connected with the crude oil economy and the creation of highly effective chemical engineering processes. In this connection, investigations performed by the Sandra National Laboratory (USA) are of special interest. This company designs enzyme mimics for catalytic activation of low-molecular gaseous alkanes in liquid fuel production [74]. Two directions of their activity should be outlined:

1. The simulation of active site structures of enzymes responsible for one-carbon substrate transformation in the organism.
2. The search for possibilities for using the unlimited resources of CO_2 in the production of gas fuels.

Another significant program implemented by the Sandra National Laboratory is methane conversion to methanol with the use of metalloporphyrin catalysts. All investigations are computerized and the synthesis of catalysts is computer designed and controlled. Structural studies of biological catalysts promoting determination of important characteristics of active sites, responsible for catalysis and encourage the general investigations.

Note that porphyrin-containing catalytic systems possess a valuable property—high activity in long-chain alkane oxidation.

Experimental studies detecting monooxygenase activity of $PPFe^{3+}OH/Al_2O_3$ catalyst in a C_3H_6—H_2O_2—H_2O system are carried out in the gas phase in flow integral reactor (plug flow), the design of which provides for unionized H_2O_2 injection directly to the reaction zone [75]. Analysis of propylene oxidation with hydrogen peroxide in the absence of catalyst at 150–250 °C indicated an almost complete absence of any substrate transformations at the contact time of 1–10 s which conforms to alternative data [57].

Figure 7.4 shows the temperature dependence of the yield of propylene catalytic oxidation with hydrogen peroxide. As follows, besides propylene oxide, its isomers (acetone, propionic aldehyde and allyl alcohol) are synthesized in the process. Neither propylene degradation products nor CO and CO_2 were detected, i.e. the process displays almost 100% selectivity per monooxygenation products. As indicated in Figure 7.4, the propylene oxide accumulation curve has a maximum. The highest is observed at $T = 160$ °C. Temperature increase to 220 °C noticeably reduces propylene oxide yield, whereas propylene isomer synthesis obeys different regularities. For example, propionic aldehyde yield sharply increases with temperature [76]. At 250–260 °C in the presence of aluminum oxide, the degree of

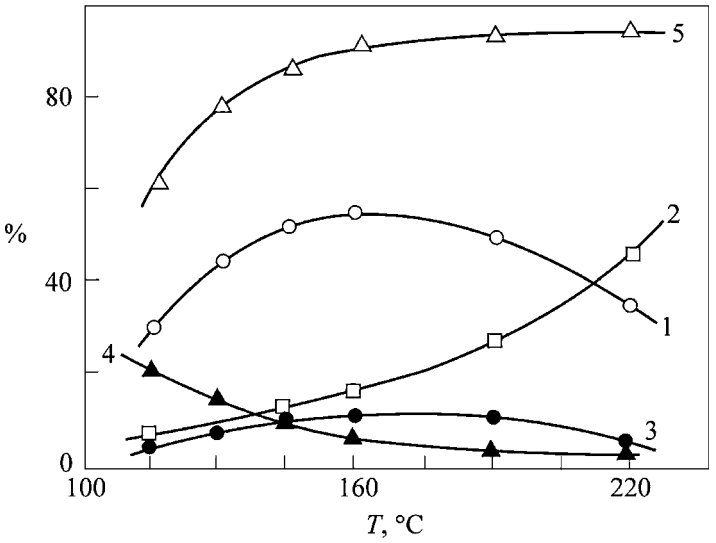

Figure 7.4 Temperature dependence of propylene oxidation product yield. C_3H_6:20% H_2O_2 = 1:1; $\nu_{C_3H_6} = 800$ ml/h; $\tau = 1.86$ s (1: propylene oxide; 2: propionic aldehyde; 3: allyl alcohol; 4: acetone and 5: total propylene conversion).

propylene oxide conversion to propionic aldehyde is higher, accompanied by synthesis of acetone traces. Hence it appears that a temperature increase above 160 °C most likely intensifies the intramolecular regrouping of propylene oxide on the catalytic matrix.

In this context, the data in Figure 7.5 showing yields of monooxygenase processes on the contact time are of interest. Long contact times (3 s or longer) cause an increase in the accumulation rate of propionic aldehyde and, simultaneously, abruptly decrease the rate of allyl alcohol synthesis, whereas propylene oxide and acetone yields pass their maxima. These results confirm that, besides temperature, the isomerization rate of propylene oxide strictly depends on the time of reaction mixture exposure in the flow reactor. Current observations are confirmed by analogous results [76], according to which at long contact times the rate of propionic aldehyde synthesis increases and the rate of allyl alcohol formation decreases. At optimal temperature (160 °C) in the contact time interval under consideration propylene conversion reaches 85–90% or higher.

The study of the substrate:reagent ratio (Figure 7.6) on the synthesis rate of propylene oxide promoted determination of optimal molar ratio C_3H_6:H_2O_2 = 1:1. As combined with the propylene conversion level exceeding 90%, this indicates the stoichiometric type of interaction between them. This circumstance confirms substrate oxidation with hydrogen peroxide by the heterolytic mechanism.

Figure 7.7 shows the dependence of monooxygenation product yields on aqueous hydrogen peroxide concentration. As indicated, 20% hydrogen peroxide in the best way of promoting propylene oxide formation, whereas higher concentrations lead to sharp increase of propionic aldehyde synthesis rate. Therefore, high sensitivity of $PPFe^{3+}OH/Al_2O_3$ catalytic activity to the reaction mixture composition is typical of enzymatic catalysis. The kinetic regularities described above allow consideration of the oxidation mechanism in the context of modern ideas about the mechanism of enzymatic analysis.

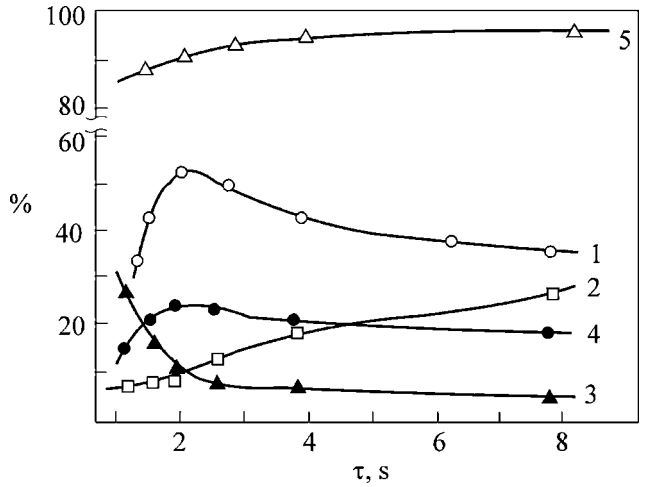

Figure 7.5 The dependence of propylene oxidation product yields on the contact time. T = 160 °C; C_3H_6:20% H_2O_2 = 1:1 (1: propylene oxide; 2: propionic aldehyde; 3: allyl alcohol; 4: acetone and 5: total propylene conversion).

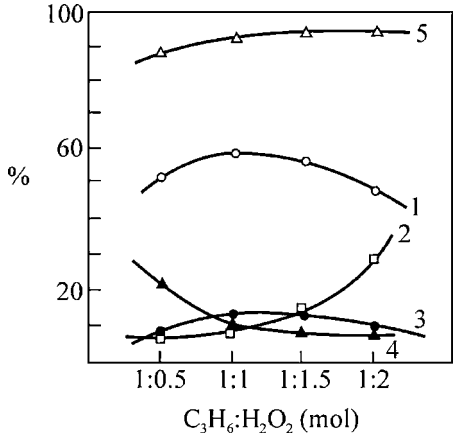

Figure 7.6 The dependence of propylene oxidation product yields on molar ratio C_3H_6:H_2O_2. T = 160 °C; 20% H_2O_2; $\nu_{C_3H_6}$ = 800 ml/h; τ = 1.86 s (1: propylene oxide; 2: propionic aldehyde; 3: allyl alcohol; 4: acetone and 5: total propylene conversion).

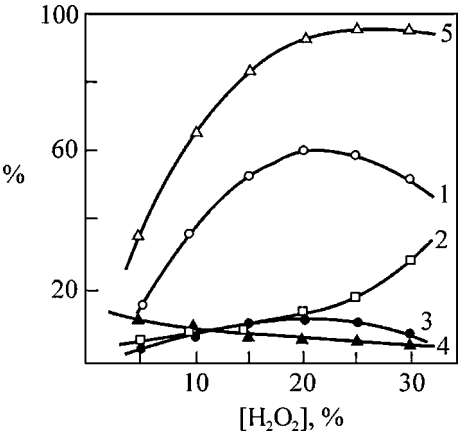

Figure 7.7 The dependence of propylene oxidation product yields on hydrogen peroxide concentration. T = 160 °C; C_3H_6:20% H_2O_2 = 1:1; $\nu_{C_3H_6}$ = 800 ml/h; τ = 1.86 s (1: propylene oxide; 2: propionic aldehyde; 3: allyl alcohol; 4: acetone and 5: total propylene conversion).

Figure 7.8 shows the principles of $PPFe^{3+}OH/Al_2O_3 \cdot H_2O_2$ complex formation in accordance with the BRC theory for catalase reaction [77–79]. In these works, Al_2O_3 is used as the matrix of the acidic–basic origin.

The complex $PPFe^{3+}OOH/Al_2O_3$ formed resembles the Chance complex $PPFe^{3+}$ OOH. The H_2O_2 substrate is heterolytically added to the metallic site so that the formal oxidation degree or coordination number of metal does not generally change. This process can be considered as the substitution of one anionic ligand by another.

According to these ideas, as a result of addition to Fe^{3+} (ligand OH^- replacement by HO_2^-) H_2O_2 forms activated intermediate $PPFe^{3+}$ OOH, which interacting with external substrate

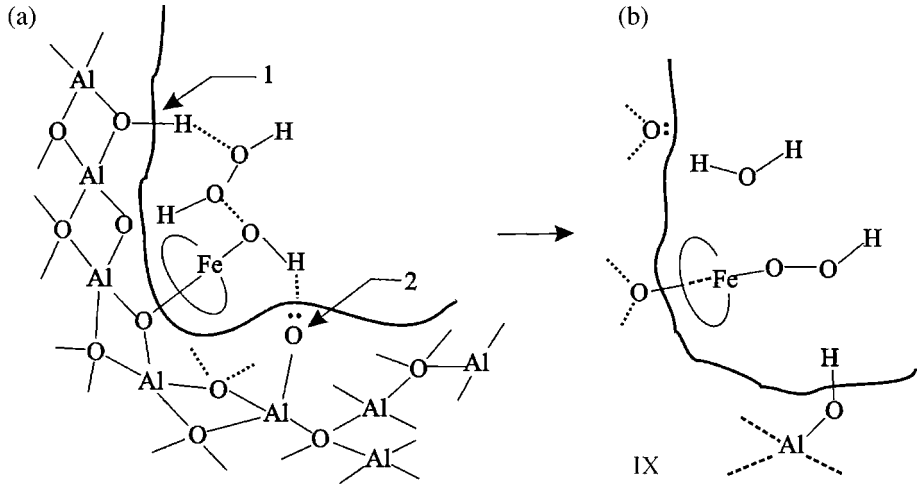

Figure 7.8 The formation mechanism of complex IX. (a) Active complex with Al_2O_3 acidic–basic sites and (b) active intermediate – complex IX (1: acidic site and 2: basic site), points-forming bonds, and continuous lines breaking bonds.

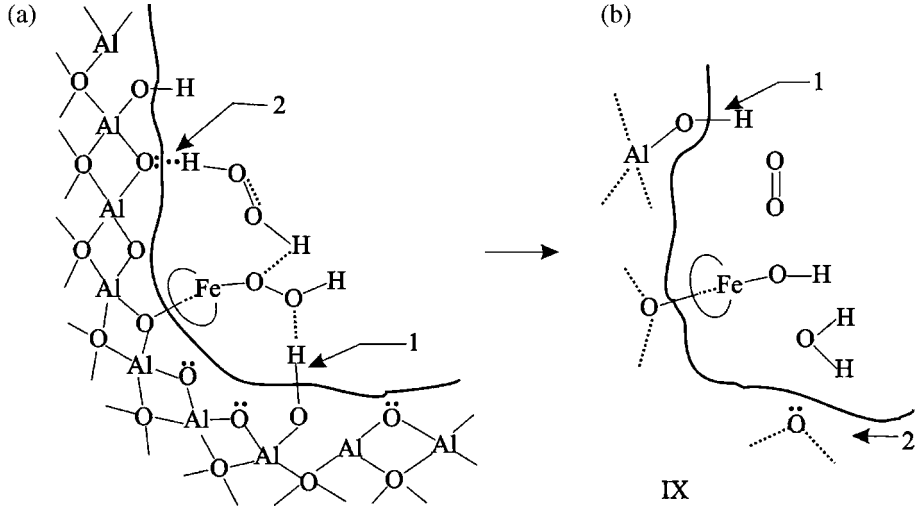

Figure 7.9 The mechanism of reaction product formation. (a) Complex IX formation with the second H_2O_2 molecule and (b) H_2O and O_2 formation, and catalyst regeneration (1: acidic site and 2: basic site).

(H_2O_2 or propylene) on Al_2O_3 carrier at the assistance of acidic–basic groups, forms stable products of the catalytic cycle. Later on, these products are detached from the catalyst (Figure 7.9). This is graphically shown in Figure 7.23, where the mechanism of allyl alcohol formation in propylene monooxygenation with hydrogen peroxide is considered in the framework of linear BRC. By analogy with cytochrome P-450, propylene is bound to the matrix. Figure 7.10 shows how H_2O_2 and, probably, ROOH perform both oxidant and reducer

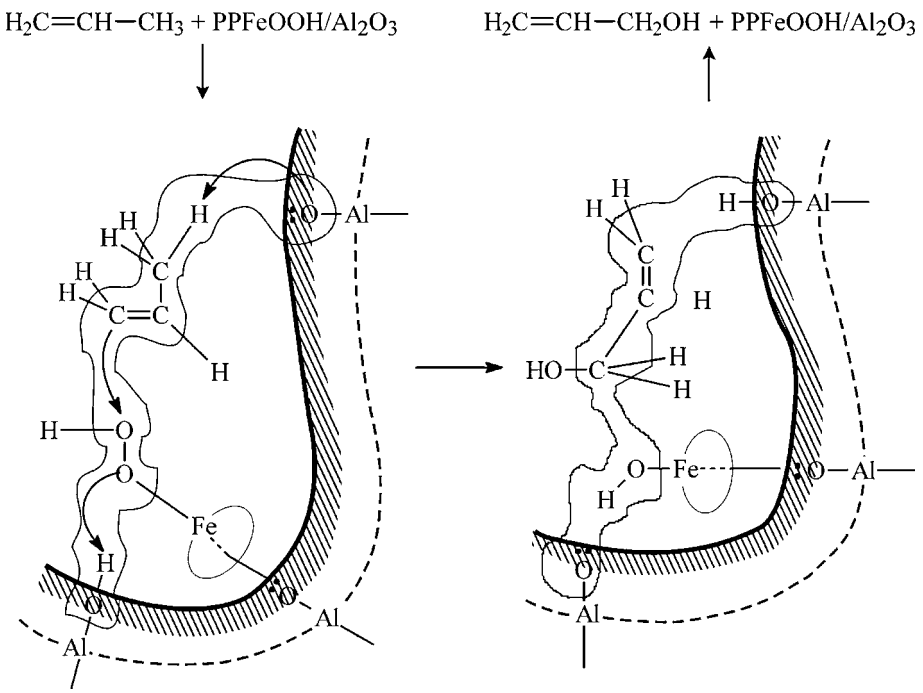

Figure 7.10 The mechanism of allyl alcohol synthesis in propylene oxidation with hydrogen peroxide, in the presence of $PPFe^{3+}OH/Al_2O_3$.

functions in monooxygenation processes. Obviously, H_2O_2 and ROOH possess dual reactivity and can play the roles of electron donors and acceptors with respect to the substrate type. It is probable that the efficiency of the mechanism shown in Figures 7.8 and 7.10 is based on their amphoteric property.

Hydroxide proton from hematin Fe(III)OH group is transferred to the Lewis basic site (B) by the first elementary stage (refer to Figure 7.8). This is accompanied by O—H bond break and electron transfer to oxygen atom, etc. At the second stage (Figure 7.9) proton bound to B is transferred to oxygen, which is accompanied by O—O bond break, etc. The sequences of electron and proton transfers to BRC are implemented simultaneously without high energy loss.

The monooxygenation mechanism depicted in Figure 7.10 consists of oxygen atom transfer from hydrogen peroxide to the C_3H_6 molecule by adding OH group to the latter. Hence, proton is simultaneously transferred from the substrate to the matrix. Thus, the oxynoid mechanism of monooxygenation is not met here. In this case, the hydrogen atom of the hydroxide radical in the allyl alcohol molecule belongs to hydrogen peroxide, which oxidizes C_3H_6. By the end of transformation at the second stage (Figure 7.10) the catalyst ($PPFe^{3+}OH$) is regenerated and, therefore, the full catalytic cycle is complete. The number of such cycles per mole of $PPFe^{3+}OH$ under optimal conditions equals 2000 per hour, approximately.

Figure 7.11 presents the mechanism of propylene oxide synthesis by allyl alcohol isomerization. This assumption correlates well with experimental data: the kinetic curve shape

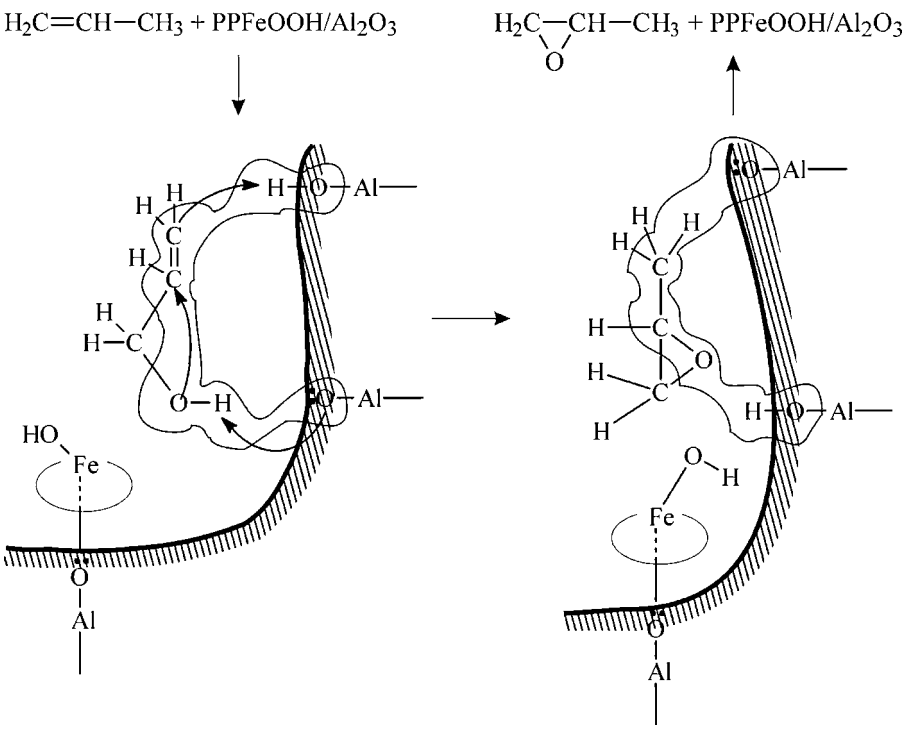

Figure 7.11 The mechanism of propylene oxide formation by propylene oxidation with hydrogen peroxide on $PPFe^{3+}OH/Al_2O_3$ catalyst.

indicates propylene oxide yield with the rate of allyl alcohol synthesis (Figure 7.12). In fact, formation of propylene oxide requires longer contact times than allyl alcohol (2 times longer or more), i.e. alcohol must be formed first, which then isomerizes on Al_2O_2 matrix of the acidic–basic type. This is confirmed by high isomerization catalytic activity of Al_2O_3.

Propylene oxidation on a $PPFe^{3+}OH/Al_2O_3$ catalyst corresponds to the case of heterogeneous catalysis, when catalyst forms a unitypical activated complex for substrate transformation in several parallel directions. Hence, the composition of the reaction products depends on the relative reaction rate, time of contact between the substrate and the catalyst, and temperature.

In the formation of propylene oxide via the stage of allyl alcohol release to the free volume and interaction with the catalyst, isomerization is of low probability because of unfavorable change in the free energy:

$$CH_2{=}CH-CH_2OH \longrightarrow CH_3-\underset{\diagdown\,O\,\diagup}{CH}-CH_2$$

$$\Delta G^0_{298} = 495\,\text{kJ/mol}$$

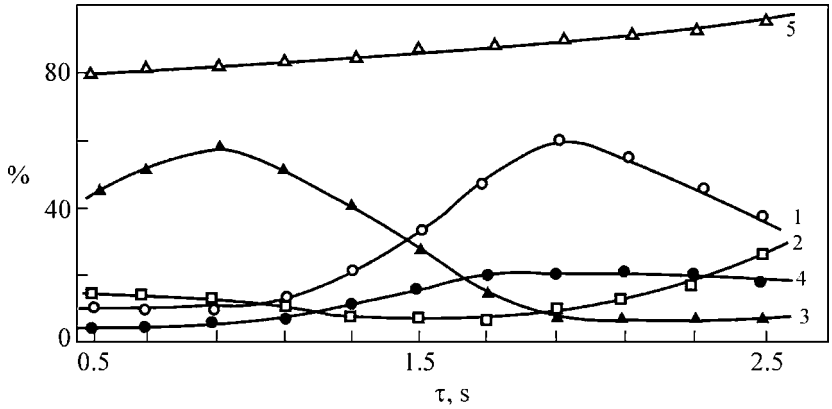

Figure 7.12 Dependencies of allyl alcohol and propylene oxide yields on the contact time on $PPFe^{3+}OH/Al_2O_3$ catalyst. T = 160 °C; C_3H_6:20% H_2O_2 = 1:1 (1: propylene oxide; 2: propionic aldehyde; 3: allyl alcohol; 4: acetone and 5: total propylene conversion).

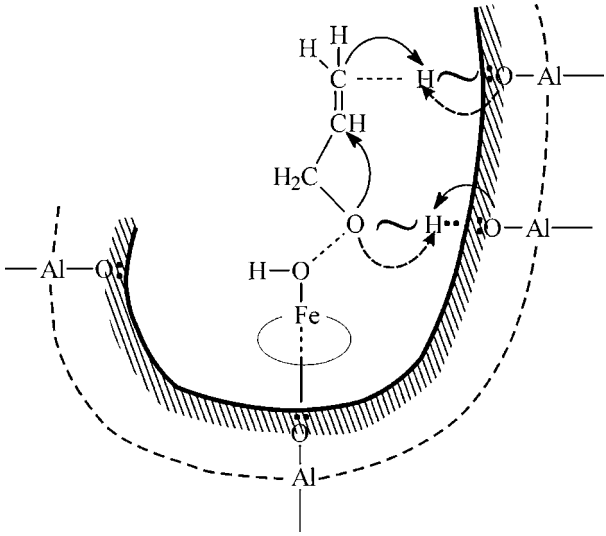

Figure 7.13 The mechanism of intermediate $C_3H_6Fe^{3+}PPOH/Al_2O_3$ transformation. Continuous arrows: propylene oxide synthesis and dashed arrows: allyl alcohol synthesis.

Therefore, this means of propylene oxide is eliminated, and another mechanism (Figure 7.13) is suggested. According to this new mechanism, allyl alcohol and propylene oxide are formed with the general intermediate $C_3H_6Fe^{3+}PPOH/Al_2O_3$, further transformation of which depends on the contact time between the substrate and the catalyst: at short time (Figure 7.12) allyl alcohol is synthesized, whereas at a longer time propylene oxide is obtained.

Propionic aldehyde and acetone formation can be represented by the two mechanisms shown in Figures 7.14 and 7.15. As follows from these mechanisms of the catalytic act, with

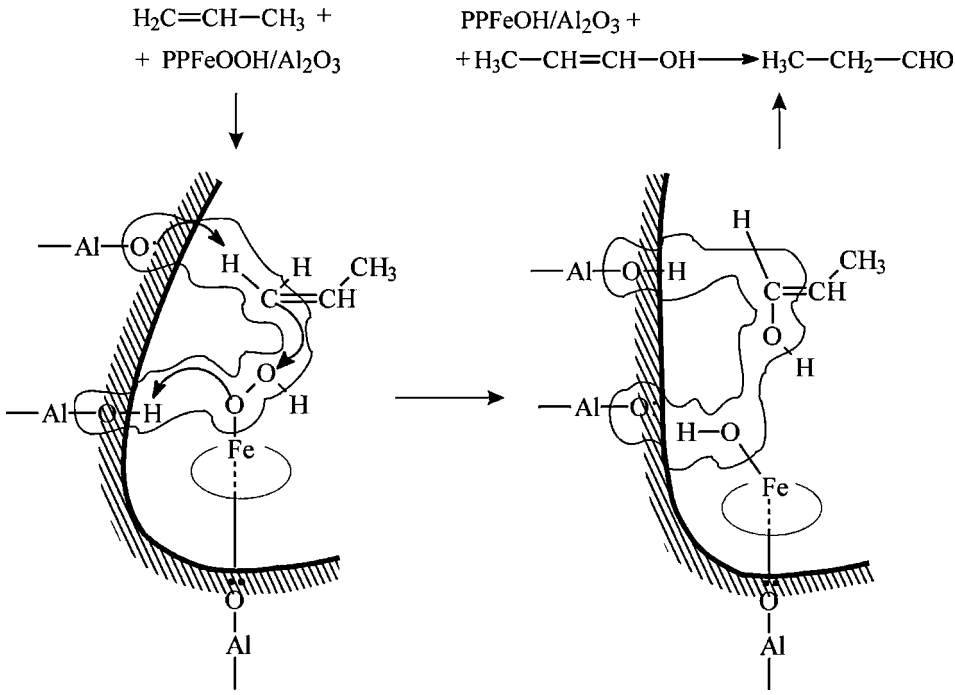

Figure 7.14 The mechanism of propionic aldehyde synthesis at propylene oxidation with hydrogen peroxide on $PPFe^{3+}OH/Al_2O_3$ catalyst.

respect to carbon atom of the propylene molecule (end at the double bond or central one) with which OOH ligand interacts, primarily, the enol form of corresponded final products is synthesized. Then under normal process conditions, it is converted to propionic aldehyde or acetone.

It is common knowledge that in the presence of iron porphyrin catalysts C_3H_6 oxidized by hydroperoxides and peroxy acids mostly produces allyl oxidation products. On the other hand, in the case of hydrogen peroxide, iron porphyrin catalyst is active on aluminum oxide in the epoxidation process. Apparently, $PPFe^{3+}OH/Al_2O_3$ promotes heterolytical dissociation of H_2O_2 with Fe—OOH complex formation, whereas iron porphyrins preferably catalyze homolytical degradation of organic peroxides. Therefore, peroxide oxygen transfer from $PPFe^{3+}$ OOH/Al_2O_3 to the substrate will differ from that with PM—ROOH [80]. As suggested for liquid-phase olefin oxidation in the presence of metalloporphyrins and ROOH, it is not fixed on the metal ion of the catalytic site. Of course, in this case olefin is not activated. Currently being the acidic–basic catalyst, aluminum oxide promotes olefin adsorption and activation.

Essentially, $PPFe^{3+}OH/Al_2O_3$—H_2O_2—H_2O—olefin is the two-substrate system with two active reaction directions:

$$PPFe^{3+}OH/Al_2O_3 + H_2O_2 \xrightarrow{\text{fast}} PPFe^{3+}OOH/Al_2O_3 + H_2O \rightarrow \xrightarrow{H_2O_2} PPFe^{3+}OH/Al_2O_3 + O_2 \quad (7.7)$$

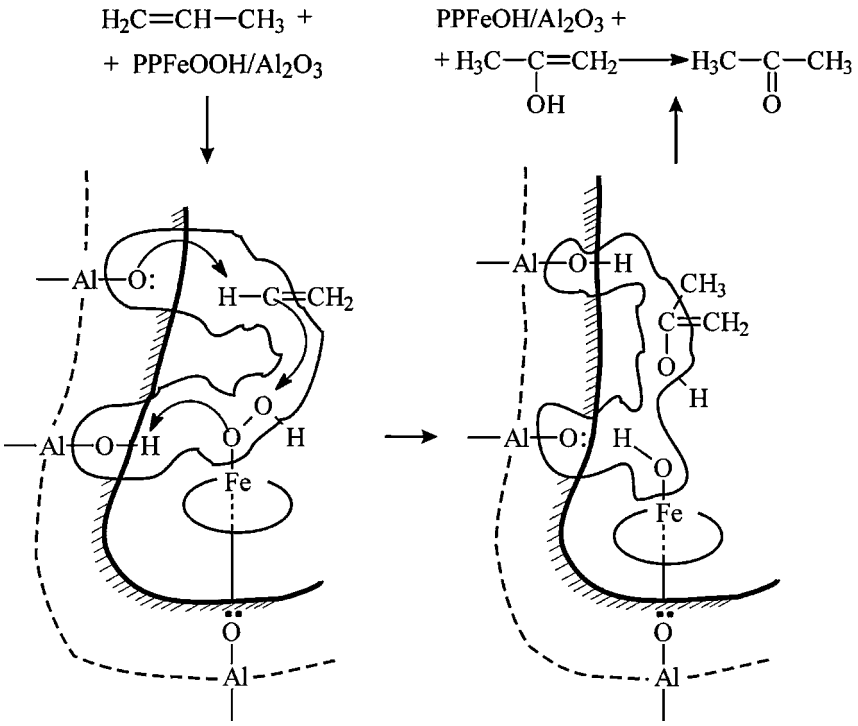

Figure 7.15 The mechanism of acetone synthesis at propylene oxidation with hydrogen peroxide on $PPFe^{3+}OH/Al_2O_3$ catalyst.

$$PPFe^{3+}OOH/Al_2O_3 + C_3H_6 \xrightarrow{\text{slow}} PPFe^{3+}OH/Al_2O_3 + C_3H_6O \qquad (7.8)$$

The present example of heterogeneous catalysis shows the unity of acidic–basic and redox mechanisms, which is typical of enzymatic catalysis.

In the framework of general BRC theory in the example of $PPFe^{3+}OH/Al_2O_3$, the unified picture of two-proton transfer to acidic–basic groups of the carrier (Al_2O_3) with electron transfer to the active site ($PPFe^{3+}OH$) is observed. Finally, the substrate is redox converted. It is typical that in enzymatic catalysis conditions without acidic–basic groups redox processes are suppressed.

Thus, it can be suggested that catalytic mechanism of $PPFe^{3+}OH/Al_2O_3$ works directly at the molecular level via the synchronous influence of catalytic groups from the active site of the catalyst on the substrate. In this connection, of special attention are studies of admixture effects on catalytic oxidation of propylene and methane. The principally important result of these studies is the detection of the gradual suppression of $PPFe^{3+}OH/Al_2O_3$ catalytic activity (to full elimination) by traces of phosphoric acid (the complexing agent), present in H_2O_2 trademarks. This indicates the central role of the Fe^{3+} ion in the act of catalysis. Moreover, phosphoric acid also affects the intraspheric processes.

However, the oxidation mechanism can also be interpreted in the framework of conjugated process theory. This requires presenting the overall equation of the secondary reaction as a sum of the complex $PPFe^{3+}OOH/Al_2O_3$ formation stage in reaction (7.7) and stage (7.8):

$$H_2O_2 + C_3H_6 \rightarrow C_3H_6O + H_2O \tag{7.9}$$

Reactions (7.7) and (7.9) are conjugated. They pass through formation of the general intermediate compound $PPFe^{3+}OOH/Al_2O_3$. Therefore, intensification of the primary reaction (7.7) always induces intensification of the secondary reaction (7.9).

Thus, turning to a kinetic description of reactions (7.7) and (7.9), it should be taken into account that the complex $PPFe^{3+}OOH/Al_2O_3$ formation is a fast stage, whereas epoxide formation (7.8) is slow and, therefore, the limiting stage.

This method of settling the kinetic task makes possible the application of Michaelis–Menten [81] to the description of propylene transformation:

$$\frac{1}{w} = \frac{1}{w_{\max}} + \frac{K_{\max}}{w_{\max}} \frac{1}{[C_3H_6]} \tag{7.10}$$

where w is the C_3H_6 transformation rate, $w_{\max}$ is the maximal rate and $K_{\max}$ is the Michaelis constant.

In equation (7.10) coordinates at all temperature points properly fit straight lines [77].

Note also that this work was one of the first to study a chemical model of a biocatalyst in the gas phase and to indicate the main possibility of process simulation.

The overwhelming majority of biological processes and their most suitable models display a heterolytical mechanism, in which the substrate is transformed without synthesis of reactive intermediates. This provides for extremely high selectivity of the process.

On the contrary, most homolytical free-radical processes display formation of reactive intermediates capable of reacting by various reaction channels, which reduces the industrial value of these processes.

Further development of the synthesis of heterogeneous catalysts with the given properties is based on the common abilities of porphyrins to targeted change of catalytic properties with respect to the central atom of metal in the porphyrin ring and origin of the axial ligand. The presence of axial ligands, as a rule, seriously affects the complex forming ability of metal ion, on which the efficiency of electron transfer to oxidant depends.

The question of iron(III) tetraphenylporphyrin mimic stabilization [44–46] is resolved by replacing all phenyl hydrogen atoms by halides, which significantly extends the lifetime of the catalyst. It is also proven that oxidants (H_2O_2, ROOH, peroxy acids and iodosylbenzene) in hydroxide solvents (diluters) dissociate heterolytically [30, 31].

Immobilization of metalloporphyrins on inorganic carriers displayed improved selectivity owing to the carrier surrounding [41, 42]. The simplicity of applied manganese catalyst preparation with high porphyrin cation adsorption to silica gel is demonstrated [42]. The exclusive activity of this compound in alkane liquid-phase hydroxylation compared with its homogeneous analog was also indicated. Electronegative substitution in iron porphyrins promotes a noticeable increase of epoxidation rate (norbornene, cyclohexene, etc.) rather than allyl oxidation [37]. It also displays high selectivity for *cis*-alkenes.

Note that the monooxygenase model reactions described above are performed in non-aqueous diluters. Therefore, hematin form is absent and only hemin is present, of which, apparently, formation of an intermediate shaped as Hm═O is typical. Model catalysts of cytochrome P-450 operate in liquids, similar to enzymes themselves. Their activity depends on many factors, including diluter origin, reaction mixture pH and cell effects. As indicated [1], the gas-phase version of the oxidation process is much freer from these effects.

It is the author's opinion that creation of heterogeneous catalysts—cytochrome P-450 analogs, for gas-phase selective oxidation will promote the development of new highly effective epoxidation and hydroxylation processes possessing all the technological advantages of heterogeneous catalytic reactions in the gas phase. In this connection, the present monograph is the first publication in which the chemical model of biocatalyst ($PPFe^{3+}$ OH/Al_2O_3) is studied in the gas phase and for which, in principle, the possibility of such a simulation is outlined. In the framework of the BRC theory a mechanism is suggested in which monooxygenation is presented as H^+-dependent oxidation reaction. The main disadvantage of this catalyst is its low resistance to the degrading effect of oxidant and increased temperature under oxidation conditions, general to all porphyrin catalysts.

Zinc(III) tetrapentafluorophenylporphyrin was synthesized via condensation of pyrrole, pentafluorobenzaldehyde and zinc acetate in 2,4,6-trimethylpyridine, according to a described technique [44, 46]. The target product, a brown-colored solid, was obtained by consecutive vacuum distillation, filtration and chromatographic separation. The product was IR analyzed, which indicated the absence of group:

NMR analysis confirmed the presence of pyrrole hydrogen atoms only.

The next stage of synthesis was the replacement of pyrrole hydrogen atoms by fluorine atoms. The zinc complex was fluorinated by cobalt fluoride according to the appropriate technique [44, 46]. The target product was extracted from reaction products by chromatographic separation in a column filled with neutral aluminum oxide.

Vacuum sublimation of a Zn(III) complex solution produced a pink-colored solid, which was Zn(III) perfluorotetraphenylporphyrin. NMR analysis of this product showed the absence of pyrrole hydrogen atoms, which is the evidence for complete replacement. Then bivalent iron chloride ($FeCl_2$) was prepared according to the common technique [17]. This compound was then used for Zn(III) ion replacement in a porphyrin ring. For this purpose, the Zn(III) complex was dissolved in dimethylformamide (DMF) and then, with the addition of an $FeCl_2$ solution, also in DMF. The reaction mixture was heated in a steam bath at water boiling point for 5 h. Finally, a dark-brown sediment was deposited, and the solution was colored blue, which is typical of iron(III) perfluorotetraphenylporphyrin (perFTPhPFe(III)) dissolved in DMF. In this case, the active weight of the catalyst iron(III) perfluorotetraphenylporphyrin equaled 47.05 mg.

Immobilized catalyst was obtained by impregnating 1.58 g of neutral active aluminum oxide shaped as spheres 1.5 mm in diameter (with specific surface over 500 m^2/g) with iron(III) perfluorotetraphenylporphyrin solution. Then the applied catalyst with 30 mg/g active

mass content in the carrier (3.0 wt.% of perFTPhPFe(III)) in an amount of 3 cm^3 was sequentially dried and annealed. After all these procedures, the model compound was ready for tests on catalytic activity in H_2O_2 dissociation reaction.

7.2.1 Catalase activity

Before monooxygenation, a preliminary typical test of synthesized catalyst on the catalase activity in liquid was performed. Such an approach is imposed by the authors' experience in work with catalytic systems [19] indicating that applied metalloporphyrins are usually more highly resistant to oxidant and intermediate influence than homogeneous analogs. The test results shown in Table 7.1 indicate high catalase of synthesized mimic. The number of cycles increases with H_2O_2 concentration, which allows orientation to higher hydrogen peroxide concentrations in propylene oxidation. In this connection, tests on detection of the catalyst resistance to high concentrations of the oxidation (H_2O_2) were continued. For a period of 6 months the mimic was regularly exposed to 30% aqueous H_2O_2. Hence during the whole period it displayed equal catalase activity, which is the evidence that the catalyst is highly stable in work and possesses the unique resistance to oxidant effect.

7.2.2 Monooxygenation of propylene

Epoxidation and hydroxylation activity of iron(III) perfluorotetraphenylporphyrin biomimic was studied in a quartz flow reactor with the reaction zone 1.7 cm long and 1.8 cm in diameter. Kinetic regularities of monooxygenase reaction were studied at 180–320 °C and molar ratios C_3H_6:H_2O_2 equal 1:0.5 and 1:2.

The search for new, highly effective systems of partial oxidation of propylene is connected to hydrogen peroxide use as selective oxidant. It should be noted that the processes of oxidation with hydrogen peroxide meet the requirements of modern technology, because they are highly selective, ecologically friendly, efficient, etc. [20]. In this connection, the ways and methods of H_2O_2 activation becomes of high importance. Obviously, catalytic activity

Table 7.1

Dependence of the number of cycles (ν) on aqueous hydrogen peroxide concentration (C) (q is H_2O_2 consumption)

C (wt.%)	q (mol/ml h)	ν (h^{-1})
5	0.12×10^{-3}	0.94×10^{3}
10	0.61×10^{-3}	0.48×10^{4}
25	0.91×10^{-2}	0.71×10^{5}
30	0.14×10^{-1}	0.11×10^{6}

Note: Test conditions: $T = 25$ °C; $V_{H_2O_2} = 3$ ml and catalyst weighing 0.005 g with active weight 0.027×10^{-6} mol.

of oxidants such as ROOH, peroxy acids, iodosylbenzene and HOCl does not require as high energy for O—O bond break as does H_2O_2. Moreover, the intermediates of the oxidants listed are more active that hydrogen peroxide intermediates.

Propylene used as a substrate in biomimic tests on epoxidation and hydroxylation activity is less suitable in the context of its transformation to oxidation products than different substances [15]. First of all, this is gas, which causes additional obstacles at liquid-phase oxidation for its accumulation in the reaction mixture compared with liquid compounds, which form the integral phase with appropriate enzymes and their models. Secondly, though propylene represents olefin, it requires higher energy for oxidation activation in the allyl position than cycloolefins. Thus, though the studied reaction system C_3H_6—H_2O_2—H_2O is less reactive than the systems considered above, when affected by a biomimic in gas such a system manifests properties that assist in achieving good results of epoxidation under soft conditions (for propylene oxidation). In experiments with hydrogen peroxide, when substrates are oxidized by the mechanism associated with chemical conjugation, of importance is the ratio $S:H_2O_2$, where S is a substrate. This kinetic aspect is comprehensively considered in the examples of free-radical chain oxidation [78, 79] and in the presence of iron protoporphyrin biomimic.

The curves in Figure 7.16 show that, all other reaction parameters being equal, the molar ratio of the reagents causes a significant effect on the product formation regularities, selectivity (by epoxide) and conversion (by substrate). The curves of epoxide yield, selectivity and substrate conversion have maxima in a narrow interval of ratio values. Under the most suitable conditions at $S:H_2O_2 = 1:1.5$ the epoxide yield equals 32 wt.% at 70% selectivity. Nevertheless, if selectivity is calculated by monooxygenase product yield, it may approach the 100% level.

The presence of maxima on the curves is explained as follows. If the ratio $S:H_2O_2$ is below 1:1.5, H_2O_2 concentration in the reaction mixture increases, which intensifies primary catalase reaction (7.7). A significant amount of general intermediate of conjugated reactions (7.7) and (7.8) is consumed in the first of them. As a consequence, the induction effect of this process on epoxidation is reduced.

Conversion of C_3H_6 in the ratio interval between 1:1.5 and 1:2 is decreased by 3 wt.%, whereas for epoxide this value equals 10 wt.%. These data show that the increase in yields of other oxidation products is caused by epoxide isomerization and the parallel proceeding of other catalytic reactions. It should be noted that chromatographic tests have detected only unreacted C_3H_6 in the gas products, whereas CO, CO_2 and other products of C_3H_6 degradation were not observed.

Plots demonstrating the dependence of propylene monooxygenation product yield on aqueous H_2O_2 concentration, supplied to the reaction zone in gas form, are shown in Figure 7.17. The selectivity curve steadily declines with H_2O_2 concentration growth, though in this case yield curves for epoxide and propionic aldehyde have clear maxima. If H_2O_2 concentration equals 25–35%, a new product—acetone, which is the epoxide isomer—is formed. As H_2O_2 approaches 35% concentration, the yield reaches 20%. These data testify once again that independently of the way H_2O_2 concentration increases, it causes a noticeable decline in epoxide yields, which, in its turn, intensifies catalase reaction (7.7). Occurrence of acetone is not an unexpected event, because it was always synthesized in similar catalytic system before [75]. However, in this case, its synthesis obeys different kinetic regularities,

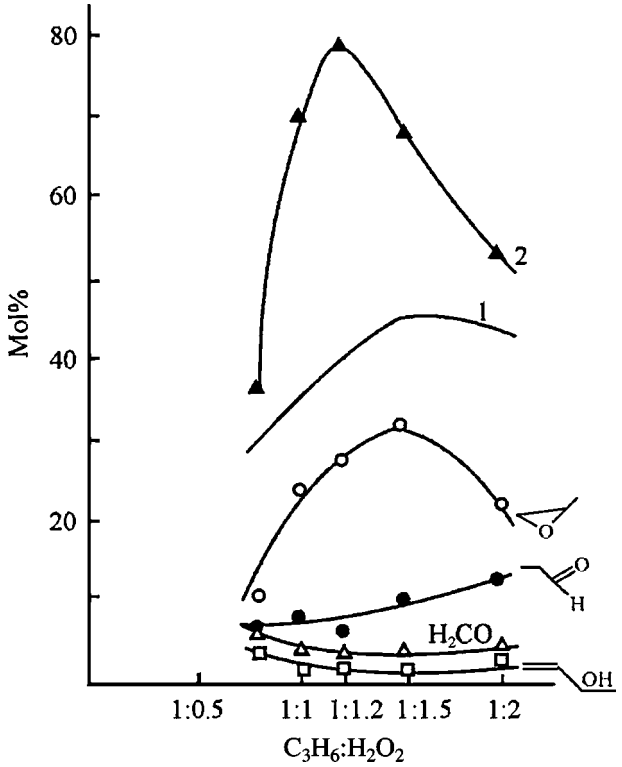

Figure 7.16 Dependencies of reaction product yield on the molar ratio C_3H_6:H_2O_2. $T = 200\,°C$; contact time $\tau = 1.4\,s$; 20% aqueous H_2O_2 (1: C_3H_6 conversion and 2: selectivity).

according to which a sharp increase in acetone yield is observed since 25% concentration of H_2O_2.

Figure 7.18 shows temperature dependencies of product yields for propylene monooxygenation with hydrogen peroxide. As indicated, propylene oxide isomers accompany the main product of the synthesis. Propylene degradation products, as well as CO and CO_2 were not detected in the whole temperature range. It is also shown in Figure 7.18 that propylene oxide, propionic aldehyde and allyl alcohol accumulation curves have maxima at 220, 300 and 260 °C, respectively. Temperature increase to 320 °C causes a noticeable decline of epoxide and allyl alcohol yields, and slightly lower yield of propionic aldehyde. On the contrary, an increase of acetone yield up to 25% is observed. It should be noted that kinetic regularities of monooxygenase product accumulation are similar in shape to those for iron protoporphyrin catalyst $PPFe^{3+}OH/Al_2O_3$ [75]. The only difference is that for current mimic the range is shifted toward higher temperatures. The selectivity curve indicates the optimal temperature range for epoxidation between 200 and 220 °C, because it corresponds to the highest yields and selectivity.

It is common knowledge that propylene oxide is isomerized to propionic aldehyde in the presence of aluminum oxide in the temperature range between 250 and 260 °C [76]. This is

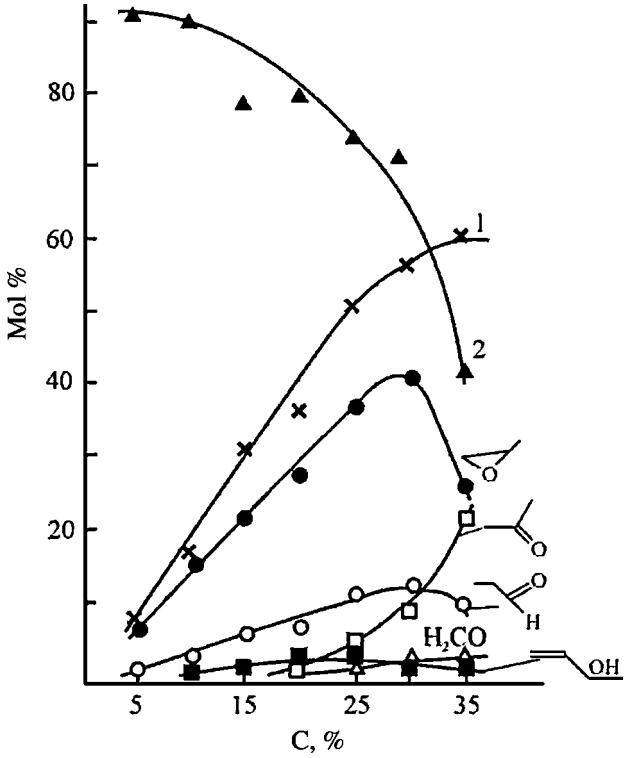

Figure 7.17 Dependencies of reaction product yield on aqueous H_2O_2 concentration (C) in the reaction zone. $T = 200\,°C$; $\tau = 1.4\,s$; C_3H_6:H_2O_2 = 1:1.2.

usually accompanied by formation of low amounts of acetone. However, acetone accumulation curves most likely indicate the existence of additional pathways of its synthesis. These data show that a definite part of propionic aldehyde is synthesized from propylene oxide at a temperature above 220 °C owing to intramolecular epoxide regrouping in the catalytic matrix.

Figure 7.19 shows the dependence of monooxygenase activity on the contact time, τ. The epoxide accumulation curve has a maximum, growing at low contact times (0.17–1.4 s) and then noticeably declining in the area of $\tau = 3.0\,s$ or longer. Thus, in the whole temperature range C_3H_6 epoxidation is most optimal at short contact times, because at long times it manages to partly isomerize [76]. In the studied time interval, propionic aldehyde accumulation curves (Figure 7.19) grow steadily, though at long contact times the dependence becomes noticeably weaker. Despite the latter fact, propionic aldehyde yields did not exceed 10 wt.%.

Acetone is the important product of the mimic's monooxygenase activity. It is synthesized at high temperature, 220 °C or higher. The yield of acetone noticeably increases with contact time and temperature, reaching 15 wt.%. In this case, two ways of acetone formation (catalytic isomerization of epoxide and direct synthesis from C_3H_6) are also probable.

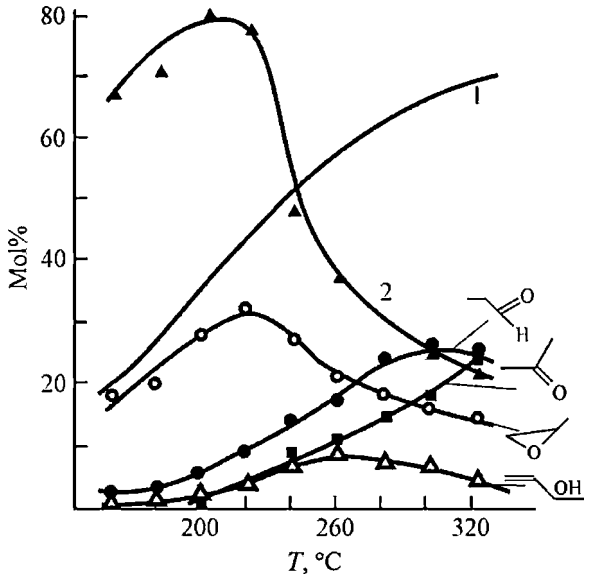

Figure 7.18 Temperature dependencies of reaction product yields. $C_{H_2O_2}$ = 20 wt.%; τ = 1.4 s; C_3H_6:H_2O_2 = 1:1.2.

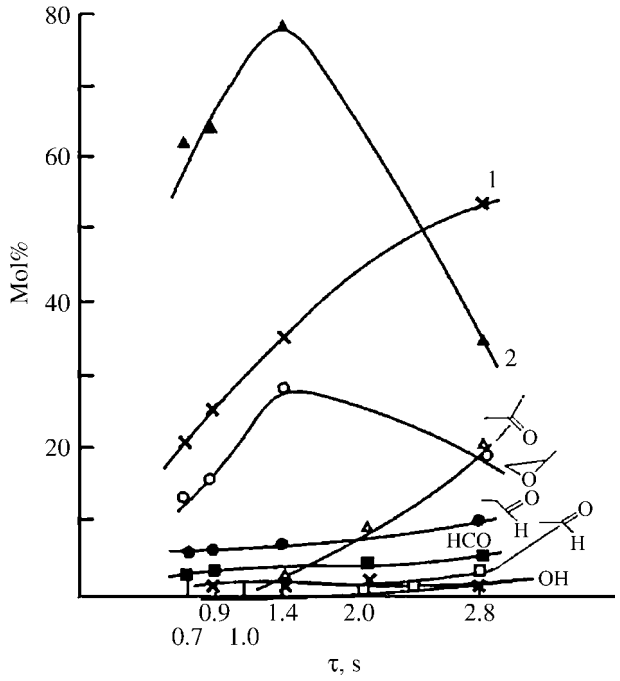

Figure 7.19 Dependencies of reaction product yields on contact time. T = 200 °C; $C_{H_2O_2}$ = 20 wt.%; C_3H_6:H_2O_2 = 1:1.2.

Figure 7.20 clearly indicates the conjugated type of two reactions (7.7) and (7.8). In fact, a decline of catalase product (O_2) accumulation rate is associated with an increasing rate of monooxygenase reaction product yield. These processes interrelate via general reactive intermediate perFTPhPFe^{3+}OOH/Al_2O_3.

The catalytic activity for a synthesized mimic [24] was also estimated by the number of catalytic cycles in two chemically conjugated reactions. Data in Table 7.2 show that, being the analog of active site of natural protein, iron protoporphyrin manifests 2 times lower activity. Resistance to the effects of oxidants and their intermediates is also higher for natural protein, because corresponded mechanisms can barely be simulated in the mimic.

Despite comparatively low amounts of catalytic cycles, the currently designed monooxygenase catalytic system is highly effective and adaptable to manufacture, which is typical of flow systems. It is also extremely resistant to the effects of oxidants and high temperature [82].

The catalyst indicated extremely high resistance to the effects of oxidants and their intermediates and relatively high temperature, e.g. it preserves the ability to epoxidize during the whole time of the biomimic tests. Owing to the mentioned properties of the mimic, kinetic regularities of current monooxygenase reaction were studied in a broad range of reaction parameters with reproducible results.

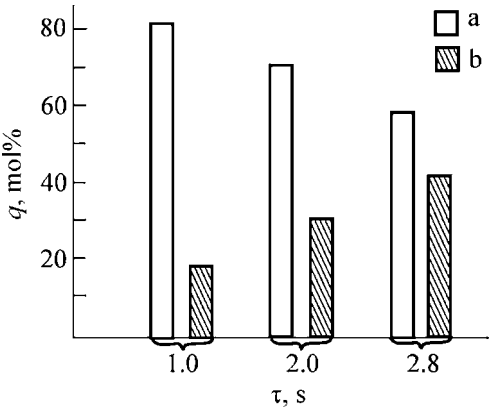

Figure 7.20 Dependence of hydrogen peroxide consumption (q) in catalase (a) and monooxygenase (b) reactions on contact time. $T = 200\,°C$; C_3H_6:H_2O_2 = 1:1.2.

Table 7.2

The number of catalytic cycles (ν) in propylene epoxidation reaction with hydrogen peroxide

Catalyst	T (°C)	n	v (mol/h)	α (%)	p (mol/(ml h))	m (mol)	ν (h^{-1})
A	220	1:1.2	1.89×10^{-2}	50.5	0.32×10^{-2}	0.400×10^{-4}	80
B [16]	160	1:1	3.57×10^{-2}	80	0.47×10^{-2}	0.315×10^{-4}	150

A: perfluorinated mimic under consideration and B: iron protoporphyrin catalyst [16]; n = C_3H_6:H_2O_2; v is the C_3H_6 injection rate; α is the conversion; p is the monoxide yield and m is the amount of active sites.

The mechanism of such mimics is discussed in detail in the literature [1]. It is indicated that monooxygenase, including epoxidation, are conjugated with the catalase process. The mandatory parameter of chemical conjugation in such chemical systems is the determinant value, calculated by the following equation:

$$D = \nu\left(\frac{W_{A_1}}{W_{Acc}} + \frac{W_{A_2}}{W_{Acc}}\right)^{-1}$$

where W_{A_1} and W_{A_2} are rates of the actor (H_2O_2) consumption in primary catalase and secondary monooxygenase reactions, respectively; W_{Acc} is the amount of consumed acceptor (C_3H_6); ν is the stoichiometric parameter of the actor (as follows from equation (7.7) $\nu = 1$, see below).

The determinant $D = 0.3$ was calculated for optimal conditions of propylene epoxidation. On the chemical interference scale this value lies in the area of chemical conjugation ($D = 0$–1). Here the peroxide intermediate is the particle conjugation catalase and monooxygenase reactions.

Based on these ideas and data on the structure of catalytic sites in cytochrome P-450 and corresponding mimics [15], the catalytic domain [83] of the biomimic was designed: perFTPhPFe(III)OH/Al_2O_3 (Figure 7.21). As observed from Figure 7.21, inorganic support (Al_2O_3) of the acidic–basic origin possesses terminal and bridge Broensted acidic sites and corresponding Brenstedt basic sites, required by the catalytic domain. The complex perFTPhPFe(III)OH with the structure stabilized by the matrix basement coordination (Al—O:) with hematin functional groups, for example, due to axial ligands [79], is the redox site of the domain.

According to data in the literature [1], catalytic monooxygenation of propylene with hydrogen peroxide in the presence of perFTPhPFe(III)OH/Al_2O_3 has an intermediate, shaped

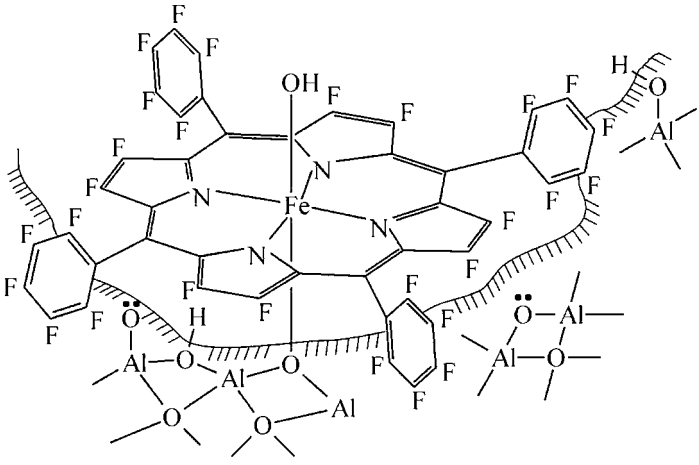

Figure 7.21 Catalytic domain design.

as perFTPhPFe(III)OOH/Al_2O_3 mimic-substrate complex. This complex is formed in the interaction of the mimic's catalytic sites with H_2O_2 at the first stage of the process:

$$\text{perFTPhPFe(III)OH/Al}_2\text{O}_3 + \text{H}_2\text{O}_2 \underset{k_{-1}}{\overset{k_1}{\rightleftharpoons}} \text{perFTPhPFe(III)OOH/Al}_2\text{O}_3 + \text{H}_2\text{O} \tag{7.11}$$

The structure of the activated complex in elementary reaction (7.11) composed in the framework of the BRC theory [14] is shown in Figure 7.22. Heterolytical addition of H_2O_2 to Fe(III) ion is implemented in a manner eliminating general change in the formal oxidation level or coordinate number of iron ion. This process can be considered to be a substitution of one anionic ligand by another (OH^- by HO_2^-). The intermediate obtained can be consumed by two alternative channels: interaction with the second hydrogen peroxide molecule giving final products of catalase reaction or propylene epoxidation according to the diagram in Figure 7.23.

According to the epoxidation mechanism shown in Figure 7.23, the oxygen atom from the hydrogen peroxide molecule is transferred to C_3H_6 by adding OH group to it. Proton in this group enters partial interaction with the basic site on the surface and, therefore, prevents complete transfer of substrate proton to the matrix.

The occurred activated complex may induce formation of either epoxide or allyl alcohol. However, under current experimental conditions the biomimic possesses exclusive epoxidizing ability, and the catalytic cycle is completed at this stage. The number of cycles per perFTPhPFe(III)OH mole under optimal process conditions is 80 per hour [82]. This example of the mimetic catalysis indicates the unity of acidic–basic and redox mechanisms typical of the enzyme catalysis.

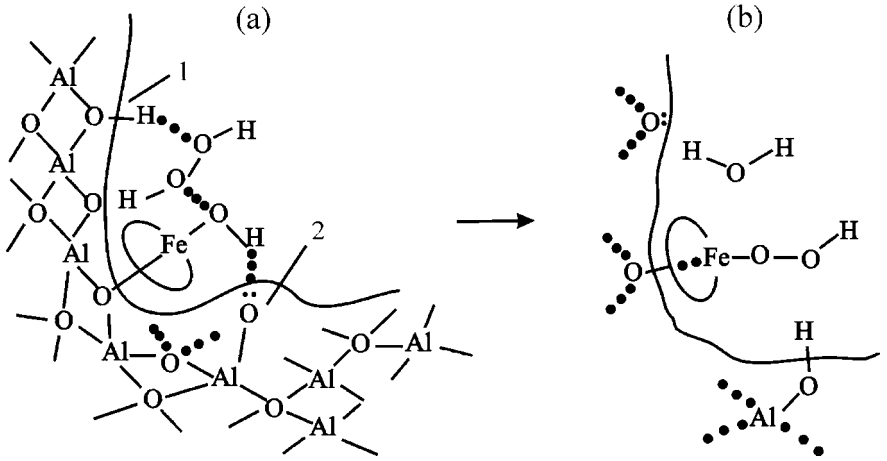

Figure 7.22 The mechanism of mimic-substrate complex formation. (a) Active complex with active Al_2O_3 acidic–basic sites and (b) active intermediate, the mimic-substrate complex (1: acidic site and 2: basic site, points-forming bonds, and continuous lines breaking bonds).

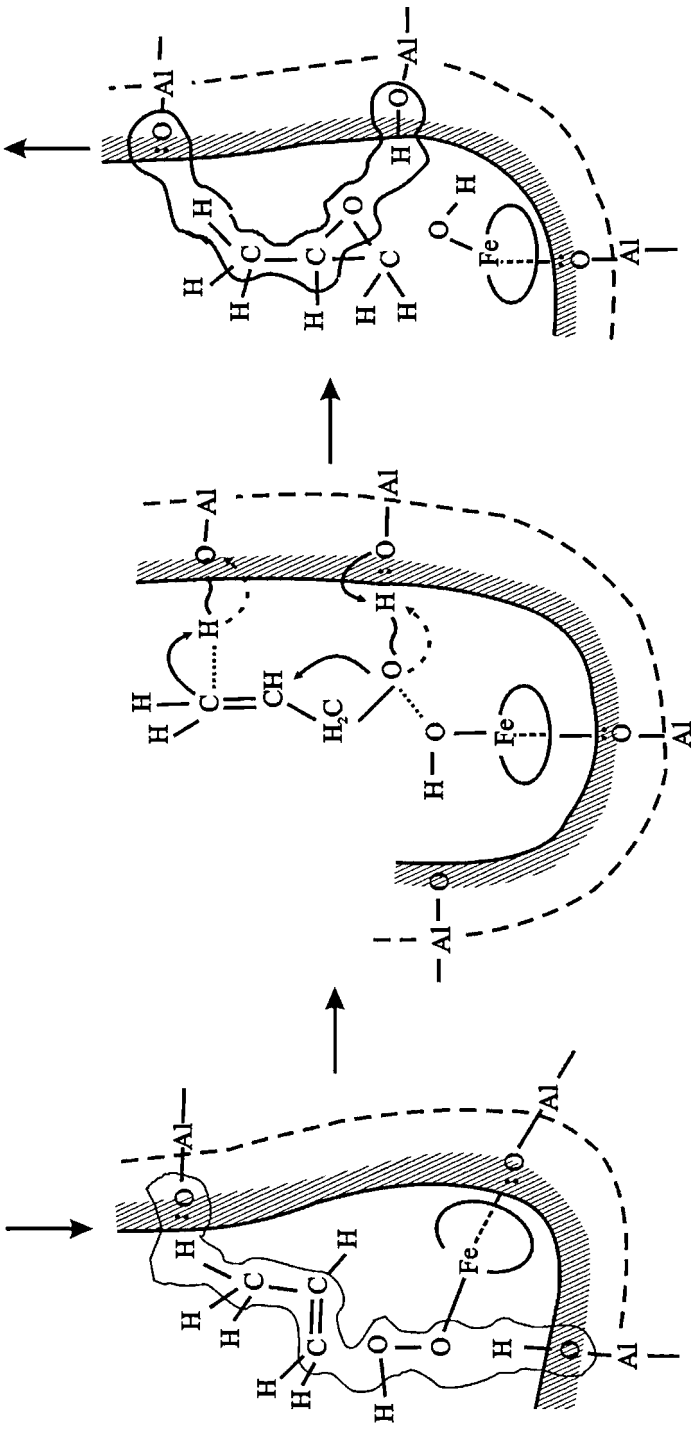

Figure 7.23 The mechanism of propylene oxide synthesis.

Thus, the probable mechanism of catalytic redox transformation of the substrate within one catalytic domain is described in the framework of the BRC theory. It is implemented owing to two-proton transfer to the acidic–basic carrier (Al_2O_3) groups with electron transfer to active site perFTPhPFe(III)OH. In this context, of special attention are data on studies of qualitative and quantitative parameters of surface acidic–basic sites of inorganic matrices, including Al_2O_3 [8].

In this study acidic–basic sites of the samples were determined by a programmed thermodesorption method: NH_3 (acidic sites) and CO_2 (basic sites). Three thermodesorption peaks are observed: weak Broensted peak and two ('moderate' and 'strong') Lewis acidic sites on Al_2O_3.

Another situation is observed for active hematin mimic ($PPFe^{3+}OH$) applied on Al_2O_3. Thermodesorptional study of $PPFe^{3+}OH/Al_2O_3$ complex detected two ('weak' (Broensted) and 'strong' (Lewis)) acidic sites and two ('weak' and 'strong') basic sites. As a consequence, hematin adsorption on Al_2O_3 causes disappearance of Lewis 'moderate' acidic sites and occurrence of a new 'strong' basic site. This testifies to hematin adsorption on 'moderate' Lewis acidic sites, whereas the new 'strong' basic site occurs due to basic properties of protoporphyrin ligand. After several hours of operation in the oxidation process the $PPFe^{3+}OH/Al_2O_3$ catalyst becomes inactive which affects the results of the thermodesorption study. Disappeared acidic 'moderate' sites in dead catalyst $PPFe^{3+}OH/Al_2O_3$ are reduced, which is probably associated with the hematin degradation process [84]. These results suggest that basic sites of adsorbed hematin may contribute to strengthening hematin bonding to Lewis 'moderate' acidic sites on Al_2O_3 surface by multisite adsorption mechanism. This suggestion is confirmed by the following conclusion [85]: metalloporphyrin structure may be stabilized by additional coordination of the polymeric carrier with hematin functional groups, for example, by means of axial or basic ligands. Actually, synthesized mimic perFTPh $PFe^{3+}OH/Al_2O_3$ displayed high temperature and oxidation resistance during propylene monooxygenation with hydrogen peroxide. It preserved initial activity during a long period (about 6 months) and was not subject to thermal degradation or poisoning. As follows from the catalyst structural diagram (Figure 7.21), such stabilization of hematin structure on Al_2O_3 carrier surface is associated with multisite hematin adsorption by axial and basic ligands. Resistance to the effects of the oxidant and intermediates is provided by hemin perfluorination.

The above-suggested biomimic mechanism conforms to modern ideas about the functioning mechanism of its biochemical analogs. Therefore, it allows passing to kinetic modeling of propylene epoxidation with hydrogen peroxide in the context of enzymatic catalysis. The reaction system C_3H_6—H_2O_2–biomimic is the two-substrate complex system, where the process proceeds in two stages (7.7) and (7.8).

Describing the reaction in kinetic terms, let us apply to the fact that the intermediate $perFTPhPFe^{3+}OOH/Al_2O_3$ formation stage (7.7) is fast, the epoxide formation stage (7.8) is slow and, consequently, limiting. For kinetic simulation of propylene oxidation to epoxide, this gives an opportunity to apply the Michaelis–Menten equation in Linuver–Berk coordinates:

$$\frac{1}{V} = \frac{1}{V_{\max}} + \frac{k_m}{V_{\max}} \frac{1}{[C_3H_6]} \tag{7.12}$$

where V is the C_3H_6 transformation rate, $V_{\max}$ is the maximal reaction rate and k_m is the Michaelis constant. In accordance with equation (7.12) for all temperatures, lines are

obtained which cut an intersect equal $1/V_{max}$ on the axis of ordinates, and an intersect equal. $1/k_m$ on the abscissa axis (Figure 7.24). For all temperatures Michaelis constants presented by the formula:

$$k_m = \frac{k_2 + k_{-1}}{k_1}$$

where k_1 and k_{-1} are rate constants of perFTPhPFe^{3+}OOH/Al_2O_3 intermediate synthesis and consumption in stage (1); k_2 is the rate constant of propylene oxide formation, were determined.

Under the condition $k_2 \gg k_{-1}$ the value $1/k_m$ makes sense of the equilibrium constant of the mimic-substrate complex formation. Under the reverse condition $k_2 \ll k_{-1}$ the value $1/k_m$ is equated to the ratio k_1/k_2 equal to the effective rate constant of the reaction. The values k_m determined from the diagram allowed calculation of the effective rate constant:

$$\frac{k_1}{k_2} = \frac{1}{k_m} \quad \frac{1}{k_m} = k_{\text{eff}}$$

Table 7.3 shows values of effective rate constants for different temperatures. Table data indicate that the epoxidation rate (7.8) is low compared with the complex formation rate (k_1/k_2) $\approx 10^2$–10^3). If we plot k_{eff} values in Arrhenius coordinates, the numerical value of effective activation energy for propylene epoxidation is determined: 8.76 kcal/mol corresponding to enzymatic processes (7–15 kcal/mol).

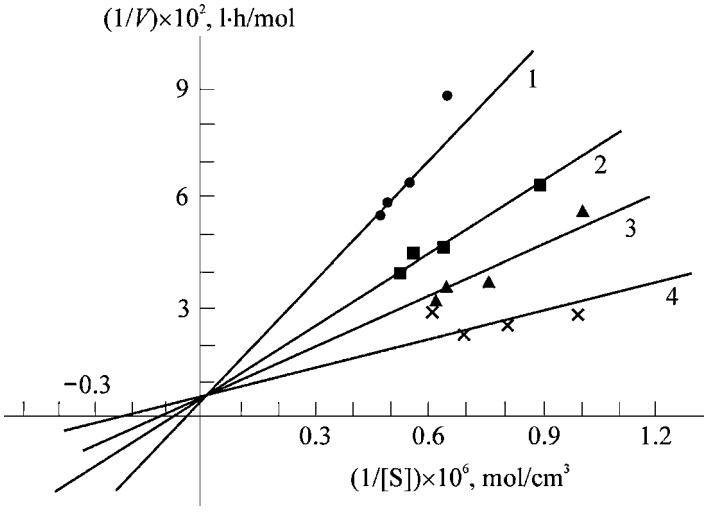

Figure 7.24 Dependencies of propylene consumption rate on propylene concentration in the epoxidation reaction at different temperatures (1: 453 K; 2: 473 K; 3: 493 K and 4: 513 K).

Table 7.3

Effective kinetic and thermodynamic parameters of propylene epoxidation with hydrogen peroxide on biomimic (perFTPhPFe(III)OH/Al_2O_3)

T (K)	$k_{eff} \times 10^{-2}$ (1h/mol)	E_{eff} (kcal/mol)	A_{eff}	$-\Delta G^*$ (cal/mol)	$-\Delta S^*$ (cal/(mol K))	$-\Delta H^*$ (cal/mol)
453	0.5	8.76	1.12×10^6	7248.9	19.14	15919.3
473	1.0			8188.7	19.23	17284.5
493	1.4			8865.8	19.29	18375.7
513	2.4			9773.5	19.39	19720.6

Contrary to simple homogeneous catalytic processes, the temperature dependence of the enzymatic reaction rate shows growth in a narrow temperature range (temperature optimum) [86].

As the pre-exponential factor is known ($A^* = 0.62 \times 10^8$ 1h/mol for the mimic-substrate complex formation), activation entropy ΔS^* is determined by the following equation:

$$A^* = \frac{kt}{h} \exp\left(\frac{\Delta S^*}{R}\right)$$

In turn, activation enthalpies were calculated from the equation:

$$\Delta H^* = \Delta G^* + T\Delta S^*$$

Thermodynamic parameter values, obtained for perFTPhPFe(III)OH/Al_2O_3 complex formation are shown in Table 7.3.

Thus, kinetic equation (7.12) adequately describes experimental data and indicates higher probability of epoxidation mechanism shown in Figure 7.23.

Catalytic activity of heterogeneously applied iron protoporphyrin biomimics in methane hydroxylation with hydrogen peroxide was kinetically studied [87].

For synthesis of biomimetic catalysts four versions of granulated carriers were used: neutral and activated Al_2O_3, NaX zeolite and synthetic amorphous aluminum–magnesium silicate and aluminum–chromium silicate.

Aluminum–metal silicate carriers were produced by the co-deposition method [87]. For obtaining aluminum–magnesium silicate, liquid silica (modulus $M = 3.9$; $d_{20}^{20} = 1.138$; [SiO_2] = 11.5%; [Na_2O] = 2.95%) was co-deposited with magnesium sulfate acidified by sulfuric acid. The hydrogel obtained was then rinsed with distilled water and activated by aluminum sulfate, and then gradually calcinated. The prepared carrier contained up to 5% Mg, 7% Al and 88% SiO_2. Aluminum–chromium silicate was prepared by co-deposition of liquid silica of the above-mentioned composition with a chromium salt solution, acidified by nitric acid. The activator is $Al(NO_3)_3$ and chromium content in the carrier was below 3%.

Hemin (BDH Company) containing 8.64% iron was used as the applied active site.

Hematin-containing monooxygenase mimics were prepared according to the known technique [1]. Hematin concentrations in obtained mimics were the following: 3.4 mg per

carrier gram for $PPFe^{3+}OH/Al_2O_3$, 2.5 mg per carrier gram for $PPFe^{3+}OH/NaX$, 0.9 mg per carrier gram for $PPFe^{3+}OH$/aluminum–magnesium silicate ($PPFe^{3+}OH/AlSiMg$) and 3.4 mg per carrier gram for $PPFe^{3+}OH$/aluminum–chromium silicate ($PPFe^{3+}OH/AlSiCr$).

For the purpose of studying the effect of the inorganic matrix origin on iron protoporphyrin biomimic activity in methane oxidation to methanol the above-mentioned carriers of the acidic–basic type were used. According to data in Tables 7.4 and 7.5, mimics derived from them simultaneously simulate catalase reaction and monooxygenase function of cytochrome P-450.

With respect to ionic additive origin (Cr and Mg ions), aluminum silicate mimics display catalase activity diametrically opposed to $PPFe^{3+}OH/Al_2O_3$ action (Table 7.4): $PPFe^{3+}OH/AlSiCr$ is the most active compound performing 700 catalytic cycles per hour. These results lead us to conclude that by changing the acidic–basic characteristics of aluminum silicate carriers, ionic additives (activators) significantly affect the catalase activity of applied metalloporphyrin mimics. However, it is not inconceivable that ionic additives themselves can participate in H_2O_2 dissociation [88].

Experimental results on monooxygenase activity of synthesized biomimics (Table 7.5) show that mimics applied on aluminum silicate carriers display higher activity for methane hydroxylation compared with Al_2O_3 and NaX zeolite. $PPFe^{3+}OH/AlSiCr$ is most active in the catalase reaction, but comes short of it in monooxygenase reaction compared with $PPFe^{3+}OH/AlSiMg$ (3 times by the number of catalytic cycles). It is apparent that high catalase activity of $PPFe^{3+}OH/AlSiCr$ is also preserved in the absence of the substrate (CH_4) which makes the monooxygenase reaction less competitive. Although high catalase activity for

Table 7.4

The number of catalytic cycles (n) in the catalase reaction

Sample	[Fe] (mol)	$W_{H_2O_2}$ (mol/h)	n (h^{-1})
$PPFe^{3+}OH/AlSiCr$	0.55×10^{-5}	0.38×10^{-2}	700
$PPFe^{3+}OH/AlSiMg$	0.7×10^{-6}	0.12×10^{-3}	171
$PPFe^{3+}OH/Al_2O_2$	0.26×10^{-5}	0.9×10^{-3}	347
$PPFe^{3+}OH/NaX$	0.2×10^{-5}	0.15×10^{-3}	75

$V_{H_2O_2} = 20$ ml; $T = 25$ °C; $m_{cat} = 0.5$ g; $[H_2O_2] = 5$ wt.% and $W_{H_2O_2}$ is hydrogen peroxide consumption rate.

Table 7.5

The number of catalytic cycles (n) in the monooxygenase reaction

Sample	[Fe] (mol)	$W_{H_2O_2}$ (mol/h)	n (h^{-1})
$PPFe^{3+}OH/AlSiCr$	0.3×10^{-4}	0.13×10^{-2}	43
$PPFe^{3+}OH/AlSiMg$	0.63×10^{-6}	0.77×10^{-3}	122
$PPFe^{3+}OH/Al_2O_2$	0.2×10^{-4}	0.19×10^{-3}	10
$PPFe^{3+}OH/NaX$	0.2×10^{-4}	0.76×10^{-4}	4

$T = 180$ °C; $[H_2O_2] = 20$ wt.%; $N_{CH_4}/N_{H_2O_2} = 1{:}0.5$; $\tau = 10$ s and W_{CH_4} is methane conversion.

aluminum oxide is observed, CH_4 molecules display rather moderate monooxygenase activity in oxidative activation. Due to the identity of the active site ($PPFe^{3+}OH$) for all synthesized samples, such behavior of the biomimic can be related to the natural properties of the carrier.

The study of biomimic functioning stability in the time interval under consideration indicates its similar decline for various complexes with no respect to the carrier origin and the quantity of adsorbed active mass (Figure 7.25). For example, activity abruptly decreases during the first hour, after which it declines monotonously to full deactivation of the mimics 6 h later.

Thus, the stability of the mimics is independent of the carrier origin and the amount of applied active mass. It depends on iron protoporphyrin complex thermal stability and resistance to oxidation (see below). This was observed in the studies performed with $PPFe^{3+}OH$/AlSiCr biomimic, which was exposed to thermal treatment in nitrogen flow at 400 °C for 1 h. Tests on hydroxiding activity ($T = 180$ °C; $N_{CH_4}/N_{H_2O_2} = 1{:}0.5$ and $[H_2O_2] = 20$ wt.%) indicated a 2.5-fold reduction of the monooxygenase activity of the mimic, induced by thermal treatment, compared with untreated complex. Meanwhile, it has previously been found [88] that thermal treatment under analogous conditions increases catalase activity of the mimic. Generalized results lead to the conclusion that thermally modified mimics cause different effects on the courses of catalase and monooxygenase reactions. Thermal treatment barely affects the resistance properties and operation stability of mimics, because they display a decay of activity during 6 h of continuous operation. Apparently, the operation stability and activity of the mimic directly depend on the oxidant origin (currently, hydrogen peroxide).

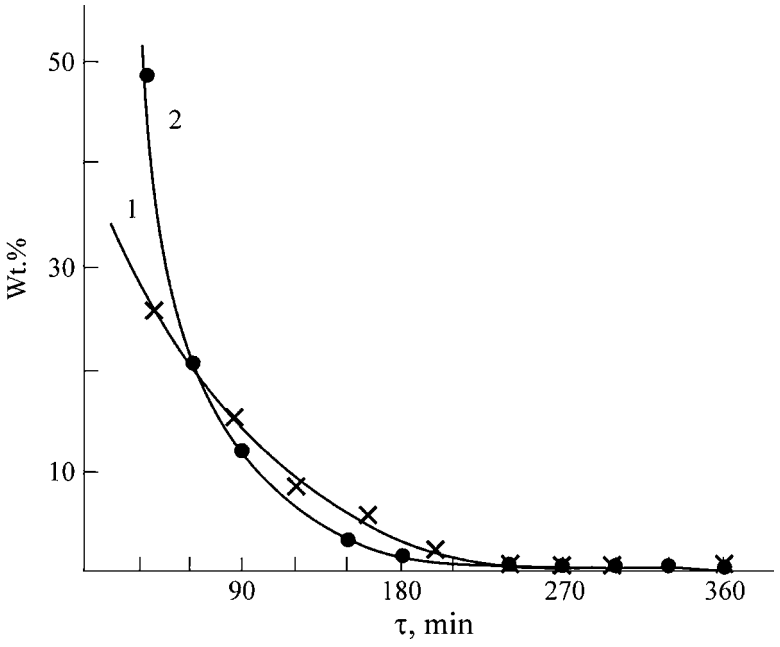

Figure 7.25 Dependencies of biomimic catalytic activity (for methane conversion) on operation time. $T = 180$ °C; $\tau = 13$ s; $V_{CH_4} = 0.086$ l/h; $V_{H_2O_2} = 0.8$ ml/h; $CH_4{:}H_2O_2 = 1{:}1.4$; $[H_2O_2] = 20$ wt.% (1: conversion on $PPFe^{3+}OH$/AlSiCr and 2: conversion on $PPFe^{3+}OH$/AlSiMg).

Unfortunately, engineering limitations do not allow biomimic sampling in the first half-hour of its operation. Figure 7.25 shows that the highest monooxygenase activity was observed in this time interval. Therefore, further experiments studying kinetic regularities of hydroxylation were only performed in this period of time (0–30 min). It should be noted that methanol yield (during 30 min) is averaged for this period, and the highest monooxygenase activity is most likely observed in shorter time intervals. Every separate test was implemented with a fresh biomimic sample.

7.2.3 Methane hydroxylation

The results shown above allowed the selection of the most active monooxygenase mimic $PPFe^{3+}OH/AlSiMg$ and its use for studying kinetic regularities of biomimetic methane hydroxylation with hydrogen peroxide under the following conditions: $N_{CH_4}/N_{H_2O_2}$ = 1:0.5–1:2.8, initial aqueous hydrogen peroxide concentration equals 10–30 wt.%; contact time τ = 2.9–11.6 s and T = 120–240 °C.

Figure 7.26 shows temperature kinetic dependencies of methanol yield possessing a maximum at 180 °C, whereas molecular oxygen yield possesses a minimum. In this experiment, methanol yield reaches 46.5 wt.% at methane conversion of 48 wt.%. Non-target products are CH_2O and HCOOH, synthesized in low amounts (~1.5%). Temperature does not noticeably affect their yield. The process selectivity by methanol is preserved at a level of 97% in the whole temperature interval.

Thus, the studied mimic catalyzes two interrelated, chemically conjugated catalase and monooxygenase reactions. The conjugation mechanism is comprehensively described by the following diagrams [11]:

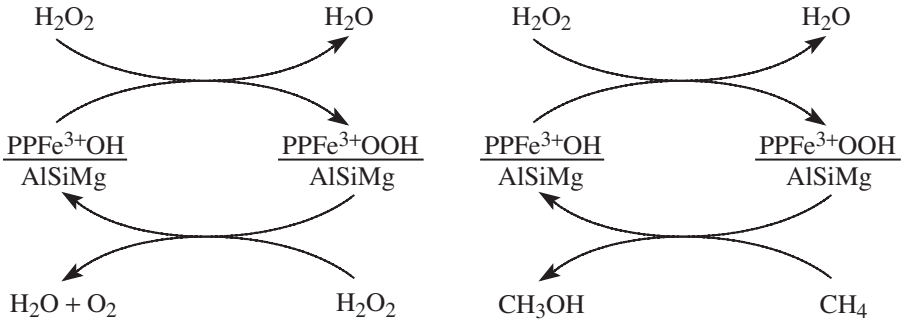

catalase reaction monooxygenase reaction

As follows from these diagrams, the chemical conjugation mechanism is realized via a general intermediate compound, which is $PPFe^{3+}OOH/AlSiMg$. It is consumed in both reactions at different rates. In all tests, H_2O_2 is consumed almost completely, and 'active oxygen' of the iron protoporphyrin complex is distributed by two channels in accordance with their kinetics. The interaction of these two reactions on kinetic CH_3OH and O_2 accumulation curves are outlined by two interdependent experimental points. Curve 5 (Figure 7.26) shows that already at 120 °C almost all hydrogen peroxide is converted to O_2; hence,

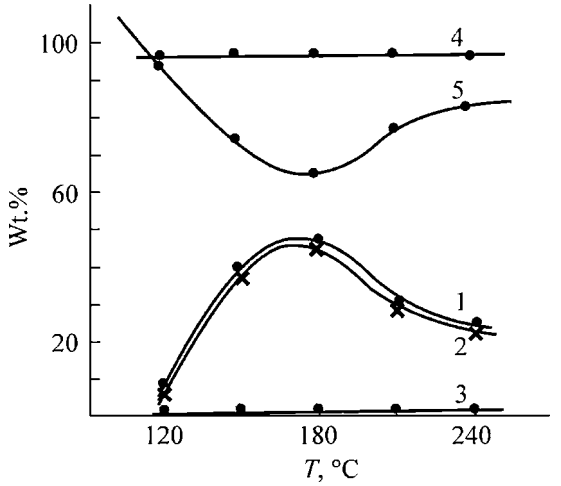

Figure 7.26 Temperature dependencies of methane hydroxylation product yields. CH_4:H_2O_2 = 1:1.4; V_{CH_4}=0.086 l/h; $V_{H_2O_2}$ = 0.8 ml/h; [H_2O_2] = 20 wt.% (1: CH_4 conversion; 2: CH_3OH yield; 3: CH_2O and HCOOH yield; 4: selectivity and 5: O_2 yield).

methanol yield equals ~6 wt.%. Side product yields were very low (below 1.4 wt.%) during the whole test, which provided for extremely high selectivity of the monooxygenase reaction (curve 4). The rate of methane hydroxylation increases with temperature, reaching a maximum at 180 °C, whereas the catalase reaction rate noticeably decreases to the minimum.

The existence of temperature optimum (kinetic curve 2, Figure 7.26) can be explained by deactivation processes, which reduce the part of really active catalytic sites. Hence, despite deactivation of a significant part of iron protoporphyrin complexes, catalase activity is preserved. Apparently, a much smaller amount of redox catalytic site is enough for H_2O_2 dissociation in this temperature range.

Kinetic curves displaying the influence of contact time (τ) on methane hydroxylation with hydrogen peroxide are shown in Figure 7.27.

As follows from the above, at short contact times (below 2.9 s) the monooxygenase activity of the mimic remains low, whereas catalase activity is maximal (molecular oxygen yield exceeds 90 wt.%). Methanol yield and methane conversion increase with contact time up to τ = 10 s and then stabilize at a level of 49–50 wt.% with ~96% selectivity. Formaldehyde and formic acid are side products, giving total 2.7 wt.%; no CO and CO_2 are detected in gaseous products.

The curve of O_2 accumulation shows that short contact times, at which the methane oxidation rate is low, are enough for complete H_2O_2 dissociation. However, as observed from shapes of O_2 and CH_3OH accumulation curves, methanol yield increases synchronously with O_2 yield decrease, and from the moment τ = 10.2 s both curves stabilize. Such stabilization and synchronization of catalase and monooxygenase reaction product yields is the experimental proof of their interaction, displayed by chemical conjugation. The existence of the stabilization zone of O_2 and CH_3OH yields is associated with full H_2O_2 dissociation.

The change of reagent molar ratio (CH_4:H_2O_2) due to aqueous H_2O_2 flow rate increase and its effect on methane conversion is shown in Figure 7.28. It is the author's opinion that

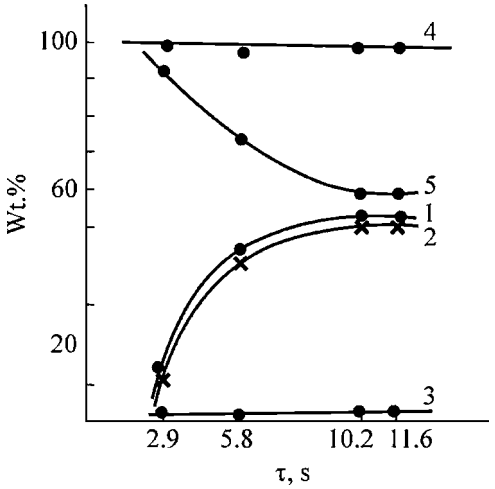

Figure 7.27 Dependencies of methane hydroxylation product yields on contact time. $T = 180\,°C$; $CH_4{:}H_2O_2 = 1{:}1.8$; $[H_2O_2] = 20$ wt.% (1: CH_4 conversion; 2: CH_3OH yield; 3: CH_2O and HCOOH yield; 4: selectivity and 5: O_2 yield).

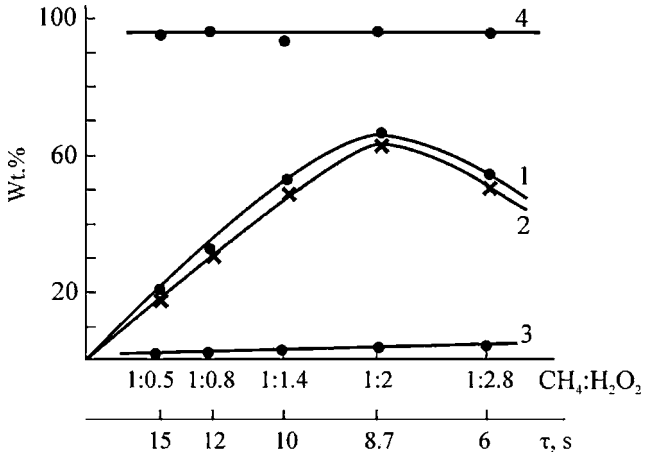

Figure 7.28 Dependencies of methane hydroxylation product yield on the molar ratio (1: CH_4 conversion; 2: CH_3OH yield; 3: CH_2O and HCOOH yield; 4: selectivity and 5: O_2 yield).

maxima observed on curves at 1:2 ratio is caused by simultaneous H_2O_2 concentration growth and contact time decrease in the reaction system. The interference of these two factors and partial deactivation of the catalyst causes the occurrence of a maximum on kinetic curve of methane hydroxylation.

To preserve the contact time $\tau = 10$ s, the molar ratio of reagents was varied by changing hydrogen peroxide concentration in the initial aqueous solution. Regularities observed from curves in Figure 7.29 can be explained in the framework of catalase and monooxygenase conjugation ideas (see above).

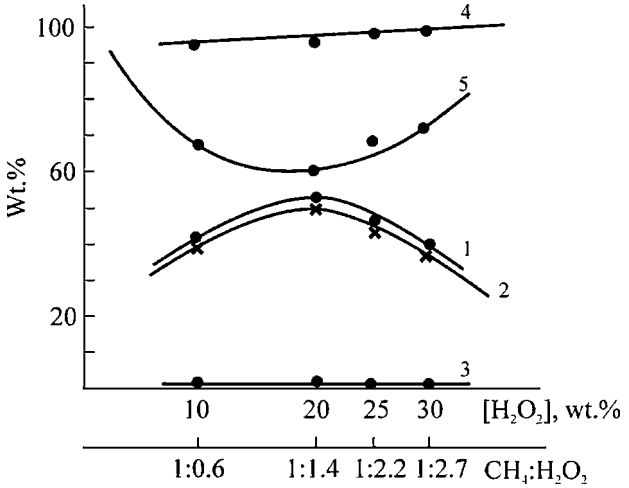

Figure 7.29 The effect of aqueous H_2O_2 concentration of CH_4 hydroxylation product yield (1: CH_4 conversion; 2: CH_3OH yield; 3: CH_2O and HCOOH yield; 4: selectivity and 5: O_2 yield).

Generalization of the experimental data lead to the conclusion that gas-phase oxidative activation of methane with hydrogen peroxide is highly effective in the presence of biomimic $PPFe^{3+}OH/AlSiMg$ in a limited time interval (high selectivity up to 97%, conversion exceeding 60 wt.%, relatively low temperature −180 °C, atmospheric pressure) [89].

The kinetic regularities observed lead to consideration of the hydroxylation mechanism in the context of modern ideas about enzymatic catalysis mechanism.

It is common knowledge that in enzymatic catalysis acidic–basic groups of the protein part of the enzyme enter the reaction with the enzyme prosthetic group. The mimic applied simulates monooxygenase function of hemin-containing enzyme cytochrome P-450, whereas the inorganic matrix (carrier) of the mimic performs acidic–basic catalytic functions of the protein part of cytochrome. Therefore, for the purpose of designing the process mechanism, acidic–basic parameters of the carrier and the mimic $PPFe^{3+}OH/AlSiMg$ were studied first with the help of the programmed thermal desorption method [90]. Acidic sites were detected with the help of NH_3 thermal desorption from the sample surfaces. Basic sites were detected by thermal desorption of CO_2 (adsorption temperature equals 25 °C, heating rate is 35 °/min in the range between 25 and 600 °C [84]).

The study of acidic sites on aluminum–magnesium silicate carrier has detected 'weak' (Broensted) and 'moderate' (Lewis) sites with thermal desorption maxima at $T_{max} = 200$ °C and $T_{max} = 400$ °C, respectively. The mimic $PPFe^{3+}OH/AlSiMg$ derived on the basis of this carrier possesses 'weak' sites only at $T_{max} = 250$ °C. The absence of 'moderate' acidic sites in the mimic indicates hematin adsorption from these mere sites, whereas 'weak' acidic sites of the carrier participate in the hydroxylation mechanism.

Basic sites of the inorganic matrix (carrier) manifest themselves in thermal desorption maxima at $T_{max} = 125$ °C and $T_{max} = 240$ °C ('weak' acidic sites). Besides the 'weak' sites of the carrier mentioned, the mimic displays an occurrence of a 'strong' basic site at $T_{max} = 415$ °C. Based on the results obtained one can conclude that the basic sites of adsorbed

hematin contribute to a strengthening of the hematin bonds with the surface, apparently, by the multisite adsorption mechanism.

The experimental data on acidic–basic sites of the mimic and ideas about the mechanism of biomimetic propylene hydroxylation with hydrogen peroxide have justified the probable mechanism of methane hydroxylation with hydrogen peroxide:

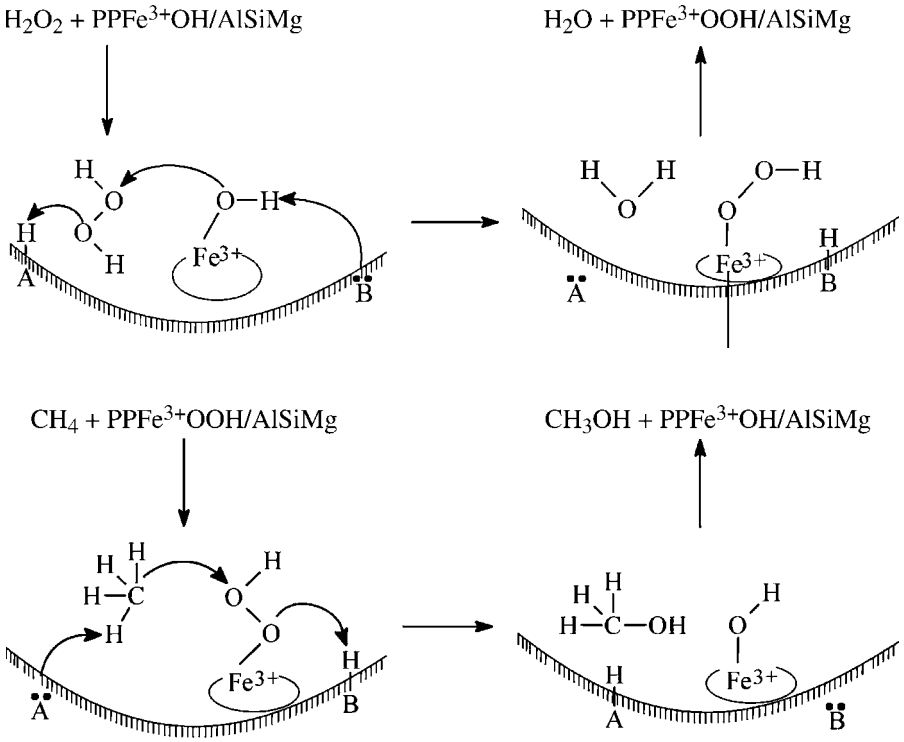

The above diagram shows A–H and B, which are acidic and basic sites, respectively. Arrows show electron transfer pathways.

According to the multisite mechanism shown, H_2O_2 heterolytically reacts with $Fe^{3+}OH$ and, with synchronous participation of acidic–basic sites of the carrier, forms a $PPFe^{3+}OOH$/AlSiMg intermediate. As interacted with methane, this intermediate forms a stable product of the catalytic cycle, methanol.

Thus, at the first stage of catalase reaction, hydroxide proton is transferred from $Fe^{3+}OH$ group to the Lewis basic site, which is accompanied by O—H bond break, electron transfer to oxygen atom, etc. At the second stage of methane hydroxylation, a proton is transferred from the Broensted acidic site of the matrix to oxygen in—OOH group of the ligand. This is accompanied by O—OH bond break and addition of OH fragment to carbon atom, from which, in turn, proton is detached with participation of the Lewis basic site of the matrix. The whole electron and proton transfer sequence in the bond redistribution system is performed simultaneously and needs no high energy consumption.

Thus, the reaction mechanism of monooxygenation (hydroxylation) consists of oxygen atom transfer from hydrogen peroxide molecule to CH_4 molecule by adding OH group to it and simultaneous proton transfer from methane molecule to the matrix. The well-known oxynoid mechanism of monooxygenation is not fulfilled.

$PPFe^{3+}OH/AlSiMg—H_2O_2—H_2O—CH_4$ is the two-substrate reaction system with two reactions proceeding:

$$\begin{aligned} PPFe^{3+}OH/AlSiMg + H_2O_2 &\xrightarrow{\text{fast}} PPFe^{3+}OOH/AlSiMg \\ + H_2O &\xrightarrow{H_2O_2} PPFe^{3+}OH/AlSiMg + O_2 + H_2O \end{aligned} \tag{7.13}$$

$$PPFe^{3+}OOH/AlSiMg + CH_4 \xrightarrow{\text{slow}} PPFe^{3+}OH/AlSiMg + CH_3OH \tag{7.14}$$

The oxidation mechanism should be interpreted in the context of the conjugated reaction theory. For this purpose, the overall equation of the methanol synthesis secondary reaction was deduced by combining the elementary stage of $PPFe^{3+}OOH/AlSiMg$ intermediate formation (7.13) and the elementary stage (7.14):

$$H_2O_2 + CH_4 \rightarrow CH_3OH + H_2O \tag{7.15}$$

The overall reactions (7.13) and (7.15) are implemented via general intermediate $PPFe^{3+}$ OOH/AlSiMg, which is the transmitter of the induction action of the primary (catalase) reaction on the secondary (monooxygenase) one. The determinant equation:

$$D = \nu\left(\frac{f_{A_1}}{f_{Acc}} + \frac{f_{A_2}}{f_{Acc}}\right)^{-1}$$

where f_{A_1} and f_{A_2} are the amounts of actor (currently, H_2O_2) consumed for final product synthesis in the primary (7.13) and the secondary (7.15) reaction, respectively; f_{Acc} is the acceptor (methane) consumption; ν is the stoichiometric coefficient, which allows quantitative identification of the interaction between reactions (experimentally obtained determinant value is $D = 0.48$), shows that reactions (7.13) and (7.15) are really conjugated, because on the chemical interference scale the value obtained lies in the chemical conjugation range ($D = 0 - \nu$, here $\nu = 1$).

Before we turn to kinetic modeling of the monooxygenase reaction, the following assumption should be made: the stage of $PPFe^{3+}OOH/AlSiMg$ complex formation is fast, and the stage of alcohol synthesis is slow, i.e. the limiting one.

Such a scenario of the kinetic task uses the Michaelis–Menten equation in Linuver–Berk coordinates to describe the methane hydroxidation reaction:

$$\frac{1}{r} = \frac{1}{r_{max}} + \frac{K_M}{r_{max}}\frac{1}{[S]} \tag{7.16}$$

where K_M is the Michaelis constant; r is the methane transformation rate; r_{max} in the maximum reaction rate and [S] is the current concentration of the substrate (methane).

Figure 7.30 shows dependencies of $1/r$ on $1/[S]$, which indicate a satisfactory description of plots from Figure 7.29 (with the exception of two points, corresponding to contact times equal 1.9 and 3.1 s) by equation (7.16). The high deviation of two points from the appropriate lines can be explained by the shortcomings of the Linuver–Berk equation, the use of which at low substrate transformations leads to overestimated values of r.

According to the data in Figure 7.30, Michaelis constants were determined for every temperature:

$$K_M = \frac{K_2 + K_{-1}}{K_1}$$

where K_1 and K_{-1} are rate constants of $PPFe^{3+}OOH/AlSiMg$ complex synthesis and degradation; K_2 is the rate constant of methyl alcohol synthesis.

Analysis of the K_M expression shows that under the condition $K_2 > K_{-1}$ the value $1\backslash K_M$ becomes the effective rate constant of the reaction. The values $K_{eff} = 1/K_M$ were calculated for two temperatures from the plot and using the Arrhenius equation the effective activation energy, E_{eff}, of the reaction was then determined (Table 7.6). The experimentally obtained

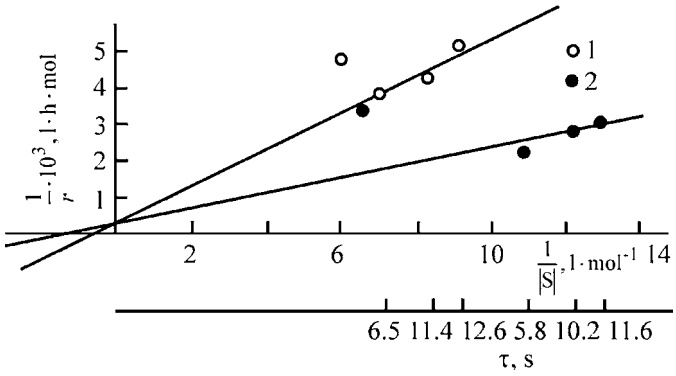

Figure 7.30 The Linuver–Berk plots for biomimetic methane hydroxidation with hydrogen peroxide.

Table 7.6

Kinetic parameters of methane hydroxidation with hydrogen peroxide

T (K)	K_M (exp.) (mol/l)	K_M (calc.) (mol/l)	K_{eff} (mol/l)	E_{eff} (kJ/mol)
423	1.25×10^{-2}	1.18×10^{-2}	0.08×10^3	49.2
453	0.48×10^{-2}	0.45×10^{-2}	0.21×10^3	49.2

$T = 180\,°C$; $\tau = 10.2$ s and $C_{H_2O_2} = 20$ wt.%.

E_{eff} value lies within the range of activation energy for enzymatic processes between 28 and 60 kJ/mol.

Thus, the adequate kinetic simulation of methane hydroxidation with hydrogen peroxide on $PPFe^{3+}OH/AlSiMg$ mimic, carried out with the help of the Michaelis–Menten equation, indicates high probability of the monooxygenation mechanism suggested [91].

Resonance Raman spectra of the synthesized $PPFe^{3+}OH/Al_2O_3$ were measured and interpreted [92]. Owing to moderate fluorescence of prepared samples (due to Al_2O_3 matrix), resonance Raman spectra were successfully composed. They are shown in Figure 7.31 for hemin chloride, $PPFe^{3+}OH/Al_2O_3$ catalyst (possessing 1% active mass) and its samples spent in the catalase reaction. Note that all samples of catalysts (distinguished by the number of adsorbed hematin) displayed identical resonance Raman spectra with a shift of heme oscillation frequencies in relation to free hemin chloride. Electron reflection spectra indicate a change of the electron ambience for the applied heme compared with the free one, which is confirmed by a change of resonance Raman spectrum intensities (*vide infra*) as a consequence of heme iron coordination change as it is fixed by the matrix. Resonance Raman spectra with π/σ -donor axial ligand in the Fe-site show that it can be AlO^- group of the aluminum oxide carcass [4]. In may be expected that injection of a π/σ-donor axial ligand (tyrosinate) to the Fe-site of the heme part of the catalase will cause charge accumulation on $d\pi$-orbitals of metal [π^--tyrosinate $\rightarrow d\pi$ (Fe)], which is reversibly transferred to free π^*-orbitals of porphyrin [$d\pi(\text{Fe}) \rightarrow \pi^*(\text{Por})$]. In turn, this may reduce porphyrin frequencies in the resonance Raman spectrum of the catalase [5]. As G. Turner suggests, an analogous phenomenon is also displayed in the case of catalase mimics. The characteristic frequencies of porphyrin ν_3 (1494 cm^{-1}) and ν_{10} (1629 cm^{-1}) are slightly underestimated compared with the appropriate frequencies of 1497 and 1632 cm^{-1} in the resonance Raman spectrum of unbound hemin chloride. Frequency ν_2 in the area of 1577 cm^{-1} is complicated by the contribution of other types of oscillations and cannot be precisely determined.

Thus, there appear to be analogies with the six-coordinate high-spin Fe(III) heme of the catalase with tyrosinate ligand [3]. The green color of Al_2O_3 with applied hemin chloride is transformed to yellow after the catalase reaction, and the resonance Raman spectrum of the spent sample indicates at least partial intactness of the heme part.

One of the difficulties appearing in the study of peroxide reactions in the presence of Fe(III) porphyrins in aqueous solutions is the deactivation of porphyrins resulting in aggregation and μ-oxydimer synthesis. The author believes that this problem is eliminated in the systems described [1], because PPFe(III) is monodisperse bound to the solid matrix. The ability of solid carrier to prevent aggregation and μ-oxydimerization itself does not provide for catalytic activity display. Similar systems [1], prepared by Fe(III) protoporphyrin fixation of carriers different from basic and neutral Al_2O_3 and silica gel, for example, acidic Al_2O_3 or cellulose, do not display even a slightly noticeable catalase activity.

The catalytic activity of hematin on the surface of alumina gel and graphitized carbon black has already been comprehensively studied by the adsorption method [93, 94]. It is shown that ‘at low filling degrees hematin molecules are placed flatly, and the iron atom contacts with the surface playing the role of the sixth ligand in this case.’ The deactivation process is associated with reorientation of the surface hematin molecule which induces iron bond break with the carrier and simultaneous formation of hematin dimer by sixth catalytically active coordinate position.

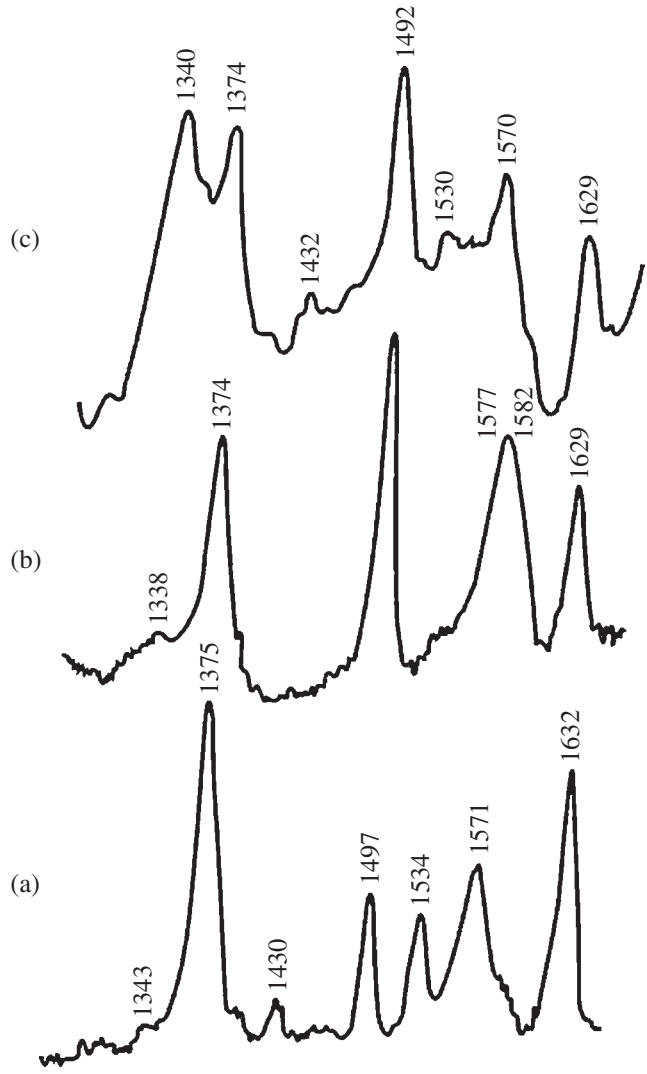

Figure 7.31 Resonance Raman spectra: (a) free hemin chloride, (b) 1% biomimic (catalyst) and (c) biomimic after reaction with H_2O_2. Soret band at 406.7 nm; laser power equals 80 mW and resolution is 2 cm^{-1}.

The studies of adsorbed hematin complex structure using the Mössbauer spectroscopy method made the selection of the adsorbed hematin structure by the author [94] more justified than in the case of the adsorbed method. Therefore, based on structural data the difference in catalytic activities of diluted and concentrated adsorptive hematin layers is justified in this work.

To prevent the poisoning action of hydrogen peroxide and catalyst life increase [51], the reaction system and the catalyst are added to by substances, i.e. stabilizers of the catalyst operation. They were: ionol, hydroquinone, diphenyl amine and diphenylguanidine.

The dependence of the catalase activity of $PPFe^{3+}OH/Al_2O_3$ catalyst on the stabilizers and methods of their injection to the reaction mixture was determined. Nevertheless, regardless of the method of injection, none of the stabilizers studied increased catalase activity of the initial iron protoporphyrin catalyst with the exception of diphenylguanidine.

Attempts were made to increase the catalase activity of synthesized hemin-containing catalysts by the thermoactivation method, where the time of thermal treatment and temperature were varied. The positive role of thermoactivation was observed: catalase activity and atomic catalytic activity (ACA) increased in activated samples and the growth of hemin-containing catalyst stability was observed (the lifetime increased almost 2-fold compared with inactivated samples) [88].

There are results [84] of the studies of acidic–basic properties of inorganic carriers and biomimics which, besides detection of the known single-site adsorption of iron(III) protoporphyrin, indicate for the first time a multisite type of hematin adsorption. The last process proceeds owing to Lewis acidic sites (moderately strong) of the carrier and hematin basic sites. The acidic–basic characteristics of biomimics and their carriers obtained in this work laid the foundation for the creation of a new heterogeneous catalytic system—cytochrome P-450 biomimics, which effectively catalyze methane hydroxylation to methanol with hydrogen peroxide. The main disadvantage of these heterogeneous catalysts is their low resistance to oxidative degradation and increased temperature in oxidation, which are typical of all porphyrin catalysts. In many aspects, this task was solved in the investigations described in the article [82]. It presents the technique of Fe(III) perfluorotetraphenylporphyrin synthesis and application on activated and neutral aluminum oxides. In the example of propylene epoxidation with hydrogen peroxide, stable monooxygenase catalyst activity was shown and kinetic regularities of substrate conversion in a broad range of reaction parameters were studied.

As can be seen from the works analyzed, modification of hemin-containing heterogeneous catalyst synthesis has been developed gradually. At present, catalysts obtained by the methods designed are being applied to complex production processes on pilot units and are approaching industrial use.

It has been suggested [95] that the synthesis of structured porphyrins with controllable steric ambience is a strategic direction in the reproduction of enzyme protein cavities, which control the selectivity and stability of biochemical reactions such as cytochrome P-450. Such an approach to the synthesis of biomimics has considerable potential, especially in their application on mineral matrices: silicon dioxide, alumina and zeolites. Data exist on the synthesis of a biomimic [96] with a complex porphyrin complex (5-pentafluorophenyl-10,15,20-tri(2,6-dichlorophenyl)porphyrin (FeMPFDCPP)) covalently linked to aminopropyl silicon dioxide, which is applied in oxidation of *cis*-cyclooctene, cyclohexene, cyclohexane and adamantane with participation of iodosylbenzene dissolved in dichloromethane.

Another method of MPFDCPP catalyst synthesis, applied in this work, was borrowed from Ref. [97]. All these catalysts displayed extremely high stability. Nevertheless, a large number of catalytic cycles was observed only at cyclooctene epoxidation. Thus, these

studies illustrate the great advantages of these catalytic systems, because they are able to regenerate, i.e. they are recyclable.

However, in the applied context, an inherent weakness of these systems is in the use of organic solvents and iodosylbenzene as the oxidant.

Iron porphyrin dimers, iron(III) μ-oxodimer iron(III) porphyrin, for example, are used as biomimetic models of oxidation catalysts [98]. It is shown that $[Fe(TFPP)]_2O$ and other modifications regioselectively oxidize adamantane and cyclohexane in the presence of iodosylbenzene (PhIO). Comparison of these results with corresponding monomeric analogs indicates the efficiency of the FeP dimer at the level of the monomeric one.

From the viewpoint of stability and resistance, the biomimics studied in Ref. [99] are also of interest.

The results of the catalytic activity of meso-*para*-carboxylphenyl and meso-*ortho*-nitrophenyl derivatives of iron(III) porphyrins in oxidation of *cis*-cyclooctene, cyclohexene and cyclohexane with iodosylbenzene. The source compounds were dissolved in dichloroethane or dichloroethane mixture with methanol:

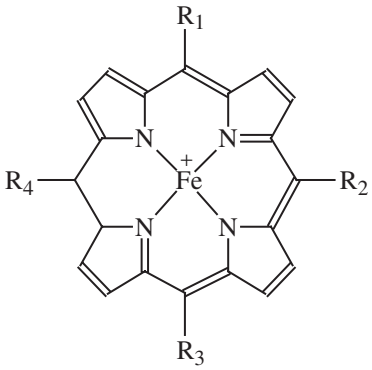

$Fe(TNMCPP)^+$ $R_1 = R_2 = R_3 = o\text{-}NO_2Ph$, $R_4 = p\text{-}COOHPh$
$Fe(DNDCPP)^+$ $R_1 = R_2(\text{or } R_3) = o\text{-}NO_2Ph$, $R_3(\text{or } R_2) = R_4 = p\text{-}COOHPh$
$Fe(MNTCPP)^+$ $R_1 = o\text{-}NO_2Ph$, $R_2 = R_3 = R_4 = p\text{-}COOHPh$

These iron porphyrin derivatives selectively catalyzed cyclohexane hydroxidation, where (FeTNMCPP)Cl displayed the higher stability. Cyclooctane epoxidation on the same mimic proceeded with multiple oxidant addition.

It is shown [100] that polyhalide derivatives of iron and manganese porphyrin catalysts applied on SiO_2 and polymeric matrices via their amino functional group were successfully synthesized.

This technique, the outstanding catalytic properties of ruthenium porphyrin systems, and the engineering advantages of heterogeneous catalysts were applied to the development [101] of polyhalide biomimic with 3-aminopropyl silica gel as the carrier:

This biomimetic catalytic system displayed high activity in hydrocarbon oxidation. For cyclohexane oxidation to cyclohexanol and cyclohexanone, the number of catalytic cycles

Ru catalyst =

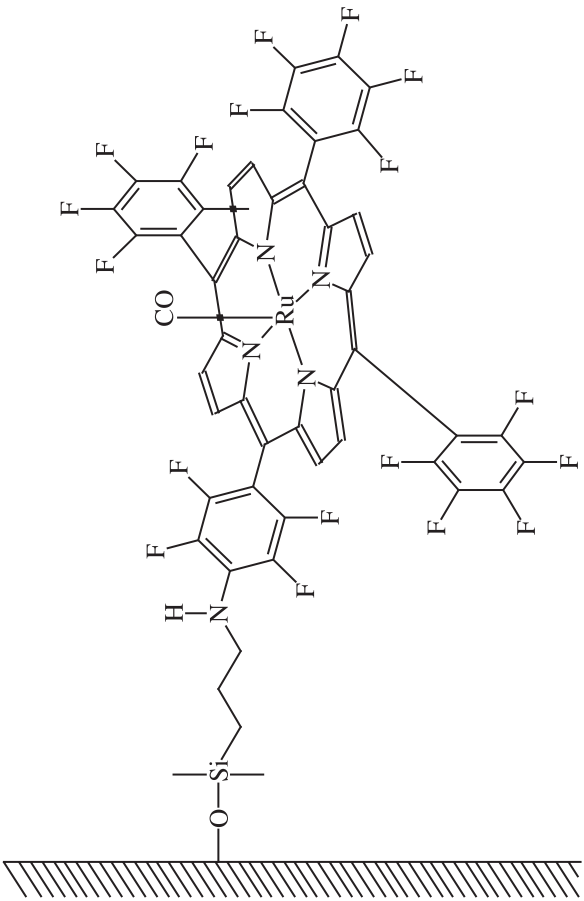

equals 2200–2800 which correlates with the homogeneous analog. The advantage of the heterogenized alternative, all other conditions being equal, consists of its manufacturability.

Perhalogenated ruthenium porphyrins are highly effective catalysts of low reactive substrate oxidation, implementing the process at high rate and selectivity under soft conditions, in the presence of 2,6-dichloropyridine N-oxide in aprotic medium [102]:

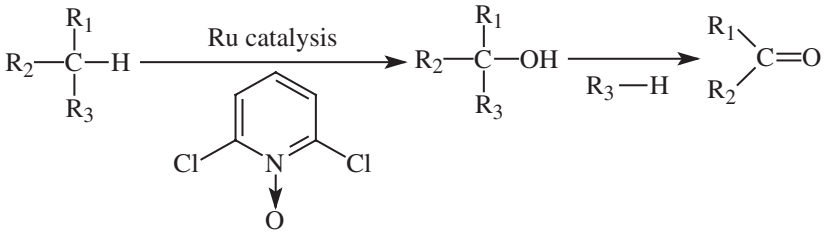

On the one hand, these catalytic systems display higher resistance to oxidative degradation and possess specific electron characteristics [103]. On the other hand, porphyrins with pentafluorophenyl functional groups possess the unique ability of replacing fluorine in the *para*-position by a nucleophilic substituting group [104]. The combination of the abovementioned properties allowed covalent addition of such catalytic systems to solid supports carrying nucleophilic groups.

With respect to the latest data obtained in biochemical studies, let us now discuss some questions about the importance of hydrogen peroxide for intracellular processes of the human organism. For example, an oxidation stress and the role of mitochondria in this event are discussed [105]. It is common knowledge that mitochondria are of dual performance: on the one hand, they provide for energy accumulation, required for vital activity of cells; on the other hand, they are active participants of the process leading to cell death. The case in hand is that resulting from their physiological activity and oxidative phosphorylation active oxygen particles—the side products of O_2 consumption process (respiration), are generated to the system. As shown in Chapter 3, H_2O_2 and $O_2^{\bullet-}$ represent aerobic respiration products, which are catalysts, unwillingly promoting hydroxide radical formation in the presence of transition metals. Glutathione (GSH) is the substance able to metabolize H_2O_2 (i.e. include it in the metabolism process), thus performing protective functions. A small part of its quantity in the cell is fixed in mitochondria on a carrier, which transports GSH from cytosol to the mitochondrial matrix. It is proved that mitochondria are sub-cellular targets for cytokines, which cause excessive production of active oxygen particles induced by the keramide-lipid intermediate of the cytokine action. Ethanol-saturated cells selectively release GSH in mitochondria due to insufficient functioning of the carrier responsible for GSH transportation from cytosol to mitochondrial matrix.

Normalization of GSH stable state levels in mitochondria opposes the oxidative stress induced by oxidative metabolism of ethanol.

The process of H_2O_2 metabolizing with the help of GSH indicates that, in spite of the common opinion about its harmfulness, it is the necessary (useful) component of the cell metabolism. This is a case of extremely complicated interaction of a number of synchronous enzymatic reactions. To perform a detailed kinetic study for the purpose of chemical

interference detection, sufficient quantitative data is required. *A priori* it may be reasoned that H_2O_2 as GSH reagent is activated in the primary reaction and consumed in the secondary (metabolic) reaction. The interaction between these synchronous reactions will provide for stable GSH concentration in the mitochondrial matrix and, therefore, affect the oxidative stress process.

Another case is associated with the role of H_2O_2 in apoptosis: the programmed cell suicide.

Recent data show that in processes of virus activation and apoptotic cell death neopterin acts owing to the presence of free oxygen radicals. In the case of AIDS, T-cell death is apparently induced by Fas/Fas ligand system, free oxygen radicals and 7,8-dihydroneopterin. Therefore, the kinetics and sensitivity of apoptotic Jurkat leukemia human T-cells were compared with these, treated by 7,8-dihydroneopterin, antiFas and H_2O_2. AntiFas-induced apoptosis increased with time up to a maximum. Combined incubation of 7,8-dihydroneopterin and H_2O_2 suppresses it. Inhibitors with antioxidant properties, such as pyrrolidinedithiocarbamate, significantly interlocked apoptosis induced by 7,8-dihydroneopterin, antiFas and H_2O_2. These results indicate that the cell death induced by these three substances may include transformation routes associated with the redox sensitivity of the system [106].

The mechanism of action of hydrogen peroxide in this process is still unclear. However, the intensification and deterioration of processes observed in the system may be explained by the ability of hydrogen peroxide to induce interference events in the system. Therefore, new tests and analysis of previous results in the context of the theory of chemical interference are required. Finally, such investigations aimed at decoding the mechanism of H_2O_2 will discover the true role of hydrogen peroxide in intracellular protective processes.

It is obvious that H_2O_2 is the intracellular component affecting processes in the cells such as protein phosphorylation, transcription and apoptosis. However, new peroxidases called peroxy redoxins (Prx) have recently been discovered. They regulate intracellular H_2O_2 concentration by its reduction in the presence of the appropriate electron donor. Prx crystalline structure of the human enzyme indicates protein containing two discrete domains and forming a dimer. Active site cysteine (Cys 47), shaped as a crystal of cysteine–sulfonic acid, is disposed at the bottom of a relatively narrow tub. The positively charged environment of Cys 47 stimulates peroxidase activity of the enzyme containing none of the redox co-factors [107]. The detection of human enzyme Prx shows how important it is to preserve H_2O_2 concentration at the physiological level.

It is suggested [108] that active oxygen particles may be involved in vascular tone regulation. This was experimentally proved by the H_2O_2 constricting action on isolated circular aortal areas in rats. The constricting effect of H_2O_2 was completely inhibited by catalase. It is the author's opinion that decoding the participation of H_2O_2 in the synchronization of biochemical processes will promote the determination of its true role in the human organism.

The disadvantages of recently synthesized model mimics as biocatalysts are discussed in the context of theoretical and applied studies [109]. In these works an attempt was made to simulate the functions of natural enzymes on extremely small peptides. However, catalysts biomimics giving interesting biological results were obtained infrequently. Owing to the discovery of catalytic RNA, this idea is now alternatively developed in the branch of gene engineering and hybridome technology.

Synthesis chemists were very inventive when they were developing effective peptide catalysts simulating definite properties of modeled enzymes. Despite a series of successful syntheses of biomimics, their action rate and selectivity were much worse than those of natural biocatalysts.

Our modern understanding of the biocatalyst modeling problem is divided into the following categories [109]:

1. entropic effects of enzyme–substrate complexes and substrate immobilization;
2. diluter elimination from the active site cavity;
3. bond energy transformation;
4. model system supply with catalytically active groups of modeled enzymes;
5. electronic 'adjustment' of the active site.

All categories are interrelated and represent very important components of the enzyme structure.

The comprehensive study of physicochemical features of the enzyme mechanism [110] led to the fundamental conclusion that, in the main, the so-called 'small peptides' may hardly approach the effectiveness and selectivity of natural enzymes.

These works were first performed with the aim of artificially obtaining as full an enzyme model as possible. Initially, the modern level of scientific knowledge was insufficient for achieving this; moreover, it should be remembered that Nature designed the enzyme for functioning under physiological conditions. Any attempt at its use as a catalyst outside physiological systems will fail. Thus, everything hinges on the intended objective. If the aim is to create an artificial enzyme simulating the appropriate natural enzyme as fully as possible, the goal is a long way off. However, if we intend to synthesize real, highly effective catalysts to be applied in many branches of science and industry, this is an achievable task. It is already under consideration in the branch of biomimetic chemistry and displays noticeable results for many technological applications. Simulation catalysis resolves similar tasks in the framework of catalysis, which is the intermediate between enzymatic and general catalyses.

Therefore, enzyme simulation using short peptides must aim at reproduction of useful functions only. They should not be adjusted to the operation mode of polypeptides (biocatalysts). To put it another way, efforts should be aimed at the synthesis of catalytic biomimics simulating corresponding enzyme action with 'non-full' parameters. It is the author's opinion that this approach will help to resolve the dead-end direction of using peptides as the main construction material.

It is common knowledge that nitroxides are effective antioxidants acting as protectors against oxidative damage in various pathological processes. It has been proved experimentally that stable nitroxide radicals manifest themselves as SOD mimics. They catalyze $O_2^{\bullet -}$ dismutation by two different routes, including redox reaction mechanisms. In these studies it is important to distinguish stoichiometric interaction and $O_2^{\bullet -}$ catalytic detoxication. For this purpose, kinetic analysis and direct ESR study of the interaction between nitroxide and $O_2^{\bullet -}$ were used. In the presence of NADH, the ESR signal of nitroxide decayed, but did not decrease with time. This proves nitroxide catalytic role in $O_2^{\bullet -}$ dismutation.

The rate constants of $O_2^{\bullet-}$ catalytic dismutation, determined for the nitroxides tested, increased with $[H^+]$, indicating that $\dot{O}OH$, but not $O_2^{\bullet-}$ oxidizes nitroxide:

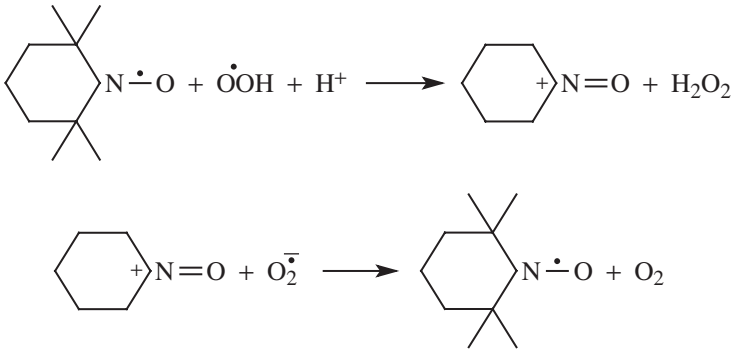

Therefore, pyridine derivatives are easily oxidized to $\dot{O}OH$ giving an ammonium cation. In the presence of the cation NADH induces full and rapid ESR signal loss as a consequence of two-electron reduction of intermediate oxo-ammonium compound to its cyclic hydroxylamine:

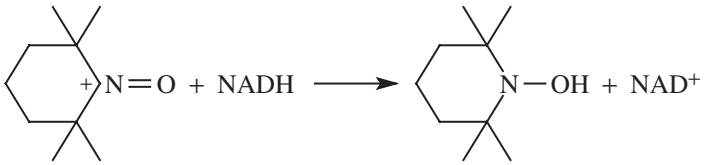

There is an uncommon feature of the SOD enzyme that distinguishes it from the other enzymes: its substrate is formed from free radicals and, therefore, its physiological concentration exceeds the substrate concentration by several orders of magnitude.

Stable nitroxide radicals represent SOD mimics with k_{cat} values over 10^7 m/s at pH 6 and, therefore, are capable of a strong influence on $O_2^{\bullet-}$ concentration in cells and tissues. Thus, it provides for effective detoxication.

Nitroxide simulation of the catalase-like activity of iron porphyrins is also considered [112].

The ability of stable nitroxide radicals to neutralize highly valent iron proteins, such as ferryl myoglobine ($MbFe^{IV}$), formed in the reactions between myoglobine ($MbFe^{III}$) and H_2O_2, was estimated by control of O_2 release, H_2O_2 consumption and redox changes in the heme prosthetic group. $MbFe^{III}$-catalyzed H_2O_2 consumption and O_2 release were accelerated by stable nitroxides. Reduction of $MbFe^{IV}$ to $MbFe^{III}$ was the decelerating stage. Nitroxide concentration excess over $MbFe^{III}$ increased the catalase-like activity by 4 times or higher. The presence of NADH induced:

(a) inhibition of H_2O_2 dissociation;
(b) rapid nitroxide reduction to corresponding hydroxide amine.

When NADH is consumed, O_2 release and the initial nitroxide concentration are restored. When transferring between two oxidized states of myoglobine ($MbFe^{III}$ and $MbFe^{IV}$), nitroxide and oxo-ammonium cation manifest catalase-mimetic activity of $MbFe^{III}$, hence, promoting $O_2^{\bullet}$ dismutation accompanied by O_2 release and protecting from highly valent iron proteins:

$$MbFe^{III} + H_2O_2 \rightarrow {}^{\bullet}MbFe^{IV}_{=0} + H_2O$$

The lifetime of the oxyferryl complex is minutes or even hours. Obviously, this reaction may not be simple, because oxyferryl myoglobine particle formation must be accompanied by a complex H_2O_2 molecule transformation. It is common knowledge that H_2O_2 never emits O_2 atom on decomposition. This happens only in the case where fixed highly active intermediates formed from it are capable of releasing oxygen atom.

The role of nitroxide in the system is in promoting catalytic cycle intensification. In this context, the interaction between reactions is indicated. Apparently, they interfere with one another, but this aspect of the problem requires more a comprehensive kinetic study of the whole system.

There is no doubt that these works promote wider investigations in the branch of heterogeneous catalysis of gas- and liquid-phase reactions using porphyrin-containing heterogeneous catalytic systems.

The synthesis of new heterogeneous catalysts derived from synthetic porphyrins is, without doubt, a profitable direction and one that will find an increasingly wide application in future.

Biological processes and their most suitable models display a heterolytical mechanism, which transforms the substrate without formation of highly reactive intermediates. In fact, this provides for exclusively high selectivity. Further development of works on biomimic synthesis with the specified properties must be based on the well-known abilities of porphyrins to purposefully change catalytic properties with respect to the origin of the central metal atom, substituting groups in the porphyrin ring and axial ligand. Usually, the presence of axial ligands causes a significant effect on the complexing ability of the metal ion, on which electron transfer to the oxidant depends. The works discussed form a good basis for widening investigations in the branch of heterogeneous catalysis of gas- and liquid-phase reactions in porphyrin-containing heterogeneous catalytic systems.

Based on the entire set of data on the important catalytic performance of this class of organic compounds in chemical and biological systems, the far-reaching conclusion can be made that biomimics will provide a foundation for catalysis chemists to solve future applied tasks of catalysis. In particular, it is the author's opinion that the unique properties of porphyrins will open new perspectives for chemical technology in the creation of highly effective chemical production.

REFERENCES

1. Nagiev, T.M., *Chemical Conjugation*, Nauka, Moscow, 1989, 216 p. (in Russian).
2. Dugat, G. and Peeney, K., *Bioorganic Chemistry*, Mir, Moscow, 1983, 512 p. (in Russian).

3. Breslow, R., Biomimetic chemistry in oriented systems, *Internet J. Chem.*, 1980, Vol. 18, pp. 187–191.
4. Breslow, R., Biomimetic chemistry, *Chem. Soc. Rev.*, 1972, Vol. 1, pp. 553–580.
5. Fife, T.H., Intramolecular nucleophilic attack on esters and amides, In: *Bioorganic Chemistry*, Vol. 1, Ch. 5, Ed. E.E. Van Temelen, Academic Press, New York, 1977, pp. 93–116.
6. Wharton, C.W., Synthetic polymers as models for enzyme catalysis—a review, *Int. J. Biol. Macromol.*, 1979, Vol. 1, pp. 3–16.
7. Breslow, R., Biomimetic control of chemical selectivity, *Accounts Chem. Res.*, 1980, Vol. 33, pp. 170–177.
8. Imanishi, Y., Intramolecular reactions on polymer chains, *J. Polym. Sci. Macromol. Rev.*, 1979, Vol. 14, pp. 1–205.
9. Lehninger, A., *Biochemistry*, Mir, Moscow, 1976, 957 pp. (in Russian).
10. Guthrie, J.P., Application of biochemical systems in organic chemistry, In: *Techniques of Chemistry Series*, Vol. 10, Pt. 2, Ch. 3, Eds J.B. Jones, C.J. Sih and D. Perlman, Wiley-Interscience, New York, 1976, pp. 627–730.
11. Sussman, J., Harel, M. and Frolow, F., *Science*, 1991, Vol. 253, No. 5022, p. 872.
12. Shilov, A.E., *Izv. AN SSSR*, *Ser. Khim.*, 1990, No. 10, p. 2407 (in Russian).
13. Poltorak, O.M. and Chukhrai, E.S., *Physicochemical Bases of the Enzymatic Catalysis*, Vysshaya Shkola, Moscow, 1971, 336 pp. (in Russian).
14. Poltorak, O.M., *Catalysis*, Izd. MGU, Moscow, 1987, p. 7 (in Russian).
15. Traylor, T.G., *Pure Appl. Chem.*, 1991, Vol. 63, No. 2, p. 266 (in Russian).
16. Momontean, M., *Ibid.*, 1986, Vol. 58, p. 1493.
17. Traylor, T.G., *New Aspects of Organic Chemistry*, Kodansha Ltd., Tokyo, 1989, p. 509.
18. Collman, J.P., Brauman, J.J., Iverson, B.L. *et al.*, *J. Am. Chem. Soc.*, 1983, Vol. 105, p. 3052.
19. Mispelter, J., Momentean, M., Lavalette, D. and Lhoste, J., *Ibid.*, 1983, Vol. 105, p. 5165.
20. Groves, J.T., Nemo, T.E. and Myers, R.S., *Ibid.*, 1979, Vol. 101, p. 1032.
21. Chang, C.K. and Kuo, M.S., *Ibid.*, 1979, Vol. 101, p. 3413.
22. Tabushi, I., *Coordin. Chem. Rev.*, 1988, Vol. 86, p. 1.
23. Ortiz de Montellano, P., *Cytochrome P-450: Structure, Mechanism and Biochemistry*, Plenum Press, New York, 1986.
24. Bruce, T.C., *Mechanistic Principles of Enzyme Activity*, Vol. 9, VCH Publishers, New York, 1989, p. 50.
25. Groves, J.T., Haushalter, R.C., Nakamura, M. *et al.*, *J. Am. Chem. Soc.*, 1981, Vol. 103, p. 2884.
26. Penner, H.J.E., Smith, E.K., McMurry, T.J. *et al.*, *Ibid.*, 1986, Vol. 108, p. 7819.
27. Sugimoto, H., Tung, H.S. and Sawyyer, D.T., *Ibid.*, 1988, Vol. 110, p. 2465.
28. Arasasingham, R.D., Balch, A.L., Cornman, C.R. and Lates-Grazynski, L., *Ibid.*, 1989, Vol. 111, p. 4357.
29. Groves, J.T. and Wanatabe, Y., Ibid., 1988, Vol. 110, p. 8443.
30. Traylor, T.G. and Ciccone, J.P., *Ibid.*, 1989, Vol. 111, p. 8413.
31. Traylor, T.G. and Xu, F., *Ibid.*, 1990, Vol. 112, p. 178.
32. Traylor, T.G., Lee, W.A. and Stynes, D.V., *Ibid.*, 1984, Vol. 106, p. 755.
33. Ortiz de Montellano, P.R., Beilan, H.S. and Kunze, K.L., *J. Biol. Chem.*, 1981, Vol. 256, p. 6708.
34. Collman, J.P., Hampton, P.D. and Brauman, J.J., *J. Am. Chem. Soc.*, 1990, Vol. 112, p. 2986.
35. Ostovic, D. and Bruice, T.C., *Ibid.*, 1989, Vol. 111, p. 6531.
36. Labeque, R. and Marnewtt, L.S., *Ibid.*, 1989, Vol. 111, p. 6621.
37. Traylor, T.G. and Mikstal, A.R., *Ibid.*, 1989, Vol. 111, p. 7443.
38. Poulos, T.L., Freer, S.T., Alden, R.A. *et al.*, *J. Biol. Chem.*, 1980, Vol. 255, p. 575.
39. Vadnstein, V.K., Melik-Adamyan, W.R., Barynin, V.V. *et al.*, *J. Mol. Biol.*, 1986, Vol. 88, p. 49.
40. Labeque, R. and Marnett, L., *Biochemistry*, 1988, Vol. 27, p. 7060.
41. Dixit, P.S. and Srinivasan, K., *Inorg. Chem.*, 1988, Vol. 27, p. 4507.
42. Battioni, P., Lalier, J.P., Barloy, L. and Mansuy, D., *J. Chem. Soc. Commun.*, 1989, No. 16, pp. 1149–1151.
43. Robert, A., Loock, B., Momentean, M. and Meunier, B., *Inorg. Chem.*, 1991, Vol. 30, p. 706.
44. Traylor, T. and Tsuchiya, Sh., *Ibid.*, 1987, Vol. 26, p. 1338.
45. Traylor, P.S., Dolphin, D. and Traylor, T.G., *J. Chem. Soc. Commun.*, 1984, No. 5, pp. 279–280.

46. Tsuchiya, Sh. and Seno, M., *Chem. Lett.*, 1989, No. 2, pp. 263–266.
47. Nagiev, T.M., *Vestnik MGU, Ser. 2, Khim.*, 1990, Vol. 31, No. 3, p. 237 (in Russian).
48. Poltorak, O.M., *Ibid*., 1971, Vol. 12, No. 6, p. 239 (in Russian).
49. Poltorak, O.M. and Chukhrai, E.S., *Ibid*., 1971, Vol. 12, No. 6, p. 639 (in Russian).
50. Veselova, M.N., Chukhrai, E.S. and Poltorak, O.M., *Ibid*., 1970, Vol. 11, No. 1, p. 14 (in Russian).
51. Nagiev, T.M., Zul'fugarova, S.Z. and Shikhiev, Yu.M., *Ibid*., 1992, Vol. 33, No. 2, p. 134 (in Russian).
52. Nagiev, T.M., Zul'fugarova, S.Z. and Shikhiev, Yu.M., *Ibid*., 1991, Vol. 32, No. 6, p. 587 (in Russian).
53. Likhtenstein, G.I., *Redox Enzymes and Their Models*, Pt. 1, Chernogolovka: Nauka, Russia, 1982, p. 7 (in Russian).
54. Nagiev, T.M., Nagieva, Z.M. and Mustafaeva, Ch.A., *Neftekhimia*, 1991, Vol. 31, No. 5, p. 67 (in Russian).
55. Alimor, P.A., *Catalysis and Inhibition of Chemical Reactions*, Mir, Moscow, 1966, p. 386 (in Russian).
56. Skibida, I.P., *Usp. Khim.*, 1975, Vol. 44, No. 10, pp. 1729–1747 (in Russian).
57. Nagiev, T.M., *Usp. Khim.*, 1985, Vol. 54, No. 10, pp. 1654–1673 (in Russian).
58. Spiro, T.G., *Iron Porphyrin*, Pt. 2, Eds A.B.P. Lever and H.B. Gray, Addison-Wesley, Reading, MA, 1983, pp. 89–160.
59. Fita, I. and Rossmann, M.G., *J. Mol. Biol.*, 1985, Vol. 185, pp. 21–37.
60. Poulos, T.L. and Kraunt, J., *J. Biol. Chem.*, 1980, Vol. 225, pp. 8199–8205.
61. Deno, N.G., Peterson, H.J. and Saines, G.S., *Chem. Rev.*, 1960, Vol. 60, pp. 7–15.
62. Adams, P.A., Baldwin, D.A., Hepner, C.E. and Pratt, J.M., *Bioinorg. Chem.*, 1978, Vol. 9, pp. 4789–4794.
63. Nagiev, T.M., *Vestnik MGU, Ser. 2, Khim*., 1984, Vol. 25, No. 3, pp. 254–258 (in Russian).
64. Traylor, T.G. and Xu, F., *J. Am. Chem. Soc.*, 1987, Vol. 109, pp. 6201–6202.
65. Bruice, T.C., Zipplies, M.F. and Lee, W.A., *Proc. Natl. Acad. Sci. USA*, 1986, Vol. 83, pp. 4646–4649.
66. Cook, B.R., Reinert, T.J. and Suslick, K.S., *J. Am. Chem. Soc.*, 1986, Vol. 108, pp. 7281–7286.
67. Karasevich, E.I., Khenkin, A.M. and Shilov, A.E., *Doklady AN SSSR*, 1987, Vol. 295, No. 3, pp. 639–643.
68. Brault, D. and Neto, P., *J. Am. Chem. Soc.*, 1981, Vol. 103, pp. 2705–2710.
69. Darr, D., Zarilla, K.A. and Fridovich, I., *Arch. Biochem. Biophys.*, 1987, Vol. 258, pp. 351–355.
70. Harriman, A., Christensen, P.A., Porter, G. *et al.*, *J. Chem. Soc. Faraday Trans.*, Pt. 1, 1986, Vol. 82, pp. 3215–3231.
71. Herron, N., Stuckey, J. and Tolman, C.A., *J. Chem. Soc. Commun.*, 1986, Vol. 108, pp. 1521–1522.
72. Herron, N. and Tolman, C.A., *J. Chem. Soc. Commun.*, 1987, Vol. 109, pp. 2837–2839.
73. Romanovsky, B.V. and Zakharov, A.N., *Catalysis*, Izd. MGU, Moscow, 1987, pp. 125–146 (in Russian).
74. Haggin, J., *Chem. Eng. News*, September 28, 1987, pp. 27–28.
75. Nagiev, T.M., Nagieva, Z.M. and Tagieva, Sh.A., *Vestnik MGU, Ser. 2, Khim.*, 1986, Vol. 27, No. 6, pp. 564–568 (in Russian).
76. Polkovnikova, A.G. and Ivanova, L.A., *Khim. Prom.*, 1966, No. 1, pp. 16–19 (in Russian).
77. Nagiev, T.M., Nagieva, Z.M. and Tagieva, Sh.A., *Vestnik MGU, Ser. 2, Khim.*, 1987, Vol. 28, No. 1, pp. 42–46 (in Russian).
78. Nagieva, Z.M., Nagiev, T.M. and Mustafaeva, Ch.A., *Vestnik MGU, Ser. 2, Khim.*, 1990, Vol. 31, No. 4, p. 356 (in Russian).
79. Nagiev, T.M., Nagieva, Z.M. and Mustafaeva, Ch.A., *Neftekhimia*, 1991, Vol. 31, No. 5, p. 67 (in Russian).
80. Shetdon, R.A., *Rev. Trav. Chim.*, 1973, Vol. 92, pp. 253–259.
81. Berezin, I.V. and Klesov, A.A., *Practical Course of Chemical Enzyme Kinetics*, Izd. MGU, Moscow, 1976, p. 298 (in Russian).
82. Nagiev, T.M., Gasanova, L.M., Zul'fugarova, S.Z. and Mustafaeva, Ch.A., *Zh. Fiz. Khim.*, 1996, Vol. 70, No. 11, pp. 2063–2068 (in Russian).

83. Nagiev, T.M., *Zh. Fiz. Khim.*, 1996, Vol. 70, No. 6, p. 967 (in Russian).
84. Abbasova, M.T., Zul'fugarova, S.Z., Shakhtakhtinskaya, A.T., Mamedova, Z.M. and Nagiev, T.M., *Vestnik MGU, Ser. 2, Khim.*, 1997, Vol. 38, No. 1, pp. 42–44 (in Russian).
85. Tsuchida, E., Honda, K. and Sato, H., *Biopolymers*, 1974, Vol. 13, No. 10, p. 2147 (in Russian).
86. Nagiev, T.M. and Gasanova, L.M., *Zh. Fiz. Khim.*, 1997, Vol. 71, No. 7, pp. 1216–1219 (in Russian).
87. Zul'fugarova, S.Z., *The Influence of Cracking Catalyst Synthesis Conditions on Their Physicochemical Properties*, Baku, 1957, p. 127 (in Russian).
88. Nagiev, T.M., Abbasova, M.T. and Zul'fugarova, S.Z., *Vestnik MGU, Ser. 2, Khim.*, 1995, Vol. 36, No. 6, p. 538 (in Russian).
89. Nagiev, T.M. and Abbasova, M.T., *Zh. Fiz. Khim.*, 1997, Vol. 71, No. 7, pp 1220–1224 (in Russian).
90. Yakerson, V.I. and Rosanov, V.V., *Physical Chemistry. Kinetics*, VINITI, Moscow, 1974, Vol. 3, p. 114 (in Russian).
91. Nagiev, T.M. and Abbasova, M.T., *Vestnik MGU, Ser. 2, Khim.*, 1999, Vol. 40, No. 1, pp. 18–21 (in Russian).
92. Nagiev, T.M., Zul'fugarova, S.Z. and Abbasov, A.A., *Azerb. Khim. Zh.*, 1998, No. 1, pp. 62–67 (in Russian).
93. Veselova, M.N., Chukhrai, E.S. and Poltorak, O.M., *Vestnik MGU, Ser. 2, Khim.*, 1969, Vol. 8, No. 6, p. 106 (in Russian).
94. Perfil'ev, Yu.D., Babeshkin, A.M., Veselova, M.N. *et al*., *Vestnik MGU, Ser. 2, Khim.*, 1973, Vol. 14, No. 1, p. 100 (in Russian).
95. Bedoui, F., *Coordin. Chem. Rev.*, 1995, Vol. 144, p. 39.
96. Assis, M.D. and Lindsay Smith, J.R., *3rd World Congress on Oxidation Catalysis*, San Diego, CA, September 21–26, 1997, Abstracts 1, 2–8.
97. Lindsey, J.S. and Wagner, R.W., *J. Org. Chem*., 1989, Vol. 54, p. 828.
98. Iamamoto, Y., Assis, M.D., Ciuffi, K.J., Sacco, H.C., Iwamoto, L., Melo, A.J.B., Nascimento, O.R. and Prado, C.M.C., *J. Mol. Catal. A Chem.*, 1996, Vol. 109, pp. 189–200.
99. Assis, M.D., Iwamoto, L.S., Iamamoto, Y. and Schiavan, M.A., *3rd World Congress on Oxidation Catalysis*, San Diego, CA, 1997, September 21–26, 1997, Abstract 1.
100. Battoni, P., Bartoli, J.F., Mansuy, D., Byun, S. and Traylor, T.G., *J. Chem. Soc. Commun.*, 1992, Vol. 15, pp. 1051–1053.
101. Shalyaev, K.V. and Groves, J.T., *3rd World Congress on Oxidation Catalysis*, San Diego, CA, September 21–26, 1997, Abstract 1.
102. Groves, J.T., Bonchio, M., Carofiglio, T. and Shalyaev, K.V., *J. Am. Chem. Soc.*, 1996, Vol. 118, pp. 8961–8962.
103. Lyons, J.E. and Elis, P.E., Catalytic Systems with Higher Resistance to Oxidative Degradation In: *Metalloporphyrins in Catalytic Oxidation*, Ed. R. Sheldon, Marcel Dekker, New York, 1994, pp. 297–324.
104. Kadish, K.M., Araullo-MsAdams, C., Han, C. and Franzen, M.M., *J. Am. Chem. Soc.*, 1990, Vol. 112, pp. 8364–8868.
105. Fernandes-Checa, J.C., Garcia-Ruiz, C., Colell, A., Morales, A., Mari, M., Miranda, M. and Ardite, E., *Biofactors*, 1988, Vol. 8, No. 1–2, pp. 7–11.
106. Wirleitner, B., Bair-Bitterlich, G., Bock, G., Widner, B. and Fuchs, D., *Biochem. Hearmacol.*, 1998, Vol. 59, No. 9, pp. 1181–1187.
107. Choi, H.J., Kang, S.W., Yang, C.H., Rhec, S.G. and Ryn, S.E., *Nat. Struct. Biol.*, 1998, Vol. 5, No. 5, pp. 400–406.
108. Yang, Z.W., Zheng, T., Zheng, A., Altura, B.T. and Altura, B.T., *Eur. J. Pharmacol.*, Vol. 334, No. 2–3, 1997, pp. 169–181.
109. Corey, M.J. and Corey, E., *Proc. Natl. Acad. Sci. USA*, 1996, Vol. 93, pp. 11428–11434.
110. Matthews, B.W., Craik, C.S. and Neurath, H., *Proc. Natl. Acad. Sci. USA*, 1994, Vol. 91, pp. 4103–4105.
111. Krishna, M.C., Russo, A., Mitchell, J.B., Goldstein, S., Dafni, H. and Samuni, A., *J. Biol. Chem. USA*, 1996, Vol. 217, No. 42, pp. 26026–26031.
112. Krishna, M.C., Samuni, A., Taira, J., Goldstein, S., Mitchell, J.B. and Russo, A., *J. Biol. Chem. USA*, 1996, Vol. 217, No. 42, pp. 26018–26025.

– 8 –

Enzymatic Biosensors and Their Biomimetic Analogs: Advanced Analytical Appliances

Construction principles and the mechanism for biosensors derived from enzymes. Combined enzymatic and electrochemical reactions proceeding on electrodes from various materials in electrolyte solutions promote development of many biosensor types for detection of glucose, amino acids, lactose, urea, pyruvate and other metabolites. Biosensors are successfully applied to environmental contamination control, medical diagnostics and the food industry.

Electrochemical system, an intermediate between bio- and chemio-sensors is developed.

Physicochemical fundamentals of construction and action of catalase- and peroxidase-biomimetic sensors are studied.

One of the most promising hi-tech directions is bio-electronics, a branch originating from the two apparently different fields of electronics and biochemistry.

Initially, analytical appliances called biosensors were developed which essentially represented the first generation of bio-electronic appliances.

Let us define biosensors: they are analytical devices, which owing to biological substances 'distinguish' separate compounds and provide quantitative estimations via electric signals.

Clark and Lyons [1] have primarily suggested a model of electrochemical sensor, based on the concept of an enzyme heterogenized on the electrode surface.

The analysis of biological fluids, blood, in particular, consisting of thousands of substances, is of interest for sensor technologies.

The creation of particular biosensors was motivated by the need for rapid qualitative and quantitative detection of the required ingredient. For example, the detection and analysis of glucose in the blood of patients with diabetes is of vital importance. Therefore, the contribution of biosensors to the rapid analysis of metabolites in human organisms, and in a broader sense, the chemical composition of any object, is now so valuable that they have revolutionized public health services.

The construction principle of any biosensor type is based on the use of two functionally different components (Figure 8.1): a bioselective membrane (a bioselector representing a biologically active, immobilized material) and a physical converter of the chemical signal (a transducer). The bioselector is applied directly to the transducer surface, which transforms

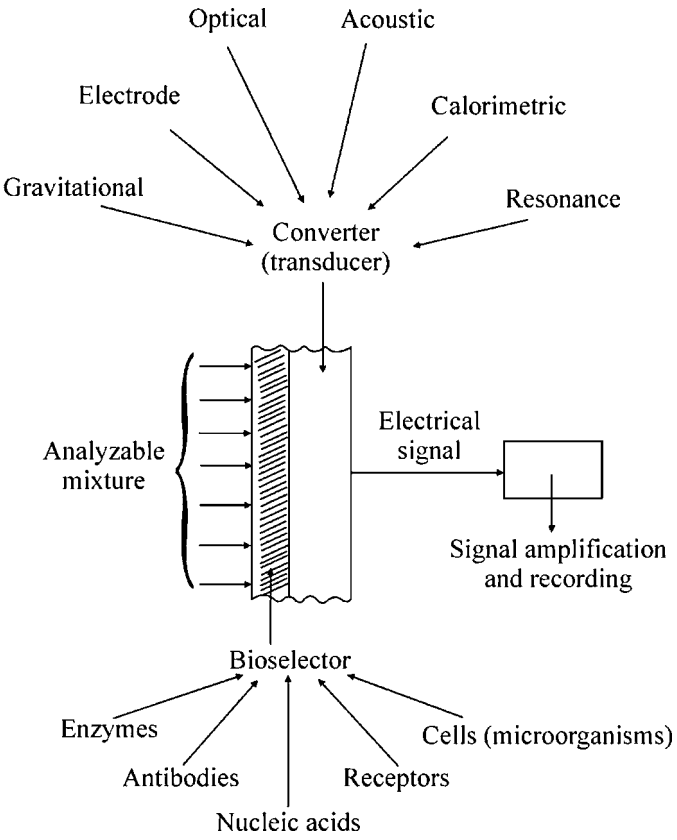

Figure 8.1 Conceptual sketch of a biosensor.

the biochemical signal to an electrical or optical signal. The physical parameter of this signal depends on the concentration of the substance analyzed in the sample.

Bioselecting structures comprise two functionally different groups:

1. those possessing catalytic properties: enzymes, cells and tissues;
2. biological materials of the affine type: antibodies, receptors and nucleic acids.

At the present time, transducers are most often electrochemical converters: electrodes (ammeter, pH meter and conductometers), various optical, calorimetric and acoustic converters. The existing variety in biosensor types is formed by varying bioselective structures with different transducers. Note that enzyme and cell biosensors are the most widespread.

Any type of biosensor can operate either stationary or kinetically. This circumstance adds more variety to biosensor appliances. Stationary operation of biosensors is stipulated by the existence of diffusion-limiting stages, at which the biochemical activity of the selector has no effect on the stability of signal decoding from the detected substance.

The kinetic mode of bioselector operation is employed when the sensitivity of the analysis depends on the activity of the biological material (i.e. on the biochemical reaction), but not on the diffusion stages of the process. Put more simply, this means that the biochemical reaction rate is limited by the substrate transformation process, but not by its transportation to the bioselector.

A transducer is selected with respect to the features of the biochemical reaction. In ammetering transducers, constant potential applied to the reference electrode and the current generated in the redox transformation of the electrochemically active compound present on the enzymatic electrode surface is measured. Electron transfer rate is controlled by increasing or reducing the potential drop between electrodes.

pH metering transducers determine the potential drop between active and reference electrodes in cases of zero current.

Semiconductor (transistor) biosensors are widely used. They possess a several process advantages over the others: small size, good reproducibility and high sensitivity, multipurpose chip design, accessibility and low price.

Bioselective membranes are mostly upgraded not by searching for new biological materials, but via modification of currently existing ones.

At present, the problems of monitoring the state of the environment are at the heart of the development of biosensor technologies.

It shall be assumed that most biosensors are designed on the basis of enzymatic working elements. In fact, two consecutive reactions proceed in such electrochemical systems: first is the enzymatic reaction, which generates electrochemically active compounds to the system; this compound acts as an intermediate or a final product of the reaction (a mediate). These compounds then enter the electron transfer reaction with conducting material.

The phenomenon of bioelectrical catalysis with direct electron transfer from electrode to enzyme active site was primarily observed in the study of electrochemical oxygen reduction in the presence of a copper-containing oxidase – laccase, adsorbed on electrodes of different origins. This work was developed with peroxidase and hydrogenase application as the working components [2].

Thus, many biosensors have been designed for the detection of glucose, lactate, pyruvate, urea, bilirubin, amino acids, sugar and other metabolites. In many cases, ammeter or pH meter measurements for enzymatic electrodes are implemented.

The most demonstrative example of detection is the operation of widespread biosensors for glucose with participation of glucose oxidase:

$$\text{glucose} + O_2 \xrightarrow[\text{glucose oxidase}]{} \text{gluconolactone} + H_2O_2 \rightarrow \text{glyconic acid}$$

The concentration of analyzed substance (glucose) in this electrochemical system is determined by recording the O_2 or H_2O_2 reduction current. The design of many commercial biosensors is based on these alternatives. It should be noted that enzymes adsorbed on a solid surface preserve their structure and activity.

The phenomenon of H_2O_2 synthesis as an intermediate product of substrate biooxidation with the participation of many oxidases has formed the foundation for the creation and development of many biosensors possessing immobilized peroxidase as the active substance [3].

In general, electrochemically realized biological processes, in which the central place is devoted to H_2O_2 synthesis and dissociation reactions, can be presented as follows:

$$\text{S (glucose, amino acids)} + O_2 \xrightarrow[\text{oxidase}]{} S' + H_2O_2$$
$$H_2O_2 \xrightarrow[\text{peroxidase}]{} H_2O + 2\bar{e}$$

As a rule, the combined immobilization of oxidase and peroxidase on the electrode allows the determination of metabolite (S) concentration, even if negligibly small. This type of biosensor is the main one used for detection of any particular compound in blood or other multicomponent system: glucose, ethanol, cholesterol, proteins, amino acids, etc. For example, for patients with diabetes a rapid analysis of their blood for glucose concentration is a vitally important procedure. We will not attempt to discuss in full all the existing types of biosensor; we will just note that enzymatic and cell biosensors are the most widespread types of these appliances. Enzymatic biosensors are more appropriate to the subject of the current monograph and, therefore, they will be discussed below.

This system is also used for detection of supertoxins and chemical war gases based on organophosphorous compounds, responsible for the blocking of acetyl cholinesterase in the central nerve system. The system of enzymatic reactions used for the brief analysis of such substances is the following [4]:

$$\text{acetylcholine} \xrightarrow[\text{acetyl cholinesterase}]{} \text{choline} + \text{acetic acid}$$
$$\text{choline} \xrightarrow[\text{choline oxidase}]{} H_2O_2 + \text{oxycholine}$$
$$H_2O_2 \xrightarrow[\text{peroxidase}]{} H_2O + 2\bar{e}$$

The catalytic activity of acetyl cholinesterases is inhibited by GB (sarin), GD (soman), Vx, and the majority of pesticides used in agriculture. The inhibition effect immediately causes a reduction of the peroxidase electric current. Biosensor sensitivity is 10^{-12} M of neurotoxin. High sensitivity and substrate specificity of sensors based on biological systems make them irreplaceable as applied measuring devices. Unfortunately, their high sensitivity to environmental impacts, short operation time and high price are the main disadvantages of the biological systems. If the active component of biosensors (biopolymers) is replaced by their chemical analogs, i.e. biomimics which are now being developed in the framework of mimetic catalysis [5], the majority of these and other disadvantages can be eliminated.

8.1 CATALASE-BIOMIMETIC SENSORS

Biomimetic analogs of existing enzymatic biosensors have been designed with broader functional abilities using inorganic biomimics, which is one of the strategic directions in the branch of super-sensitive analytical systems. The development of model systems is the

only means of succeeding in this direction. Following achievements in mimetic catalysis, biomimetic electrodes of the catalase, peroxidase and monooxygenase type have been effectively designed [5].

For example, phenol oxidation [6] was implemented with the help of immobilized catalase monomer. It has been proved experimentally that catalase monomers are stable and possess high activity at pH 3.02, when usual peroxidases become inactive. This capability of heterogenized catalase monomers may be used for the construction of biochemical electrodes for biosensors.

Additional sufficient capabilities also occur as a result of the chemical conjugation mechanism, on which the overwhelming majority of enzymatic reactions are based. There is a firm belief that, in principle, a sequence of conjugated chemical processes can be selected for any reagent, starting from the substance to be detected and ending with an active product of enzymatic reaction. To put it another way, the corresponding enzymatic electrode may always be prepared.

Figure 8.2 shows an electrochemical system – a model of a catalase-biomimetic sensor, consisting of the reference electrode (Ag/AlCl/Cl^-) and biomimetic electrode. In this system, the electrochemical potential changed as a result of mimetic electrode interaction with

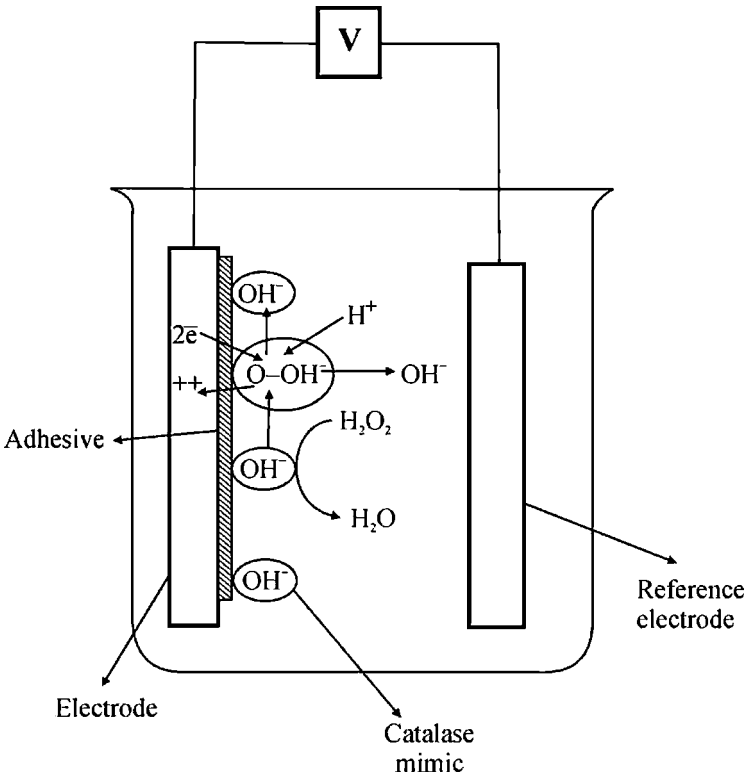

Figure 8.2 Catalase-mimetic electrochemical cell.

H_2O_2 injected into the system. Initially, the system potential is measured in twice distilled water (the background solution) and then, as a definite amount of H_2O_2 is added, a change of aqueous H_2O_2 potential is observed.

Biomimetic electrode was prepared according to two techniques:

1. inorganic biomimic-catalase adhesion to aluminum foil;
2. based on the active fragment of catalase (the most complicated way to obtain the working element of biomimetic sensor).

In order to obtain a fragment of catalase, it was immobilized by adsorption on various organic and inorganic carriers (such as aluminum oxide, diasorb DEAE, agarose), with further trypsine treatment. Aluminum wire or foil was used as the electrode. Such electrodes were selected because of their low price and inertness in relation to hydrogen peroxide. The binding agent between the electrode and biomimic was *Pattex* adhesive and 7.5% polyacrylamide gel.

Inorganic mimic of catalase was prepared according to the well-known technique [5]. Partly purified catalase of human blood erythrocytes and trypsine (Sigma Company) were used for the catalase sources.

To obtain the active site of the biomimic, consisting of an enzyme fragment with a prosthetic group, catalase preparation was treated by dialysis with 0.1 M potassium-phosphate buffer (pH 7.0) in the ratio 1:10 during 18 h at 4 °C. It was first centrifuged then equal (by weight) quantities of various carriers (aluminum oxide, diasorb DEAE) were added and incubated, being continuously mixed, for 24 h at 4 °C. This method of adsorptive immobilization provides for a more uniform filling of the carrier surface with the adsorbed enzyme.

Enzyme immobilized on the carrier was multiply rinsed from nonsorbed protein in distilled water then 0.2 M tris–HCl buffer (pH 8.0) was added to deposits and, finally, treated by 0.025% trypsine in 1:1 ratio during 1 h at 37 °C. When hydrolysis was finished, the deposit was washed in distilled water and dried on a filtering paper at room temperature.

A biomimetic sensor was created with electrodes from aluminum wire (2 mm thick) and aluminum foil (size $20 \times 10 \times 1$ mm), to which the working element was applied by two methods:

1. on an adhesive covering the electrode with a thin layer;
2. mixed with adhesive.

The change of electrode potential (E) of the catalase reaction with time was measured by a voltmeter. pH and E values for aqueous hydrogen peroxide were determined simultaneously for possible correlations between pH metric and potentiometric results of enzymatic activity of catalase-biomimetic sensors. The electrochemical unit was also equipped with a magnetic mixer.

For the purpose of determining low hydrogen peroxide concentrations, the authors have designed the most cost-effective and simple to use potentiometric-biomimetic sensors based on immobilized catalase mimics. These sensors possess high hydrodynamic properties and the fastest speed of response. Figure 8.3 shows experimental data on catalase activity of biomimetic electrode in 0.03% aqueous H_2O_2. For the sake of comparison, catalase activities of aluminum electrode and aluminum electrode with applied adhesive are also shown.

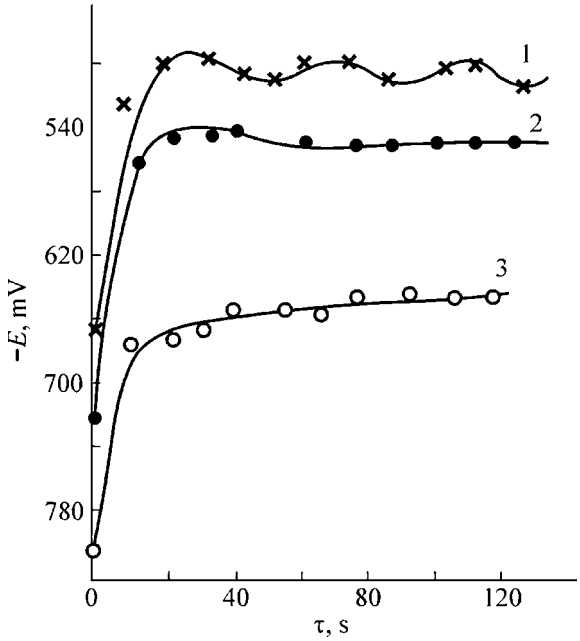

Figure 8.3 Time dependence of electrochemical potential in the system. $T = 20\,^{\circ}C$, 0.03 wt.% H_2O_2 (1: biomimetic electrode; 2: aluminum electrode; 3: aluminum electrode with applied adhesive).

In all three cases (Al, Al with applied adhesive and biomimetic electrode), as observed from Figure 8.3, the presence of hydrogen peroxide in the system causes an initial sharp increase of the system potential. This is most likely associated with the formation of a new surface layer at the electrode–solution interface. Some time later an equilibrium surface layer is formed and the potential at Al–solution and Al–adhesive–solution barely changes. Refractometric analysis shows that Al does not cause dissociation of H_2O_2 at low concentration of the latter, whereas electrochemical potential in biomimetic electrode–H_2O_2–Cl^-–AgCl–Ag system continues changing to almost full H_2O_2 dissociation (Figure 8.2). Dissociation of H_2O_2 was tested by solution titration with potassium permanganate.

According to the author's ideas and experiments, the following reactions are implemented in electrochemical system:

Catalase reaction

$$2H_2O_2 \xrightarrow{\text{biomimic}} 2H_2O + O_2 \tag{8.1}$$

Electrochemical reaction

$$O_2 + 4\bar{e} + 2H^+ \xrightarrow{\text{electrode}} 2OH^- \tag{8.2}$$

It is common knowledge that hydrogen peroxide is a soft dibasic acid. Therefore, catalase activity of biomimetic electrodes may change the pH of the H_2O_2 solution by both

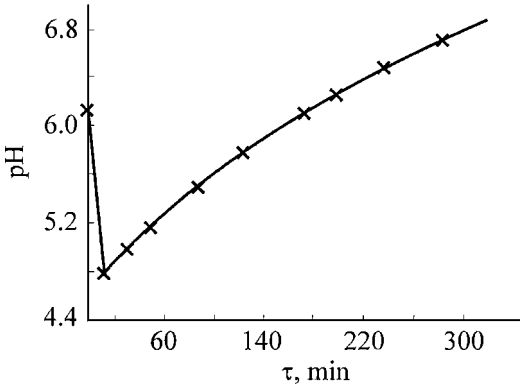

Figure 8.4 Time dependence of pH for aqueous H_2O_2 dissociation. $T = 20\,^{\circ}C$, 0.01 wt.% H_2O_2.

reactions (8.1) and (8.2). If these reactions take place on the biomimetic electrode, at the end of the process the pH of the solution will equal the pH of the distilled water.

For the purpose of determining H_2O_2 dissociation mechanism on the electrode, the authors followed up the pH variation dynamics in the system until complete hydrogen peroxide dissociation. Some time after the start of the process the course of the curve in Figure 8.4 indicates a pH higher than for redistilled water (background solution) approaching 7. Titration by $KMnO_4$ showed that a trace concentration of hydrogen peroxide below the sensitivity of biomimetic electrode still remained in the solution.

The fact that the pH of the reaction mixture exceeds the value for redistilled water testifies to the implementation of both reactions (8.1) and (8.2) in the system. Note that in the absence of reaction (8.2) and full H_2O_2 dissociation, the pH observed for the solution must correspond to the pH of the redistilled water (6.2).

These data present an experimental proof of process (8.1) and (8.2) run on the biomimetic electrode and the consequences:

1. A definite quantity of oxygen molecules accumulated on the surface of the biomimetic electrode (catalase reaction) must diffuse to the volume of the adhesive layer, toward the electrode surface. Hence, the specific requirements to the adhesive follow: on the one hand, it must provide strong enough adhesion of a mimic to electrode; on the other hand, it must possess low oxygen adsorption ability.
2. The adhesive must be highly inert in the catalase reaction.
3. OH^- anions, formed in electrode reaction (8.2), must display higher adsorption ability to the adhesive.
4. The exclusive role of surface oxygen in electrochemical reaction (8.2).

The additional experimental proof of the last statement is given by data in Figure 8.5. Curve (a) shows the change of pH and potential in the 'mimetic electrode–H_2O_2–Cl^-–AgCl–Ag' system. Curve (b) shows the results of tests carried out for the mimic applied on the electrode surface. According to these data, the potential abruptly decreases in the system, whereas curve (a) indicates its increase.

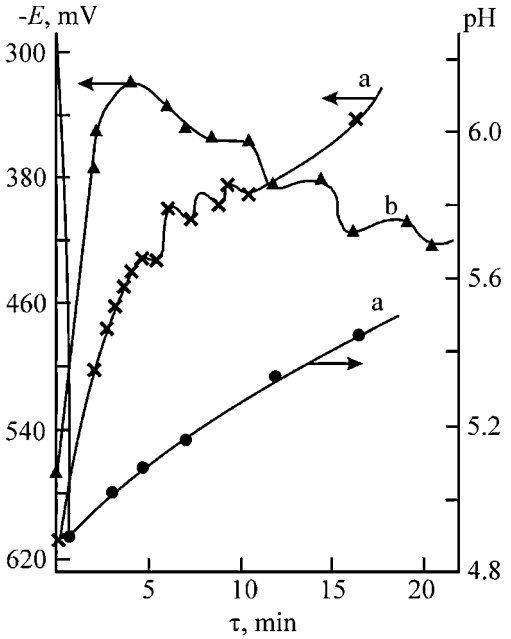

Figure 8.5 Time dependence of electrochemical potential in the system and aqueous H_2O_2. pH: $T = 20\,°C$, 0.01 wt.% H_2O_2 (a: biomimic is adhered to aluminum foil; b: biomimic is present in aqueous H_2O_2).

With regard to the above, of special interest are test results for unmixed system (in all other experiments the system was mixed by a magnet mixer). It turns out that part of the molecular oxygen synthesized in the catalase reaction (8.1) releases from the solid, and forms a gas 'cover' around the mimetic electrode in the interface layer between the solid and the reaction mixture. This circumstance will decelerate H_2O_2 diffusion to the biomimetic electrode and decrease the rate of the catalase reaction (8.1), hence promoting electric potential drop. Most of these hindrances can be eliminated by mixing the reaction system. The efficiency of the system mixing is illustrated by data in Figure 8.6.

Although mixing of the solution reduces the diffusion effect on the course of the catalase reaction, a special experiment must be set up to determine the predominance of one of two possible limitations of diffusion and kinetic origin. For this purpose, knowing that the diffusion rate is almost independent of temperature in the system and the chemical reaction rate increases with temperature by 2–4 times for every 10 K, the temperature influence on the change of potential and pH in the system was studied. The results of the experiments are presented in Figure 8.7. The pH curves are practically unchanged, although the temperature of the mixture was twice increased. Such regularity is typical of reactions proceeding under diffusion complication conditions, where the catalase reaction rate is limited by diffusion (i.e. depends on H_2O_2 delivery to and elimination from the mimetic electrode), but not by kinetics of the catalase reaction. Apparently, electrochemical indices deteriorate as a consequence of an increase in the molecular oxygen desorption rate in the volume

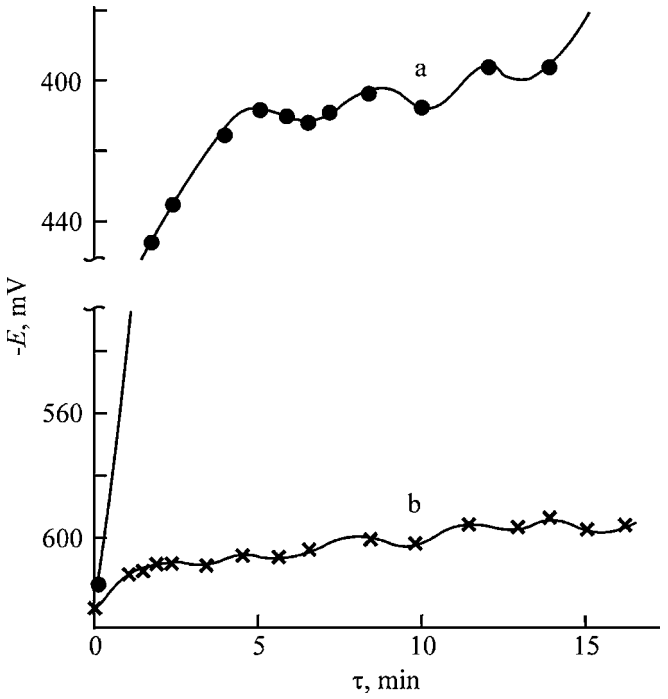

Figure 8.6 The mixing effect on the change of electric potential in the system. $T = 20\,^{\circ}C$, 0.01 wt.% H_2O_2 (a: mixed system; b: without mixing).

which reduces the rate of electrochemical reaction (8.2). It is also probable that temperature causes any other effect on the physical conditions of the electrode.

In all Figures electrochemical potentials possess clear maxima and minima. Such curve shapes conform to the shape for catalase and electrochemical reactions in the diffusion zone of the system. As mentioned above, molecular oxygen accumulated on the surface of the mimetic electrode during catalase reaction (8.1) diffuses through the adhesive and mimic layers to the electrode surface, where it is activated and interacts with H^+. Anions OH^- formed in this process may set the electrode surface free for the next portion of oxygen by diffusion only. Thus, the rate of electrochemical reaction (8.2) will be defined by the ratio of the rates of molecular oxygen diffusion to the electrode surface and reverse diffusion of OH^- anions from the surface.

The maxima observed on E curves correspond to the highest rates of electrochemical reaction (8.2), which are functions of O_2 concentration on the electrode, testifying to its highest values under current conditions. During reaction (8.2) the O_2 concentration decreases and the rate of electrochemical reaction (8.2) is reduced simultaneously. It begins increasing as soon as a new portion of molecular oxygen reaches the electrode surface, set free from OH^- anions. Finally, this catalytic process connected to diffusion events will have a sinusoidal shape until H_2O_2 is fully dissociated, and the reaction is terminated.

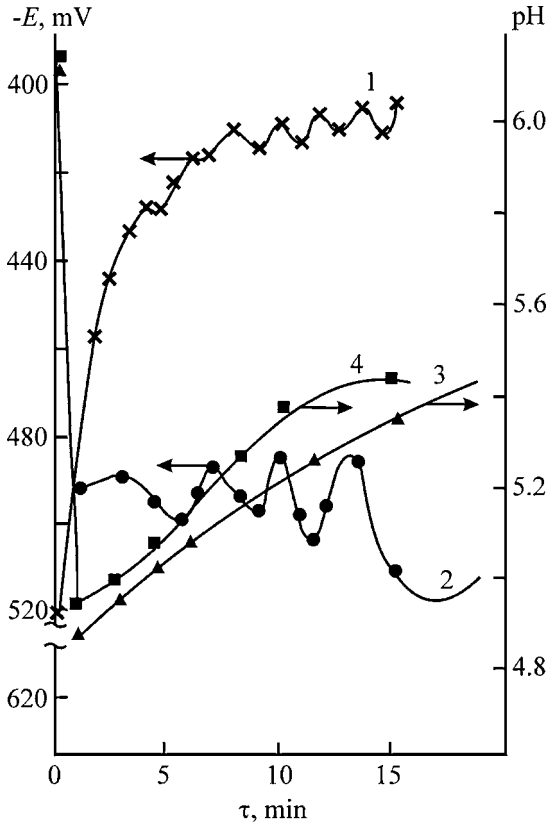

Figure 8.7 Temperature dependencies of electrochemical potential (1, 2) and pH (3, 4) at 20 °C (1, 3) and 40 °C (2, 4); 0.01 wt.% H_2O_2.

Based on the analysis of the obtained experimental regularities of the electrochemical process, it may be fundamentally concluded that the process at electrode displays a self-oscillation mechanism. Obviously, self-oscillations happen due to internal diffusion of the surface components of the mimetic electrode, which is not affected by solution mixing intensity. Mixing causes a strong influence on the external diffusion and OH^- anion drainage from the interface layer.

The suggested mechanism of catalase-biomimetic electrode operation is shown in Figure 8.8. As observed from the figure, the mechanism consists of several stages. At the first stage a hydroperoxide active particle is formed, which is responsible for electron transfer from cathode to iron ion with further redistribution of it. As a result, in the final stage hydroxide anions are generated to the volume (the reaction mixture), and the biomimic is regenerated simultaneously. This mechanism clearly indicates the reaction manner in which the pH increases to a value exceeding the distilled water level (pH 6.2) in the system.

Biomimetic sensors, prepared from catalase adsorbed on diasorb and Al_2O_3, treated with trypsine and adhered to an aluminum electrode surface using 7.5% polyacrylamide gel of

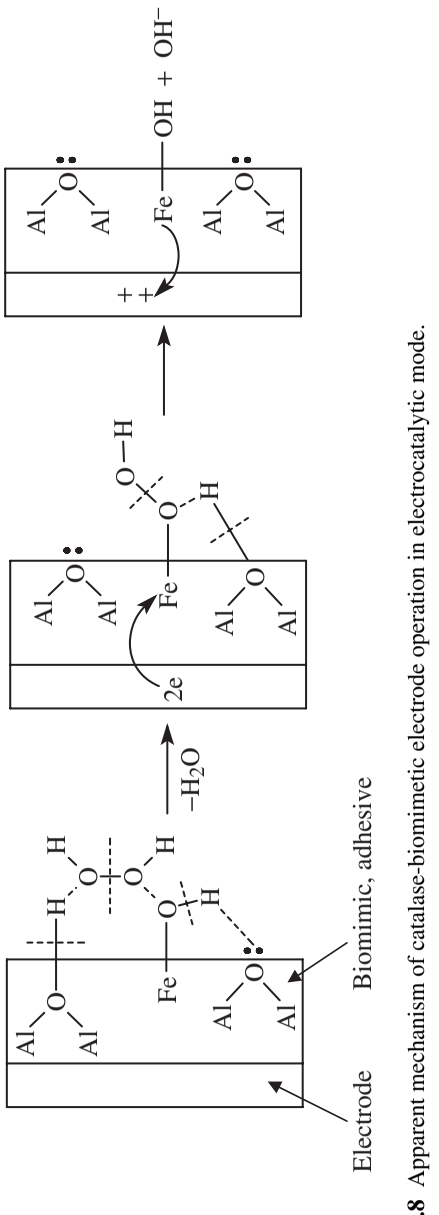

Figure 8.8 Apparent mechanism of catalase-biomimetic electrode operation in electrocatalytic mode.

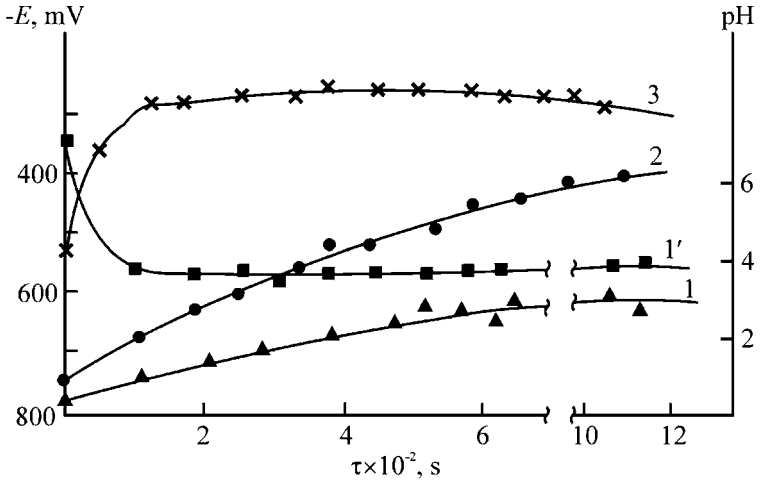

Figure 8.9 Time dependencies of electrochemical potential (1–3) and pH of aqueous H_2O_2 (1′) in the system. $T = 20\,^{\circ}C$, 0.06 wt.% H_2O_2.. Catalase is adsorbed on diasorb (1, 1′) or Al_2O_3 (2, 3), treated by trypsine and adhered to aluminum foil with 7.5% polyacrylamide gel (1, 1′, 2) or *Pattex* (3).

Pattex adhesive, were found to be the most effective sensors among appliances of this type (Figure 8.9). These biomimetic sensors are distinguished by high hydrodynamic properties, operation stability and rapid speed of response. A tendency to an increase of the electrode potential is observed for biomimetic sensors, derived from catalase adsorbed on diasorb (without trypsine treatment), agarose (treated with trypsine and without it), and adhered to an aluminum electrode surface by 7.5% polyacrylamide gel. It is also observed for biomimetic sensors, derived from catalase adsorbed on diasorb (without trypsine treatment), Si_2O_3 (treated with trypsine and without it), and adhered to aluminum electrode surface by *Pattex* adhesive.

Biomimetic sensors, prepared by catalase adsorption on diasorb and agarose (treated with trypsine) and adhered to an aluminum electrode surface by *Pattex* adhesive, displayed an abrupt decrease of the electrode potential. Sensors prepared by catalase adsorption on Al_2O_3 (without trypsine treatment) and adhesion to the aluminum electrode with *Pattex* adhesive displayed a high oscillation of the electrode potential, which induces extreme instability of the operation. Hence, it should be noted that sensor operation was always better in the case of enzyme treatment with trypsine.

When the carrier is selected, aluminum oxide should be preferred, because biomimetic sensors on it display higher characteristics (Figure 8.9). Moreover, they are low in price, long lived and stable, and possess high hydrodynamic properties.

Pattex adhesive combines well with such carriers as Al_2O_3 and Si_2O_3, but is absolutely useless for agarose and diasorb.

Thus, two reactions (catalase and electrochemical) are implemented in the biomimetic electrode–H_2O_2–Cl^-–AgCl–Ag system. In the case of inorganic support, it is not the kinetic but the diffusion (external and internal) factor that is predominant, owing to which the electrochemical reaction is of a self-oscillation type [7, 8].

8.2 PEROXIDASE-MIMETIC SENSOR FOR DETECTION OF ETHANOL IN LOW CONCENTRATIONS IN AQUEOUS SOLUTIONS

At the present time, qualitative and quantitative determination of lower aliphatic alcohols, e.g. a mixture of methanol with ethanol, is being performed with the use of enzymatic and enzyme-based biosensor methods [9, 10].

The investigations of catalase-mimetic sensors allow continuation of studies in the field of biomimetic sensors of peroxidase type.

As shown below, the basic principles of peroxidase-mimetic sensor appliance operation are developed using the example of model peroxidase reaction of ethyl alcohol electrochemical oxidation to aldehyde.

Studies on ethanol trace detection in aqueous solutions were carried out in an electrochemical cell of peroxidase-mimetic sensor of the potentiometric type, consisting of a reference electrode (Ag/AgCl) and a biomimetic electrode. Redistilled water was used for the background solution. The biomimetic electrode was prepared by adhering hematin-containing meroxidase mimetic to aluminum foil with *Pattex* adhesive [7, 8].

The peroxidase mimetic and its enzymatic analog consist of two components: active and carrying. The carrier represents neutral activated aluminum oxide, on which active site (hematin with 8.6 wt.% iron), produced by Sigma Company, is applied [11, 12]. The biomimetic was synthesized according to the known technique.

The peroxidase mimetic electrode was studied as follows: redistilled water (the background solution) potential was measured first, then the required quantity of C_2H_5OH was added, and the electrode potential change was observed. After that a definite quantity of H_2O_2 (oxidant) was added to the solution, and the change of electrochemical potential was observed. The potential of the electrochemical system was changed as a result of coherent–synchronous reactions (catalase and peroxidase) proceeding in it. The potential drop on the electrode was measured by voltmeter F4834.

The electrode was selected with respect to the accessibility and low price of the material needed for it, as well as its inertness to H_2O_2. All tests were performed with the use of a magnetic mixer.

The need to develop concise methods for determining the concentration of C_2H_5OH in aqueous solutions arises from the requirements imposed by the quality control of alcohol drinks.

Another reason for developing these sensors is for detecting microquantities of C_2H_5OH in aqueous solutions of various origins.

The authors devoted their investigations to the development of a peroxidase-biomimetic sensor for determining trace quantities of ethyl alcohol in various solutions. In all tests the reaction system represented a mixture of microamounts of hydrogen peroxide and ethyl alcohol in an aqueous medium. The task was to determine the effect of the H_2O_2:C_2H_5OH ratio on the detection ability of the biomimetic electrode.

In a series of experiments, the concentration of ethyl alcohol varied from 10^{-8} to 5 wt.%, whereas hydrogen peroxide was constant, equal to 1 wt.%. The results obtained are shown in Figure 8.10, where the curve for redistilled water is given for comparison. Since the electrochemical reaction mixture [7, 8] possesses catalytic activity, Figure 8.10 also shows a curve of the electrochemical potential change for 1% aqueous H_2O_2 in the absence of C_2H_5OH.

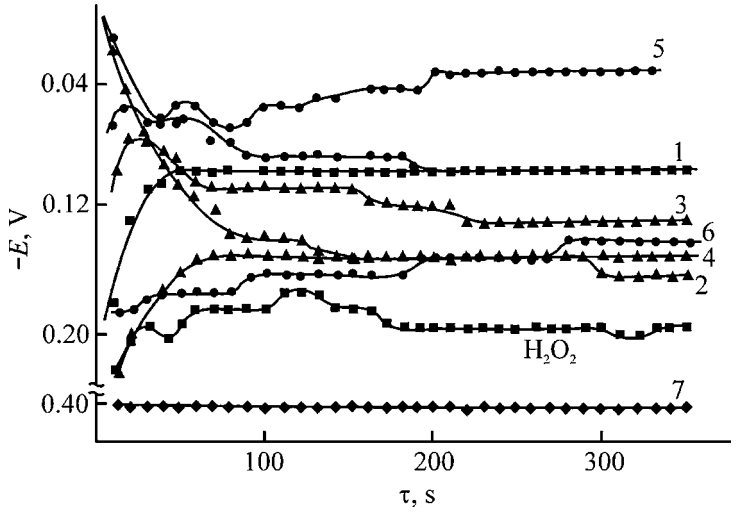

Figure 8.10 Time dependencies of electrochemical potential at 1 wt.% H_2O_2 and different C_2H_5OH concentrations (1: 5×10^{-6}; 2: 5×10^{-5}; 3: 5×10^{-4}; 4: 5×10^{-2}; 5: 5×10^{-1}; 6: 5 wt.%; 7: redistilled water).

As might be expected [7, 8], the curve of the electrochemical potential of the catalase reaction in relation to the water potential shifts to positive values.

To analyze the curves of peroxidase reaction, one should measure the electrochemical potential of 1% aqueous ethyl alcohol. Its value coincides with the redistilled water potential. Thus, the aqueous–alcoholic mixture is inert in relation to the electrode. The peroxidase curves (Figure 8.10) of the potential change in the $C_2H_5OH + H_2O_2$ reaction mixture in the case of constant H_2O_2 concentration (1 wt.%) and variable C_2H_5OH concentration in the range between 10^{-6} and 5 wt.% indicate a higher shift of the potential to greater values than for the H_2O_2 catalase curves. The greatest difference between the potentials of the H_2O_2 and $C_2H_5OH + H_2O_2$ mixture is observed at $\tau = 10$ s. For 1% H_2O_2 and C_2H_5OH solutions, $\Delta E \approx 0.2$ V. At the initial stage of peroxidase reaction, the potentials were found to be higher compared with later stages. Note that the mixture $C_2H_5OH + H_2O_2$ potential never coincided with the H_2O_2 potential and more often was not lower. Hence an important conclusion can be made: there is a reaction between C_2H_5OH and H_2O_2, obviously proceeding in the system. This reaction is responsible for the increase in the peroxidase reaction potential, which is greater than for the catalase reaction. In the absence of a peroxidase reaction the observed potential in the system must coincide with that of the catalase reaction. However, the disposition of the peroxidase potential curves indicates a definite periodic behavior with respect to low concentrations of ethyl alcohol. Such a disposition may be associated with the methodological imperfection of peroxidase mimic fixation on the surface of the aluminum electrode. Apparently, this question may be resolved only in the case where possible systematic errors caused by biomimetic electrode are eliminated.

It is common knowledge that acetaldehyde in the system $C_2H_5OH + H_2O_2$ can be synthesized not only in peroxidase reaction in the presence of a catalyst, but also according to

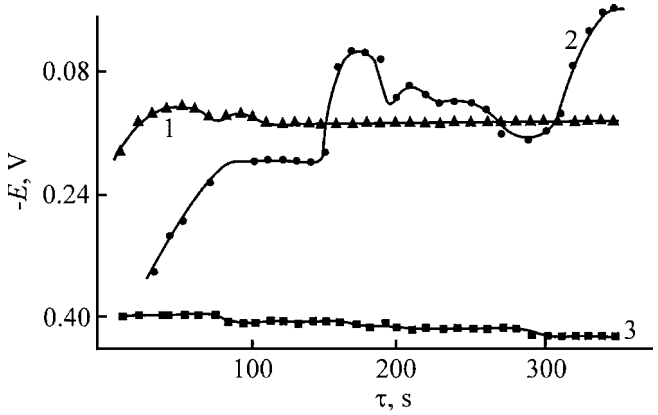

Figure 8.11 Time dependencies of peroxidase electrode potential for 1 wt.% H_2O_2 and different CH_3CHO concentrations – the product of electrochemical reaction (1: 0.25; 2: 0.25 + 10^{-2}; 3: 0.025 wt.% C_2H_5OH).

the monooxygenase mechanism. This question can be resolved by a standard identification method for peroxide reaction [13]. For this purpose, a thymolphthalein indicator was added 1% aqueous H_2O_2 with a weighing of a biomimic. Hence, the solution color change from transparent to dark blue identified the peroxidase mechanism of acetaldehyde synthesis.

The next series of experiments studied the influence of acetaldehyde on electrochemical potential of the system.

Curve 3 for acetaldehyde in Figure 8.11 is located below the potential curves for water and ethyl alcohol, because acetaldehyde is a nonpolar substance. Curve 1 of the potential change of the reaction mixture $CH_3CHO + H_2O_2$ is located above the hydrogen peroxide curve. This, apparently, testifies to the reaction (possibly, monooxygenase) between H_2O_2 and CH_3CHO, in which polar substance CH_3COOH is synthesized.

The experimental data shown in Figure 8.11 (curve 2) were obtained as follows: aqueous H_2O_2 was added to the reaction mixture $C_2H_5OH + CH_3CHO$ with $\tau = 130$ s. Curve 2 shows that the potential of the aqueous $C_2H_5OH + CH_3CHO$ solution (up to $\tau = 130$ s) is much higher than the potentials of these substances separately, which are usually at the level of the water potential or lower. The observed phenomenon can be explained by the formation of a new surface layer on the electrode. If C_2H_5OH and CH_3CHO separately were to form an electrode surface, curve 2 could hardly be obtained (Figure 8.11) with the area up to $\tau = 130$ s, typical of it. In all likelihood, ethyl alcohol with acetaldehyde form associates in water, and the activity of these formations is higher than for each of them separately. Injection of H_2O_2 to the $C_2H_5OH + CH_3CHO$ mixture at $\tau = 130$ s induces a noticeable, jump-like increase of the potential and occurrence of maxima and minima typical of complex electrochemical reactions. One can suggest the presence of two shapes of acetaldehyde molecules in the system. One of them synthesized in the peroxidase reaction is fixed on the electrode surface or in the surface layer of the mixture, where the CH_3CHO concentration is higher than in the volume. The second shape occurs when CH_3CHO is present in the volume. It is the author's opinion that the combination of these two shapes is responsible for the maxima and minima observed in curve 2 (Figure 8.11).

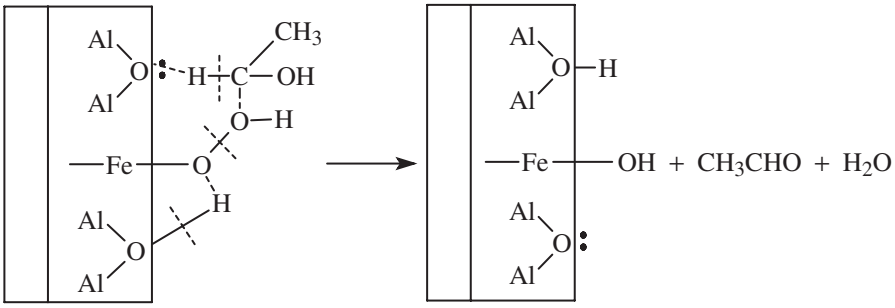

Figure 8.12 The apparent mechanism of peroxidase-mimetic electrode operation in electrocatalytic mode.

Besides the catalase reaction, a peroxidase reaction synchronous to that mentioned proceeds in the electrochemical system studied. These two reactions interact (are conjugated) with one another via the general intermediate $PPFe^{3+}OOH/Al_2O_3$.

By analogy with the mechanism of the catalase reaction, the probable mechanism of the peroxidase reaction is considered (Figure 8.12). Note that a proton transferred to the active site of the biomimetic electrode can be replaced by H^+ from the reaction mixture volume. The mechanisms of catalase and peroxidase reactions provide an insight into the ways of their realization in the electrochemical mode. The ratio of products synthesized in both reactions (O_2 and CH_3CHO) depends on the ratio of the H_2O_2 and CH_3CHO interaction rates with the surface intermediate.

Figure 8.13 shows the results of experiments in which the aqueous H_2O_2 concentration varied between 0.01 and 1 wt.% at constant C_2H_5OH concentration (1 wt.%). It is observed that the electrode potential in the reaction mixture $C_2H_5OH + H_2O_2$ increases with H_2O_2 concentration. This, apparently, is associated with the fact that the rates of all three reactions mentioned above increase with H_2O_2 concentration. The observed complex shape of the potential change curves and experimental data spreading can be explained in the framework of the biomimetic electrode preparation procedure, i.e. each time it is produced with the help of an adhesive and the active mass is applied non-uniformly with varying thickness of the layer.

The experimental data on the sensitivity threshold of the peroxidase-mimetic sensor designed for detecting microquantities of C_2H_5OH are shown in Figure 8.14. The electrode potentials in Figure 8.14 correspond to different microquantities of C_2H_5OH and represent the highest ΔE values, selected from the experimental curves in Figure 8.10. It should be noted that the entire experimental material was obtained for a single sample of aluminum electrode. Each time, when preparing a new peroxidase mimetic electrode, the old one was mechanically removed from the aluminum support and the new portion was then adhered with an adhesive to the same place. Of course, this technique of biomimetic electrode preparation may cause systematic errors. For example, the aluminum electrode can be worn out or some part of the old material can remain on the surface. Therefore, the alteration of maxima and minima observed in Figure 8.14 may reflect systematic errors associated with the preparation of the biomimetic electrodes or complex physicochemical processes proceeding on the surface.

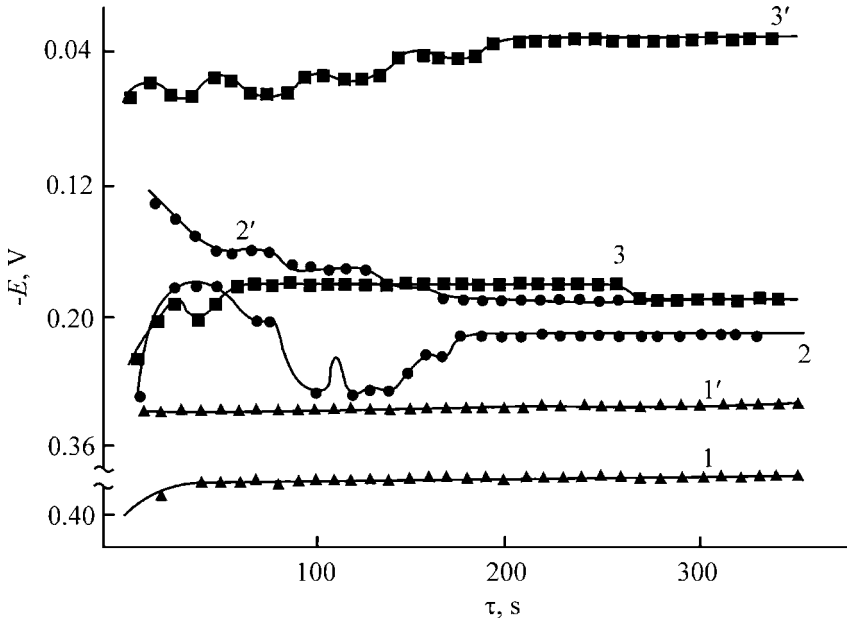

Figure 8.13 The dependence of catalase (1–3) and peroxidase (1′–3′) reaction potentials on H_2O_2 concentration in the mixture with 1 wt.% C_2H_5OH (1, 1′: 0.01; 2, 2′: 0.1; 3, 3′ 1 wt.% H_2O_2).

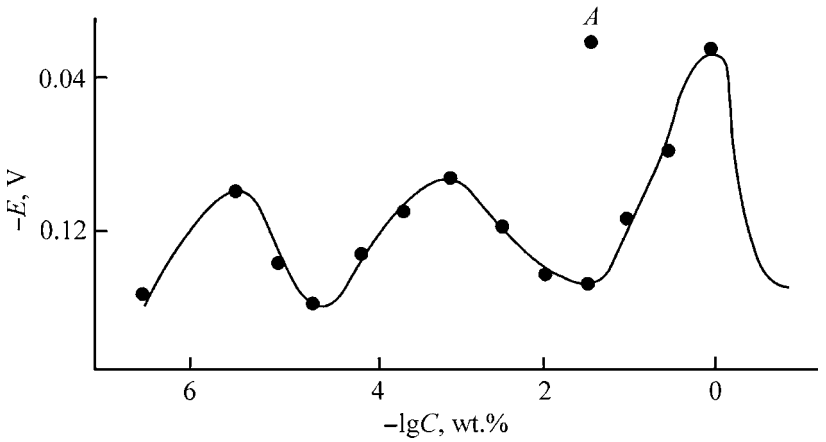

Figure 8.14 The dependence of peroxidase sensor potential on ethanol concentration (*C*) in aqueous solution with 0.01 wt.% H_2O_2 (A: result of the test with new aluminum electrode).

To check these suggestions, the authors conducted an experiment with a peroxidase-mimetic sensor prepared on a new aluminum electrode under conditions corresponding to one of the minima in Figure 8.14. As shown by the plot of this experiment (point A in Figure 8.14), the minimum at C_2H_5OH concentration equal 10^{-3} wt.% depends on aluminum foil conditions: for a fresh electrode a sharp, jump-like increase of the potential is detected.

Of course, this fact outlines ways to improve the physicochemical parameters of biomimetic sensor design and, consequently, the technological modernization of biomimetic electrode preparation. As concluded from the data in Figure 8.14, the sensitivity threshold of the designed sensor is very high (10^{-8} wt. % aqueous ethyl alcohol) [14].

New approaches to the creation and analytical use of biosensors and their analogs allowing concise information about the chemical composition of the analyzed object shaped as an electrical signal are rapidly being developed.

In the context of commercial use, progress in sensor technologies will be fully defined by their price and usability. To make biosensors competitive with existing methods of analysis, the price of single-use biosensors should be below US$ 2, and for non-expendable devices should be US$ 0.50 per analysis. It is obvious that the introduction of sensor technologies will promote the increase of qualitative and quantitative indices of medical analyses and, hence, diagnostics, monitoring of food and the environment, and technological processes.

REFERENCES

1. Clark, L. and Lyons, C., *Ann. Ny. Acad. Sci.*, 1962, Vol. 102, pp. 29–45.
2. Berezin, I.V., Bogdanovskaya, V.A. and Varfolomeev, S.D., *Dokl. Akad. Nauk. SSSR.*, 1978, Vol. 240, pp. 615–619 (in Russian).
3. Varfolomeev, S.D., Kurichkin, I.N. and Aropolov A.I., 1996, Vol. 11, No. 9, pp. 863–871.
4. Varfolomeev, S.D., Evdokimov, Yu.M. and Ostrovsky, M.A., *Vestn. Ros. Akad. Nauk.*, 2000, Vol. 70, No. 2, pp. 99–108 (in Russian).
5. Nagiev, T.M., *Zh. Fiz. Khim.*, 1996, Vol. 70, No. 6, p. 967 (in Russian).
6. Horozova, E., Dimcheva, N., Jordanova Z., *3rd World Congress on Oxidation Catalysis*, SanDiego, CA, September 21–26, 1997, Abstracts 2, L-10.
7. Nagiev, T.M., Abbasova, M.T., Baba-zade, S.N., Stepanova, E.V. and Agamamedova, L.M., *Zh. Fiz. Khim.*, 1999, Vol. 73, No. 12, p. 2261 (in Russian).
8. Nagiev, T.M., Abbasova, M.T., Baba-zade, S.N., Kuliev, S.A., Stepanova, E.V. and Agamamedova, L.M., *J. Appl. Biochem. Biotechnol.*, 2000, Vol. 88, p. 275.
9. Sorochinsky, V.V. and Kurganov, B.I., *Prikl. Biokhim. Mikrobiol.*, 1997, Vol. 33, No. 6, p. 579 (in Russian).
10. Glazkov, V.V., Mizgunov, U.M., Zolotova, G.A. and Dolmanova, I.F., *Zh. Analit. Khim.*, 1997, Vol. 52, No. 1, p. 83 (in Russian).
11. Nagiev, T.M., Zul'farova, S.Z. and Shikhiev, Yu.M., *Vestn. MGU, Ser. 2, Khim.*, 1992, No. 33, p. 134 (in Russian).
12. Nagiev, T.M., *Chemical Conjugation*, Nauka, Moscow, 1989, 215 pp. (in Russian).
13. Waker, J.F., *Formaldehyde*, Goskomkhimizdat, Moscow, 1957, 423 pp. (in Russian).
14. Agamamedova, L.M., Abbasova, M.T. and Nagiev, T.M., *Zh. Fiz. Khim.*, 2002, Vol. 76, No. 12, pp. 2194–2198 (in Russian).

This page intentionally left blank

– 9 –

General Issues of Selectivity and Flexibility of Chemical Systems

To clearly demonstrate the tendency and outlook for the practical application of conjugated processes in the near future, our theoretical knowledge must be integrated with application capabilities. According to well-known reasoning, it is appropriate that we perform such 'working out' using the example of conjugated oxidation reactions with hydrogen peroxide. In this connection, the variety of its technical applications is of special interest.

The production volume of hydrogen peroxide is in hundreds of thousands of tons. It is one of the most widespread and valuable products in modern chemistry. All over the world hydrogen peroxide is widely applied in epoxidation and hydroxylation processes, for example, in glycerol production from allyl alcohol or organic peroxides, which are polymerization and vulcanization initiators.

At present, the economic conditions of hydrogen peroxide production and consumption clearly indicate the customers' wish for a rapid increase in its manufacture to the construction of large-tonnage enterprises with high productivity of every single unit. This will significantly reduce the cost price of H_2O_2 and form a good basis for a further broadening of its intensified introduction in the economy. Relatively stable prices would also increase manufacturers' profits (at the time of writing, the cost price per 1 ton of 35 wt.% hydrogen peroxide is about US$ 45–50).

On the one hand, these data impress on low costs of H_2O_2 production by the existing technology and, on the other hand, they justify the increasing role of H_2O_2 in modern production.

Chemical processes associated with the application of hydrogen peroxide meet the requirements of modern engineering, namely, they are highly selective, economic, ecologically friendly, productive, etc.

In previous chapters an attempt was made to summarize theoretical and experimental results, which present modern ideas of chemical conjugation. Special attention was paid to free radicals – the intermediates participating in the 'radical induced attack' of substrate molecules in oxidation reactions with hydrogen peroxide. Hence, the phenomenon of induced two-electron oxidation of the substrate proceeding in one stage with hydrogen peroxide, both in gas and liquid (biological systems) phases was also particularly considered. It has been shown that because of the spin prohibition, oxygen is unable to implement oxidation in one stage and that hydrogen peroxide has such abilities. This is the principal difference between the oxidation mechanisms.

Despite the differences between the functions implemented by hydrogen peroxide in gas, liquid and biological oxidation processes, they are united by a specific feature: H_2O_2 first transforms to a higher reactive form in which the donor–acceptor properties of the original compound are preserved, and then only (in this new form) oxidizes the substrate according to the conjugated mechanism.

Developing the ideas of the enzymatic catalysis mechanism, Poltorak [1] formulated a scientific statement about the meeting of chemical mechanisms of homogeneous, heterogeneous and enzymatic catalysis in the framework of the concept of a linear bond redistribution chain suggested by him.

Zamaraev *et al*. [2] have concluded that there are 'deep analogies in the structure and the mechanism of active sites in homogeneous, heterogeneous and enzymatic systems: the reason is the coincidence of unitypical active site properties in different systems and qualitatively equal types of the environmental influence on the mechanism of the rate of the key stage of catalysis'.

Emphasizing the community of active site mechanisms in homogeneous, heterogeneous and enzymatic catalyst, the authors of the above works became catalytic chemists and introduced a new methodology, which consists in the existence of a somewhat ideal catalyst for substrate transformation. Therefore, the main objective is to model this catalyst for homogeneous or heterogeneous and enzymatic reactions (depending upon the particular tasks facing the investigators).

Apparently, a 'portrait' of the ideal catalyst should be designed for every type of catalytic reaction, and an object-oriented construction of the real catalyst able to implement catalytic transformations by the single mechanism, supplemented with particular details in respect of the reaction mixture and the process regime, should be implemented.

Let us discuss the questions outlined in more detail using the example of conjugated substrate oxidation with hydrogen peroxide. Hydrogen peroxide concentration in the reaction mixture is reduced in the course of the reaction, followed by the change of the key active sites ($HO_2^{\bullet}$ and $^{\bullet}OH$ radical) and, correspondingly, the physicochemical situation is changed not for the benefit of selective transformation of the raw material.

Let us remind ourselves briefly of the essence of oxidation and why the consequences caused by a change of its mechanism are so catastrophic for the selectivity of the process.

Seemingly, the situation is very simple: H_2O_2 concentration usually decreases in the course of oxidation and, therefore, $HO_2^{\bullet}$ radical synthesis is hindered. Thus, $^{\bullet}OH$ radicals as active sites dominate in the system with all the ensuing consequences, which are an abrupt decrease of efficiency and selectivity of oxidation. Such a change of the key active sites in the chemical system transforms the oxidation mechanism and provides a gradual transition from the two-electron stages to single-electron radical reactions, i.e. transition from selective to random oxidation.

What added measures can be taken to avoid this seemingly fatal fate of the free-radical processes with hydrogen peroxide participation? As with any other process, selective oxidation with hydrogen peroxide can be divided into three-conditional stages: ripening (the initial reaction stage), mature period (stable, stationary area of the fullest reaction proceeding) and expiration (deterioration and degeneration of selective oxidation). After the initiation of the reaction active oxidation sites are synthesized, accumulated and fixed. When this period in the development is finished, the reaction mixture formed is ready for selective oxidation of

the substrate. To put it more vividly, this is the most spacious time and the fullest life of the reaction. Then gradual attenuation of the catalytic activity is initiated in the reaction mixture. In the case of hydrogen peroxide, this means the change of the oxidation mechanism and degeneration of the process, followed by its natural end – deterioration of the oxidation parameters.

Needless to say, such division of the process is conditional; all stages follow one another without abrupt interfaces, but physicochemical characteristics clearly distinguish them at any time. Elementary $HO_2^{\bullet}$-dependent reactions are the first to be sensitive to H_2O_2 deficiency, which affects the selectivity of the substrate oxidation. Naturally, the increase of $^{\bullet}OH$ radical concentration in the reaction mixture is damaging for the substrate (i.e. it intensifies the degradation reactions).

This is the key problem of selective oxidation with hydrogen peroxide. Is there a way out of this situation? Of course, we are talking about creating conditions for highly selective substrate transformation to the required product. In the context of the applied tasks, this is already highly valuable.

In due course, radicals $^{\bullet}OH$ were the subject of great attention however, no practical results were obtained. For example, the main 'factories' producing $^{\bullet}OH$ radicals, which are Fenton and similar redox systems, manifested themselves as initiating systems, i.e. operates as the 'triggers' of radical polymerization.

Since the main reason for selectivity decrease of oxidation with hydrogen peroxide is associated with $^{\bullet}OH$ radical accumulation in the system, the search for ways to eliminate this event, i.e. liquidating the reason but not the consequence, should consist in the following:

- sectional H_2O_2 delivery to a pipe (flow) reactor;
- reasonable time decrease of reagent exposure in the reaction zone (in order to eliminate the reaction at low H_2O_2 concentration, if possible);
- development of effective catalytic systems that model separate principles of enzyme operation.

In this context, the most successful will be the branch of 'pure' catalysis of oxidation where the substrate is oxidized in close connection with the catalyst, i.e. the catalyst forms an active intermediate with the substrate or oxidant (or, probably, with both).

Thus, there may be an unlimited increase in selectivity by the elimination of free-radical intermediates. For example, selectivity of liquid-phase epoxidation with organic hydroperoxides depends on two factors [3]:

1. if electrons are transferred between the catalyst and the substrate (strong oxidants), homolytical ROOH dissociation reducing selectivity of the entire process is implemented;
2. as the substrate is heterolytically added to the catalyst (weak oxidants), e.g. if electron transfers are absent, selective oxidation is the predominant process.

However, despite a clear understanding of the homogeneous-type problems, the development of practically suitable catalysts for homogeneous or heterogeneous catalysis face difficulties associated with resolving particular questions of targeted catalyst design.

Meanwhile, currently existing radical reactions are important for organic synthesis and catalysis. They successfully compete with other synthesis techniques based on heterolytical reactions [4].

The problems occurring in the study of oxidative reactions in different phases and systems are complex and, therefore, make the composition of the 'principal layout' of the oxidation mechanism very complicated.

In this context, homolytical oxidation reactions (autooxidation) proceeding by the free-radical mechanism seem to be the most suitable model. In autooxidation reactions ROOH dissociation catalysis (in the most reduced case, H_2O_2) plays the key role, but does not eliminate selectivity. This is the most urgent problem of homolytical oxidation.

In the autooxidation system, the initial stage only (dissociation) is catalyzed. Other stages are usually insensitive or less sensitive to the catalyst action. This situation strictly limits the abilities of catalyst selection for selective homolytical oxidation.

For high-temperature homolytical oxidation of hydrocarbons, it should be taken into account that the difference in reactivities of different C—H-bonds in relation to radical attack becomes insignificant, which provides for formation of many different reaction products.

One of the important solutions to the known difficulties should be found among conjugated catalytic systems which simulate oxidation enzyme operation. In this branch all the research and attempts are aimed at immobilizing transition metal complexes – enzyme active site analogues.

It is apparent that in future a combination of catalysis and chemical conjugation will be an important direction in the search for ways of selective substance transformation according to the oxidative mechanism.

In the oxidation reactions the problem of oxidant activation is frequently met (in the general case, activation of small molecules [5]). For example, comparatively low reactivity of O_2, H_2O_2 and O_3 under soft conditions requires their prior thermal or catalytic activation, for instance, with the help of transition metal complexes or irradiation. Activation of molecular oxygen by one-electron reduction consumes energy:

$$O_2 + \bar{e} \rightarrow O_2^{\bullet -}, \quad \Delta G^0_{298} = 15.4\,\text{kJ/mol}$$

$$O_2 + RH \rightarrow HO_2^{\bullet} + R^{\bullet}$$

This is a thermodynamically unprofitable way due to the simultaneous transfer of two or more electrons.

An important detail should be mentioned: molecular oxygen, representing a triplet (biradical) in the main state, enters only single-electron reactions with organic compounds. Therefore, in homogeneous oxidation free radicals are necessarily generated to the reaction system. Activation of O_2 by transition metals, iron ions, in particular, provides for formation of linked oxygen shaped as a 'superoxide' ion:

$$Fe^{2+} + O_2 \rightarrow Fe^{3+} + O_2^{\bullet -} \tag{9.1}$$

which, usually, does not add a proton. However, cooperating with Fe^{2+}, it forms another complex of the peroxide type ($Fe^{4+}\,O_2^{2-}$) which easily reacts with protons in the acidic medium.

The overall reaction is presented by the following equation:

$$Fe^{3+}\,O_2^{\bullet-} + Fe^{2+} + 2H^+ \rightarrow 2Fe^{3+} + H_2O_2 \qquad (9.2)$$

Active forms of oxygen, formed by reactions (9.1) and (9.2), are not yet ready for selective interaction with the substrate because, in principle, they may enter various reactions, including undesired processes:

$$Fe^{3+}\,O_2^{\bullet-} + RH \rightarrow Fe^{3+} + HO_2^- + R^{\bullet} \qquad (9.3)$$

$$Fe^{3+}\,O_2^{\bullet-} + RH \rightarrow Fe^{2+} + HO_2^{\bullet} + R^{\bullet} \qquad (9.4)$$

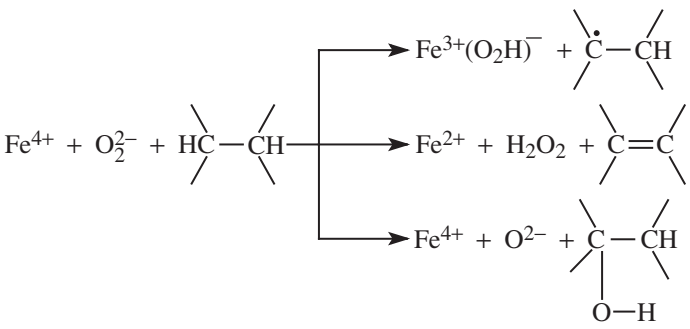

(9.5)

(9.6)

(9.7)

It is obvious from the mechanism (9.1)–(9.7) that oxidation condition variation may direct the process towards selective formation of a definite product. For example, oxygen-containing compounds can be obtained in one highly selective stage (monooxygenation) by the reaction channel (9.7). The comparative simplicity of these reactions is also associated with the fact that metal complexes, representing something like 'weak acids', coordinate 'weak' bases, such as olefins, N_2, CO, etc. with formation of unstable complexes, which provide for catalytic transformation of the substrate [5].

Another class of substrate selective oxidation processes is the synchronous transfer of two electrons according to reaction (9.6), which indicates the principal possibility of weak and selective oxidation of organic substances, which is urgent for the creation of new oxidation technologies.

Of interest is that in some cases O_2 replacement by H_2O_2 in the systems under consideration promotes a significant increase of the selective oxidation rate [6]; in other cases, it promotes synthesis of new, previously undetected products [7]. This may be explained by the fact that in oxidation with molecular oxygen H_2O_2 is always an endogenic intermediate product, playing a key role in the substrate conversion mechanism and O_2 reduction to H_2O. Moreover, H_2O_2 is the endogenic product of the metabolic cycle. This circumstance has attracted the interest of biochemists in new theoretical ideas concerning oxidation with

hydrogen peroxide and model redox systems, which include exogenic hydrogen peroxide, because the mechanism of these systems is principally equal to endogenic H_2O_2 action.

Therefore, the questions associated with the ways and methods of exogenic H_2O_2 activation also become urgent. Model systems simulating separate properties and functions of biological analogues also help in their resolution: biooxidation by catalase, peroxidase and monooxygenase enzymes. On the other hand, progress in decoding some details of catalase and peroxidase chemical mechanisms with the help of model systems will finally provide for effective modernization of model catalyst structures for selective oxidation.

It should be noted that this problem has been the subject of great interest for many years and publications on this topic are so abundant that we cannot discuss them comprehensively here. The majority of these papers show that transition metal–H_2O_2 systems have the greatest potential for studying the redox processes.

The mechanism of two-electron iron ion oxidation with hydrogen peroxide performed in one stage was already suggested in 1932 [8] and experimentally proved [9] by determination of the following mechanism:

$$Fe^{2+} + H_2O_2 \rightarrow Fe^{4+}\,O^{2-} + H_2O$$

$$Fe^{4+}O^{2-} + Fe^{2+} \rightarrow Fe^{3+} + Fe^{3+}OH$$

These theoretical suggestions were found to be very useful for further stages in the development of the oxidation mechanism: up to now ferryl-ion ($Fe^{2+}O$) has been considered in biooxidation as the intermediate hydroxiding intermediate [10].

At the present time, the one-stage two-electron oxidation mechanism with hydrogen peroxide has been unambiguously determined for iron ions [11] and lanthanide elements [12]. This compares favorably the oxidation mechanism with hydrogen peroxide to the oxidation mechanism with molecular oxygen, because in the latter case, $^{\bullet}OH$ radicals are necessarily formed in the system. The singularity of ferryl-ion reactivity consists in displaying chemical properties typical of atomic oxygen, $^{\bullet}OH$ radical or superoxidized iron ion (the two-electron acceptor) with respect to redox and steric characteristics of the substrate, owing to the existence of the following interconvertible states:

$$LFe^{2+}\,O \leftrightarrow LFe^{3+}O^{\bar{\bullet}} \leftrightarrow LFe^{4+}\,O^{2-}$$

where L is organic or inorganic ligand. There are indications that in aqueous solution this particle easily dissociates to single-electron transfer products synthesizing $^{\bullet}OH$ free radicals in the system.

As follows from the above, to activate O_2 and H_2O_2 transition metal ions must be reduced. Therefore, several recommendations for modernizing oxidation catalysts can be formulated:

- superoxidized transition metal ions must be used; they are able to implement two-electron oxidation in one stage (i.e. it is reached by metal oxidation with oxygen or H_2O_2);
- transition metals must possess properties of moderate oxidants and reducers, otherwise obstacles will occur in the course of the catalytic cycle;

- if possible, substrates should be reducers able to be oxidized according to the two-electron mechanism in one act;
- it is desirable to inject superoxidized metal ions into the reaction system;
- the steric structure of the substrate and the catalyst must not prevent their interaction.

In fact, the implementation of highly selective two-electron processes of catalytic oxidation with H_2O_2 provides for the development of a principally new technology for substrate conversion to target products bypassing the formation stages of the substrate intermediates, which initiate additional channels of substrate consumption for side product synthesis.

Single-electron reactions are widespread in chemistry. They are usually described in the framework of chain radical reaction theory. However, selective conversion may barely be obtained in such systems, because substrate intermediates are consumed in many directions.

In general, the solution of the selectivity question for chain radical reactions depends on a favorable combination of various process conditions. Unfortunately, a desirable combination is not always to be found. The profound improvement of chain oxidation parameters towards higher selectivity should be reached via synchronous two-electron oxidation. An attempt to induce two-electron substrate oxidation without its transition to intermediate using complex free radicals is always sensible.

Different forms of active oxygen [13, 14] are present on the surface of a heterogeneous catalyst. Under appropriate conditions, these forms can convert the substrate in several directions. The qualitative and quantitative characteristics of these forms usually depend on catalyst preparation and activation techniques and may be difficult to control, i.e. unresolvable obstacles can occur on the way of selectivity increase.

In this respect, metallocomplex catalysis is most preferable. In this process, variations of ligand and diluter types allow control of the catalyst activity. When combined with soft conditions, this provides for high selectivity of the process.

Nevertheless, metallocomplex catalysts display a series of principal disadvantages compared with heterogeneous catalysts: the necessity to separate reaction products from the catalyst, relative thermal instability and, in the majority of cases, relatively low productivity of the catalyst.

Thus, the present monograph presents the range of typical technical approaches to and kinetic estimations of conjugated processes, representing 'the thread of Ariadne' which shows the direction in which to search for a solution to the question of 'active site amplification'—the increase of unitypical active site concentration in the reaction mixture. All this is merely a guideline as sufficient information can only be obtained by experiments. The increased level of experimental technology and theoretical knowledge define recent progress in determining the chemical origin of intermediates, operating *in situ*, and reduces to a minimum the number of various suggestions about the mechanism of conjugation reactions. In this context, of great importance is a kinetic model of the conjugated processes which reflects their dynamics. It is not simply a supplement to the research, but allows conditions to be foreseen for the best 'counter adaptation' of interfering reactions.

It is the author's opinion that the method of oxidation in the oscillation-kinetic mode gives an opportunity to resolve effectively the problem of establishing chemical processes that can be flexible and capable of being adjusted to the manufacture of different products in a very short time. Recently, production flexibility has been associated with 'flexibility of

space': plants, workshops and areas that allow low-cost reconstruction in a short time [15–18]. We wonder why universalization, which has transformed many branches of industry, did not touch upon chemical technology.

However, 'truly flexible technology' usually means a transition from laboratory tests to pilot experiments, when reconstruction is almost unnecessary. This question is harmonized with universalization of chemical production. Therefore, such a solution seems improbable and is unsatisfactory for chemical engineers. This is because every introduced chemical reaction is distinguished by a specific feature, which does not allow the unification of entire chemical processes and separate process assemblies.

Taking into account all the above-said, the authors think it of interest to suggest one more solution for chemical production unification. It consists not in designing separate chemical engineering processes, differing in both chemical and engineering bases, but in the creation of chemical systems in which chemical reactions with abundant general properties can be realized.

A chemical system, in which a series of unitypical reactions can be implemented, will possess the properties suitable for the unification of the entire reaction system, though minor additions and exclusions are allowed. There is no doubt that conjugated oxidation reactions of various substrates with hydrogen peroxides are related to these chemical systems. Finally, this will help in the creation of principally new processes of chemical oxidation, which will meet modern requirements such as the economic use of energy and mineral resources, specific productivity increase of chemical reactors, and the maximum possible elimination of environmental contamination.

***

To conclude the discussion, it is desirable to emphasize that the previous monograph [19] concluded with the same ancient Latin epigram that begins the present monograph is started. When I was working on the previous book, I felt that I was climbing a mountain. The monograph was published, but the investigations still continued. The ensuing years have been full of intensive research which has allowed me to contribute to the development of the chemical interference theory, phase shifts, and coherence of synchronized reactions, and to give an experimental proof of the theory.

Most of this monograph presents scientific results, and when I finished it, I felt that my climb was over and that I had conquered the mountain. However, I also thought about the next mountain to conquer and whether I have enough strength for the task, and more importantly, if I even wanted to do it.

It is clear to me that the current height is not in the Himalayas. It may be in my beloved Caucasus, but you can take my word for it: 'The thing better than mountains is the mountains you have not yet visited'.

REFERENCES

1. Poltorak O.M. and Chukhrai E.S., *Physicochemical Fundamentals of Enzymatic Catalysis*, Vysshaya Shkola, Moscow, 1971, 331 pp. (in Russian).

2. Zamaraev K.I. and Zhidomirov G.M., *V International Symposium on Connections between Homogeneous and Heterogeneous Catalysis*, Vol. 1, Novosibirsk, 1986 (in Russian).
3. Masters K., *Homogeneous Catalysis with Transition Metals*, Mir, Moscow, Mir, 1983, 300 pp. (in Russian).
4. Nikishin G.J., *Abstract, VI International Conference on Organic Synthesis*, Moscow, 1986, p. L-02.
5. Shilov A.E., *Kinetika i Kataliz*, 1980, Vol. 31, No. 1, pp. 26–32 (in Russian).
6. Breslow R. and Lukens J., *J. Biol. Chem.*, 1969, Vol. 235, pp. 292–296.
7. Normann R.O.C. and Rodder G.K., *Biol. Chem. Soc.*, 1962, Vol. 237, No. 4, pp. 138–144.
8. Bray W.S. and Gorin M.H., *J. Amer. Chem. Soc.*, 1932, Vol. 54, pp. 2324–2328.
9. Cahill A.F. and Taube H., *Ibid.*, 1952, Vol. 74, pp. 2312–2325.
10. Czapski G., Samumi A., and Meisel D., *J. Phys. Chem.*, 1971, Vol. 75, p. 3271.
11. Shtamm E.V., '*Catalysis of Ascorbic Acid Oxidation with Copper Ions'*, PhD Thesis, MGU, Moscow, 1975, 120 pp. (in Russian).
12. Lupenok-Burmakina A.V., Lezina G.G., Emelianov V.B. *et al*., *Zh. Fiz. Khim.*, 1974, Vol. 48, No. 12, pp. 3013–3016 (in Russian).
13. Kazansky V.B., *Kinetika i Kataliz*, 1977, Vol. 18, No. 1, pp. 43–54 (in Russian).
14. Czandern A.W., *J. Coll. Interf. Sci.*, 1967, Vol. 21, p. 500.
15. Legasov V.A. and Safonov M.S., *Khim. Prom.*, 1985, No. 3, pp. 22–29 (in Russian).
16. Gross man J.E., Halemane K.P., and Swaney R.E., *Comp. Chem. Eng.*, 1983, Vol. 7, pp. 439–442.
17. Morrari M., *Ibid.*, pp. 423–427.
18. Rippin D.W.T., *Ibid.*, pp. 463–466.
19. Nagiev T.M., *Chemical Conjugation*, Nauka, Moscow, 1989, 216 pp. (in Russian).

This page intentionally left blank

Index

This page intentionally left blank